



UWS Academic Portal

Science and Art: A Future for Stone

Hughes, John; Howind, Torsten

Published: 01/01/2016

Document Version

Publisher's PDF, also known as Version of record

[Link to publication on the UWS Academic Portal](#)

Citation for published version (APA):

Hughes, J., & Howind, T. (Eds.) (2016). Science and Art: A Future for Stone: Proceedings of the 13th International Congress on the Deterioration and Conservation of Stone, Volume 2. Paisley: University of the West of Scotland.

General rights

Copyright and moral rights for the publications made accessible in the UWS Academic Portal are retained by the authors and/or other copyright owners and it is a condition of accessing publications that users recognise and abide by the legal requirements associated with these rights.

Take down policy

If you believe that this document breaches copyright please contact pure@uws.ac.uk providing details, and we will remove access to the work immediately and investigate your claim.



SC16

SCIENCE and ART: A Future for Stone

**Proceedings of the 13th International Congress on the
Deterioration and Conservation of Stone – Volume II**

**Edited by
John Hughes & Torsten Howind**

SCIENCE AND ART: A FUTURE FOR STONE

PROCEEDINGS OF THE 13TH INTERNATIONAL CONGRESS ON THE
DETERIORATION AND CONSERVATION OF STONE

6th to 10th September 2016, Paisley, Scotland

VOLUME II

Edited by
John J. Hughes and Torsten Howind



UNIVERSITY OF THE
WEST of SCOTLAND
UWS

© University of the West of Scotland, Paisley, 2016

Licensed under a Creative Commons Attribution 4.0 International License.



ISBN: 978-1-903978-58-0

ISBN: 978-1-903978-55-9 (eBook)

ISBN: 978-1-903978-59-7 (Set: Volume 1&2)

ISBN: 978-1-903978-56-6 (eBook-Set: Volume 1&2)

Hughes J.J. and Howind T. (Editors), “Science and Art: A Future for Stone. Proceedings of the 13th International Congress on the Deterioration and Conservation of Stone”, University of the West of Scotland, Paisley, September 6th to 10th, 2016.

Cover image: The front door of the Paisley Technical College building, now University of the West of Scotland. T.G. Abercrombie, architect 1898. Photograph and cover design by T. Howind.

PREFACE

Standing under the portico of the Paisley Town Hall, completed in 1882, and looking south east towards the West Façade of Paisley Abbey, built in the 13th to 15th Century, it is possible to compare two historical periods in Scottish building where the use of stone was unavoidable. Walking further into the historic centre of Paisley, or any other town or city in Scotland, reveals the ubiquitous use of uncovered natural stone in our architecture, and also the problems that it faces. The challenge in maintaining the essential integral character of our towns for the future, and to recognise and enhance their values is a complex one, but not our challenge alone. Much hard work is still needed to characterise, assess and propose conservation approaches that are compatible with the existing fabric and prevailing philosophies, in Scotland and around the world.

We sought to bring the 13th Congress to a damp Scotland of decaying stone structures, to share our stone-built heritage with the conservation community and also to focus on the needs of stone conservation for our built heritage in Scotland. We hope that by bringing some global attention to the issue, in the country where, arguably, modern geology began, we demonstrate the sharing of our common heritage and our values in seeking its understanding and protection.

In these volumes you will find the proceeds of the work of many people, the conservators, practitioners and even academics and researchers whose concern is the protection of our stone-made cultural heritage. The Permanent Scientific Committee (PSC) of the Stone Congresses worked to review each contribution followed by revision by the authors. The editing effort by ourselves involved direct improvements to text, in many cases, and by one of us in particular to the formatting. However, beyond the title pages and abstracts, after review by the PSC and revision by the authors, proof correction was limited. The contents and accuracy of the papers are therefore the responsibility of the authors.

John J. Hughes and Torsten Howind

Paisley, Scotland, August 2016

Permanent scientific committee

Christine Bläuer

Conservation Science Consulting Sàrl, Fribourg, Switzerland

Ann Bourgès

Ministère de la culture et de la communication, Paris, France

Susanna Bracci

Italian National Research Council, Rome, Italy

Philippe Bromblet (Vice-President)

Centre Interdisciplinaire de Conservation et Restauration du Patrimoine (CICRP), Marseille, France

Hilde De Clercq (President)

Royal Institute for Cultural Heritage, Brussels, Belgium

Eric Doehne

Scripps College, Claremont, CA, United States of America

Miloš Drdúcký

Academy of Sciences of the Czech Republic, Prague, Czech Republic

Christoph Franzen

Institut für Diagnostik und Konservierung an Denkmälern in Sachsen und Sachsen Anhalt e.V.,
Dresden, Germany

Jadwiga Łukaszewicz

Department for Conservation of Architectonic Elements and Details, Faculty of Fine Arts,
Nicolaus Copernicus University, Toruń, Poland

Antonia Moropoulou

School of Chemical Engineering, National Technical University of Athens, Greece

Stefan Simon

Institute for the Preservation of Cultural Heritage (IPCH), Yale University, West Haven, CT,
United States of America

Ákos Török

Department of Construction Materials and Engineering Geology,
Budapest University of Technology and Economics, Budapest, Hungary

Johannes Weber

Institute of Art and Technology, Conservation Science, University of Applied Arts Vienna, Austria

George W. Scherer

Civil and Environmental Engineering Department, Princeton University, United States of America

David A. Young

Heritage Consultant, Melbourne, Australia

ACKNOWLEDGEMENTS

Historic Environment Scotland, for their assistance and support in the hosting of the Congress Dinner at the Kelvingrove Art Gallery and Museum, Glasgow. Ewan Hyslop, Maureen Young and Christa Gerdwilker are thanked for their voluntary input to the organisation of technical visits to Largs and Glasgow.

The British Geological Survey.

Our commercial sponsors: SINT Technologies, Surface Measurement Systems, GC Laser Systems, Fokus GmbH Leipzig and Remmers.

Renfrewshire Council and the staff of the Town Hall.

The community at Paisley Abbey.

Alexander Collins, excursion guide.

Drew Wilson, Richard Potts and Stuart Johnson of UWS's Corporate Marketing for design and layout of the Congress Logo, programmes and other printed matter.

Finally, thanks must go to Alison Wright (formerly of Glasgow University), who bravely bore our application to host the Congress to New York in 2012, without complaint. On this occasion we must also thank the team at the University of the West of Scotland; Georgia Adam, Irene Edmiston, Gaia Frola, Matt Gilmour and Emma Paterson, without whose efforts the Congress could not have been held.



This page has been left intentionally blank.

CONTENTS

Volume I

Damage	1
Traffic-induced Emissions on Stone Buildings.....	3
<i>M. Auras, P. Bundschuh, J. Eichhorn, D. Kirchner, M. Mach, B. Seewald, D. Scheuvsens and R. Sneathlge</i>	
Weathering Patterns of the Carved Stone and Conservation Challenges - World Heritage Site of Qutb Complex, New Delhi	13
<i>S.S. Bais and S.C. Pandey</i>	
Effect of Microorganism Activities in a Polluted Area on the Alteration of Limestone used in Historical Buildings	25
<i>C. Balland-Bolou-Bi, M. Saheb, N. Bousserhine, S. Abbad-Andalousi, V. Alphonse, S. Nowak, A. Chabas, K. Desboeufs and A. Verney-Carron</i>	
Granite and Marine Salt Weathering Anomalies from Submerged and Inter-tidal and Coastal Archaeological Monuments in Ireland	33
<i>J. Bolton</i>	
Decay of Mesozoic Saltrio and Viggiù Limestones: Relationship between Micro- structural, Compositional and Environmental Characteristics	41
<i>G. Cavallo, R. Bugini, D. Biondelli and S. Franscella</i>	
Role of Hydro-mechanical Coupling in the Damage Process of Limestones Used in Historical Buildings	49
<i>F. Cherblanc, J. Berthonneau and P. Bromblet</i>	
The Contribution of Traditional Techniques to New Technology to Evaluate the Potential Risk of Stone Deterioration by Microorganisms	57
<i>E. Sirt-Ciplak, A. Cetin-Gozen and E.N. Caner-Saltik</i>	
Porosimetric Changes and Consequences for Damage Phenomena Induced by Organic and Inorganic Consolidation Treatments on Highly Porous Limestone.....	67
<i>P. Croveri, L. Dei, J. Cassar and O. Chiantore</i>	
Alteration of Marble Stones by Red Discoloration Phenomena	75
<i>O.A. Cuzman, S. Vettori, F. Fratini, E. Cantisani, S. Ciattini, L. Chelazzi, M. Ricci and C.A. Garzonio</i>	
Quantifying Salt Crystallization Dynamics in Sandstone Using 4D Laboratory X- ray Micro-CT	83
<i>H. Derluyn, M.A. Boone, J. Desarnaud, L. Grementieri, L. Molari, S. de Miranda, N. Shahidzadeh and V. Cnudde</i>	

Investigation of Salt Solution Behaviour in Building Stones Using Paper Pulp Poultices Under Laboratory Conditions.....	91
<i>I. Egartner and O. Sass</i>	
Experimental Study of the Ageing of Building Stones Exposed to Sulfurous and Nitric Acid Atmospheres	99
<i>S. Gibeaux, C. Thomachot-Schneider, A. Schneider, V. Cnudde, T. De Kock, V. Barbin and P. Vazquez</i>	
Geological Studies on Volcanic Tuffs Used as Natural Building Stones in the historical Center of San Luis Potosi, Mexico	107
<i>R.A. López Doncel, W. Wedekind, N. Cardona-Velázquez, P.S. González- Sámamo, R. Dohrmann, S. Siegesmund and C. Pötzl.</i>	
Weathering and Deterioration of Building Stones in Templo Mayor, Mexico City	117
<i>G. Mora Navarro, R.A. López Doncel, M. Espinosa Pesqueira and W. Wedekind</i>	
Decay Products of the Kersantite Building Stone in the Monument of the Small Staircase at the Kalemegdan Park (Belgrade, Serbia).....	125
<i>N. Novaković, M. Franković, V. Matović, K. Šarić and S. Erić</i>	
Relationship between the Durability and Fabric of Pasargadae Carbonate Stones (Archaeological Site from Achaemenid Period, South of Iran)	133
<i>A. Shekofteh, H. Ahmadi and M. Yazdi</i>	
Biodeterioration of Limestone Built Heritage: A Multidisciplinary Challenge	139
<i>P.J.A. Skipper, H. Schulze, D.R. Williams and R.A. Dixon</i>	
Characterisation of a Pink Discoloration on Stone in the Pnom Krom Temple (Angkor, Cambodia)	147
<i>M. Tescari, F. Bartoli, A. Casanova Muncichia, T. Boun Suy and G. Caneva</i>	
Influence of the Villarlod Molasse Anisotropy on Cracking Advances in the Comprehension of the Desquamation Mechanisms	155
<i>M. Tiannot, A. Bourgès and J.-D. Mertz</i>	
Decay phenomena of marbles in the archaeological site of Hierapolis of Phrygiae (Denizli, Turkey)	165
<i>S. Vettori S. Bracci, P. Caggia, E. Cantisani, O.A. Cuzman, T. Ismaelli, C. Riminesi, B. Sacchi, G. Scardozzi and F. D'Andria</i>	
Freezing-thawing Phenomena in Limestones and Consequences for their Physical and Mechanical Properties.....	173
<i>C. Walbert, J. Eslami, A.-L. Beaucour, A. Bourgès and A. Noumowe</i>	

Rapid Degradation of Stylolitic Limestones Used in Building Cladding Panels	181
<i>T. Wangler, A. Aguilar Sanchez and T. Peri</i>	
Swelling Clay and its Inhibition in the Villarlod Molasse	189
<i>T. Wangler</i>	
First Investigations of the Weathering and Deterioration of Rock Cut Monuments in Myra, Lycia (Turkey)	197
<i>W. Wedekind, R.A. López Doncel, B. Marié and O. Salvadori</i>	
Contour Scaling at the Angkor Temples: Causes, Consequences and Conservation.....	205
<i>W. Wedekind, C. Gross, A. van den Kerkhof and S. Siegesmund</i>	
Georgia Marble at the Minnesota State Capitol: Examining the Correlations between Marble Composition, Local Climate, Climate and Durability	215
<i>P.G. Whitenack and M.J. Scheffler</i>	
Investigation Methods	223
The Effect of Salt Crystallisation on the Mechanical Properties of Limestone: Statistical Correlation between Non-Destructive and Destructive Techniques	225
<i>N. Aly, A. Hamed, M. Gomez-Heras, D. Benavente and M. Alvarez de Buergo</i>	
Computational simulation: Four Important Structural Elements to Protect the Buildings in Ancient Persian Engineering	233
<i>A. AmirShahkarami, M. Mehdiabadi and H. Ashooriha</i>	
Material Analysis of Tarsus' (Mersin, Turkey) Traditional Buildings for the Development of Conservation Strategies.....	243
<i>M.C. Atikoğlu, A. Tavukçuoğlu, B.A. Güney, E.N. Caner-Saltık, O. Doğan, M.K. Ardoğa and M. Mayhar</i>	
Artificial Ageing Techniques on Various Lithotypes for Testing of Stone Consolidants	253
<i>M. Ban, A.J. Baragona, E. Ghaffari, J. Weber and A. Rohatsch</i>	
Applications of Image Analysis to Marble Samples	261
<i>R. Bellopede, E. Castelletto, N. Marcone and P. Marini</i>	
The Effects of Commercial Ethyl Silicate Based Consolidation Products on Limestone	271
<i>T. Berto, S. Godts and H. De Clercq</i>	
Field Exposure Tests to Evaluate the Efficiency of Nano-Structured Consolidants on Carrara Marble.....	281
<i>A. Bonazza, G. Vidorni, I. Natali, C. Giosuè, F. Tittarelli and C. Sabbioni</i>	

Electrophoresis as a Tool to Remove Salts from Stone Building Materials – Results from Lab Experiments and an On-site Application.....	289
<i>H. De Clercq, S. Godts, L. Debailleux, Y. Vanhellemont, N. Vanwynsberghe, L. Derammelaere and V. De Swaef</i>	
Salt Weathering of Sandstone During Drying: Effect of Primary and Secondary Crystallisation	299
<i>J. Desarnaud, H. Derluyn, L. Grementieri, L. Molari, S. de Miranda, V. Cnudde and N. Shahidzadeh</i>	
Handheld X-Ray Fluorescence Analysis (HH-XRF): A Non-Destructive Tool for Distinguishing Sandstones in Historic Structures	309
<i>P.A. Everett and M.R. Gillespie</i>	
Intrinsic Parameters Conditioning the Formation of Mn-rich Patinas on Luneville Sandstones	317
<i>L. Gatuingt, S. Rossano, J.-D. Mertz, B. Lanson and O. Rozenbaum</i>	
Smart Hydrophobic TiO ₂ -nanocomposites for the Protection of Stone Cultural Heritage	325
<i>F. Gherardi, A. Colombo, S. Goidanich and L. Toniolo</i>	
Salt Extraction by Poulticing Unravelling?.....	333
<i>S. Godts, H. De Clercq and L. Debailleux</i>	
Quantifying the Damage and Decay for Conservation Projects: Identification, Classification and Analysis of the Decay and Deterioration in Stone	343
<i>P.T. Janbade N. Thakur and B.N. Tandon</i>	
The Potential of Laser Scanning to Describe Stone degradation	353
<i>R. Janvier, X. Brunetaud, K. Beck, S. Janvier-Badosa and M. Al-Mukhtar</i>	
Application of Colorimetry for the Post-Fire Diagnosis of Historical Monuments	361
<i>S. Janvier-Badosa, K. Beck, X. Brunetaud, Á. Török and M. Al-Mukhtar</i>	
Developing Application Technology of Infrared Thermography for Documentation of Blistering Zone.....	369
<i>Y.H. Jo and C.H. Lee</i>	
Stability Evaluation and Behaviour Monitoring of Songsanri Royal Tomb Complex in Gongju, Korea	375
<i>S.H. Kim, C.H. Lee, Y.H. Jo and S.H. Yun</i>	
Simulated Weathering and Other Testing of Dimension Stone	381
<i>D. Kneezel</i>	

IR Thermography Imaging of Water Capillary imbibition into Pourous Stones of a Gallo-Roman Site	391
<i>J. Liu, J. Wassermann, C.-D. Nguyen, J.-D. Mertz, D. Giovannacci, R. Hébert, B. Ledesert, V. Barriere, D. Vermeersch and Y. Mélinge</i>	
Investigation of Urban Rock Varnish on the Sandstone of the Smithonian Castle	399
<i>R.A. Livingston, C.A. Grissom, E.P. Vicenzi, Z.A. Weldon-Yochim, N.C. Little, J.G. Douglas, A.J. Fowler, C.M. Santelli, D.S. Macholdt, D.L. Ortiz-Montalvo and S.S. Watson</i>	
Petrophysical Characterization of Both Original and Replacment Stone Used in Archtectural Herritage of Morelio (Mexico)	407
<i>J. Martinez-Martinez, A. Pola Villaseñor, L. García-Sánchez, G. Reyes-Agustín, L.S. Osorio Ocampo, J.L. Macías Vazquez and J. Robles-Camacho</i>	
Assesment of a Non-Destructive and Portable Mini Permeameter Based on a Pulse Decay Flow Applied to Historical Surfaces of Porous Materials	415
<i>J.-D. Mertz, E. Colas, A. Ben Yahmed and R. Lenormand</i>	
Monitoring of Salts Content in Monuments of Toruń Old Town Complex	423
<i>W. Oberta and J.W. Łukaszewicz</i>	
Comparability of Non-Destructive Moisture Measurement Techniques on Masonry During Simulated Wetting	431
<i>S.A. Orr, H.A. Viles, A.B. Leslie and D. Stelfox</i>	
Water Absorption and Pore-Size Dtribution of Silica Acid Ester Consolidated Porous Limestone	439
<i>Z. Pápay and Á. Török</i>	
Conservation Status and Behaviour Monitoring System of Gongsanseong Fortress Wall in Gongju, Korea	445
<i>J.H. Park, K.K. Yang, C.U. Park, Y.H. Jo and C.H. Lee</i>	
Ground Penetrating Radar and the Detection of Structural Anomalies of High Historical Value: A Case Study of a Burgher House in Toruń, Poland	451
<i>M. Pilarska, J. Rogóż, A. Cupa, K. Krynicka-Szroeder and P. Szroeder</i>	
Strategies for the Conservation of Built Heritage Based on the Analysis of Rare Events	459
<i>Y. Praticò, F. Girardet and R.J. Flatt</i>	
Direct Measurement of Salt Crystallisation Pressure at the Pore Scale	467
<i>N. Shahidzadeh, J. Desarnaud and D. Bonn</i>	

Drilling Resistance Measurement in Masonry Buildings: A Statistical Approach to Characterise Non-homogeneous Materials	475
<i>E. Valentini and A. Benincasa</i>	
<i>In situ</i> Assessment of the Stone Conservation State by its Water Absorbing Behaviour: A Hands-On Methodology	483
<i>D. Vandevoorde, T. De Kock and V. Cnudde</i>	
Surface hardness Testing for the Evaluation of Consolidation OF POROUS STONES	491
<i>W. Wedekind, C. Pötzl, R.A. López Doncel, T.V. Platz and S. Siegesmund</i>	
Other Materials.....	501
Long-term Monitoring of Decay Evolution in Bricks and Lime Mortar Affected by Salt Crystallisation.....	503
<i>C. Colla, E. Gabrielli and F. Grüner</i>	
Assessment of the Physical Behaviour of Historic Bricks and their Mechanical Characteristics via Absorption and Ultrasound Tests	511
<i>C. Colla and E. Gabrielli</i>	
Acrylic-based Mortar for Stone Repair: A Viscoelastic Analysis of the Thermal Stresses	521
<i>T. Demoulin, G.W. Scherer, F. Girardet and R.J. Flatt</i>	
Characterization and Test Treatments of Cast-Stone Medallions at the Smithsonian	529
<i>C.A. Grissom, E. Aloiz, E.P. Vicenzi, N.C. Little and A.E. Charola</i>	
Composition of Stone Plasters and Pigmented Plasters Applied in the 1920s and 1930s in Berlin, Germany	537
<i>S. Laue</i>	
Recovering the Architectural Heritage of the Nueva Tabarca Island (Spain) by Studying the Durability of Original and Repair Mortars	545
<i>J. Martinez-Martinez and A. Arizzi</i>	
Stone-mortar Interaction of Similar Weathered Stone Repair Mortars Used in Historic Buildings	553
<i>B. Menendez, P. Lopez-Arce, J.-D. Mertz, M. Tagnit-Hamou, S. Aggoun, A. Kaci, M. Guiavarch and A. Cousture</i>	
Restoration of Weathered Load Bearing Masonry with Optimised Gypsum based mortars	561
<i>B. Middendorf and U. Huster</i>	

Acquisition and Analysis of Petrophysical Properties of the Rock of the Masonry of the Cathedral of Aguascalientes, Mexico	569
<i>R. Padilla Ceniceros, J. Pacheco Martínez and R.A. López Doncel</i>	
The Assessment and Treatment of Two Cast Stone Fountains from the 1920's in Palm Beach, Florida, USA: Technical and Theoretical Issues in the Preservation of Aged Cast Stone	575
<i>M. Rabinowitz, J. Sembrat and P. Miller</i>	
Dating the Pre-Romanesque Church of San Miguel de Lillo, Spain: New Methods for Historic Buildings	583
<i>A. Rojo, L.L.Cabo, C.M. Grossi and F.J. Alonso</i>	
Swelling Inhibition of Clay-Bearing Building Materials used in Architectural Monuments	591
<i>A. Stefanis and P. Theoulakis</i>	
Long-term Mechanical Changes of Repair Mortar Used in Restoration of Porous Limestone Heritage.....	599
<i>B. Szemerey-Kiss and Á. Török</i>	
Proprietary Mortars for Masonry Repair: Developing a Predictive Framework for Assessing Compatibility	607
<i>C. Torney</i>	
Study of Efficiency and Compatibility on Successive Applications of Treatments for Islamic Gypsum and Plaster from the Alhambra	613
<i>R. Villegas Sanchez, F. Arroyo Torralvo, R. Rubio Domene and E. Correa Gomez</i>	
Comparative Studies on Masonry Bricks and Bedding Mortars of the Fortress Masonry of The Teutonic Order State in Prussia: Malbork, Toruń, and Radzyń Chelmiński Castles	621
<i>K. Witkowska and J.W. Łukaszewicz</i>	
Organic Additives in Mortars: An Historical Tradition through a Critical Analysis of Recent Literature	631
<i>K. Zhang, L. Rampazzi, A. Sansonetti and A. Grimoldi</i>	
Abstracts.....	639
Impact of Heat Exposure (Fire Damage) on the Properties of Sandstone.....	641
<i>T. Howind, W. Zhu and J.J. Hughes</i>	
Sandstone Weathering: New Approaches to Assess Building Stone Decay	642
<i>J. Dassow, M. Lee, P. Harkness, S. Hild and A.B. Leslie</i>	

Pore-scale Freeze-Thaw Experiments with Environmental Micro-CT	643
<i>T. De Kock, H. Derluyn, T. De Schryver, M.A. Boone and V. Cnudde</i>	
Conservation Study of Stone Masonries Using IRT: Discover Hidden Information by Thermal Properties.....	644
<i>C. Franzen and J.-M. Vallet</i>	
Active IRT and Theoretical Simulation Inputs for the Voids Determination in Building Material.....	645
<i>K. Mouhoubi, C. Franzen, J.-M. Vallet, V. Detalle, O. Guillon and L. Bodnar</i>	
Evaluation of Harmfulness of Traditional Cleaning Techniques of Stone with 3D Optical Microscopy Profilometry	646
<i>C. Tedeschi, M.P. Riccardi, S. Perego and M. Taccia</i>	
Multifunctional Polymers for the Restoration of the Deteriorated Mineral Gypsum (Selenite) of the Minoan Palatial Monuments of Knossos.....	647
<i>I.E. Grammatikakis, K.D. Demadis and K. Papathanasiou</i>	
Consolidant Efficiency of Newly Developed Consolidant Based on the Soluble Calcium Compounds.....	649
<i>A. Pondelak, L. Škrlep, T. Howind, J.J. Hughes and A. Sever Škapin</i>	
List of Authors	XXI
List of Keywords.....	XXV

Volume II

Conservation	651
Analysis, Testing and Development of Safe Cleaning Methods of Rusted Stone Material.....	653
<i>J. Aguiar, S. Bracci, B. Sacchi and B. Salvadori</i>	
Preliminary Studies in Using Lime with Additives as a Substitute for Resins as Adhesives in Stone Conservation	663
<i>J. Alonso and M. Franković</i>	
Freeze Thaw and Salt Crystallisation Testing of Nanolime Treated Weathered Bath Stone.....	671
<i>R.J. Ball and G.L. Pesce, M. Nuño, D. Odgers and A. Henry</i>	
Thermosetting Methyl Methacrylate Adhesive for Stone: Charcterisation, Application Techniques and Long-term Performance Elevation.....	679
<i>Z. Barov</i>	

Consolidation Effects on Sandstone Toughness	687
<i>M. Drdácáký, M. Šperl and I. Jandejsek</i>	
Is the Shelter at Hagar Qim in Malta Effective at Protecting the Limestone Remains?	695
<i>C. Cabello-Briones and H.A. Viles</i>	
Assessment of the Cleaning Efficiency of a Self-cleaning Coating on Two Stones Under Natural Ageing.....	703
<i>P.M. Carmona-Quiroga, S. Kang and H.A. Viles</i>	
Exploitation of the Natural Water Repellency of Limestones for the Protection of Building Façades	711
<i>C. Charalambous and I. Ioannou</i>	
The Use of New Laser Technology to Precisely Control the Level of Stone Cleaning.....	719
<i>B. Dajnowski and A. Dajnowski</i>	
Cleaning Stone – The Possibilities for an Objective Evaluation.....	729
<i>J. Ďoubal</i>	
The Natural Weathering of an Artificially Induced Calcium Oxalate Patina on Soft Limestone.....	737
<i>T. Dreyfuss and J. Cassar</i>	
A Comparison of Three Methods of Consolidation for Claceros Mixed Stones	745
<i>J. Espinosa-Gaitán and A. Martín-Chicano</i>	
Seasonal Stone Sheltering: Winter Covers	753
<i>C. Franzen and K. Kraus</i>	
Performance and Permanence of TiO ₂ -based Surface Treatments for Architectural Heritage: Some Experimental Findings from On-site and Laboratory Testing	761
<i>E. Franzoni, R. Gabrielli, E. Sassoni, A. Fregni, G. Graziani, N. Roveri and E. D'Amen</i>	
The Impact of Science on Conservation Practice: Sandstone Consolidation in Scottish Built Heritage.....	769
<i>C. Gerdwilker, A. Forster, C. Torney and E. Hyslop</i>	
Use of Local Stone in the Midwestern United States: Successes, Failures and Considerations	777
<i>E. Gerns and R. Will</i>	
Laser Yellowing of Hematite-Gypsum Mixtures: A Multi Scale Characterisation	785
<i>M. Godet, V. Vergès-Belmin, C. Andraud, M. Saheb, J. Monnier, E. Leroy and J. Bourgon</i>	

The Use of Hydroxyapatite for Consolidation of Calcareous Stones: Light Limestone Pińczów and Gotland Sandstone (Part I).....	793
<i>A. Górnjak, J.W. Łukaszewicz, B. Wiśniewska</i>	
Marble Protection by Hydroxyapatite Coatings.....	803
<i>G. Graziani, E. Sassoni, E. Franzoni and G.W. Scherer</i>	
Use of Consolidants and Pre-Consolidants in Sandstone with Swelling Clay at the Municipal Theatre of São Paulo.....	811
<i>D. Grossi, E.A. Del Lama and G.W. Scherer</i>	
Assessing the Impact of Natural Stone Burial upon Performance for Potential Conservation Purposes.....	817
<i>B.J. Hunt and C.M. Grossi</i>	
Study of Protective Measures of Stone Monuments in Cold Regions	825
<i>T. Ishizaki</i>	
Study of Consolidation of Porous and Dense Limestones by Bacillus Cereus Biomineralization	831
<i>J.M. Jakutajć, J.W. Łukaszewicz and J. Karbowska-Berent</i>	
Assessment of Dolomite Conservation by Treatment with Nano-Dispersive Calcium Hydroxide Solution	839
<i>F. Karahan Dağ, Ç.T. Mısır, S. Çömez, M. Erdil, A. Tavukçuoğlu, E.N. Caner-Saltık, B.A. Güney and E. Caner</i>	
European Project “NANO-CATHEDRAL: Nanomaterials for conservation of European architectural heritage developed by research on characteristic lithotypes”.....	847
<i>A. Lazzeri, M.-B. Coltelli, V. Castelvetro, S. Bianchi, O. Chiantore, M. Lezzerini, L. Niccolai, J. Weber, A. Rohatsch, F. Gherardi and L. Toniolo</i>	
New Polymer Architectures for Architectural Stone Preservation	855
<i>A. Lazzeri, S. Bianchi, V. Castelvetro, O. Chiantore, M.-B. Coltelli, F. Gherardi, M. Lezzerini, T. Poli, F. Signori, D. Smacchia and L. Toniolo</i>	
Trials of Biocide Cleaning Agents on Argillaceous Sandstone in a Temperate Region.....	863
<i>E. S. Long and D.A. Young</i>	
Development of a methodology for the Restoration of Stone Sculptures using Magnets	871
<i>X. Mas-Barberà, M.A. Rodríguez, L. Pérez and S. Ruiz</i>	

The Rock Reliefs “ <i>Steinerne Album</i> ” of Großjena, Germany – Problems of Deterioration and Approaches for a Lasting Preservation	879
<i>J. Meinhardt, T. Arnold and K. Böhm</i>	
Ethyl-silicate Consolidation for Porous Limestone Coated with Oil Paint – A Comparison of Application Methods.....	889
<i>M. Milchin, J. Weber, G. Krist, E. Ghaffari and S. Karacsonyi</i>	
Electro-desalination of Sulfate Contaminated Carbonaceous Sandstone – Risk for Salt Induced Decay During the Process.....	897
<i>L.M. Ottosen</i>	
Permeable POSS-based Hybrids: New Protective Materials for Historical Sandstone.....	905
<i>A. Pan, S. Yang and L. He</i>	
Differential Effects of Treatments on the Dynamics of Biological Recolonisation of Travertine: Case Study of the Tiber’s Embankments (Rome, Italy).....	915
<i>S. Pascucci, F. Bartoli, A. Casanova Muncicchia and G. Caneva</i>	
Statistical Analysis at the Service of Conservation Practice: DOE for the Optimisation of Stone Consolidation Procedures	923
<i>Y. Praticò, F. Caruso, T. Wangler and R.J. Flatt</i>	
Vacuum-Circling Process: A Innovative Stone Conservation Method.....	931
<i>E. Pummer</i>	
Sustainable Conservation in a Monumental Cemetery	939
<i>S. Salvini</i>	
Consolidation of Sugaring Marble by Hydroxyapatite: Some Recent Developments in Producing and Treating Decayed Samples	947
<i>E. Sassoni, G. Graziani, E. Franzoni and G.W. Scherer</i>	
Application of Ethyl Silicate Based Consolidants on Sandstone with Partial Vacuum: A Laboratory Study.....	955
<i>H. Siedel, J. Wichert and T. Frühwirt</i>	
Mould Attacks! A Practical and Effective Method of Treating Mould Contaminated Stonework.....	963
<i>B. Stanley, N. Luxford and S. Downes</i>	
Injection Grouts based on Lithium Silicate Binder: A Rview of Injectability and Cohesive Integrity.....	971
<i>A. Thorn</i>	

Innovative Treatments and Materials for the Conservation of the Strongly Salt-contaminated Michaelis Church in Zeitz, Germany	981
<i>W. Wedekind, R.A. López-Doncel, J. Rüdrieh and Y. Rieffel</i>	
Field Trials of Desalination by Captive-head Washing	991
<i>D. Young</i>	
Digitisation	997
Digital Mapping as a Tool for Assessing the Conservation State of the Romanesque Portals of the Cathedral of our Lady in Tournai, Belgium	999
<i>J. De Roy, S. Huysmans, L. Hoornaert, L. Fontaine and N. Verhulst</i>	
Digital Field Documentation: The Central Park Obelisk	1009
<i>C. Gembinski</i>	
Computational Imaging Techniques for Documentation and Conservation of Gravestones at Jewish Cemeteries in Germany	1017
<i>C.A. Graham and S. Simon</i>	
A Metadata-supported Database Schema for Stone Conservation Projects	1025
<i>E. Kardara and T. Pomonis</i>	
3D Photo Monitoring as a Long-term Monument Mapping Method for Stone Sculptures	1031
<i>B. Kozub and P. Kozub</i>	
Emerging Digitisation Trends in Stonemasonry Practice	1041
<i>S. McGibbon and M. Abdel-Wahab</i>	
Digitalisation and Documentation of Stone Deterioration, Using Close-Range Digital Photogrammetry	1051
<i>M.Á. Soto-Zamora, R.A. López-Doncel, G. Araiza-Garaygordobil and I.E. Vizcaino-Hernández</i>	
Recording, Monitoring and Managing the Conservation of Historic Sites: A New Application for BGS SIGMA	1059
<i>E.A. Tracey, N. Smith and K. Lawrie</i>	
Case Studies.....	1067
Condition Survey of Aquia Creek Sandstone Columns From the U.S. Capitol Re-Erected at the U.S. National Arboretum	1069
<i>E. Aloiz, C. Grissom, R.A. Livingston and A.E. Charola</i>	
The Black Surfaces of the Porta Nigra in Trier (Germany) and the Question of Cleaning	1077
<i>M. Auras, H. Ettl, W. Hartleitner and T. Meier</i>	

The Conservation of Giovanni Labus’s Sculpture of Bonaventura Bavallieri (1844) and Antonio Galli’s Sculpture of Carlo Ottavio Castiglione (1855)	1089
<i>I. Ruiz Bazán, V. Bresciani, A. Balloi, A. Quarto, I. Marelli, M. Colella, C. Sotgia and F. Arosio</i>	
Restoration Off-set by the Public Exhibition of Decorated Stone Elements Rescued from the demolished Vacaresti Monastery, Romania.....	1097
<i>C. Bîrzu</i>	
Rosslyn Chapel - A Review of the Conservation & Access Project	1103
<i>N. Boyes</i>	
Laboratory and in situ evaluation of restoration treatments in two important monuments in Padua: “Loggia Cornaro” and “Stele of Minerva”	1111
<i>V. Fassina, S. Benchiarin and G. Molin</i>	
Investigations Guiding the Stone Restoration of the “Schöner Erker” in Torgau, Germany	1119
<i>C. Franzen, H. Siedel, S. Pfefferkorn, A. Kiesewetter and S. Weise</i>	
Ananalysis and Treatment of the Fire-Damaged Marble Plaque from Thomas Jefferson’s Grave Marker	1129
<i>C. Grissom, E. Vicenzi, J. Giaccai, N.C. Little, C. France, A.E. Charola and R.A. Livingston</i>	
The Diagnostic and Monitoring Approach for the Preventive Conservation of the Façade of the Milan Cathedral	1137
<i>D. Gulotta, P. Fermo, A. Bonazza and L. Toniolo</i>	
Enviromental Monitoring and Surface Treatment Tests for Conservation of the Rock-Hewn Church of Üzümlü, Cappadocia	1145
<i>C. Iba, Y. Taniguchi, K. Koizumi, K. Watanabe, K. Sano C. Piao and M. Yoshioka</i>	
Time Tested Repairs: A Review of 11 Years of Cementery Stone Repair	1153
<i>M. Jablonski</i>	
The Current State and Factors of Salt Deterioration of the Buddha Statue Carved onto a Cliff at Motomachi in Oita Prefecture of Japan	1163
<i>K. Kiriyama, S. Wakiya, N. Takatori, D. Ogura, M. Abuku and Y. Kohzuma</i>	
The Durbar Square and the Royal Palace of Patan, Nepal – Stone Conservation Before and after the Great Earthquake of April 2015	1171
<i>G. Krist, M. Milchin and M. Haselberger</i>	

Restoring the Past Experience of Stone Masonry in Burkina Faso for Fostering the use of Local Materials.....	1181
<i>A. Lawane, A. Pantet, R. Vinai and J.H. Thomassin</i>	
Protection of Medieval Tombstones (Stećci) with Ammonium Oxalate Treatment	1189
<i>V. Marinković and D. Mudronja</i>	
Influence of Water Evaporation on the Degradation of Wall Paintings in Hagia Sophia, Istanbul	1201
<i>E. Mizutani, D. Ogura, T. Ishizaki, M. Abuku and J. Sasaki</i>	
Conservation of Magai-Wareishi-jizo, A Buddha Statue Carved into a Granite Rockface on the Seashore	1211
<i>M. Morii, N. Kuchitsu, T. Kawaguchi, H. Matsuda and S. Tokimoto</i>	
Evaluation of the Preservation State of the Holy Aedicule in the Holy Sepulchre Complex in Jerusalem.....	1219
<i>A. Moropoulou, K. Labropoulos, E. Alexakis, E.T. Delegou, P. Moundoulas, M. Apostolopoulou and A. Bakolas</i>	
Conservation of Machu Picchu Archaeological Site: Investigation and Experimental Restoration Works of the “Temple of the Sun”	1227
<i>T. Nishiura, I. Ono, A. Ito, H. Fujita, M. Morii, F. Astete and C. Cano</i>	
Las Casas Tapadas de Plazuelas – Structural Damage, Weathering Characteristics and Technical Properties of Volcanic Rocks in Guanajuato, Mexico.....	1237
<i>C. Pötzl, R.A. López-Doncel, W. Wedekind and S. Siegesmund</i>	
Desalinating the Asyut Dog in the MUSÉE DU LOUVRE.....	1247
<i>O. Rolland, V. Vergès-Belmin, M. Etienne, H. Guichard, S. Duberson and P. Bromblet</i>	
Investigation of Salt Crystallisation in a Stone Buddha Carved into a Cliff with a Shelter by Numerical Analysis of Heat and Moisture Behaviour in the Cliff.....	1255
<i>N. Takatori, D. Ogura, S. Wakiya, M. Abuku, K. Kiriya and Y. Kohdzuma</i>	
Scientific Examination of a Painted Thracian Tomb Discovered Near Alexandrovo Village, Bulgaria	1263
<i>V. Todorov, K. Frangova and T. Marinov</i>	
Case Study of the Episcopal Group of Frejus (France): Diagnosis and Treatment of Clay Containing Sandstones in Marine Environment.....	1271
<i>M. Trubert, B. Brunet-Imbault, P. Bromblet and C. Guinamard</i>	
The Polychromed Bethlehem Portal of Huy, Belgium: Evaluation and Maintenance of a 25 Year Old Treatment.....	1279
<i>J. Vereecke, L. Rossen, K. Raymakers and M. Stillhammerova</i>	

Exploring the Performance of Pompignan Limestone as Exterior Cladding and Pavers in the Mid-Atlantic Region of the United States	1287
<i>R. Wentzel and M. Coggin</i>	
Abstracts.....	1295
Mechanisms of Carbonate-oxalate Transformation: Effectiveness of Protective Treatments for Marble based on Oxalate Surface Layers	1297
<i>A. Burgos-Cara, C. Rodríguez-Navarro and E. Ruiz-Agudo</i>	
Preservation of Built Cultural Heritage Using Nanotechnology Based Coatings: Responding to Conservation Values?	1299
<i>J.J. Hughes, L.P. Singh, P.C. Thapliyal, T. Howind and W. Zhu</i>	
Innovative Developments in the Field of Stone Conservation by the Acrylic Resin Total Impregnation Process of Natural Stones by the JBACH Company	1300
<i>G. Scholz, R.J.G. Sobott, H.W. Ibach</i>	
MONUMENTUM: Digital 3D Modelling and Data Management for the Conservation of Decorated Stone Buildings	1301
<i>L. De Luca, J.-M. Vallet, P. Bromblet, M. Pierrot-Desseilligny, X. Brunetaud, F. Dubois, M. Bagneris, M. Al Mukhtar, F. Cherblanc, O. Guillon and J. Tugas</i>	
Investigation of Building Stones Used in the Al-Azhar mosque (Historic Cairo, Egypt)	1303
<i>N. Aly, A. Hamed, Á. Török, M. Gomez-Heras and M. Alvarez de Buergo</i>	
The Effect of Reburial on Stone Deterioration: Experimental Case Study, Oxford, England	1304
<i>N. Zaman and H. Viles</i>	
List of Authors	XXIII
List of Keywords.....	XXVII

This page has been left intentionally blank.

CONSERVATION

This page has been left intentionally blank.

ANALYSIS, TESTING AND DEVELOPMENT OF SAFE CLEANING METHODS OF RUSTED STONE MATERIAL

J. Aguiar¹, S. Bracci², B. Sacchi² and B. Salvadori^{2*}

Abstract

Rust stains are a widespread problem for natural stones of both civil buildings and cultural heritage, particularly for white marbles. For this reason, the aim of this work was to develop new methods of treatment/application, in order to identify a safe protocol for cleaning rusted marbles. Three different treatments were applied on several specimens of both dolomitic and calcitic marble, properly stained with rust to mimic real situations (the stone specimens were exposed to the natural environment for about six months in contact with rusted iron). Marble specimens were characterized before and after treatment and monitored during the cleaning tests. The specimens were characterized by SEM-EDS (Scanning Electron Microscopy coupled with Energy Dispersive System), XRD (X-Ray Diffraction), XRF (X-Ray Fluorescence), FTIR (Fourier Transform Infrared Spectroscopy) and color measurements. In addition, microscopic and macroscopic analyses of the stone surface along with tests of short and long term capillary absorption were carried out. A series of test trials were conducted in order to identify the best conditions in terms of concentrations and contact time, starting from the data reported in literature. New methods of treatment application were verified, substituting the usual Cellulose Poultice with Agar. The latter is a gel already used in many other contexts, being something new in this field, which possesses great applicability in the field of conservation of stone materials. After the application of the cleaning method, the specimens were characterised again in order to understand which treatment was more effective and less harmful. The study indicates that for a very intense and deep penetration into the stone, a solution of 3.5% (w/v) of Sodium Dithionite buffered with Ammonium Carbonate to *pH* 7 applied with Agar support would be appropriate.

Keywords: stone, rust removal, sodium dithionite, ammonium citrate, sodium hexametaphosphate

¹ J. Aguiar

Department of Conservation and Restoration, Nova University, Lisbon, Portugal,

² S. Bracci , B. Sacchi and B. Salvadori*

CNR-ICVBC Institute for the Conservation and Valorization of Cultural Heritage, Sesto Fiorentino (Florence), Italy

b.salvadori@icvbc.cnr.it

*corresponding author

1. Introduction

Rust stains in stone are mostly caused by iron corrosion of architectonic elements such as grades, nails and supports (Matero and Tagle 1995). The cleaning methodology should improve the visual appearance of the stone, promoting its stability (Selwyn and Tse 2009), while preventing physical and/or chemical changes such as abrasion of the surface and introduction of soluble salts (Aires-Barros 2001) (Amoroso and Fassina 1983). While many researchers tested different chemical compounds, there is no definitive comparative assessment identifying an efficient and safe method. This paper reports the preliminary results of an investigation carried out to setup a proper methodology for rust removal from both calcitic and dolomitic marbles, largely used in the construction of built heritage. Some promising chemical products reported in the literature were used, exploring different application procedures. Studies about this topic are not recent and a clear definition of a good treatment is not still defined. It comes out from the literature that for appropriate treatment of marble the *pH* has to be adjusted to *pH* 7-8, being this the fundamental point to avoid the dissolution of the calcite (Cushman and Wolbers 2007). Another crucial factor to be controlled is the contact time between the sample and the poultice (Amoroso and Fassina 1983). Because of its insolubility in water, rust is difficult to remove (Matero and Tagle 1995; Irwin 2011). The removal may be performed by dissolution in acids, complexation or chemical reduction with or without complexing agents (Burgess 1991). The choice of appropriate chelating agents should enable the removal of the metal ion, avoiding the dissolution of calcite (Selwyn and Tse 2009; Burgess 1991). For instance, EDTA is far too strong a chelator to use for this application, as calcium will be taken up and brought into solution (Tab. 1); on the other hand, Citrate should be safer for the marble surface, but neither of these materials, EDTA included, is able to efficiently bind the iron species (Cushman and Wolbers 2007).

Tab. 1: Solubility product (pK_{sp}) of prevalent calcium and iron species in the marble matrix and in the iron staining and constants of chelate formation (pK_f) of Ca(II), Fe(II) and Fe(III) (CRC Handbook 2003)

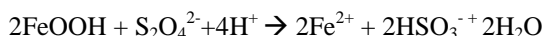
	pK_{sp}	pK_f (Citrate)	pK_f (EDTA)
Ca(II)	8.3 ^a	4.7	11.0
Fe(II)	16.3 ^b	3.1	14.3
Fe(III)	38.6 ^c	12.5	24.2

^a CaCO₃; ^b Fe(OH)₂; ^c Fe(OH)₃

Sodium Hexametaphosphate is a deflocculant/chelating agent used in the field of conservation for the cleaning of stone materials, due to its neutral *pH* which makes it safe for marble. It is a weaker chelating agent than EDTA and for this reason it is indicated for calcareous stones. Good results in rust removal after several applications have been reported (CTS newsletter 2006).

Reducing agents can be used as well, to convert the orange-red Fe(III) form to the much more water soluble Fe(II) form. (Selwyn and Tse 2009; Irwin 2011) (Vanýsek 1991). To this aim, the use of the reducing agent Sodium Dithionite, Na₂S₂O₄, to remove iron stains was first suggested in 1968 (Stambolov 1968) and it is currently applied to clean a variety

of inorganic materials (Selwyn and Tse 2009) (Irwin 2011). Its reaction with goethite yields the more soluble $\text{Fe}(\text{OH})_2$ which can be removed with water:



Also Ammonium Citrate has been reported as an effective chelating agent in removing iron stains (Matero and Tagle 1995). However, the literature points out that the Citrate is able to attack the calcareous stone (Gervais *et al.*, 2010).

2. Materials and methods

2.1. Stone specimens

Two types of marble, with different resistance against acids, were used: one calcitic (CaCO_3), which quickly reacts with acids, and one dolomitic ($\text{CaMg}(\text{CO}_3)_2$), less reactive. XRD analyses confirmed the composition of the selected specimens (data not reported). Eighteen specimens of each lithotype (size $5 \times 5 \times 2$ cm) were exposed outdoors for about six months in contact with rusted iron. The specimens were washed with water before performing the tests.

2.2. Investigation techniques

The specimens were characterized before and after cleaning treatments to monitor changes in terms of color, iron and/or salt residues. Color measurements (Hunt 1991) were performed according to the procedure described in (EN 15886:2010) using the CIELAB 1976 method, with the standard illuminant D65 and observer 10° . The color coordinates L^* , a^* and b^* were recorded for each selected area ($\varnothing \sim 8$ mm), using a Minolta cm-700d spectrophotometer. For each specimen, four spots of interest were selected corresponding to rust stains and five measurements were taken on each area. A mask properly prepared for each specimen enabled the repositioning of the instrument on the same areas during the monitoring steps. The colorimeter was calibrated against a SPECTRALON® prior to each measurement. Surface changes were monitored through photographic documentation, with a digital reflex camera Canon 7D equipped with Canon EFS 60 mm macro lens, and a Stemi 2000 (Zeiss) stereomicroscope with ACT 1 software. Elemental characterization of the surfaces was performed with a portable X-Ray fluorescence spectrometer Tracer III-SD (Bruker) using the following conditions: Rh source, Pd slit, Ti and Al filter, 40 KV, 30 μA , 60 seconds. Chemical analyses were performed with a portable Bruker Optics ALPHA FT-IR spectrometer equipped with SiC Globar source and DTGS detector. For non-invasive chemical characterization of the surface compounds, the instrument was equipped with a front-reflection module and a video camera. The spectra were acquired in total reflection mode collecting 256 scans, with 4 cm^{-1} resolution in the $4000\text{--}400 \text{ cm}^{-1}$ range and a measuring spot of 6 mm in diameter. Powders taken from the surface of the specimens were analyzed through an attenuated total reflection module (ATR) with diamond crystal. The collected IR spectra were processed using OPUS 7.2 software. On the same powdered samples, XRD analyses were performed using a X-ray diffractometer X'Pert PRO PANalytical with anticathode Cu ($\lambda = 1.54 \text{ \AA}$), investigated 2θ $3\text{--}70^\circ$, step size 0.017° , time per step 50 s), equipped with a multidetector X'Celerator. Data processing was performed using HighScore software and ICDD database.

2.3. Reagents

All chemicals were used as supplied. Sodium Dithionite $\text{Na}_2\text{S}_2\text{O}_4$ (technical grade, 85%, SDT) and Ammonium Hydroxide NH_4OH (20.0-30.0%, AM) were purchased from Sigma-Aldrich; Ammonium Citrate dibasic $\text{HOC}(\text{CO}_2\text{H})(\text{CH}_2\text{CO}_2\text{NH}_4)_2$ ($\geq 99.0\%$, AC), Ammonium Carbonate $(\text{NH}_4)_2\text{CO}_3$ ($>99.7\%$, AmmC) and Sodium Hydrogencarbonate NaHCO_3 ($\geq 99.7\%$, SodHC) were purchased from Fluka Analytical; Sodium Hexametaphosphate NaPO_3 (technical grade, HMP) was supplied by CTS srl (Florence, Italy).

2.4. Cleaning tests

Each cleaning agent was used in different concentrations and contact times (Tab. 2) selected after a series of preliminary tests. The solutions were buffered at $\text{pH} \approx 7$ to avoid the dissolution of calcite which is favoured at $\text{pH} < 7.6$ (Thorn 2005). Ammonia was used for Sodium Hexametaphosphate and Ammonium Citrate solutions. As suggested by some authors (Mehra and Jackson 1960) (Lem and Wayman 1970), Sodium Hydrogencarbonate was used for the SDT solutions, slowing down the decomposition of the Sodium Dithionite which is faster at acidic pH. To reduce the amount of sodium in solution and contamination of the surfaces, the use of Ammonium Carbonate instead of Sodium Hydrogencarbonate was also tested. Besides the traditional Cellulose poultice, Agar gel was used as well (Campani *et al.*, 2006, Gulotta *et al.*, 2014). With Sodium Hexametaphosphate, the Agar film did not form: since this cleaning agent acts as a deflocculant, it does not allow the folding of the Agar fibers.

Tab. 2: Cleaning treatments applied on stained marble samples.

Cleaning agent	Concentration % (w/v)	Contact time (hours)	pH	Buffer agent	Poultice ^a
Sodium Dithionite (SDT)	3.5	6	6 / 7	SodHC or AmmC	Ce, Ag
	7	5			
		3			
Sodium Hexametaphosphate (HMP)	10	2	7	AM	Ce
Ammonium Citrate (AC)	2	24	8	AM	Ce, Ag
	5				

^a Ce: Cellulose; Ag: Agar

3. Results and discussion

The comparison of the two lithotypes showed a different appearance of rust stains, also visible in cross section (not reported). Rust formed large spots on dolomite, while a sort of finely distributed, light staining was found on calcite. This could be due to the slightly different porosity of the two lithotypes and different crystals size (larger in dolomite than calcite). However, the penetration depth was quite similar, ranging from 10 to 25 μm .

3.1. Sodium Dithionite

Fig. 1 shows the effects of the SDT cleaning intervention. Less concentrated solution applied for longer contact time (3.5% solution, 6 hours) removed the rust stains more efficiently than the more concentrated solution applied for shorter contact time (7% solution, 3 hours), especially in the case of dolomite. FT-IR analyses of the marble surface did not reveal any residual cleaning product, while XRF analyses showed minimal amount of iron on dolomite, not visible to the naked eye (Fig. 2).

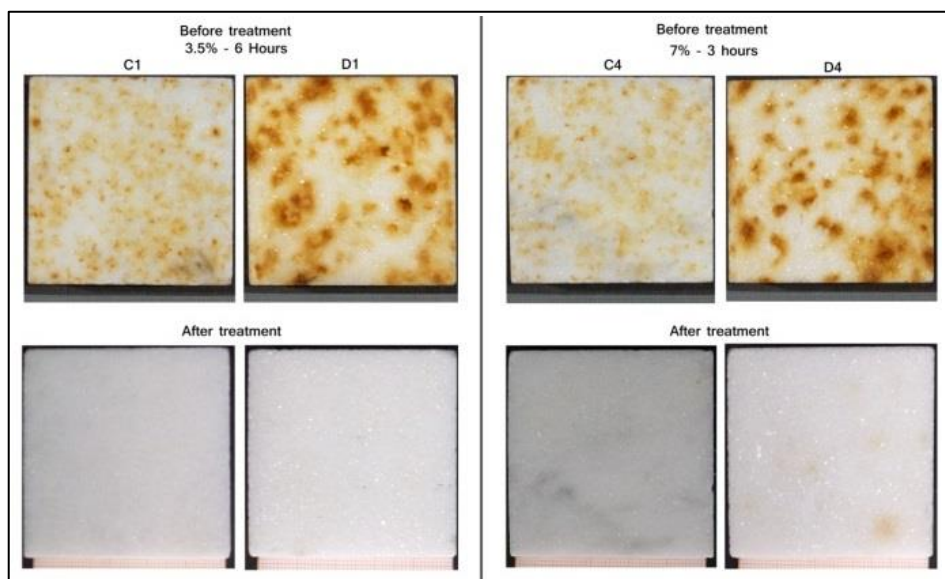


Fig. 1: Comparison between treatments on calcitic (C) and dolomitic (D) samples with SDT.

This confirms the importance of an appropriate washing of the stone substrate after applying the treatment, to completely remove iron(II) ions, avoiding eventual re-staining (colourless, remaining iron(II) ions may be oxidized back to rust-coloured iron(III)oxyhydroxides). After treatment, colour measurements ascertained the regression of the chromatic coordinates to those registered on unstained surfaces (Tab. 3 and Tab. 4). This was particularly evident on calcitic samples treated for 6 hours with SDT 3.5%, in Cellulose poultice. However, some yellowing (increase of b^*) was also detected after most of the treatments.

Good results were also achieved through the use of Agar gel to support the cleaning solution. Indeed, the Agar allowed faster removal of stains with respect to Cellulose poultice, also permitting the monitoring in real time due to the transparency of the gel (Fig. 3).

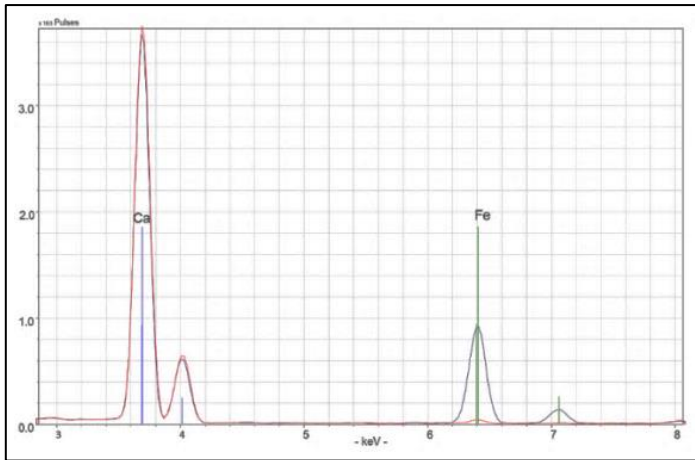


Fig. 2: XRF spectra of the dolomite specimen treated with SDT 3.5%-6hours before (---) and after cleaning (---).

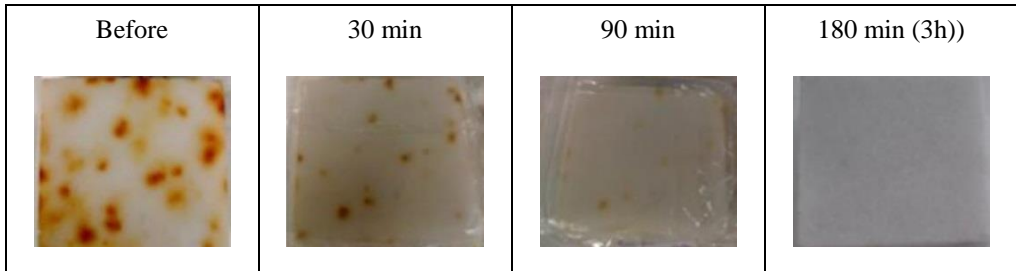


Fig. 3: Timeline SDT 3.5% with Agar poultice.

Tab. 3: Color measurements of the stained (t_0), cleaned (t_1) and reference unstained (Ref.) calcitic specimens.

Cleaning product	% (w/v)	contact time (h)	Poultice	buffer	L^*		a^*		b^*	
					t_0	t_1	t_0	t_1	t_0	t_1
SDT	3.5	5	A	AmmC	79.6	83.9	2.5	-0.6	20.4	1.0
SDT	3.5	5	C	AmmC	66.1	84.2	11.8	-1.0	28.3	2.9
SDT	7	3	C	SodHC	75.7	81.1	3.2	-1.0	23.1	1.6
SDT	3.5	6	C	SodHC	78.6	84.6	2.5	-0.9	16.5	-0.7
Ref.	-	-	-	-	-	83.4	-	-0.7	-	-1.0

Tab. 4: Color measurements of the stained (t_0), cleaned (t_1) and reference unstained (Ref.) dolomitic specimens.

Cleaning product	% (w/v)	contact time (h)	Poultice	buffer	L^*		a^*		b^*	
					t_0	t_1	t_0	t_1	t_0	t_1
SDT	3.5	5	A	AmmC	70.5	86.4	11.3	-0.1	32.9	4.6
SDT	3.5	5	C	AmmC	65.1	85.7	14.1	0.4	34.3	4.6
SDT	7	3	C	SodHC	70.5	83.2	10.0	1.2	28.3	10.1*
SDT	3.5	6	C	SodHC	71.5	86.5	11.3	-0.5	27.1	4.2
Ref.	-	-	-	-	-	83.4	-	-0.7	-	-1.6

*N.B.: Rust stain after cleaning

3.2. Sodium Hexametaphosphate and Ammonium Citrate

Fig. 4 shows the results of cleaning with HMP and AC. Although the highest concentration and longest contact time reported in the literature were used for both of the products, the methods appeared less effective than SDT. The use of Agar instead of Cellulose did not improve the results. It can be noticed that only the most superficial rust stains were removed, particularly for AC, which resulted safe for the marble surfaces.

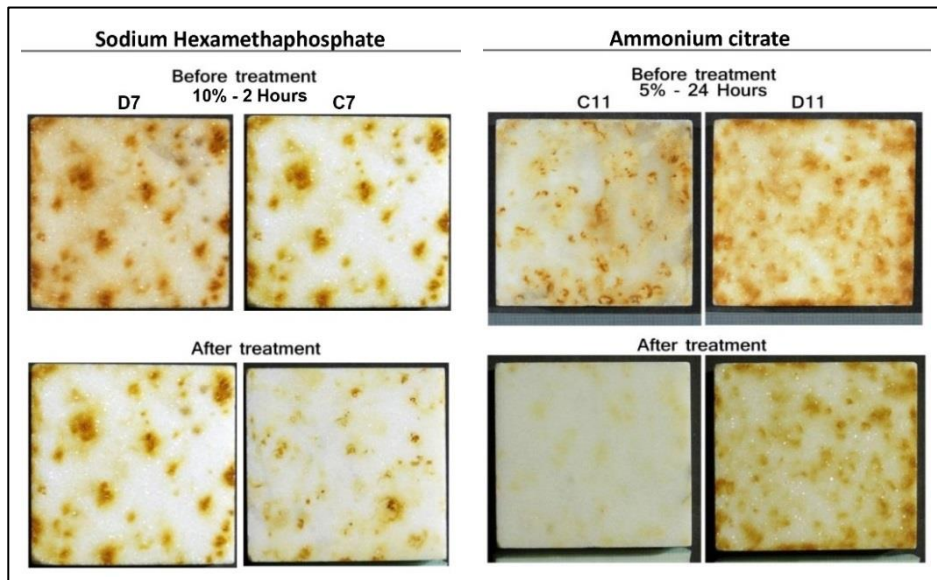


Fig. 4: Calcitic (C) and dolomitic (D) samples before/after application of Sodium Hexametaphosphate 10% (left) and Ammonium Citrate 5% (right).

4. Conclusions

The use of Sodium Dithionite proved to be the most effective product for rusted stone cleaning, compared to Sodium Hexametaphosphate and Ammonium Citrate. Contact time and concentration were the key factor in the removal process. Sodium Dithionite acts as a reducing agent, making possible to wash away the reduced Fe(II) iron from the stone. The combination with a proper buffer, such as Ammonium Carbonate, allowed to prolong the cleaning agent's life (which decomposes rapidly in the presence of oxygen), raise the *pH* to a safe value for stone and minimize the amount of sodium salts on the cleaned surface. Rust stains were removed from the surfaces, leaving no or minimal iron residues. The use of Sodium Hexametaphosphate was not effective, while Ammonium Citrate showed some results on light or superficial stains. The use of Agar gel instead of Cellulose poultice enabled the monitoring of the treatment without touching the poultice, which is really advantageous on sensitive substrates. In conclusion, based on the present results, for rust removal from marble the 6-hour application of Sodium Dithionite 3.5%, buffered with Ammonium Carbonate, in Agar, followed by accurate washing of the stone surface is advisable. However, further studies will allow for checking the depth of rust cleaning and the complete absence of harmful effects on the surfaces.

References

- Aires-Barros, L., (2001), "As Rochas dos Monumentos Portugueses, Lisboa: Instituto Português do Património Arquitectónico, Coleção Cadernos", Vol. I e II. ISBN 9728087810.
- Amoroso, G.G. and Fassina, V., (1983), "Stone Decay and Conservation: Atmospheric Pollution, Cleaning, Consolidation and Protecting", Materials Science Monographs, 11. Elsevier Science Publishing Company Inc., New York, ISBN 9780444421463, 453pp.
- Burgess, H., 1991, The use of chelating agents in conservation treatments, *The Paper Conservator* 15, 36-44.
- Campani, E., Casoli, A., Cremonesi, P., Saccani, I., Signorini, E. (2006), "Use of Agarose and Agar for preparing "Rigid gels"". CESMAR 7, Quaderno 4, Il Prato, Padova, Italy, ISBN 8889566655, 52pp.
- Cremonesi, P., 2006, Applicazione di metodologie di intervento più recenti per la pulitura del materiale cartaceo. Atti delle giornate di studio Problemi di Restauro – Giornate di Studio per storici d'arte, ispettori di Soprintendenza, conservatori e operatori museali. 39-46.
- CTS Srl., 2006, Una vecchia ruggine [<http://www.ctseurope.com/site/dettaglio-news.php?id=45> Accessed 23rd August 2015].
- Cushman, M. and Wolbers, R., 2007, A new approach to cleaning iron-stained marble surfaces, *WAAC Newsletter*, 29 (2), 23-8.
- Doehne, E. and Price, C. A., (2010), "Stone Conservation, An Overview of Current Research", 2nd edition, Getty Publications, Los Angeles, CA, ISBN 9781606060469, 160pp.

- EN 15886:2010, Conservation of Cultural Property. Test Methods. Color Measurement of Surfaces, 2010.
- Erhard, M. W., (1994), "Stone in Architecture: Properties, Durability in Man's Environment", 3rd ed., Springer Verlag, Berlin, ISBN 978366210072, 309pp.
- Gervais, C., 2010, Cleaning marble with ammonium citrate, *Studies in Conservation*, 55, 164-176.
- Gulotta, D., Salviello, D., Gherardi, F., Toniolo, L., Anzani, M., Rabbolini, A. and Goidanich, S., 2014, Setup of a sustainable indoor cleaning methodology for the sculpted stone surfaces of the Duomo of Milan, *Heritage Science*, 2:6, 1-13.
- Hunt, R.W.G. (1991), "Measuring Colour", 2nd edition, Ellis Horwood, Chichester, ISBN 013567686X, 313pp.
- Irwin, S., 2011, A comparison of the use of sodium metabisulfite and sodium dithionite for removing rust stains from paper, *American Institute for Conservation, The Book and Paper Group Annual*, 30, 37-46.
- Lem, W.J. and Wayman, M., 1970, Decomposition of aqueous dithionite. Part II. A reaction mechanism for the decomposition of aqueous sodium dithionite, *Canadian Journal of Chemistry*, 48, 782-7.
- Lide, D. R., (2002), "CRC Handbook of Chemistry and Physics", 83rd Edition, CRC Press, Boca Raton, FL, ISBN 0849304830, 2664pp.
- Matero, F.G. and Tagle, A. A., 1995, Cleaning, iron stain removal and surface repair of architectural marble and crystalline limestone: The Metropolitan Club, *Journal of the American Institute of Conservation*, 34, 49-68.
- Mehra, O.P. and Jackson, M.L., 1960, Iron oxide removal from soils and clays by a dithionite-citrate system buffered with sodium bicarbonate. *Proceedings of the Seventh National Conference on Clays and Clay Minerals*, Swineford, A. (ed.), Washington D.C., Pergamon Press, 317-327.
- Selwyn, L. and Tse S., 2009, The chemistry of sodium dithionite and its use in conservation, *Studies in Conservation*, 54 (Supplement 1), 61-73.
- Stambolov, T., 1968, Notes on the Removal of Iron from Calcareous Stone, *Studies in Conservation*, 13 (1), 45-7.
- Thorn, A., 2005, Treatment of heavily iron-stained limestone and marble sculpture, *Proceedings of the ICOM Committee for Conservation 14th Triennial Meeting*, Verger, I. (ed.), the Hague, Netherlands, James & James, London, 888-894.
- Zaini, N. 2009, Calcite-Dolomite mapping to assess dolomitization patterns using laboratory spectra and hyperspectral remote sensing: a case study of Bédarieux Mining Area, SE France, Master of Science Thesis, International Institute for Geo-Information Science and Earth Observation Enschede, The Netherlands.

This page has been left intentionally blank.

PRELIMINARY STUDIES IN USING LIME WITH ADDITIVES AS A SUBSTITUTE FOR RESINS AS ADHESIVES IN STONE CONSERVATION

J. Alonso^{1*} and M. Franković²

Abstract

The use of synthetic resins as adhesives is very common in stone conservation based on its good performance and gluing speed, even though it is known for irreversibility and different characteristics compared to natural stone. The main goal of this paper is to explore the possibilities of using lime with different organic additives as adhesives in stone conservation, considering that the bond should be slightly weaker than the stone. Six different adhesive mixes were designed for preliminary evaluation using the following ingredients: lime putty, NHL3.5, casein, acrylic colloidal dispersion, butadien-styrol latex, fumed silica, distilled water. Properties of adhesive mixes that were evaluated were shrinkage, wrapping, rigidity, brittleness, water absorption and weathering performance. Samples of limestone and marble were glued and tested with cantilever to evaluate its performance. Based on those preliminary results, three adhesive mixes were selected for further testing. To evaluate the structural performance of adhesives, limestone semi-circular specimens were bonded and tested under the Brazilian nut test. This test measures indirect tensile and shear of the interfacial material and allows the inspection and interpretation of the fracture patterns. Preliminary tests and assessment of adhesive mixtures performance gave promising results, since the mechanical resistance and weathering properties of adhesives match the requirements searched, even though further investigation and discussion should be developed.

Keywords: cultural heritage, stone, conservation, additives, adhesives, lime

1. Introduction

Many different natural products are described in conservation literature as glues for bonding different materials since ancient times. Use of natural resins or animal glues is well known throughout history. Since 17th century, adhesion systems using different mixes, based on casein, rosin or “mistura” (Mix of colophony resin and beeswax) were in wide use as stone adhesives. However, when at the beginning of the 20th century, synthetic resins were invented, they quickly substituted these traditional methods.

¹ J. Alonso*
PROSKENE SLP. Madrid, Spain
estudio@proskene.com

² M. Franković
Central Institute for Conservation in Belgrade, Serbia

*corresponding author

Use of epoxy resins as adhesives is very common in stone conservation, even though its known irreversibility and different characteristics compared to natural stone. Good performance and gluing speed make it an easy and useful product. Comparing properties of epoxy resins to limestone and hydraulic lime mortar properties show that mechanical properties (i.e. compressive, tensile and flexural strength) of epoxy resin is up to 10 times higher than those of limestone or hydraulic lime mortars. On the other hand, their porosity, permeability and water absorption are approximately zero (Sikadur product data sheet. SikaCorporation). As an intermediate solution to irreversibility, some authors have studied an interface of acrylic resin (Paraloid B72) to achieve reversibility of the bond (Podany *et al.* 2001). We believe, and so is confirmed by other authors in recent papers (Podany *et al.* 2009), that as a general stone bonding criteria, mechanical results obtained by gluing two pieces of stone should be equivalent or slightly lower than the original. Creating “weak” bonds from a mechanical point of view ensures that, if the stone breaks again, it would be in the same place, thus avoiding creating new damages. To this “weak” adhesions some pins could be added if necessary, improving the final resistance of the joint (Devreux and Spada 2015). We consider these criteria more reasonable from a stone conservator point of view than gluing with high performance adhesives. Starting from the idea that adhesive properties should match stone properties, this preliminary study is exploring possibilities of using lime with different organic additives as adhesives in stone conservation. Study was aimed at gluing limestone with the lime based adhesives, in order to best match the properties of the stone. It relied on traditional recipe for lime-casein mixture, which was then modified by changing or replacing main ingredients to better suit practical requests of quality control and availability of materials. Performance of the mixtures was compared to the performance of traditional lime-casein mixture and to mechanical performance of the limestone. The objective of this study was to assess the potential of using lime based mixtures as adhesives for stone in order to create a base on which more in depth research could be founded. Apart from the mechanical performance of adhesives, which was the main criteria for their evaluation, mixtures were evaluated by other properties that can be of interest from the conservation point of view, such as their workability, ease of application, appearance, water absorption and resistance to weathering.

2. Methodology

This study consisted of several stages, which had the objective to assess properties of adhesive mixtures, their weathering behaviour and to evaluate their structural performance.

2.1. Adhesive mixtures

In the first stage, six adhesive mixtures were designed and their properties observed. Traditional recipe for lime putty-casein mix was a starting point in designing adhesive mixtures. Recipe was then modified by replacing lime putty with natural hydraulic lime (Lafarge NHL 3.5 Z®) and by replacing casein with two different synthetic additives - butadien-styrollatex (Policem®) and acrylic colloidal dispersion (Primal 60A®). Diluting or thickening agents were added in order to achieve good working properties of adhesive mixtures. Distilled water was used to dilute mixtures and fumed silica (Aerosil®) as a thickener. Composition of adhesive mixtures is given in Tab. 1.

Tab. 1: Composition of adhesive mixtures and observation of fresh mixtures properties.

Adhesive mixture No.	Composition	Proportion (Vol.)
1	Lime putty+casein	1:1
2	NHL 3.5+casein+distilledwater	1: 1:0.5
3	NHL 3.5+butadien-styrol latex	2:1
4	NHL 3.5+butadien-styrol latex fumedsilica	1:1:0.5
5	NHL 3.5+ acrylic colloidal dispersion + fumedsilica	1:1:0.5
6	NHL 3.5+ acrylic colloidal dispersion	1:1

2.2. Observation of adhesive mixtures properties

Samples of adhesive mixtures were poured into PE circular moulds, 2 mm thick and 50 mm in diameter and left to cure at room temperature for 7 days. Their appearance, curing behaviour and properties after curing were then assessed in order to collect additional information about the mixtures. Shrinkage was assessed by comparing changes in sample dimensions before and after drying. For water absorption, water drop test was performed. Wrapping and brittleness of dried samples, as well as consistency of fresh mixtures were assessed by macroscopic visual examination.

2.3. Structural performance

Gluing limestone samples with adhesive mixtures and performing tensile tests assessed structural performance of the adhesive mixtures. Testing was done in two steps. In order to select the most promising adhesive samples to be tested in laboratory, preliminary cantilever test was performed. Three adhesive mixtures were then selected for further testing.

2.3.1. The cantilever test

The cantilever beam test is a method used to measure the flexural strength of a material. A cantilever beam is clamped at one end and the other remains free. A load is applied progressively to the free end until failure. The beam breaks at the fixed side, where maximum effort is happening. Top of the beam is in tensile effort and bottom in compression.

$M = P \times L$ where M is the bending moment, P is the applied load and L is the distance to the support.

$\sigma = M/W$ where σ is the stress, M is the bending moment and W the resistant moment.

Specimens of 340×32×22 mm, made of limestone with stylolites (commercial name Sunny), were cut in half using mosaic's hammer and anvil. Adhesive mixtures were applied to both sides; samples were joined and left to cure in vertical position for 7 days and then tested (Fig. 1, Tab. 2).

Tab. 2: Cantilever load test data at 7 days.

Sample No.	P , N	M , Nmm	W , mm ³	σ , N/mm ²
1	-	-	-	-
2	137.34	16480.80	2581.33	6.385
3	78.48	9417.60	2581.33	3.648
4	78.48	9417.60	2581.33	3.648
5	78.48	9417.60	2581.33	3.648
6	107.91	6474.60	2581.33	2.508



Fig. 1: Preparing samples and cantilever test: a – limestone samples; b – applying the adhesive mixture 1; c – setting of samples; d and e – cantilever test.

2.3.2. The Brazilian nut test

Based on results of preliminary cantilever test, three adhesive mixtures (samples 1, 2, and 6) were selected to be tested in laboratory under the Brazilian nut test. Brazilian Test is a geotechnical laboratory test for indirect measurement of tensile strength of rocks. Due to its simplicity and efficiency, it is amongst the most commonly used laboratory testing methods in geotechnical investigation (Amadei 2015). In the Brazilian test, two opposing normal strip loads at the disc periphery load a disc shape specimen of the rock. The standard used is ASTM D3967-95, used by Jorjani to assess the potential adhesive for marble repair (Jorjani *et al.* 2008). The load is continuously increased at a constant rate until failure of the sample occurs. The loading rate depends on the material and may vary from 10 to 50 kN/min. At the failure, the tensile strength of the rock is calculated as follows.

$$\sigma_t = 2P / (\pi DL) \quad \text{where } \sigma_t \text{ is the tensile stress, } P \text{ is the load, } D \text{ is the diameter of the sample and } L \text{ is the thickness.}$$

The above equation uses the theory of elasticity for isotropic continuous media and gives the tensile stress perpendicular to the loaded diameter at the centre of the disc at the time of

failure. For every adhesive three samples were prepared. The stone samples were made of oolitic limestone (commercial name Capri). Cylinders with a diameter of mean value 83.8 mm and a height of 21 mm were cut in halves with electrical saw. The surface was smooth, clean and semi polished. After preparing the surfaces, the adhesive mixtures were applied to both sides of the wetted samples with a spatula, two pieces were then pressed together and excess adhesive was brushed away. Samples were clamped and left to cure at room temperature for 28 days. After specimen preparation was complete, tensile tests were conducted by the authors using a "Controls" – Advantest 9, frame range 0-100 kN, with the adapter for tensile testing for concrete and concrete blocks at The Highway Institute in Belgrade, Serbia. The applied load P was increased at a rate of 0.03 MPa/s (Fig. 2)



Fig. 2 Preparing samples and Brazilian nut test: applying adhesive mixture (a and b); setting of samples (c); Brazilian nut test (d and e).

2.4. Weathering behaviour

Resistance of adhesive mixtures to weathering was assessed by leaving the samples exposed to elements for one year and monitoring their decay. Adhesive mixtures 2 and 6 were tested on site. They were used to reattach broken fragments on limestone gravestones at the medieval necropolis Crkvine in Priboj, Serbia. Necropolis is located in the southwest part of Serbia, in the valley of the river Lim, at the 400-500 m altitude. The climate is continental, with an average annual temperature of 9.3°C, a mean precipitation value 752 mm and 15% of snowfall. Fragments of limestone were reattached in October 2014. On one gravestone adhesive mixture 2 was used, on another mixture 6. After reattachment of fragments, wider cracks were pointed with hydraulic lime mortar. They were assessed after one year's exposure to the elements.

3. Results and discussion

3.1. Observation of adhesive mixtures properties

Observations of adhesive mixtures properties are given in Tab. 3. Properties of fresh and cured mixtures were assessed. In fresh mixtures, viscosity changed significantly in samples where thickening agent was added, but difference in viscosity between the sample with butadiene-styrol latex (sample 3) and the one with acrylic colloidal dispersion (sample 6) was noticeable as well.

Tab. 3: Observation of adhesive mixtures properties

Adhesive mixture No.	Fresh mixture	Cured mixture			
		Shrinkage	Wrapping	Flexibility	Water drop absorption
1	viscous	7%	noticeable	rigid, brittle, break easily	some absorption
2	viscous	5%	noticeable	rigid, brittle, break easily	some absorption
3	thick paste	2%	no, cracked	flexible, resiststobraking	total absorption
4	thick paste	2%	no	flexible, resiststobraking	medium absorption
5	paste	7%	slight	rigid, veryhardtobrake	no absorption
6	viscous	5%	slight, cracked	flexible, hardtobrake	no absorption

All the samples shrank upon curing, but to the different degree. Shrinking manifested as wrapping and cracking. From the observations of cured samples, it could be concluded that properties of the mixtures can be related to the additive - butadiene-styrol latex samples being the most flexible and casein samples being the most brittle. Presence of fumed silica in the mixtures did not seem to have the effect on preventing shrinking or cracking. Presence of cracks might have affected shrinkage, i.e. it can be suspected that sample number 6 would have shrunk more if it did not crack. Water drop absorption test showed that samples with acrylic colloid dispersion (5 and 6) did not absorb water at all, ones with casein (1 and 2) showed some absorption, while ones with butadiene-styrol latex (3 and 4) completely absorbed water drop within 1 minute.

3.2. Observation of the structural failure by indirect tensile (Brazilian Test)

Compressive strength applied on both sides of the circular specimens creates tensile efforts that cause diametric vertical cracks coincident with the load axis (isotropic rocks). Specimens numbered one (limestone glued with adhesive mixture 1 - lime putty and casein) broke on the adhesive layer, clean and fragile break and adhesive remains on both sides. The range of the results is very wide, can't be considered consistent, possibly lime putty setting problems happened. Specimens numbered two (limestone glued with adhesive mixture 2 - NHL 3.5 and casein) broke on the adhesive layer, clean and fragile break and adhesive remains on both sides. Specimens numbered six (limestone glued with adhesive mixture 6 - NHL 3.5 and acrylic dispersion) broke on the adhesive layer. The adhesive remained on both sides but the elasticity of the bond deformed till definitive fracture (no fragile fracture). Using lime putty and casein as an adhesive presents very diverse tensile results. One result is very close to the ones reached with NHL, but the other two are significantly lower. This could be due to setting problems. Adhesives composed of Natural Hydraulic Lime and casein or acrylic dispersion perform mostly equal. They perform almost 70% of the natural stone tensile resistance.

Tab. 4: Brazilian nut test data at 28 days.

Sample No.	Adhesive mixture no.	P, N	s, N/mm ²	Average
1-1	1	5.071	1.796	
1-2	1	2.425	0.859	2.612
1-3	1	14.624	5.181	
2-1	2	18.035	6.389	
2-2	2	13.004	4.607	5.504
2-3	2	15.572	5.516	
3-1	6	15.107	5.352	
3-2	6	17.535	6.212	5.687
3-3	6	15.514	5.496	

3.3. Weathering behaviour

Adhesive mixture samples were left exposed to elements in the beginning of December 2013. After two months sample 1 broke in half. After 4 months upon exposure, sample 1 disaggregated completely while sample 2 started cracking and flaking. The other samples were unchanged. After 6 months sample 2 also disaggregated, while the other samples started to be colonized by microorganisms. Samples did not show any visible decay effects. When handled while wet, they all showed certain degree of flexibility, but stiffened again upon drying. Fifteen months upon exposure, samples 3, 4, 5 and 6 still did not show any significant decay effects; on their surface only a thin reddish bio-film could be noticed (Fig. 3).

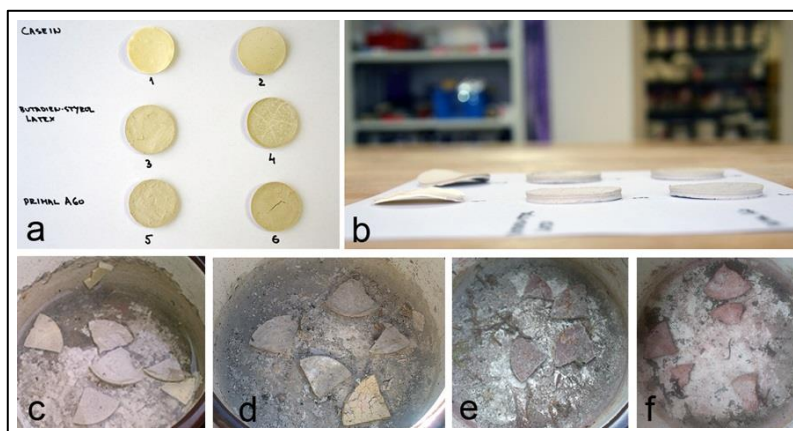


Fig. 3: Properties of adhesive mixtures: samples after curing (a and b); monitoring weathering of samples (c 1/2014, d 3/2014, e 5/2014, f 11/2014).

After a year's exposure to elements on site, fragments reattached with both adhesive mixtures (2 and 6) are in good condition. There are no noticeable signs of decay. It can be argued that, if used for bonding and not directly exposed to the elements, both adhesive mixtures perform well after one year. Monitoring should be continued in a longer period of time in order to attain more data on the behaviour of adhesive mixtures applied on site.

4. Conclusions

Study in using lime with additives as a substitute for resins as adhesives in stone conservation gave promising preliminary results. Resistance of the bond is always lower than the natural stone, but strong enough to be considered. Samples broke on the joint line, therefore no additional damage to stone is made. Adhesives composed of NHL with either casein or acrylic dispersion, perform almost 70% of the natural stone tensile resistance. Adding pins to the bond could make the bond even more resistant. Tested adhesives do not require using solvents; they are health and eco friendly. They are compatible with natural stone and can be used on wet surfaces. Although setting time is longer than epoxy resin, they are relatively easy to work with. Last, they could be removed, thus allowing for the reversibility of the treatment. Further research should be developed, in order to better understand long-term behaviour and resistance of the mixes to weathering and biodeterioration.

References

- Amadei, B., 2015, Principles and procedures of the Brazilian test, University of Colorado, CVEN 5768, Lectures notes 8.
- Devreux, G. and Spada, S., 2015, Experiences in anchoring systems in the restoration of stone artefacts, IIC, News in Conservation, Issue 50, pp. 11-14.
- Jorjani, M. *et al.*, 2008, An evaluation of adhesives for marble repair, The American Institute for Conservation of Historic & Artistic Work, Objects Specialty Group Postprints, Volume Fifteen, pp.95-07.
- Podany, J., *et al.*, 2001, Paraloid B-72 as a Structural Adhesive and as a Barrier within Structural Adhesive Bonds: Evaluations of Strength and Reversibility, Journal of the American Institute for Conservation, Vol. 40, No. 1, pp.15-33.
- Podany, J., Risser, E. and Sanchez E., 2009, Never forever: assembly of sculpture guided by the demands of disassembly, Holding it All Together: Ancient and Modern Approaches to Joining, Repair and Consolidation, Ambers, J. *et al.* (eds.), Archetype Publications, ISBN: 9781904982470, pp. 134-142.
- Wang, R., Lackner, R and Wang, P.-M., 2011, Effect of Styrene-Butadiene Rubber Latex on Mechanical Properties of Cementitious Materials Highlighted by Means of Nanoindentation, Strain 47, doi: 10.1111/j.1475-1305.2008.00549, pp 117-126.

FREEZE THAW AND SALT CRYSTALLISATION TESTING OF NANOLIME TREATED WEATHERED BATH STONE

R.J. Ball^{1*} and G.L. Pesce¹, M. Nuño¹, D. Odgers² and A. Henry³

Abstract

This paper describes the effects of freeze thaw and salt crystallisation on weathered Bath stones treated with nanolime. Specimens were characterised using drilling resistance measurements to evaluate the variation in surface and subsurface integrity following application of nanolime and subsequent testing. A number of different regimes used to apply the nanolime are reported. The tests did not suggest any negative impacts due to the presence of nanolime on the freeze-thaw tested specimens, however evidence of sub-surface damage was observed on some specimens subjected to salt crystallisation.

Keywords: weathered stone degradation, freeze thaw, nanolime, salt crystallisation, drilling resistance

1. Introduction

Many historic and new buildings are built using natural limestone due to its availability workability and aesthetic appearance. However, since the industrial revolution the level of atmospheric pollutants has increased substantially and this had resulted in an acceleration of degradation of stone surfaces. Common pollutants such as sulphur dioxide and oxides of nitrogen form acids that etch the surface reducing mechanical strength and also, for certain stone types, result in the formation of a crust, commonly gypsum (Nuno *et al.*, 2015). Such crusts are often much less permeable compared to the underlying stone and lead to the undesirable trapping of moisture and salts in the subsurface layer. In addition to the effect of pollutants, erosion from weathering plays an important part in stone decay.

To consolidate surfaces of decayed stone, treatments are commonly applied aiming to restore or maintain a desirable level of strength and integrity. There is a wide variety of treatments available based on a range of different chemical systems including organosilicon compounds, ethyl silicate or ethyl-methacrylate. (Ferreira Pinto and Delgado Rodrigues 2012; Karatasios *et al.*, 2009; Esbert *et al.*, 1991). However it is generally accepted that when identifying a suitable consolidant, materials which have some chemical compatibility with the stone to be consolidated have a reduced risk of undesirable effects. All, chemical,

¹ R.J. Ball*, G.L.A. Pesce and M. Nuño
BRE Centre for Innovative Construction Materials, Department of Architecture and Civil
Engineering, Bath, United Kingdom
r.j.ball@bath.ac.uk

² D. Odgers
The Old Stable, Peacock Hill House, Barton St. David, Somerton, United Kingdom

³ A. Henry
Historic England, Engine House, Fire Fly Ave, Swindon, United Kingdom

*corresponding author

physical and mechanical properties are important, and in the case of limestone, lime (calcium hydroxide) based materials may offer such compatibility. For many years *lime water* and *milk of lime*, have been applied as a consolidant. The former is a clear solution of lime in water whereas the latter consists of micro-sized particles of calcium hydroxide as a suspension in a saturated aqueous solution of calcium hydroxide. When either product is applied to stone, evaporation of the liquid carrier results in the deposition of calcium hydroxide which subsequently carbonates depositing calcium carbonate on the surface and within the pores of the stone providing an increase in strength. However this particular approach has several drawbacks including: (i) the micro sized calcium hydroxide particles of milk of lime may be larger than the stone pores reducing the amount of lime deposited within the stone; (ii) although lime dissolved in the lime water may enter the stone the actual amount deposited upon evaporation is only about 1.8g per litre of water; (iii) in order to deposit a sufficient quantity of calcium hydroxide to give a reasonable level of consolidation the process of applying the *lime water* must be repeated numerous times, in some cases up to forty. Aside from the labour intensive nature of such a treatment repeatedly wetting and drying the stone with water (the most important natural solvent) can mobilise soluble salts contained within the stone. In some instances this can lead to further damage, negating any increase in strength arising from the use of the consolidant.

In the late 1990's researchers at the University of Florence including Baglioni, Dei and Salvadori synthesised nanometre sized calcium hydroxide to be used in the field of cultural heritage. This was added to an organic carrier, often an alcohol, forming what is now commonly called *nanolime* which generally has a particle size <150nm. Properties such as rapid evaporation of the solvent, small particle size and a liquid carrier that does not dissolve salts within the stone, have generated much interest from the conservation industry. Originally formulated for the restoration of deteriorating fresco paintings, in the last few years this material has been used as a stone consolidant in a number of countries including the UK.

Due to its relatively recent introduction and the lack of research there still remain many unanswered questions regarding its medium to long term effects. Recent studies focussed on weathered stones (Pesce *et al.*, 2013) and findings from the *International Workshop on the Application of Nanolime for Consolidation of Weathered Stone*, held at the University of Bath in September 2015, have highlighted the importance of factors such as application technique, environmental conditions and stone type on the effects of treatments. Depths of penetration and formation of surface crusts are extremely hard to predict on site, yet can have a significant influence on the post-treatment behaviour of the stone. Previous studies often highlight the adverse effects of treatments that result in accelerating the onset of damage (Dei and Salvadori, 2006). Salt crystallisation and freeze-thaw cycling are two mechanisms to which many of the stones treated with nanolime in the UK will be subjected. In this paper we report on the likely effect of nanolime on stones subject to freeze/thaw cycling and salt crystallisation.

2. Experimental methods

2.1. Preparation of specimens

Cube shaped specimens approximately 100 mm in each direction were cut from carefully selected pieces of weathered Bath stone. The weathered surface of each stone was treated with commercial nanolime CaLoSiL® E25, containing 25g/l calcium hydroxide in ethanol. A detailed analysis of porosity in the Bath stone used is given in Pesce (2013). A reduction in porosity of around 6% was reported when comparing weathered to un-weathered stone. A number of different treatment regimens including: different numbers of applications, period between applications, post treatment spraying with water during curing and variations in relative humidity during curing was chosen to represent methodologies and conditions expected in the UK. In total 15 individual treatments were applied, labelled A to O, and given in Tab. 1. The surface and sub-surface characteristics of each specimen before treatment with nanolime, after treatment with nanolime and following freeze-thaw and salt crystallisation testing was evaluated. A SINT Technology s.r.l. Drilling Resistance Measurement System (DRMS) was used to characterise mechanical properties of each stone to a depth of 30 mm (and therefore to evaluate the penetration depth of the consolidant). Due to the natural heterogeneity of stone in order to obtain a representative measure of the surface and sub-surface properties, each stone was drilled three times using a 5 mm diameter flat ended diamond drill bit and results were averaged to produce a single drilling resistance profile. All tests were undertaken using a 600-rpm rotational speed and penetration rate of 10 mm/min.

Tab. 1: Relative humidity during curing, number and timing of applications and details of water spraying during curing of test specimens.

Relative humidity		90	90	90	60	30
Post application water spraying		3 sprays/ day (1 day)	3 sprays/ day (4 days)	-	-	-
	1	B	C	A	J	M
Number of applications of nanolime	6 within 2 hours	E	F	D	K	N
	6 in a day	H	I	G	L	O

Letters A – O indicate the specimen identification and treatment conditions

Two of each specimen type were produced providing one for freeze-thaw and the other for salt crystallisation testing. Specimens were subjected to 15 individual freeze-thaw cycles where each cycle consisted of firstly saturating the stone surface with water followed by placing it in a freezer at -22°C for 48 hours. In order to promote unidirectional freezing from the nanolime treated surface into the bulk of the specimen (simulating the natural process of freezing that occurs in stone on a building), the remaining 5 untreated faces of the cubes were covered in a 60 mm layer of rigid phenolic foam insulation, Fig. 1a. Following freezing, the specimens were removed from the freezer and thawed at 19°C and 76% relative humidity.

An epoxy coating was applied to four faces of the salt crystallisation specimens leaving top and bottom faces uncoated Fig. 1b. Salt crystallisation within the surface of the specimens was initiated by firstly allowing a saturated solution of sodium sulphate to diffuse into the nanolime treated surface. This was achieved by immersion in a tray of the liquid to a height of 35 mm with the nanolime treated face in the vertical orientation, specimen turned onto side as shown in Fig. 1c, therefore leaving the remaining 65 mm of treated surface out of the solution. The 48 hour immersion period was sufficient to allow saturation of the stone surface above the liquid level by capillary action. Each specimen was then removed and allowed to dry for 48 hours at 19°C and 76% relative humidity. The epoxy resin coating ensured that the evaporation of moisture and flow of salts were towards, and out of, the nanolime treated surface. Three cycles were sufficient to cause a range of different severities of damage over the different of specimens, and therefore to allow comparison between the treatment regimes.

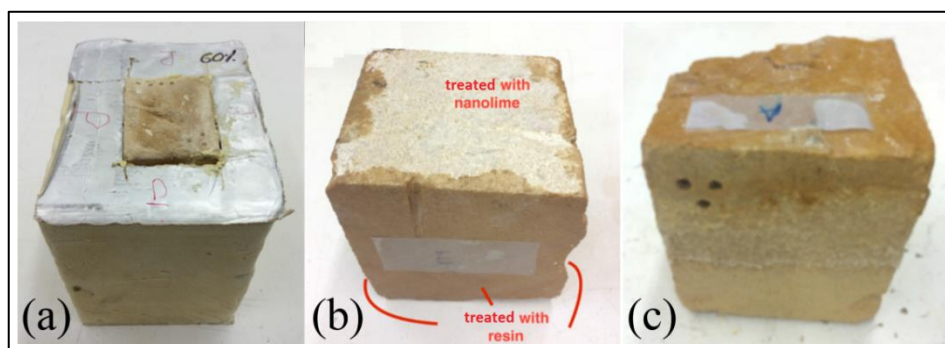


Fig. 1: Stone specimens: (a) freeze thaw, (b & c) salt crystallisation.

3. Results

3.1. Freeze thaw cycling

Visual examination of the specimen surfaces subjected to freeze thaw cycling revealed a variation in the severity of damage observed on different areas. This was attributed to natural variations of the stone surface. To evaluate this effect on drilling resistance, measurements were taken in both areas of severe and areas of low damage. Each stone behaved slightly differently and comparisons of the drilling resistance measurements taken at different stages of the specimen's treatment are given in Tab. 2. All specimens except those subject to a single application in low RH (30% and 60%) showed an increase in the stone integrity after application of nanolime. An (*) is shown where an increase in the stone integrity after application of nanolime was not detected. This was defined as when the drilling resistance of the nanolime treated stone increased compared to the untreated stone. In almost all cases a sharp increase in the drilling resistance of the treated stone signified that a nanolime crust had been formed. The exceptions were those specimens indicated by the symbol (\$) in the table. Where the drilling resistance of the stone subjected to freeze thaw cycling was greater than that of the original stone, but generally less than the treated stone this was classed as an improvement, and denoted by the symbol †. In this case the application of nanolime had mitigated against the effects of freeze thaw cycling. Fig. 2 shows the drilling resistance profiles for stone H. It is clear that the application of nanolime has increased the hardness of the surface crust and a modest increase in the resistance of the

sub surface layer to a depth of approximately 9 mm. Following the freeze thaw cycling the drilling resistance is seen to drop. However for the area classed as ‘less damaged’ the resistance is still greater than that of the untreated stone. In the ‘more damaged’ area the drilling resistance has dropped below that of the untreated stone.

Tab. 2: Summary of DRMS profiles from specimens subjected to freeze thaw cycling

Relative humidity		90	90	90	60	30
Post application water spraying		3 sprays/ day (1 day)	3 sprays/ day (4 days)	-	-	-
No. of applications of nanolime	1	†	†		* §	* §
	6 within 2 hours		†		†	
	6 in a day	†	†		§	†

* = No detectable increase in integrity of stone after application of nanolime, § = No crust formed on stone, † = Improvement in the stone resistance to freeze thaw cycling attributed to the application of nanolime.

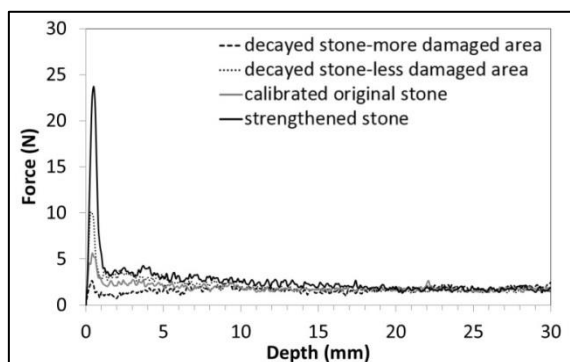


Fig. 2: Drilling resistance profiles of stone H subjected to freeze thaw cycling.

3.2. Salt crystallisation

A summary of the drilling resistance measurements from the salt crystallisation tests are given in Tab. 3. An (*) is given where the application of nanolime led to an increase in the drilling resistance before immersion in the salt solution. A number of the specimens showed an increase in the drilling resistance following salt crystallisation cycles. Visual examination attributed this to the precipitation of salts in the surface pores resulting in the increased drilling resistance, as indicated by the Greek letter ϕ in Tab. 3. A further effect that was observed on a number of the stones was a decrease in the drilling resistance within the subsurface at a depth between 5 and 10 mm. This is denoted in the table by symbol (\ddagger).

Fig. 3 shows the drilling resistance profiles for stone G subjected to salt crystallisation, which can be considered as a successful treatment. The application of nanolime has resulted in an increase in the drilling resistance to a depth of 6 mm. Following salt crystallisation

cycling the drilling resistance was reduced, however it is still greater than that of the untreated stone, and therefore the presence of nanolime has been beneficial. In comparison the drilling resistance profiles from stone D subjected to salt crystallisation are shown in Fig. 4. The application of nanolime has increased the drilling resistance to a depth of approximately 8 mm, however it has also produced a surface crust, indicated by the peak at a depth <1mm. Following salt crystallisation cycles the strength of this crust has increased, however a weakening of the stone is observed in the subsurface layer.

Tab. 3: Summary of DRMS profiles from specimens subjected to salt crystallisation

Relative humidity		90	90	90	60	30
Post application water spraying		3 sprays/ day (1 day)	3 sprays/ day (4 days)	-	-	-
No. of applications of nanolime	1	§ φ ‡	* ‡	‡	* §	* §
	6 within 2 hours	§ φ ‡	* § ‡	φ ‡		φ
	6 in a day	* § φ	* φ		§	

* = No detectable increase in integrity of stone after application of nanolime, § = No nanolime crust formed on stone, φ = evidence of a salt crust, ‡ = subsurface weakening

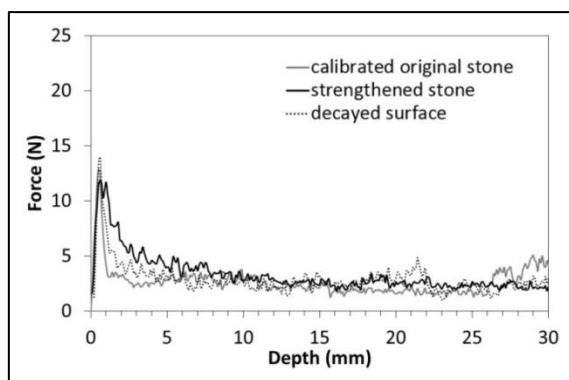


Fig. 3: Drilling resistance profiles of stone G subjected to salt crystallisation cycling.

4. Discussion

Examination of the drilling resistance profiles for the stones before and after treatment with nanolime revealed that an increase in drilling resistance, between 5 and 10 mm, was observed on the majority of stones. Stones J and M, which received 1 application of nanolime and were cured in an atmosphere of relative humidity 60% and 30%, respectively, did not show an improvement. This result highlights the importance of the presence of water in promoting the carbonation of nanolime through the formation of carbonic acid. Stones C, F, H and I that were used in the salt crystallisation tests also did not show an increase in drilling resistance following treatment with the nanolime. Further work is

required to determine the cause of this observation especially considering that the equivalent stones which were used for freeze thaw tests did show an increase in drilling resistance.

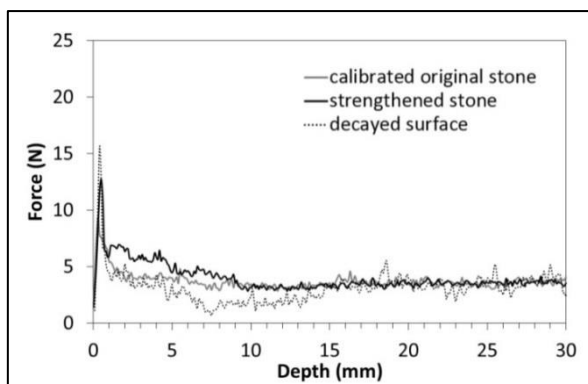


Fig. 4: Drilling resistance profiles of stone D subjected to salt crystallisation cycling.

The majority of specimens used to evaluate the effect of freeze thaw cycling had evidence of crust formation on the surface. From the specimens where the nanolime treatment appeared to have been beneficial following freeze thaw cycling the most consistent effect was observed in the specimens that, after application of nanolime, were sprayed with water 3 times a day for 4 days. Such treatment, which would be expected to maintain a high humidity in and around the stone, could again be enhancing the effect of carbonic acid formation and thus carbonation.

From the specimens treated with nanolime and subjected to salt crystallisation, a much larger proportion did not show evidence of an improvement as a result of the application of nanolime, prior to the salt tests. As there was little correlation with the equivalent specimens prepared for the freeze thaw tests this difference must be attributed to natural variations in the weathered stone. This is perhaps not unexpected and a common problem associated with tests using natural materials. However as a result some caution must be exercised when drawing more specific conclusions.

Perhaps the most noticeable difference between the freeze thaw and salt crystallisation tests was an increase in drilling resistance of the surface crust following salt crystallisation. This increase would be consistent with the precipitation of sodium sulphate within a pre-existing naturally formed gypsum or consolidant induced (nanolime) crust. Consideration of all the specimens shows a definite pattern in which salt crystallisation to nanolime treated surfaces results in a weakened subsurface region. This may be due to the crust on the surface being less permeable but further tests would be required to establish the exact mechanism. Changes in the surface permeability attributed to the nanolime treatment may restrict the flow of salt solution out of the surface during the drying cycle. This could therefore promote an enhanced precipitation, and therefore accelerated deterioration of the stone.

5. Conclusions

This paper provides a summary of results obtained from a study to evaluate the effects of freeze thaw and salt crystallisation on nanolime treated stone. A total of 30 different specimens were conditioned and 315 holes were drilled. Despite the extensive data obtained natural variations in the stone means caution must be exercised when drawing conclusions. The key findings are summarised below:

- High relative humidity of 90% enhanced the consolidating effect of nanolime compared to equivalent specimens exposed to a lower humidity of 60 and 30%.
- Spraying nanolime treated surfaces with water immediately after application can, in some circumstances, improve the consolidation effect by providing a humid environment where carbonation is promoted.
- All stones treated with nanolime, and subjected to freeze thaw cycling, either showed an improvement in drilling resistance as a result of the presence of nanolime or no improvement. Within this study there was no evidence which suggested a negative effect on drilling resistance due to the presence of nanolime being applied to the surface.
- In a number of the tests performed to investigate the effect of salt crystallisation, drilling resistance measurements indicated that a weakened sub surface layer was formed. This suggests that damage from salt crystallisation may be exacerbated by changes in surface properties of stone which can be attributed to treatment with nanolime.

References

- Dei, L. and Salvadori, B., 2006, Nanotechnology in cultural heritage conservation: nanometric slaked lime saves architectonic and artistic surface from decay. *Journal of Cultural Heritage* 7(2): 110–115.
- Esbert, R. M., Montoto, M., and Ordaz, J., 1991, Rock as a construction material: durability, deterioration and conservation. *Materiales De Construcción* 41(221): 61–73.
- Ferreira Pinto A. and Delgado Rodrigues J., 2012, Consolidation of carbonate stone: influence of treatment procedures on the strengthening action of consolidants. *Journal of Cultural Heritage* 13(2): 154–166.
- Karatasios, I., Theoulakis, P., Kalagri, A., Sपालidis, A., and Kilikoglou, V., 2009, Evaluation of consolidation treatments of marly limestones used in archaeological monuments. *Construction and Building Materials* 23(8): 2803–2812.
- Nuño, M., Pesce, G. L., Bowen, C. R., Xenophontos, P. and Ball, R. J., 2015, Environmental performance of nano-structured Ca(OH)₂/TiO₂ photocatalytic coatings for buildings. *Building and Environment* 92: 734–742.
- Pesce, G. L., Morgan, D., Odgers, D., Henry, A., Allen, M., and Ball, R. J., 2013, Consolidation of weathered limestone using nanolime. *Proceedings of the ICE - Construction Materials* 166(4): 213–228.

THERMOSETTING METHYL METHACRYLATE ADHESIVE FOR STONE: CHARACTERISATION, APPLICATION TECHNIQUES AND LONG-TERM PERFORMANCE ELEVATION

Z. Barov^{1*}

Abstract

A two-component thermosetting adhesive for fractured stone and ceramic objects is composed of polymethyl methacrylate copolymer (powder) containing hardener, and a liquid monomer. When the two components are mixed the powder rapidly dissolves in the monomer and the mixture begins to cure. The powder/liquid ratio can vary considerably allowing the formation of an adhesive with various viscosities. The resulting syrup or paste can be used as adhesive, gap-filler and reconstruction material for marble restoration. After polymerization it produces a resin with Tg of 74 - 85°C, depending on the presence of inert filler. This, together with its photochemical stability, makes it quite appropriate for outdoor applications. The complete polymerization occurs in 24 hours. but after 40-50 minutes the connection is sufficiently strong to allow handling. The polymer produces sufficiently strong joint that is also resistant to air pollutants. It remains totally reversible in a variety of solvents even after long time. This allows disassembling of complex pinned joints, usually quite difficult to achieve with other adhesives. A special technique has been developed for reassembling complex joints. It consists of fixing the fragment to a sled mounted on tracks, allowing moving it back and forth without losing the alignment. This permits application of the adhesive, placing of pins and then fast and precise reassembling. When pressure is applied the excess adhesive is squeezed out of the joint. Because the shrinkage upon curing is minimal all the gaps that may be present stay filled. When mixed with some pigments it can be used as an external gap filler and reconstruction material for restoration of missing marble elements. It produces matt surface that can be additionally carved and patinated. The system has been applied on several artifacts and has withstood outdoor exposure for decades.

Keywords: reversible stone adhesive, thermosetting polymethyl methacrylate, technical investigations, application techniques, fill material

¹ Z. Barov*

ETHOS, conservation of ancient art, United States of America
barov.ethos.art@mac.com

*corresponding author

1. Introduction

When in the early 1970's there was a need to remove the lid of a newly discovered medieval sarcophagus without employing tools that could damage the stone, it was decided to adhere hooks to it with the use of a reversible adhesive. Veselin Vekov and Alexandar Savov of the National Institute for the Monuments of Culture in Sofia, Bulgaria were responsible for the choice of the adhesive. Two-component, solvent reversible polymethyl methacrylate system (PMMA), Colacryl, made by ICI, was selected by them, tested and successfully employed on the project. The same type of adhesive but made by different manufacturer was tested for long-term application and used by the author routinely, in various projects, for stone and ceramic reassembly (Barov, 1985). After more than 30 years of outdoor exposure it proved to be excellent glue, resisting high temperature fluctuations and direct sunlight. Its high glass transition temperature (T_g) held the joins firmly even when the surface temperatures of a black diorite sculpture reassembled with it reached, in many occasions, the levels of 60-63°C. Subsequently, it became clear that because of its photochemical stability it could be used as a fill material for surface gaps and for rebuilding missing areas on marble objects. Being a thermosetting resin it exhibits very low shrinkage upon curing, which is a useful property for gluing fragments with worn interfaces, where missing sections must be filled to insure continuous surface contact of the adhesive film with the substrate. The fast curing time allows layering when thick fills must be applied. That helps avoiding excessive temperature increase during the curing of large masses. It is also very useful for achieving colour matches when building restored parts because the resin is semi translucent and allows achieving subtle colour nuances with the addition of small amount of pigments in each layer. Finally, its prompt reversibility in many solvents, even after decades of outdoor exposure, insures the separation of joins reinforced with one or several pins, even when they are deeply embedded into the substrate.

2. Use of PMMA as an adhesive

The first attempts of reassembling stone artifacts with PMMA were made only on the bases of manufacturers information about the characteristics of the product. The resin was developed mainly for use in dentistry. It is supplied as a two-component system: The polymer, polymethyl methacrylate is in powder form. It is usually based not only on a pure methyl methacrylate but is copolymerized with other acrylates (2-ethyl hexyl acrylate) to decrease the T_g of the polymer and to improve some of its physical properties (W.H.A. Plastics, 2002). The brand we usually employ, *Teets Cold Cure Denture Material*, manufactured by *Co-Oral-Ite Dental Manufacturing Company* in the USA, has a T_g of 74°C (our measurements). The polymer contains small amount of plasticizer, dialkyl phthalate and a hardener, organic peroxide. The second ingredient of the two-part system is a liquid methyl methacrylate monomer (manufacturers' data). When mixed with the powder it forms a syrup or paste that is used as an adhesive or fill material. It is stabilized with a small amount of inhibitor, hydroquinone, to prevent spontaneous polymerization.

Upon combining, the powder dissolves in the monomer quite fast – after one to two minutes of mixing. At the same time the monomer reacts with the hardener, present in the powder, initiating the curing process. The ratio between the two components can vary considerably allowing the production of mixtures with different viscosity. The ratio suggested by the manufacturer is 2 parts of powder to 1 of liquid but the mixture is too thick for normal gluing purposes and is usually reduced to 1:1 or even with less amount of

polymer. When applied over the interfaces the substrate absorbs part of the monomer. To avoid the initial loss of liquid, especially in highly porous materials, is a good practice to brush the surfaces with small amount of pure monomer, before the application of the glue. Some monomer evaporates during the preparation and application processes that also increase the viscosity of the mixture.

The curing is exothermic and initiates 15-20 min. after the mixing of the components. The temperature increases rapidly, but most of it is absorbed by the substrate. The reaction takes 10-15 minutes after which the heat generation stops and the adhesive film becomes hard. Theoretically the complete curing occurs after 24 hrs. but the join becomes sufficiently strong after 30-40 min. to allow manipulation of the glued fragments, if necessary. It is better, however, to allow complete curing before applying substantial stress on the joint.

Although the adhesive is sufficiently strong and at the same time resistant to high environmental temperatures it should not be presumed unconditionally reliable for very long outdoor exposure where the temperature fluctuations generate continuous stress on the joints. Its longevity could be affected mainly by the differences of the coefficients of thermal expansion of the film and the substrate. The stress could be aggravated by the position of the attached fragment that can protrude horizontally and add the negative effect of vibrations, especially those caused by earthquakes that can increase significantly the vulnerability of the joints. Although the author has not noticed separations after 30 years of outdoor exposure, this does not mean that the perfect adhesion will continue indefinitely. For these reasons the connections are reinforced with the addition of rigid pins that have several positive effects: To increase the gluing surface and the general strength of the joint; To increase its rigidity and *especially* to prevent the fragment(s) from falling off if the adhesive fails completely. Disassembly of pinned joints in the future could be a difficult task because if the pins are selected and placed properly (an issue not covered in detail here) makes a future separation very difficult to accomplish if other adhesive has been used.

The system is composed of two parts (powder and liquid) to speed up the preparation of the mixture, to decrease the evaporation of the monomer and especially to decrease the curing time. Using only monomer and curing agent as an adhesive is much more difficult even if thickened with fumed silica and after several unsuccessful attempts it was decided to exclude it from our tests and practical work.

In normal temperature (20-25°C) the working time of the *Teets Cold Cure* adhesive is around 15 min. including mixing the two components together, applying the mixture on the interfaces, filling the pin holes, coating the pins and aligning correctly the fragments. For large and complex joins this time could be not sufficiently long and there is a chance that imperfect connections could result from the hurried manipulation. Initially it was attempted to slow down the curing process by adding the inhibitor hydroquinone. It however changed the colour of the PMMA, from transparent to pink and was dimmed inappropriate. Two other inhibitors were also tested, the antioxidants Butylated hydroxyanisole (BHA) and 2,6-D tert-butyl d-methylphenol but the results were again unsatisfactory.

2.1. Alignment technique

To compensate for the relatively short working life of the system some mechanical improvements of the gluing process were developed and implemented in several projects. One of the most time consuming operation is to align correctly a large and heavy broken

detail to an immovable object (statue) especially if the joint must be reinforced with one or several pins. The operation includes application of the adhesive its injection into the holes where the pins will be inserted and then the fragment must be aligned correctly and pressed strongly until the complete curing of the resin takes place. The fragment could be positioned above the immovable object (the best case), or protruding sideways, beneath the object vertically or in an angle.

In order to shorten the reassembling process, the fragment is installed onto a sled that is mounted on a track with two or four members. Both the sled and the track are made of wood. The track is parallel to the axis of the fragment and to the pin, if such is present, and is firmly connected to a supporting structure. It allows the sled to move back and forth along the axis of the fragment but restricts movements in any other direction. The track and the sled are aligned so that the fragment and the object fit correctly together before any glue is applied. Subsequently the sled/detail assembly is moved away from the object far enough to expose the two interfaces. The adhesive is applied with brush on both sides then the assembly is moved back to the object and pressed firmly until the adhesive sets. In some cases we have used ratchet straps to accomplish the movement and the pressure and other times – a bottle jack. Usually some excess adhesive is pressed out of the joint and must be wiped off with acetone-soaked rag from the visible areas. In some cases the sled should have some polyethylene sheet lining to prevent gluing the stone to it.

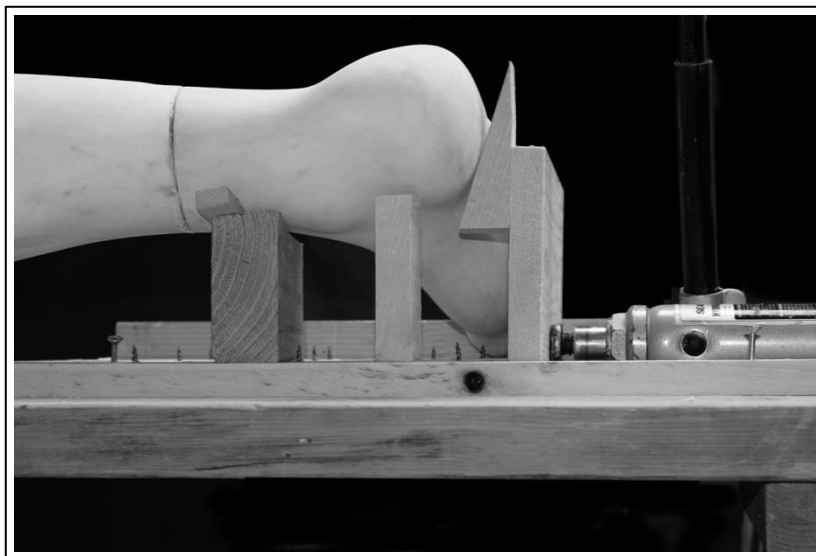


Fig. 1: The detail to be bonded is mounted on a wooden sled and pressed with bottle jack. The small elements of the wooden support are attached to themselves and to the sled with cyanoacrylate gel.

If a pin is required, the hole must be drilled first in the object, before installing the tracks. Subsequently the tracks are built and the fragment, attached to the sled, is dry-fitted to the object. To mark the place where the hole should be drilled into the fragment, a ball of cotton is inserted in the hole of the object, prior to the dry fitting, so that some of it protrudes slightly above the surface of the interface. The visible side is painted with

gouache or acrylic colour and when the fragment is pressed to the object the whet colour leaves a paint mark on the other interface, indicating the drilling spot. The same technique could be applied if there is more than one pin. After drilling the second hole, the pin is glued to the fragment and while the adhesive is still in the stage of hardening the fragment, fixed to the sled, is fitted to the object so that the pin is correctly positioned for the final assembly. After the curing, the fragment is pulled back and adhesive is injected into the hole of the object as well as applied over the pin. To prevent the adhesive to run out it could be thickened and made jell-like with the addition of fumed silica. The rest of the gluing proceeds as described above.

2.2. Reversibility

Being soluble in many solvents the PMMA can be removed not only from the joins but also from the holes where the pins are embedded. In simple cases wrapping solvent containing compresses, covered with polyethylene foil around the joins could dissolve the adhesive. For more complicated joints building a temporary container around the glue line allows to keep large amount of solvent in contact with the glue and the surrounding substrate for a long time. Such container can be build out of aluminum-lined cardboard, shaped around the fragment and adhered to it with substance insoluble to the solvent to be used. If acetone is employed a thickened with fumed silica polyvinyl alcohol (PVOH) or hide glue can be used. These two adhesives are easily removable afterward with water or steam. The container is made out of several pieces of cardboard joined together with staples, cyanoacrylate gel, etc. Before use, the joints are sealed with thickened PVOH or animal glue. The aluminum-lined side faces the object and prevents excessive absorption of the solvent by the cardboard. If aluminum faced cardboard is unavailable the internal surface can be coated with a layer of 15% PVOH. For large and complicated joins the author applies the adhesive on stripes over the interfaces in order to leave narrow unglued channels that facilitate the penetration of the solvent used for eventual disassembling in the future.

2.3. Characteristics of the adhesive

From aesthetic point of view there are two positive qualities unique to this system. First, it does not darken the surface of the stone, unlike dissolved acrylics, epoxies and polyesters that form slightly darker margins or intensified colour of the non-white stones or terracotta at the glue boundaries. Second, it produces totally mat surface that blends quite well with the surrounding original material and requires very little additional work to finish when used as fill or as reconstruction material.

From technical point of view, the adhesive power of the cured film to the substrate appears to be inferior to the cohesion forces of most stones used in the architecture and in the arts. This is an important issue, especially for outdoor objects (or architectural details), which joins are going to fail, sooner or later, as discussed above. Indoor objects are not totally immune either to joint failures caused by vibrations, earthquakes, etc. In both cases adhesives stronger than the substrate will cause detachment of a thin layer of original off the surface of the interfaces. In our tests most of the epoxies as well as Paraloid B72 develop very strong adhesion to stone and ceramics causing breakage of the substrate. In most cases the PMMA separates cleanly from the inorganic surfaces.

From purely practical point of view the system provides very fast final results that is quite convenient when reassembling objects with multiple breaks. Because of the fast initial

curing, the connection becomes sufficiently strong after 40-50 min. and one can proceed to the next join or to any kind of other manipulation. For very large objects, of course, is advisable to wait 24 hrs. before proceeding.

Some of the most important properties of the cured adhesive were tested to determine the numeric values of its performance and become aware of the resin's limits. It was important to determine, in a first place, the adhesive power of the system to stone and ceramic substrates. Two different tests were performed: lap shear adhesive strength (ASTM D 905-49) and tensile strength of the stone/adhesive joint. The results show that the PMMA system is weaker than the cohesion of the substrate. At the same time it is sufficiently strong to hold large and heavy fragments together: the result of the lap shear test is 2.45 MPa (25 kg/cm²) (Barov, 1986).

The resin was also tested to determine several other properties that were important for the design of the different applications. The tensile strength is 55 MPa (561 kg/cm²) quite strong and at the level of the epoxy resins. The elongation is 7%, again close to some popular epoxies and Young's modulus is 1280 MPa (13052 kg/cm²). The T_g was determined with Differential scanning calorimetry (DSC) and the result is 74°C. The addition of glass microspheres increases the T_g of the cured resin to 85 for 10% w/w of added filler. These results were obtained during series of tests performed for the selection of the materials for the restoration of the Nine Muses Sarcophagus in the Hearst Castle, CA. The report prepared by Ethos, conservation of ancient art partnership and the Chemistry department of Cal Poly, San Luis Obispo is not published. Some technical data, not mentioned here were covered by the author in the material "The Restoration And Subsequent Earthquake-Safe Mounting Of Four Sculpted Columns Broken During An Earthquake At The Hearst Castle" in the 12th International Congress on the Deterioration and Conservation of Stone, New York 2012.

2.4. Long-time behavior

The first time the adhesive was used for the reassembling of an outdoor fractured stone object was on one of the heads of the Sekmet fountain and the ceramic Persian tile panel in the Hearst Castle in California, more than 30 years ago (Barov, 1986). The head sculpted in dark gray, almost black diorite is displayed on the southern side of the main terrace under daily exposure of sunlight. The air temperature reaches the maximum of 44°C during the summer and drops occasionally under the freezing point during the winter months with daily fluctuations averaging 8°C with an average of the sunny days of 186/year in this region, according to the local records. The surface temperature of the dark gray stone, however, have reached 63°C on the side directly exposed to the sun while the temperature of the north side was 23.5°C, according to our measurements. The numerous joins of the two objects have held perfectly since 1985, for a period of more than 30 years resisting the temperature and humidity fluctuations and the dynamic stress produced by frequent earthquakes, including the 6.6 tremor of 2003. All joins were made with *Teets Cold Cure*.

3. PMMA as a gap filler and reconstruction material

In addition to the use of the system as an adhesive its qualities of colour stability and ease of application make it an appropriate material for gap filling and reconstruction of missing details, especially on marble. If no inert fillers are added the cured resin is almost

completely transparent. With the addition of inert powders, such as glass microspheres, it becomes translucent light grey, almost white. For achieving of a close colour matching to the surrounding original material it is often necessary to add small amounts of colour stable pigments that are already pre-mixed in small amount of monomer.

3.1. Application technique and esthetic issues

As stated before, the curing process is exothermic. The temperature increase is quite small when the resin is employed as an adhesive because the film is usually quite thin. When used as a fill or reconstruction material however, the mass of resin is much larger and that could lead to fast and substantial increase of the temperature to the point that the resin could start boiling. Large missing areas must be filed gradually, on several layers, because the temperature increase is proportional to the mass of resin employed. Diminishing the thickness of single application insures faster dissipation of the heat and avoidance of deformations caused by boiling. The fast curing allows building large reconstructions quite fast. New layer, 1-2 cm thick, can be placed about one hour after the application of the previous.

The colouring of the fills or reconstructions is also facilitated by the fast curing process. Fine colour nuances are achieved by adding thin layers with slight colour differences between them. Because the resin is translucent, the under-layers transpire through the surface layer, creating colour nuances that can approximate quite well the complex patinated surface of the surrounding original. Obtaining white colour values requires adding large amounts of glass microspheres, which decreases the strength of the cured fill.



Fig. 2: Reconstructed detail (tip of the nose) before and after. The head is approximately 25% over life-size.

This can be quite positive for indoor applications, but such fills are not strong enough to resist the outdoor deterioration agents. Fortunately there are PMMA systems available on the market today that are premixed with titanium dioxide that makes obtaining of a base light colour much easier. One such product is Bosworth Duz-All All-Purpose Self-Cure Acrylic Repair Material, Keystone industries, USA. The amount of pigment in the mixture is very small and its presence virtually does not diminish the strength of the fill.

Not staining the stone is another very important quality of the PMMA fills. They do not produce a darker shade on the stone at the boundary of the fills or reconstructions, which elimination is always a problem when using other organic materials.

In our practice we usually adjust the translucency of the fills to that of the original, especially when working on marble. In our measurements a one cm thick slab of Thasos marble blocks approximately 97.4% of the light. Five cm thick slab does not transmit visibly any light in normal environment but some thin sections and small details look much more convincingly integrated with the original if they match the translucency of the original. Toot Col Cure resin mixed with 10% of glass microspheres w/w has a translucency virtually identical to that of this particular marble. Duz-All system, premixed with titanium dioxide, has lower translucency, blocking 99.4% of the light. It can be adjusted by mixing the white with translucent Duz-All, also produced by Keystone.

4. Conclusion

In a 30 years outdoor exposure the PMMA two-component system has performed quite well as a stone adhesive. It has some of the epoxy characteristics mainly low shrinkage after curing and excellent gap-filling properties but at the same time is reversible, non-yellowing and has a higher Tg. It produces weaker bonds, which in most cases is a positive quality and sets fast that could be restrictive in some complicated applications. A gluing technique, in which the smaller fragment is mounted on a sled, accelerates the process of reassembly and produces precise joins. Its reversibility allows disassembling pined joins even after long periods of time. There are many manufactures worldwide that produce this type of system and the author has not explored most of them in search of a product with longer working time. Nevertheless the PMMA systems described here are applicable in large variety of cases and could be a preferred alternative where reversibility, non-yellowing and high Tg are important.

Acknowledgements

The author would like to acknowledge the contribution of Veselin Vekov, structural engineer and the late Alexandar Savov, scientist, National Institute for the Monuments of Culture, Sofia, Bulgaria who first applied the PMMA system in the early 1970's. Tanks are also due to Eddy de Witte, IRPA and Dane Jones, Cal Poly, San Luis Obispo for valuable advice regarding the use of inhibitors.

References

- Barov, Z. "The Use of Methyl Methacrylate as an Adhesive in the Conservation of Two Objects from the W. R. Hearst Collection" in Preprints of the contributions to the Bologna Congress, Case Studies in the Conservation of Stone and Wall Paintings, Brommelle, N. and Smith, P. (eds.), IIC, London (1986) 112-115.
- W. H. W. Plastics. Cold Cure Denture material, MSDS, 2002
www.whwplastics.com/downloads/msds/Cold-Cure%20Combined.pdf.

CONSOLIDATION EFFECTS ON SANDSTONE TOUGHNESS

M. Drdáký^{1*}, M. Šperl² and I. Jandejsek³

Abstract

The paper presents a methodology for investigating fracture phenomena in sandstone treated for consolidation. It demonstrates the preparation of test specimens with a cyclic loading generated crack, monitoring of the test specimen preparation and verification by means of X-ray microCT and DIC techniques. Finally, the influence of various consolidation agents on the toughness of cracked specimens is demonstrated.

Keywords: cracks in stone, consolidation, toughness

1. Introduction

Cracks in stone monuments are a very common defect. In addition to naturally arising cracks due to geological and tectonic processes, cracks in many historical structures indicate the action of external forces accompanied by internal strain gradients. This is usually a repetitive process, and damage accumulation may occur in porous brittle or quasi-brittle materials. The authors (Drdáký, Šperl, Jandejsek 2016) performed a study of environmental fatigue effects on sandstone from Božanov (one of the typical medieval rock materials used in Charles Bridge in Prague, the Czech Republic) due to the accumulation of damage. An investigation was performed with the Young modulus and the Poisson number, using a verified methodology for testing stone in simple tension and in cycling simple tension/compression loading. They developed a methodology suitable for testing historical stone subjected to repeated tension strains. The results show that the first tension load-displacement can be approximated very satisfactorily by a power function, and the optical DIC method demonstrated once again its capacity and suitability for measuring complex deformation fields on porous surfaces and on naturally well-structured surfaces. Nevertheless, the methodology used required painstaking specimen preparation and highly-skilled staff and can be recommended only for special small-series tests.

Crack propagation and sandstone toughness has been experimentally investigated by several researchers in the past using test specimens of various shapes and dimensions provided with crack initiation notches. In papers by Le, Bažant and Bazant 2011, Le & Bažant 2011, Kirane and Bažant 2015, and Le, Manning and Labuz 2014, many basic references are presented. From these papers it follows that size effect plays an important role in fracture and must be considered in toughness research. In our case, in which comparative tests on the influence of various consolidants on crack propagation were carried out, the size effect was supposed not to influence the results substantially. However, Nara *et al.* 2012 demonstrated the influence of the moisture content and relative humidity

¹ M. Drdáký*, M. Šperl and I. Jandejsek
Academy of Sciences of the Czech Republic, Prague, Czech Republic
drdacky@itam.cas.cz

*corresponding author

on the fracture toughness of stones and therefore these parameters were carefully controlled in the present tests.

The aim of this experimental study was to investigate the effects of consolidation on cracked sandstone behaviour, particularly its toughness (Šperl *et al.* 2016). Experimental investigations on specimens with cracks have very rarely been published. One such study by Feng *et al.* 2015 was focused on experimental research into strength restoration of cracked sandstone. Only one consolidation agent was applied – a high polymer adhesive called MEYCO 364, with a very fast setting and hardening time. The approach was based on crushing cylindrical sandstone specimens, placing them carefully in a special cylindrical mould that was then injected with the adhesive polymer. Subsequently, the specimens were released from the mould and tested again after maturing. Naturally, such an approach was not suitable for the purposes of the present study.

2. Božanov Sandstone

Božanov Sandstone is one type of medieval stone used in the construction of the 14th-century Charles Bridge in Prague. Božanov stone is a greyish-beige gross quartz grain strong arkose sandstone without marked layering (Fig. 1). The material tested was extracted from the 11th arch of the Charles bridge parapet wall, which had to be replaced during recent repair because it has a rather deeply located detachment crack parallel to the surface, probably due to some previous surface treatment which locked moisture inside the stone. The material can be characterized as a quasi-brittle inelastic silicate composite.

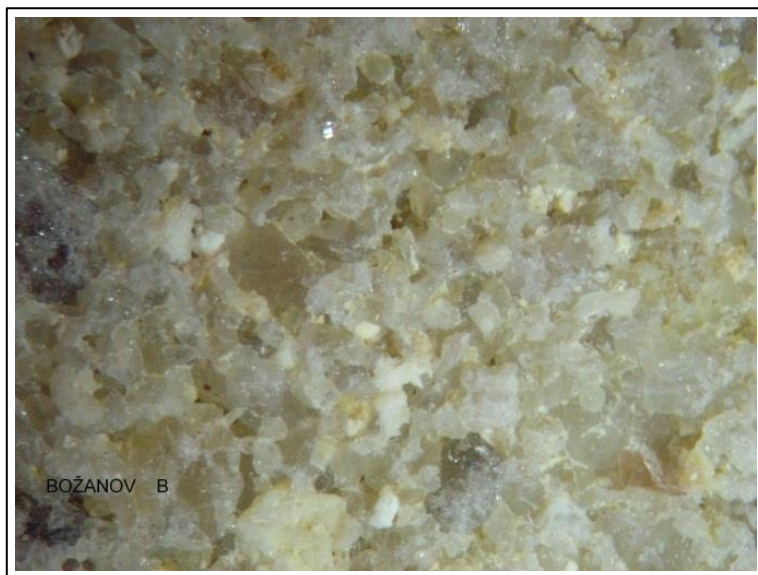


Fig 1: Composition of the Božanov sandstone.

3. Methodology

Test specimens with dimensions of $20 \times 20 \times 100 \text{ mm}^3$ were placed on one side in the centre with an initiation notch 1 mm thick and 2 mm deep. Then the specimens were cyclically loaded in three-point bending generated by a resonance pulsating Rumul Mikrotron frame (Fig. 2). The initiation notch was placed on the side in tension and the load pulsated in a mode with the asymmetry of the cycle being $R = 0.0385$ – i.e., with a nearly vanishing load cycle. The resonance loading frame started cycling with an initial force impulse and then the loaded specimen acted as an elastic member in the system. The cycling at a given force was controlled by a resonance frequency which was dependent on the stiffness of the test specimen (Vavřík *et al.* 2013). Then, a change in stiffness of the specimen was followed up during the loading, which signalled the crack initiation and propagation, and enabled control of the crack depth. To this end, a change in loading frequency was measured. In this way it was possible to prepare a series of test specimens with approximately the same damage in front of the initiation notch. However, a series of preliminary tests had to be carried out in order to identify a suitable level for the loading force. They included a static three-point bending test (3PB) and a series of fatigue tests on various low-force levels to determine the approximate fatigue behaviour of the test material.

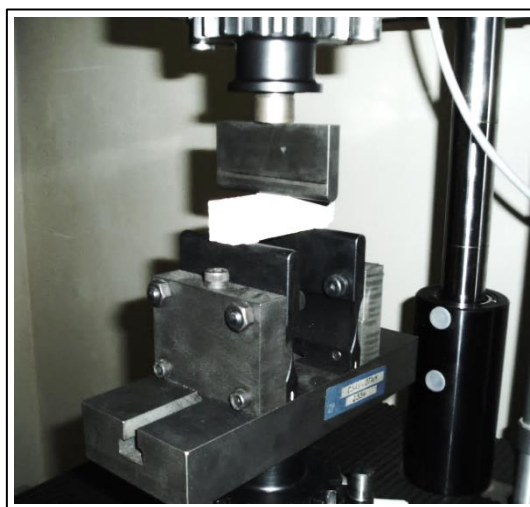


Fig. 2: Cyclic loading of the test specimen in an electromagnetic resonance frame.

Then, in order to ascertain the depth of the initiated cracks X-ray micro-tomography was applied. A special table-top loading device allowing simultaneous X-ray imaging of the test specimen during loading was employed. A specimen was loaded in a cylindrical chamber made of a high-strength composite which had a low attenuation for X-rays and allowed observation from all directions. Both simple 2D transmission images and CT acquisitions could be acquired in individual loading steps. The focal spot of the X-ray source was approximately $50 \mu\text{m}$ with this setting, which was sufficient with respect to the desired resolution. A scintillation flat panel detector of 2048×2048 pixels resolution and $200 \mu\text{m}$ single pixel size was used. The resulting imaging geometry allowed $\times 4$ magnification, which entailed the resolution of $50 \mu\text{m}$ at one pixel. The standard three-point bending test was performed with the specimen. The load was applied only until the moment when the

crack was observable by simple transmission radiography. In this position CT data (1200 projections per 360°) was acquired. The acquisition time of one projection was 2s. The images obtained were corrected with regard to beam hardening effect by a set of aluminium filters and subsequently a final CT reconstruction was carried out. A 3D visualization of the reconstruction obtained was performed in a VG studio.

Then, specimens with similar cracks were consolidated and the most typical agents were applied: elastified Steinfestiger 300 (cca 30% concentration of the active substance), Paraloid B72 (2% concentration), Funcosil 100 (10% concentration of the active substance); and after maturing they were tested in static standard three-point bending. The products were applied by immersing the specimens up to one half of the profile cross-section height in the agent bath for 4 hours, then wrapped in a plastic foil after removal from the bath, which protected the specimens from drying quickly.

4. Results and Discussion

Cycling the specimens in the high frequency resonance loading frame helped to understand fatigue behaviour of the Božanov sandstone. At a given force level (3PB arrangement under point load cycling from -10 N to -260 N) the majority of specimens exhibited fatigue life in a range between 90 000 and 140 000 cycles. However, there were specimens with one order lower or higher fatigue life due to the heterogeneity of the sandstone. To prepare the test specimens, a lower number of loading cycles was applied (between 32 000 and 40 000), and only specimens exhibiting behaviour similar to those of the above mentioned majority were accepted for further experiments. A typical record of the change of resonance frequency is presented in Fig. 3. Visible steps are the results of the regulation loop reaction which keeps the mean loading value within an interval of +/- 2 N.

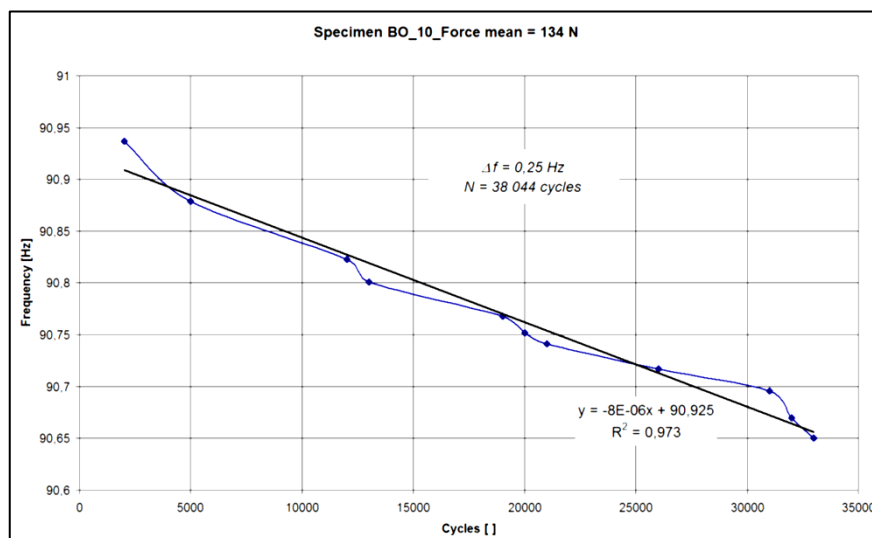


Fig. 3: Decrease of loading frequency during cycling of the specimen BO_10 (for 134N).

The character of the damage after cycling was determined by means of X-ray CT. It was not possible to identify the crack originating in the granular structure of the sandstone without applying a slight 3PB loading to the specimen and opening the crack. Thus, the specimen under investigation (BO_5 after 140,300 cycles) was loaded with 200 N and under such loading scanned with the X-ray CT. Then the DIC method was used to identify similar situations within the sections in the specimen depth. DIC proved to be a useful tool for crack propagation studies, e.g. Lin and Labuz 2013. A comparison of crack visualisations for loaded and unloaded specimens is shown in Fig. 4.

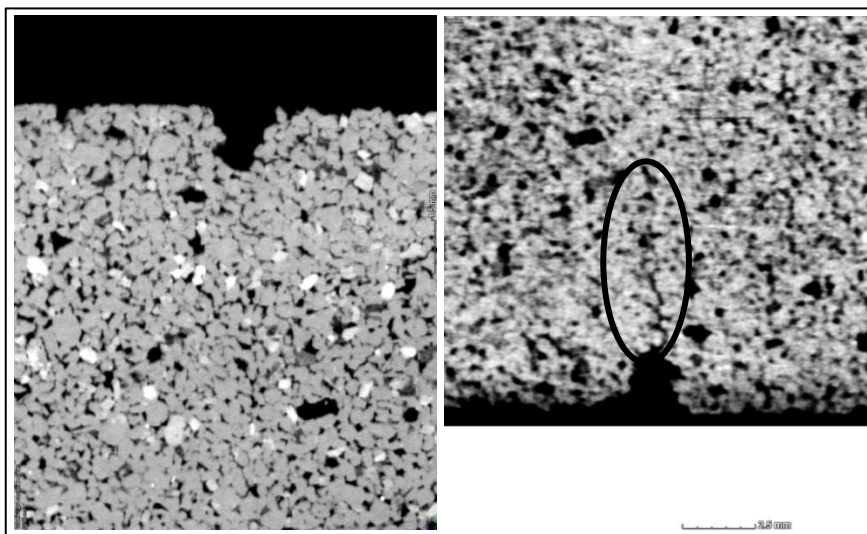


Fig. 4: X-ray pictures of unloaded (left) and loaded (right) sandstone specimen BO_5

Then, three types of specimens were tested with regard to three point bending - notched beams, notch beams with cracks generated by cycling and notched beams with cracks after consolidation. The test results are presented in Tab. 1. The results show the beneficial influence of consolidation on the cracked sandstone specimens. The reference specimen with the initiation notch attained an average bending strength of 5.05 MPa, the notched specimen with cycled crack one of 4.56 MPa and the consolidated specimens one of about 6 MPa. The broken halves of the test beams were used for comparative tests on full profile beams after prolongation by the prothesis method (Drdácký 2007). The results were influenced by cycling; however, it may be seen that consolidation eliminated the influence of crack degradation effects (Fig. 5).

For all specimens the absorbed energy needed to create the critical macrocrack was calculated. The specimen without a crack exhibited the maximum energy, as expected. The specimens with cracks exhibited lower energy, which was almost constant for all specimens. From these results and the load displacement diagrams it follows that the consolidated material becomes stronger but more brittle with a lower capacity of deformation absorption.

Tab. 1: Results of three point bending tests for Božanov sandstone.

Spec. No.	F_{max} [N]	Height [mm]	Width [mm]	Span [mm]	Number of cycles [-]	Bending strength [MPa]	Treatment
BO_N	433.26	20.82	20.66	60	0	5.26	None
BO_20	363	20.45	20.68	60	0	4.83	None
<i>Average bending strength of the notched specimens</i>						5.05	None
BO_9	393.15	20.74	21.6	60	32,248	4.56	None
<i>Bending strength of the notched beam with crack</i>						4.56	
BO_10	487.33	20.86	21.02	60	38,044	5.70	KSE 100
BO_11	509.78	21.02	20.69	60	35,000	6.09	KSE 100
BO_16	562.18	20.82	19.32	60	43,457	6.61	KSE 300
BO_19	515.49	20.94	19.18	60	42,236	6.10	Paraloid

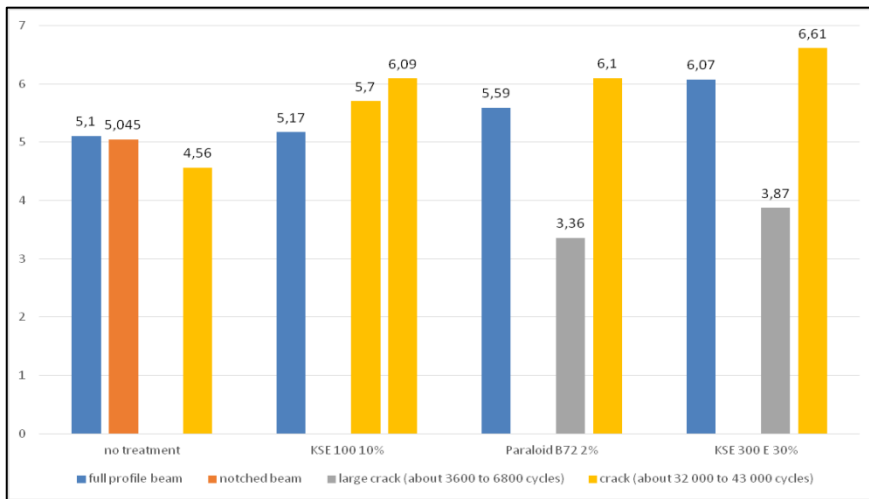


Fig. 5: Results of 3PB tests on four types of test specimens.

Load displacement diagrams together with changes in the deformability (apparent modulus of elasticity) were recorded; one example is presented in Fig. 6. The modulus of elasticity gradually degraded during the course of loading; however, in the case of the consolidated sandstone, the decrease started to be very slight rather early and the modulus was almost constant up to the failure.

The acquired ultimate loads were used to calculate K_{IC} toughness (Gross 1965), which attained the value of 0.331 for the notched beam, 0.349 for the notched beam with the crack and from 0.449 to 0.561 for the consolidated cracked beam in $\text{MPam}^{0.5}$. The toughness values are approximate estimates based on an engineering approach to the crack depth assessment from the above mentioned X-ray CT scans and the DIC reconstructions.

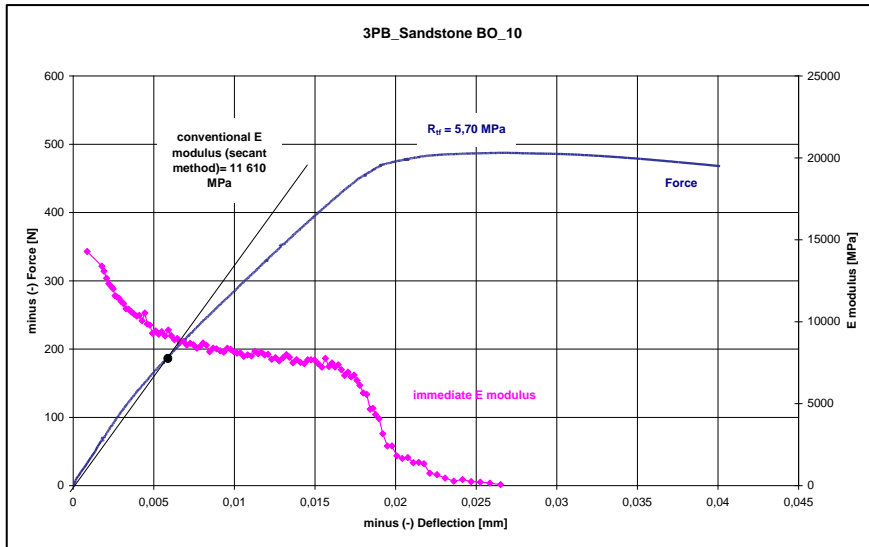


Fig. 6: Summary diagram for 3PB test of the specimen BO_10.

5. Conclusions

The described methodology involving the use of the resonance loading frame to generate cycled cracks in stone was demonstrated. It enables the successful creation of well-defined and controlled crack damage in stone.

The computer X-ray microtomography is a useful tool for visualizing and measuring generated cracks in combination with the digital image correlation technique. The crack is usually close and to identify its depth the specimen must be loaded slightly in order to open the crack and make it more visible.

The tests with consolidated specimens proved the positive effects of consolidation with regard to strength and toughness. All notched and cracked specimens after consolidation with ethylsilicates KSE 100, KSE 300 and Paraloid B72 attained values above full profile strength.

The full profile specimen exhibited the greatest energy absorption necessary to create a critical macrocrack leading to overall loss of stability of the specimen. The notched and cracked specimens after consolidation with ethylsilicates needed less energy, which in the case of the increased strength of the consolidated sandstone, shows that the material becomes stiffer and more brittle with a higher modulus of elasticity and a lower capacity to absorb deformation energy. Consolidation with Paraloid B72, on the other hand, required much more energy (3.5 times more than with ethylsilicates).

The toughness of untreated notched and cracked specimens reached almost same values, which means that with such heterogeneous material we cannot expect stress concentration factors similar to those of metals. Consolidation with the abovementioned agents increases the toughness of Božanov quartz sandstone substantially (up to 70%).

Acknowledgements

Support from the GAČR P105/12/G059 & the SADeCET NPU I project is acknowledged.

References

- Drdácký, M., Šperl, M., Jandejsek, I. (2016) Pilot experiments on cumulative tensile damage to stone monuments. (to be published by Cambridge Scholars Publishing), 8 p.
- Feng, X., Zhang, N., Zheng, X., Pan, D. (2015) Strength restoration of cracked sandstone and coal under a uniaxial compression test and correlated damage source location based on acoustic emission, *PLoS ONE* 10 (12): e0145757. doi: 10.1371/journal.pone.0145757, 20 p.
- Gross - NASA TN D-3092, 1965 Stress-Intensity Factors for 3PB Specimens by Boundary Collocation.
- Kirane, K., Bažant, Z.P. (2015) Size effect in Paris law for quasibrittle materials analyzed by the microplane constitutive model M7, *Mechanic Research Communications*, 68, 60–64.
- Le, J.-L., Bažant, Z.P., Bazant, M.Z. (2011) Unified nano-mechanics based probabilistic theory of quasibrittle and brittle structures: I. Strength, static crack growth, lifetime and scaling, *J. of the Mech. and Phys. of Solids*, 59, 1291–1321.
- Le, J.-L., Bažant, Z.P. (2011) Unified nano-mechanics based probabilistic theory of quasibrittle and brittle structures: II. Fatigue crack growth, lifetime and scaling, *J. of the Mech. and Phys. of Solids*, 59, 1322–1337.
- Le, J.-L., Manning, J., Labuz, J.F. (2014) Scaling of fatigue crack growth in rock, *Int. J. of Rock Mechanics & Mining Sci.*, 72, 71–79.
- Lin, Q., Labuz, J.F.: (2013) Fracture of sandstone characteristics by digital image correlation, *Int. J. of Rock Mechanics & Mining Sci.*, 60, 235–245.
- Nara, Y., Morimoto, K., Hiroyoshi, N., Yoneda, T., Kaneko, K., Benson, Ph.M. (2012) Influence of relative humidity on fracture toughness of rock: Implications for subcritical crack growth, *Int. J. of Solids and Structures*, 49, 2471–2481.
- Šperl, M., Drdácký, M., Jandejsek, I. (2016) Experimental study of consolidation effects on sandstone toughness, *Proc. of the 17th International Conference on Experimental Mechanics (ICEM 17) – E.E.Gdoutos (ed.)*, Rhodos, July 3-7, 2016, 2p.
- Vavřík, D., Jandejsek, I., Fíla, T., Veselý, V. (2013) Radiographic observation and semi-analytical reconstruction of fracture process zone silicate composite specimen, *Acta Technica CSAV*. 2013, Vol. 58, No. 3, pp. 315–326, 2013.

IS THE SHELTER AT HAGAR QIM IN MALTA EFFECTIVE AT PROTECTING THE LIMESTONE REMAINS?

C. Cabello-Briones^{1*} and H.A. Viles¹

Abstract

Shelters are structures built over archaeological sites to protect the remains from decay. They may prevent direct sunlight and rainfall reaching the remains, but they may also enhance decay by modifying microclimatic conditions. Lightweight, open shelters (without lateral cladding) are a popular preventive conservation strategy for sites in the Mediterranean basin but there have been few scientific assessments of the impacts of shelters on limestone decay. Hagar Qim in Malta is a UNESCO World Heritage Site containing the remains of a megalithic temple constructed of local limestone. The effectiveness of the shelter at Hagar Qim, built in 2009 with a fiberglass and PTFE membrane, was evaluated during a 1 year campaign using two methods: (a) monitoring microclimatic conditions outside and inside the shelter (centre and periphery) and (b) monitoring soiling and decay of small limestone blocks located outside and inside the shelter (centre only). Microclimatic conditions were monitored using i-button® loggers to record temperature and *RH* over the whole year, with shorter term monitoring of dust deposited on horizontal surfaces. Soiling and decay of *Globigerina* and *Coralline* limestone blocks (9×3×3 cm) over the year were quantified by comparing a number of stone properties before and after exposure. Results are presented here for weight, surface hardness and surface colour. This research demonstrated that, in general, the shelter at Hagar Qim is effective at reducing limestone decay and the site would be exposed to more damaging conditions if it was not sheltered. However, the shelter has also been found to enhance some decay mechanisms such as dust deposition under the central part of the shelter and NaCl crystallisation events on the periphery.

Keywords: shelters, archaeological sites, limestone decay, monitoring, Hagar Qim

1. Introduction

The prehistoric site of Hagar Qim consists of megalithic buildings built between 3600 and 3200 BC. It is situated at the top of a hill, less than 1 km away from the sea, on the south western coast of Malta (location: lat. N 35.8277, long. E 14.4417). The site was inscribed on the UNESCO World Heritage list in 1992 because of its significance for human history. The temple was built exclusively with *Globigerina* limestone, probably quarried near the site, which is a relatively soft bioclastic limestone still widely used for construction in Malta. *Globigerina* limestone is prone to powdering and alveolisation, mainly due to salt weathering (Cassar, 2007). These patterns are defined respectively as granular disintegration and formation of cavities on the stone surface (ICOMOS International

¹ C. Cabello-Briones* and H.A. Viles

Oxford University Centre for the Environment, University of Oxford, United Kingdom
cristina.cabello-briones@ouce.ox.ac.uk

*corresponding author

Scientific Committee for Stone ISCS, 2008). An open shelter (without lateral cladding) was installed over the remains in 2008 to reduce environmental risks (Fig. 1).



Fig. 1: Shelter over the megalithic temples at Hagar Qim, Malta.

Before sheltering Hagar Qim, Istituto di Scienze dell'Atmosfera e del Clima (CNR-ISAC) carried out a study on the microclimate and stones of the site, which determined that the main decay mechanism at Hagar Qim was salt weathering from marine aerosols (unpublished report for Heritage Malta, 2006). High solar radiation, wind and *RH* fluctuations were thought to enhance salt dissolution and recrystallization. In addition, high diurnal temperature ranges and solar radiation were hypothesized to produce mechanical stresses on the ruins. An open shelter made of a fiberglass and PTFE membrane was thought to be the best conservation solution until further research could be undertaken (Stroud, 2010). Membrane structures are considered lightweight as they require minimal supporting elements (Zanelli *et al.*, 2013). Light-weight, open shelters have increasingly been proposed as medium-term preventive conservation methods due to, for example, their high flexibility and modularity. However, as yet there has been little specific research on their effects on archaeological remains (Demas, 2013).

2. Materials and methods

2.1. Monitoring of microclimatic conditions and dust deposition

Shelters should provide protection for the stone remains by reducing the frequency and/or range of microclimatic fluctuations which cause stone decay. The impact of the open shelter at Hagar Qim on microclimatic conditions was evaluated by monitoring temperature, *RH* and dust deposition inside (centre and periphery) and outside the shelter from 29th July 2013 to 22nd July 2014. The monitoring of the peripheral location started later than the others, on the 18th October 2013, for logistical reasons. The most central location possible under the shelter was selected as a fully protected position and was compared with a fully exposed (outside) and a partly exposed location (periphery) (Fig. 2). The chosen peripheral location is located towards the edge of the site (SW), where possible inadequacies in the coverage of the shelter were detected after a rapid visual assessment.

Low-cost and easy to hide temperature and *RH* loggers (i-button® hygrochron dataloggers, accuracy = $\pm 0.5\%$ *RH* and $\pm 0.5^\circ\text{C}$) were synchronised to record at all three positions every 60 minutes. From the data collected, the number of times a day *RH* crossed the 75% threshold was used as proxy for NaCl crystallisation events. The amount of dust deposited on horizontal surfaces inside and outside the shelter was studied using self-adhesive,

transparent vinyl film patches (10×10 cm) during one week in October 2013 and for three months between October 2013 and January 2014. The adhesive part of the patch was left exposed and a small area (10×3.5 cm), which remained covered, was used as a control. After exposure, they were analysed by imaging processing techniques. Pictures of the samples were taken with a camera (DFK 51BU02.H, Imaging Sources, sensor Sony CCD, sensibility 0.15 lx) set with a fixed exposure. An integrating sphere light source, which provides spatially uniform luminance, was placed on the other side of the film. Mean opacity values were calculated by studying the amount of light that passed through the samples (transmittance) in comparison to the control area. Mean values refer to the amount of pixels in the processed images (1280×960).



Fig. 2: Monitoring positions – 1: centre, 2: periphery and 3: outside of the shelter.

2.2. Monitoring of decay with limestone blocks

The degree and nature of decay and soiling were determined by measuring dry weight, surface hardness and surface colour in Globigerina and Coralline limestone blocks before and after exposure for one year. Four replicates (9×3×3 cm) of each stone type were exposed from 17th July 2013 to 22th July 2014 inside (centre) and outside the shelter. Because of potential visibility of blocks to tourists it was not possible to place a set of replicates in the peripheral location. In addition, three blocks per stone type were left in the laboratory and used as controls. The tests to evaluate change in stone properties were carried out under the same conditions before and after exposing the blocks. Comparison of changes in stone properties between locations permitted an assessment of the different rates of deterioration and soiling outside vs. inside the shelter. The reason for using small blocks was to obtain representative information about decay within a short exposure period without invasive sampling of the remains themselves. The stone types used in this study present different vulnerabilities to decay (Tab. 1). Globigerina is very soft and porous and a greater degree of weathering was expected. Both are commonly used in Maltese cultural heritage.

Tab. 1: Physical properties of the stone samples used.

Standard test	Property	Globigerina	Coralline
BS EN 3755:2008	Water absorption at atmospheric pressure (A_b)	14.75%	3.36%
BS EN 1936:2006	Open porosity (P_o)	31.18%	11.01%
BS EN 1936:2006	Apparent density (ρ_b)	1789.72 kg/m ³	2356.52 kg/m ³

Weight was quantified using a balance (Sartorius AG Göttingen, ± 0.01 g accuracy) and weight change expressed as a percentage of initial dry weight. This method has been extensively used to calculate the amount and rate of stone weathering, for example in relation to salt accumulation and erosion (Moses, 2000). Surface hardness was assessed using an Equotip 3 (Proceq), an electronic rebound hardness testing device often used to study stone deterioration (Moses *et al.*, 2014). After a pilot study based on the study of Viles *et al.*, (2011), 18 single impacts for Globigerina and 36 for Coralline were determined to be adequate sample sizes. The median of hardness readings from each stone block was used to summarise the data. Colour changes were measured with a spectrophotometer (CM-700d, Konica Minolta) and the results expressed using the International Commission on Illumination (CIE) L^*a^*b system. Ten measurements (SCE) per stone block were taken on different points of the top horizontal surface and the mean used to summarise the data set. Two-way ANOVA tests were undertaken to determine if there were statistically significant differences in stone properties between positions and stone type. These analyses were complemented with post-hoc all multiple comparison tests (Holm-Sidak method).

3. Results

3.1. Monitoring of microclimatic conditions

3.1.1. Temperature

The temperature inside the shelter (centre and periphery) followed the temperature outside and exhibited similar daily and seasonal fluctuations. However, there were some significant differences between locations within the site. Non-parametric Mann-Whitney-Wilcoxon tests on daily mean temperatures showed that in summer, the outside was warmer than the centre of the shelter ($U=561$, $P=2.328e^{-10}$) and the centre was significantly warmer than the periphery ($U=406$, $P=3.986e^{-06}$). In winter, the central part of the shelter was warmer than outside ($U=454$, $P=2.398e^{-10}$) but the temperatures on the periphery were higher than in the centre of the shelter ($U=455.5$, $P=6.787e^{-10}$). Therefore, the outside had the most extreme environment with higher temperatures in summer and lower in winter. In spring and summer, the centre was warmer than the periphery due to higher temperatures at night. In addition, the periphery was slightly warmer than the centre in winter. This result can be related to a problem with the shelter covering area, which allows direct solar radiation on the ruins towards the edge. Differences between maximum and minimum temperatures per day were calculated to examine temperature fluctuations (Fig. 3). The daily temperature range was higher outside over the whole year, especially in spring and summer. The daily temperature range in the periphery of the shelter was higher than in the centre during autumn and winter and closer to the outside values.

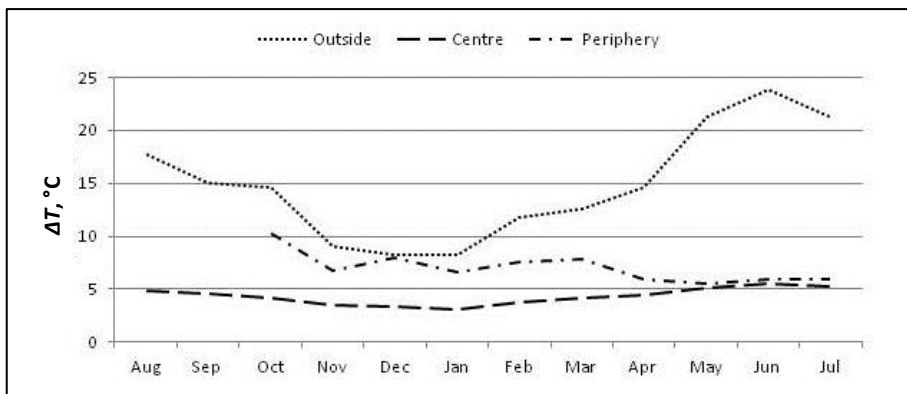


Fig. 3: Monthly means of diurnal temperature range outside, in the centre and on the periphery of the shelter.

A multilevel linear model with day as random effect for the diurnal temperature ranges was fitted in order to find out if the differences depended upon location. The statistical analysis indicates significant differences in diurnal temperature ranges between outside and the periphery of the shelter ($t = -25.497$, $DF = 1661$, $P < 0.001$) and between the periphery and centre of the shelter ($t = -14.638$, $DF = 1661$, $P < 0.001$). As expected, the central part of the shelter had a more stable microclimate in terms of temperature than outside and on the periphery. The more variable microclimate in autumn and winter in the peripheral parts of the shelter illustrates the limitations to the sheltering effect.

3.1.2. NaCl crystallisation events

The daily number of salt crystallisation events was relatively constant in all positions during the majority of the year, with a slight decrease in winter (when RH is often above 75%). The number of times the NaCl threshold was crossed in a year was fitted as the response in a Poisson Generalised Linear Model (GLM) with 'Position' as explanatory variable and with 'Day' as the second level. The results showed significant differences in the number of events between outside and the centre ($t = 2.695$, $DF = 1590$, $P = 0.007$) and between outside and the periphery of the shelter ($t = 5.305$, $DF = 1590$, $P < 0.001$). There were more NaCl crystallisation events in the central part of the shelter (daily mean = 2.10) than outside (daily mean = 1.83), and more at the periphery (daily mean = 2.45) than in the centre ($t = 2.837$, $DF = 1590$, $P = 0.004$). This unexpected finding illustrates the more variable microclimate (in terms of RH fluctuations crossing the 75% threshold) found in the peripheral parts of the shelter.

3.1.3. Dust deposition

Malta is characterised by high daily wind speeds. The shelter reduces wind speeds inside the site but there is turbulence probably due to the effect of the monument itself (Farrugia and Schembri, 2008). Opacity data collected from the vinyl film patches showed that there was more dust deposition inside the shelter than outside. The sheltered samples showed less light transmittance values (i.e. higher opacity) than the ones located outside the shelter for the same amount of time (Tab. 2). After three months, the sample located inside the shelter showed 381% less light transmittance than the control area. The amount of dust deposition

is probably an underestimate as the surface of the film became fully covered before the end of the experiment and could not collect more.

Tab. 2: Mean opacity (%) values of unsheltered and sheltered samples.

Unsheltered		Sheltered	
1 week	3 months	1 week	3 months
-0.80	54.42	10.34	381.68

3.2. Monitoring of decay with limestone blocks

3.2.1. Dry weight

All Globigerina blocks lost weight, especially those located under the shelter. In comparison, Coralline samples located outside gained in weight whereas the ones inside lost weight (Fig. 4). Globigerina samples lost significantly more weight inside than outside the shelter ($t=3.225$, $P=0.005$) and those inside the shelter lost more weight than Coralline blocks in the same position ($t=3.708$, $P=0.002$). The difference between inside and outside Coralline blocks is also significant ($t=5.639$, $P<0.001$).

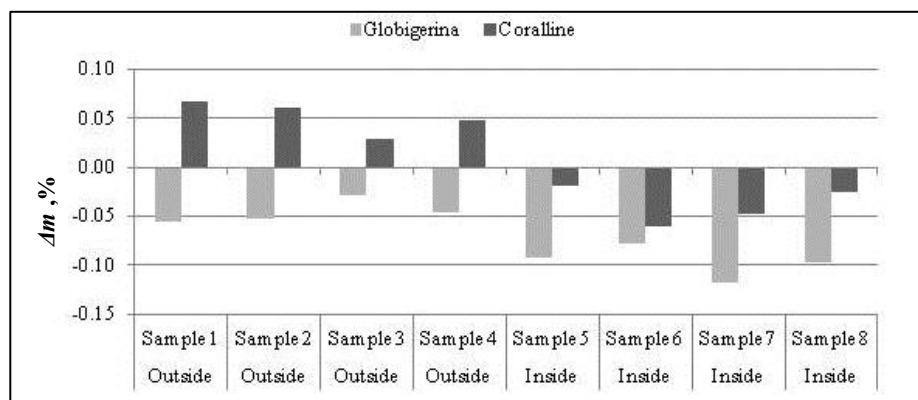


Fig. 4: Weight change as percentage of initial dry weight of the Globigerina and Coralline replicates placed outside and inside the shelter after 12 months.

3.2.2. Surface hardness

All the samples increased in hardness, especially Coralline blocks outside the shelter. However, the blocks did not change significantly in hardness over the one year period. As a result, there were no significant differences in behaviour between those located inside and those outside.

3.2.3. Surface colour

Most of the stone blocks showed an overall colour difference over 3.8 dE*ab, which indicates that the change is distinctively perceptible to the naked eye (Bieske and Vandahl, 2008). Globigerina samples located outside the shelter changed significantly more in colour

than the blocks placed inside ($t=7.641$, $P<0.001$). In addition, Globigerina blocks outside changed more in colour than the Coralline ones in the same position ($t=9.483$, $P<0.001$). The difference in colour change in Coralline blocks between inside and outside is not significant ($t=0.125$, $P=0.903$). In addition, CIELAB differences in dL^* (lightness/darkness) and db^* (yellow/blue) were examined to determine the characteristics of the colour changes. Globigerina and Coralline blocks became yellower and darker in both positions, with the Globigerina blocks outside showing the greatest change (Tab. 3).

Tab. 3: Mean colour difference in Globigerina and Coralline blocks after 12 months.

	Position	dE^*_{ab} (D65)	dL^* (D65)	db^* (D65)
Globigerina	Outside	12.88	-8.22	8.70
	Centre	6.59	-4.55	4.22
Coralline	Outside	5.08	-4.49	0.40
	Centre	5.18	-5.03	0.17

4. Discussion and Conclusions

Temperatures outside the shelter fluctuated more than in the centre and on the periphery showing higher maximum temperatures in summer and lower in winter. The maximum differences between inside and outside were registered during the hottest months. The shelter was able to reduce daily temperature differences and keep the temperatures in the centre of the shelter lower and stable. The temperature on the periphery varied more than in the centre, and a fault in the shelter design allowed direct solar radiation to significantly increase temperatures at this point during winter. As temperature is not as high in this season than in summer the risk of thermal stress is reduced. However, the probability of having more NaCl crystallisation events on the periphery than outside the shelter is higher due to daily *RH* fluctuations. On the other hand, there was more dust deposition inside than outside the shelter. Dust from the arid surroundings is likely to access the area under the shelter driven by wind and accumulate when wind reduces velocity and increases turbulence under the shelter. However, the risk of salt weathering inside the shelter is lower than outside because the microclimate is more stable.

Globigerina and Coralline limestone samples inside and outside the shelter turned darker and yellower after a year of exposure. Although colour change could be due to natural weathering, the conditions outside the shelter might have enhanced it as the chromatic alteration was observed mainly on Globigerina blocks located outside.

Samples inside the shelter lost more weight than those outside. The great temperature ranges outside could have had a low effect on weathering. However, it is more likely to assume that there was an increase in weight due to, for example, accumulation of salts, and the combined effect with temperature fluctuations resulting in a final slight change of weight. In addition, Coralline samples outside the shelter gained in weight and all of the Coralline samples but mainly those outside the shelter increased in hardness. This suggests that great temperature ranges outside the shelter in combination with the effect of salts are the main cause of decay. This study has demonstrated that the shelter reduced temperature

fluctuations, minimizing the risk of physical weathering. Therefore, the shelter at Hagar Qim is effective at reducing limestone decay and the site would be exposed to more damaging conditions if it was not sheltered. This research has also proven that small stone samples provide an effective, rapid and non-invasive method to monitor deterioration at sheltered archaeological sites.

Acknowledgments

We thank Heritage Malta, especially Dr. Katya Stroud and Mario Galea, for their help and support. We also acknowledge Dr. Daniel Lunn and Dr. Javier Muñoz for sharing their knowledge. This research was funded by EPSRC and La Caixa Foundation.

References

- Bieske, K. and Vandahl, C., 2008, A Study about Colour-Difference Thresholds, in proceedings of Lux et Color Vespremiensis, Veszprem, Virtual Environments and Imaging Technology Laboratory of the Faculty of Technical Informatics.
- Cassar, J. 2007. Malta: buildings, materials and deterioration, STONE. Newsletter on stone decay, 2, 3-4.
- Demas, M., 2013, Protective Shelters for Archaeological Sites, in *Mosaics In Situ. An Overview of Literature on Conservation of Mosaics In Situ*, Roby, T. & Demas, M. (eds.), Los Angeles: The Getty Conservation Institute (http://hdl.handle.net/10020/gci_pubs/lit_review, accessed 24th November 2015).
- Farrugia, S. and Schembri, J. A., 2008, Wind funnelling underneath the Hagar Qim protective shelter. *Malta Archaeological Review*, 9, 51-59.
- ICOMOS International Scientific Committee for Stone, 2008, ICOMOS-ISCS: Illustrated glossary on stone deterioration patterns = Glossaire illustré sur les formes d'altération de la pierre, Paris: ICOMOS, ISBN: 978-2-918086-00-0.
- Moses, C., 2000, Field rock block exposure trials. *Zeitschrift für Geomorphologie Supplementband*, 120, 33-50.
- Moses, C., Robinson, D. and Barlow, J., 2014, Methods for measuring rock surface weathering and erosion: A critical review. *Earth-Science Reviews*, 135, 141–161.
- Stroud, K., 2010, Hagar Qim & Mnjdra Prehistoric Temples (Qrendi), in *Malta Insight Heritage Guides*, Heritage Malta, Midsea Books, ISBN: 978-99932-7-317-2.
- Viles, H., Goudie, A., Grab, S. and Lalley, J., 2011, The use of the Schmidt Hammer and Equotip for rock hardness assessment in geomorphology and heritage science: a comparative analysis, *Earth Surface processes and Landforms*, 36, 320–333.
- Zanelli, A., Rosina, E., Beccarelli, P., Maffei, R. and Carra, G., 2013, Innovative solutions for ultra-lightweight textile shelters covering archaeological sites, in *Structures and Architecture: New concepts, applications and challenges*, Cruz, P. (ed.), CRC Press, ISBN: 978-0-415-66195-9.

ASSESSMENT OF THE CLEANING EFFICIENCY OF A SELF-CLEANING COATING ON TWO STONES UNDER NATURAL AGEING

P.M. Carmona-Quiroga^{1*}, S. Kang² and H.A. Viles¹

Abstract

Implementation of preventive treatments to protect built heritage from soiling is of particular value given the high cost of cleaning practices, which sometimes may put in danger the already weathered materials and the limited financial resources available for conservation. In different fields, including construction, TiO₂ dispersions have been gaining ground as a self-cleaning treatment because of their photocatalytic activity. When irradiated with UV light, crystalline nanoparticles are able to photo-oxidise and decompose bacteria, organic and inorganic compounds. Moreover, they prevent, due to a superhydrophilic effect, contact between dirt and the material's surface. However, in the field of architectural heritage research on the application of these coatings to stones is still limited. The present study explores the efficiency and durability of a self-cleaning coating on Portland limestone (Dorset, England) and Locharbriggs sandstone (Dumfries, Scotland) over time under natural weathering conditions in the South of England (Wytham Woods, Oxford). One or two coats of the treatment were applied on the surface of 8.5×6.5×1 cm³ slabs of these two materials by spraying. Colour, gloss, and self-cleaning efficiency of the surface of the slabs (photodegradation of methylene blue stain) were analysed before and after the treatment was applied to assess how compatible the treatment is with the stones. To evaluate how permanent is the photocatalytic activity under a rainy regime, the photodegradation test was also performed on coated stones naturally aged for 4 and 6 months in the field site.

Keywords: self-cleaning coating, TiO₂, ageing, natural weathering, photocatalytic activity

1. Introduction

Soiling of surfaces through air pollution (SO₂, NO_x, O₃, HNO₃, particulate matter and acid rainfall) can be very severe for urban cultural heritage objects. The corrosion products not only accelerate erosion rates of building materials and cause aesthetic damage (Varotsos *et al.*, 2009; Viles *et al.*, 2002) but also cleaning procedures with either water, abrasive or chemical methods or combined procedures can themselves alter the roughness and porosity of already weathered surfaces (Vazquez-Calvo *et al.*, 2012) making them more susceptible to the penetration of future dirt (Doubal 2014). In fact, cleaning of stone is considered one of the most critical processes in monument restoration (Doubal 2014).

¹ P.M. Carmona-Quiroga* and H.A. Viles

School of Geography and the Environment, University of Oxford, United Kingdom
paula.carmona-quiroga@ouce.ox.ac.uk

² S. Kang

Department of Cultural Heritage Conservation Sciences, Kongju National University, South Korea

*corresponding author

The conviction that prevention is an effective option to the soiling problem is gaining ground. In fact, since the early 1990s, self-cleaning (anti-soiling) coatings have been used on some building materials such as tiles, paving gloss, cement mortar, glass, PVC fabric, etc. (Chen and Poon 2009). However, on stones (of historic and contemporary building and monuments) their uses are quite limited in spite of their potential benefits (Munafò *et al.*, 2015).

Self-cleaning effect is obtained by two photochemical phenomena of TiO₂ nanoparticles under UV irradiation: a) the photocatalytic one that promotes the decomposition of air pollutants and bacteria that darken the surface of building materials via redox reaction and b) the super-hydrophilic one that flattens water droplets on the surface of titania film preventing the adhesion of dirt.

Up to date research on the value of these coatings for protection of stone cultural heritage objects has been principally based on studying their compatibility (physical properties of the substrates such as colour, permeability, superficial morphology and water absorption), and evaluating their efficiency in de-polluting, self-cleaning and decomposing bacteria (Munafò *et al.*, 2015; Licciulli *et al.*, 2011; Pinho and Mosquera 2011; Quagliarini *et al.*, 2012). However, their durability has been much less explored (Munafò *et al.*, 2015) and such studies have been carried out under accelerated (lab) weathering conditions, with salt crystallisation (Bergamonti *et al.*, 2015; Pinho *et al.*, 2013), UV-A light irradiation (La Russa *et al.*, 2012), or combined procedures (UV-A irradiation and simulated rain, Munafò *et al.*, 2014). Of all the weathering agents, UV exposure is considered one of the most important (Munafò *et al.*, 2014), whereas the effect of rain is more uncertain since it could improve the performance of titania instead of increasing its weathering (washing) due to regenerative effect of water on TiO₂. In any case, the photocatalytic efficiency of the coatings is related to the type and duration of the weathering conditions and the interaction between coatings and substrates (Munafò *et al.*, 2014).

The aim of this study is to extend current knowledge of the performance of self-cleaning coatings on natural stones by exploring the durability of one of these products using a long-term exposure trial under natural weathering conditions. Samples of Portland limestone (Dorset, England) and Locharbriggs sandstone (Dumfries, Southern Scotland) have been left outdoors for 4 and 6 months at a test site in the South of England (Wytham Woods, Oxford) to test the evolution of the photocatalytic efficiency of a TiO₂ coating.

2. Materials and methods

Two stone types widely used in the built heritage of UK were selected to study the durability of a self-cleaning coating under outdoor conditions. Locharbriggs is a Permian red sandstone of fine to medium grain-size and distinctive aeolian cross lamination (Pandey *et al.*, 2014) mainly composed of quartz, with some feldspars and clays and very few little rock fragments as shown in the polarized microscope images of Fig. 1a taken with a DP30 digital camera fitted to a Meiji ML9000 microscope. Portland limestone (Whitbed) is a Jurassic white oolitic limestone, with subspheric and subelongated oolites from 0.1 to 0.5 mm in diameter, some of them with a quartz nucleus, low proportion of micritic matrix and big and scattered fossil fragments (Fig. 1b).

The two stone types were characterised with FTIR. KBr pellets were analysed on a Nicolet 6700 infrared spectrophotometer with the following settings: range, 4000-400 cm⁻¹; scans,

10; spectral resolution, 4 cm⁻¹. The FTIR spectrum of sandstone only exhibited the bands characteristic of quartz (1169-467 cm⁻¹) whereas the limestone spectrum contained vibration bands from the CO₃²⁻ in calcite (1433, 874 and 714 cm⁻¹), along with very low intensity bands attributable to the vibrations generated by Si-O bonds (1165-1003 cm⁻¹) (Fig. 1). In addition, the water-accessible porosity of the samples was measured to EN 1936:2006 standard. Mean values of open porosity were slightly higher for limestone (12 vol% vs. 10 vol% of the sandstone).

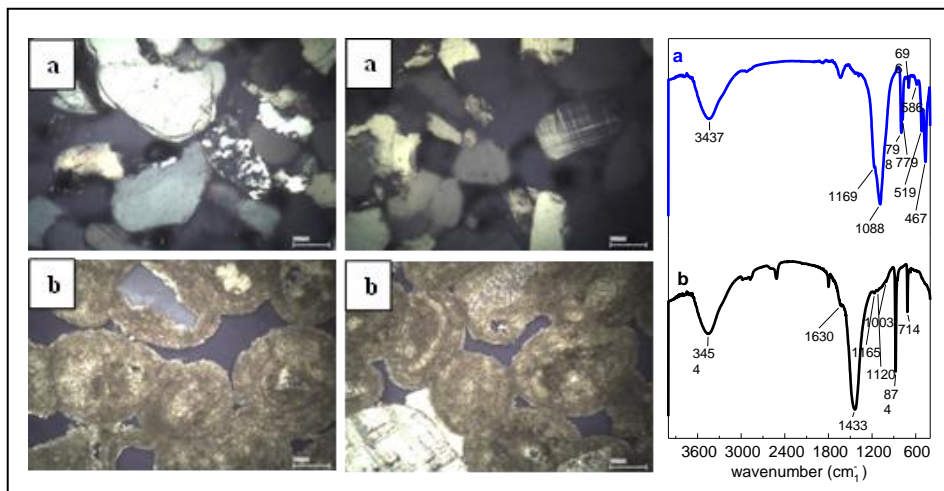


Fig. 1: Polarisating optical microscope images and FTIR spectra of a) Locharbriggs sandstone and b) Portland limestone - Whitbed (scale bar: 100 µm).

To apply the self-cleaning coating a commercial aqueous dispersion of TiO₂ (anatase) nanoparticles (10-40 nm) was sprayed at room temperature onto one face of stone slabs of 8.5 cm×6.5 cm×1 cm. One or two coats were applied on consecutive days (in triplicate) and the product uptake (dry weight) was measured.

Before and after applying the self-cleaning product, colour coordinates of the stones were recorded (5 measurements per slab) with a Minolta cm-700d spectrophotometer using the L* a* b* colour standard (CIE 1976). L* values measure lightness; a* measures the red (+)/green(-)hue and b* denotes the yellow (+)/blue (-) hue. The chromatic changes in the samples after coating were also expressed in terms of total colour variation $\Delta E^* (\Delta E^* = (\Delta L^{*2} + \Delta a^{*2} + \Delta b^{*2})^{1/2}$, CIE 1976).

A TQC glossmeter was used to determine changes in gloss at a reflection angle of 85° (Garcia and Malaga 2012); 3 measurements per slab. The peak-to-valley height of the surfaces was measured with a PosiTector SPG surface profile gauge also before and after coating application (20 measurements per slab).

Coated specimens were naturally exposed in Wytham Woods (5 miles away from central Oxford in a non-polluted area) on a rack facing south for 4 and 6 months. Climatic conditions over the period were taken from the nearby Radcliffe Meteorological Station of the University of Oxford. After the end of each exposure period the cleaning efficiency of the coating was assessed though the methylene blue test adapted from the literature (UNI

11259:2008; Graziani *et al.*, 2014) in which rhodamine B stain (artificial dirt) was replaced by methylene blue because the former produces no contrast on the red surface of the sandstone. 24 h after applying the dye on the TiO₂-coated and uncoated surfaces (2 ml on the sandstone slabs and 3 ml on limestone of a 0.1 wt% aqueous solution), the specimens were irradiated with a 20 W UV-A ($\lambda = 365$ nm) black light for up 190 hours. Coating distribution before and after ageing was examined with a JEOL JSM -5910 scanning electron microscope (SEM) equipped with a 20-kV Oxford INCA energy-dispersive X-Ray spectrometer (EDS).

3. Results and discussion

3.1. Physical characterization of the coated stones

The physical properties of the surface of the stones before and after being coated with one or two layers of the self-cleaning product are given in Tab. 1. The average roughness of the limestone is lower than the sandstone in spite of having limestone voids on the surface, this would condition the differences in the (already low) product consumption between the two stones, with sandstone being the substrate that on an average absorbed more in spite of being a less porous material (10 vol% vs 12% of the limestone).

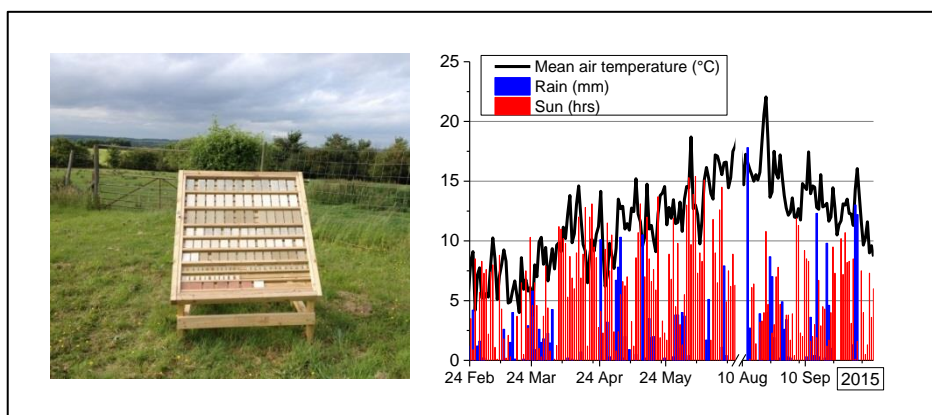


Fig. 2: Rack for outdoor exposure of the samples and climatic conditions for the exposure period.

One coat of the product did not change the surface colour of the specimens, however two coats on the red sandstone slightly whitened the surface (L^* increased) enough to be perceptible to the naked eye ($\Delta E^* > 3$, Berns 2000) but acceptable in conservation studies ($\Delta E^* \leq 5$, Berns 2000). As found in the literature titania modified the colour of dark-coloured stones more than lighter ones (Munafò *et al.*, 2015). The treatment did not modify the gloss of the specimens, nor their surface roughness.

Tab. 1: Physical properties of the stones untreated and treated with the self-cleaning coating.

		limestone uncoated	1 coat	2 coats
product uptake (residue, g/m ²)			5.24 ± 1.90	7.06 ± 1.58
roughness (peak to valley height, µm)		58 ± 35	58 ± 45	57 ± 50
colour	<i>L</i> *	77.82 ± 1.22	77.75 ± 1.27	77.96 ± 1.22
	<i>a</i> *	2.06 ± 0.22	1.87 ± 0.27	1.62 ± 0.28
	<i>b</i> *	8.95 ± 0.62	9.75 ± 0.60	10.73 ± 0.64
	ΔE^*		0.88	1.84
gloss units at 85°		1.8 ± 0.7	2.1 ± 0.8	2.1 ± 0.9
		sandstone uncoated	1 coat	2 coats
product uptake (residue, g/m ²)			6.60 ± 1.80	8.82 ± 1.79
roughness (peak to valley height, µm)		103 ± 51	111 ± 49	120 ± 43
colour	<i>L</i> *	53.23 ± 1.82	55.18 ± 2.01	55.90 ± 1.75
	<i>a</i> *	13.96 ± 0.89	13.09 ± 0.68	12.15 ± 1.26
	<i>b</i> *	17.45 ± 1.39	16.70 ± 1.00	16.03 ± 1.27
	ΔE^*		2.17	4.12
gloss units at 85°		0.4 ± 0.1	0.4 ± 0.1	0.4 ± 0.1

3.2. Durability of the self-cleaning coating

Coated stones were naturally weathered in a non-polluted area (Wytham Woods; Oxford), under a rainy-regime for 4 and 6 months from February to October 2015 and the climatic conditions were monitored (Fig. 2). During these two periods of time the samples were exposed to 750 and 1022 hours of sunshine, 135 and 255 mm of rain, respectively, and a range of temperatures between 3.8 and 22.1°C (Fig. 2). After each of the exposure times the photodegradation of methylene blue (staining agent) was determined in the lab under UV-A radiation at different time intervals (up to 190 h) through measuring the colour variation of the surfaces (Fig. 3) (the reference colour value was measured after methylene blue was applied and let dry for 24 hours). The results reveal that on limestone the photodegradation of the organic stain is more effective than on sandstone. This may be because of the different amount of dye applied on the surfaces. Even though on the most porous material, limestone, more stain was applied (3 ml vs 2 ml on sandstone) it was more easily absorbed and less was retained on the surface (as illustrated in Fig. 3). On both substrates two layer coatings promoted faster degradation of the stain than one layer, however once the coated substrates were naturally weathered for 6 months these differences no longer existed, as Munafo *et al.* (2014) also found on artificial weathering conditions, and the surfaces ended up exhibiting a very low (residual) photoactivity.

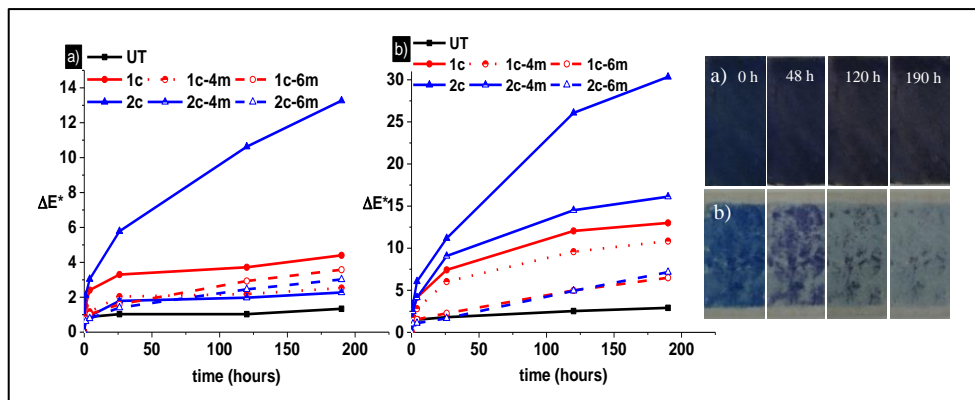


Fig. 3: Colour variation (ΔE^*) of a) sandstone and b) limestone during photo degradation of MB: uncoated (UT), treated (1 and 2 coats) and weathered (for 4 and 6 months). On the right, photodegradation of MB on unweathered coated stones (2 layers).

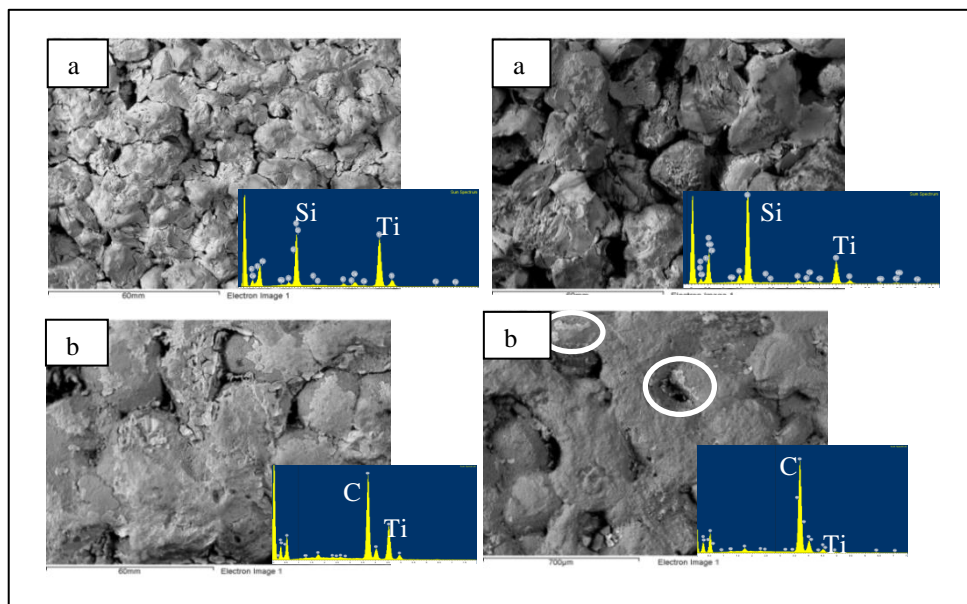


Fig. 4. SEM images and EDS analysis of the coated (2 layers) sandstone (a) and limestone (b) before (1) and after (2) six months of weathering (traces of the coating marked with a circle)

Coated samples were examined with SEM (equipped with EDS analyser) before and after being weathered for 6 months in order to examine the distribution of the self-cleaning product (Fig. 4). Titania coating is observed semi-continuously across both surfaces before weathering. On sandstone, it is cracked (Fig. 4a1) whereas on limestone it partially covers the oolites surfaces as a sort of crust (Fig. 4b1). The EDS spectra of the areas analysed

show a higher content of Ti on the surface on sandstone than on limestone, corresponding to the higher product uptake (Tab. 1). However after the outdoor exposure (6 months) the content of Ti decreases significantly on both surfaces (Fig. 4a2, b2). Only small traces of TiO₂ still remain but the coating has been mostly removed. This explains the loss of photocatalytic effectiveness previously determined.

4. Conclusions

An aqueous dispersion of TiO₂ nanoparticles did not alter the aesthetic of either Locharbriggs sandstone or Portland limestone when applied in one layer, however on the red sandstone the application of 2 coats of the product whitened the surface slightly but to an admissible level in conservation studies.

Regarding its durability under natural environmental conditions in a rainy regime, the coating after 6 months of exposure in the South of England is gradually removed from the surfaces of both stones and the photocatalytic activity is lost regardless of the amount of product applied (1 or 2 layers).

Acknowledgements

Funding from the Marie Curie Action (FP7-2013) under REA grant agreement PIEF-GA-2013-622417 is gratefully acknowledged. Sanha Kang wishes to thank Kongju National University (Republic of Korea) for funding her research stay.

References

- Bergamonti, L., Alfieri, I., Lorenzi, A., Predieri, G., Barone, G., Gemelli, G., Mazzoleni, P., Raneri, S., Bersani, D. and Lottici, P.P., 2015, Nanocrystalline TiO₂ coatings by sol-gel: photocatalytic activity on Pietra di Noto biocalcarene, *J. Sol-Gel Sci. Technol.* 75, 141-151.
- Berns, R.S., 2000, Billmeyer and Saltzman's Principles of Color Technology, Wiley-Interscience, New York.
- Chen, J. and Poon, C-S., 2009, Photocatalytic construction and building materials: From fundamentals to applications, *Building and Environment* 44, 1899-1906.
- Commission Internationale de l'Eclairage (CIE), 1976, Colorimetry, Bureau central de la CIE, Paris.
- Ďoubal, J., 2014, Research into methods of cleaning silicate sandstones used for historical monuments, *J. of Architectural Conservation* 20, 123-138.
- EN 1936:2006, Natural stone test methods - Determination of real density and apparent density, and of total and open porosity, European committee for standardization.
- García, O. and Malaga, K., 2012, Definition of the procedure to determine the suitability and durability of an anti-graffiti product for application on cultural heritage porous materials, *J. of Cultural Heritage* 13, 77-82.
- Graziani, L., Quagliarini, E., Bondioli, F. and D'Orazio, M., 20014, Durability of self-cleaning TiO₂ coatings on fired clay brick façades: Effects of UV exposure and wet & dry cycles, *Building and Environment* 71, 193-203.
-

- La Russa, M.F., Ruffolo, S.A., Rovella, N., Belfiore, C.M., Palermo, A.M., Guzzia, M.T. and Crisci, G.M., 2012, Multifunctional TiO₂ coatings for Cultural Heritage, *Progress in Organic Coatings* 74, 186-191.
- Licciulli, A., Calia, A., Lettieri, M., Diso, D., Masieri, M., Franza, S., Amadelli, R. and Casarano, G., 2011, Photocatalytic TiO₂ coatings on limestone, *J. Sol-Gel Sci. Technol.* 60, 437-444.
- Munafò, P., Goffredo, G.B. and Quagliarini, E., 2015, TiO₂-based nanocoatings for preserving architectural stone surfaces: an overview, *Construction and Building Materials* 84, 201-218.
- Munafò, P., Quagliarini, E., Goffredo, G.B., Bondioli, F. and Licciulli, A., 2014, Durability of nano-engineered TiO₂ self-cleaning treatments on limestone, *Construction and Building Materials* 65, 218-231.
- Pandey, S.C., Pollard, A.M., Viles, H.A. and Tellam, J.H., 2014, Influence of ion exchange processes on salt transport and distribution in historic sandstone buildings, *Applied Geochemistry* 48, 176-183.
- Pinho, L. and Mosquera, M.J., 2011, Titania-silica nanocomposite photocatalysts with application in stone self-cleaning, *J. Phys. Chem. C* 115, 22851-22862.
- Pinho, L., Elhaddad, F., Facio, D.S. and Mosquera, M.J., 2013, A novel TiO₂-SiO₂ nanocomposite converts a very friable stone into a self-cleaning building material, *Applied Surface Science* 275, 389-396.
- Quagliarini, E., Bondioli, F., Goffredo, G., Cordini, C. and Munafò, P., 2012, Self-cleaning and de-polluting stone surfaces: TiO₂ nanoparticles for limestone, *Construction and Building Materials* 37, 51-57.
- UNI 11259:2008, Determination of the photocatalytic activity of hydraulic binders e Rodamina test method, Ente nazionale italiano di unificazione.
- Varotsos, C., Tzani, C. and Cracknell, A., 2009, The enhanced deterioration of the cultural heritage monuments due to air pollution, *Environ. Sci. Pollut. Res.* 16, 590-592.
- Vazquez-Calvo, C., Alvarez de Buergo, M., Fort, R. and Varas-Muriel, M.J., 2012, The measurement of surface roughness to determine the suitability of different methods for stone cleaning, *J. Geophys. Eng.* 9, S108-S117.
- Viles, H.A., Taylor, M.P., Yates, T.J.S. and Massey S.W., 2002, Soiling and decay of N.M.E.P. limestone tablets, *The Science of the Total Environment* 292, 215-229.

EXPLOITATION OF THE NATURAL WATER REPELLENCY OF LIMESTONES FOR THE PROTECTION OF BUILDING FAÇADES

C. Charalambous¹ and I. Ioannou^{1*}

Abstract

Natural stone is one of the oldest building materials used all over the world. However, almost all existing stone buildings and monuments show clear evidence of decay and weathering. One of the most common causes contributing towards the weathering of stones and porous materials in general is the presence of moisture. As such, the process of water movement within this geomaterial should be fully understood in order to assess potential damages and subsequently minimize the deterioration of stone buildings and façades. In previous research work, limestone has been shown to possess an inherent water repellency. This was attributed to the presence of organic contaminants, such as fatty acids, in the pore network of the material. In this paper, the natural water repellency of limestones is revisited and exploited to further reduce the wettability of building and decorative stone from Cyprus. A laboratory treatment based on the inherent composition of the samples under investigation is proposed. This succeeds in significantly and permanently reducing the water capillary absorption, and hence the wettability of limestones, without modifying their composition or appearance. The results provide strong evidence that the aforementioned treatment may be potentially used in practice to protect stone façades.

Keywords: limestone, wettability, fatty acid, sorptivity, Cyprus, water repellency

1. Introduction

Natural stone is susceptible to water-mediated decay processes, such as salt crystallization and frost weathering, induced by alternate cycles of wetting and drying. While some researchers (e.g. Walker *et al.*, 2012) suggest the use of hydrophobic surface coatings in order to protect existing stonework in monuments and cultural heritage sites, others (e.g. Thomas *et al.*, 1993; Taylor *et al.*, 2000; Ioannou *et al.*, 2004) have noted that stones, and in particular limestones, have a natural resistance to water absorption; the latter is indicated by an observed anomaly during water capillary absorption experiments, suggesting a low affinity for water and consequently a reduced water wetting index ($\beta < 1$). Taylor *et al.* (2000) and Ioannou *et al.* (2004) agree that there is no indication of microstructural change or reactivity in the limestone samples they have tested to explain the low water absorption observed. Instead, capillary absorption tests with aqueous organic solutions (i.e. ethanol, 2-propanol, n-heptane) suggested that the low affinity of the limestone samples for water was a contact angle effect, possibly due to a layer of organic contaminants favouring partial wettability to water (Ioannou *et al.*, 2004). It is worth noting that, according to the

¹ C. Charalambous and I. Ioannou*

Department of Civil and Environmental Engineering, University of Cyprus, Cyprus
ioannis@ucy.ac.cy

*corresponding author

literature, the most severe modification of calcite surfaces is attributed to the absorption of carboxylic and especially fatty acids. A number of researchers (e.g. Zullic and Morse, 1988; Rezaei Gomari *et al.*, 2006) agree that fatty acids are irreversibly adsorbed by a calcite surface. Traube's rule states that "*adsorption increases strongly and regularly with increasing homolog chain length*" (Zullic and Morse, 1988). As a result, short chain fatty acids (C₄ to C₁₂) are not permanently absorbed on calcite surfaces. In contrast, strongest affinity for carbonate surfaces is shown by medium-to-long chain fatty acids and carboxylated polymers (Thomas *et al.*, 1993). The long, straight chains of some fatty acids and the small size of the carboxyl groups allow them to form a nearly close-packed hydrocarbon layer above the calcite surface, which excludes water and prevents desorption and carbonate dissolution (Thomas *et al.*, 1993). The aforementioned layer is formed due to the alkyl units of the long straight chains of the fatty acids, which are considered to be hydrophobic (Zullic and Morse, 1988; Thomas *et al.*, 1993; Ioannou *et al.*, 2004). This hydrophobicity primarily controls the solubility of fatty acids and provides an additional mechanism for chemical interactions with carbonate surfaces.

In this paper, the natural water repellency of limestones is revisited and exploited to further reduce the wettability of building and decorative stones from Cyprus. A laboratory developed hydrophobic treatment, based on the inherent composition of the samples under investigation, and in particular the presence of naturally occurring organic contaminants, such as fatty acids, is proposed. This treatment may be potentially used to protect stone façades in monuments and historic buildings, as well as in contemporary structures.

2. Experimental Work

Four different, freshly quarried calcareous rocks from Cyprus were used in this study (Tab. 1). These rocks were quarried in the areas of Lympia, Anogyra, Agios Theodoros and Kivides. Cubic specimens (70×70×70 ± 5 mm) were used in all the tests, to better facilitate result comparison. Initially, the sorptivity (*S*) of all specimens was measured at different temperatures using both water and organic liquids. The results were plotted against $(\sigma/\eta)^{1/2}$, where σ [N m⁻¹] is the surface tension and η [N s m⁻²] the viscosity of the wetting liquids at each temperature. From the graphs, the so-called *intrinsic sorptivity* (*S_I*) and the wetting index (β) of each specimen were estimated (Taylor *et al.*, 2000):

$$S = S_I (\beta * \sigma/\eta)^{1/2} \quad (Eq. 1)$$

All the samples were then heated in a furnace at 400 °C for approximately 5 hours, so that any organic contaminants could be removed. The target temperature of 400°C was gradually reached during the heating procedure (i.e. by increasing the temperature by 100°C every one hour). In order to minimize the risk of damage, all samples were pre-heated at 105°C. At the end of the heat treatment, the specimens were allowed to cool down to room temperature, before repeating the sorptivity measurements using water and organic liquids. Sodium oleate was then applied to the limestone specimens under pressure. Cylindrical cores measuring 27 mm in diameter and 70 mm in length were used for the sodium oleate treatment. These were drilled out of the original heat treated samples. The cores were dried to constant weight at 105 °C in an air oven and were then vacuum saturated with de-ionised water. Following vacuum saturation, they were loaded into a Hassler cell and a containing pressure of 34 bar was established. Sodium oleate was then injected into the cores by a chromatography pump. Two pore volumes of 0.5% w/w sodium

oleate were used. This was based upon the pore volume of an average core and the amount of sodium salt required to form a monolayer. After the injection of sodium oleate, 8-9 pore volumes of de-ionised water were also pumped into the cores to remove any residual salt. The samples were left to dry at room temperature. All the specimens were subjected to thermal analyses using a TG-DTA instrument, both before and after the heat and sodium oleate treatments. A dry, clean, non-heat-treated Lympia stone was further treated with sodium oleate by brushing its top surface. The concentration of sodium oleate used in this surface treatment was also 0.5% w/w. Following brushing, the treated sample was allowed to dry at room temperature. Its sorptivity was measured before and after the treatment to observe the effect of sodium oleate treatment on its water wettability.

Tab. 1: Physical properties and mineralogical composition of the limestones under study.

Specimen	Open Porosity (EN 1936)	Water Sorptivity (EN 1925)	Mineralogy (XRD)
	%	mm·min ^{1/2}	
Lympia	41	1.21	calcite (98%), quartz (2%)
Anogyra	23	0.08	calcite (89%), quartz (5%), illite (traces), albite (4%), heulandite (2%)
Agios Theodoros	28	0.30	calcite (56%), quartz (7%), montmorillonite (traces), pyroxene (10%), illite (traces), plagioclase (18%), heulandite (2%), aragonite (7%), analcime (5%)
Kivides	31	0.13	calcite (82%), quartz (4%), plagioclase (9%), pyroxene (2%), montmorillonite (traces), aragonite (3%), illite (traces)

3. Results and discussion

3.1. Sorptivity measurements

For each specimen and for all liquids, the cumulative absorption per unit surface area i increased linearly with the square root of time $t^{1/2}$. Consequently, the sorptivity $S (=i/t^{1/2})$ was derived from the slopes of the graphs. When sorptivity values were plotted against $(\sigma/\eta)^{1/2}$, the data points fell into two groups, which lied on separate straight lines (Fig. 1). Despite the fact that both the organic liquids and the water sorptivity values increased linearly with $(\sigma/\eta)^{1/2}$, the water data lied on a line with a lesser slope. This confirms previous related work (Ioannou *et al.*, 2004), and demonstrates a marked water anomaly in the case of limestone specimens.

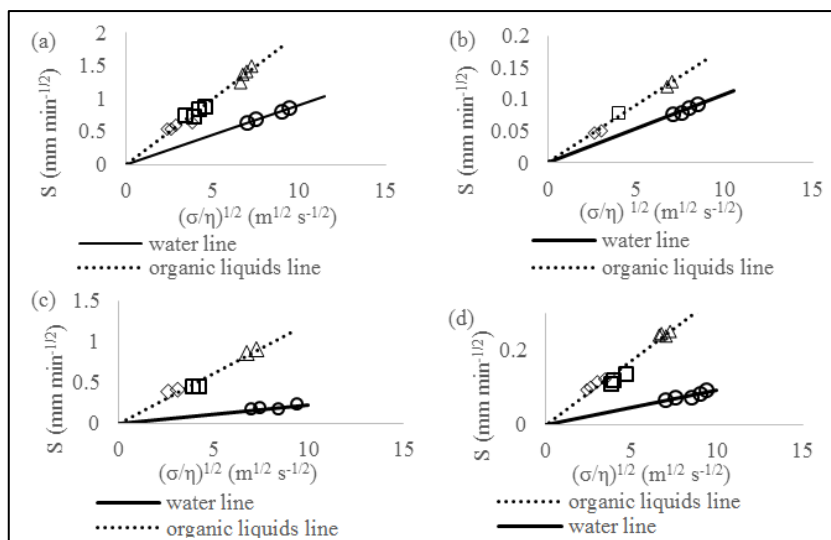


Fig. 1: S versus $(\sigma/\eta)^{1/2}$ for water and organic liquids for all limestones under study: (a) *Lympia*, (b) *Anogyra*, (c) *Agios Theodoros* and (d) *Kivides*.

It is worth noting that pure organic liquids have low energy tensions and, thus, exhibit complete wetting (Fox and Zisman, 1950; Taylor *et al.*, 2000). Partial wetting therefore seems to exist when water is used as the acting liquid; the slopes of the respective lines are markedly lower ($\beta < 1$). This can be explained by a degree of hydrophobicity of the calcite surface of limestones, which seems not to have a good affinity for water. The gradients of both lines in Fig. 1 were used to estimate the so-called *intrinsic sorptivity* of each specimen (Taylor *et al.*, 2000). Using the values of intrinsic sorptivity and Eq. 1, the water wetting index (β) of each stone was calculated. Water wetting indices before and after each treatment and intrinsic sorptivity values for each sample are shown in Tab. 2. The highest original water wetting index was observed in the case of *Anogyra* stone, while the lowest one was estimated for the *Agios Theodoros* stone. This can be attributed to the mineralogy of this stone (Tab. 1) and in particular to the presence of clay minerals, which are known to contain significant amounts of organic impurities (Sayyoub *et al.*, 1990).

3.2. Heat treatment

Fig. 2 shows that the organic liquid S versus $(\sigma/\eta)^{1/2}$ lines after heat treatment do not vary from the ones before heat treatment in all cases; the water lines, however, have a significantly higher slope, which in the cases of *Agios Theodoros* and *Kivides* limestones increased with the number of heat treatments (not shown in the graph for clarity reasons). This confirms that the intrinsic sorptivity of all samples remains unchanged, whereas their water wetting indices change (Tab. 2). The results strongly indicate that the heat treatment managed to “remove” a large amount of organic contaminants from the specimens, while their inorganic mineralogical composition was not affected. According to the literature, thermal degradation of organic contaminants occurs at temperatures $>400^\circ\text{C}$, while CaCO_3 is stable until 400°C (Gaffey *et al.*, 1991). Therefore, organic contaminants are most likely charred rather than removed at the target temperature of the heat treatment adopted in this study (Love and Woronow, 1991). This is confirmed by the black crust layer, probably a

carbon residue, which appeared on the top surface of all samples after the 5 hour heat treatment. It is worth noting that after a single heat treatment at 400°C, Anogyra limestone appeared almost hydrophilic ($\beta = 0.92$). The samples from Lympia, Agios Theodoros and Kivides, albeit showing a significant increase in their water wetting indices after the 1st heat treatment, were still very much partially wetted. Nevertheless, after a 2nd treatment, Kivides stone was nearly fully wetted by water ($\beta = 0.97$). As for the Agios Theodoros stone, although its water wetting index was also further increased after the 2nd heat treatment, a 3rd treatment was carried out. At the end of this treatment, the sample was fully wetted by water since its water wetting index was 1 (Tab. 2); this suggests that whatever organic contaminants this stone contains, they are strongly bound to its surface and it is therefore difficult to remove them.

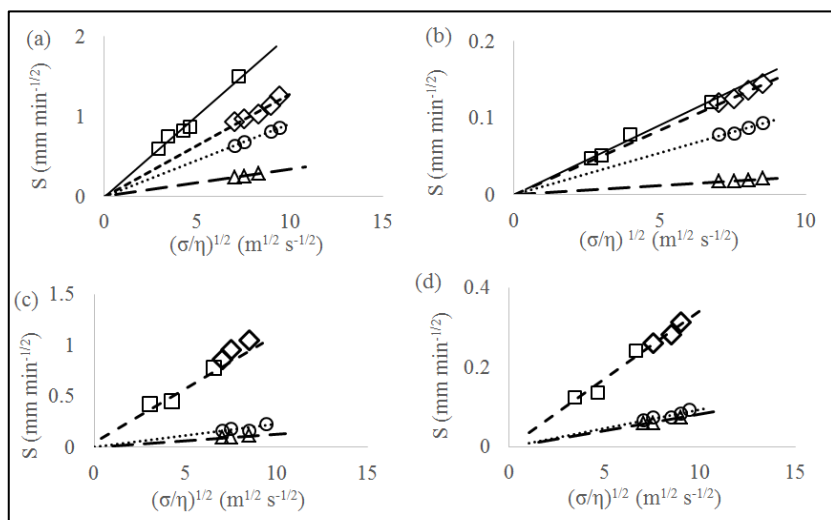


Fig. 2: S versus $(\sigma/\eta)^{1/2}$ for organic liquids and water before and after all treatments. (\square) organic liquids line, (\circ) water before treatments, (\diamond) water after final heat treatment, (\triangle) water after treatment with sodium oleate and flushing de-ionised water (see section 3.3). (a) Lympia, (b) Anogyra, (c) Agios Theodoros and (d) Kivides limestone.

3.3. Treatment with Sodium Oleate

The results of the capillary absorption experiments after treatment with sodium oleate and subsequent flushing with de-ionised water are also shown in Fig. 2. The organic liquids line remained generally unchanged after treatment with sodium oleate, whereas the water line had a much lower slope. Hence, there was a significant reduction in the water wetting indices of the specimens (Tab. 2). These results provide strong evidence that sodium oleate adsorbs well on calcite surfaces, causing a reduction in their wettability. Better diffusion of sodium oleate was achieved by flushing de-ionised water through the treated samples. The largest difference in water wetting index after treatment with sodium oleate was observed for Anogyra limestone, which had been converted from a nearly fully water-wetted stone ($\beta = 0.92$) to a nearly hydrophobic stone ($\beta = 0.02$), before flushing amounts of de-ionised water through it. The sodium oleate treated stones from Agios Theodoros, Lympia and

Kivides reached down to almost the same β with Anogyra stone after flushing with de-ionised water; however, Lympia stone originally had a water wetting index $\beta = 0.42$ (after heat treatment).

Tab. 2: Water wetting indices before and after each treatment for all limestones under study.

Specimen	Intrinsic Sorptivity $\times 10^{-4} \text{ mm}^{1/2}$	Water Wetting Indices			
		Original	After final heat treatment	After treatment with sodium oleate	After flushing de-ionised water
Lympia	8.11	0.21	0.42	0.16	0.03
Anogyra	0.75	0.35	0.92	0.02	0.02
Agios Theodoros	5.04	0.03	1.00	0.33	0.01
Kivides	1.41	0.07	0.97	0.08	0.05

In order to investigate the practical applicability of the treatment with sodium oleate, the surface of a freshly quarried specimen of Lympia limestone was repeatedly brushed with sodium oleate (0.5 % w/w). After a single brushing, the sorptivity of this specimen was reduced by 10%. Further treatments reduced its sorptivity by nearly 90%, while flushing with de-ionised water led to a final reduction of 95% (compared to the original sorptivity). The results strongly indicate that sodium oleate reduces the water absorption of limestone by modifying its surface wettability. Through brushing with sodium oleate (0.5 % w/w), the calcite surface of Lympia stone has turned from hydrophilic to almost hydrophobic. Sodium oleate chemically adsorbed on the CaCO_3 surface of Lympia stone, which interacted in itself with oleate anions, thus giving the surface a Ca-oleate product. Ca-oleate is water insoluble and remains on the CaCO_3 surface. The chemical reaction can be described according to Eq. 2 and 3. The chemisorption is not reversible and the reaction takes place only in one direction.



The unsaturated bond of sodium oleate affects the close packing of carbon chains at the surface of the stone (Sayan, 2005; Alinnor and Enenebeaku, 2014).

3.4. Thermal analysis

The differential thermal analyses (DTA) results of the original stone samples showed a small exothermic peak near 300°C ; this peak disappeared after heat treatment and re-appeared after the treatment with sodium oleate (see for example Fig. 3).

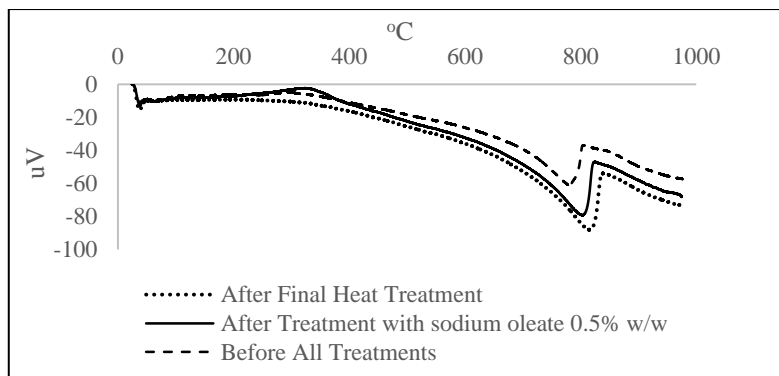


Fig. 3: DTA results for Agios Theodoros limestone.

Weight loss at this temperature, followed by an exothermic peak, is indicative of a double bond (C=O) cleavage and of the formation of intermediate products, which are rich in oxygen (Middendorf *et al.*, 2005; Roonasi and Holmgren, 2009). This can be linked to the presence of organic impurities and sodium oleate in particular. It is worth noting that the original peak was more prominent in the Agios Theodoros stone; this was the sample that needed three heat treatments to remove its naturally occurring organic contaminants.

4. Conclusions

The anomalously low water absorption of limestones from Cyprus has been confirmed by the data illustrated in this paper. When the specimens were subjected to capillary absorption experiments with water and organic liquids, a significant differentiation in S vs $(\sigma/\eta)^{1/2}$ graphs was observed: water data were evidently on a line of lesser slope compared to organic liquid data. Heat treatment led to a significant increase of the water wetting indices of the stones under study. This strongly suggests that the stones' anomalously low original water absorption may be attributed to the presence of a hydrophobic organic contaminants adlayer below their surface. The latter was charred (and hence became inactive) at temperatures around 400°C. The apparent natural water repellency of limestones from Cyprus was exploited through chemical modification of their surfaces using sodium oleate. This strongly adhered to the stones' calcite surfaces, rendering them water repellent. DTA results provided evidence that sodium oleate (or other similar fatty acid products) may be responsible for the anomalously low water absorption of untreated limestones. This work has practical significance, since the durability of stone masonry is largely controlled by processes mediated by water. Partial wettability of limestones is desirable, in order for their durability to be boosted. Treatments based on naturally occurring organic contaminants can therefore be used to induce partial wettability to limestones.

References

- Alinnor I.J. and Enenebeaku C.K., 2014, Adsorption Characteristics of Sodium Oleate onto Calcite, *Int. J. of Pure and Applied Chemistry* 4, 88-96.
- Fox H.W. and Zisman W.A., 1950, The spreading of liquids on low energy surfaces. I. polytetrafluoroethylene, *J. of Colloid Science* 5, 514-531.

- Gaffey S.J., Kolak J.J. and Bronnimann C.E., 1991, Effects of drying, heating, annealing and roasting on carbonate skeletal material, with geochemical and diagenetic implications, *Geochimica et Cosmochimica Acta* 55, 1627-1640.
- Ioannou I., Hoff W.D. and Hall C., 2004, On the role of organic adlayers in the anomalous water sorptivity of Lepine limestone, *J. of Colloid and Interface Science*, 279, 228-234.
- Love K.M. and Woronow A., 1991, Chemical changes induced in aragonite using treatments for the destruction of organic material, *Chemical Geology*, 93, 291-301.
- Middendorf B., Hughes J.J., Callebeaut K., Baronio G. and Papayianni I., 2005, Investigation methods for the characterisation of historic mortars. Part 1: Mineralogical Characterisation, *Materials and Structures*, 38, 761-769.
- Rezaei Gomari K.A., Denoyel R. and Hamouda A.A., 2006, Wettability of calcite and mica modified by different long-chain fatty acids (C18 acids), *J. of Colloid and Interface Science* 297, 470-479.
- Roonasi P. and Holmgren A., 2009, A Fourier transform infrared (FTIR) and thermogravimetric analysis (TGA) study of oleate adsorbed on magnetite nanoparticle surface, *Applied Surface Science*, 255, 5891-5895.
- Sayan P., 2005, Effect of sodium oleate on the agglomeration of calcium carbonate, *Crystal Research and Technology*, 40, No. 3, 226- 232.
- Sayyoun M.H., Dahab A.S. and Omar A.E., 1990, Effect of clay content on wettability of sandstone reservoirs, *J. of Petroleum Science and Engineering*, 4, 119-125.
- Taylor S., Hall C., Hoff W.D. and Wilson M., 2000, Partial wetting in capillary absorption by limestones, *J. of Colloid and Interface Science*, 224, 351-357.
- Thomas M., Clouse J.A. and Longo J.M., 1993, Adsorption of organic compounds on carbonate minerals: 1. Model compounds and their influence on mineral wettability, *Chemical Geology*, 109, 201.
- Walker R., Wilson K., Lee A., Woodford J., Grassian V., Baltusaitis J., Rubasinghe G., Cibin G. and Dent A., 2012, Preservation of York Minister historic limestone by hydrophobic surface coatings, *Scientific Reports*, 2:880, 1-5.
- Zullig J.J. and Morse J.W., 1988, Interaction of organic acids with carbonate mineral surfaces in seawater and related solutions: I. Fatty acid adsorption, *Geochimica et Cosmochimica Acta*, 52, 1667-167.

THE USE OF NEW LASER TECHNOLOGY TO PRECISELY CONTROL THE LEVEL OF STONE CLEANING

B. Dajnowski^{1*} and A. Dajnowski¹

Abstract

Laser ablation cleaning has significantly evolved over the years and offers unique solutions to monumental and architectural stone cleaning problems. Laser cleaning, when applicable, is an attractive technology because it does not involve the use of any chemicals or abrasive media, which can often be logistically problematic and require significant efforts for containment and disposal. With a proper understanding of the ablation threshold of the material and the damage threshold of the stone substrate, it is possible to safely clean a soiled stone surface without affecting the substrate. It is also possible to precisely control the level of cleaning and achieve consistent results ranging from fully clean to partially clean surfaces. This level of control can be particularly useful in situations where a fully clean surface is not desirable and some level of historic patina needs to be preserved or matched in the cleaning process. This research will demonstrate different levels of laser cleaning that can be achieved on a variety of stone surfaces by fine-tuning laser parameters such as fluence, pulse duration, and pulse frequency. The GC-1 Laser Cleaning System, a new laser cleaning technology developed specifically for art and architecture conservation will be introduced. In addition to findings from research performed at the Conservation of Sculpture & Objects Studio conservation lab, real world treatment examples such as the laser cleaning of the over 3,500 year-old ancient Egyptian obelisk of Pharaoh Thutmose III in Central Park, NY will be presented.

Keywords: laser cleaning, ablation, GC-1, conservation, obelisk, stone, granite, limestone

1. Introduction

Many years in the making, the first GC-1 Laser Cleaning System (Fig. 1) was built by Bartosz Dajnowski in 2014 to meet the conservation needs of the 3,500 year old Egyptian obelisk in Central Park, NY. This new cutting edge system is the result of over a decade of hands on laser experience, laser research, professional training, optical engineering, and frustration with the shortcomings of existing laser systems. The compact and portable 1064 nm GC-1 laser system is air-cooled, has no consumable parts, and plugs into any standard 110 V or 220 V outlet in the world. This system was built specifically to meet the needs of art and architecture conservation and is being used on cultural heritage projects across North America, and has led to the formation of a new company called G.C. Laser Systems Inc. (www.GCLasers.com) that specializes in evolving laser applications technology for the world of cultural heritage preservation. This paper will go over some of

¹ B. Dajnowski* and A. Dajnowski

Conservation of Sculpture & Objects Studio, Inc, (CSOS), United States of America
BDajnowski@CSOSinc.com

*corresponding author

the practical applications of this system and illustrate how its unique features make it an effective tool for cleaning stone.

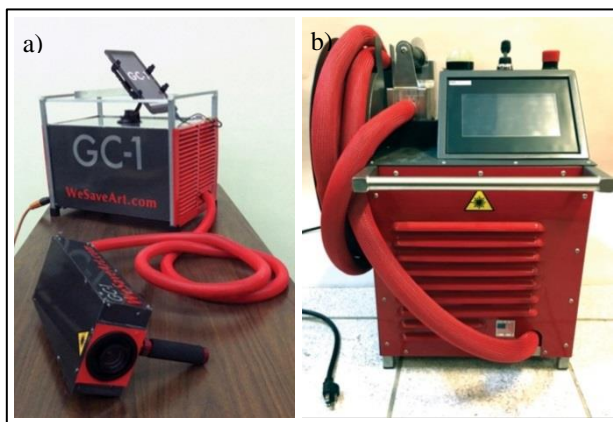


Fig. 1: a) First GC-1 Laser Cleaning System Prototype; b) New generation of the GC-1 which measures: W=41.3 cm/L=74 cm/H=56 cm. (Multiple patents pending worldwide).

2. Working principle of laser cleaning

The method of laser cleaning relies on taking advantage of the fact that various materials will absorb different wavelengths of light depending on properties such as their color and chemical composition. Laser parameters such as wavelength, pulse duration, and energy density/fluence can be tuned to selectively excite a layer of unwanted material in order to remove it from an original surface that does not get affected by the same laser parameters. Examples of unwanted layers of material include corrosion, soiling, graffiti, and coatings on monuments. The atoms and molecules of the contaminant get so excited by the laser energy they absorb that molecular bonds are broken, particles are ejected, and the contaminant is vaporized/ablated. Unlike mechanical or abrasive cleaning methods which rely on mechanically impacting the surface to get contaminants to break free, this method relies on exciting the contaminant so that it separates from the surface on its own.

Tuning a laser cleaning system can result in a variety of photomechanical, photothermal, and photochemical effects that can aid in the removal of an unwanted layer such as contaminants, corrosion, coatings, or paint. The goal is for the laser to discriminate between the unwanted layer and the substrate. Ideally the unwanted layer absorbs the laser pulses while the original substrate reflects them. Once the laser reaches the substrate, it does not absorb into it and simply reflects off the surface. Laser cleaning relies on calibrating laser parameters to selectively remove unwanted layers of material or coatings. Fig. 2 shows the following steps:

- 1.) The contaminant layer (red) needs to be removed from the original substrate (green).
- 2.) Laser parameters are calibrated to ablate away the contaminant without damaging the substrate.
- 3.) The substrate is uncovered to reveal a clean and undamaged surface.

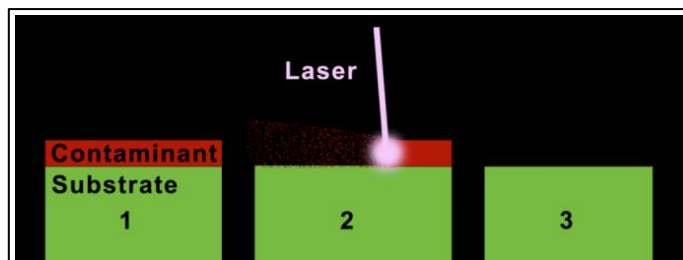


Fig. 2: Laser cleaning of a contaminant off of a substrate.

3. Precision of Laser cleaning

The efficacy and precision of a properly tuned laser to discriminate between a contaminant and a substrate is illustrated in Fig. 3, where blue tape is used to mask of a test area on discolored architectural limestone for laser cleaning tests. This orange colored limestone is from the historic façade of the Oklahoma State Capitol Building. The building had a silicon-based coating applied in the 1980s, which has since discolored orange and proved difficult to remove with other methods. CSOS conducted laser-cleaning tests on the façade under the supervision of Treanor Architects in 2015. The image shows that something as simple as paper or blue painters tape can be used to mask off an area while laser cleaning tests were performed (Fig. 3).

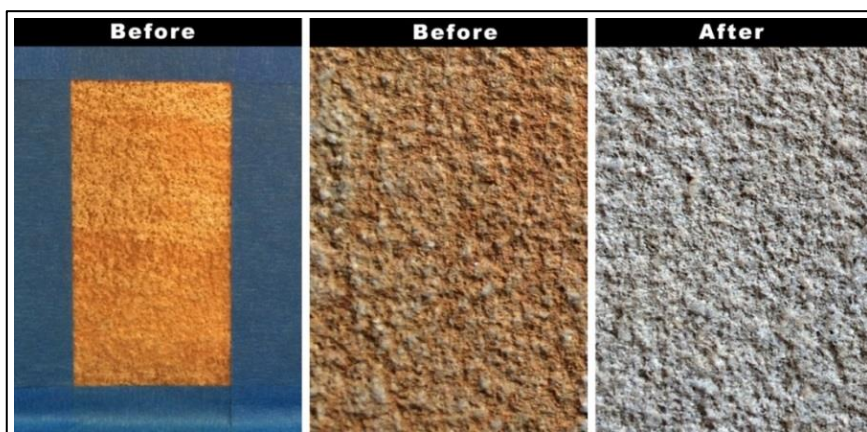


Fig. 3: Using blue tape to mask off areas for laser of a discolored coating from architectural limestone (left), and detail of cleaning results (right).

The laser settings used here did not damage or penetrate through the blue tape, and they did not damage or alter the surface texture of the limestone while removing the discolored orange film. The laser does not affect the area covered by the tape, resulting in a much defined border during cleaning. Tape or other optical barriers can be used to strategically mask off parts of a stone structure from being exposed to the laser. For example, window seals can be easily masked off during laser cleaning. By comparison, chemical cleaning of architectural stone could compromise window seals while air abrasive methods could etch

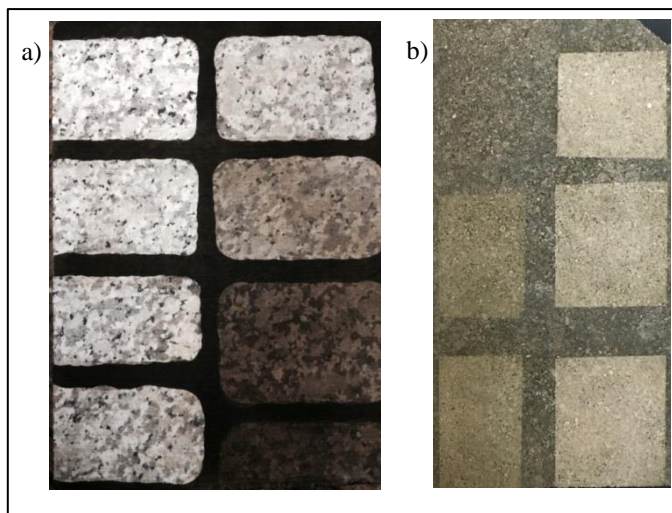
glass, not to mention potentially erode the stone surface. The GC-1 laser system has a red aiming beam feature that can be activated to show exactly where the laser will fire (Fig. 4). When the trigger is pulled, the red aiming beam is replaced with the 1064 nm laser beam that does the ablation.



Fig. 4: The red aiming beam of the GC-1 is used to target an area of architectural marble before firing the laser to remove dark gypsum crust.

4. Precise control over laser parameters

The lasers typically used for such treatments have very short pulses in the nanosecond range. It is common practice and very important that laser cleaning case studies to report the fluence of the laser pulses being used. Fluence, also known as energy density, is simply the ratio of energy per pulse over the surface area of the pulse, and is typically measured in Joules/cm². The concentration of laser energy should be set to give satisfactory cleaning results while remaining below the damage threshold of the substrate. However, there are many other parameters to take into consideration such as pulse duration. In general, shorter pulses result in more of a photomechanical effect and longer pulses result in less photomechanical effect, more plasma formation and the potential for more photothermal effect. For example, a 10ns pulse generates more photomechanical shock on a surface than a 100 ns pulse because the laser energy is delivered over a much shorter period of time. Longer pulses result in longer reactions and more plasma formation. Depending on the nature of the soiling/contaminant being removed and the characteristics of the substrate, a shorter or longer pulse duration may be optimal for effective cleaning. A 1064 nm laser emitting 10 ns pulses can give completely different cleaning results than a laser system emitting 100 ns pulses. Longer pulses in the nanosecond region are more gentle on fragile surfaces than shorter pulses. Unlike other laser systems that have a set pulse duration, the GC-1 laser cleaning system is unique because it allows the conservator to select a wide range of pulse durations ranging from 10ns – 250 ns [additional pulse duration options and laser systems are in development by G.C. Laser Systems Inc.], and those pulse durations are independent of pulse frequency. Pulse frequency is finely tunable from 1 kHz – 1 MHz. For example, the operator could chose to have the laser emit any desired exact number of pulses, such as 202,542 or 202,543 pulses per second. Laser energy, fluence, and scan speed are also precisely controlled and tunable via a touch screen user interface. Spot size can be changed simply by changing focal lenses in the scanner, allowing for an extended range of fluence options.



*Fig. 5: a) Different levels of consistent cleaning of fire damaged granite;
b) Historic limestone with dark biological growth by tuning laser parameters.*

The granite sample in Fig. 5 was exposed to fire and soot and then washed to remove superficial loose soot from the stone. This process was repeated 8 times until a dark and well-adhered soot layer remained on the surface. Precise tuning of critical laser parameters can allow a conservator to control the level of cleaning of stone to achieve very uniform and consistent results. Fig. 5 illustrates the wide range of levels of “clean” that can be achieved on fire-damaged granite. The Indiana limestone sample on the right is covered with dark biological growth from being exposed to the elements for many years. Both biological growth and atmospheric pollution can be removed from stone with laser ablation, and the laser system will not clean beyond a certain level that it has been tuned to. Partial cleaning can be useful when the treatment goal is not to make a surface look like new, but to leave behind some level of patina. For example, if a large historic stone building has an overall level of historic patina, but suddenly experiences a fire in one area. It could be undesirable to over clean the fire-damaged area, which would then look too new relative to the rest of the façade. With a well-tuned laser it is possible to precisely control the level of cleaning to better match the tonality of the rest of the building.

5. Unique scanning system

Conservators use either low pulse frequency lasers or high pulse frequency lasers for treatments. Low frequency lasers typically generate a maximum of less than 50 pulses per second (50 Hz) and are commonly used on small-scale projects or objects. High frequency lasers generate thousands or hundreds of thousands of pulses per second, delivered via a scanning system, and are more efficient for use on larger conservation projects. A common scan system uses for high frequency lasers is a line scan system. The line scan is typically created by an oscillating galvanometer mirror that directs the laser beam back and forth along one axis, resulting in a line. Such line scanners can be effective tools for conservation; however they can have inherent difficulties. When the beam reaches the endpoint, the mirror has to physically stop and change direction. Although this process of

changing direction is extremely fast, lasting only a small fraction of a second, it is still long enough for more laser energy to be delivered to the endpoints of the scan line, resulting in “hot spots” as are shown in Fig. 6. Hot spots in a cleaning system can produce uneven results. By comparison, the unique circular scan pattern of the GC-1 laser system delivers a continuous even distribution of laser energy over the path of the scan. There is no stopping or changing direction of the beam and therefore no end point hot spots. Fig. 6 and Fig. 7 illustrate how a circular scan pattern is a geometrically more efficient solution. A line scan pattern, as shown in Fig. 6a, will expose every point on a surface once as it moves past an area. In contrast, as a circular scan moves over a surface, the leading edge of the circle passes over an area first (1) and then the trailing edge passes over the same area again (2). There are two separate exposures of the laser beam to any given point with each movement of the laser across the surface. This can make cleaning twice as fast, particularly in cases where multiple passes of the laser are often needed. The probability of thorough cleaning is significantly increased because anything that might be missed or under cleaned by the leading edge (1) will be exposed to the laser parameters again as the trailing edge (2) reaches it. In short, this process results in two passes of the laser with any given physical movement where a line scan only offers one pass of the laser per physical movement.

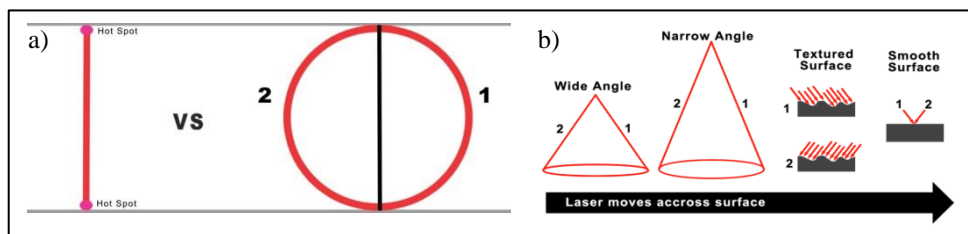


Fig. 6: a) Comparison of a typical line scanner to the GC-1 circular scan pattern; b) Multiple angles of exposure as the laser moves across a surface.

The laser beam comes out of the scanner as an expanding cone (Fig. 6b). As the circle/oval moves over a surface, the leading edge (1) of the cone hits the surface from one angle, and then as the laser keeps moving the trailing edge (2) of the cone hits the same area from the exact opposite angle. Textured surfaces are efficiently cleaned by this process because the laser is able to reach multiple facets of a complex surface with just one pass. The angle of the cone can be custom modified as well. By comparison, a line scanning system essentially emits a flat plane of laser light that offers only one angle of incidence per pass. During actual cleaning trials on various surfaces we have found the rate of cleaning of the GC-1 to range from five to sixty square feet per hour, depending on the nature of the material being removed and the substrate being cleaned. For example, carbon deposits are very quickly removed from a variety of stone surfaces.

6. Limitations

A laser system is simply an additional tool in the toolbox of the conservator. It is by no means a magic wand and the parameters of the laser need to be thoroughly understood. The same laser systems can provide excellent results as well as cause irreversible damage to a surface depending on how it is used, how it is tuned, and the skill of the operator. Not understanding laser the properties of a laser and the physics behind laser cleaning can lead to undesirable results or misinterpretations of what is happening during the process.

Fig. 7 addresses the issue of yellowing of stone that many have observed after laser cleaning stone, and one reason why this may appear to happen.

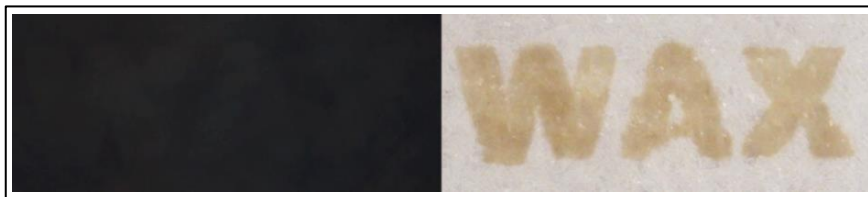


Fig. 7: Removing fire damage soiling from a marble surface that was completely black with soot before laser cleaning (left). The word WAX remains as an actual film of wax on the surface after cleaning (right).

When the soiling is removed from the white marble with laser, a dark yellow word WAX is uncovered. Wax was in fact used to spell out the word WAX which was applied prior to soiling the sample. In this case the laser was tuned to remove the soiling, but the parameters were not sufficient to remove wax from the surface. An inexperienced operator may think they have turned the stone yellow, when in fact they have simply failed to remove a layer of wax residue from the surface that was beneath the soiling. This wax residue can be removed with different laser parameters or with poulticing and/or chemical methods. It is not uncommon for stone objects to have been waxed, to have accumulated oily organic pollutants, or to have been oiled during their history to make them look more polished. Laser cleaning should not necessarily be considered as a stand-alone technique. There are many situations in which laser cleaning is most effective when it is part of a process that involves other conservation methods and treatment steps. It should also be understood that laser cleaning is a surface cleaning technique and that it is not always applicable. If the damage threshold of the substrate is exceeded by the available laser parameters, then it is not safe to laser clean. This is why testing on samples is always recommended. It is critical to understand that laser cleaning will not extract stains from a stone and attempting to remove, for example, iron or copper stains from a stone with a laser can cause permanent damage and discoloration to the stone. Stains should be removed with traditional poulticing methods, and occasionally a laser may be used to remove the final thin layer of stain residue from a stone surface after a poulticing campaign. A common hurdle to incorporating laser cleaning into a project is that the equipment can initially be relatively expensive when compared to other methods such as pressurized media blasting. However, with this new technology the increased rate of cleaning, the precise control over the level of cleaning, and the lack of chemical and abrasive media waste disposal costs makes it a competitive option to consider.

7. The obelisk of Pharaoh Thutmose III

The ancient Egyptian Obelisk that stands in New York's Central Park behind the Metropolitan Museum of Art is made of one piece of solid Aswan granite, weighs approximately 220 tons, and is over 21 meters tall. This amazing object has a rich history that involves Thutmose III, Ramses II, Cleopatra, Julius Caesar, the Egyptian government, the Vanderbilts, masons, and an epic transatlantic voyage to the USA in 1880. This obelisk is one of a pair of two obelisks, and the second one stands in London. The Central Park Conservancy (CPC) cares for and maintains the obelisk. After extensive research and

testing of chemical cleaning, micro-abrasive cleaning, and laser cleaning methods and options, the Central Park Conservancy concluded that laser cleaning provided the safest, most environmentally friendly, and most uniform level of cleaning for the fragile stone surface. For example, chemical cleaning was uneven and runoffs were difficult to control. Scanning electron microscopy showed that micro abrasive cleaning abraded the stone surface while laser cleaning resulted in more thorough cleaning with no impact on the granular structure of the stone. CSOS was selected to perform the laser cleaning of the entire obelisk surface, the granite plinth on which it stands, and the four replica bronze crabs wedged in its corners. CSOS was asked to first conduct tests on loose samples that had fallen off over time, which were examined by the CPC and by Dr. George Wheeler at the Metropolitan Museum of Art to ensure that there was no damage being done to the stone. It was critical not to damage the black biotite inclusions in the granite or to cause micro shattering of the quartz while removing the dark soiling from the granite. The tests confirmed that it was possible to safely clean the granite without causing any damage. More tests were conducted onsite on the obelisk and then the project moved forward under the supervision of the CPC. To ensure that the project went smoothly, CSOS had one 100 W and three 120 W line scanning laser systems onsite. These systems were custom modified by CSOS to eliminate hot spots that could potentially damage the stone. This project was catalyst for the creation of the GC-1, as the first prototype was made to meet the needs of this project. The GC-1 was the only scanning laser system that could be carried by one or two people to the top of the scaffold due to its light weight and compact size. The 70W GC-1 outperformed the other more powerful 100-120 W laser systems on the project and was proven to clean twice as fast as the line scanning systems. Due to its efficiency and speed, the GC-1 was used to clean over 60% of the granite surface, despite the fact that there were typically two line-scanning systems in operation at all times. Overall, depending on the level of soiling, 100-200 ns pulses were used at a fluence of 1-3 J/cm². The entire laser cleaning process was done wet by misting the surface with distilled water just prior to firing the laser, which gives a micro-steam cleaning effect as the laser vaporizes water that enters the pores of the stone. The wet ablation allows for deeper cleaning of the surface and also helps protect the surface from potential phase changes by minimizing plasma exposure to oxygen as the reaction happens under a film of water. The laser cleaning treatment was a success and Fig. 8 shows that legibility of the hieroglyphs significantly improved after cleaning as the natural shadows of the carvings are no longer masked by dark soiling.

The granite surface was examined with a portable USB microscope during treatment to ensure that no damage was being done to the surface. Photomicrographs were taken to document the cleaning results. Fig. 9 shows a one area before and after laser cleaning in regular light and infrared light. IR light helps show carbon on a surface. The images show that the soiling was successfully removed and that the black biotite inclusions, pink quartz, white quartz, and other minerals were not damaged during the cleaning process. In fact, the green arrows point to two small grains of quartz on the surface which are not disrupted at all by the cleaning process and remain intact.



Fig. 8: Overall and detailed results of laser cleaning the obelisk.

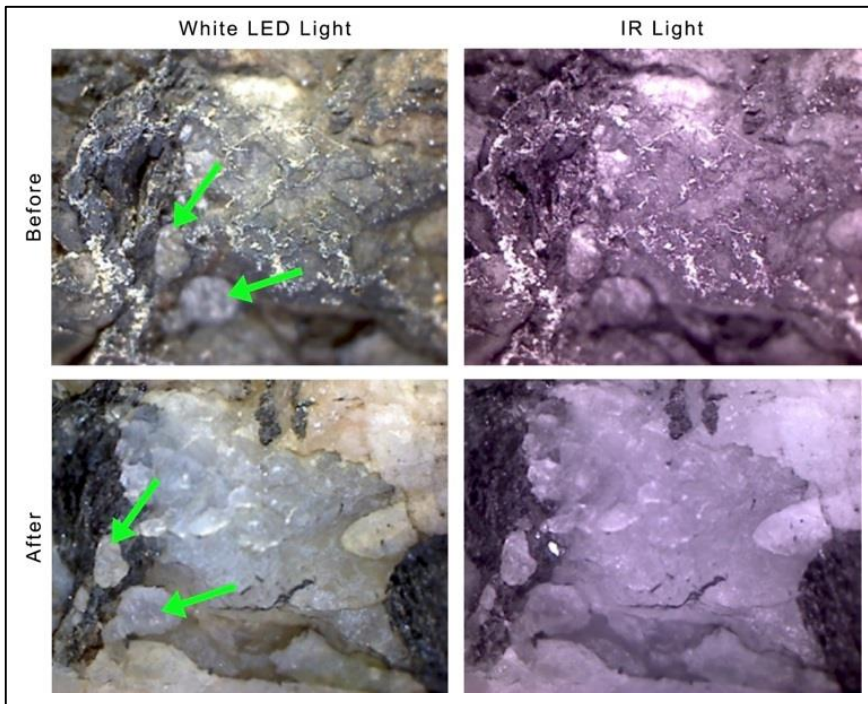


Fig. 9: Photomicrographs (magnification: $\times 40$) of the surface before and after laser cleaning. The green arrows point at delicate small grain features that were preserved during laser cleaning.

8. Conclusion

Laser cleaning is becoming more popular because it is environmentally friendly and very precise. The unique GC-1 laser cleaning system is a versatile new tool for cleaning stone. The GC stands for “Game Changer,” because of its’ compact size, tunability, and reliability. It offers unmatched parameters and control over cleaning which, in the right hands, means consistent results on both large and small projects.

Acknowledgements

We would like to thank the conservation staff at CSOS for their work and dedication to these projects and to the many projects that led up to this point. A special thanks is owed to Robert Zarycki, Christopher Ciaston, Tadeusz Mlynarczik, and Rosanna Ioppolo. We would like to thank Tri-State Stone and Brick Co for supplying us with a variety of historic and new stones for our research. We are grateful to architectural firms such as Wiss, Jenny, Elstner Associates Inc., Treanor Architects, Kiewit Building Group, Grunley Construction Company, Atwill-Morin Inc. and the government agencies and cultural institutions such as the Architect of the Capitol and the Smithsonian that give us the opportunity to test and use this technology on a variety of unique cultural heritage projects. We are particularly grateful to the Central Park Conservancy for trusting us to treat the obelisk in Central Park, especially since this project motivated us to bring the GC-1 laser cleaning system into existence. Bartosz Dajnowski would like to express his sincere gratitude to the team at the Laser Applications Lab at the Military University of Technology Institute of Optoelectronics, Laser Applications Lab in Warsaw for the education and training they provided him, and in particular the mentorship and friendship of the late Prof. Dr. Hab. Inz. Jan Marczak.

References

- Castillejo, M., 2007, *Lasers in the Conservation of Artworks*. The Netherlands: CRC Press.
- Nimmrichter, J. 2005. *Lasers in the Conservation of Artworks, LACONA VI* Proceedings, Vienna, Austria, Sept. 21-25, 2005. Germany: Springer.
- Koss, A. and Marczak, J., 2005, *Application of Lasers in Conservation of Monuments and Works of Art*. Warsaw, Poland: Oficyna Drukarska.
- Radvan, R., 2009, *Lasers in the Conservation of Artworks VIII*, Proceedings of the International Conference on Lasers in the Conservation of Artworks VII (LACONA VIII), 21-25 September 2009, Sibiu, Romania. The Netherlands: CRC Press.

CLEANING STONE – THE POSSIBILITIES FOR AN OBJECTIVE EVALUATION

J. Ďoubal¹

Abstract

The cleaning of monuments is one of the most common and at the same time most risky procedures when conserving or renovating monuments. Cleaning monuments can be carried out only if based on solid knowledge of the actual monument issues, its origin and character of soiling (using X-rays, FTIR and Raman spectrometry or optical microscopy) as well as of the substrate material (using for instance SEM, SEM-EDS and petrological analyses of the cut using polarizing microscopy). The aim of this paper is to present some of the recent options of objective cleaning results assessment. The paper focuses both on the description and assessment of instrumental measurement of changes in physical properties (water uptake, water-vapour permeability, cohesion after testing using a peeling test) and on optical methods facilitating assessment of cleaning effectivity and the restoration intervention impact on the substrate (SEM, optical microscopy). The overview of objective possibilities of evaluating cleaning methods is based on many years of experience of assessing the results of cleaning on real objects, as well as in laboratory testing.

Keywords: stone, cleaning, evaluation, conservation, compatible treatment

1. Introduction: Cleaning stone monuments

The cleaning of monuments is one of the fundamental and most important aspects of monument conservation. It is a crucial step both from the point of view of the philosophy of conservation and from the perspective of the technology and techniques of conservation.

The cleaning of monuments can only be carried out based on in-depth knowledge of the aspects of the monument in question, of the origin and nature of the soiling and of the state of the underlying material. The evaluation of the necessity and level of cleaning is essentially based on assessment from two basic aspects:

In what manner the soiling of the surface influences the state of the underlying material. When assessing this aspect, it must be considered, based on the survey, whether the surface soiling could pose a risk to the future life of the monument. It is inspected whether the change of the physical properties of the surface (such as water uptake, water-vapour permeability, changes in thermal and moisture expansion, etc.) is not the source of damage, and if it is, the severity of the risk is examined. Another important criterion for evaluating the necessity of cleaning is the question to what extent soiling is a source of substances harmful to the stone, e.g. water-soluble salts, etc.

¹ J. Ďoubal*

Faculty of Conservation – University of Pardubice, Czech Republic
Jakub.doubal@upce.cz

*corresponding author

In what manner the soiling of the surface compromises the artistic and aesthetic value of the monument. The impurities may cover the surface as a thick layer which obscures the surface relief and often alters the sculpting. Soiling is practically always accompanied by a significant change in colouring. Depending on the type of pollutant, the source of soiling and the substrate material, impurities also sediment unequally and the resulting effect may be very far from the original intent of the sculptor. On the other hand, a certain level of alteration of the original appearance of the monument is generally accepted when assessing aesthetic positions. This alternation gives rise to the historical value of the monument and is connected in its life in time - this type of changes in the surface layer is called a patina. The definition of patina and the necessity of preserving it have been subject to discussions ever since modern monument care has existed.

It follows from the nature of both aspects that, while with the first one a relatively objective assessment can be carried out at today's level of understanding, the other one will always entail a subjective assessment depending on the time period, aesthetic feelings and point of view of the assessor. The fact is, however, that both these basic aspects are equally relevant when it comes to works of art.

There is a broad range of techniques ranging from highly effective ones that are used on large façades, to sensitive and precise ones that are used on the smallest details of a sculptor's work (Fassina 1994, Andrew *et al.* 1994, Normandin *et al.* 2005, Ďoubal 2014). The individual techniques and technologies have their own respective and irrefutable advantages, but they are also connected with certain risks, when it comes to their application. When choosing a suitable technology of cleaning, all aspects of the use of the given method should be taken into account, including its effectiveness, the effect it has on the substrate and how demanding it is economically.

2. Assessing the results of cleaning

In practice, the results of cleaning are mostly assessed subjectively based on visual inspection. Objective possibilities of assessment have been described by a large number of authors (Andrew *et al.* 1994, Kapsalas *et al.* 2007, Hauff 2008, Werner 1991, Verges-Belmin 1996, Ďoubal 2014).

When assessing the change in appearance (i.e. of the effect of cleaning), it is impossible to avoid individual assessment since it is aesthetic qualities, which are by their very nature impossible to measure, that are assessed.

While there are not many instrumental tools for the assessment of appearance, there are a number of possibilities for assessing possible changes in the characteristics of the surface after cleaning and of measuring the level of material loss (Ashurst 1994). The principles for assessing the effect of cleaning (Tab. 1) are based on requirements that have already been drawn up in the past. In 1997, WTA - *The Scientific-Technical Society for the Rehabilitation of Buildings and for Monument Care* drew up a technical regulation called "The Assessment of Cleaned Stone Surfaces (Goreczky, L. and Hoffmann 1997), which evaluates measures aimed at cleaning the surfaces of buildings and stones. The system of assessing interventions introduced by the WTA regulation is based on the evaluation of selected physical-mechanical parameters, but also on the evaluation of changes in the chemical composition of material and of alterations in its structure and surface.

Table. 1: Decisive material characteristics for the assessment of cleaning

Characteristic	Name of quantity measured/unit	Methods, norms and recommendations for trials		Criteria for positive assessment
		<i>In labo</i>	<i>In situ</i>	
Chemical and mineralogical characteristic (of the material as well as of the soiling)	-	Optical microscopy in polarized and non-polarized lights, (SEM-EDS), X-ray diffraction (XRD)	Micro chemical tests	No changes (material)
Surface water uptake	Capillary water uptake coefficient C ($\text{kg}\cdot\text{m}^{-2}\cdot\text{min}^{-1/2}$)	EN 101518:2009	EN 16302:2013	$C_i > C_0$
Microstructural properties: thickness of the layer of deposits, surface changes after cleaning	-	Optical microscopy, SEM, X-ray tomography	-	Reducing the thickness of the layer of deposits, without disruptions and changes in surface
Colour of the soiled surface and the referential colour of the material (determined by agreement)	L^* , a^* , b^* , ΔE , ΔC^*	EN 15886:2010	-	Criteria must be defined individually for the respective case
Surface cohesion (weight of torn-off material)	Weight of torn-off material	-	Peeling test	No changes (material)
Surface roughness	Roughness depth, R	DIN 4768, 4772, E-DIN 4760 Optical microscopy, SEM	-	No changes (material)

The quality of the cleaning carried out is in practice mostly assessed based on the change in water uptake, which should increase after the cleaning. However, its level cannot be quantified with more precision, as the level of cleaning depends on other qualities of the surface (e.g. it carries shape; underneath the layer of soiling, the stone is completely decayed and the layer of impurities hardens it, etc.). In practice, the capillary water uptake is usually determined *in situ* using Karsten tube test (or its more recent modifications), or on samples in a laboratory. From the point of view of the mechanism, it is obvious that absorption power increases when the layer of soiling is made thinner, or when it is completely removed. Even in that case, the rate of removal is individual and it is necessary to consider its rate in relation to other characteristics of the surface (especially cohesion and grain size).

With regard to an aesthetic evaluation of the artwork after cleaning, the assessment of the colouring of the surface of the material is an important macro-characteristic. These changes in colouring and other aspects are in practice mostly evaluated visually by comparing the

cleaned surface to a referential surface of material (surrounding surface, architecture, other elements within the set, polychromy, etc.). In the case of a need for a more objective assessment (again with some limitations given by the quality and morphology of the surface), it is possible to assess the overall change in colouring by means of a portable spectrometer. Deviations acceptable within the intervention are listed in literature in absolute values as the changes in colouring. However, for cleaning the exact limits for a positive evaluation of the intervention have not been published - for understandable reasons.

2.1. Characteristic of the substrate and deposition of soiling

In order to obtain a basic characteristic of the soiling, the thin section of a representative sample collected, including soiled surface, will be used. A thin section collected in this manner allows for a petrological analysis of the stone which will determine the basic characteristic properties of the rock and help determine the manner of deposition of the impurities, or the depth of seepage into the substrate, which is an essential property for the selection of the appropriate rate and method of cleaning. Examination in a polarizing microscope allows the petrologist to carry out a detailed analysis of the examined stone, including its mineralogical composition and porous structure. The chemical as well as mineralogical characteristic of both the substrate and the layer of soiling itself, i.e. the chemical or phase composition and their microscopic characteristics (e.g. thickness, binding to substrate, cracks, porosity, etc.) will be provided by a wide range of optical examination methods supplemented with analytical methods that focus on the elemental and substance composition. Visual assessment, examination under a stereo magnifying glass or under a USB microscope is used to assess changes in macro-scope - these examinations are ordinarily carried out *in situ*. More exact information, in particular with regard to assessing changes in the substrate in micro-scope will be provided by microscopic methods on collected micro samples, processed into cross sections or thin sections (Fig. 1). Microscopic methods include optical microscopy in polarized light (PLM) and in non-polarized light, scanning electron microscopy used independently for the study of changes in surface (change of the thickness of the layer of impurities, changes in the distribution of impurities, creation of cracks, etc.), but also for the determination of substance composition, in which case microscopy is used in connection with energy-dispersing X-ray analysis (SEM-EDS). This method is designed particularly for characterizing the compositions of the layer of deposits, the effect of cleaning, chemical changes on the surface after the use of the respective cleaning method (e.g. in the case of chemical cleaning, or the removal of crusts or of coats of paint etc.). The methods that can be used in these cases include also X-ray diffraction, or spectroscopic ones such as mid-FTIR and Raman spectroscopies also coupled to microscopy (Martínez-Arkarazo 2008, Potgieter-Vermaak 2005).

Additional analyses which can contribute to the knowledge of the state of the substrate underneath the soiling include the measurement of drilling resistance and ultrasound transmission. These methods can discover for instance a possible decrease of the firmness of the substrate underneath the crust, or in the layer near the surface, which can influence the planning of a conservation intervention (e.g. pre-consolidation before cleaning, etc.).

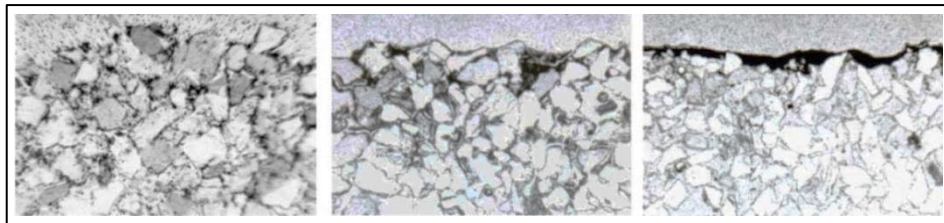


Fig. 1: Optical microscopy - thin section, deposition of soiling on different sandstones. On the thin section we can see how deep into the substrate the impurities had penetrated, or if they close the porous structure of the substrate.

2.2. Selected methods of evaluating cleaning trials

Each cleaning must be preceded by trials on a small surface of historical material. The results of these trials can be evaluated in the following manner:

Visual inspection: Visual inspection is the essential and indispensable tool for inspecting the results of cleaning. It provides a relatively clear idea of the resulting aesthetic effect of the cleaned surface, and based on trials, the most suitable intensity can be chosen from the perspective of the resulting aesthetic impression. Although visual inspection, possibly accompanied by the use of simple magnifying tools, such as magnifying glass, photography and macrophotography, can discover more significant damage to the substrate caused during cleaning, it is still often insufficient for the evaluation of all possible risk to the substrate.

Optical surface microscopy: Optical surface microscopy is a highly suitable and widely available tool for examining the effects of cleaning on the surface of the substrate. It can be carried out either in non-destructive manner using a USB microscope that allows sufficient magnification and that can store images, or *in situ* using a modified field microscope. Another possibility is to collect samples and examine them using an optical microscope. Stationary devices provide better-quality images and allow for greater magnification, or for examination in various types of lighting conditions. Ideal information is provided by means of comparison photography from before and after cleaning from the same location, or images of partial cleaning.

Optical Microscopy of a Cross Section: Another tool used to examine the effect of cleaning on the substrate is optical microscopy of a cross section. This method requires the collection of a representative sample of the surface, and it provides a reasonably good idea of the success of cleaning, and with larger magnification, it is possible to discover also possible negative effects on the substrate, which could become source of problems in the future. The success rate of this method depends to a large extent on the quality of the collected sample and of the executed cross section. It is rather a supplementary method of assessment.

Optical Microscopy of a Thin Section: Very valuable information about the sensitivity of cleaning and about the interaction with the substrate can be provided by microscopy of a thin section. Thanks to very good readability, which is significantly higher than in the case of a cross section, relatively clear conclusions can be drawn from the examination. The thin

section can also be subjected to polarizing microscopy, which broadens the range of information acquired. The disadvantage of this method is the difficulty of preparing the sample, which needs to be prepared at a specialized workspace and is costly.

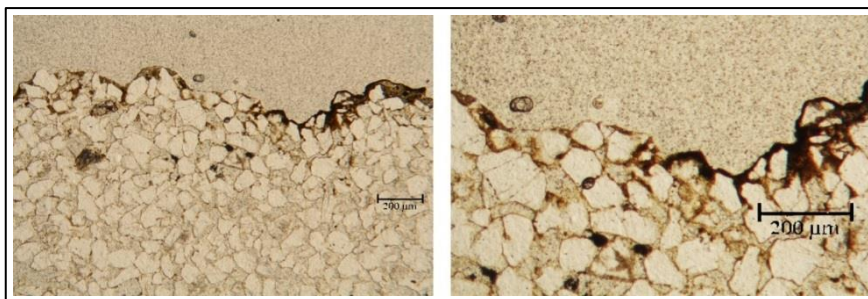


Fig. 2: Stereoscopic microscope. Thin section - Yellow sandstone - left half of both figures after cleaning by laser - even after cleaning, there are remains of the patina on the surface.

Surface electron microscopy – SEM: Surface electron microscopy provides a detailed look at the changes in the surface morphology. With smaller magnification, the changes can be examined in the overall appearance of the surface, and with greater magnification it is possible to get to the level of the individual grains. It is one of the best tools for evaluating the effect of cleaning on the substrate even though it is still necessary to compare the results with other methods of examination.

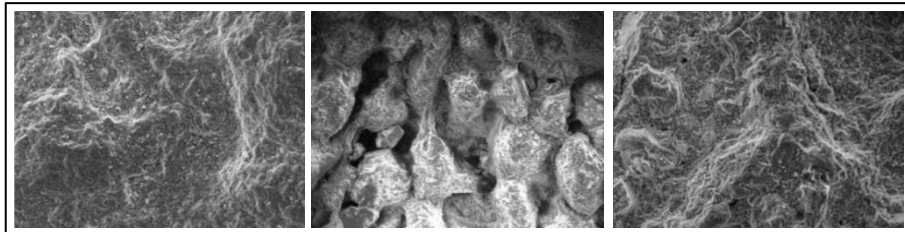


Fig. 3: SEM; magnified 200x. left: uncleaned; middle: micro-sandblasting; right: laser cleaning. This examination allows for the monitoring of changes in surface morphology. These changes have a fundamental effect on the behaviours of the surface in the future.

Elemental Analysis SEM –EDS: Some electron microscopes are equipped with a tool that allows for elemental analysis through energy-dispersive by an X-ray detector. The tool can be used for the analysis of the individual points, as well as on the entire monitored surface. Thanks to elemental analysis, it is possible to monitor the elemental composition of the deposits, or changes in elemental composition before and after cleaning, and to use this tool as a supplementary analysis for the evaluation of the sensitivity of the cleaning process and for characterizing the deposits.

2.3. Examining physical properties after cleaning

Measuring the water uptake of cleaned surfaces: It is common practice to assess the effect of cleaning on the basis of determining the physical-mechanical characteristics of the surface and their changes after cleaning. It concerns in particular the determination of the

capillary activity of the surface, i.e. of the capillary water uptake, which is essential for the restoration of natural properties that concern the transport of water and water vapour through the material. Their improvements further influence the successful implementation of further restoration interventions (e.g. consolidation, filling, retouches, etc.). It is carried out by determining the coefficient of capillary water uptake on laboratory samples of regular shape (e.g. drilling cores), or more often *in situ* using the Karsten tube by comparing the capillary flow or coefficient of capillary water uptake before and after cleaning on the given location (or by comparing to other cleaning methods and water uptakes on the fracture surface). Another significant characteristic is the assessment of water-vapour permeability and its changes after cleaning. However, this method cannot be implemented without the collection of a sufficiently large quantity of samples, for which reason it is not used in practice.

Peeling test: The so-called peeling test can be carried out in order to determine surface cohesion after cleaning. This test measures the cohesion of material in its lower layers, which is expressed as the quantity of material that remains stuck to adhesive tape. The test entails the application of both sided adhesive tape onto the substrate and in measuring the differences in weight before and after the application. This test is also a comparison test and it may provide information about a possible change in surface cohesion after cleaning (Drdáček 2012).

3. Conclusion

The presented methods do not, by far, include all the possibilities of assessing a cleaned surface. The methods had been selected with regard to their contribution to the assessment of the results of cleaning, and they are also limited by the author's experience with assessing cleaning trials. As far as optical methods are concerned, electron microscopy of a cross section or a thin section was omitted, even though it can surely provide important information. As regards other methods, certain information could be provided by measuring the morphology of the surface by means of a needle profilometer, or directly by a machine for the measurement of surface topography by means of a holographic microscope, the possibilities of which are currently being tested. Interesting comparison information could possibly be provided by a sensitive 3D scanner, which would scan the surface before and after cleaning. The limit of all these methods is that, as opposed to optical methods, the information about changes in, or loss of material is not closely linked to the possibility of examining to what extent this loss is limited to impurities, and to what extent it affects the original substrate. It is obvious that the examination and comparison of various instrumental methods which could provide relevant information about the effect of cleaning on the substrate is not concluded yet, nor can it be with regard to the development of new analytical methods.

Acknowledgements

This contribution is based on the findings and experience gained on the basis of a grant of the Ministry of Culture of the Czech Republic "Conditions and Requirements of Compatible Care for Porous Inorganic Materials" DF12P01OVV018.

References

- Andrew, C.A., Young, M.E. and Tonge, K.H., 1994, *Stone Cleaning: A Guide for Practitioners*, Historic Scotland and The Robert Gordon University. ISBN 0 7480 0874 8, 122pp.
- Ashurst, N., (1994), *Cleaning historic buildings*, Donehead, ISBN 18-733-9412-8, 258pp
- Drdácký, M., Lesák, J., Rescic, S., Slížková, Z., Tiano, P., and Valach, J., 2012, Standardization of peeling tests for assessing the cohesion and consolidation characteristics of historic stone surfaces, *Materials and Structures*, 45 (4), 505-520.
- Ďoubal, J., 2014, Research into the methods of Cleaning the Silicate Sandstones Used for Historical Monuments, *Journal of Architectural Conservation*, 20 (2), 123-138.
- Fassina, V., 1994, General criteria for the cleaning of stone: Theoretical aspects and methodology of application. In *Stone Material in Monuments: Diagnosis and Conservation*, Mario Adda (ed.), Heraklion, Crete, Scuola universitaria C.U.M. conservazione dei monumenti, 131–138.
- Goreczky, L. and Hoffmann, M. 1997, WTA 3-9-95-D: Bewertung von gereinigten Werksein – Oberflächen=Assessment of cleaned stone surfaces. Baierbrunn: WTA publications.
- Hauff, G., Kozub, P. and D'Ham, G., 2008, Which cleaning method is the most appropriate one? A systematic approach to the assessment of cleaning test panels in 11th International Congress on Deterioration and Conservation of Stone, Niemcewicz P. (red.), Torun, Poland, Uniwersytetu Mikołaja Kopernika, 381–388 .
- Kapsalas, P., Maravelaki-Kalaitzaki, P., Zervakis, M., Delegou, E. T. and Moropoulou, A., 2007, Optical inspection for quantification of decay on stone surfaces. *NDT & E International*, 40, 2–11.
- Martínez-Arkarazo, I., Sarmiento, A., Usobiaga, A., Angulo, M., Etxebarria, N., and Madariaga, J.M., 2007, Thermodynamic and Raman spectroscopic speciation to define the operating conditions of an innovative cleaning treatment for carbonated stones based on the use of ion exchangers, *Talanta*, 75(2), 511-516.
- Normandin, K.C., Weiss, N.R. and Slatonm, D., (2005), *Cleaning techniques in conservation practice*, Donhead, ISBN 978-187-3394-748, 146pp.
- Potgieter-Vermaak, S.S., Godoi, R. H. M., Van Grieken, R., Potgieter, J.H. , Oujja, M., and Castillejo, M., 2005, Micro-structural characterization of black crust and laser cleaning of building stones by micro-Raman and SEM techniques, *Spectrochimica Acta Part A: Molecular and Biomolecular Spectroscopy*, 61(11-12), 2460-2467.
- Verges-Belmin, V., 1996, Towards a definition of common evaluation criteria for the cleaning of porous building materials, *Science and Technology for Cultural Heritage*, 5, 69-83.
- Werner, M., 1991, *Research on cleaning methods applied to historical stone monuments in Science, technology, and European cultural heritage: proceedings of the European symposium*. Boston: Published for the Commission of the European Communities by Butterworth-Heinemann Publishers, 688–691.

THE NATURAL WEATHERING OF AN ARTIFICIALLY INDUCED CALCIUM OXALATE PATINA ON SOFT LIMESTONE

T. Dreyfuss^{1*} and J. Cassar¹

Abstract

This paper focuses on the effects of natural weathering on Globigerina Limestone (Malta) which was treated with ammonium oxalate to produce a calcium oxalate surface layer. This study includes the first two phases of a larger research programme. Laboratory samples were considered first. These were treated and tested in a controlled environment (Phase 1). Identical samples sets were prepared for Phase 2. These were treated *in situ* and exposed to site conditions for the period of one year. In an attempt to simulate site conditions, for both Phase 1 and Phase 2 samples, the limestone was contaminated with soluble salts before treatment took place. These included three separate types; sodium chloride, sodium sulfate and sodium nitrate. Desalinated samples were also included in the study. Scanning Electron Microscopy (SEM) was carried out on the Phase 1 samples while Drilling Resistance Measurement System (DRMS) was carried out on the samples of both phases. This paper focuses on the results from the SEM and correlates these with those results from the DRMS in light of the influence of natural weathering on an artificial calcium oxalate layer, induced in the presence of soluble salts.

Keywords: oxalates, consolidation, protection, limestone, treatment durability

1. Introduction

The Maltese Islands, a small island archipelago measuring 316 square kilometres and located 93km south of Sicily and 288km north of Africa have a large collection of historic limestone buildings and monuments that span the millennia. These are built in Maltese Globigerina Limestone - a highly porous calcareous stone which naturally deteriorates in an environment that is exposed to both water and soluble salts. These buildings and monuments inevitably require conservation action at certain points in their lifetime which may include consolidation and/or protective treatments. Many of the historic stone edifices (pre-1850s) in Malta and Gozo were built without the insertion of a damp proof course, thus allowing water entry in the form of rising damp together with any soluble salts present. Additionally, wall construction generally utilised soil infill, usually salt laden, between two masonry wall leaves. The island environment further enhances salt contamination through wind driven and aerosol borne salts. The context is therefore a porous limestone which has a continual supply of water and soluble salts.

¹ T. Dreyfuss* and J. Cassar

Department of Conservation and Built Heritage, Faculty for the Built Environment,
University of Malta, Malta
tdrey01@um.edu.mt

* corresponding author

Consolidation of exposed Globigerina Limestone which has lost cohesion, manifested as powdering/ granular disintegration, must therefore take this context into account. The aim must be to bridge the loose powder/ grains together and to the sound stone beneath with a compatible material that retains both the water and salt transport properties of the stone that is being consolidated. Ammonium oxalate treatment on calcareous stone has been studied as a surface treatment providing protection from acid attack together with possible consolidating properties (Matteini *et al.*, 1994; Matteini 2007), even on Globigerina Limestone (Croveri 2004; Mifsud *et al.*, 2006; Dreyfuss *et al.*, 2012 and 2013), which to date has revealed promising results suggesting its potential use in this respect. The actual study of ammonium oxalate treatment on Globigerina Limestone *in situ* and its relationship with soluble salts present in the stone was the next step. This was to take this research to a point where the actions and mechanisms of ammonium oxalate treatment are understood in terms of the parameters presented by a historical building. The two parameters identified here are the presence of salts and site exposure whilst stone pathology is considered in other parts of the larger research project (Phase 3). To this end, the parameters included here were desalinated versus salt contaminated conditions and controlled versus uncontrolled environments.

2. Methodology

2.1. Globigerina Limestone

The material considered, Globigerina Limestone, of the *franka* type (Cassar 2004), is a fine-grained limestone, sedimentary in origin with few to abundant fossils including planktonic and benthonic foraminifera especially globigerinae which is from where it gets its name. It is primarily composed of calcium carbonate in the form of calcite crystals cemented together by non-crystalline calcium carbonate. Besides calcite, Globigerina Limestone also contains clay minerals, quartz, feldspars, apatite and glauconite. A large part of the clay minerals consists of kaolinite with smectite, illite-smectite, illite and vermiculite also being present (Cassar 2002). The porosity is high and varies between 24% (Cassar 2004) and 41% (Cassar *et al.*, 2001) whilst the majority of pores $\leq 4 \mu\text{m}$ (Vannucci *et al.*, 1994).

2.2. Sample preparation

The samples were prepared as $50 \times 50 \times 10 \text{ mm}^3$ (for the SEM samples) and $50 \times 50 \times 50 \text{ mm}^3$ (for the DRMS samples) cut from stone blocks (approximately $w=410 \text{ mm} \times D=230 \text{ mm} \times H=267 \text{ mm}$) obtained from the quarry area known as *Ta' l-Iklin* in Qrendi (coordinates 51,500; 66,500) at a depth of 12 m below ground level. The horizontal (downward facing direction) bedding plane was noted in all cases and retained as the treatment and testing surface for all samples.

The samples consisted of quarry samples with different salt contents, namely desalinated samples, samples contaminated respectively with saturated solutions of sodium chloride, sodium sulfate and sodium nitrate. Desalination was carried out by immersion of the samples in distilled water, repeatedly changing the water until its conductivity revealed that soluble salts were no longer present ($\leq 3 \mu\text{S/cm}$). All of the samples were thus desalinated and then oven dried for 24 hours at a temperature of 105°C then cooled in the laboratory to constant mass at 20°C room temperature. One fourth of the samples were then retained to represent the desalinated type samples, while the remaining samples were divided into three sets and each set was salinated with a saturated solution of sodium chloride, sodium sulfate

and sodium nitrate respectively by immersion for 2 hours. Following immersion, the samples were air dried.

2.3. Ammonium oxalate treatment

Treatment was carried out to all sides of the samples using a 5% ammonium oxalate monohydrate solution applied in a cellulose pulp poultice for 24 hours at 20°C; conditions were 74% RH in the case of the laboratory samples and at 26°C, 70% RH on site. Following treatment the poultice was manually removed and the samples left to air dry. The excess pulp was brushed off with a soft nylon brush. Untreated samples were prepared for all treated sample types.

2.4. Site exposure

The one-year site exposure of the Phase 2 samples included temperatures ranging from 5.6°C to 37.5°C, a total rainfall of 350.7 mm, 3059.4 hours of sunshine, an average Relative Humidity of 72.4%, 35 days with thunderstorms, 12 days with hail, 4 days with fog and 4 days with “dust haze”. The samples were retrieved after one year for DRMS testing which was carried out in a laboratory.

3. Testing

The Scanning Electron Microscopy (SEM) samples measured 10×10×10 mm³ and were cut out of the larger 50×50×10 mm³ samples using a surgical blade. The treated and untreated samples were examined under identical magnifications for each sample type, for direct comparison at ×100 and ×2000. The surface morphology, surface topography, surface features, surface texture, and crystal arrangement were analysed.

Drilling Resistance Measurement System (DRMS) was carried out on the 50×50×50 mm³ cube samples. The depth of the calcium oxalate layer was evaluated through the Drilling Resistance Measurement System (DRMS). Desalination was carried out before DRMS testing for all samples that were treated with ammonium oxalate in the presence of a soluble salt. In the case of untreated samples however, salt free and salinated types were tested.

4. Results & discussion

The DRMS results for the Phase 1 samples revealed a treatment depth of up to 1.60 mm for samples treated in a salt free environment and 0.70 mm - 1.00 mm in the case of samples treated in the presence of the soluble salts considered. The depths for the Phase 2 samples were 0.80 mm in the first instance and 0.70 mm - 0.90 mm in the second (Dreyfuss *et al.*, in preparation). Therefore, while salt-free conditions induced deeper formations with treatment (1.60 mm) when compared to salinated conditions (0.70 mm-1.00 mm), this depth was reduced (from 1.60 mm to 0.80 mm) over the year of site exposure which indicates that the calcium oxalate formed in this sample type was being weathered away. Conversely, the depths achieved with treatment in salt-contaminated conditions (0.70mm-1.00 mm) were still maintained one year after exposure (0.70 mm-0.90 mm), possibly suggesting improved durability.

The maximum drilling resistances at the corresponding depths of treatment were also recorded. The results showed that the increased depths of 1.60 mm in the samples treated in a salt-free environment were coupled with reduced values of drilling resistance (13.52 N) when compared to those samples treated in the presence of soluble salts which had

shallower treatment depths (0.70 mm-1.0 mm) but a greater drilling resistance (14.79 N-21.62 N), (Dreyfuss *et al.*, in preparation). This implies that the newly formed calcium oxalate in the salt contaminated samples has improved strength characteristics when compared to the calcium oxalate formed in salt-free environments. These DRMS results were further analysed and correlated to SEM observations as discussed below.

For SEM analysis a Merlin FESEM with Carl Zeiss optics and Gemini II column (s/n: 4216) was used. In the SEM images of the desalinated untreated samples at $\times 100$, individual calcite crystals/granules were observed together with globigerinae and other fossils. In the treated samples, the microfossils were still visible and the previously individual crystals/granules were seen to be more compact. These findings suggest that treatment results in an improved and more compact surface texture without blocking the globigerinae/fossils. At higher magnifications ($\times 2000$) the desalinated untreated samples showed that individual crystals/granules (A) were clearly distinguishable, (Fig. 1). In the treated samples (Fig. 2), the newly formed calcium oxalate was observed to take the form of flat crystals/plates which were arranged in a layered arrangement/stacked parallel to the sample surface (B). This arrangement is schematically illustrated in Fig. 4.

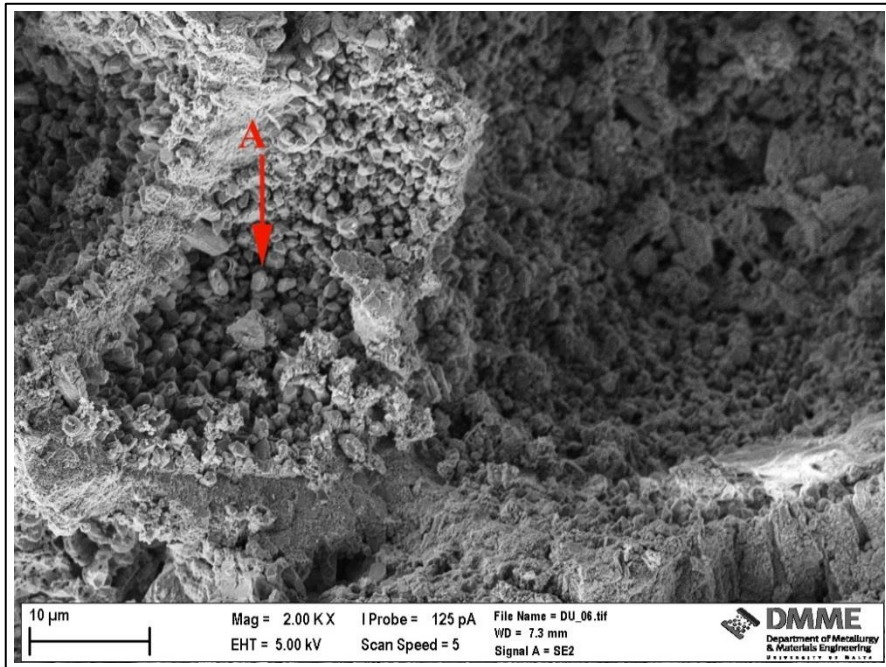


Fig. 1: SEM image ($\times 2000$) for desalinated untreated laboratory sample.

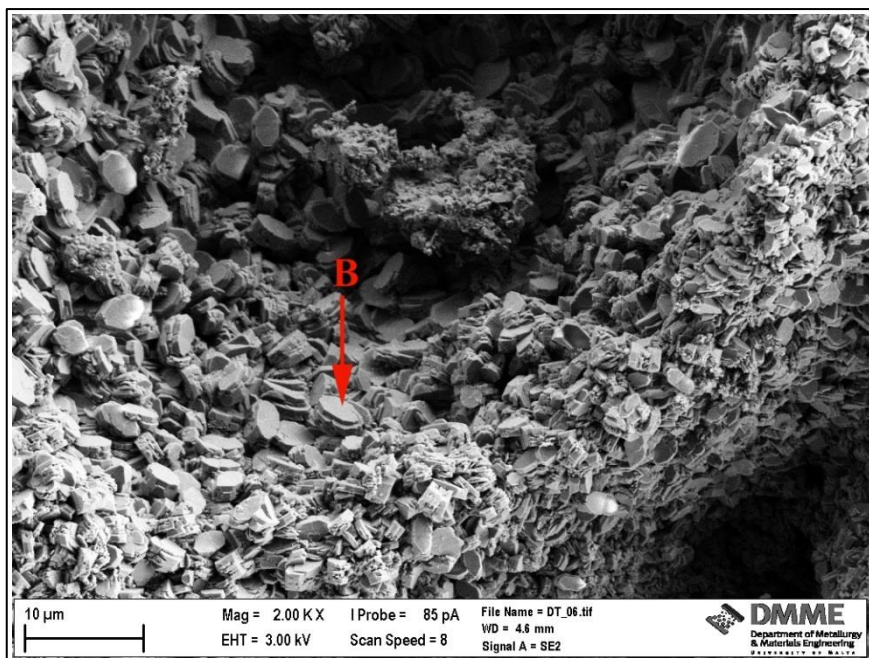


Fig. 2: SEM image (x 2000) for desalinated treated laboratory sample.

In the untreated salt contaminated samples, salt crystals were seen to completely cover the sample surface in the sodium chloride and sodium nitrate contaminated samples respectively. Sodium sulfate was also seen to substantially cover the sample surface although to a lesser extent since globigerinae were still visible after salt contamination. These findings confirm that salt contamination has a “pore blocking/coating” effect which probably inhibits the ammonium oxalate from penetrating deeper resulting in shallower calcium oxalate formations as observed in the DRMS results above.

After treatment, the amount of surface salt was seen to be greatly reduced in the sodium chloride and sodium sulfate contaminated sample types. The reduction in surface salt in the sodium nitrate contaminated samples was seen to occur to a lesser extent (C in Fig. 3) confirming the blocking/coating behaviour of this salt, also seen in the results from the DRMS where surface salt concentrations were still present after one year of site exposure (Dreyfuss *et al.*, in preparation). These conclusions indicate a reduction in salt content during treatment probably through the water-based poultice.

The morphology observed in the treated, salt contaminated samples showed calcium oxalate to be formed in a different configuration to that developed in the desalinated samples. The calcium oxalate was observed as individual crystals (not layered) which were organised in a vertical arrangement (not horizontal), predominantly perpendicular (not parallel) to the sample surface (D in Fig. 3). This configuration, which is schematically illustrated in Figure 5 may be understood to withstand erosion and natural weathering better than the arrangement of calcium oxalate formed in salt-free conditions (Figure 4), where the configuration may be more susceptible to erosion. The difference between the newly formed calcium oxalate crystal orientation in relation to the salt conditions during treatment

is currently being investigated further. This physical difference in calcium oxalate crystal orientation may account for the reduced depths, the increased drilling resistance and the improved durability achieved in salt laden samples.

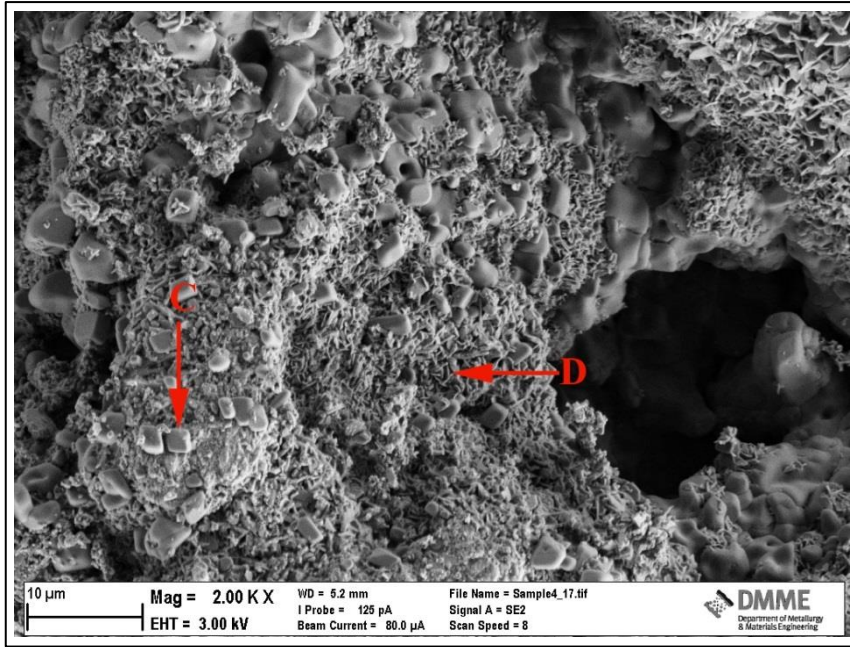


Fig. 3: SEM image (x 2000) for sodium nitrate contaminated treated laboratory sample.

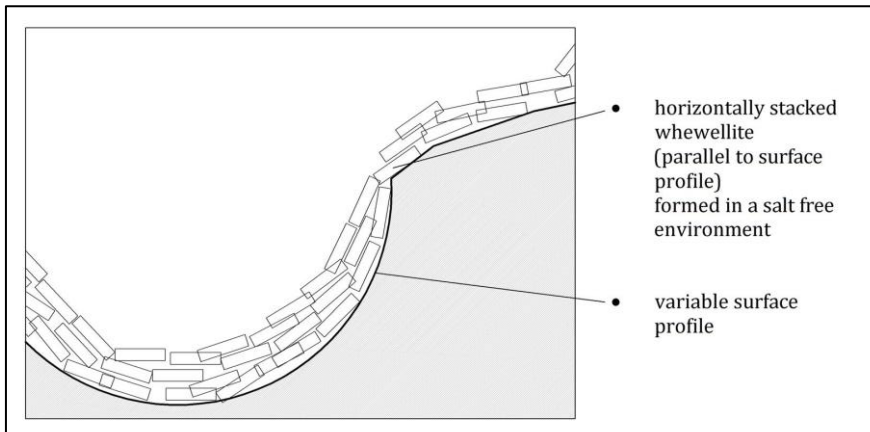


Figure 4: Schematic illustration of the whewellite formed in salt free environments.

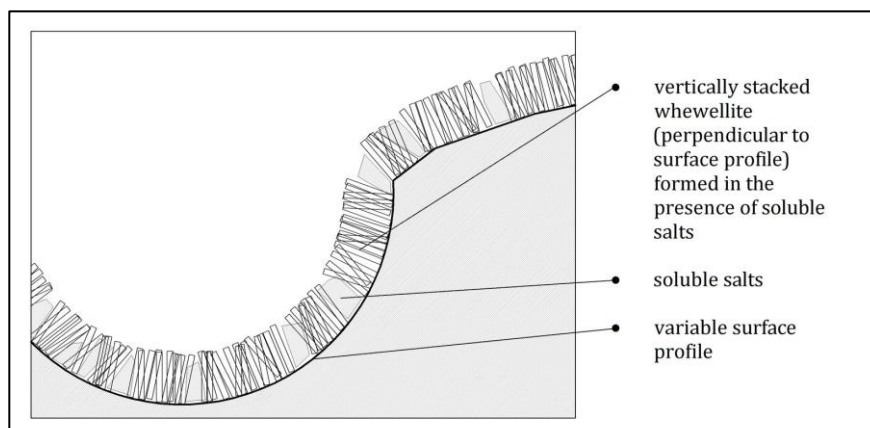


Figure 5: Schematic illustration of the whewellite formed in the presence of soluble salts.

5. Conclusions

When compared to treated desalinated samples of the same type, the treated salt contaminated samples recorded shallower calcium oxalate depths and higher values for the drilling resistance. This resulted in an increased durability during the one year of site exposure, after which the depth of induced “hardness” decreased from a range of 0.70 mm to 1.0 mm to a range of 0.70 mm to 0.90 mm. In the desalinated samples this decreased from 1.60 mm to 0.80 mm. This difference was explained through the SEM images where calcium oxalate was seen to form in horizontally stacked layers, parallel to the sample profile, in the desalinated samples, the physical configuration of which is probably differently susceptible to erosion. The calcium oxalate formed in the presence of soluble salts was arranged in a vertical manner, perpendicular to the sample profile, creating an interlocked network of whewellite crystals. Further research into the reasons for this varying orientation, as well as treatment and testing of exposed historic limestone is currently ongoing.

Acknowledgement

The authors widely appreciate the fact that this research work is being funded by the REACH HIGH Scholars Programme – Post-Doctoral Grants. The grant is part-financed by the European Union, Operational Programme II — Cohesion Policy 2014- 2020 Investing in human capital to create more opportunities and promote the wellbeing of society - European Social Fund. Furthermore, the authors would like to express the gratitude towards the Department of Metallurgy and Materials Engineering, Faculty of Engineering, University of Malta for carrying out the SEM analysis under the direction of Ing. J. Camilleri funded under ERDF (Malta) through the project: “Developing an Interdisciplinary Material Testing and Rapid Prototyping R&D Facility (Ref. no. 012)”. Further thanks also to Dr Silvia Rescic at the CNR-ICVBC (Consiglio Nazionale delle Ricerche Istituto per la Conservazione e Valorizzazione dei Beni Culturali) in Florence, Italy for assisting us with the Drilling Resistance Measurements was carried out under the direction of.

References

- Matteini, M., Moles, A., Giovannoni, S., (1994). Calcium oxalate as a protective mineral system for wall paintings: methodology and analyses. In: 3rd International Symposium on the Conservation of Monuments in the Mediterranean Basin, Venice, Italy, pgs 155-162.
- Matteini, M., (2007). Conservation of stone monuments and artefacts: new possibilities offered by the ammonium oxalate based treatment. <http://www.eu-artech.org/files/CUBA/MATTEINI.pdf>
- Croveri, P., (2004). Metodologie di consolidamento di materiali lapidei nell'area Mediterraneo: La Globigerina Limestone maltese – degrado e consolidamento. Dottorato di Ricerca in Scienza per la Conservazione dei Beni Culturali XVII ciclo, Università degli Studi di Firenze, unpublished.
- Mifsud, T., Cassar, J., (2006). The treatment of weathered Globigerina Limestone: the surface conversion of calcium carbonate to calcium oxalate. Proceedings of Heritage, Weathering and Conservation, Madrid, pgs 727-734.
- Dreyfuss, T., Cassar, J., (2012). The performance of an induced calcium oxalate surface on Globigerina Limestone. In: 12th International Congress on the Deterioration and Conservation of Stone, New York.
- Dreyfuss, T., Cassar, J., (2013). Ammonium oxalate treatment application in the presence of soluble salts: laboratory results on soft limestone. Built Heritage 2013 Monitoring Conservation Management, Milan, pgs 403-412.
- Cassar, J., 2002. Deterioration of the Globigerina Limestone of the Maltese Islands. In: Siegesmund, S., Weiss, T., and Vollbrecht, A. (eds). Natural Stone, Weathering Phenomena, Conservation Strategies and Case Studies, Geological Society London, London, 2005, pgs 33-49.
- Cassar, J., (2004). Composition and property data of Malta's building stone for the construction of a database. Architectural and Sculptural Stone in Cultural Landscape, R. Prikrl, Siegl, P. (Eds), The Karolinum Press, pgs 11-28.
- Cassar, J., Vannucci, S., 2001. Petrographical and chemical research on the stone of the megalithic temples. In: Malta Archaeological Review, 5, pgs 40-45.
- Vannucci, S., Alessandrini, G., Cassar, J., Tampone, G., Vannucci, M.L., 1994. Templi megalitici Preistorici delle isole Maltesi: cause e processi di degradazione del Globigerina Limestone. In: Fassina, V., Zezza, F., (Eds), 3rd International Symposium, "La Conservazione dei Monumenti nel Bacino del Mediterraneo, Venezia, Italia, pgs 555-565.
- Dreyfuss, T., Cassar, J., (in preparation). Consolidation of a soft and porous limestone: from the laboratory to the field.

A COMPARISON OF THREE METHODS OF CONSOLIDATION FOR CLACEROUS MIXED STONES

J. Espinosa-Gaitán^{1*} and A. Martín-Chicano²

Abstract

In this paper, three stone conservation treatments (alcoxisilanes (TEOS), a combination of nanolime and TEOS, and microbial carbonate precipitation) have been studied on Puerto stone, a biocalcarenite with a high presence of coarse quartz grains, high porosity and low cementation. Several tests were undertaken in order to evaluate and compare the effectiveness of these treatments, according to EU standards where possible, and following the most commonly used procedures found in the literature. Changes in colour and appearance, porosity and hydric properties (water absorption, water desorption, water vapour permeability) of the stone caused by treatments were measured, in order to determine their compatibility with the stone. The performance of the products was evaluated using various tests, such as microdrilling (DRMS), measurement of ultrasound pulse velocity (UPV), and peeling test. In addition to that, samples were analysed using scanning electron microscopy (SEM/EDS), providing graphic information of how consolidants were deposited on the stone surface. This first set of results show that the combination of nanolime and TEOS offers the best performance as stone consolidant.

Keywords: stone consolidation, TEOS, nanolime, biomineralization, Puerto stone

1. Introduction

There is no doubt that consolidation is one of the most important actions to be taken when approaching the conservation of built heritage. Building materials are exposed to a broad variety of elements which may alter their nature, making them weaker and more susceptible to decay, endangering the structure (Young *et al.* 1999, Wheeler 2005, Doehne & Price. 2010). Many solutions have been offered from ancient times, using different substances with the goal of restoring materials their original properties. Stones have been treated with beeswax, plants extracts or limewash, and a great variety of synthetic substances, resulting in different degrees of success. Consolidation aims at restoring cohesion, compactness and mechanic properties to aged stone, without significantly altering other properties such as colour and hydric properties.

This work aims to determine what consolidant is more suitable for a calcareous mixed stone (Puerto stone) that was used as building material in several monuments in SW Spain. There are several stone consolidants commercially available, although not all of them are used

¹ J. Espinosa-Gaitán*

Andalusian Institute of Cultural Heritage (IAPH), Seville, Spain
jesus.espinosa@juntadeandalucia.es

² A. Martín-Chicano

University of Granada, Spain

*corresponding author

with the same frequency for different reasons. It was important for the study to test consolidation products that were easy to apply, available, affordable, and with low or null toxicity. After carrying out a characterisation of the stone, three consolidation treatments were considered to be tested: alcoxisilanes, nanolime, and biomineralization. Alcoxisilane based consolidants are the most popular ones. These products are applied diluted in a volatile solvent, and once the solvent evaporates a sol-gel reaction occurs, leading to polymerisation inside the pores of the stone, consolidating the damaged material (Wheeler 2005). These products are easy to use, affordable and fairly efficient, in spite of presenting some problems such as cracking of the silica layer, or incompatibilities when there is presence of clay or carbonates in the stone. Lime is a natural choice for carbonate stones, although its low penetration rate is an issue, a problem that was solved with the use of nanolime. Due to their size, nanolime particles are able to penetrate more deeply into the stone matrix. Its use is based on the reaction of calcium hydroxide with atmospheric carbon dioxide in presence of water, resulting in precipitation of calcium carbonate inside the damaged stone. A combination of alcoxisilanes and nanolime has been proposed as a consolidation method with better results than the two methods separately (Ziegenbalg and Piaszczyński 2012). The third tested method consists of inducing the deposition of a calcium carbonate layer on the surface of the stone, generated by some microorganisms under the right conditions. Two approaches to this method have been proposed, one takes advantage of the existing microbiota in the stone (Jiménez-López et al 2007), applying only a nutrient solution to the damaged stone, whereas a nutrient solution containing bacteria is sprayed onto the surface of the stone in the other method. The three consolidation methods were tested in the laboratory.

2. Experimental: Material and Methods

2.1. Stone

The material subject of the present study is Puerto stone, a biocalcarenite with a high presence of coarse quartz grains (30-40%), high porosity (>30%) and low cementation. It is a very soft and crumbly rock. This stone is extracted from the San Cristobal quarries, in Cádiz, SW Spain (Jiménez-Pintor *et al.* 2002), and has been extensively used in the construction of several monuments in the area, such as the Cathedral of Seville, Cathedral and Cartuja of Jerez, etc. It is an Upper Miocene ivory colour biosparite (Folk 1965), with a large proportion of clastic particles (30-40%), basically formed of coarse quartz grains and microfossils (bryozoans, algae and foraminifera). The cement of the rock is sparry calcite, representing 50-60% in the most compact varieties. This is a highly porous stone with an open porosity of about 35%, predominantly macropores.

Samples for this study were obtained from two fragments of decontextualized ashlar found in the Cartuja de Jerez, belonging to a demolished part of the building. This fact is very important for the study, because samples present the same characteristics and degree of alteration than the actual stone in the building, making results even more relevant than if samples had been obtained from freshly extracted stone from the quarry.

Two types of test specimens were obtained from the ashlar, planar samples of 4×4×2 cm, and cubic samples of 4 cm edge according to the recommendations of European standards for testing materials of Architectural Heritage (CEN/TC-346 Conservation of Cultural Property: Test methods). The stone in this monument is deteriorating mainly on its surface

by granular disaggregation, sanding, scaling, loss of cement, biological attack, efflorescence, and cracks (ICOMOS-ICMS, 2008), so a consolidation process is needed.

2.2. *Treatments and application procedure*

The method of application of treatments replicate the way these products are applied in situ, so results could relate as much as possible to a work situation rather than to a laboratory environment (Young *et al.* 1999, Theoulakis *et al.* 2008). Application with flat brush was chosen, being one of the most widespread in the field of conservation and restoration. Cubic samples were treated on all sides, while planar samples were treated only on one of the squared sides, depending of the type of test to be performed.

The treatments and mode of application are:

W (SILRES® BS OH 100 (Wacker)): Ethyl silicate as supplied by the manufacturer. Three applications with a flat brush with a 15 min interval between each application under laboratory conditions ($T=23\pm 2^{\circ}\text{C}$ and $RH=50\%\pm 5\%$).

NR+W (NANORESTORE® (C.T.S) + SILRES® BS OH 100 (Wacker)): Nanorestore is supplied as a dispersion of nanolime particles in isopropyl alcohol. Application procedure as follows: an ethanol:water solution (1:1 v/v) solution was applied to samples in order to facilitate the absorption of the consolidant. Nanorestore was applied afterwards with a flat brush, three times with a 15 min. interval. 24 hours later SILRES OH was applied in the same way.

KBYO I and **KBYO II** (KBYO Biological): Nutrient aqueous solution. I and II refers to the same product obtained under two different fabrication methods. Samples were treated at the manufacturer's facilities, according to the method developed and optimised there.

2.3. *Laboratory tests*

The methodology for assessing the efficiency of the treatment was based on the study of issues related to compatibility and effectiveness of treatment (The Charter of Krakow, 2000). Samples were cleaned and left to dry in the oven for 24 hours at 60°C . Treatments were applied according to the method previously described, and samples were left on a rack at laboratory conditions for three months. UNE-CEN standard tests for conservation of cultural heritage were performed when possible, following procedures for natural stone when unavailable. Otherwise, proposed tests in literature were carried out.

2.3.1. *Compatibility*

Measurement of colour was done according to UNE-EN 15886 procedure, with a Minolta CR-200 colorimeter (diffused lighting, 0° viewing angle, specular component included, and D65 standard illuminant). Results are expressed according to the CIE $L^*a^*b^*$ colour space (CIELAB 1976), that measures three aspects of the object chromaticity. The parameter ΔE^* ($\Delta E^* = \sqrt{(\Delta L^*)^2 + (\Delta a^*)^2 + (\Delta b^*)^2}$) provides an idea of global colour change by the difference in values before and after treatment. When its value exceeds 5 it is assumed that change is perceptible by the human eye (Delgado-Rodriguez and Grossi 2007, Pérez-Ema *et al.* 2013).

The change in *Open porosity* values was obtained following the procedure described in UNE-EN 1936: 2006, measuring water content under pressure. *Determination of drying properties* test was performed according to EN 16322:2013-1 standard. The test is

performed on cubic specimens placed on a grid, so that evaporation affects all sides equally. *Water absorption by capillarity* was performed following standard UNE-EN 15801: 2010, also on cubic specimens. *Water vapour permeability* changes (WVP) were evaluated following standard UNE-EN 15803:2010. Planar samples were used for this test. Samples were fitted to the lid of a plastic container of similar dimensions, half filled with silica gel for dry test mode, or a saturated KNO₃ solution for wet test mode. Water vapour may only go through the stone samples, so the lid is sealed with Permagum, a waterproof sealant.

2.3.2. Effectiveness

The *ultrasound pulse velocity* test was carried out following the UNE-EN14579: 2005 standard. This technique has been successfully used in determining the effectiveness of stone consolidation treatments (Sebastián *et al.* 1999, Pérez-Ema *et al.* 2013). The equipment was a Ultrasonic Steinkamp BP-7 tester, with a wave frequency of 40 MHz. Measurements were determined in the three perpendicular directions of the specimens, in order to avoid any anisotropy. Values from 15 samples in total were obtained, and the media of each group of specimens was calculated.

The *Peeling tape test* was performed in order to establish the granular cohesion degree of the stone surface and the treatments effects. This test is a method for evaluating the adhesion of a coating to a substrate. A pressure-sensitive tape is applied to an area of the surface. In this case recommendations suggested by Drdácĕy *et al.* (2012) were followed, due to the absence of published standards. This process was carried out on two sides of each sample, three strips per side, and the average was calculated for each type-group of specimens.

Finally, the *DRMS test* (Drilling Resistance Measurement System) was performed, in order to measure the resistance of the stone to be perforated with a drill, keeping a constant rotation speed and degree of penetration of the drill throughout the test duration. The equipment was a DRMS Cordless Version 4 device, manufactured by SINT Technology, with a 5 mm diameter drill. Test conditions were established at 300 rpm rotational speed, 20mm/min of penetration rate, and 20 mm penetration depth. The test was performed on one specimen of each group, making three perforations on two opposite sides of each specimen.

In addition, surface-coating characteristics, distribution of the treatments, and microtexture of stone before and after being treated with consolidants were identified with a *Scanning Electronic Microscopy (SEM)* using a JEOL JSM-5600LV microscope with a wolfram filament and an X ray energy dispersion microanalysis system (EDS) Inca x-sight from Oxford Instrument.

3. Results and discussion

3.1. Compatibility

Hydric properties results indicate that Puerto stone has a water accessible porosity of 33%, presenting a high water absorption rate (4cm high samples reach saturation in 2.5 minutes). Drying rate is also high, about 90% of water content evaporates in one day. This might be caused by its open porosity which makes absorption and evaporation of water fairly easy. Tab. 1 presents changes in water content under pressure and open porosity for treated and untreated samples.

Tab. 1: Water content (W_{max}) and open porosity values.

Property	Untreated	NR+W	W	KBYO I	KBYO II
W_{max} under vacuum (weight-%)	18.37	14.26	16.21	18.05	17.25
Open porosity (volume-%)	33.41	26.95	29.71	32.47	31.42

There is a general decrease in open porosity values and water content, higher for the *NR+W* treated sample, which may be caused by the closure of smaller pores by the action of consolidants. These samples show the same behaviour in the capillary absorption test, reaching saturation at an earlier stage than the other treatments. The drying rate is not altered, and samples lost about 90% of water in a day. The water vapour permeability test showed little change in the values of the permeability coefficient before and after treatment, very similar in all cases.

Variation in *Colour* is presented in Tab. 2. A value greater than 5 for ΔE^* means that the change in colour is visible for the human eye. Results show that none of the treatments alter this property significantly.

Tab. 2: Change in colour parameters.

Treatment	ΔL^*	Δa^*	Δb^*	ΔE^*
W	-1.76	0.43	1.55	2.38
NR+W	-0.66	0.50	1.84	2.02
KBYO I	-0.22	0.26	1.28	1.32
KBYO II	-1.64	0.41	1.82	2.48

3.2. Effectiveness

Results obtained by the *Ultrasound Pulse Velocity* show higher UPV values for all treated samples compared to untreated specimens. A higher velocity means more compactness, and it is related to a decrease in open porosity. This is very clear for *W* and *NR+W* treatments, but not so for *KBYO*, where open porosity values were similar to those for untreated stone.

The *Drilling resistance measurement (DRMS)* test usually offers consistent results for homogeneous rocks, but not for polymineral, heterogeneous ones, like Puerto stone. The resistance to perforation varied greatly for the same sample as the test was being carried out, with a great value dispersion as a result of the variety of minerals and compactness within the rock, which made very difficult to quantify this property. In spite of this limitation, an index of global resistance “F” (Newton) for each group of samples was determined and its standard deviation (σ) was established, considering the average values of all the measurements from 1 mm to 20 mm of depth. The results obtained were: *Untreated*: F (3.49), σ (1.18); *NR+W*: F (6.50), σ (1.58); *W*: F (5.48), σ (1.68); *KBYO I*: F (4.21), σ (1.00) and *KBYO II*: F (4.80), σ (1.29). It could be observed that *NR+W* offered greater resistance to perforation than the rest of them.

The *Peeling test* gives best results for *NR+W*, as shown in Fig. 1. All these treatments improved the cohesiveness of the damaged stone, giving away less matter on the adhesive tape.

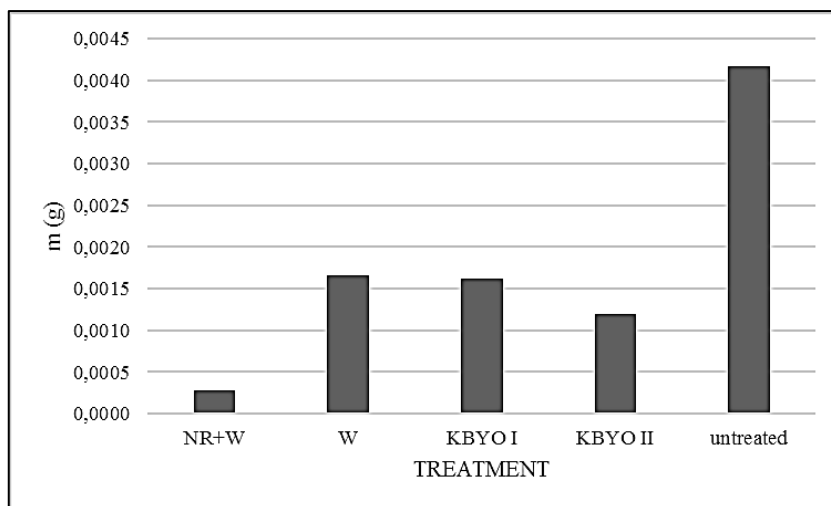


Fig. 1: Mass of adhered matter on adhesive tape for each treatment.

3.3. Microscopic observation

SEM images allow the observation of how the products are deposited on the stone surface. Fig. 1 shows the *NR+W* (a and b) and *W* (c and d) samples. A layer of product can be observed, presenting a similar aspect, even with the appearance of some cracks in the layer.

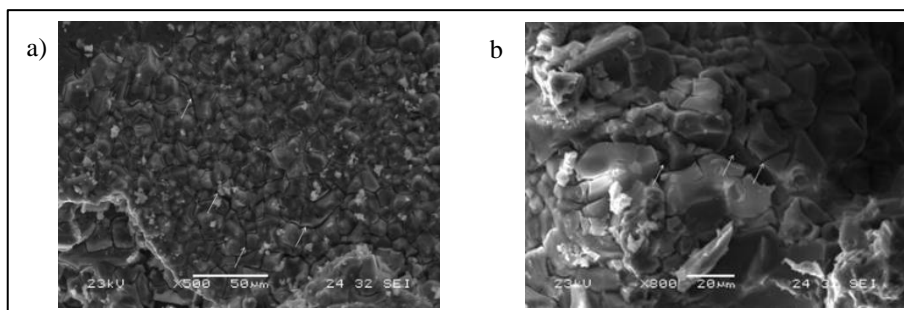


Fig. 1: SEM-EDX images of treated stone (a for *NR+W* and b for *W*).

Images for *KBYO* treated samples show a similar aspect to untreated samples, as can be seen in Fig. 2, which could explain the apparently little effect these treatments have on this stone. Some spheroid granules could be observed (b image), maybe caused by the treatment, although this was not tested.

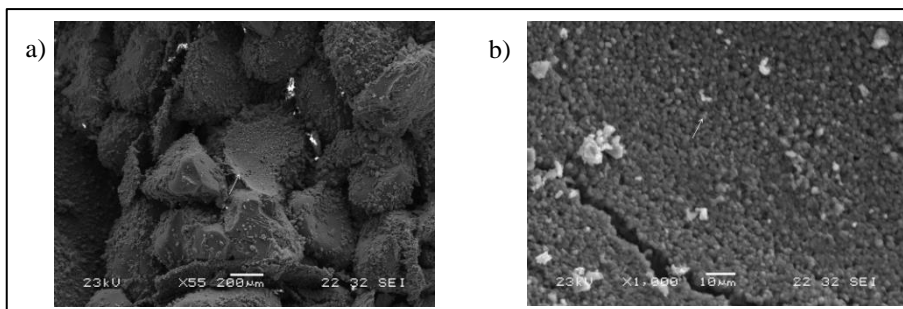


Fig. 2: SEM-EDX images of KBYO I (a) and KBYO II (b) treated samples.

4. Conclusions

In this work, the effectiveness of three consolidation treatments has been tested on Puerto stone, by looking at changes in hydric properties of the stone, its colour and appearance, cohesion, compactness, and resistance to perforation, before and after the application of the treatments. Results obtained from the tests show that the most effective treatment is **NR+W**, that is, the combination of Nanorestore and Wacker OH, since it did not alter hydric properties and colour significantly, and improved compactness, cohesion and resistance to perforation. It is easy to apply, safe and does not require specific instruments or installations strange to any standard intervention. The presence of microfractures in the silica gel layer three months after the application of the product is, however, a fact worth studying so it can be avoided.

Results obtained for the biomineralization treatments (**KBYO**) do not match those published for a different type of carbonatic stones (Jiménez-López *et al.* 2008, Jroundi *et al.* 2010), being in this case most unexpected. This suggests that either this treatment does not suit this stone or the application method must be tailor made to the stone characteristics, which could indicate the need to optimize the method according to the characteristics of each type of stone.

Finally, it is necessary to stress the importance of carrying out preliminary tests before performing an intervention on any heritage object. An evaluation study of the candidate treatments in order to assess the best possible one allows more accuracy in interventions.

References

- Delgado-Rodriguez, J. and Grossi, A. (2007): Indicators and ratings for the compatibility assessment of conservation actions. *Journal of Cultural Heritage*, 8(2007), 32-43
- Doehne, E. and C.A. Price. 2010. Stone Conservation: An overview of current research. Second edition. *The Getty Conservation Institute*. Los Angeles.
- Drdáček M., J. Lesák, S. Rescic, Z. Slížková, P. Tiano and J. Valach. 2012. Standardization of peeling tests for assessing the cohesion and consolidation characteristics of historic stone surfaces. *Materials and structures*, 45:505-520.

- Folk, R.L.: 1965, *Petrology of Sedimentary Rocks*, Hemphill ICOMOS-ICMS, 2008. Illustrated glossary on stone deterioration patterns.
- Jiménez-López C., C. Rodríguez-Navarro, G. Piñar, F.J. Carrillo-Rosúa, M. Rodríguez-Gallego and M.T. González-Muñoz. 2007. Consolidation of degraded ornamental porous limestone stone by calcium carbonate precipitation induced by the microbiota inhabiting the stone. *Chemosphere*, 68 (10), pp. 1929-1936.
- Jiménez-López C., F. Jroundi, M. Rodríguez-Gallego, J.M. Arias and M.T. González-Muñoz. 2007. Biomineralization induced by Myxobacteria. *Communicating current research and educational topics and trends in applied microbiology*. A. Méndez-Vilas (Ed.), FORMATEX.
- Jiménez-López C., F. Jroundi, C. Pascolini, C. Rodríguez-Navarro, G. Piñar-Larrubia, M. Rodríguez-Gallego and M.T. González-Muñoz. 2008. Consolidation of quarry calcarenite by calcium carbonate precipitation induced by bacteria activated among the microbiota inhabiting the stone. *International Biodeterioration & Biodegradation* 62, 352-363.
- Jroundi F., E.J. Bedmar, C. Rodríguez-Navarro and M.T. González-Muñoz. 2010. Consolidation of ornamental stone by microbial carbonatogenesis. *Global Stone Congress* 2010.
- Pérez-Ema N., M. Álvarez de Buergo, R. Bustamante. 2013. Integrated studies for the evaluation of conservation treatments of building materials from archaeological sites. Application to the case of Merida (Spain). *International Journal of Conservation Science*. Vol. 4, Special Issue, 693-700.
- Sebastián E. M., M. J. de la Torre, O. Cazalla, G. Cultrone, C. Rodriguez-Navarro. 1999. Evaluation of treatments on biocalcarenes with ultrasound. *The e-Journal of Non-Destructive Testing*, 4, 12.
- The Charter of Krakow, 2000: Principles for Conservation and Restoration of Built Heritage
- Theoulakis P., I. Karatasios, N. Stefanis. 2008. Performance criteria and evaluation parameters for the consolidation of stone. In: *Proceedings of the international symposium: Stone consolidation in cultural heritage*. Lisbon, 6-7 May, 2008.
- Wheeler, G. 2005. Alkoxysilanes and the Consolidation of Stone. The Getty Conservation Institute. Los Angeles.
- Young, M.E., M. Murray and P. Cordiner. 1999. Sandstone consolidants and water repellents. *Stone consolidants and chemical treatments in Scotland. Report to Historic Scotland*. - <http://www2.rgu.ac.uk/schools/mcrg/miconsol.htm>
- Ziegenbalg G. and E. Piaszczyński. 2012. The combined application of calcium hydroxide and silicic acid esters – A promising way to consolidate stone and mortar. In: *12th International Congress on the Deterioration and Conservation of Stone*. New York.

SEASONAL STONE SHELTERING: WINTER COVERS

C. Franzen^{1*} and K. Kraus²

Abstract

Protective winter sheltering is a tradition for high grade stone decorations of some cathedrals and castles in Central Europe. During winter, the often delicate sculptures or reliefs exposed outdoors in parks and gardens are sheltered by wooden cladding applied since the 1980s. Different systems of protective sheltering by winter covers can be distinguished. These include wrapping techniques and several types of box used to cover the surfaces or objects requiring protection. The distributions of different winter cover types in Europe seem to reflect local traditions. Recently, systems made from new materials have come to market. We evaluate different seasonal shelter types and give some general recommendations for making decisions for the application of protective winter covers. New environment data measurements, inspection of different materials in use, considerations about the work load and summer storage are presented.

Keywords: preventive conservation, weathering, protection, winter cover, risk assessment

1. Introduction

It is said the application of protective sheltering systems has a long standing tradition in European parks and gardens. Objects of art, often of natural stone, are encased during the cold winter period. In areas north of the Alps valuable marble sculptures were sheltered with protective winter covers while the citrus fruits of baroque gardens hibernated in orangeries. Also for sculptures made from sandstone this technique of preventive conservation came into use. Despite this widespread practice, there is an open question about the precise time that this form of preventive action started in general, and even for some specific first class parks and gardens. For example, the documentation of the seasonal winter sheltering in the park of Versailles, near Paris, winter sheltering can be dated initially to the beginning of the 1980s. Scientific examination of that preventive conservation action was started by Berry (2005) with climate measurements in several British parks and complemented by Rüdrieh *et al.* (2011). Rüdrieh (op cit.) addressed a new development of protective winter covers for the monumental marble statuaries on the Schlossbrücke in Berlin. Looking at the different kinds of protective sheltering systems a wide variety can be found. Materials used are metal, fabric and synthetic materials, quite often in material combinations that mean that a differentiation of winter shelter systems based on material criterion is not helpful. The main distinction that can be made between

¹ C. Franzen*

Institut für Diagnostik und Konservierung an Denkmälern in Sachsen und Sachsen-Anhalt e.V.
(IDK), Schloßplatz 1, D-01067 Dresden, Germany
franzen@idk-denkmal.de

² K. Kraus

Institut für Steinkonservierung e.V., Große Langgasse 29, D-55116 Mainz, Germany

*corresponding author

protective winter covers is the bearing mode. Most box type shelters compensate their own weight with posts in the ground, whereas in most wrapping techniques the cover is carried by the sculpture. The distribution of several winter protection types in Europe is dominated by local traditions. Some new types of shelter, fabricated from modern materials are now coming to the market. In this paper we evaluate different shelter types and give some general recommendations for decisions making about the application of protective winter covers. Data from new environment measurements, the inspection of different materials in use, considerations about the work load and summer storage is discussed.

2. Protective winter covers

The study presented here focusses on seasonal sheltering free standing pieces in parks, gardens and in castle areas e.g. on balustrades. We will not consider fountains, permanent shelters, protection shelters for events or building construction bound winter covers. All the protective winter covering systems are handled twice a year: with some local differences the system is applied in November and dismantled in March. As a simple consequence of this, the protective system is employed in-situ for approximately a third of the year and has to be stored for the remaining time. Summer storage arrangements must be taken into account. Moreover in terms of workload the installation team is occupied for twice. There are winter protection systems which have standard dimensions and use standardised exchangeable structural elements. Others are constructed bespoke for single art objects, using components that cannot be interchanged easily. In such cases a durable labelling system is advisable to ensure a consistency and appropriateness of the relation between the object and its cover. This is even more important if the shelter system consists of several parts. This may seem rather to be too simple to mention but has serious implications in the total handling of work planning and the labelling should not get lost during winter conditions or summer storage. The winter cover is erected by trained garden personal or specialist subcontractor companies. In several cases stone restorers are involved in planning or advising the works. Thus, in financial terms there are costs for system planning and buying, for summer storage and transportation, working time for set up and dismantling multiplied by the number of workers, repair and time of use.



Fig. 1: Dresden (D), Blüherpark, wooden boxes.



Fig. 2: Dresden, Großer Garten, wooden boxes.



Fig. 3: Wooden box, City of Leipzig(D).



Fig. 4: Wood and tarboard box, Großharthau.

2.1. The general idea

The idea of winter sheltering is an extra protection of the stone material against deterioration action in winter. The commonly and vaguely defined aim is to avoid weathering action from specific winter related damage factors. The sometimes rather airily enumerated principles and processes are worth considering in some more detail. With respect to protection from rain, which is ensured in all cases, it is also certain, that in some parts of Europe, where winter covers are applied, there is more rainfall summer than in winter. Nevertheless, water coming down in snow does not rest direct on the material. Looking at temperature one has to acknowledge that as long as the shelter is not heated the ambient temperature will equilibrate in the shelter and to the stone. Also, frost action is not eliminated. Obviously the interaction of the object with solare radiation is prevented, but here the question can be raised about the relevance of the solar insolation in general weathering action. A similar approach can be taken to the deposition of aerosols on the surface, especially with respect to the effects of deposition in wind shaded areas. Biological action is most often mentioned as a risk, and can be increased with the winter cover. However, if winter shelters do not protect effectively from all the weathering actions that we assume take place, they do prevent frost action in the wet stone state, if certain factors are fulfilled. As nearly all published climate measurements demonstrate, in, in the sheltered volume environmental changes of temperature and humidity adjust in a damped manner (e. g. Berry 2005, Rieffel 2009).



Fig. 5: Barockschloss Rammenau (D).



Fig. 6: Rheinsberg (D).



Fig. 7: Stockholm, Stadthuset, wooden box.

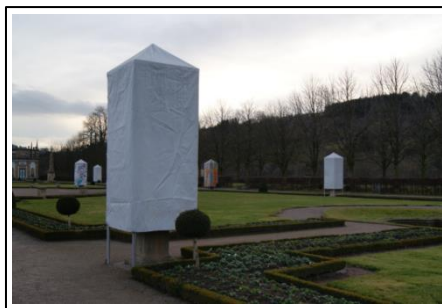


Fig. 8: Weikersheim (D), tents.

2.2. All Solutions?

In our study we counted that seasonal protective winter sheltering is these days regularly applied at more than one thousand free exposed stone art objects in central Europe. There is no standard for the technique and oral or written recommendations (e.g. Wölbert 2005) are quite vaguely formulated. For protective winter covers applies what of Agnew (2002) states for shelters in archaeological sites: it is “not a simple matter, although it may appear so to some stakeholders.” Thus we can find countless solutions, depending on the local options. This is true for innumerable kinds of box constructions, e.g. from wood (Fig. 1 to Fig. 7), boxes with metal planes (Fig. 9, Fig. 10) or other framework constructions like tents (Fig. 8). The varieties continue with coating and wrapping in fabric (Fig. 11, Fig. 12), with or without an underconstruction (Fig. 15). Also, to a certain extent, shells of polyurethane are to be found (Fig. 13). Most often in one park one type of cover is applied to all items, and that method is unique to that park. At the beginning of our survey of the topic and, not yet aware of the total variability in the solutions applied in practice, it was decided to focus attention on three different types: wooden construction, wrapping in fabric with an underconstruction and polyester shell.



Fig. 9: Biebrich Castle (D), metalcover.



Fig. 10: Berlin (D), metal house.



Fig. 11: Versailles (F), cotton wrapping.



Fig. 12: Moritzburg (D.)



Fig. 13: Weimar, Ilmpark (D) Ciccum.

3. Field tests

Three types of winter covers were constructed for and applied over trial stone sculpted columns installed at a site of a research station of the IÖZ Freiberg, Erzgebirge, to obtain measurement results from different covering options. The trial objects are reused original columns from the Zwinger in Dresden, set on aged pedestals (Fig. 14). The columns are comprised of Cotta type Elbe sandstone. Each column was equipped with climate loggers. Winter covers were applied in November and dismantled in March. One column named “Frühling” was wrapped in a procedure as developed in Moritzburg 1999 (Franzen 2011), the second “Sommer” encased in the Ciccum®, a polyurethane hard foam shell, the third gets a wooden shelter original from Barockgarten Großedlitz “Herbst” and the fourth “Winter” is not protected at all.



Fig. 14: Four test columns at the research station: anticlockwise starting right in front: Frühling (fabric), Sommer (light-weight), Herbst (wood) and Winter (without covering).



Fig. 15:
Underconstruction



Fig. 16:
Wrapping in fabric



Fig. 17:
Polyestershell



Fig. 18:
Wooden box

4. Results

The experience from the practical handling of the different systems were documented and evaluated. Compared to the other methods, the wooden sheltering requires the most substantial effort, while wrapping demands the discreet application of the underconstruction directly on the surface of the stone object. In terms of reparability wood allows for the remediation of small defects on site, while all of the other systems need to be brought to a workshop for maintenance. In terms of the durability of the solutions our experience, for most methods indicate that the real life cycle is shorter than the period that is aspired to. This also has an impact on the cost calculations, a key element in decisions about winter sheltering. Costs consist of the equipment acquisition, adequate storage of that equipment the, work in application, repair and maintenance.

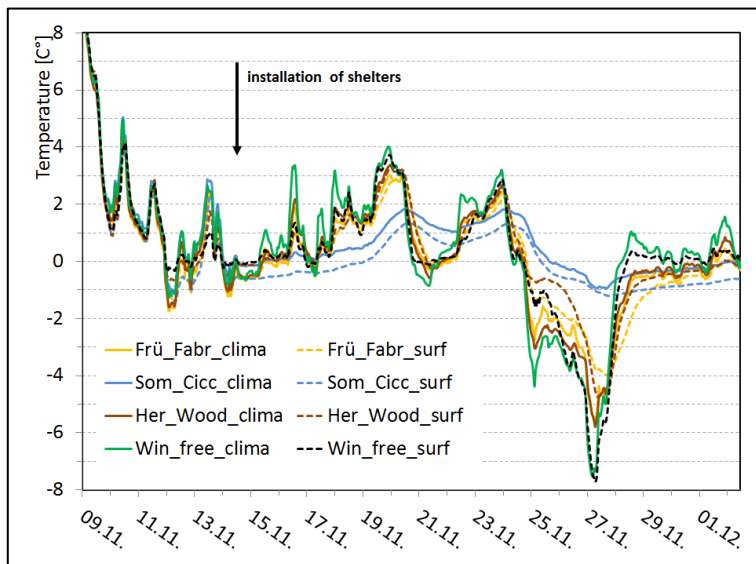


Fig. 1: Cutout of climate measurements in the field test ensemble.

However, from the environmental parameter data logging some more important conclusions can be drawn. Fig. 1 presents a revealing sub-set of the climate measurements made on the four experimental stone columns. Winter covers were applied on the 14th of November. Until that date the data for all the specimens are very hard to separate. In detail it can be seen that the surface temperatures, given in dotted lines, fluctuate closely to the environmental temperature data. With the installation of the winter covers a microclimate arises under the cover. The outer climate is damped to different extents. The temperature changes beneath the wooden box are reduced, and under the wrapping even more. The strongest damping can be observed under the polyester shell. These effects are probably influenced by the material used, but the main regulating parameter is the ventilation. To assess this, the ventilation number, the complete air exchange per hour, was approximated by fitting model data. The wooden cover stands on posts giving an unhampered air exchange, a ventilation number of more than 30 h⁻¹, whilst Ciccum allows the lowest ventilation about 4 h⁻¹, wrapping in fabric is in between with a ventilation number of about 8 h⁻¹. Those huge differences in air exchange have major control on humidity and moisture exchange. Stone sculptures that have a low water uptake (low permeability and sorptivity) do not need to have a drying environment when sheltered. But stone that absorbs relatively a lot of water in the pore system needs an interaction with the air, allowing the stone to dry out. Theoretically therefore there is the recommendation to shelter the material solely in dry conditions, which is in practice not always possible. Thus wet state sheltering is a possible risk, the shelter system has to cope with. Therefore, ventilation has to be adapted to those possible risks. Ventilation is to be regarded as the key parameter to distinguish different shelter systems, as it is a key factor for possible material drying. As this is a material property the factor has to be related to the material, an important approach which remains to be researched.

All protective winter shelter systems prevent precipitation falling on the protected sculptures during winter. Also, the damped microclimate flattens the gradients of temperature changes; this is to be considered also with respect to direct wind action, which accelerates the material temperature transformation significantly. With respect to temperature changes the vulnerability is also material related.

Comparing all different winter shelter systems consisting of various materials, major distinctive features are not due to those materials but to the grade of ventilation the construction enables. Both deterioration related parameters of temperature changes and dehumidification are significantly controlled by the ventilation in opposite directions: high ventilation enables drying but invokes intense temperature fluctuations, while prevented ventilation stabilises the temperature and impedes any drying. The dimension or degree of ventilation has to be referred to the material properties of the sculpture to be sheltered.

Acknowledgements

The project was funded by Deutsche Bundesstiftung Umwelt (DBU) grant: Az 30415.

References

- Agnew, N. (2002) Methodology, conservation criteria and performance evaluation for archaeological site shelters, *Conservation and Management of Archaeological Sites* 5(1-2):7-18, DOI: 10.1179/cma.2002.5.1-2.7
- Berry J. (2005) Assessing the performance of protective winter covers for outdoor marble statuary—pilot investigation. In: Verger I, Coccia Paterakis A, Chahine C, Kardes K, Eshoj B, Hackney S, de Tagle A, Cassar M, Thickett D, Villiers C, Wouters J (eds) 14th Triennial Meeting The Hague, 12–16 September 2005, Preprints. Earthscan/James & James, London, pp 879–887.
- Franzen, C. (2011) Winter shelter systems for garden sculptures, in: Marcel Stéfanaggi & Véronique Vergès-Belmin (eds): *Jardins de Pierres, Conservation of stone in Parks, Gardens and Cemeteries*, SFIIC Paris ISBN: 2-905430-17-6, p. 132 - 141.
- Rieffel, Y. *et al.* (2009) Entwicklung und Überprüfung von Einhausungssystemen zur Reduzierung umweltbedingter Schädigungen von außenexponierten Marmorobjekten mit dem Ziel des langfristigen Erhalts in situ an einem national bedeutenden Objektkomplex, den Schlossbrückenfiguren Unter den Linden, Berlin, Abschlussbericht zum DBU Projekt 24000-45.
- Rüdrich, J., Rieffel, Y., Pirskawetz, S., Alpermann, H., Joksch, U., Gengnagel, C., Weise, F., Plagge, R., Zhao, J., Siegesmund, S. (2011) Development and assessment of protective winter covers for marble statuary of the Schlossbrücke, Berlin (Germany), *Environ Earth Sci*, Vol. 63/ 7, pp 1823-1848 DOI 10.1007/s12665-010-0765-2, online 19. Okt. 2010.
- Wölbert, O. (2005) Winterschutzverkleidungen für witterungsgefährdete Objekte. in: Matthias Exner, Dörthe Jakobs (Hrsg.) *Klimastabilisierung und bauphysikalische Konzepte*, Tagung ICOMOS, Reichenau Nov. 2004, S.185 - 190.

PERFORMANCE AND PERMANENCE OF TiO₂-BASED SURFACE TREATMENTS FOR ARCHITECTURAL HERITAGE: SOME EXPERIMENTAL FINDINGS FROM ON-SITE AND LABORATORY TESTING

E. Franzoni^{1*}, R. Gabrielli², E. Sassoni¹, A. Fregni¹,
G. Graziani¹, N. Roveri³ and E. D'Amen³

Abstract

The possibility of providing historic façades with self-cleaning ability in urban polluted environments by means of treatments based on photocatalytic nano-TiO₂ dispersions, has recently received growing attention. The potential impact of these treatments for the protection of heritage buildings is evidenced by the high number of papers where the performance of TiO₂-based nanocoatings on stone (mainly marble, travertine and limestone), mortar and brick were investigated by laboratory tests. The results seem encouraging, even if the nature of the treatments, the kind of substrate and the methods used for assessing the coatings' performance differ greatly from one study to the other, thus making the results difficult to compare or even contradictory. Several aqueous titania nanodispersions are already available in the market and some applications of these treatments as trial testing in real heritage buildings are known, but information about their performance (colour change, self-cleaning ability, etc.) on real substrates and in real outdoor environments are still very scarce. In particular, the long-term permanence of TiO₂ nanoparticles on outdoor exposed surfaces, also in relation with strategies for promoting the adhesion between nanoparticles and substrate, has also not been fully elucidated yet. In the present paper, some experimental findings collected during last years from on-site and laboratory testing campaigns are reported, as a contribution towards a better assessment of the behaviour of TiO₂ treatments when exposed to real and accelerated environmental conditions.

Keywords: self-cleaning, historic building materials, protection, rain, leaching

¹ E. Franzoni*, E. Sassoni, A. Fregni and G. Graziani
Dept. of Civil, Chemical, Environmental and Materials Engineering (DICAM),
University of Bologna, Italy
elisa.franzoni@unibo.it

² R. Gabrielli
Leonardo S.r.l., Casalecchio di Reno, Italy

³ N. Roveri and E. D'Amen
Chemical Center S.r.l., Castello d'Argile, Italy

*corresponding author

1. Introduction

While current strategies for surface protection of historic monuments involve the use of sacrificial layers (as in the past) or water repellents, an 'active' kind of protection has been recently proposed, based on the use of photocatalytic materials (Licciulli *et al.* 2011, La Russa *et al.* 2012). TiO₂ nano-particles, in particular, have been investigated for application on façade materials, as they are expected to catalyse deterioration of several pollutants that threat building materials and to provide self-cleaning action (Pinho *et al.* 2013, Quagliarini *et al.* 2013, Munafò *et al.* 2014, Franzoni *et al.* 2014). Different kinds of substrate, representative of the historic ones, were treated with different nano-titania dispersions and tested in laboratory, with positive results (as shown in the review paper Munafò *et al.* 2015). Porosity, roughness and composition of the substrate were found to be important for the treatments performance, as well as the composition and particle size of the dispersions. Nevertheless, the test methods employed in the laboratory studies necessarily involve simplified conditions with respect to the complex conditions experienced by historic materials on site. For instance, the self-cleaning ability is determined as the capacity of a treated surface to discolour a standard organic stain under a standard UV light exposure, but the on-site exposure is obviously very different, due to the occurrence of complex urban atmospheres (gases, particulate matter, etc.) and environmental conditions (temperature, humidity, sun, rain, wind, etc.). Hence, the collection of data from real historic buildings treated with TiO₂ is crucial to assess the actual performance of these finishings, and their compatibility with the original substrates (colour change, microstructural variations, etc.).

Moreover, it is very important to assess the durability of these treatments. In particular, the permanence of the TiO₂ nanoparticles on the surfaces is a key parameter to investigate, as most of the current treatments are constituted by aqueous nano-dispersions, only occasionally preceded by primer application, hence the nanoparticles are expected to adhere to the substrate only mechanically and by weak physical bonding and could be removed by environmental agents (Franzoni *et al.* 2014, Graziani *et al.* 2014). The issue of TiO₂ removal by rain is important also from an environmental point of view (Kaegi *et al.* 2008).

This paper aims at presenting the results of some studies performed in laboratory and on-site, as a contribution to a better understanding of the aspects highlighted above. Firstly, the permanence of nano-TiO₂ on render and marble samples was investigated in laboratory, by subjecting the samples to an artificial rain system, in order to understand whether the nanoparticles and their photocatalytic activity are lost after exposure to rain. Then, aqueous nanodispersions of TiO₂ were applied to three heritage buildings in Bologna (an Istrian stone decoration of a XX Cent. building, a repair render of a XVIII Cent. portico and some sandstone ashlar of a XIII Cent. building; Fig.1) and the effects and permanence of the treatments were investigated.



Fig. 1: The places selected in Bologna for testing the nano-TiO₂ application. From left to right: the limestone sculpture in the Mathematics Dept.; the new renders of the former Del Corso Hotel; sandstone ashlars in 'Palazzo del Podestà' during the treatment application.

2. Laboratory testing

2.1. Materials and methods

Dispersions of nano-TiO₂ were applied on two kinds of substrates, characterised by different composition, porosity and surface roughness: a painted render (similar to those used in historic buildings) and Carrara marble. The render was manufactured mixing natural hydraulic lime (NHL2, EN 459-1:2010), quartz sand <2 mm, ground brick powder <1 mm and water, according to the volume proportions: 1-1-1-0.5. Render slabs 1.8 cm thick were manufactured and cured for 4 weeks at $T=20^{\circ}\text{C}$ and $RH=50\%$, then they were painted by two brush strokes with an inorganic paint (slaked lime, 5 wt% inorganic pigments and 5 wt% acrylic polymer). Immediately after paint application, a commercial aqueous dispersion of TiO₂ nanoparticles (anatase, mean size 20-50 nm), with concentration 3.4 wt% and containing 0.1 wt% of NaOH, was applied by two brush strokes: a better adhesion of the nanoparticles is expected thanks to the carbonation process of the paint. Some samples were left untreated (REF). Tests were performed after 2 weeks curing.

Freshly quarried Carrara marble slabs with thickness 2 cm were used for the tests. A 2 wt% hydro-alcoholic dispersion (20 wt% isopropyl alcohol) of TiO₂ nanoparticles (anatase, mean size 10-20 nm) was applied by brushing. One stroke was considered enough due to the low porosity of marble. Some samples were left untreated (REF), for comparison.

Half of the samples was subjected to the methylene blue discolouration test, consisting in dripping 100 mg of a solution of methylene blue in ethanol (50 mg/l) on the treated and REF samples and comparing the discolouration after exposure to UV light. Marble samples were exposed to UV light for 2 hours, while render samples were exposed for 5 hours due to the difficulty in observing the blue discolouration in such porous samples, where the blue drop was mainly absorbed by the substrate. The other half of the samples was exposed to an artificial dripping system aimed at simulating the action of rain on the treated surfaces. Given the nature of the treatments under testing, that are aqueous dispersions of TiO₂ nanoparticles (with no primer), the resistance to rain impact and flow was considered a key deterioration process to investigate. The samples, having a surface of about $3 \times 3 \text{ cm}^2$, are positioned under the artificial rain system with a slope of 45° from the horizontal plane. Two drips of distilled water fall on each sample from a height of about 4 cm, flowing along

the surface. The rate of artificial rain on each sample is about 350 ml/hour. The artificial rainfall was performed for a total of 20 hours (10 cycles of 2 hours rain followed by 22 hours drying) on marble samples and for 4.5 hours of continuous dripping on the render samples. A continuous dripping instead of rain cycles was preferred for render, for keeping the substrate in a saturated condition and hence for maximising the water flowing on the treated surface. Moreover, a shorter exposure was preferred for render, in order not to cause an excessive leaching of the mortar substrate (not fully carbonated yet). Considering the average rainfall in the Italian city of Bologna (80 cm/year), the artificial rain performed corresponds to an exposure of about 2 years for render and 6 years for marble.

After the exposure to artificial rain and subsequent drying, the samples were observed by SEM and the amount of Ti still present on the surface was analysed by EDS (SEMLEO EVO 40XVP-MZeiss; EDS analysis system INCA Energy 250, Oxford Analytical Instruments). Moreover, the methylene blue discolouration test was carried out on the samples subjected to artificial rain, following the same procedure described above.

2.2. Results and discussion

The results of the methylene blue discolouration test on the render and marble samples are reported in Fig. 2. After the application of the TiO₂-based treatment, both substrates exhibit some discolouration of the methylene blue under UV exposure (Fig. 2: b and e), differently from the untreated samples (a and d), thus confirming the photocatalytic action of the treatment. After exposure to artificial rain, the photocatalytic behaviour of the treatment seems almost unaltered in the render samples (Fig. 2: c), although the EDS analysis reveals that the amount of TiO₂ on the surface has decreased (two representative EDS spectra before and after artificial rain are reported in Fig. 3 left and centre). Notably, the amount of titania deposited by the treatment on the surface is high (Fig. 3 left), probably due to the higher amount of nanodispersion absorbed by the samples in the two brushing applications. The TiO₂ persistence on the surface can be ascribed to the render roughness, the enhancement of the nanoparticles adhesion due to paint carbonation and the adsorption capacity of silicatic fractions in the paint towards nano-TiO₂ (although this is a complex phenomenon depending on the nanoparticles size and concentration (Dietrich *et al.* 2012)).

In marble samples, the photocatalytic effect seems more limited than in render, according to visual observations (Fig. 2), although a direct comparison cannot be made between the two substrates, given the different UV exposure times (2 hrs for marble and 5 for render). In the case of marble, the TiO₂ amount is however quite limited (Fig. 3 right), probably due to the limited retention capacity of marble in the single brush stroke. After artificial rain, the photocatalytic action is further reduced (Fig. 2: f) and the Ti presence is barely detectable by EDS, which points out that possible nano-TiO₂ removal is an important issue in marble.

3. On-site testing

3.1. Istrian stone sculpture in the Department of Mathematics in Bologna (XX Cent.)

The carved limestone slab under testing (Fig. 1 left, sculptor Alfonso Leoni) was placed at the extremity of the portico of the Dept. of Mathematics of the University of Bologna in 1971. The slab is made of Istrian stone, a compact limestone whose aspect and properties are very similar to marble. In the 2009 conservation works, a commercial nanodispersion of TiO₂ was applied to the sculpture, after cleaning, to investigate its self-cleaning action in a heavily trafficked area. A primer was applied to promote nanoparticles adhesion (aqueous

dispersion of silica gel, surfactants, acrylic polymers and NaOH), by single spraying (pressure 0.3-0.4 bar; distance nozzle/surface 20-25 cm; expected amount of product deposited 70 g/m²). Then, a 3.4 wt% aqueous dispersion of anatase nanoparticles (particle size not reported in the technical datasheet; 0.1 wt% of NaOH; expected amount of product deposited 50 g/m²) was applied by double spray application (same tool used for the primer).

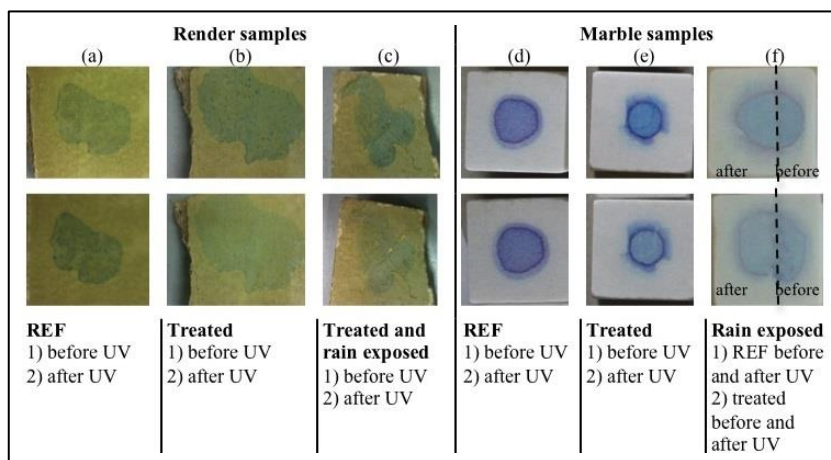


Fig. 2: The samples subjected to the methylene blue discolouration test.

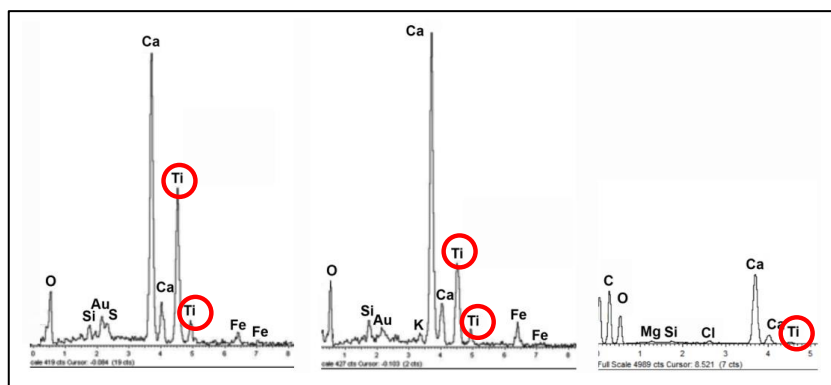


Fig. 3: EDS of the treated surface of: the render before (left) and after (centre) exposure to artificial rain; marble before exposure to artificial rain (right) (area analysed $\sim 300 \mu\text{m}^2$)

Three years after the treatment, the treated face of the slab (the external one, exposed to direct rain) appeared substantially unaltered, while the untreated one (the internal one, under the portico and hence sheltered) exhibited some visible darkening, as shown in Fig. 4 (comparison between 1 and 2 and between 5 and 6). As the treated face was substantially clean also in the cavities of the sculpture, a combined action of rain wash and self-cleaning ability can be envisaged. Small samples were taken by chisel from the sculpture, in both internal and external surfaces, and they were observed by polarised light microscope (PLM) and ESEM/EDS. A thin layer (1-8 μm) very rich in Ti was found on the treated external face, hence TiO₂ was still present on the surface after 3 years since application (Fig. 4: 3-4).

On the untreated internal surface a layer of deposited particulate matter was detected (Fig. 4: 7-8).

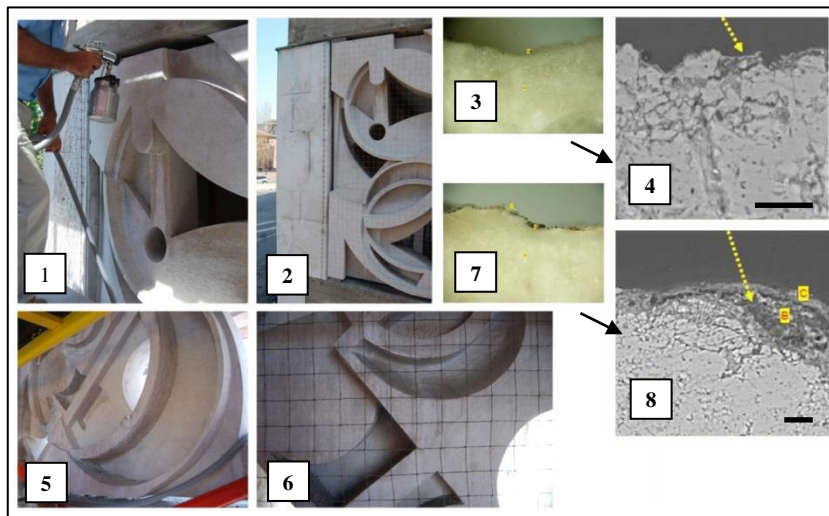


Fig. 4: External surface of the slab: 1) state at 2009; 2) state at 2012; 3) cross section observed by PLM and 4) by ESEM (marker 50 μm). Internal surface of the slab: 5) state at 2009; 6) state at 2012; 7) cross section observed by PLM and 8) by ESEM (marker 50 μm).

3.2. Renovation render of a XVIII Cent. building in Bologna

The 18th Century building selected for the tests was the former *Del Corso Hotel* in Bologna (Fig. 1-centre), a neoclassical building affected by a severe degradation of the existing façade renders, facing a street characterised by intense car and bus traffic. In 2012, the renders were replaced, using new renders and paint of the same kind of the existing ones (same materials used in laboratory tests on render samples: § 2.1). Finally, a photocatalytic self-cleaning finishing (the same used for renders in § 2.1) was applied by a single spray application to some pillars of the portico, after complete hardening of the paint. In 2015, some samples of the treated repair renders were collected (Fig.5), in order to evaluate the amount of TiO_2 still present on the surface after 3 years of exposure to the weathering agents.

The samples were observed by SEM and the presence of Ti was determined by EDS (SEM LEO EVO 40XVP-M Zeiss; EDS INCA Energy 250, Oxford Analytical Instr.). The EDS analysis in Fig. 6 shows that a very small amount of TiO_2 is still present in the samples taken from the external face of the pillars, directly exposed to rain (samples A, C), while samples B and D, taken from the sheltered faces show a notably higher TiO_2 amount.

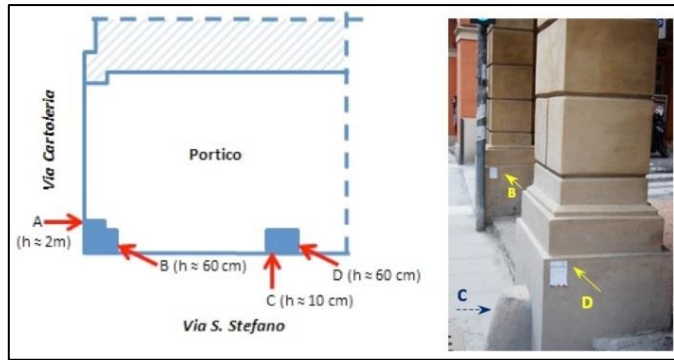


Fig. 5: Sampling points (and heights) in the two treated pillars.

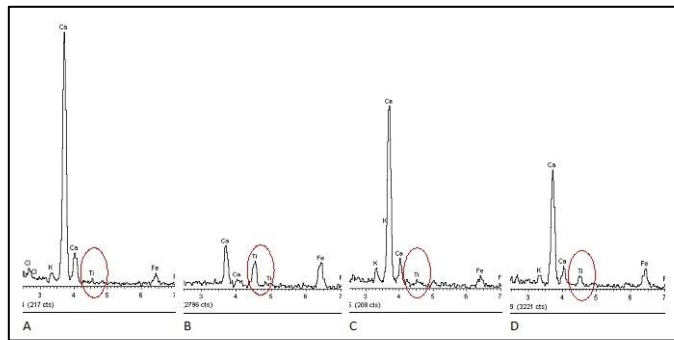


Fig. 6: EDS spectra of the surfaces of the collected samples (area analysed $\sim 3.5 \text{ mm}^2$).

3.3. Sandstone ashlars of Palazzo Podestà in Bologna

The application of a TiO_2 nanodispersion identical to that used for marble samples in the laboratory tests was carried out (on 24th July 2015) in some sandstone ashlars of Palazzo Podestà, a XVI Century building which faces the central square of Bologna and is one of the most prominent monuments in the city. Despite the dark yellow colour of the stone, no visible colour change was observed after two subsequent spraying applications (Fig. 7). The monitoring of the presence of TiO_2 is presently in progress.



Fig. 7: The sandstone before (left) and 30' after the TiO_2 application (right).

4. Conclusions

The laboratory tests show that the aqueous dispersions of nano-TiO₂ exhibit some photocatalytic behaviour even after few hours of UV exposure. Nevertheless, depending on the amount of nanoparticles deposited on the surface (higher for render than for marble) and the technology used for promoting nanoparticles adhesion (none for marble, fixing through lime carbonation for render), artificial rain significantly affects TiO₂ permanence. In fact, artificial rain decreases the TiO₂ amount in both substrates, but more markedly for marble. The on-site tests highlight the aesthetical compatibility of the treatments, but show that, depending on the method used for enhancing the nanoparticles adhesion, rain may differently affect TiO₂ removal. In the Istrian stone sculpture a primer was used before the TiO₂ application and a thin layer of titania is still present after 3 years. Conversely, in the repair render directly exposed to rain (where the treatment was applied on the carbonated lime paint) a limited amount of TiO₂ was found, despite the high substrate porosity. Further monitoring of the buildings is presently in progress.

References

- Dietrich, L. A. S., *et al.*, 2012, Experimental study of TiO₂nanoparticle adhesion to silica and Fe (III) oxide-coated silica surfaces, *Chemical Geology*, 332, 148-156.
- Franzoni, E., *et al.*, 2014, Compatibility of photocatalytic TiO₂-based finishing for renders in architectural restoration: a preliminary study, *Build Environ*, 80, 125-135.
- Graziani, L., *et al.*, 2014, Durability of self-cleaning TiO₂ coatings on fired clay brick facades: Effects of UV exposure and wet & dry cycles, *Building and Environment*, 71, 193-203.
- Kaegi, R., *et al.*, 2008, Synthetic TiO₂nanoparticle emission from exterior facades into the aquatic environment, *Environmental Pollution* 156, 233–239.
- La Russa, M.F., *et al.*, 2012, Multifunctional TiO₂ coatings for Cultural Heritage, *Progress in Organic Coatings*, 74, 186–191.
- Licciulli, A., *et al.*, 2011, Photocatalytic TiO₂ coatings on limestone, *J of Sol-Gel Science and Technol*, 60, 437–444.
- Munafò, P., *et al.*, 2014, Durability of nano-engineered TiO₂ self-cleaning treatments, *Construction and Building Materials*, 65, 218-231.
- Munafò, P., Goffredo, G.B. and Quagliarini, E., 2015, TiO₂-based nanocoatings for preserving architectural stone surfaces: An overview, *Construction and Building Materials*, 84, 201–218.
- Pinho, L., *et al.*, 2013, A novel TiO₂-SiO₂nanocomposite converts a very friable stone into a self-cleaning building material, *Applied Surface Science*, 275, 389–396.
- Quagliarini, E., *et al.*, 2013, Self-cleaning materials on Architectural Heritage: compatibility of photo-induced hydrophilicity of TiO₂ coatings on stone surfaces, *J of Cultural Heritage*, 14, 1–7.

THE IMPACT OF SCIENCE ON CONSERVATION PRACTICE: SANDSTONE CONSOLIDATION IN SCOTTISH BUILT HERITAGE

C. Gerdwilker^{1*}, A. Forster², C. Torney¹ and E. Hyslop¹

Abstract

Scotland's extensive sandstone-built heritage is an irreplaceable cultural and material asset which suffers increasing weathering decay that necessitates the consolidation of friable surfaces to delay material loss. Many academic studies of sandstone consolidants have been carried out but long-term field performance monitoring is rarely undertaken. Currently only two types of consolidants, the acrylic resin Paraloid B72 and alkoxy silanes, are commonly applied to sandstone, both associated with inherent risks that could irreversibly accelerate decay. Scotland's conservation community has the technology and expertise to carry out compatibility and performance testing of consolidants but is hampered by typical restrictions on access, project funding and time. The use of science in the context of risk assessment rather than guarantee of compatibility is suggested to enable timely and solution orientated results that inform the decision-making process. The research highlights the need for conservation science to be routinely and more effectively integrated into conservation planning and processes from the outset. The architect's role as client representative and project manager is identified as critical to achieving this. Training, outreach activities and an accessible platform for the collation and dissemination of research and treatment documentation are considered possible means of improving collaboration between scientists and conservators and advancing conservation technology and processes.

Keywords: sandstone, consolidation, compatibility, risk assessment, conservation planning

1. Introduction

Scotland's Historic Environment Audit 2012 identifies 90% of pre- 1919 buildings as requiring some repair (Historic Scotland, 2012), the vast majority of these adopting mass sandstone construction (Urquhart, 2007). Climate change is likely to accelerate the decay of masonry due to moisture transfer mechanisms and long term saturation in porous materials (Smith *et al.*, 2011) caused by increasing levels of rainfall and low potential evaporation associated with a northern maritime climate. Given that almost all the quarries that historically supplied Scottish building stone are currently closed this places greater pressure to arrest decay, and a presumption to consolidate as opposed to replace stone may be favoured. These decisions also aid application of the philosophical and technical

¹ C. Gerdwilker*, C. Torney and E. Hyslop
Historic Environment Scotland, United Kingdom
christa.gerdwilker@hes.scot

² A. Forster
Heriot Watt University, United Kingdom

*corresponding author

requirements associated with best practice conservation (BS7913, 2013; ICOMOS, 2013), and more specifically issues surrounding minimal intervention and authenticity.

Price (2006) describes consolidation as ‘the process of strengthening and reinforcing’ and, given the potential scale of application Panagiotis *et al.* (2008) consider consolidation as a major conservation activity which presents particular risks due to the irreversibility of the consolidation processes affecting the stone matrix (De Clerq *et al.*, 2008; Ferreiro Pinto & Delgado Rodrigues, 2008). Subsequently, a clear evidence-based understanding of the benefits and risks associated with the application of consolidants is necessary for objective and informed treatment decisions to be taken. This research aims to identify how conservation science supports Scotland’s building conservation community in their decision-making process in regards to the use of stone consolidants. The research identifies factors impacting on effective collaboration between conservators and scientists and means of improvement.

2. Method

A review of recent literature determined key requirements for and evaluated currently used sandstone consolidation treatments. Means of testing the efficacy and compatibility of consolidants were identified. The applicability of the review findings for the Scottish stone conservation sector was tested during subsequent questionnaires and interviews. A small, yet representative group of six practising stone/building conservators and six conservation scientists in Scotland from different public and private organisations were chosen as interviewees and grouped into scientists and conservators. The interview process combined small scale quantitative with qualitative research to gain understanding of:

- the type and extent of consolidation treatments carried out in Scotland,
- the extent to which they are determined and evaluated by scientific investigations,
- the type of investigations used,
- their impact on the treatment decision making process and
- respective attitudes towards and experiences of collaboration between conservation scientists and conservators.

A meta-synthesis examined six conservation project case files of properties throughout Scotland. Their study compared the interview findings with the factual application of conservation science in relation to stone consolidation in Scotland.

2.1. Literature research

Examination of current literature identified key requirements for sandstone consolidants as

- to not alter the physical and visual nature and behaviour of the stone in the short or long-term (Young *et al.*, 2003; Doehne & Price, 2010).
- being effective in slowing down the rate of decay (Price, 2006).
- the ability to penetrate to a sound core (Weber & Zinsmeister, 1991).

Given the great variability of sandstones, the review surprisingly identified only two types of currently prevalent sandstone consolidation treatments: the acrylic resin Paraloid B72 is used to re-adhere surface delaminations, while alkoxy silanes are applied to soft powdering sandstone surfaces. As an irreversible surface-applied material, alkoxy silanes have the greatest potential to cause harm and are the most tested type of consolidant (Weber &

Zinsmeister, 1991; De Clerq *et al.*, 2008). The main advantages of silanes are their chemical compatibility with sandstone and potential ability to achieve deep penetration (Price, 2006). While useful on disaggregating stonework their brittle and non-adhesive nature cannot achieve the re-adhesion of delaminating surfaces. This common problem is overcome by the theoretically reversible acrylic resin Paraloid B72. Its disadvantage is that the resin has poor penetration and significantly reduces the permeability of consolidated stone. It is also noted for poor performance in damp settings (Price 2006; Odgers & Henry, 2012).

Ultrasound velocity (US), infrared (IR) thermography and measuring water adsorption are identified as effective non-destructive field techniques to monitor the impact of consolidants (Haake *et al.*, 2004; Ruedrich *et al.*, 2004; Ferreira Pinto & Delgado Rodrigues, 2008; Moropoulou *et al.*, 2013). A rebound hammer can also provide information on surface hardness (Török, 2010). The difficulty and importance of correlating laboratory and field test results, to ensure the former relates to practical situations and the latter are correctly interpreted, are highlighted. Thin section petrography of core samples is seen as an important initial step in understanding stone petrology and decay phenomena (Nwaubani & Dumbelton, 2001) while drill resistance (DRMS) can detect a hardness profile (Cnudde *et al.* 2007; Pamplona *et al.*, 2008). Furthermore, the above are often combined with strength, permeability and colorimetric tests (Young *et al.*, 2003). Academic research also allows access to more sophisticated laboratory equipment, e.g. neutron radiography and X-ray tomography (Cnudde *et al.*, 2007; Graham *et al.*, 2014).

In spite of the evidently available technology and academic research, little published field data is available on the long-term performance of project applied consolidants (Calia, 2004; Wheeler, 2005).

2.2. Interviews

2.2.1 Interviews with conservators

The conservators represent the private and public sector in equal measure and carry out the bulk of stone conservation in Scotland. Consolidation forms 25 – 50% of all conservation work and >75% of consolidation treatments are applied to sandstone. The conservators most commonly use Paraloid B72 and non-hydrophobic silanes as sandstone consolidants. Conservators rarely commission material testing due to lack of funding, time or the inability to take destructive samples. If undertaken, this usually involves thin section petrography to identify decay mechanisms. More commonly, comparative hardness and water absorption tests are carried out by the conservators themselves. While all conservators keep and archive treatment records, these are not generally accessible to others and rarely include long term performance monitoring results as this is usually also prevented by lack of funding, access to the site and restraints on destructive sampling.

Four of the six conservators wish to work more closely with conservation scientists while two question the scientists' ability to relate their findings to the context of their projects. They also bemoan a lack of conclusive answers to their questions on treatment compatibility within project timeframes and budgets. Limited awareness of available investigative technology is singled out as inhibiting their collaboration with conservation scientists by the majority of conservators, followed by restricted funding and access to scientists. The commercial conservators in particular feel that their clients' lack of

awareness of conservation science impacts on their willingness to pay for such services and client development is identified as key to improving collaboration, combined with 'access to conservation science research' and 'access to scientists' themselves.

2.2.2 Interviews with conservation scientists

Six building conservation scientists are interviewed, representing approximately 60% of the sector in Scotland. One scientist works in the commercial sector while the remainder are employed by academic and public institutions. All scientists spend over 75% of their time on conservation related work, three scientists primarily on academic research while the other three are conservation project focused. Combined, the scientists are able to offer all of the analytical techniques identified by the literature research as potentially useful for consolidant testing. Nonetheless, they confirm that such testing is very rare. Only the three most experienced scientists have ever tested consolidants and only one scientist has applied such findings to conservation projects while the other tests form part of academic research. Petrographic analysis, water absorption and hardness are considered the most effective stone consolidant tests to have been used by each of the above three scientists. In addition, DRMS followed by US are seen as potentially useful techniques, but had not been used.

Like the conservators, the conservation scientists see performance monitoring of consolidation treatments as imperative but the interviews reveal that this tends to be carried out only in response to treatment failures and positive outcomes are likely to go uninvestigated. Nonetheless, the scientists feel that their research findings influence conservation practice and agree that effective conservation science research requires involvement in practical conservation projects. Limited contact and communication difficulties, due to lack of funding, are identified as the biggest obstacles to collaboration between conservation scientists and practitioners. Four main themes recur when asked how collaboration between conservators and conservation scientists might be improved: education, communication, contact and funding; with time being considered only a minor factor.

2.3. Meta-synthesis of conservation projects

The meta-synthesis examines six stone conservation projects carried out over the last approximately 30 years in Scotland to compare stone consolidation practice with interviews and literature review findings (Tab. 1).

The meta-synthesis aims to identify:

- the investigative processes involved,
- their impact on the decision making process,
- the consolidation treatment and application methodology,
- the decision makers in these processes,
- whether performance monitoring is carried out, and
- treatment outcome.

Analytical investigations were carried out in 80% of the examined cases to determine decay causes but rarely to test consolidant compatibility. Paraloid B72 is the main consolidant used with silane being the only other identified substance in use, confirming the findings of the interviews and literature review. The cases indicate that consolidants do not return stone to 'as new' condition but that they might only last a few years before requiring re-treatment. Thin section petrography followed by moisture related investigations are the

primary means of establishing decay causes, but X-ray diffraction (XRD) and IR thermography are also commonly used. Hill House is the only project to have involved consolidant testing but, seemingly, findings were not applied to the project. Performance monitoring tends to be limited to visual observations. As a preventive alternative to remedial consolidation treatment, stabilisation of environmental conditions appears to have slowed down the decay of internal stone at Skara Brae and this approach is currently being trialled and monitored at Skelmorlie Aisle. While stone conservators determine treatments, their decision tends to require the approval from the architect (as client representative) as well as statutory bodies when applied to listed buildings and scheduled monuments.

Tab. 1: Summary of meta-synthesis.

	Hill House	Linlithgow Palace	Skara Brae	Holyrood Abbey	Melrose Abbey	Skelmorlie Aisle
	Petrography	Petrography	Petrography	Petrography	No	Petrography
	Moisture content (MC)		Porosity Sorptivity	Moisture survey		Moisture survey
Analysis	Strength			IR thermography		IR thermography
			XRD	XRD		XRD
			Environmental			Environmental
Applied to project	No	Yes	Yes	Yes	N/A	Yes
Treatment	Silane injection	Paraloid B72	Environmental	Paraloid B72	Paraloid B72 Silane	Environmental
Decision maker	Architects	Architect Conservator Inspector	Architect Conservator Inspector	Conservator	Conservator	Architect Conservator Scientist
	Visual	Visual	Visual	Visual	Visual	Visual
Perfor- mance monitoring	MC		Environmental			Environmental
	XRD					Laser scan
	IR thermography					
Outcome	Failed	Re-treated	Slowing of decay rate	No access	Paraloid partially failed; Silane stable	Too early

3. Discussion

Currently only two products are applied to address two main forms of sandstone decay: granular de-cohesion and surface delamination. Of these, Paraloid B72 has been shown by the literature review and meta-studies to have poor long-term performance, particularly in

exterior settings. Like all other resinous consolidants, Paraloid B72 is an impermeable adhesive and was never developed as a consolidant. At the same time, silanes are unable to re-adhere detached surfaces. Consolidation is a major conservation activity yet, investigating its impact on sandstone has been shown as not being routinely carried out, in spite of available technology and expertise. Impregnation depth, hardness, water absorbency and strength have been identified as key parameters for the compatibility assessment of consolidants. A lack of awareness by budget holders and subsequent failure to commission compatibility testing, combined with constraints on site access, time and sampling from heritage sites, mean that these consolidant parameters are rarely known in a project context and treatment decisions are predominantly influenced by user familiarity as opposed to most effective testing regime and treatment. The short-term effect of most consolidation treatments is seen as positive but without monitoring, misleading assumptions about their long-term performance might be made which puts remote or inaccessible parts of buildings or monuments at particular risk of unobserved decay. The limited life span of consolidants necessitates periodic re-treatment which will undoubtedly pose new compatibility problems.

The research reveals a discrepancy between the conservator perceived lack of access to conservation science research and the conservation scientist's feeling that their research informs conservation practice. The majority of research participants would like to see more project collaboration to support each other's work which would resolve this discrepancy.

4. Conclusion

The long-term effects of consolidants on heterogeneous sandstone masonry in Scotland are poorly understood due to a lack of compatibility and performance testing. Given the limited range of consolidants, such testing might only seek to answer whether to consolidate or not. Research and testing of other potentially suitable or adaptable products and the development of new commercially available and purpose-designed products is urgently required.

Science cannot necessarily clearly answer, within a project restricted timeframe, whether consolidation is going to be effective and compatible. Realistic expectations of what consolidants can achieve and what questions scientists can usefully answer within a given timeframe need to be established.

Consequently, conservation science might be more realistically used as an evidence-based risk assessment tool to reduce treatment uncertainty by identifying existent risk factors in the stone e.g. low strength, high porosity, presence of clays etc. in relation to prevalent environmental factors e.g. soluble salts, moisture content, climatic conditions, etc. to produce a stone decay risk factor. By subsequently assessing the physical properties of consolidated stone in the context of improved environmental conditions, the risk factors of treated and un-treated stone might be compared, taking the intrinsic and extrinsic properties of stone into consideration.

The routine integration of purposeful analytical investigations into conservation projects from the start would permit effective planning of resources to allow informed treatment decisions to be made. This should involve both analyses prior to treatment as well as post treatment and longer term monitoring. The significance of architects and other professionals influencing this process must be recognised and addressed to improve

awareness of how conservation science can aid their client's project outcomes, e.g. through outreach events, formal training, publications and guidance. The lack of long-term performance monitoring of consolidants leads to high-risk treatments with potentially costly outcomes and results in missed opportunities to learn from past experiences. The combined collation and dissemination of conservation science research and conservation case studies through accessible and non-judgmental publications and online portals is advocated but has both a resource and administrative requirement.

References

- Australia ICOMOS, 2013, The Burra Charter: The Australia ICOMOS Charter for Places of Cultural Significance, 2013 (<http://australia.icomos.org/wp-content/uploads/The-Burra-Charter-2013-Adopted-31.10.2013.pdf>, accessed 20.04.14) articles 3.1, 4.
- BSI Group. BS 7913:2013. Guide to the conservation of historic buildings - 2013, paragraphs 6.5 – 6.7.
- Calia A., Lettieri M., Quarta G., Laurenzi Tabasso M., Mecchi A. M., 2004, Documentation and assessment of the most important treatment carried out on Lecce stone monuments in the last two decades. In: Kwiatkowski D., Loefvendahl R. (eds.), 10th International Congress on Deterioration and Conservation of Stone, 27 June – 2 July 2004, Stockholm Vol. 1, ICOMOS Sweden, pp. 431 – 438.
- Cnudde V., Dierick M., Vlassenbroeck J., Masschaele B., Lehmann E., Jacobs P., Van Hoorebeke L., 2007, Determination of the impregnation depth of siloxanes and ethylsilicates in porous material by neutron radiography. *Journal of Cultural Heritage*, 8, Elsevier, pp. 331 – 338.
- De Clerq H., De Zanche S., Biscontin G., 2008, TEOS and Time: Influence of Application Schedules on the Effectiveness of Ethyl Silicates Based Consolidants. In: Delgado Rodrigues J., Mimoso J. M. (eds.) *Proceedings of the International Symposium Stone consolidation in cultural heritage – research and practice*, 6 – 7 May 2008, Laboratorio Nacional de Engenharia Civil, Lisbon, pp. 399 – 408.
- Doehne E., Price C. A., 2010, *Stone Conservation – an overview of current research*, 2nd edition, Getty Institute, Los Angeles, pp. 39, 36, 40.
- Ferreira Pinto A. P., Delgado Rodrigues J., 2008, Stone consolidation: The role of treatment procedures. *Journal of Cultural Heritage*, 9, Elsevier, pp. 38 – 53.
- Graham C., Martin L., Vernon P., Young M., 2014, Conserving Scotland's Built Heritage: A Petrographic Investigation on the Effects of Deicing Salts on Scottish Sandstones, *Engineering Geology for Society and Territory*, Vol. 8, pp 487 – 490.
- Haake S., Simon S., Favaro M., 2004, The Bologna Cocktail – evaluation of consolidation treatments on monuments in France and Italy after 20 years of natural ageing. In: Kwiatkowski D., Loefvendahl R. (eds.), 10th International Congress on Deterioration and Conservation of Stone, 27 June – 2 July 2004, Stockholm Vol. 1, ICOMOS Sweden, pp. 423 – 430.
- Historic Scotland, *Scotland's Historic Environment Audit 2012*, pp. 3,9; (<http://www.historic-scotland.gov.uk/sheareport2012-2.pdf>, accessed 27.10.2015).

- Moropoulou A., Labropoulos K. C., Delegou E. T., Karoglou M., Bakolas A., 2013, Non-destructive techniques as a tool for the protection of built cultural Heritage. *Construction and Building Materials*, 48, Elsevier, pp. 1222 – 1239.
- Nwaubani S. O., Dumbelton J., 2001, A practical approach to in-situ evaluation of surface-treated structures. *Construction and Building Materials*, 15, pp. 199 – 212.
- Odgers D., Henry A. (eds.), 2012, *Practical Building Conservation – Stone*, English Heritage, London, p. 222.
- Pamplona M., Kocher M., Snethlage R., Wendler E., 2008, Consolidation effectiveness of TEOS on Ança limestone from Portugal. In: Delgado Rodrigues J., Mimoso J. M. (eds.) *Proceedings of the International Symposium Stone consolidation in cultural heritage – research and practice*, 6 – 7 May 2008, Laboratório Nacional de Engenharia Civil, Lisbon, pp. 183 – 192.
- Panagiotis T., Karatasios I., Stefanis N. A., 2008, Performance Criteria and evaluation parameters for the consolidation of stone. In: Delgado Rodrigues J., Mimoso J. M. (eds.) *Proceedings of the International Symposium Stone consolidation in cultural heritage – research and practice*, 6 – 7 May 2008, Laboratório Nacional de Engenharia Civil, Lisbon, pp. 279 – 288.
- Price C., 2006, Consolidation. In: Henry A. (ed.) *Stone Conservation – Principles and Practice*, Donhead Publishing, Dorset, pp. 102, 104, 107.
- Ruedrich J., Hertrich M., Just A., Siegesmund S., Yaramanci U., Jacobs F., 2004, Construction physics of the market gate of Miletus discovered by non-destructive tools. In: Kwiatkowski D., Loefvendahl R. (eds.), *10th International Congress on Deterioration and Conservation of Stone*, 27 June – 2 July 2004, Stockholm Vol. 2, ICOMOS Sweden, pp. 745 – 752.
- Smith B. J., McCabe S., McAllister D., Adamson C., Viles H. A., Curran J. M., 2011, A commentary on climate change, stone decay dynamics and the ‘greening’ of natural stone buildings: new perspectives on ‘deep wetting’. *Environmental Earth Science*, 63, pp. 1691 – 1700.
- Török Á., 2010, In situ methods of testing stone monuments. In: Boştenaru Dan M, Prikryl R, Török Á (eds.) *Materials, Technologies and Practice in Historic Heritage Structures*, Part II, Springer Verlag, pp. 177 – 193.
- Urquhart D., 2007, Stonemasonry skills and materials - a methodology to survey sandstone building facades, Technical Advice Note No. 31, Historic Scotland, Edinburgh, p. 5.
- Weber H., Zinsmeister K., 1991, *Conservation of Natural Stone – Guidelines to Consolidation, Restoration and Preservation*. Expert Verlag, Ehningen, Germany, p. 54.
- Wheeler G., 2005, Alkoxysilanes and the consolidation of stone. Getty Conservation Institute, Los Angeles, p. 113.
- Young M., Cordiner P., Murray M., 2003, Chemical Consolidants and Water Repellents for Sandstones in Scotland. *Historic Scotland*, Edinburgh, pp. 54 – 62, 242.

USE OF LOCAL STONE IN THE MIDWESTERN UNITED STATES: SUCCESSSES, FAILURES AND CONSIDERATIONS

E. Gerns^{1*} and R. Will¹

Abstract

Until relatively recently, locally available stone was used almost exclusively in construction, due to availability, limited transportation options and economics. Historically, naturally formed field stone was used for foundations, localized cladding features and in some instances entire building façades. Stone, perhaps more than any other natural building material, has numerous varieties and characteristics within its broader classifications. Many of these local stones were not necessarily appropriate for some applications and environmental conditions. Since around 1880, and continuing for perhaps 40 years, as quarrying techniques mechanized, the use of some local stones in larger and thinner individual units as cladding in multi-wythe exterior wall systems were replacing traditional monolithic field stone wall systems. As these “newer” wall systems have aged, these applications introduced challenges including unanticipated weathering characteristics, residual stresses and detrimental inclusions. Where and how these unique local stones are installed as well as climate and weathering patterns certainly contribute to the potential deterioration and serviceability challenges. This paper will focus on three local limestones used in the Midwestern United States between the 1850s and early 1900s that have variable performances in various applications.

Keywords: façade cladding, Joliet limestone, Carthage marble, Platteville limestone

1. Introduction

Stone has been used as a building material for thousands of years. Its aesthetics and sense of permanence have made it a popular material, especially among builders and architects. Many of the significant buildings throughout history have been constructed of stone. Early stone monuments constructed of non-local material have been the source of numerous theories regarding how this material was transported over great distances. In reality, the method of extracting and transporting may be as simple as basic physics, in combination with inexpensive and available labor and the expectation that construction can be a generational endeavour, rather than the highly accelerated pace required in today’s economic climate. The days of monumental royal constructions are mostly long over, but the desire to construct buildings using stone remains universal. The evolution of stone clad buildings closely parallels the evolution of building construction and technologies. Monolithic wall assemblies were the standard for thousands of years. Modern construction techniques attempt to minimize the amount of stone used to maintain the aesthetics a particular stone provides, to save weight and money. This change is a result of the evolution

¹ E. Gerns* and R. Will

Wiss, Janney, Elstner Associate, Chicago, Illinois, United States of America

*corresponding author

of structural and manufacturing technology allowing stone to be used and quarried in thinner applications than had historically been feasible. Historic quarrying and fabrication techniques relied on both local labor forces, local stone sources and basic transportation systems.

Historically stone was used for both decorative and functional purposes. With few exceptions, building systems incorporate inexpensive backup materials in combination with more expensive facing. Early stone structures were typically solid, multi-wythe, load bearing assemblies combining high quality facing stone finished to very tight tolerances with a looser rubble or brick backup. Once again, economics was critical to the development of exterior enclosure systems.

The Industrial Revolution of the mid-19th Century dramatically changed the building industry. Economics certainly still was the primary driving factor in almost all building construction, but mechanization provided advancements in the construction industry from machines to transportation. This resulted in the wider use of stone since it was now more economical in some respects. Transportation remained a major factor in the selection and use of stone throughout the world.

2. Midwestern United States geology

In the Midwestern United States large stores of limestone exist. Beginning in the 1850s, the use of locally quarried limestone for civil structures and building foundations became common. The stone was readily available and the physical properties were found to be desirable for civil and foundation applications. In these applications, the stone was quarried in relatively large blocks and installed with the bedding planes oriented parallel to the ground (naturally oriented).

Unlike foundations, when some of these sedimentary stones were used for cladding, the geological composition of the stone became more critical to the durability and workability and therefore appropriateness of the applications. As a cladding, the desire to use the stone in less natural applications was greater, thus resulting in situations with higher exposure and less redundancy in the material. Workability with respect to carving, and the desire for larger units used in alternate aesthetics to random coursing, began to expose the limited durability of some of the stone.

3. Midwestern United States stone

This paper will focus on three commonly used stones in the Midwestern region of the United States between 1850 and 1910 including Joliet Limestone, Platteville Limestone and Carthage “Marble”. Each is extensively used in civil and building applications between 1850 and 1910 in the areas close to their natural source. The material was rarely transported out of the area for use in other parts of the United States. Use of these stones as a building stone has all but stopped, but many examples remain in each respective area of their natural formations.

3.1. Joliet limestone

In the Chicago area, a cream-colored dolomitic limestone known as Joliet limestone was widely used prior to 1870. Laid down during the Silurian age, roughly 425 million years ago, the stone was often marketed as marble to improve the perception of quality of the material. Joliet limestone was first encountered when the I&M Canal was being built in the late 1830s. The density and low absorption characteristics of the stone were ideal for lining the walls of the canal. Being local, the stone was relatively inexpensive and readily available. Buildings built adjacent to the canal were often constructed using the stone (Kubal 2013). The Great Chicago Fire of 1871, however shifted the popularity of Joliet limestone toward Indiana limestone. Newspaper accounts from the time unbelievably reported that during the fire, limestone ‘seemed as though [it] actually burned like wood.’ Certainly not the case. By the 1870s exposed applications of the stone revealed that Joliet limestone was subject to exfoliation and weathering. Thus, many of the older buildings of the time that used the stone for the exterior walls were showing signs of age that also put a damper on new construction (Kubal 2013). Further, many of the stone masons that had worked with the stone since it was first used were no longer in the industry having retired or passed away. Thus, the rise of popularity of Indiana limestone occurred since the stone provided a more uniform appearance, had good weathering characteristics, was easier to work with and was more consistent with the change of architectural aesthetic that was beginning around 1890. In addition, Joliet limestone became more popular and economical as an aggregate rather than a building stone since the processing and skilled labor force required was less than that of building stone. With few exceptions, the stone has not been used as a building stone since around 1910.

Many examples of Joliet Limestone buildings and structures remain throughout the Chicago area to this day including the I&M canal, the Chicago Water tower, the Scottish Rite Cathedral, and Second Presbyterian Church (Fig. 1).

Common characteristics of the stone that often must be addressed in repair work is exfoliation and face bedding. Few options exist to address these issues and often substitute stone is used to replace deteriorated components. The weathering of the stone can be mitigated to an extent by maintaining or improving the water shedding characteristics of the building with the use of gutters and downspouts. Watertables and drip courses often were constructed of regional sandstone (Fig. 1) in-lieu of the limestone since it was easier to work, but more expensive to procure. These features tend to exhibit more deterioration from run off, requiring higher percentages of repair and replacement than units within the field of the wall. Replacement material that is similar to the original remains available when replacement is necessary.

Another unique nature feature is asphaltic inclusions in the stone giving the stone the mistaken appearance of being stained by roofing mastics or careless repair activities. Understanding that this is a natural occurring feature of the stone is critical to developing appropriate and necessary repairs rather than ill-advised approaches such as surface treatments or aggressive cleaning techniques. Even gentle cleaning methods, such as water soaking, can cause significant levels of the friable surface to release from buildings clad with Joliet limestone as the stone begins to soften and ‘protective’ crust formed by years of atmospheric soiling is removed.

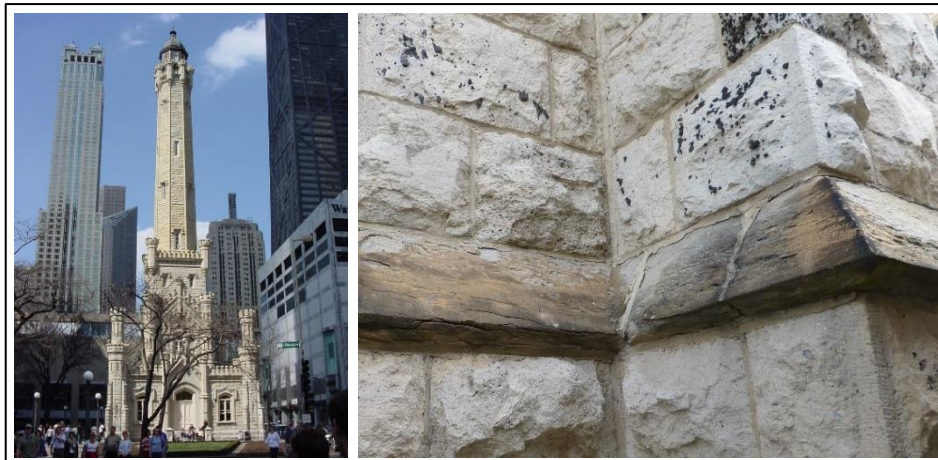


Fig. 1: Representative example of Joliet limestone with sandstone drip course. Image on the left is of the Chicago Water Tower (1869) and the image on the right is from Second Presbyterian Church (1874) also located in Chicago. Note the asphaltic inclusions that are common in some of the limestone quarried in the area of Joliet Illinois.

3.2. Carthage “Marble”

In Missouri, a metamorphic limestone, known as Carthage marble was popular for both foundations and cladding beginning in the 1880s. Carthage deposits are part of the Burlington group of the Mississippian Carboniferous strata that was formed during the Silurian and Carboniferous periods, roughly 360 million years ago. The ledges are horizontal and vary from three to twelve feet thick, the thickness increasing with depth. The ledges are separated by mud seams (Strong 1908). The peak of production for Carthage marble was the early 1900s at which point more than 750,000 cubic feet were quarried per year which was second in the United States only to Indiana limestone (Hiller 1910).

The stone in the Carthage quarries has a gray and bluish-gray color, and the lithologic characteristics of the quarry beds. Stylolites are prominent in the ledges and usually lie in the direction of the planes of bedding. They are spaced in vertical intervals that vary in thickness from 1 to 18 inches. The texture of the stone is essentially of uniform crystallinity, with only slight variations in grain sizes in the stone between the stylolite ‘veins’ (Perazzo 2015).

Carthage marble is similar to limestone in appearance with the exception of the pronounced stylolites and bedding planes (Fig. 2). When used in exterior wall applications, face spalling and visible pronounced stylolites are susceptible to freeze-thaw related deterioration in areas of high exposure. Carved building elements are also more susceptible to weathering since more of the bedding planes and stylolites are exposed. In addition, random hairline map cracks are common. These cracks are likely the result of the residual stresses in the stone being released during quarrying operations. The combination of the factors listed above resulted in a relatively short use of the stone for building applications. Once again, the use of Indiana limestone usurped a locally available stone. Most of the original quarries

have been converted to gravel facilities. Repair of this stone introduces similar challenges as Joliet limestone. Water shedding façade features can be protected by installing a metal flashing or cap on the top exposed surfaces of the features. With few exceptions, replacement material options are limited to higher quality and more consistent limestone. A common approach that helps maintain the aesthetics and original building fabric is to replace architectural features, such as water tables and drip courses, in their entirety with similar matching material. While all of the stone in a particular feature may not be significantly deteriorated, the likelihood of such deterioration is often unavoidable. By replacing the features, these areas of high weathering achieve a much greater service life cycle.

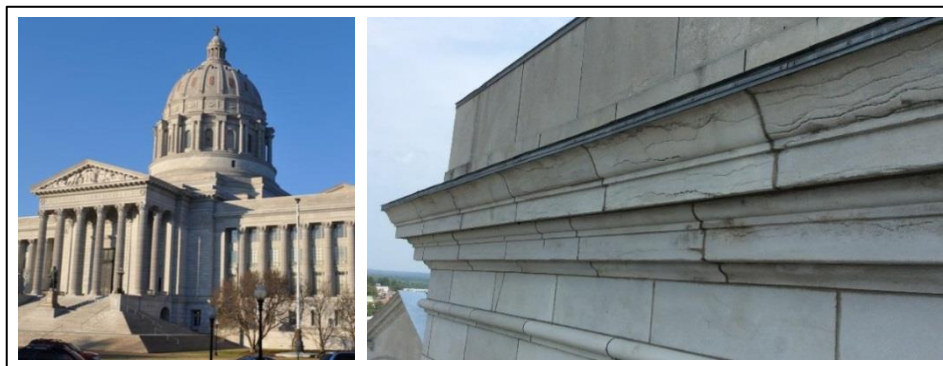


Fig. 2: Representative example of Carthage marble. Photograph is of the Missouri State Capitol (1917). Note pronounced bedding planes in image on the right.

3.3. Platteville limestone

In the Minneapolis area, a dolomitic limestone, known as Platteville limestone was widely used for foundations and cladding beginning in the 1880s. Platteville Limestone is part of the Ordovician limestone formation and overlies a layer of Glenwood Shale, which overlies a much thicker layer of Saint Peter Sandstone. Platteville limestone was deposited during the Ordovician period of the Paleozoic era, roughly 485 million years ago. Platteville was used widely in the Minneapolis for a period of about 30 years. The lower bed of the formation was first used for building stone as early as 1823 and was generally characterized to consist of interlaminated dense or semicrystalline blue-gray limestone with irregular shaly bands. The upper bed which is fine-grained limestone was found to be more durable than the lower layers but its use was still limited to foundations and walls not exposed to view (Sardeson 1914). Over time, in wall applications, all layers of the limestone have not performed well in a severe cyclical climate such as Minneapolis. When used in a confined application, such as foundation walls, the stone has performed reasonably well over the years. In unconfined applications that are exposed to water, the inclusions in the bedding planes form calcium sulfate dihydrate (gypsum) that will expand when exposed to moisture, resulting in often dramatic displacements and bowing of building components such as window sills and parapets (Fig. 3). The gypsum will also result in efflorescence forming on the surface of the stone as it dries. Like the other two stones, little can be done to address the stone itself in these instances and replacement is often the only viable repair option.

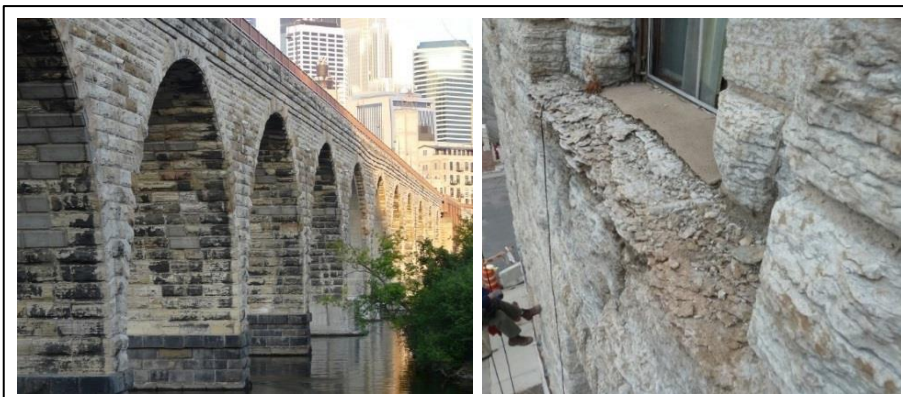


Fig. 3: Representative examples of Platteville limestone. Image on the left is of the Stone Arch Bridge (1883) located in Minneapolis, Minnesota; image on the right is from the Pillsbury A-Mill (1881) also in Minneapolis.

4. Causes of deterioration

All stone is susceptible to deterioration from various causes including: moisture shedding characteristics, lack of proper maintenance, organic growth, inappropriate previous repairs, and inappropriate cleaning techniques. Freeze-thaw durability has long been known as a source of stone deterioration and a significant issue in the Midwestern United States. In the case of dolomitic limestones, clay laden bedding planes are far more susceptible to freeze-thaw deterioration than oolitic limestone as the clay will readily absorb water (Winker, 1997). Most importantly, relative to the stone described above is a general vulnerability of the materials based on application. This issue is further exacerbated when the stone is installed in a face-bedded orientation. Face-bedding is an economic-driven fabrication method that is commonly used when the proportions of the stone are greater in elevation than in plan. This creates a greater potential for face delamination and exfoliation of units when exposed to temperate weathering patterns. While the stones presented above provided an economical solution for particular application in localized areas of the Midwestern United States, time has provided the best indication that there are clear disadvantages to using these local stones in many applications.

5. Repair approaches

While it is often desirable from a preservation philosophy perspective to replace as little deteriorated stone with the same stone as necessary, yet in some instances this is not practical or appropriate. Often, the stone is no longer available and for good reason. Replacing severely deteriorated units or façade elements with an alternate stone in most instances is the accepted approach. In the case of the stones presented in this paper, a stone that is often substituted for Platteville and Joliet limestone is known as Lannon stone. First quarried in the 1830s, Lannon was used in throughout the Midwestern United States. The stone is a dolomitic limestone quarried in southeast Wisconsin and is part of the Niagara Escarpment from the Silurian Period (Young 2012). The stone is generally a gray to cream color and is quarried close to the surface and has excellent durability and very low

absorption. This stone has been found to blend well with the both Joliet and Platteville limestone (Fig. 4). Indiana limestone has been found to be good substitute for Carthage marble, aside from some of the aesthetic concerns regarding uniformity described above. The material has a long successful track record of successful applications and the color is generally consistent Platteville and Carthage with the exception of the lack of pronounced bedding planes and stylolites. Using these alternate stones for water shedding façade elements as well as deteriorated façade features enable many of the buildings clad with these poor performing stones to remain in service.



Fig. 4: Representative examples Lannon stone used as a substitute for Platteville stone. Image on the left is a replacement sill and image on the right is a reconstruction of a parapet.

As with any building façade repair project, developing an appropriate repair approach is a multi-faceted process. A typical investigation should include a review of available documents related to the façade including drawings, maintenance records and previous reports, a thorough inspection, an investigation of concealed conditions and field and laboratory testing of the constituent façade components including the stone and mortar. Based on the findings of the investigation, appropriate repairs, scope and prioritized phasing can be developed. These repairs may principally include stone replacement, but in addition consideration of envelope water management provisions, including roof drainage, repointing and crack repair are often necessary. Finally, appropriate cleaning and biogrowth treatment often helps to mitigate accelerated deterioration, yet in the Joliet limestone could cause further deterioration. Other repairs that are sometimes considered include patching, application of consolidants, pinning and re-sculpting of weathered elements. Each of these need to be approached with great care. Often times these techniques are ineffective at best and in some instances detrimental to the stone.

6. Conclusions

When considering these three stones or other local stones that have not been recently used in building construction, it is critical to understand the properties which make them unique. This understanding helps to prioritize repairs and determine the appropriateness of using the same material, if it is available, or using an alternate material without significantly

compromising aesthetic and providing proven durability. Because stone is not a man-made product, its physical and aesthetic characteristics can vary significantly even within the same quarry, thus just because it appears to be the same material, does not mean it will behave as such.

Traditionally recognized stone properties include compressive, flexural, shear, and tensile strengths, density, abrasion resistance, coefficient of thermal expansion, and modulus of elasticity and rupture. In addition to these established properties, other properties that are frequently overlooked can contribute to premature failure of a stone cladding system. These properties include permanent volume change or hysteresis, freeze-thaw weathering, chemical weathering, thermal weathering, effects of stone finish, orientation and permeability. Simply stated, these properties may reduce the strength and durability of the particular stone, which can lead to significant maintenance and repairs of the stone façades in the not-so-distant future.

References

- Hiller, J. C., 1910, “Annual Report of the Bureau of Labor Statistics, the State of Missouri...”, Volume 32”, Hugh Stephens Printing Company, Jefferson City, MO, p. 627, <https://books.google.com/books?id=7RkoAAAAYAAJ>, (accessed November 1, 2015).
- Kubal, J., 2013, “One Stone to Another”, http://www.esconi.org/esconi_earth_science_club/2013/04/what-do-you-know-about-joliet-lemont-limestone-.html, (accessed November 1, 2015).
- Perazzo, P., 2015, “Stone Quarries and Beyond”, <http://quarriesandbeyond.org/states/mo/Missouri.html>, (accessed November 1, 2015).
- Sardeson, F., 1914, “Description of the Minneapolis and St. Paul District”, pubs.USGS.gov/gf/201/text.pdf, p. 13, (accessed November 1, 2015)
- Strong, R. S., 1908, “Carthage Limestone: Its Production and Characteristics”, Mine and Quarry, Chicago, pp. 179-182.
- Winkler, E. M., 1997, “Stone in Architecture: Properties Durability”, p.254
- Young, E. 2012, “Home-grown Limestone”, Masonry Edge, Masonry Advisory Council, <https://masonryedge.com/site/mim-archives-thestorypole-vol-38-no-6/372-homegrown-limestone>, (accessed November 1, 2015).

LASER YELLOWING OF HEMATITE-GYPSUM MIXTURES: A MULTI SCALE CHARACTERISATION

M. Godet^{1*}, V. Vergès-Belmin¹, C. Andraud², M. Saheb³,
J. Monnier⁴, E. Leroy⁴ and J. Bourgon⁴

Abstract

Nd:YAG Laser cleaning at 1064 nm of limestone monuments covered by black gypsum crusts is sometimes associated with yellowing. This unwanted yellow discoloration is still not fully explained by the scientific community. During laser irradiation of black crusts a lot of particles are ablated, forming a visible smoke. One possible explanation of the yellowing phenomenon is that some yellow iron-rich nanoparticles formed by irradiation and present in the smoke are redeposited on the surface of stone during the cleaning. To investigate this hypothesis, previous research has been conducted on simplified model crusts containing only gypsum and hematite. However this research always focuses on the analysis of the substrate after cleaning and never on the ablated particles. In the investigation presented here, we have characterised the particles ablated during the laser cleaning of a model gypsum crust containing hematite. As the particles of interest are rare and submicronic we have elaborated a multi-scale analytical methodology. Light digital microscopy reveals that the ablated particles are essentially gypsum crystals with a slightly yellow hue, plus red and black micro-particles interpreted as being hematite and magnetite. When focusing on the yellow gypsum crystals at the nanoscale, electron microscopy allows us to highlight the presence of two types of iron-rich nanoparticles covering the surface of gypsum crystals. One type of nanoparticle measure several tens of nanometres and contain iron, calcium and oxygen whereas the other type of nanoparticles measure less than ten nanometres and seem to contain only iron and oxygen. These results ascertain the link between the presence of iron containing nanoparticles and the yellowing effect.

Keywords: laser, cleaning, gypsum crust, nanoparticle, iron yellowing, TEM

¹ M. Godet* and V. Vergès-Belmin

Laboratoire de Recherche des Monuments Historiques (CRC-LRMH USR 3224), France
marie.godet@culture.gouv.fr

² C. Andraud

Centre de Recherche et Conservation des Collections (CRC-CRCC USR 3224), France

³ M. Saheb

LISA, UMR CNRS 7583, Université Paris-Est Créteil and Université Paris-Diderot, France

⁴ J. Monnier, E. Leroy and J. Bourgon

Université Paris-Est, ICMPE Institut de Chimie et des Matériaux Paris-Est, UMR 7182
CNRS-UPEC, Thiais, France

*corresponding author

1. Introduction

The Nd:YAG (1064 nm) laser cleaning of historical monuments covered by black gypsum crusts sometimes induces a yellowing of the underlying stone (Pouli, 2012). In the 2000s, this yellowing phenomenon raised a widespread aesthetic controversy (Délivré, 2003), especially in France where the market of laser cleaning for historical monuments has almost totally disappeared nowadays (Vergès-Belmin *et al.*, 2014). Since 2001, many studies on the yellowing effect have been conducted on model gypsum crusts (Klein *et al.*, 2001; De Oliveira *et al.*, 2015; Gracia *et al.*, 2005). As a reminder, a natural black crust is a complex system composed of a gypsum matrix entrapping soot, iron oxides, ashes; basically all the particles present in the atmosphere. Thus studying the interactions between this system and the laser beam is difficult. The problem has therefore been simplified by focusing on simplified model crusts. Model crusts studied to date are mixtures of synthetic gypsum and lamp black, graphite, or hematite with various quantities of each component. These mixtures are applied as a coating on various substrates such as marble or plaster. By irradiating these model crusts, scientists have managed to simulate in a very simplified way the laser induced yellowing obtained on site. The irradiated model crusts have then been analysed with various techniques. For instance for model crusts containing only hematite, it was found with SEM-EDS that the surface of the post-irradiated yellow substrate was covered by iron-rich nanoparticles measuring a few tens of nanometres (Klein, 2001).

During laser irradiation of black crusts, a lot of particles are ablated, forming a visible smoke (Vergès-Belmin *et al.*, 2003). One possible explanation of the yellowing phenomenon is that some yellow iron-rich nanoparticles are redeposited on the stone surface during cleaning. To investigate this hypothesis, yellow phases may be searched for either on the substrates or in the smoke itself. Most of the researches conducted to date focus on the analysis of the substrate and never on the ablated particles (Klein *et al.*, 2001; Gracia, 2005; Potgieter-Vermaak *et al.*, 2005).

The only investigations performed on smoke are related to health hazards. Feely *et al.* (2000) and Kush *et al.* (2003) for instance, have evidenced the presence of micro to nanoparticles in the smoke generated by laser during natural black crust elimination. They had to face the difficulties of developing a pertinent observation methodology as the particles are present in very low quantities. These studies were not focussed on yellowing, and in any case a great number of phases not implicated in the yellowing phenomenon may be generated in such conditions. Starting from this statement we have decided in the present study to simplify the system and to focus on particles ejected from a model crust based on gypsum and hematite. We have elaborated a multiscale approach wherein the morphology and the structure of the ejected particles were analysed at a macro- to nanometric scale using complementary analytical tools in order to link these multi-scale observations with the yellowing effect.

2. Materials and methods

2.1. Sample preparation

The sample used in this study is a model gypsum crust elaborated with a procedure already described by De Oliveira *et al.* (2015). A white gypsum plate (7×3 cm) is synthesised by hydration of a powder of calcium sulphate hemihydrate $\text{CaSO}_4 \cdot 0.5\text{H}_2\text{O}$ (ALDRICH 97%) in distilled water. Before the plate becomes totally dry, a mixture of the same calcium sulphate hemihydrate and red hematite $\alpha\text{-Fe}_2\text{O}_3$ (ALDRICH 99%) powders (70:30 wt %) is

sprinkled over the plate through a coarse-meshed sieve (about 1 mm). The remaining water in the plate is absorbed by the powder and leads to the crystallization of a gypsum crust entrapping particles of hematite. The crust is left to dry for 24 hours. The name of the sample is GH30 for Gypsum-Hematite-30_{wt%}. The amount of iron oxide has been deliberately chosen much higher than the amount present in a natural black crust (1-2_{wt%} according to Ruffolo *et al.* (2014)) in order to increase the probability of the detection of the yellow particles. Indeed De Oliveira *et al.* (2015) has shown that the more concentrated in hematite the model crusts are, the more yellow they become after laser irradiation. We operate under the assumption that the more yellow is the surface of model crusts, the larger will be the amount of particles responsible of the yellowing. Particulate materials from the sample GH30 are obtained using a Nd:YAG laser. The irradiation conditions have been chosen because they are similar to those used by restorers-cleaners. (see Tab. 1).

Tab. 1: Experimental parameters for laser irradiation of model black crust GH30.

Parameters	Unit	Value
Energy	J	0.4
Frequency	Hz	10
Duration/cm ²	min·cm ²	3
Fluence	J·cm ²	0.4-0.6

The laser is operating at a wavelength of 1064 nm and producing discrete pulses of laser energy up to 0.4 J with a pulse length of 15×10^{-9} seconds. The pulse is delivered using an articulated mirrored arm and a hand-piece equipped with a 70 cm focal converging lens. The fluences used slowly increase from 0.4 to 0.6 J·cm² during the cleaning with a frequency of 10 Hz and a duration of irradiation of three minutes per cm². In other words, about 1800 pulses per centimetre are used to clean the sample. The surface is water sprayed before irradiation. The particles are collected on a clean glass slide (76×26 mm) and a round adhesive carbon tab (diameter: 6 mm) put vertically aside the sample at a distance of about 1 cm. (see Fig. 1). The slide and the carbon tab are then stored in an airtight box to prevent contamination.

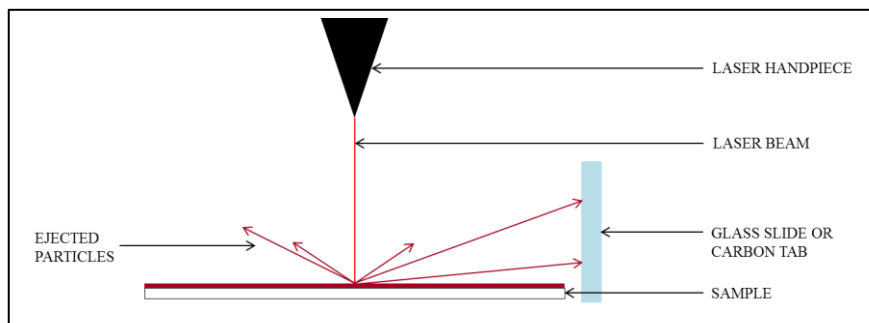


Fig. 1: Experimental set-up used to collect particles ejected from the model crust.

2.2. Characterization techniques

The morphology and colour of particulate materials have first been observed with a light digital microscope Keyence 3D VHX-5000. We then use scanning electron microscopy (SEM) to study the morphology at a micro and sub-micron scale. The SEM observation is performed with a SEM-FEG MERLIN coupled with an energy dispersive X-ray spectrometer Aztec EDS Advanced to give a first approximation of the chemical composition. The adhesive carbon tab covered by ablated particles is directly put in the microscope. Transmission electron microscopy (TEM) analysis is used to identify the chemical composition and the structure of the particles at a nanoscale. TEM analysis is performed at 200 keV with a FEI TECNAI F20 equipped with a STEM device coupled with an EDS spectrometer EDAX R-TEM Sapphire and with a Gatan GIF 2001 Electron Energy Loss Spectrometer (EELS). The EELS and EDS capabilities are used to determine the chemical compositions of the particles. Energy-filtered transmission electron microscopy (EFTEM) technique is also used to select a precise range of electron energies to provide elemental maps. The sample is prepared by rubbing gently the surface of the glass slide with a copper grid covered with a holey amorphous carbon film.

3. Results and discussion

3.1. Digital microscope

During laser cleaning of model black crust, the surface of the cleaned sample GH30 becomes yellow (see Fig. 2) and a lot of particles are ablated and are transferred to the glass slide or the adhesive carbon tab.

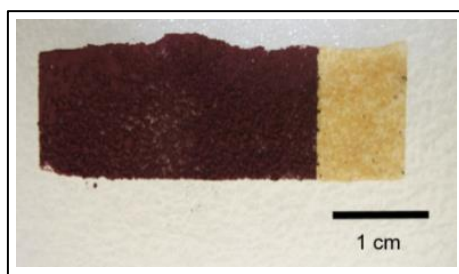


Fig. 2: GH30 sample before (red) and after (yellow) laser irradiation.

With naked eye observation, we are able to see a dust deposit. The digital microscope observation reveals the simultaneous presence of various particles together with a high quantity of euhedral gypsum crystals having a slightly yellow colour (see Fig. 3). In addition to the gypsum crystals we can see two other types of particles:

- Irregular agglomerated red particles ranging from a few to several tens of micrometers interpreted as being hematite which has not reacted with the laser beam.
- Sub-rounded and often agglomerated black particles ranging from a few to several tens of micrometers interpreted as being magnetite formed from the transformation of hematite under the laser beam (Da Costa, A. R., 2002; Gracia, 2005).

The gypsum crystals are recognizable thanks to their morphology: they usually form long and white transparent rods or platelets as shown by De Oliveira *et al.* (2015). In our case,

most ablated gypsum rods or platelets show a diffuse yellow colour but the microscope resolution is too low to see more clearly their details. It seems therefore that, during laser irradiation, at least two transformations take place: the hematite transforms into magnetite and the white transparent gypsum rods acquire a yellow hue.

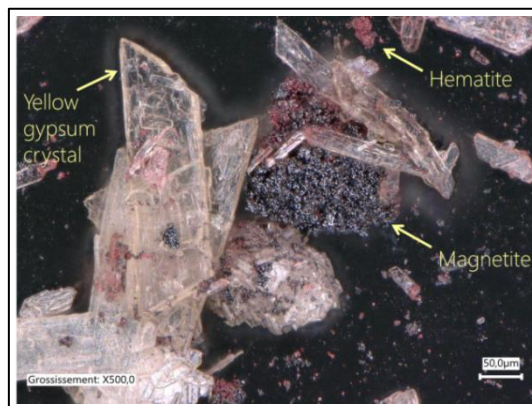


Fig. 3: Ejected particles collected on a glass slide (digital microscope picture).

3.2. Scanning electron microscope

The SEM investigation we conducted permitted to better understand the structure of the yellow hue observed with the digital microscope. The ablated yellow gypsum platelets are actually covered by two types of objects: a large number of spherical nanoparticles and a rough nanometric film. The size of the nanoparticles is very variable: they range from several tens of nanometres to more than a few hundreds of nanometres. The rough nanometric film is covering irregularly the surface of gypsum rods and platelets (see Fig. 4). The SEM resolution is too low to distinguish more clearly the morphology of the nanometric film. Based on EDS analyses, we found that the surface of the ablated gypsum rods and platelets contains calcium, sulphur, oxygen and iron.

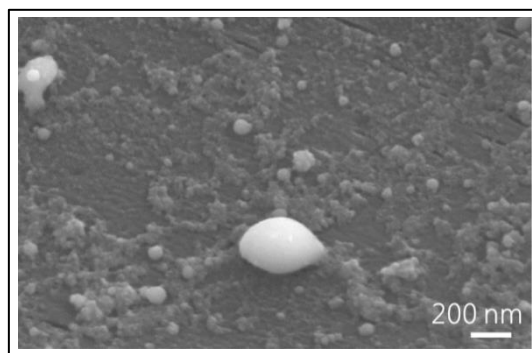


Fig. 4: Nanoparticles and rough nanometric film at the surface of a gypsum platelet (SEM picture, secondary electron mode).

Our SEM observations are in line with those made by Klein *et al.* (2001) and De Oliveira *et al.* (2015) on model gypsum crusts containing hematite which present a yellow hue after laser irradiation. The two authors have shown that after irradiation the surface of the gypsum substrate is covered by nanophases containing iron. Here we found that the laser ablated gypsum crystals presenting a slight yellow hue are covered by nanoparticles and by a rough nanometric film both containing iron. Our SEM analysis thus tends to indicate that the yellow hue observed on the gypsum substrate and on the ejected gypsum crystals after laser irradiation may both originate from the formation of similar nanometric phase(s) containing iron.

3.3. Transmission electron microscope

TEM analysis was conducted to explore the surface of the gypsum rods and platelets at the nanoscale. Two types of particles were observed (see Fig. 5):

- Spherical nanoparticles measuring several tens of nanometres which we will call “big” nanoparticles.
- Sub-rounded nanoparticles measuring less than ten nanometres which we will call “small” nanoparticles. The small nanoparticles are often agglomerated and may cover a big nanoparticle.

The big nanoparticles observed by TEM probably correspond to what was described as “nanoparticles” on SEM observation. The small nanoparticles most probably correspond to the basic unit of the rough nanometric film previously described.

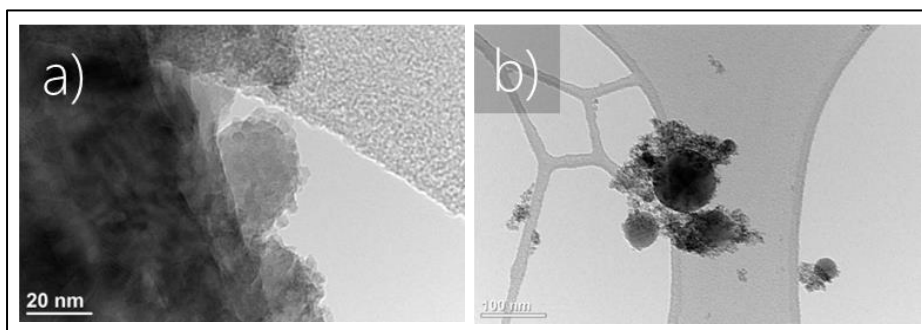


Fig. 5: a) Small nanoparticles agglomerated on the surface of a gypsum rod; b) Isolated big nanoparticles covered by a lace of small nanoparticles (TEM pictures); note: the grey network observed behind the nanoparticles corresponds to the carbon holey film.

The chemical composition of some nanoparticles was determined using EDS and/or EELS. We mostly looked for isolated nanoparticles to avoid the contribution of gypsum chemical components to their chemical composition. The localized isolated nanoparticles have probably detached from the gypsum rods or platelets when we rubbed the copper grid on the glass slide surface. Two types of particles were detected: nanoparticles containing iron and oxygen and nanoparticles containing iron, oxygen and calcium. The TEM image in Fig. 6 shows a big nanoparticle partially covered with an aggregate of small nanoparticles. The EFTEM maps of calcium, iron and oxygen clearly show that the big nanoparticle contains iron, oxygen and calcium while the small nanoparticles contain iron and oxygen. The absence of calcium may be due to the fact that calcium is present in too low quantity to

be detected. The absence of sulphur is most probable, as sulphur was not detected by EDS and it cannot be detected by the EFTEM set up because sulphur energy is too low for the electron energy loss spectrometer (GIF GATAN) we worked with. However as sulphur is very difficult to detect at the nanoscale we do not exclude the possibility of its presence.

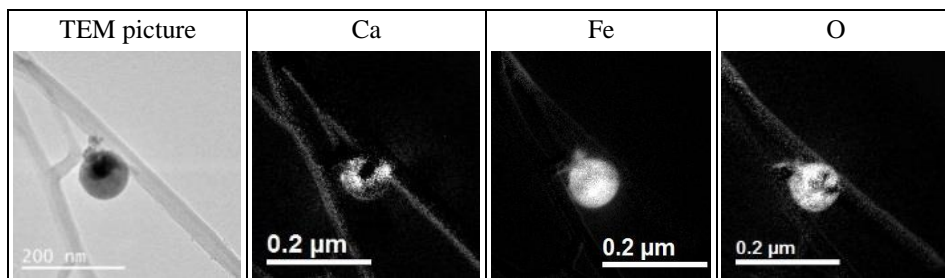


Fig. 6: EFTEM cartography of an isolated big nanoparticle covered by an aggregate of small nanoparticles.

4. Conclusion

In order to understand the laser-induced yellowing phenomenon, we have studied the ablated materials ejected during the laser irradiation of a model crust composed of gypsum and hematite. We used a multi-scale approach to link the colour to the morphology at a micro and nanoscale. The digital microscope aids the identification of yellow gypsum crystals in the form of rods or platelets associated with red and black micro-particles interpreted as being respectively hematite and magnetite. SEM/EDS analysis enabled us to observe the surface of the ablated yellow gypsum rods or platelets at a sub-microscale. Those crystals are covered with isolated nanoparticles and a rough nanometric film both containing iron. TEM analyses show that in addition to the isolated nanoparticles observed with SEM, the presence of smaller nanoparticles measuring less than ten nanometres is ascertained. These smaller nanoparticles may correspond to the basic unit of the rough nanometric film observed with SEM but it has not been evidenced yet. Using TEM coupled with EDS, EELS and EFTEM techniques we have determined the chemical composition of the observed nanoparticles. The composition seems to depend on the size of the particle: the “small” nanoparticles measuring less than 10 nanometres contain iron and oxygen whereas the “big” nanoparticles measuring 20 to 100 nanometres contain iron, oxygen, calcium and possibly sulphur. The next step of the investigation on those neoformed nanophases is now to link these multi-scale observations with the yellow colour observed on the surface of gypsum rods. Further study will undoubtedly reveal more information about the precise identification of the nanophases and their relation with the yellow colour. Understanding the laser induced yellowing is a major challenge as it will help the laser manufacturers to build new cleaning lasers which will not discolour the stone and thus give the cleaning method a fresh start.

Acknowledgements

Many thanks to the SILLTEC company which is partly funding this PhD research.

References

- Da Costa, A. R., 2002, Ultra-fast dehydration and reduction of iron oxides by infrared pulsed radiation, *Scripta Materialia*, 47, 327-330.
- Délivré, J., 2003, Laser cleaning: Is there specific laser aesthetics?, *Journal of Cultural Heritage*, 4, 245-248.
- De Oliveira, C., Vergès-Belmin, V., Demaille, D. & Bromblet, P., 2015, Lamp black and hematite contribution to laser yellowing: a study on technical gypsum samples, *Studies in Conservation*, online DOI:10.1179/2047058415Y.0000000003
- Feely, J., Williams, S., Fowles, S., 2000, An initial study into the particulates emitted during the laser ablation of sulphation crusts, *Journal of Cultural Heritage*, 1, 65-68.
- Gracia, M., Gavino, M., Vergès-Belmin, V., Hermosin, B., Nowik, W. & Saiz-Jimenez, C., 2005, Mössbauer and XRD Study of the Nd-YAG Laser Irradiation at 1.06 μm on Haematite Present in Model Samples, *Proceedings of the Laser in the Conservation of Artworks Congress (LACONA V)*, Dickmann, K., Fotakis, C. and Asmus, J. F. (eds.), Osnabrueck, Germany, 341-346.
- Klein, S., Fekrsanati, F., Hildenhagen, J., Dickmann, K., Uphoff, H., Marakis, Y. & Zafiropoulos, V., 2001, Discoloration of Marble During Laser Cleaning by Nd:YAG Laser Wavelengths, *Applied Surface Science*, 171(3-4), 242-51.
- Kusch, H.-G., Heinze, H., Wiedemann, G., 2003, Hazardous emissions and health risk during laser cleaning of natural stones, *Journal of Cultural Heritage*, 4, 38s-44s.
- Pouli, P., Oujja, M., Castillejo, M., 2012, Practical issues in laser cleaning of stone and painted artefacts : optimisation procedures and side effets, *Applied Physics A : Materials Science & Processing*, 106, 447-464.
- Potgieter-Vermaak, S.S., Godoi, R.H.M., Van Grieken, R., Potgieter, J.H., Oujja, M., Castillejo, M., 2005, Micro-structural characterization of black crust and laser cleaning of building stones by micro-RAMAN and SEM techniques, *Spectrochimica Acta Part A*, 61, 2460-2467.
- Ruffolo, S., Comite, V., La Russa, M., Belfiore, C., Barca, D., Bonazza, A., Crisci, G., Pezzino, A., Sabbioni, C., 2014, An analysis of the black crusts from the Seville Cathedral: A challenge to deepen the understanding of the relationship among microstructure, microchemical features and pollution sources, *Science of the Total Environment*, 502, 157-166.
- Vergès-Belmin, V., Wiedemann, G., Weber, L., Cooper, M., Crump, D., Gouverne, R., 2003, A review of health hazards linked to the use of lasers for stone cleaning, *Journal of Cultural Heritage*, 4, 33-37.
- Vergès-Belmin, V., De Oliveira, C., Rolland, O., 2014, Investigations on yellowing as an effect of laser cleaning at Chartres Cathedral, France, *Proceedings of the ICOM-CC 17th Triennial Conference*, Bridgland, J. (eds.), Melbourne, art. 1703.

THE USE OF HYDROXYAPATITE FOR CONSOLIDATION OF CALCAREOUS STONES: LIGHT LIMESTONE PIŃCZÓW AND GOTLAND SANDSTONE (PART I)

A. Górniak¹, J.W. Łukaszewicz^{2*}, B. Wiśniewska¹

Abstract

Carbonate stones have been widely used to create works of art and architecture, due to their mineral composition which is extremely sensitive to weathering mechanisms. The corrosion processes results in density reduction and loss of mechanical integrity, often accompanied by an increase in porosity. Structural consolidation aims at restoring the original physical properties of the stone and at the same time making them more resistant to weathering agents. Since the second half of the 20th century, after many years of using organic, synthetic resins for this purpose, there is now a tendency to return to inorganic consolidants, which are chemically compatible with stone building minerals. One goal of this research is to examine the possibility of using diammonium hydrogen phosphate (DAP) for consolidation of light limestone and calcareous Gotland sandstone, often used in Polish architecture and sculpture. Another aim is to determine the best conditions for the procedure.

Keywords: Pińczów limestone, Gotland sandstone, consolidation of calcareous stone, hydroxyapatite, diammonium hydrogen phosphate (DAP), SEM/EDS

1. Introduction

Apatite coatings have been identified on ancient monuments. Good preservation of these layers and the stone underneath, was an impulse to start research on consolidation and increasing acid dissolution resistance by causing formation of apatite in the structure of carbonate stones. These works commenced in 2009 by a research team under the direction of Professor George W. Scherer, Princeton University, New Jersey, USA.

This paper investigated the possibility of using diammonium hydrogen phosphate (DAP) as a consolidant for a structural treatment of Pińczów limestone and Gotland sandstone. Conditions affecting the effectiveness of the reaction between DAP and calcium carbonate and its impact on the properties of treated stones were defined.

¹ A. Górniak and B. Wiśniewska
conservator-restorer

² J.W. Łukaszewicz*

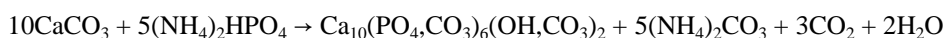
Department for Conservation of Architectonic Elements and Details, Faculty of Fine Arts,
Nicolaus Copernicus University, Toruń, Poland
jwluk@umk.pl

*corresponding author

The effectiveness of structural consolidation is affected by stone properties, like their chemical and mineralogical nature, type of porous structure (pore distribution, their diameter and shape) and also by the method and materials used. The most significant requirements for consolidants are (Łukaszewicz 2002, s. 63-64):

- Short time of solution penetration, depending on its low viscosity;
- Evenly distributed in stone structure, lack of migration to the surface;
- High degree of amplification of the disintegrated material, while maintaining the porosity;
- Not affecting any visual changes, especially on the surface;
- Absence of harmful side effects, like introduction of water-soluble salts;
- High resistance to erosion and corrosion factors, like water, UV radiation, air pollution, biological agents.

The method of carbonate stone consolidation with hydroxyapatite (HAP) is based on exposing calcite to an diammonium hydrogen phosphate (DAP) solution, as schematically shows the chemical reaction (Kamiya *et al.* 2004, s. 56)



The structure of the final product depends on many factors including solution concentration, temperature, *pH* and presence of foreign ions. During this transformation intermediate, metastable phosphate phases other than hydroxyapatite are formed (identification of their structure will be studied in Part II of current research).

In this study the impact of the type of the stone, DAP solution concentration and temperature on the possibility of reaction between calcium carbonate contained in Pińczów limestone and DAP was investigated.

2. Methodology

2.1. Materials

2.1.1. Stone samples

Two types of carbonate stones were used, both popular in Polish monuments and sculptures, Pińczów limestone and Gotland sandstone. Pińczów is a porous light limestone with bulk density $d = 1.73 \text{ g/cm}^3$, water penetration up to 5 cm within 30-36 min., water absorption $N = 13.9\%$, open porosity $P_o = 22.61\%$ and compressive strength $R_c = 10.9 \text{ MPa}$.

Gotland is a porous sandstone with carbonate binder with varying amount of calcium carbonate, with bulk density $d = 2.11 \text{ g/cm}^3$, water penetration up to 4 cm within 28-60 min., water absorption $N = 5.9-6.2\%$, open porosity $P_o = 12.7\%$ and compressive strength $R_c = 17.9 - 38.2 \text{ MPa}$. In this research two types of Gotland sandstone were used, one with 8.42-10.67% calcium carbonate content, and another with 13.32 - 14.02%.

Ground Pińczów limestone fractions <0.16 mm, 0.16-0.25 mm and 0.25-0.40 mm were used. The crushed limestone was placed in cylindrical containers having 3.5 cm diameter and 5cm high. In the second part of the research cubic samples were used (5 side).

2.1.2. Consolidant

Both stones were consolidated with water solution of diammonium hydrogen phosphate (DAP) - $(\text{NH}_4)_2\text{HPO}_4$, purchased from Polskie Odczynniki Chemiczne S.A., Gliwice, 5% and 15% solutions were prepared.

2.2. Consolidation

Ground Pińczów limestone was impregnated by capillarity with 5% and 15% DAP solutions. After a fully saturation, part of the cylindrical containers were placed in a tightly covered vessel for 48h in laboratory conditions (293-294 K) and the second part in a heat chamber (303K). This treatment was repeated 1, 2, 3 and 5 times. Pińczów limestone and Gotland sandstone cubic samples were consolidated by partial immersion with 5 in 15% DAP solutions. Calcium phosphate phases and bridges between grains formed after treatment were assessed with ATR-FTIR and SEM/ EDS. The effectiveness of the consolidation was evaluated by the capillary impregnation time change and impregnability change after treatment, also by improvement of mechanical properties and freezing resistance of the stone.

3. Results

3.1. Impact of DAP solution concentration and multiple saturation on properties of ground Pińczów limestone

After just one saturation cycle with 5% DAP in every ground cylindrical sample bridges between grains emerged as a product of DAP and calcium carbonate reaction. This merger allowed samples to be released out of the cylindrical containers and to be cut in pieces (Fig. 1). An increase in weight occurred, depending on aggregate fraction, from 0.54% (<0.16 mm) to 1.08% (0.25-0.40 mm), due to different solution absorption of the samples of different grain size. The sharp increase of phosphate phases content in the samples occurred after repetition of the saturation and increasing the concentration of DAP (Tab. 1).

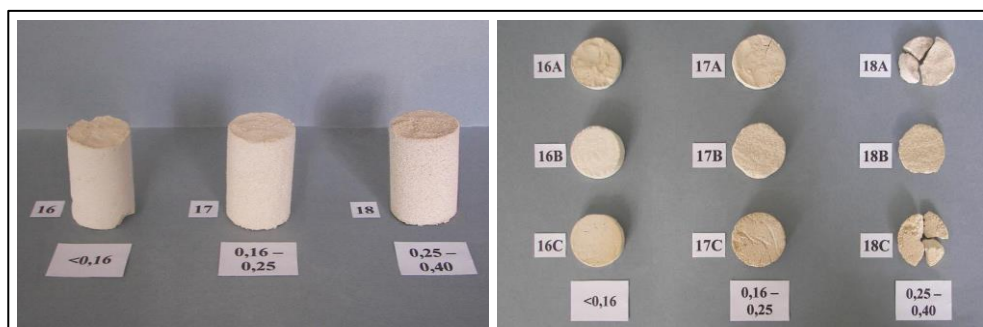


Fig. 1: Ground Pińczów limestone after consolidation.

Tab. 1: *Influence of concentration and numbers of DAP application on time of capillary rise, absorption and changes in weight.*

Fraction of aggregates	Number of application of DAP	Time of capillary rise up to 4 cm	Absorption	Increase of weight
mm		s	%	%
0.16-0.25 5% DAP	I	58	43.99	0.82
	II	36	40.08	3.08
	III	31	38.39	3.97
	V	26	35.68	4.62
0.16-0.25 15% DAP	I	1'21''	54.04	5.94
	II	46''	32.50	12.51
	III	35''	32.23	13.31
	V	37''	30.53	14.26

The decrease of capillary penetration time and absorption during the subsequent impregnation of ground limestone is clearly demonstrated. The number of separated phosphate phases depends on both the concentration of the solution as well as the number of impregnation cycles, with the highest value (14.26%) for fivefold impregnation with 15% DAP solution. Samples after triple impregnation with 15% DAP were analyzed by SEM/EDS to determine their texture, identify phosphate phases and define their distribution in micro regions (Fig. 2 to Fig. 4). The results indicate that phosphate phase distribution is evenly throughout the sample, also on the surface of limestone and in free spaces between grains.

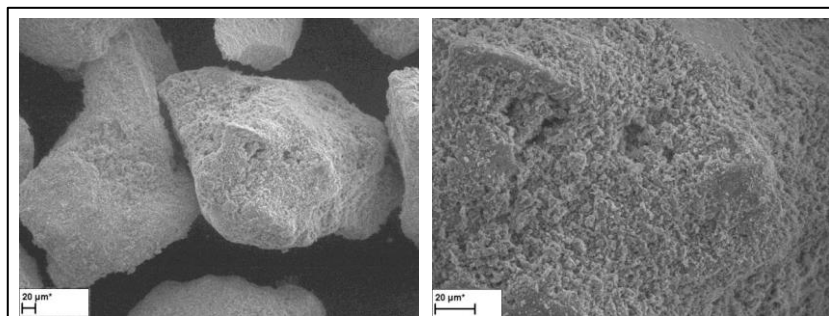


Fig. 2: *Texture of limestone grain before treatment.*

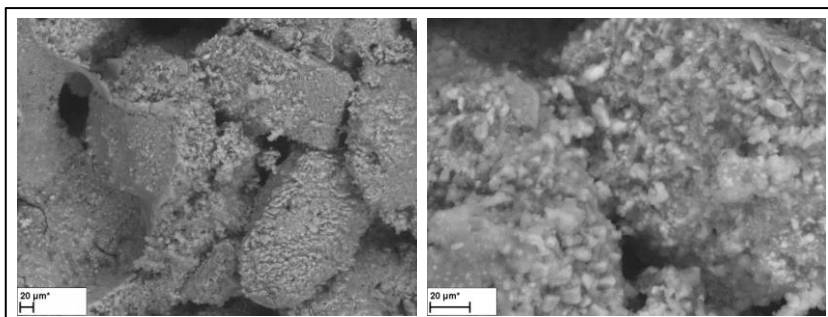


Fig. 3: Texture of treated limestone grains by 15% DAP – middle part of the sample.

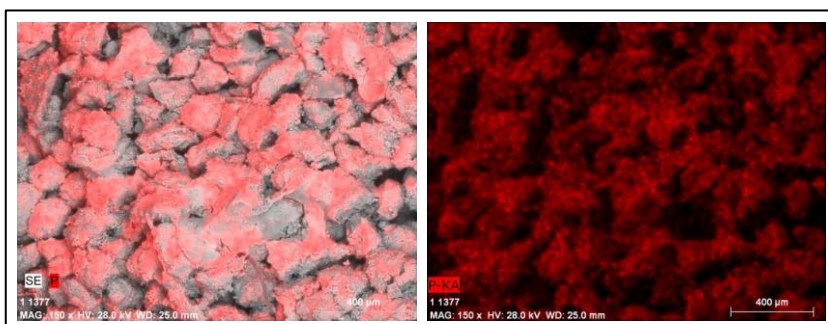


Fig. 4: Distribution of phosphorus.

ATR-FTIR was used as an analysis method to investigate the newly formed phosphate phases. As a comparative model untreated ground Pińczów limestone and calcium phosphates synthesized in the reaction of lime water and a 15% solution of DAP were used. For carbonates analytical bands with wave number 1396 cm^{-1} , 871 cm^{-1} , and for phosphates 1031 cm^{-1} , 560 cm^{-1} were adopted. With increasing degree of conversion into phosphate phases the carbonate absorbance bands decreased whilst phosphates were increasing. The Fineness of Pińczów limestone together with the solution concentration clearly influences this process. Additionally, temperature has also a small effect on the conversion of carbonates into phosphate phases.

3.2. The impact of stone type on consolidation effectiveness

3.2.1. Stone impregnation

Pińczów limestone and Gotland sandstone were impregnated by capillarity from a partial immersion in 5% and 15% DAP solution. Impregnation time of the limestone was quite short, but the solutions moved slower in the sandstone (Tab. 2). It depends on the type of stone but also on the concentration of the solutions. An extremely long time was needed for the 15% DAP solution to saturate Gotland sandstone. Absorption of DAP solutions in different concentrations and water absorption were similar (approx. 13% for Pińczów limestone and approx. 6.2% for Gotland sandstone). It must therefore be concluded that these two lithotypes were fully saturated with the investigated solutions, regardless of their concentration.

Tab. 2: Influence of type of stone for consolidation possibility.

Stone	Concentration of DAP solution	Capillary rise up to 4 cm	Absorption of DAP solution	Increases of weight
	%	min.	%	%
Limestone	5	39	13.19	0.16
	15	46	13.19	0.33
Sandstone	5	44	6.05	0.14
	15	151	6.16	0.40

After impregnation a slight increase in weight of the samples was noted, depending on the DAP solution concentration used. Despite the fact that after impregnation the samples were kept in a closed system, the reaction products migrated to the surface, having a significant impact on esthetic values of the stone, which is difficult to accept. Surfaces of both, the limestone and the sandstone were covered with a white coating (Fig. 4 and Fig. 5), also the color of the stones was darker. The standard tests for color changes in a L^*a^*b system showed a large color change after consolidation for Pińczów limestone (ΔE from 5.6 to 6.5).

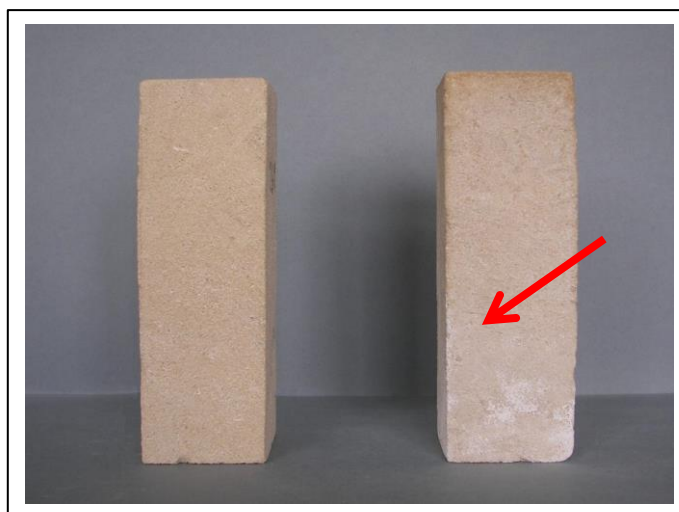


Fig. 4: White coatings after consolidation of limestone (right), before consolidation (left).



Fig. 5: White coatings after consolidation of Gotland sandstone by 15% DAP.

2.1.1. Properties of consolidated stones

Properties of consolidated stones were investigated on Pińczów limestone impregnated one and two times with 5% and 15% DAP, and Gotland sandstone impregnated with 5% DAP. 15% DAP solutions were abandoned in Gotland sandstone impregnation due to a strong crystallization of reaction products on the surface of the stone, hence the inability to use this solution concentration in conservation practice. The effectiveness of the process is obtained by changes in water absorption, porosity, compressive strength (R_c) and breaking strength (R_b). The results are presented in Tab. 3.

Tab. 3: Properties of treated stones.

Stone	Concentration of DAP solution/ Number of applications	Increase of weight	Water absorption	Decrease of water absorption	Open porosity	Decrease of porosity	R_c	ΔR_c
	%	%	%	%	%	%	MPa	%
Lime-stone	5%/2×	0.18	12.47	4.15	21.84	3.41	13.51	24.17
	15%/1×	0.33	12.74	2.6	22.21	1.78	13.67	25.64
	15%/2×	0.68	12.52	4.28	21.85	3.36	16.47	51.38
Sand-stone	5%/1×	0.14	5.75	7.56	12.01	4.93	31.38	6.32
						$R_b=$	0.45	25

The use of DAP to consolidate Pińczów limestone and Gotland sandstone, and as a consequence formation of calcium phosphates phases inside the stone pores (with not fully examined chemical structure) caused only a slight decrease in water absorption and porosity of both stones, which should be considered as an advantage of the proposed method. Mechanical strength increase depends on the amount of phosphate phases introduced into the pores of the stone. Increasing numbers of phosphate phases were

obtained by increasing the concentration of DAP solution and the number of solution applications. There was a greater percentage increase in mechanical strength of limestone than sandstone, which is connected to the initial high, but also diverse mechanical properties of the sandstone. This occurrence is known and confirmed in other studies on Gotland sandstone, where breaking strength had a slightly higher gain than presented in this paper, due to lower initial values.

4. Conclusions

The current study shows that the use of diammonium hydrogen phosphate (DAP) to structural consolidation of porous carbonate stones is possible, the method fulfils many of the criteria stated in the introduction. It does not require the use of environmentally harmful toxic solvents, aqueous DAP solutions move relatively quickly in the pores, allowing a complete saturation. Seasoning after the procedure takes only two days during which no substances harmful for the stones are emerged, the consolidated materials also retain their hydrophilic properties.

The research has shown that the phosphates forms were evenly distributed throughout the volume of all treated samples, wherein the water absorption and the open porosity decreased only slightly, which allows resaturating the consolidated stone in the future if needed. However, a partial migration of the reaction products to the surface, especially in Gotland sandstone, has caused reliable sealing of the surface and produced white coatings, and darkening of the surface of both stones, which of course is harmful. The mechanical properties depend on the number of newly created phosphate phases, which form in the pores of the stones, and their number depends on the concentration of the DAP solution and the number of repetitions of the process. The highest increase in compressive strength was obtained after a double impregnation of 15% DAP solution, 51%, with 0.68% weight increase after the treatment. Consolidation of Gotland sandstone also gives good results.

Preliminary studies on freezing resistance of treated stones showed that samples of consolidated limestone after 25 freezing-thawing cycles endured it better than not consolidated samples. The decrease in mechanical properties in the first case was 33%, while in the second 42%.

With increasing reaction temperature the degree of conversion of calcium into phosphate forms in Pińczów limestone increases, therefore the treatment should be carried out, if possible, at higher temperature (approx. 25-40°C).

In conclusion:

- Diammonium hydrogen phosphate (DAP) solutions can be interesting consolidates for Pińczów limestone and Gotland sandstone.
- Time of capillary rise of DAP solutions depends on their concentration and the structure of the stone.
- Reaction effectiveness depends on the mineralogical composition of the treated stones and the conditions of seasoning after treatment.
- Increase in mechanical strength properties depends on the concentration of the solution and the number of procedures performed.
- Due to migration of phosphate phases to the surface, which follows its seal and coatings forming, at this stage of the research the method cannot be used in conservation practice.

Future research should be continued, primarily on further explaining the mechanism of DAP and calcium carbonate reaction in different stones (including the impact of metal ions presence) and the reduction of phosphate phases migration to the surface.

Acknowledgements

The authors would like to thank Dr. Grażyna Szczepańska (Instrumental Analysis Laboratory, Faculty of Chemistry, NCU) for helping with the SEM-EDS analysis and Mr. Krzysztof Lisek for technical assistance during the project.

References

- Kamiya M., Hatta J. Shimada E., Ikuma Y., Yoshimura M., Monma H., 2004, AFM analysis of initial stage of reaction between calcite and phosphate, *Materials Science and Engineering B*, 111.
- Łukaszewicz J. W., 2002, *Badania i zastosowanie związków krzemoorganicznych w konserwacji zabytków*”, Wydawnictwo UMK, Toruń, ISBN 83-231-1445-5, pp. 257.
- Rodrigues J. D., Pinto A. P. F., 2015, Laboratory and onsite study of barium hydroxide as a consolidant for high porosity limestones, *Journal of Cultural Heritage*, paper in press.
- Sassoni, E., Naudi S., Scherer, G. W., 2010, Preliminary Results of the Use of Hydroxyapatite as a Consolidant for Carbonate Stones, Paper WW4.5, *Materials Research Society Symposium WW, Materials Issues in Art and Archaeology IX*, November 29 - December 2, Boston, s. 189-196.

This page has been left intentionally blank.

MARBLE PROTECTION BY HYDROXYAPATITE COATINGS

G. Graziani^{1*}, E. Sassoni¹, E. Franzoni¹ and G.W. Scherer²

Abstract

Hydroxyapatite (HAP) based treatments have been proposed for the protection of marble artifacts against acidic rain corrosion, because of the much lower dissolution rate and solubility of HAP with respect to calcite. Results obtained so far are promising, but optimization is necessary to make the treated layer complete, non-cracked and non-porous. In this study, ethanol addition was proposed to enhance surface coverage while avoiding crack formation, thus increasing the acid attack resistance of the substrate. The investigation of the best formulation and treatment procedure to be used was determined on calcite powders, then the acid resistance of the most promising treatments was evaluated on Carrara marble specimens by a specifically designed simulated rain apparatus, allowing to drop a continuous flux of acidic solution onto the samples, thus being closer to real weathering conditions on site. Results obtained show that HAP is a valuable option for marble protection, being able to slow down marble decay due to acid rain and exhibiting a better performance than ammonium oxalate, currently the most investigated inorganic protective for marble.

Keywords: calcium phosphate, acid attack, ammonium oxalate, calcite, dissolution

1. Introduction

Dissolution of marble surfaces due to the interaction with rain is a severe issue regarding cultural heritage preservation, as it results in the loss of precious material from stone artworks. Marble dissolution is linked to the solubility of calcite, its principal constituent (Naidu *et al.* 2015; Bonazza *et al.* 2009). However, all stone protectives currently available, both organic and inorganic, exhibit drawbacks that limit their efficacy. For this reason the research for a suitable product to be employed for stone protection is a primary goal in cultural heritage conservation.

The use of hydroxyapatite (HAP) as a protective for marble has been recently investigated (Naidu *et al.* 2014; Naidu *et al.* in press), as HAP has a very low solubility and dissolution rate compared to calcite. For this reason, creating a layer of HAP on top of marble would prevent calcite dissolution, provided that the layer is continuous, non-porous and uncracked. HAP can be formed by a mild chemical route by reacting diammonium hydrogen

¹ G. Graziani*, E. Sassoni and E. Franzoni
Department of Civil, Chemical, Environmental and Materials Engineering (DICAM),
University of Bologna, Italy
gabriela.graziani2@unibo.it

² G.W. Scherer
Department of Civil and Environmental Engineering (CEE), Princeton University,
United States of America

*corresponding author

phosphate (DAP) with calcium ions (Sassoni *et al.* 2011), deriving either from partial dissolution of the stone or externally added. Results obtained so far were very promising, but the treatment still needs to be optimized.

Ethanol has been found to be a calcite growth modifier and to adsorb on calcite and HAP (Ji *et al.*, 2015, Sand *et al.* 2010). For this reason, in this study, ethanol addition to the DAP solution was investigated, with the aim of increasing surface coverage without causing crack formation, and hence improving acid resistance of HAP-treated marble. Solutions of DAP and ethanol in different concentrations and in single and double applications were used and their efficacy was compared. At this step, treatments were applied to calcite powders and acid attack testing was performed by exposing samples to a finite volume of acid solution. Powders, having very high specific surface, undergo much faster dissolution, so this method allowed faster evaluation of the treatments. Moreover, it allowed exposure of a high number of grains that differ in crystallographic orientation and impurities, which otherwise would have required a high number of coarse samples. First, the most suitable ethanol concentration and treatment procedure were selected based on resistance to acid attack. Results were compared to those obtained by treating samples with ammonium oxalate (AmOx), currently the most used inorganic material for marble protection. Mixtures of AmOx and HAP were investigated too, with and without ethanol addition, as AmOx is effective in uniformly covering the substrate, but its solubility is significantly higher than that of HAP. Morphology and composition of the coatings were also investigated. The most promising coatings were applied on Carrara marble prisms, to get closer to the real situation, and a different type of acid attack test was used, consisting in a simulated runoff apparatus. Cycles, each consisting in continuous dripping of acidic solution over the samples followed by drying, were performed to prevent too high an accumulation of calcium ions near the dissolving marble surface, which would reduce the marble dissolution rate (Kaufmann G., *et al.*, 2007, Sjöberg E.L. *et al.*, 1985).

2. Materials and Methods

Calcite powders (30-50 White, Imerys) were sieved to select the fraction with particle size between 500 and 595 μm . Particles in this range would allow several nucleation sites on each particle, while providing a high specific surface area for dissolution tests. Carrara marble samples (Imbellone Michelangelo s.a.s.) had $30 \times 30 \times 20 \text{ mm}^3$ size. DAP (> 99%, Sigma Aldrich), calcium chloride (assay > 99.0%, Sigma Aldrich), ethanol (Fisher-Scientific) and ammonium oxalate ($\geq 99.99\%$, Sigma Aldrich) were used for the treatments. Prior to treating and characterization, powders and prisms were rinsed with water and ethanol to remove possible surface impurities and dried overnight.

2.1. Treatments on calcite powders

Reference samples were treated with a 0.1 M DAP solution (sample D0.1M) and with a 5 wt.% AmOx solution, according to Doherty *et al.*, 2007 (sample AmOx). To evaluate the effect of ethanol on the formation of HAP, ethanol was added in different concentrations to the 0.1 M DAP solution and its effects were evaluated (samples with the letter "E"). To boost surface coverage, ethanol addition was tested in combination with higher DAP concentration (namely 1M, samples D1E) and in double treatments (samples D1E+D1). In all DAP-treated samples (with and without ethanol addition), calcium ions were externally added by adding CaCl_2 to the solution, to prevent dissolution of the substrate. All treatments were performed by immersion (reaction time 24 hours). Compositions of the

most significant solutions are presented in Tab. 1. Second treatments were performed exactly as the first ones, but on pre-treated powders. Surface coverage, morphology and composition of the layers were investigated for the most promising treatments by FT-IR (Nicolet 6700) and SEM/EDS (FEI Quanta 200 FEG ESEM with Oxford EDS probe).

Tab. 1: Composition and nomenclature of the most significant treatments.

Specimen	Treating solution
D0.1	0.1 M DAP + 0.1 mM CaCl ₂
D0.1E	0.1 M DAP + 0.1 mM CaCl ₂ + 0.5 wt.% ethanol
D1E	1 M DAP + 1 mM CaCl ₂ + 0.5 wt.% ethanol
AmOx	5 wt.% Ammonium Oxalate
AmOxE	5 wt.% Ammonium Oxalate + 0.5 wt.% ethanol

The efficacy of the treatments was evaluated in terms of acid attack resistance, determined by exposing powders to an aqueous solution of HNO₃ at *pH* 5, such *pH* being chosen based on current and future values of rain *pH* (Bonazza *et al.*, 2009a, Bonazza *et al.*, 2009b). Powders were put in a beaker with the acidic solution kept stirring at a constant speed and *pH* variations in time were recorded. Morphology was re-examined for relevant samples.

2.2. Treatments on Carrara Marble prisms

Treatments D0.1M, D0.1ME and double treatment D0.1ME+0.1M were applied on Carrara Marble prisms. Untreated and AmOx treated samples were also examined for comparison's sake. Treatments were performed by immersion as for the powders.

As calcite dissolution depends on the concentration of Ca²⁺ ions in the solution, a custom designed setup providing a continuous dripping of solution onto the samples was preferred for the acid resistance test. Deionized water (at initial *pH* 6.8) was dripped onto the samples at a rate of 500 mL/h, alternating periods of dropping (2.5 h) and drying. After 24 wet/dry cycles (2 cycles per day), each sample had been exposed to an average solution volume of 29 L. Considering the annual average rain in Bologna (800 mm) and the size of the specimens, this volume of solution corresponds to about 40 years of rain. Runoff water was collected at each cycle and Ca²⁺ and PO₄³⁻ concentrations in the solutions were determined after cycles 1, 2, 8 and 24, to evaluate the dissolution of both the substrate and the coating. Ca²⁺ concentration was determined by HPLC, PO₄³⁻ by spectrometer. SEM/EDS was performed after the acid resistance test on the most promising formulation, to evaluate the treated layer morphology after artificial weathering.

3. Results and discussion

The treatment efficacy was evaluated on powders in terms of acid resistance (Fig. 1). The acid resistance of samples treated with 0.1M DAP solution is not satisfactory and accordingly several uncoated areas can be observed when powders are examined by SEM (Fig. 2a). These areas can act as preferential points for acid attack and, in fact, after acid attack it is visible that acid has undercut the substrate under the coating (Fig. 3b).

When ethanol is mixed to the solution, acid attack resistance of samples remarkably increases (Fig. 1a). Ethanol additions are beneficial in terms of acid resistance; no benefits are obtained by increasing the concentration above 0.5 wt.-%, while values of 20 wt.-% make the solution too diluted and the acid resistance decreases; hence 0.5 wt.-% was the selected concentration. SEM observations of ethanol-treated samples show that surface coverage has been remarkably improved by ethanol addition; however, some sparse uncoated areas can still be spotted (Fig. 2a). For this reason, ethanol-doped solutions at higher DAP concentration were tested.

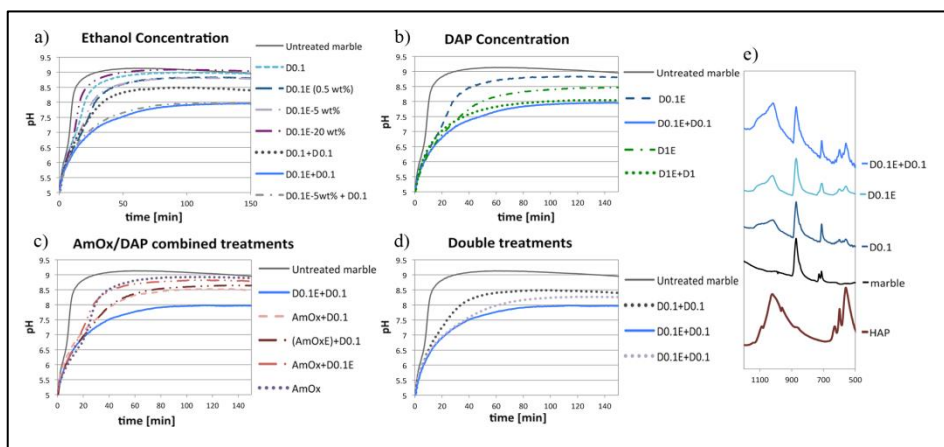


Fig. 1: Acid resistance (pH vs. time) for: a) different concentrations of ethanol in single and double treatments, b) different DAP concentrations, c) AmOx and DAP combined treatments, d) double treatments with and without ethanol addition. In e) the composition of the treated layer of the most promising formulations is investigated by FTIR.

In terms of acid resistance (Fig. 1b), D1E samples are much more resistant than D0.1E samples. However, when the morphology of the treated layer is observed, cracks are evident (Fig. 2c) thus raising concerns about long time performance of the coating. Cracks might occur during drying due to excessive thickness of the coating. Hence, double treatments were investigated, with the aim of creating two superimposed layers of reduced thickness instead of a thicker one, so as to avoid the crack formation. Double treatments with and without ethanol addition were investigated and the best one in terms of acid resistance was selected (Fig. 1c and d). Double treated samples at 0.1M concentration (D0.1+D0.1) have a better acid resistance than single D 0.1M treatment with and without ethanol addition (Fig. 1b). However, the efficacy can be further enhanced by ethanol addition: the most promising formulation being that where ethanol is used in the first layer, as no further increases in acid resistance were obtained by ethanol addition in the second layer (Fig. 1d). Double treatments at higher ethanol concentration in the first layer were also examined, as well as double treatments at higher DAP concentration (Fig. 1b). None of the tested treatments exhibits a better behaviour with respect to D0.1E+D0.1, which was then selected as the most promising and subjected to further characterization.

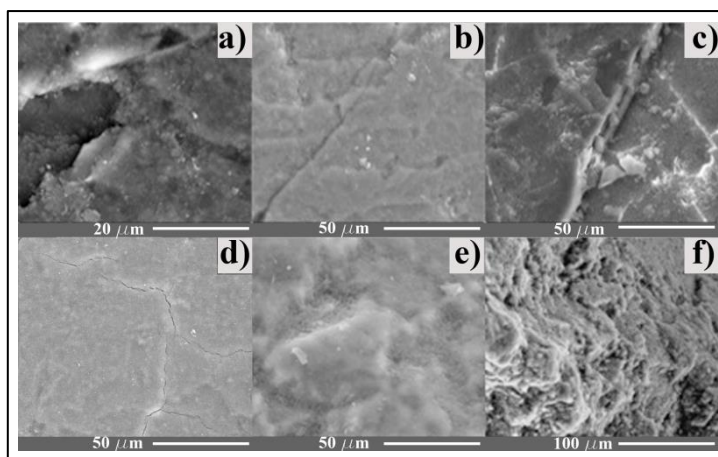


Fig. 2: Morphology of treated powders: a) sample D0.1; b) sample D0.1E; c) sample D1E; d) sample D1E+D1; e) sample D0.1E+D0.1; f) sample AmOx.

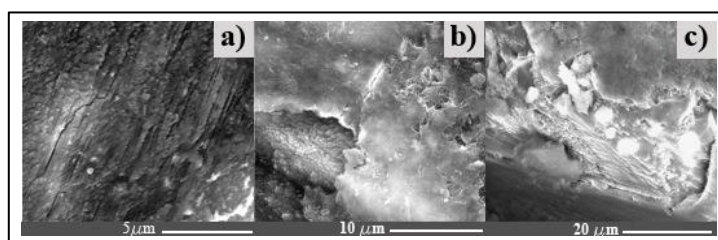
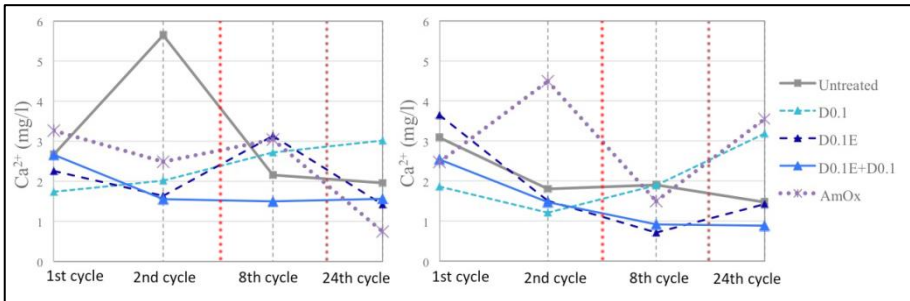
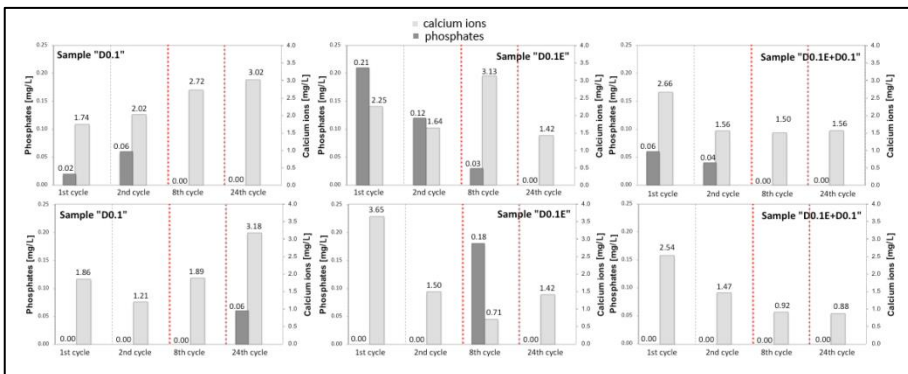


Fig. 3: Morphology of treated powders after acid attack test: a) untreated powder; b) sample D0.1; c) sample D0.1E+D0.1.

Acid resistance of D0.1E+D0.1 sample is much higher than that of ammonium oxalate treated samples, despite the uniformity of AmOx coating on powders (Fig. 2f), due to high solubility of calcium oxalate with respect to HAP and to the porosity of the layer. AmOx and HAP mixed treatments exhibit a better behaviour than AmOx treatment alone. However, they are still more soluble than D0.1E+D0.1 treated samples. No substantial benefits were obtained by adding ethanol to ammonium oxalate (Fig. 1c). When sample D0.1E+D0.1 morphology was examined by SEM, the coating appeared continuous and uncracked (Fig. 2e). After acid attack, however, some sparse uncoated areas were found close to the grain edges (Fig. 3c). The composition of the treated layer was determined for the most promising samples: D0.1, D0.1E and D0.1E+D0.1 by FT-IR (Fig. 1e). Bands relative to HAP formation can be assessed for all of the samples. These treatments were then applied to massive samples, again in comparison with AmOx, using the described dripping apparatus, so that data would not be affected by the finite volume of acid. Dissolution of samples was evaluated by determining the Ca^{2+} concentration in the runoff solution; values are reported in Tab. 2 and Fig. 4.

Tab. 2: Ca^{2+} concentrations (values are averages for duplicate samples).

Specimen	Ca^{2+} (mg/L)
Untreated	2.59±1.34
D0.1	2.21±0.69
D0.1E	1.97±0.98
D0.1E+D0.1	1.64±0.65
AmOx	2.69±1.18

Fig. 4: Ca^{2+} ion concentration in the runoff solutions for duplicate samples.Fig. 5: Ca^{2+} and PO_4^{3-} ion concentrations in the runoff solutions for duplicate samples.

The lowest calcium ions concentration can be assessed for samples D0.1E+D0.1, thus indicating slower dissolution (Fig. 4). Ethanol addition alone results in an improvement with respect to the sample treated with 0.1M solution but, for massive samples, its effect is much less visible than for powders. D0.1E+D0.1 also exhibits the lowest standard deviation between the two samples and in the different cycles, indicating that the behaviour is more dependent on that of the coating than the substrate. Phosphate concentration was also investigated to assess whether the dissolution would affect only the substrate or also the coating (Fig. 5). As HAP is expected to be insoluble for the given pH, high PO_4^{3-} contents indicate the presence of soluble phases together with HAP. Non-negligible phosphate

amounts in sample D0.1E might hence suggest that soluble phases have formed together with HAP, hence Ca^{2+} ions found in the solution might derive from the dissolution of both the substrate and the coating. Sample D0.1E+D0.1 exhibits the lowest dissolution and a negligible presence of PO_4^{3-} ions, hence indicating that HAP and not soluble phases were obtained by the treatment. In particular, Ca^{2+} concentration is much lower than that of AmOx samples, where, however, Ca^{2+} ions in solution derive from dissolution of both the substrate and the coating, given the higher solubility of AmOx with respect to HAP.

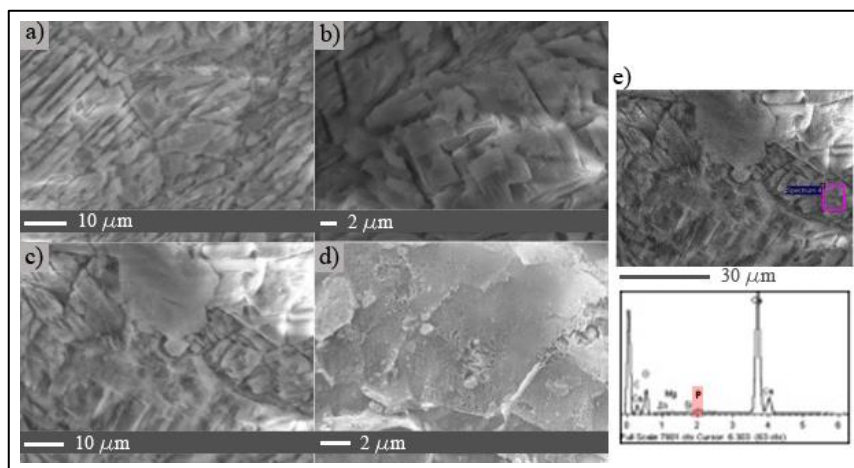


Fig. 6: Morphology of samples after simulated rain test: a) untreated marble, b) AmOx, c,d) D0.1E+D0.1; e) EDS on sample D0.1E+D0.1 in one area that seems uncoated.

Ca^{2+} ion concentration in D0.1E+D0.1 is lower than that of untreated marble; however, as some dissolution occurs in the samples, SEM was performed after the simulated rain test (Fig. 6). Images of untreated marble and AmOx are also reported for sake of comparison.

After acid attack, untreated samples appear etched, as does AmOx, where the surface seems essentially bare, thus suggesting that both dissolution of the coating and of the substrate has occurred. After acid attack, large areas of D0.1E+D0.1 appear uncoated and etched, though etching seems less severe than in the untreated reference. Some thick areas of the coating remain visible. However, when EDS is performed, phosphorous signal is detected in all the areas of the sample, including those that seem bare. For this reason it might be presumed that a layer of nanometric thickness is preserved: this would be consistent with the fact that, despite the treated layer being almost entirely consumed, the dissolution of the sample is still lower than that of the untreated reference, hence some protection is still maintained. Further tests are currently in progress to verify the presence of this layer and for further optimization of the treatment.

4. Conclusions

A novel HAP-based treatment for marble protection was proposed: ethanol addition was investigated to enhance surface coverage and acid resistance of the coating. The treatment proposed (D0.1E+D0.1), consisting in a double application of the solution with ethanol addition in the first layer, was successful in providing good coverage on powders without leading to the formation of cracks and hence to slow down dissolution.

The treatment gave promising results also when applied to Carrara Marble specimens, slowing down the dissolution of treated samples. The treatment still offered protection after prolonged simulated rain (corresponding to a period of 40 years in Bologna, Italy): however, further optimization is currently in progress to enhance the coating resistance.

Acknowledgements

We thank Dr. J. Schreiber for assistance on SEM analysis and Prof. A. Bocarsly and Dr. J. Pander for FT-IR analysis (Princeton University), M.Eng. M. Glorioso for collaboration on dripping tests and Dr. L. Guadagnini on HPLC (University of Bologna).

References

- Bonazza, A. Sabbioni C., Guaraldi C., De Nuntiis P., 2009a, Climate change impact: Mapping thermal stress on Carrara marble in Europe, *Sci Total Environ*, 407, 4506-4512.
- Bonazza A., Messina P., Sabbioni C., Grossi C.M., Brimblecombe P., 2009b, Mapping the impact of climate change on surface recession of carbonate buildings in Europe, *Sci Total Environ*, 407, 2039-2050.
- Doherty B., Pamplona M., Selvaggi R., Miliani C., Matteini M., Sgamellotti A., Brunetti B., 2007, Efficiency and resistance of the artificial oxalate protection treatment on marble against chemical weathering, *Appl Surf Sci*, 253, 4477-4484.
- Ji X., Su P., Liu C., Li J., Tan H., Wu F., Yang L., Fu R., Tang C., Cheng B., 2015, A novel ethanol induced and stabilized nanorods: hydroxyapatite nanopeanut, *J Am Ceram Soc*, 98, 1702-1705.
- Kaufmann G., Dreybrodt W., 2007, Calcite dissolution in the system $\text{CaCO}_3\text{-H}_2\text{O-CO}_2$ at high undersaturation, *Geochim Cosmochim Acta*, 71, 1398-1410.
- Matteini M., 2008, Inorganic treatments for the consolidation and protection of stone artifacts, *Conserv Sci Cult Herit*, 8, 13-27.
- Naidu, S., Liu C., Scherer G.W., 2015, Hydroxyapatite based consolidants and the acceleration of hydrolysis of silicate-based consolidants, *J Cult Herit*, 16, 94-101.
- Naidu, S., Scherer G.W., 2014, Nucleation, growth and evolution of calcium phosphate films on calcite, *J Colloid Interf Sci*, 435, 128-137.
- Naidu, S., Blair J., Scherer G.W., Acid attack mechanism on Carrara marble and efficacy of a protective hydroxyapatite film, *J Am Ceram Soc* (in press).
- Sand K.K., Yang M., Makovicky E., Cooke D.J., Hassenkam T., Bechgaard K., Stipp S.L.S., 2010, Binding of ethanol on calcite: the role of the OH bond and its relevance to biomineralization, *Langmuir*, 26, 15239-15247.
- Sassoni E., Naidu S., Scherer G.W., 2011, The use of hydroxyapatite as a new inorganic consolidant for damaged carbonate stones, *J Cult Herit*, 12, 346-355.
- Sjoberg E.L., Rickard D.T., The effect of added calcium on calcite dissolution kinetics in aqueous solutions at 25°C, *Chem Geol* 49, 1985, 405-413.

USE OF CONSOLIDANTS AND PRE-CONSOLIDANTS IN SANDSTONE WITH SWELLING CLAY AT THE MUNICIPAL THEATRE OF SÃO PAULO

D. Grossi^{1*}, E.A. Del Lama¹ and G.W. Scherer²

Abstract

Swelling clay is a problem in the stone cultural heritage of some countries, such as the United States, Germany and Switzerland. This expansive mineral increases the rate of stone degradation and puts the monuments at risk. As such, we need to test products for increasing the durability of these stones. Itararé Sandstone was used to build important historical and cultural heritage buildings, such as the Municipal Theatre of São Paulo – a 100-year-old building that has undergone three restorations. Ethylenediamine anhydrous and 1.3 Diaminopropane (DAA) were used as pre-consolidants, and tetraeth oxysilane (TEOS) and diammonium hydrogen phosphate (DAP) were used as consolidants. The results showed that the products closed the pores slightly and the stones become resistant to water degradation.

Keywords: swelling clay, Itararé sandstone, pre-consolidants, consolidants, surfactants

1. Introduction

Sandstones with swelling clays used in heritage buildings and monuments constitute a challenge for conservation. This is due to a rain-induced wetting-and-drying phenomenon, and to increasing moisture levels causing movement of the clay layers and generating a granular disintegration and weakening of the structure of the rock, causing the rock to degrade faster. The object of study is Itararé Sandstone, which is a layered rock, formed in a deltaic environment and of a fine-to-coarse grain. Mineralogically, it is a feldspathic sandstone with a clayey matrix consisting of clay minerals of the smectite group, including chlorite and illite. This rock is a constituent of the Municipal Theatre of São Paulo – an important building in the history of the development of the city – which is used for events up to the present day. As an attempt to inhibit or reduce the clay swelling behaviour, we pre-consolidated the rock using surfactants, ethylenediamine anhydrous and 1.3 diaminopropane (DAA).

Jiménez González and Scherer (2004) evaluated the use of surfactants to decrease the expansion of rocks that contain swelling clays, and found good results for Portland Brownstone. Wangler and Scherer (2008) worked on understanding the behaviour of the

¹ D. Grossi* E.A. Del Lama
Institute of Geosciences, University of São Paulo, Brazil
danigrossi@usp.br

² G.W. Scherer
Department Civil & Environmental Engineering, Princeton University, United States of America

*corresponding author

clays and identified two main types of expansion, with intracrystalline expansion causing more damage. The latter authors developed a method for the characterization of this type of expansion in sandstones.

Water is considered one of the most damaging agents for stone. The harm is greater when the stone has small pores, which increasing capillarity and carry the water deep into the stone. This behaviour is most harmful when the water freezes or when the stone has salts or swelling clays.

The methods used for the evaluation of the products were ultrasonic velocity measurement, dilatometry, sorptivity, mercury porosimetry and wetting and drying cycles. With these tests, performed on fresh and treated samples, it was possible to compare the action of products, simulating the passage of time and the deterioration caused by water.

2. Itararé Sandstone

Itararé Sandstone is poorly consolidated, deposited in a deltaic environment between the Paleozoic and Mesozoic eras. Today the quarry from which the samples were taken is a nature conservation area, known as National Forest of Ipanema. It is located in the municipality of Iperó, in the state of São Paulo (Brazil). The stone is a yellow sandstone, with fine-to-coarse grains, formed in a deltaic environment. Petrographically, Itararé Sandstone is feldspathic, with clayey matrix constituted by the smectite group with illite and chlorite (Del Lama *et al.*, 2009).

3. Methodology

The fresh samples were cut and dried before treatment with pre-consolidants, consolidants, or pre-consolidants and consolidants sequentially. The pre-consolidants are aminoalkanes with hydrocarbon chains of varying lengths (DAA). The aim of this phase was to decrease the volume and the depth of water penetration and increase the resistance of the clays in contact with water without the application of the hydrophobic products that prevent the ingress of the water and sometimes close the pores, making retreatment or application of other products impossible. The consolidants were diammonium hydrogen phosphate (DAP) prepared at 1 molar concentration and oligomers of tetraethoxysilane (Conservare 100, PROSOCO), hereafter identified as TEOS, diluted in 99.5% ethanol in the proportion 1:3.

The products were applied by capillary rise to penetrate the stone and avoid trapping air inside it. After it rose to the top, the samples were covered by the product and left to impregnate for 24 hours. After that, they were removed from the liquid and left to dry in a chemical hood. In the case of TEOS, the manufacturer indicates that the hydrolysis takes three weeks. After three weeks, the samples were submerged in a solution of 1:4 ethanol:deionized water for 24 h to complete the hydrolysis of the TEOS and render the sample hydrophilic (Naidu *et al.*, 2015). After this period, the samples were left to dry naturally under the fume hood. The product was completely hydrolyzed when the weight of the sample stabilized.

To summarize, the treatments were two pre-consolidants (DAA) successively, DAP only, DAA + DAP, TEOS only and DAA + TEOS.

3.1. Mercury porosimetry

Mercury porosimetry was used to measure the pore sizes and the cumulative intrusion volume, aiming to compare the results of untreated and treated samples. The size tested was 1×1×1.5 cm.

3.2. Sorptivity

The equipment to perform this test was used by Jiménez González and Scherer (2002). The sample is suspended from a balance and its bottom surface is in contact with water, so the balance shows the weight gain caused by the ingress of water into the pores. The sorptivity is calculated from the slope of the curve of weight gain versus square root of time. Measurements were made parallel to the bedding and perpendicular to the bedding. The size of the samples was 1×1×1.5 cm.

3.3. Ultrasound velocity

The velocity of sound decreases on passing through fractures, larger pores and any kind of discontinuity, so it is a good parameter for following the degradation of stone. The equipment measures the transit time, t (s), of the sound wave through the sample, and the velocity, V (m/s), is given by $V = d/t$, where d = sample thickness (m). The equipment used was a Pundit machine with 54kHz transducers. The size tested was 2.5×2.5×8.5 cm.

3.4. Wetting-and-drying cycles

To simulate the stress caused by hygric expansion, wetting-drying cycles were performed in a machine developed by Jiménez González and Scherer (2006). Samples are attached to a belt that passes through a bath containing tap water to saturate the stone and then under a set of fans to produce rapid drying. The samples were submerged in water for 20 minutes and dried for 40 minutes in each cycle. This process was repeated for one month, which amounts to about 700 cycles. The ultrasonic velocity was measured before and after the cycles. The samples size was 2.5×2.5×8.5 cm.

4. Results and Discussion

Mercury porosimetry showed that the total porosity was not affected by the products, but the TEOS closed the small pores (diameters near 10 nm) (Fig. 1), and drastically reduced the volume of pores with diameters near 1 μm . All the results are shown in Tab. 1.

The sorptivity of the bare stone was about 0.0045 $\text{g}/\text{cm}^2 \cdot \text{min}^{1/2}$ perpendicular to the bedding, and varied by about a factor of 2 parallel to the bedding (from a value similar to that perpendicular to the bedding to about half as much). The DAA increased the sorptivity from 0.0038 $\text{g}/\text{cm}^2 \cdot \text{min}^{1/2}$ (fresh) to 0.0060 $\text{g}/\text{cm}^2 \cdot \text{min}^{1/2}$ perpendicular to the bedding and from 0.0043 $\text{g}/\text{cm}^2 \cdot \text{min}^{1/2}$ (fresh) to 0.0051 $\text{g}/\text{cm}^2 \cdot \text{min}^{1/2}$ parallel to the bedding direction. This may reflect expansion of the body as DAA intercalates into the clay in the stone (Wangler and Scherer, 2008). DAP reduced swelling by 29% perpendicular to the bedding and raised it 23% parallel to the bedding direction. Treatment with DAA + DAP reduced swelling by 91% perpendicular to the bedding, and TEOS reduced it by 42% perpendicular to the bedding and by 10% parallel to the bedding. DAA + TEOS reduced the sorptivity by 50% perpendicular to the bedding direction and increased it by 27% parallel to the bedding. (Tab. 2). The greatest decrease was caused by the treatment with DAA+DAP, which is in contrast to results on other stones (e.g., Naidu *et al.*, 2015), where the silicate consolidant caused a much greater change.

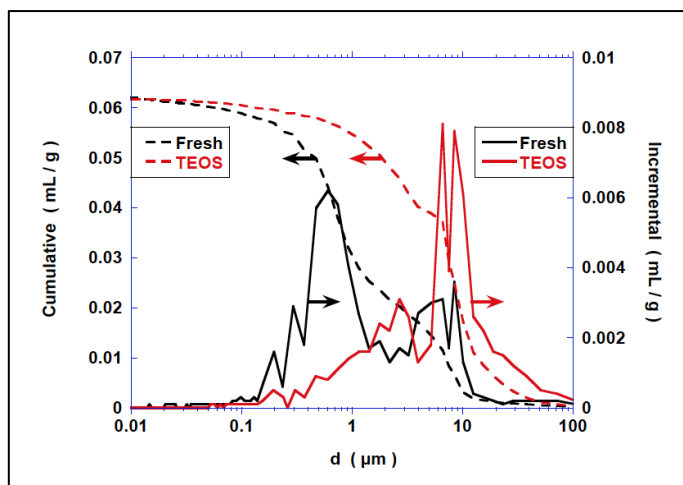


Fig. 1: Comparison of mercury intrusion curves for fresh stone and sample consolidated with TEOS.

Tab. 1: Results of mercury porosimetry.

Treatment	Porosity (%) – (100 – 10000 nm)	Porosity (%) – (10 – 100 nm)
Bare	17.09	14.15
DAA	16.09	15.13
DAP	29.66	14.39
DAA + DAP	17.01	9.65
TEOS	13.09	1.80
DAA + TEOS	14.53	10.80

We tested six samples for each treatment in wet and dry cycles, totalling 30 samples. The best results were obtained by using aminoalkanes followed by silicate-based and phosphate-based products (Fig. 2). The range of ultrasonic wave velocity before wetting-and-drying cycles was 2.7 to 3.6 km/s and 1.9 to 3.1 after the cycles. The sample treated with DAA + DAP shows the highest velocity before and after the treatment. Even though it did lose a lot of stiffness after cycling, it is still much better than the untreated stone, and better than the one treated with TEOS. The biggest negative factor for DAP is the decrease in sorptivity, which probably indicates that it reacted with the DAA and precipitated a product that blocks the pores. In all cases, the velocity decreases following wetting-drying cycles were lower for treated stones than for fresh samples. It shows that all products were of benefit to the stone. The DAA + TEOS was not cycled, because the sorptivity result showed that this product blocked the pores.

Tab. 2: Results of sorptivity.

Treatment	Bedding direction	Sorptivity (g/cm ² •min ^{1/2})	Average (g/cm ² •min ^{1/2})
Bare	Perpendicular	0.0057	0.0038
	Perpendicular	0.0043	
	Perpendicular	0.0026	
	Perpendicular	0.0025	
	Parallel	0.0043	0.0043
	Parallel	0.0039	
	Parallel	0.0050	
	Parallel	0.0040	
DAA	Perpendicular	0.0050	0.0060
	Perpendicular	0.0069	
	Parallel	0.0042	0.0051
	Parallel	0.0060	
DAP	Perpendicular	0.0027	0.0027
	Parallel	0.0053	0.0053
DAA+DAP	Perpendicular	0.0004	0.0004
TEOS	Perpendicular	0.0017	0.0022
	Perpendicular	0.0027	
	Parallel	0.0039	0.0039
DAA+TEOS	Perpendicular	0.0024	0.0019
	Perpendicular	0.0014	
	Parallel	0.0043	0.0055
	Parallel	0.0067	

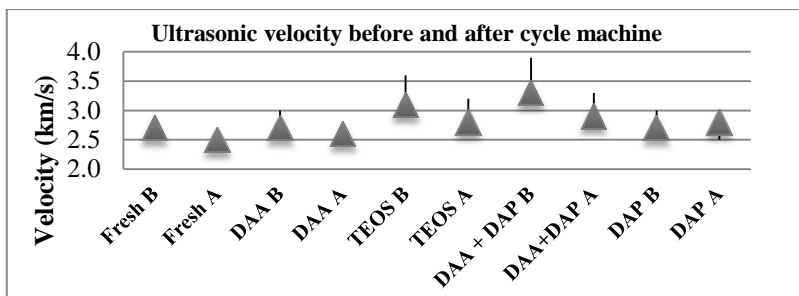


Fig. 2: Ultrasonic wave velocity before and after wetting-and-drying cycles. B: Before, A: After the cycles. The line represents the range of values and the triangle is the average.

5. Conclusions

Treatment with diaminoalkane (DAA) is expected to suppress swelling of the clay, but it had a negligible effect on the stiffness of the stone and on the retention of stiffness after cycling. When used in combination with diammonium hydrogen phosphate (DAP), there seems to be a detrimental chemical reaction that reduces the sorptivity, but it provides a considerable increase in stiffness, much of which is retained after cycling. The best results were obtained with TEOS alone, which caused less reduction in sorptivity than DAA + DAP and had higher stiffness than untreated stone after cycling. All of these tests were performed on unweathered stone, which may account for the modest impact of the treatments on the properties. Future studies will focus on samples that have already been damaged by hydric or thermal cycles.

Acknowledgements

The authors thank FAPESP (2012/24067-4 and 2013/24833-1) for the financial support.

References

- Del Lama, E.A., Dehira, L.K., and Reys, A.C., 2009, Visão geológica dos monumentos da cidade de São Paulo, *Revista Brasileira de Geociências*, 39 (3), 409-420.
- Jiménez González, I. and Scherer, G.W., 2002, Hygric Swelling of Portland Brownstone. *MRS Proceedings*, 712, II 2.4.
- Jiménez González, I. and Scherer, G. W. 2004, Effect of swelling inhibitors on the swelling and stress relaxation of clay-bearing stones, *Environmental Geology*, 46, 364-377
- Jiménez González, I. and Scherer, G.W. 2006, Evaluating the potential damage to stones from wetting and drying cycles, in *Measuring, Monitoring and Modeling Concrete Properties*, Konsta-Gdoutos M.S. (ed.), Springer, 685-693.
- Naidu, S., Liu, C. and Scherer, G.W., 2015, Hydroxyapatite-based consolidant and the acceleration of hydrolysis of silicate-based consolidants, *J. Cultural Heritage*, 16, 94-101.
- Wangler, T. and Scherer, G.W. 2008, Clay swelling mechanism in clay-bearing sandstones, *Environmental Geology*, 56, 529-534.

ASSESSING THE IMPACT OF NATURAL STONE BURIAL UPON PERFORMANCE FOR POTENTIAL CONSERVATION PURPOSES

B.J. Hunt^{1*} and C.M. Grossi²

Abstract

Historic England is researching the performance of natural stone subjected to burial. The primary reason driving the research is a need to reduce the costs of preserving natural stone monuments and structures where there may not be the immediate funds to carry out more extensive preservation works. Stone burial is poorly researched and the possible benefits and risks are neither known nor understood. The research involves testing designs for burial, known as clamps, over a minimum three-year period to determine the optimum design. A range of stone types is being tested to develop guidance as to when such an approach is appropriate. Clamps have been set up at an exposed site using four different burial media for eight different stone types set at both shallow and deeper levels. Probes set within the stone blocks directly measure the temperature and moisture contents, which is being compared with data from a weather station at the test area. Two sets of the stone blocks have also been left out in the open, one set being free of ground contact, the other simply sitting upon the ground. Exposure began in November 2014 and this paper considers the first nine months of readings. It is already indicated that the stone blocks do not easily dry out within clamps once saturated and that shallow buried stones undergo more rapid freezing than deeper buried stones. Current indications are that the depth of burial along with the ability of a stone to take on board and retain moisture will be critical. This suggests that burial sites will need to be well drained and ventilated with direct moisture contact reduced.

Keywords: stone, burial, frost, monitoring, preservation, cultural heritage

1. Introduction

Funds for the upkeep of the many buildings and monuments of historical importance that come under the auspices of Historic England rarely are sufficient. Unfortunately there are many situations where the building fabric is left unprotected whilst funds for necessary major interventions are awaited. To this end Historic England considered ways in which fabric deterioration could be slowed whilst awaiting such intervention. Part of the solution has been the removal of fabric to controlled storage facilities, which can involve substantial capital costs and significant limitations to what can be achieved effectively. The other part

¹ B.J. Hunt*

IBIS Limited, 10 Clarendon Road, South Woodford, London, E18 2AW, United Kingdom
barry.hunt@ibis4u.co.uk

² C.M. Grossi

School of Health Sciences, University of East Anglia, Norwich NR4 7TJ, United Kingdom

*corresponding author

of the solution has been the on-site burial of fabric in what have become known as ‘clamps’.

Clamps are believed to provide protection from the principally maritime environment of the UK, especially cyclic frost attack, allowing fabric to be stored until funds can be made available for proper intervention. The need for storage for many structures is believed to be measurable in decades. Therefore, clamps may buy considerable time for a structure whilst significantly reducing long term preservation costs. Having received enquiries from owners of historic structures concerning the use of clamps Historic England realised that there was no tangible research or other technical backup available to support the promotion of clamp use without taking a significant unknown risk. Therefore in late 2005 Historic England undertook the burial in sand of some 600 stone elements at Riveaulx Abbey, incorporating sensors to monitor the burial environment. A principal conclusion of this initial research was that further and more in depth research was required; this prompted the current project.

A literature search reveals a lack of significant research into the conditions and performance of buried natural stone. There has been some work concerning archaeological site reburial (Canti & Davis, 1999) and research into the geochemical conditions of archaeological sites and effects upon various materials (Lillie & Smith, 2006) but this is of minimal relevance to the current study. Apocryphal stories from stone quarriers about the protection by burial of stone over winter periods and general geological observation of natural stone resources within the UK environment were thus used to formulate how clamps might be constructed in order to provide protection from the elements. General experience of how different stones and the structures built from them suffer deterioration was also considered. Thickett *et al* (2008) carried out X-ray fluorescence and near infrared spectroscopy on a variety of sandstones in order to rank their potential durability prior to burial and to help monitor the stone condition once buried. This non-destructive approach had only very limited use.

The two principal factors believed to exert the greatest influence upon a clamp environment were considered to be stone temperature and moisture content. How these two factors interacted over time, particularly with respect to the degree of saturation at the time of freezing, and possibly the rate of freezing, was considered to be important. The amount of cover to the stone and the nature of the burial media were believed to be significant controlling factors of both the moisture content and temperature, so some variation in these was required. The most obvious variation was the stone itself and thus eventually eight stones representing a range of British types were selected for testing. It was considered that the clamps needed to be drained whilst the top surface of the burial media remained uncovered. Two sets of control stones were deployed, one set sitting 200 mm off the ground on a wooden pallet and thus exposed on all sides, and another set laid directly upon the ground and thus exposed on five sides.

The monitoring comprises combined temperature/moisture sensors set into two of the eight stone types taking readings on the hour that will continue for a period of at least three years. These readings are being compared with those from a small weather station set up within the area of the test clamps. The readings include air temperature, humidity, rainfall, wind speed, wind direction and sunlight. Statistical analyses are being applied to the results in order to assess the number of actual freezing events inside the clamps, and the influence of

temperature lag, moisture changes and other potential factors. At the end of the monitoring period in early 2018 the stones will be assessed for changes using petrography and electron microscopy, and possibly using mercury porosimetry at different levels from surfaces.

2. Trial set-up

2.1. Principal considerations

There were believed to be five principal considerations for setting up the trial variables: 1) an apocryphal history of stone burial suggested this provided protection; 2) deeper burial would provide more stable temperatures and potentially a lower number of freeze-thaw cycles; 3) different burial media might increase/decrease the rate of saturation, the level of saturation, and the rate of drying; 4) different burial media might exhibit differences in lateral moisture creep and 5) the variables were applicable to porous stones. Assessments of the level of damage to the various stone test blocks will only be undertaken at the end of the trial. Assessment of the current findings is based on comparison of data and the limited visual observations that have been made so far.

2.2. Stone selection

The majority of historical structures built in England used local stones that inevitably included sandstone and/or limestone. The following eight stone types were selected to represent the range of available materials. Included are basic descriptions along with density (D, g cm⁻³), water absorption (W, %) and saturation coefficient (S) values as appropriate.

Jordan's Whitbed Portland limestone: medium grade, oolitic (D: 2.16 W: 6.3 S: 0.73)

Jordan's Basebed Portland limestone: medium grade oolitic (D: 2.18 W: 6.9 S: 0.76)

Appleton sandstone: high grade, arenitic (D: 2.38 W: 2.9 S: 0.63)

Stanton Moor sandstone: medium grade, arenitic (D: 2.32 W: 3.8 S: 0.67)

St Bees sandstone: medium grade, calcareous (D: 2.09 W: 6.8 S: 0.66)

Red Lazonby sandstone: medium grade, iron-rich (D: 2.34 W: 2.4)

Creeton Hard White limestone: low grade, oolitic (D: 2.25 W: 7.0 S: 0.93)

Cadeby White Magnesian limestone: medium grade (D: 2.17 W: 7.3 S: 0.83)

Blocks of a significant size (300 mm length, 200 mm width and 200 mm height) were used, given that in practice masonry blocks to be buried typically would be relatively large. Larger blocks would also allow the taking of samples at the end of the monitoring period whilst leaving significant material to continue the burial exercise if required. The blocks were also cut to ensure that the natural bedding would run perpendicular to the small end faces.

2.3. Site and burial media

The test site is located in Helmsley, North Yorkshire, and has an oceanic climate. The nature of the burial media was considered to be a potential factor in the performance of the clamps, especially in relation to moisture transmission in and out of the clamps. Four different stone burial media were selected for the clamp construction as follows:

- a) coarse 20 mm single sized crushed granite with poor packing and low absorption;
- b) coarse 20 mm single sized crushed limestone with poor packing and high absorption;
- c) crushed igneous rock fines with good grading but poor packing, and
- d) natural building sand with continuous grading and good packing.

A bed of 150 mm depth was laid first before the lower layer of stone test blocks was installed by simply placing them on top of that layer. The stone test blocks remained isolated from each other. The area around the stone test blocks was then filled with the aggregate and this was continued until the stone test blocks were completely covered by a 150 mm thick layer of the aggregate. The upper layer of stone test blocks was then placed upon the aggregate, the area around them filled and the stone test blocks finally covered to at least 150 mm. Additionally, two sets of the eight stones were placed outside of the clamps. One set was left sitting upon the ground via a thin bed of the building sand to ensure full contact. The other set was left sitting upon a wooden pallet about 200 mm above the ground and exposed.

2.4. Monitoring Equipment

The temperature and moisture content of the stone within the clamps and on the outside set in contact with the ground were monitored using Delta-T SM300 sensors set into the samples. A pair of nominal 7 mm diameter holes were drilled into each stone test block, the centres 25 mm apart, and the wire probes inserted into the holes and set using a proprietary masonry grout to ensure full contact with the stone fabric. A weather station was set up at the centre of the clamps that incorporated instrumentation supplied by Delta-T: a) RHT2nl-02 Relative Humidity/Precision air temperature sensors (2K Thermistor); b) RG2+BP-06 Raingauge, Compact; c) ES2-05 Solar Energy Flux Sensor, and d) AN-WD2 combined wind speed and direction sensor. The instrumentation of the clamps and weather station was linked to a Delta-T DL2e Data Logger that was set to take measurements every hour. With a total of 43 measurements being taken each hour, a total of 1,130,040 measurements would be obtained over the course of a continuous three year monitoring period.

2.5. Clamp design

It was assumed that any clamps to be constructed realistically would require a location that was either free-draining or with some form of drainage installed. It was considered that the retention of moisture within a clamp would be a function of the trickle down of moisture from above and the absorption and packing of the burial media. Ideally it would have been preferred to construct the trial clamps within a pit that was then drained, but this created a number of serious problems at the proposed trial site. It was agreed that the clamps could be constructed above ground, which was considered to be potentially a straightforward and more realistic methodology for constructing actual clamps. Fig. 1 below shows how the clamps were constructed, with some of the materials stripped away. The use of exposed sides was considered to be potentially more realistic but likely to increase the damage potential due to an increased rate of heat loss and reduced ground heat storage effects. The base of the clamps was left in direct contact with the ground so that moisture was able to flow out from the construction. The top of the clamps was left open, leaving the possibility that at some time the clamps might be covered and the findings before and after covering them might be compared and contrasted.

3. Data analysis

A descriptive statistical analysis of the stone temperature and moisture content in the different situations and their variation during the time of exposure was carried out. Time series analysis was used to compare stone temperature and moisture with air temperature, relative humidity and precipitation by estimating autocorrelation and cross-correlation of the stones and their lags with the environmental parameters. The percentage of frost hours

was determined by counting the hours where temperatures were lower than 0° C. Clustered multivariable regression models with robust standard errors using the channel as panel variable (16 clusters) were carried out. The response variables were stone temperature, stone moisture as continuous variables, and frost event in the stone as a binary variable (yes or no). The stone type (Appleton or Creeton), type of clamp (limestone, sand, granite sand or crushed granite) and levels (upper or lower) were used as covariates. Linear regression was used for the analysis of stone temperature and moisture and logistic regression was used for frost occurrence. The statistical analysis was carried out using STATA 14 software.

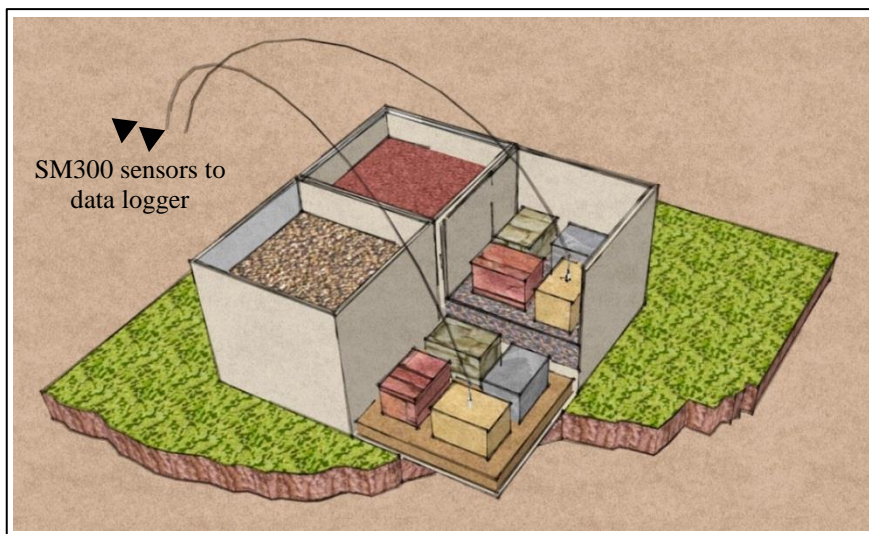


Fig. 1: design of the trial clamps using four different burial media and four of the eight stones set at two different levels; typical positioning of the SM300 sensors is shown.

4. Initial results

4.1. Monitoring

Monitoring was begun on 05 November 2014, just prior to the winter period and before the first frosts occurred. At the time of writing monitoring has been carried out for nine months, to 27th August 2015, with a total of 7073 hourly records. During this monitoring period the number of freezing events affecting the external environment numbered 48 and the total number of hours with temperature $\leq 0^{\circ}\text{C}$ (and potential frost occurrence) totalled 289. Precipitation totalled 501 mm, the daily average being 1.69 mm.

One of the most important occurrences affected the Creeton limestone left sitting upon the ground, which obviously suffered relatively catastrophic breakdown. This demonstrated that the local climate over the winter period had been particularly harsh. It was also apparent that this would provide a good basis for comparison with the performance of the Creeton limestone within the various clamps under the different storage and exposure conditions.

4.2. Current indications

The temperature within the clamps is both strongly auto-correlated and correlated with the air temperature. The clamp temperature also varies according to the level with the upper level exhibiting temperatures closer to the air temperature than those of the lower level. The time lag in temperature change is smaller in the upper level than in the lower level (Tab. 1). The percentage of variance by stone type is very small and this does not appear to be a significant factor (Tab. 2). Changes in humidity also appeared to be more stable within the finer burial materials.

Tab. 1: Summary of winter temperature (November to February).

Levels	Number of observations	Mean °C	St Dev °C	Min °C	Max °C	Corr with Air T	Lag with Air T**
Air T	2,767	4.9	3.7	-5.5	14.5	--	--
Overground	5,534	4.1	3.6	-5.1	13.1	0.99	0
Upper level	22,136	3.9	2.8	-2.0	10.8	0.77	5 (2)
Lower level	22,136	4.3	2.5	-0.2*	9.9	0.67	9 (3)

* Lower level: temperatures $< 0^{\circ}$ C were only recorded in the coarse limestone clamp;

** Mean and Poisson standard deviation (brackets); Lag = Number of hours to reach the best correlation between Air and clamp temperature (i.e. time of response to external temperature conditions).

Tab. 2: Regressions of T, moisture and frost occurrence vs type of stone, clamp and level.

		Temp*	Temp	Moisture*	Moisture	Frost occurrence**	Frost occurrence
		Coef	P > t	Coef	P > t	O.R.	P > t
Stone	<i>Appleton</i>	base	---	base	---	base	---
	<i>Creeton</i>	0.06	0.468	4.78	<0.001	1.07	0.880
Clamp	<i>CC limestone</i>	base	---	base	---	base	---
	<i>Building sand</i>	-0.11	0.486	2.38	0.102	0.41	0.263
	<i>Granite sand</i>	0.002	0.988	2.53	0.091	0.45	0.181
	<i>CC granite</i>	0.17	0.245	5.00	0.009	0.45	0.063
Level	<i>Lower</i>	base	---	base	---	base	---
	<i>Upper</i>	-0.37	0.001	-1.35	0.173	16.2	0.002
R ²		0.01	---	0.58	---	---	0.10

* Clustered linear regression with robust errors;

** Clustered logistic regression with robust errors

No autocorrelation or environmental factors were included in these regressions. Freeze events coded as No-Yes. P values ≤ 0.1 indicate significant relationship with 10% error. O.R. are odds ratios where O.R. > 1 indicate positive relationship and O.R. < 1 indicate negative relationship. Coefficients > 0 indicate positive relationship and coefficients < 0 indicate negative relationship.

The upper levels of the clamps were more susceptible to the outside frost events (Tab. 3) mostly due to the shorter time lag in temperature change. The clamp that employed the coarse limestone burial material appeared to achieve freezing conditions more rapidly.

The stones within the clamps initially took on board moisture, which then stabilised to a degree and then slowly reacted to outside moisture variations (Fig. 2). Drying occurred only very slowly during prolonged drying periods. The indications are that over the period of monitoring the moisture content has been slowly growing, especially within the Appleton sandstone. Outside of the clamps the Appleton sandstone was more reactive to the changes in the amount of precipitation.

The Creton limestone placed externally that suffered breakdown saw a disruption in the temperature data, probably suggesting a loss of contact between the stone and grout, and possibly other factors. It also appeared the Creton limestone within the clamps may have failed at the same time, most likely within the coarse limestone and granite burial media, and potentially in the granite sand clamp.

Tab. 3: Cross-tabulation of the external environment frost occurrence (number of hours with $T \leq 0^\circ\text{C}$) and frost occurrence at different exposures from Nov 2014 to Feb 2015.*

Air Frost occurrence	Overground stones			Upper level clamps			Lower level clamps		
	$T \geq 0$	$T \leq 0$	%**	$T \geq 0$	$T \leq 0$	%**	$T \geq 0$	$T \leq 0$	%**
Air $T \geq 0$	4837	203		19714	446		20122	38	
Air $T \leq 0$	6	488	99	1718	258	13	1969	7	0.35

* Freeze events in the lower level only were registered in the coarse crushed limestone clamps. ** Number of hours with stone $T \leq 0^\circ\text{C}$ / number of hours with Air $T \leq 0^\circ\text{C}$ as percentage (e.g. overground stones = $488/(488+6) \times 100$), two significant figures.

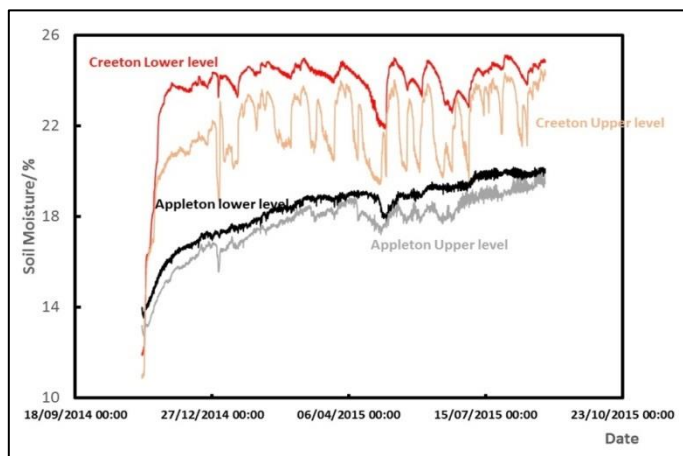


Fig. 2: Moisture content of the trial clamps for Appleton and Creton stones at lower and upper levels during the first nine months of exposure.

5. Initial Conclusions and Recommendations

The findings to date suggest that a burial environment does alter the effects of local weather upon the stone by slowing the rate at which a frost event occurs. This may increase the ability of stone to combat the potential build up of internal pressures and subsequent damage experienced. Therefore there is already strong evidence that clamp environments do provide protection, though the potential level of this protection is yet to be determined.

It would appear that leaving the upper surface uncovered has made the stones within the clamps more susceptible to taking on board moisture, which then takes a long time to reduce during drier periods. It is indicated that more deeply buried stone takes longer to dry out. This reduction in the rate of drying out may counteract some of the apparent benefits of burial, which needs to be investigated further.

During the second half of the current monitoring period it is proposed to incorporate a cover to the clamps and to direct moisture away from the buried stones. This may help to better determine whether different burial media produce different burial climates, especially in response to possible lateral transfer of moisture.

The rate of take up and release of moisture and temperature changes at different depths from the outer surface of a stone block may be important factors in the assessment of the long term performance. Future research might incorporate probes at different positions within larger and differently shaped pieces of masonry to assess such potential effects. The moisture content readings will require conversion to actual moisture content values, which will be undertaken at the end of the monitoring period.

Acknowledgements

The Authors would like to thank Historic England for the opportunity to carry out this research on their behalf, and also the opportunity to produce this on-going summary of the findings. The Authors would also like to thank Zoë Davis for her assistance with the manuscript. Thanks also go to various staff members of Albion Stone, Cadeby Stone, Marshalls and Stancliffe Stone for the supply of stone materials for the project, and especially to Gordon Hines and Michael Poultney.

References

- Canti M.G. & Davis, M., 1999, Tests and Guidelines for the Suitability of Sands to be used in Archaeological Site Reburial, *J. of Archaeological Science*, 26, 775-781.
- Lillie, M. & Smith, R., 2006, The *in situ* preservation of archaeological remains: using lysimeters to assess the impacts of saturation and seasonality, *J. of Archaeological Science*, 34, 1494-1504.
- Thickett, D., Lambarth, S. and Wyeth, P., 2008, Determining the stability and durability of archaeological materials, 9th International Conference on NDT of Art, Jerusalem, Israel, 25-30 May 2008.

STUDY OF PROTECTIVE MEASURES OF STONE MONUMENTS IN COLD REGIONS

T. Ishizaki ^{1*}

Abstract

In cold regions, stone monuments located outside deteriorate due to the freeze and thaw cycles in winter. The main factors for the deterioration of stone are material property, water content and temperature. The stone deteriorates severely if the stone is frost susceptible. There is a stone gateway (*Torii* in Japanese) at the entrance to a Shinto shrine in Yamagata city. The stone gateway was built in Heian Period (from 8 to 12 centuries ago) and is designated as an important cultural property. For the protective measures, the stone gateway is covered with plastic film with insulation and straw mat in winter. In order to measure the temperature of the stone surface, the temperature sensor was set on the stone surface inside of the cover. The environmental temperature decreased to -5.3 °C at the end of January, but the surface temperature of the stone was -0.8 °C. The experimental result showed that a large amount of water was not frozen at -1 °C. Therefore, it can be said that the freezing pore water in stone in the winter cover did not have big effect on the stone damage during this period. From these results, this is considered to be a quite effective method for the protective measures of stone monuments in cold regions. The present author observed the microclimate condition in the glass shelter for the stone monument in Hokkaido. The shelter is quite effective to reduce the water content of the stone monuments. The laboratory experiment showed that the freezing temperature decreases greatly with the decrease of the water content of the stone. In this condition the water content of the stone monument is kept quite low, which leads to low freezing temperature and results in low risk of frost damage.

Keywords: frost damage, frost heave phenomenon, protective measure, water content, shelter

1. Introduction

In cold regions, stone monuments deteriorate due to the freezing and thawing cycles in winter season. The degree of the deterioration depends on the stone type, moisture content and temperature. The freezing temperature decreases with decreasing moisture content of the stone. Therefore it is one of the protective measures to reduce the moisture content of the stone. The installation of a shelter around a stone monument or applying water repellent material on the monument is an effective protective measure to prevent deterioration. Another protective measure is to avoid the exposure of the stone to low temperatures by using thermal insulation material.

¹ T. Ishizaki*

Institute for Conservation of Cultural Property, Tohoku University of Art & Design, Japan
ishizaki.takeshi@aga.tuad.ac.jp

*corresponding author

For these purposes in Germany stone monuments made of marble are covered with wood shelter during the winter season. In Japan one example of protective measures is to cover stone monuments with straw mat. Fig. 1 shows the stone shrine gate with winter cover in Motoki, Yamagata city. The stone shrine gate was built around 1000 years ago in Heian Period and it was designated as an important cultural property in Japan. The procedure for the winter cover is as follows. First the stone was covered with vinyl sheet with insulation layer, then covered with straw mat and finally covered with vinyl sheet. To evaluate the validity of this winter cover, temperatures of stone surface and cover surface were measured in winter season. The temperature and relative humidity of the environmental condition were also measured. The time lapse camera was installed to take photos of the stone gate to observe the snow accumulation on the stone gate.



Fig. 1: Stone shrine gate with winter cover in Motoki, Yamagata city.

2. Results of Temperature Measurement

Air temperature and relative humidity of the surrounding environment were measured for two month from January 26 to March 27, 2015. The air temperature around the stone gate is shown in Fig. 2a. Based on the temperature measurement, the air temperature recorded minimum value of $-5.3\text{ }^{\circ}\text{C}$ at 5:30 on January 29. The stone surface temperature inside the winter cover is shown in Fig. 2b. The surface temperature on the stone surface inside the winter cover recorded $-0.8\text{ }^{\circ}\text{C}$ at 3:30 on January 29. On February 5, the minimum air temperature was $-4.3\text{ }^{\circ}\text{C}$ and the temperature on the stone surface inside the winter cover was $-0.2\text{ }^{\circ}\text{C}$. Fig. 3 shows daily minimum air temperature and the minimum surface temperature of the stone surface inside the winter cover. In this figure, positive temperature

values were omitted. During this period, the minimum air temperature was $-5.3\text{ }^{\circ}\text{C}$ and the minimum temperature on the stone surface was $-0.8\text{ }^{\circ}\text{C}$.

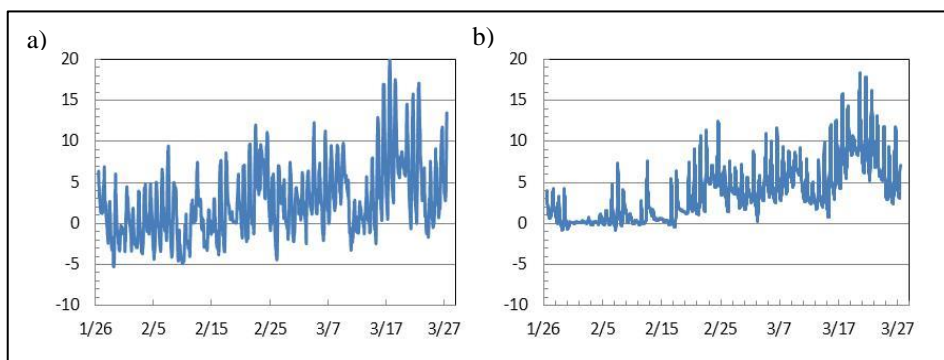


Fig. 2: a) Air temperature change around the stone shrine gate in Motoki, Yamagata city; b) Temperature change of the stone surface inside the winter cover.

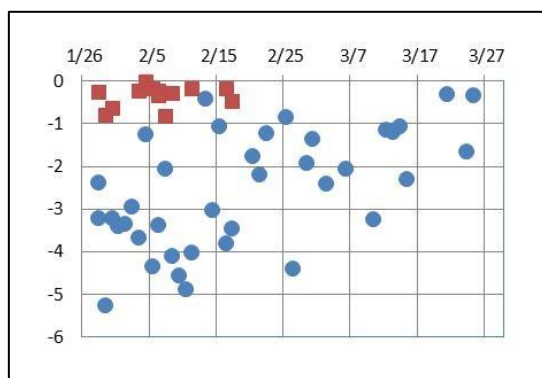


Fig. 3: Daily minimum air temperature (●) and daily minimum surface temperature (■)

3. Discussion

The stone deteriorates due to the freezing and thawing cycles. Based on the laboratory experiment, Fukuda (1984) concluded that the number of temperature change cycles between $+4$ and $-4\text{ }^{\circ}\text{C}$ is important for the frost damage of the stone. Ishizaki (2000) carried out measurement of unfrozen water content of Oya tuff stone which was used for the stone monument in Japan by the pulsed NMR technique. The experimental result showed that large amount of water was not frozen at $-1\text{ }^{\circ}\text{C}$. Therefore, it can be said that the freezing pore water in stone in the winter cover did not have big effect on the stone damage during this period based on the temperature data shown in Fig. 2b and Fig. 3. As shown in Fig. 3, the surface temperature of the stone was around $4\text{ }^{\circ}\text{C}$ higher than the air temperature. The reason can be due to the winter cover in which straw mat was covered with vinyl sheet on both sides. This structure prevented cold air to flow into the winter cover. Therefore this

method is simple and effective way to reduce the risk of frost damage of stone monument in winter.

The minimum air temperature in Yamagata city was $-7.5\text{ }^{\circ}\text{C}$ on December 28, 2014 based on the meteorological data from Yamagata Meteorological Agency. This method of winter cover is considered to be effective in the area where winter temperature is not so low, such as in Yamagata city. However, it would be difficult to reduce the risk of frost damage by this winter cover method in the area where winter coldness is much severe. In Hokkaido area, where the minimum temperature reaches $-20\text{ }^{\circ}\text{C}$ and stone freezes even if the stone monument is covered with insulation materials.

For further studies, it is necessary to obtain thermal properties of stone and materials used for the winter cover and carry out thermal analysis for the precise estimation of the stone surface temperature change with environmental conditions.

The present author has been doing research on the frost damage of earthen wall of Shiwa-jo in Morioka City, Iwate prefecture (Fig. 4). The degree of damage to the earthen wall depended on the volumetric water content of the soil. The earthen wall was damaged greatly where the volumetric water content measured by TDR (Time Domain Reflectometer) apparatus exceeded 30%. The earthen wall was not damaged where the volumetric water content was low. Laboratory experiments were carried out to clarify the relationship between the freezing temperature of the soil and the volumetric water content (Ishizaki, 2015). From these research results, it was found that the risk of frost damage becomes low if the water content of the earthen wall is kept at lower value than 20%.



Fig. 4: Earthen wall of Shiwa-jo in Morioka City, Iwate prefecture

4. Conclusions

Use of plastic film with straw insulation in winter keeps the surface temperature of the stone around 4 °C higher than the air temperature. This is a simple and effective way to reduce the risk of frost damage to stone monuments in winter, if the climate is not severe. For further studies, it is necessary to obtain thermal properties of stone and materials used for the winter cover and carry out thermal analysis for the precise estimation of the stone surface temperature change with environmental conditions.

Acknowledgement

The present Author would like to thank Ms. Kaoru Uematsu and people in Board of Education of Yamagata city to help this research for the preservation of stone monument.

References

- Fukuda, M., 1984, Frost shattering of the carving in Temiya Cave, Otaru, *Low Temperature Science, Ser. A*, 43, 171-180.
- Ishizaki, T., 2000, Frost deterioration of historical stone monuments and brick buildings and its preventive measures, *Proc. of the international Symposium on Ground Freezing and Frost Actions in Soils, Belgium*, 79-83.
- Ishizaki, T., 2015, Deterioration of cultural properties with earthen materials and their protective measures, *Proc. 2015 International Symposium on Conservation of East Asian Cultural Heritage in Nara*, 26-29.

This page has been left intentionally blank.

STUDY OF CONSOLIDATION OF POROUS AND DENSE LIMESTONES BY BACILLUS CEREUS BIOMINERALIZATION

J.M. Jakutajć¹, J.W. Łukaszewicz^{2*} and J. Karbowska-Berent²

Abstract

The research was focused on the evaluation of the possibility of using commercially available materials and biomineralisation technology, which is based on the ability of *Bacillus cereus* to precipitate calcium carbonate for consolidating high porous stones and infilling micro-cracks in dense limestones. The effectiveness of the treatment was verified indirectly by the evaluation of physical properties of consolidated stones and directly by identification of calcium carbonate on sandstone slabs with SEM/EDS analysis. The results show that the bacteria are able to induce calcium carbonate precipitation and the new cement alters the strength properties of the stone. Nevertheless the consolidating effect is superficial and biomineralisation procedure is linked with some side effects. The evaluation of suitability of this treatment for use on dense stones demonstrated that it is possible to fill micro-cracks and create colour patina on the stone surface.

Keywords: biomineralisation, bacillus cereus, consolidation, infilling cracks, carbonate stones, porous and dense limestone

1. Introduction

Carbonate stones are very susceptible to decay due to the chemical nature of their main component – calcite. Symptoms of weathering and corrosion of limestones may cause defacing of a relief and a sculpture form or may even lead to full destruction of a stone artwork (ed. Domasłowski 2011). Consolidation treatment is needed in some cases to avoid such damage. Since the second half of the 19th century, consolidation of stone artworks has been one of the basic conservation problems. Since that time, a wide variety of materials have been used for strengthening weathered monuments. A majority of these materials are inorganic: lime, nano-lime (Ziegenbalg 2008), barium hydroxide (Lewin 1971) and organic polymers: epoxy resins (Domasłowski, Strzelczyk 1986), acrylic polymers (Domasłowski, Łukaszewicz 1983), alkoxysilanes (Łukaszewicz 2002). Unfortunately, some of these materials are not effective enough or may cause irreversible changes in the chemical structure of a stone. The research towards new treatments based on compatibility of the consolidant with the stone substrate has led to the development of an alternative conservation treatment based on the phenomenon of MICP (Microbially Induced Calcite

¹ J.M. Jakutajć
Conservator – Restorer, Poland

² J. W. Łukaszewicz* and J. Karbowska-Berent
Department for Conservation and Restoration of Architectonic Elements and Details,
Faculty of Fine Arts, Nicolaus Copernicus University, Toruń, Poland
jwluk@umk.pl

*corresponding author

Precipitation). MICP has been investigated for consolidation and protection of sculpture and architecture made from carbonate stones for more than twenty years (Castanier *et al.* 1999, Le Metayer-Levrel *et al.* 1999, Rodriguez-Navarro *et al.* 2003, De Muynck *et al.* 2010). The method known as calcium carbonate biomineralisation or biodeposition is the development of the lime-water treatment, the purpose of which is to recreate the binder in deteriorated calcareous stones. The first biomineralisation technology was developed and industrialised by the French research group (Adolphe and Billy 1974, Adolphe *et al.* 1989, 1990, Castanier *et al.* 1999) which was patented as Calcite Bioconcept (CB) technology, where the *Bacillus cereus* activity is used. The success of the method encouraged different research groups to develop alternative approaches for the bacterial biomineralisation. A Spanish research group proposed the use of *Myxococcus xanthus* (Rodriguez-Navarro *et al.* 2003) or the use of microorganisms inhabiting the stone (Jimenez-Lopez *et al.* 2007) to consolidate carbonate stones. Another main biomineralisation technology was developed by the Ghent University research group, which proposed the microbial hydrolysis strategy to obtain a calcite layer by *Bacillus sphearicus* (De Muynck *et al.* 2010).

2. Materials and methods

2.1. Stone samples

In this experiment two groups of stones were chosen: porous stones (Pińczów limestone, Żerkowice sandstone) and nonporous stones (Rosso Verona marble, Dębnik limestone). The Pińczów limestone is one the most popular Polish carbonate stones, which was widely used in architecture and sculpture, especially in the 16th century. It is a fine-grained limestone of ecru or light beige colour with high porosity (25-27%) and high water absorption (14-18%) (ed. Domaśłowski 2011). The Żerkowice sandstone is a Polish coarse-grained sandstone with clay binder, porosity 12-14% and water absorption 6-7.5% (ed. Domaśłowski 2011). The porous stones were used for the examination of the consolidation effect of microbial induced calcite precipitation. Considering the superficial nature of strengthening effect due to the biomineralisation (De Muynck *et al.* 2010, Rodriguez-Navarro *et al.* 2003), the research on the changes of physical properties of stones was conducted on slabs 0.4-0.5×1×10 cm in size, as the bacteria could penetrate the whole structure of the sample. To enable the detection of newly formed calcite crystals in the stone structure by SEM/EDS analysis, the sandstone samples were used. In the experiment concerning the possibility of infilling cracks and fissures in dense limestones, the decayed slabs of the Dębnik limestone and the Rosso Verona marble were chosen. The samples were devoid of polish and were rich in micro-cracks and fissures. Considering the real conditions of historical stones, the treatment was applied on non-sterile stone slabs.

2.2. Biodeposition procedure

The study was based on the CB biomineralisation technology (Adolphe *et al.* 1990). The bio-preparation used in the experiments consists of two compounds: freeze-dried bacteria isolates – *Bacillus cereus* and dry culture medium (nutrition). The compounds were hydrated by distilled water and applied on the stone samples using a brush or spray, according to the five-day procedure that was recommended by the producer. The application procedure is shown in Tab. 1. The new liquids were prepared daily due to the risk of undesired growth of microorganisms from the air.

Tab. 1: The application programme of Calcite Bioconcept treatment.

Day	Compounds	Amounts
1	Inoculation of <i>Bacillus cereus</i> in liquid nutrition	0.25 g bacteria 1.25 g nutrition 50 cm ³ distilled water
2	Application on stone of 16h old inoculated culture medium (CB+)	—————
3	2× Application on stone of sterile culture medium (CB-)	2.5% in distilled water
4	1× Application of CB-	2.5% in distilled water
5	1× Application of CB-	2.5% in distilled water

Considering the possibility of creating a colour patina due to CB technology (Le Metayer-Levrel *et al.* 1999), the use of the biomineralisation with pigments for infilling cracks and fissures in the dense stones was proposed. In this experiment, pigments matched to the colour of the stone were added to the culture medium during the 3rd, 4th and 5th day of the biomineralisation procedure. The coloured liquids were applied on the stone surfaces by spraying, brushing, or local application into cracks by syringe. An extra test was performed to evaluate the effect of bio-patina and cracks filling, when the colour liquid is applied before the biomineralisation procedure.

All the experiments were performed in laboratory conditions at a temperature between 20-30°C. In contrast to the original method, the condition of increased relative humidity of the air (70-80%) was proposed during the application procedure and 7 days after to retard water vaporisation from the stone surfaces. Considering the high content of soluble salts in the culture medium, a desalination procedure (24 hour in the static bath in distilled water) was proposed three weeks after the end of the biomineralisation procedure.

Tab. 2: An overview of the types of treatment.

Humidity conditions	Trials
conditions of normal humidity (40-50%)	CB treatment
	CB treatment and desalination procedure
conditions of increased humidity (70-80%)	CB treatment
	CB treatment and desalination procedure

2.3. Evaluation methods

To investigate the changes on *Bacillus cereus* cells during the biomineralisation process the Scanning Electron Microscope (LEO Electron Microscopy – model 1430 VP) was used.

The consolidation effect of the biomineralisation technique was evaluated by the verification of physical properties of treated Pińczów limestone: colour changes, weight increase, soluble salts content, and mechanical properties. The colour changes were verified by comparison of treated samples and control samples. The total weight increase was calculated from the difference in weight before and after the treatment on samples dried to constant mass at 60°C. The hypothetical weight increase of calcium carbonate was calculated from the difference in the dry weight before treatment and after the desalination of treated samples. The contents of soluble salts were measured by the conductometric method before and after the treatment and also after the desalination of treated samples. To verify mechanical properties of the treated samples, the resistance to bending was measured by using the “Dynstat” instrument. The measurement was performed two months after the biomineralisation procedure for the control samples, treated samples and treated desalinated samples. Considering the heterogeneous texture of the stone slabs the investigation was conducted on 44 consolidated samples and two highest and two lowest results were rejected. The mechanical properties were calculated using the formula:

$$R_{zg} = \frac{6M * 98.07}{bh^2} \quad (Eq. 1)$$

where R_{zg} is the resistance to bending, M is the bending moment, b is the width of the sample and h is the thickness of the sample. The detection of newly formed calcium carbonate and the evaluation of penetration depth of the new carbonate cement was performed on the treated Żerkowice sandstone samples by SEM/EDS analyses (Quantax 200 with the XFlash 4010 detector, Bruker AXS). The evaluation of the filling of cracks in the dense stones was based on the microscopy conducted before and after the treatment.

3. Results

3.1. Observation of *Bacillus cereus* growth

The inoculation of *Bacillus cereus* in CB culture medium results in very fast growth of the bacteria. After 16 hours of incubation, most of the bacteria are still in a spore phase (Fig. 1a), which allows to introduce them deeper to the structure of the stone; however, after the 2nd day of the procedure all of the bacteria are already in the advanced stage of evolution (Fig. 1b). The vegetative bacteria cells always arrange themselves around the organic matter from the nutritional solution (Fig. 2a). The bacteria firstly organize themselves into chains, but then establish structures, sometimes highly organized. The SEM observation showed that 4 days after inoculation of bacteria in the culture medium, the solid products (in the form of patches) start to appear on the bacteria cell walls (Fig. 2b).

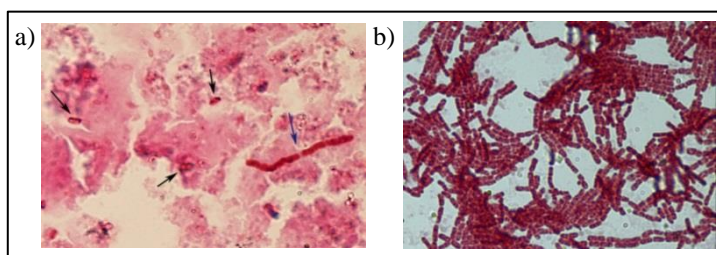


Fig. 1: a) *Bacillus cereus* at the spore phase, b) *Bacillus cereus* at the evolution stage (zoom $\times 100$).

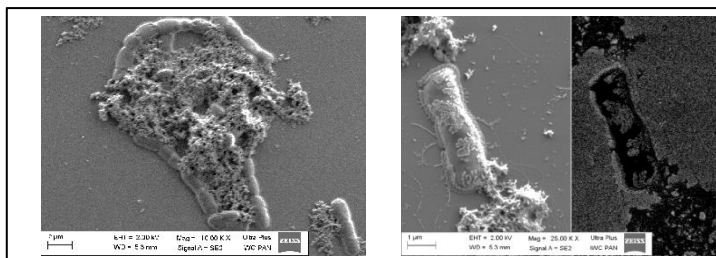


Fig. 2: a) Congregating of *Bacillus cereus* bacteria around organic matter, b) inorganic precipitants on the bacterial cell wall.

3.2. Changes of physical properties of Pińczów limestone

Colour changes: After the treatment, the darkening and yellowing of the specimens were reported mostly on the evaporation side of the stone samples. Less visible changes of colour were noticed on the specimens treated in the conditions of increased relative humidity of the air (70-80%). After the desalination the visual aspects of the stone surfaces returned to the original.

Weight increase: The CB treatment resulted in significant weight increase of Pińczów limestone samples (2-3%). The bigger changes of mass properties were noticed on the samples treated in the conditions of normal relative humidity of the air (40-50%). Nevertheless, after the desalination procedure the weight increase amounted to about 0.2%.

Soluble salts content: The content of soluble salts was significant for all of the treated specimens (Tab. 3). The treatment in normal conditions of air humidity resulted in twice as high a content of soluble salts when compared to the treatment that was performed in conditions of increased humidity. After the desalination, the soluble salts content decreased to 0.4%.

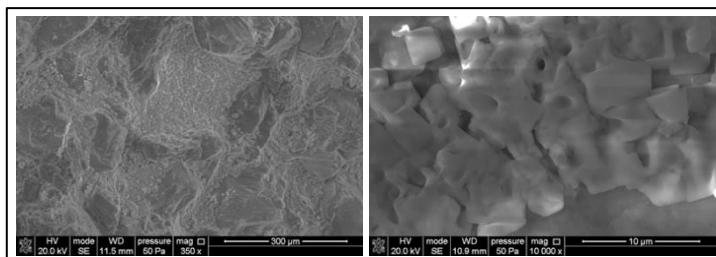


Fig. 3: Crystallisation of NaCl in the porous structure of the limestone.

Mechanical properties: The CB treatment increased resistance to bending for all the limestone samples. The highest strengths were obtained for the samples treated in normal humidity (5.72 MPa). After the desalination, the resistance to bending decreased but was still 15-16% higher than before the treatment. After the desalination, the change in humidity did not result in significant influence on the mechanical properties.

Tab. 3: Summary of changes of physical properties of Pińczów limestone according to CB procedure.

Condition	Specimen	Total weight increase	CaCO ₃ weight increase	Soluble salt content	Resistance to bending	Increase of bending resistance
		%	%	%	MPa	%
laboratory	untreated	-	-	0.05	2.85	-
	treated	3.17	-	2.44	4.63	62
	treated and desalinated	-	0.21	0.37	3.3	16
increased humidity	treated	2.17	-	1.18	5.72	101
	treated and desalinated	-	0.21	0.2	3.29	15

3.2.1. Identification of calcium carbonate

The SEM/EDS analyses showed the presence of calcium carbonate crystals on the surface of treated sandstone samples. The accumulation of the calcium carbonate is especially apparent on the superficial layer up to 300 µm in depth.

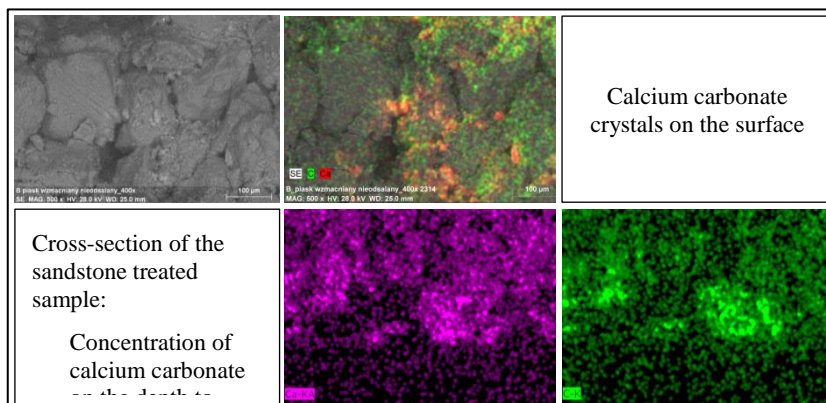


Fig. 4: Żerkowice sandstone.

3.3. Infilling cracks and fractures in dense stones

The CB treatment with the addition of the pigments gave different outcomes depending on the method of application. The pouring of the coloured culture medium resulted in a more homogeneous effect of patina on the stone surface than applying it by brush. Microscopy showed that the micro-cracks were partially or completely infilled. Nevertheless, the created patina was not resistant to abrasion. The local application of bio-preparation using the syringe did not increase the effectiveness of the micro-cracks infilling. The application of the pigments mixed with distilled water before CB procedure resulted in the creation of

homogenous colour patina and its resistance to abrasion; however, the filling of micro-cracks was not completed. A side effect was noticed during and after the procedure: white crystals of salts were precipitated on the stone surfaces after the water evaporated.

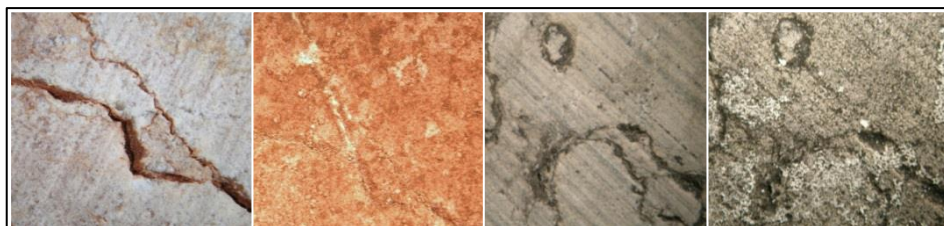


Fig. 6: The filling of micro-cracks on the Rosso Verona marble and the Dębnik limestone due to the biomineralisation procedure

4. Discussion

The CB biomineralisation treatment had significantly altered the physical properties (weight, strength) of the Pińczów limestone. Nevertheless, structural consolidation was not obtained due to the superficial effect of calcite precipitation. Moreover, the procedure was linked to some side effects, like the colour changes and the soluble salt crystallisation due to the composition of the culture medium. However, the desalination procedure, proposed in this research, made it possible to remove them. After the desalination, the stone samples returned to their original colour and were still more resistant to bending (15-16%) than the untreated ones. The introduction of the conditions of increased humidity limited colour changes of the stone. The high humidity of the air retards the vaporisation of water from the stone structure and may decrease migration of the unused nutritional solution to the stone surface, which can cause the colour change. The present preliminary study shows that biomineralisation is able of infilling micro-cracks on the surface of dense stones. The micro-cracks were probably infilled by the grains of pigment bonded by the calcium carbonate cement. However, the homogenous colourful patina was difficult to obtain due to the separation of the suspension of the pigments in the culture medium. Among the negative effects were the crystallisation of the soluble salts (NaCl) and the lack of resistance to abrasion. It might have been a result of the insufficient yield of the calcium carbonate precipitation to bind all the grains of pigments. The biggest homogeneity and resistance of the patina was obtained in the treatment where the pigments were applied on the stone surface before the CB procedure. Although the filling of micro-cracks was not complete, it is believed that the repetition of the procedure may bring better results.

5. Conclusion

The CB procedure results in a very fast growth of *Bacillus cereus* and the precipitation of inorganic crusts on the bacteria cell walls. In the porous stone the calcium carbonate precipitation is obtained only on the surface up to 300 μm . The changes of physical properties of the Pińczów limestone due to the CB were evident, although it was attended by precipitation of a significant amount of soluble salts. The desalination treatment removed this side effect, but caused a decrease in the mechanical properties compared to the value obtained after the CB treatment. It may be a result of the finely crystalline

structure of the calcium carbonate, which elutes from the stone along with the salts. The further research should be concerned with the evaluation of the harmfulness of the soluble salts introduced to the stone during the biomineralisation procedure. An explanation for the decline of the mechanical properties after the desalination procedure should also be investigated.

References

- Adolphe, J.-P., Loubie`re, J.-F., Paradas, J., Soleilhavoup, F., 1990. Procé`de´ de traitement biologique d'une surface artificielle, European patent No. 90400G97
- Castanier S., Le Metayer-Levrel G., Perthuisot J-P., 1999, Ca-carbonates precipitation and limestone genesis – microbiogeologist point of view, *Sedimentary Geology*, 126.
- De Muynck W., De Belie N., Verstraete W., 2010, Microbial carbonate precipitation in construction materials: A review, *Ecological Engineering*, 36, 118-136.
- Domasłowski, W. (ed.), 2011, Zabytki kamienne i metalowe, ich niszczenie i konserwacja profilaktyczna, Toruń.
- Domasłowski W., A. Strzelczyk, 1986, Evaluation of applicability of epoxy resins to conservation of stone historic monuments, *Case Studies in the Conservation of Stone and Wall Paintings: Preprints of the Contributions to Bologna Congress*, ed. N. S. Brommelle and P. Smith, 126-132.
- Domasłowski W., Łukaszewicz J. W., 1983, Badania nad strukturalnym wzmacnianiem wapienia pińczowskiego termoplastycznymi żywicami sztucznymi, *AUNC Zabytkoznawstwo i Konserwatorstwo X, Nauki Humanistyczno-Społeczne*, 129, Toruń.
- Jimenez-Lopez, C., Rodriguez-Navarro, C., Pinar, G., Carrilo-Rosua, F. J., Rodriguez-Gallego, M., Gonzalez-Munoz, M.T., 2007, Consolidation of degraded ornamental porous limestone by calcium carbonate precipitation induced by microbiota inhabiting the stone, *Chemosphere*, 68 (10), 1934.
- Le Metayer-Levrel G., Castanier S., Oriol B., Loubiere J-F., Perthuisot J-P., 1999, Applications of bacterial carbonatogenesis to the protection and regeneration of limestones in buildings and historic patrimony, *Sedimentary Geology*, 126, 25-34.
- Lewin, S. Z., 1971, Recent experience with chemical techniques of stone preservation, *The Treatment of Stone, Proceedings of the Meeting of the Joint Committee for the Conservation of Stone*, Bologna, Italy.
- Łukaszewicz J. W., 2002, Badania i zastosowanie związków krzemooorganicznych w konserwacji zabytków kamiennych, Toruń, Poland.
- Rodriguez-Navarro, C., Rodriguez-Gallego, M., Ben Chekroun, K., Gonzalez-Munoz, M. T., 2003, Conservation of ornamental stone by *Myxococcus Xanthus* – induced carbonate biomineralization, *Applied Environmental Microbiology*, 69 (4).
- Ziegenbalg, G., 2008, Colloidal calcium hydroxide: A new material for consolidation and conservation of carbonatic stones, *Proceedings of the 11th International Congress on Deterioration and Conservation of Stone*.

ASSESSMENT OF DOLOMITE CONSERVATION BY TREATMENT WITH NANO-DISPERSIVE CALCIUM HYDROXIDE SOLUTION

F. Karahan Dağ^{1*}, Ç.T. Mısır¹, S. Çömez¹, M. Erdil¹, A. Tavukçuoğlu¹, E.N. Caner-Saltık¹, B.A. Güney¹ and E. Caner²

Abstract

In recent years, compatible stone consolidation treatments have gained a special importance. This study concerns the treatment of microcrystalline dolomite, a building stone that has been widely used in Anatolian monuments, with nano-dispersive calcium hydroxide solutions and monitoring the efficiency of those treatments. Sound dolomite pieces from the new quarries of Midyat-Mardin were used for the experiments. Samples were cut to the sizes of 5×5×2 cm. A nano-dispersive calcium hydroxide solution in ethyl alcohol prepared in the laboratory was applied through the surface of stone samples by capillary suction. The aim was to establish a compatible calcite network within the dolomite structure. The efficiency of the treatment was assessed by using standard laboratory tests through monitoring the progress in main physical and physicochemical properties of samples in terms of bulk density, total porosity, water absorption capacity, water vapour permeability, thermal and moisture expansion, ultrasonic pulse velocity and modulus of elasticity before and after treatments. Depth of consolidation and calcite formation in the microstructure of dolomite were examined by using SEM/EDS, XRD and optical microscopy. Treatment with a nano-dispersive calcium hydroxide solution resulted in considerable increase in ultrasonic pulse velocity of dolomite indicating improvements in physicochemical properties. No significant change in water vapour permeability and dilation properties after treatment promise advantages for future compatibility of treated and untreated parts of stone. Microstructural investigations with optical microscopy and SEM/EDS at high magnification showed integration of newly formed calcite crystals with existing dolomite crystals of the stone. Additional investigations with repeated treatments will help for further evaluation of treatments for historical dolomitic structures

Keywords: dolomite, consolidation, efficiency tests for conservation treatment, nano-dispersive calcium hydroxide solutions, XRD, SEM/EDS

¹ F. Karahan Dağ*, Ç.T. Mısır, S. Çömez, M. Erdil, A. Tavukçuoğlu, E.N. Caner-Saltık and B.A. Güney
Middle East Technical University (METU Materials), Department of Architecture, Ankara, Turkey
flykarahan@gmail.com

² E. Caner
Department of Conservation and Restoration of Cultural Heritage, Pamukkale University Denizli, Turkey

*corresponding author

1. Introduction

Stone consolidation treatments have a major role in the field of conservation science. Stone consolidation treatments are expected to slow the decay mechanisms, be compatible with the stone structure in the long run and improve physical and physicomaterial properties of the deteriorated stone. Consolidation of the historic stones by the formation of a compatible network within the microstructure of the stone is a requirement for the compatibility of the treatment. However, there is limited knowledge on the efficiency of various consolidation products in terms of their performance, compatibility and durability in relation to the stone type and state of deterioration. Therefore, it was necessary to develop some tests to assess the effectiveness of stone consolidation treatments by measurable parameters before their application and prove their success in time.

There are numerous studies on application of calcium hydroxide solutions on several materials like limestones, wall-paintings, mortars or plasters (Daehne and Herm, 2013, Caner *et al.*, 2013, Caner, 2011, Daniele *et al.*, 2008, Dei and Salvadori, 2006, Giorgi *et al.*, 2000, Ambrossi *et al.*, 2001). Treatments with nano-dispersive calcium hydroxide solution are favourable due to their high penetration depth, the final product calcium carbonate having the same chemical and mineralogical composition with limestone, lime mortars and plasters.

Carbonation of calcium hydroxide is closely affected by relative humidity of the environment, its CO₂ enrichment, the type of dispersing medium, and the calcium hydroxide concentration. Tests that are performed before and after treatments are expected to show the changes in physical and physicomaterial properties and the microstructure of stone. The results of the tests should be directly correlated with the compatibility and durability properties of stone.

In this study, nano-dispersive calcium hydroxide solution was applied to dolomite samples obtained from quarries of Midyat-Mardin and some tests were conducted to evaluate effectiveness and compatibility of treatment. Dolomite mineral has a unit cell of rhombohedral shape with chemical formula CaMg(CO₃)₂. Minerals of dolomite are similar in structure to those of calcite having unit cell of rhombohedral shape. Dolomite has layers of carbonate alternating with layers calcium and magnesium. The insertion of magnesium atom for half of the calcium atoms makes dolomite with a lower degree of symmetry compared to calcite. The regular alternating layers of calcium-magnesium in its unit cell make dolomite a difficult mineral to be synthesized in the laboratory under normal atmospheric conditions. Even though, it is a very stable mineral thermodynamically, its formation is not favored in terms of kinetic factors (Morrow, 1982). Since the treatment of dolomite with dolomite nanoparticles has not yet been achieved, nano-dispersive calcium hydroxide solution was used for the treatment of dolomite where the carbonation product, calcite, having similar crystalline shape can be an appropriate choice for the consolidation of dolomite.

2. Materials and Methods

Dolomite samples were obtained from Midyat-Mardin. They were cut to the size of 5×5×2 cm. Those samples were used in all experiments before and after the treatments. Nano-dispersive calcium hydroxide solution in ethyl alcohol was prepared at METU Materials Conservation Laboratory with the concentration of 30g/L. The size of the nano-

dispersed particles was measured by Malvern Nano ZS90 instrument. The average particle size was found to be in the range of 350-600nm (Caner, 2011, Caner *et al.*, 2013).

Samples were treated by putting them on filter papers saturated with nano-dispersive calcium hydroxide solution. By this way, the solution penetrated through samples by capillary suction. Samples were left on filter paper for half an hour. Treated samples were then kept in a chamber (Thermo Scientific MIDI 40 CO₂ incubator) under 90% relative humidity and 20% CO₂ environment during one month and then dried in oven at 60°C.

Effectiveness of consolidation treatment in dolomite samples were studied by examining them for their physical, physicomechanical and microstructural properties before and after the treatments. Bulk density (ρ), porosity (ϕ) of samples were determined by RILEM standards (RILEM, 1980). Ultrasonic pulse velocity (UPV_{direct}) in dry condition was measured via PUNDIT Plus 220Hz equipment. Modulus of elasticity was calculated indirectly by using average UPV_{direct} values and densities of dry samples (RILEM, 1980; Topal & Doyuran, 1995) (Tables 1 and 2). Water vapor permeability properties of stone samples were determined according to the standards (RILEM, 1980, Teutonico, 1988). An experimental set up was constructed and equivalent air thickness of vapor permeability (SD) and water vapor diffusion resistance coefficient (μ) of treated and untreated stone samples were determined (Tab. 3). Linear expansion-shrinkage behaviour of dolomite samples (5×5×2 cm dimensions) were observed at a dry ambient environment having a constant relative humidity (30%) during cooling from 40 to 20°C and then immersing in water (Fig. 1) by recording the movement vs time with sensitive probes of LVDT (Linear Variable Differential Transformer) which works with a data collector (ASTM D5335-14: 2010). Mineralogical and microstructural properties of dolomite samples before and after the treatment were studied by XRD (Bruker D8 Advance Diffractometer), stereomicroscope (Leica Z16 APO A model stereomicroscope), and SEM/EDS analyses.

3. Results and Discussion

Effectiveness of consolidation with nano-dispersive calcium hydroxide solution in ethyl alcohol was evaluated through comparison of basic physical and physicomechanical properties, water vapour permeability, linear dilation properties and microstructural views before and after the treatments.

3.1. Physical and Physicomechanical Properties

Average bulk density of untreated dolomite samples were 1.89 ± 0.02 g·cm⁻³, porosity values being $27.6\pm 0.9\%$ by volume. Those properties were not measured after the treatment to avoid damage to treated samples. Samples were thoroughly examined for their ultrasonic pulse velocity characteristics by direct UPV measurements in three axes. Average UPV_{direct} values of dry samples were between 3127 ± 219 ms⁻¹ (Tab. 1). Values for modulus of Elasticity, E_{mod} , calculated by using bulk density and UPV_{direct} were found to be 19.6 ± 2.7 GPa (RILEM, 1980; Topal & Doyuran, 1995). Average UPV_{direct} values of treated samples in three axes did not show any significant difference in the samples treated with nano-dispersive calcium hydroxide solution (Tab. 2). Although the changes in average ultrasonic velocity values were near the range of standard deviation, some increase was noticed in the capillary direction after the treatments (4%-15%). Obtaining variable changes in UPV_{direct} values in three axes indicated heterogeneous distribution of nano-dispersive solution in the sample by capillary suction.

Tab. 1: Physical and physicomechanical properties of dolomite samples.

Stone sample	ρ g·cm ⁻³	φ Vol.-%	UPV _{dry} m·s ⁻¹	E_{mod} GPa
Dolomite (M)	1.89±0.02	27.6±0.9	3127±219	19.6±2.7

Tab. 2: Average UPV values of dolomite samples before and after treatment with nano-dispersive Ca(OH)₂ solutions.

Stone samples	Direct UPV values before treatment		Direct UPV values after treatment		Rel. Change	
	UPV*	UPV _Z **	UPV*	UPV _Z **	Δ UPV*	Δ UPV _Z **
	m·s ⁻¹	m·s ⁻¹	m·s ⁻¹	m·s ⁻¹	%	%
MII-1	3331	3430	3187	3583	-4	4
MII-2	3491	3498	3537	4006	1	15
MII-3	3538	3435	3373	3877	-5	13
MII-4	3463	3365	3364	3826	-3	14
Average	3455	3432	3365	3823		

* average UPV values of x-y-z directions

** UPV values in z direction being parallel to the direction of capillary suction

Water vapor permeability of the samples before and after the treatments was thought to be a useful parameter to show the compatibility between the treated and untreated parts of stone in consolidation applications for the evaluation of treatment's compatibility. It was observed that water vapor permeability characteristics of untreated and treated samples were in quite the same range indicating that the treatment did not significantly affect the breathing behavior (Tab. 3).

Tab. 3: Water vapor permeability properties of treated and untreated dolomite samples.

Stone samples		S_0^* m	SD^{**} m	μ^{***}
MII	Untreated(average)	0.0197	0.199	10.39
MII-1	Treated	0.0195	0.247	12.68

* thickness of sample

** equivalent air thickness of water vapor permeability (SD)*** water vapor diffusion resistance coefficient (μ)

3.2. Linear Thermal Expansion Properties Related to Thermal Changes

Linear expansion/shrinkage behavior of dolomite related to temperature and water suction changes were first examined with a preliminary experiment during cooling from 40°C to 20°C followed by immersion in water. Considerable shrinkage during cooling from 40°C to 20°C was observed, whereas, the immersion of the sample in water did not cause any dimensional change (Fig. 1). Those results indicated that linear expansion behavior of dolomite samples related to thermal change was more important.

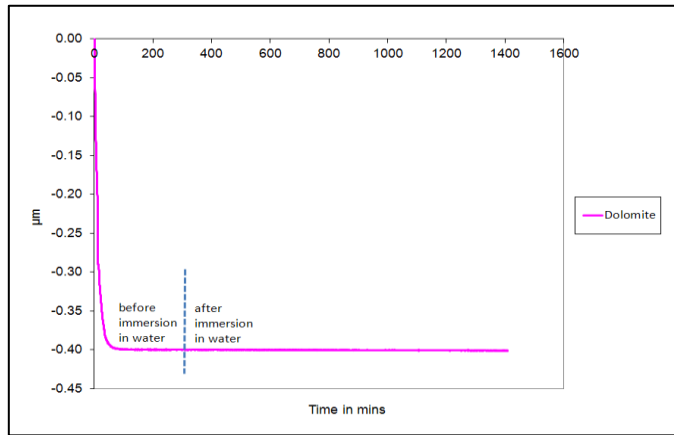


Fig. 1: Linear shrinkage of 5 cm dolomite sample during cooling from 40°C to 20°C and immersion in water.

Therefore linear expansion of the dolomite samples related to thermal changes was examined before and after the treatment with nano-dispersive solution. Before treatment, dolomite samples of 5 cm length had linear expansion of about 0.015 mm during heating from 10°C to 50°C. Expansion of the same sample after the treatment was observed to be around 0.016 mm. The results indicated that treatments did not cause any significant difference in the expansion properties of dolomites during temperature changes (Fig. 2). The results showed the treatment's compatibility in terms of linear expansion.

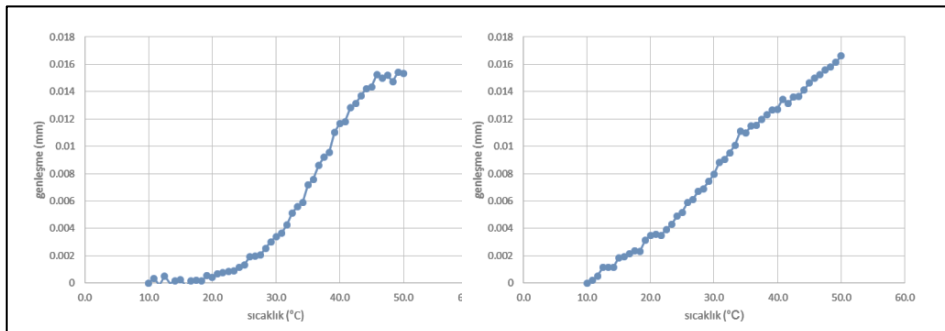


Fig. 2: Thermal expansion graph of dolomite sample before (left) and after (right) treatment.

3.3. Mineralogical and Microstructural Characteristics

Mineralogical composition of dolomite was identified by XRD. The dolomite samples obtained from new quarries of Midyat-Mardin, are purely dolomite as followed by XRD traces. Impurities within the dolomite were more likely to be in minor amounts.

Microstructural changes by the treatments were followed by stereomicroscope and SEM/EDS. Untreated and treated samples were viewed by a stereomicroscope at its highest zoom, It was observed that calcite crystals formed by nano-dispersive $\text{Ca}(\text{OH})_2$ solution gathered within the bigger pores; covering the areas with a white layer whereas in untreated samples, large dolomite crystals belonging to original stone were observed within the pores.

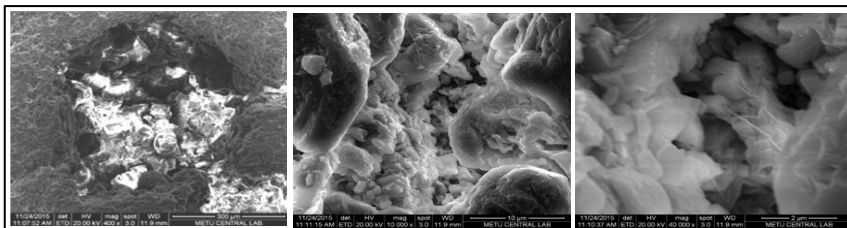


Fig. 3: SEM images of treated dolomite cross-sections: General view ($\times 100$) of bigger pores (left); Detailed view ($\times 10000$) of crystals inside the pores (center); Dolomite crystals ($\times 40000$) can be observed in structure after treatment (right).

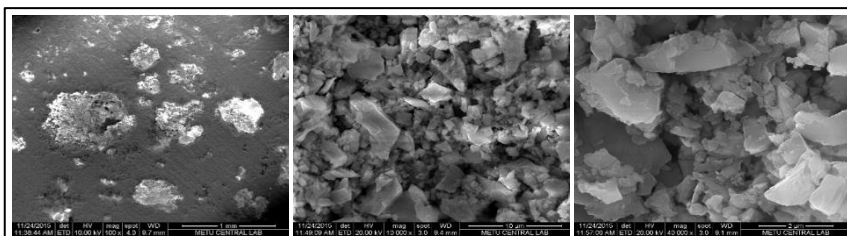


Fig. 4: SEM images of treated dolomite cross-sections: General view ($\times 100$) of bigger pores (left); Detailed view ($\times 10000$) of crystals inside the pores (center); Nano calcite crystals ($\times 40000$) can be observed in structure after treatment (right).

The changes in the microstructure of dolomite were better observed in secondary electron images of gold /palladium coated samples before and after treatments. Cross-section views of big pores before the treatments are seen in Fig. 3. Micritic size dolomite crystals are well observed in the pores of the stone. Cross-section views of big pores after the treatments are seen in Fig. 4. Newly formed calcite crystals after the treatments are well observed in the pores as being integrated with the dolomite crystals. Straight lines of crystal edges are indicative of surface controlled precipitation of calcite by treatment with nano-dispersive $\text{Ca}(\text{OH})_2$ solution. Dissolution and precipitation reactions of calcium carbonate are supposed to be controlled by surface reactions in a wide pH range of 4 to 14 (Morse and Arvidson, 2002). Alkaline solutions at pH larger than about 13.5 are considered to be in favor of aragonite precipitation (Kitamura *et al.*, 2002). Aragonite formation is also favored in presence of magnesium ions (Bischoff and Fyfe, 1968., Lipmann, 1973). Morphological characteristics of precipitated calcium carbonate in SEM images indicate the presence of rhombohedral calcite but not orthorhombic aragonite. The precipitation of calcite must have

occurred in a medium with *pH* lower than 13.5 and where magnesium ion concentration was not noticeable. Therefore, dedolomitization of dolomite was unlikely to occur during the treatments with nano-dispersive Ca(OH)₂ solution (Caner *et al.*, 1985).

4. Conclusion

In this study, consolidation of dolomite with nano-dispersive calcium hydroxide solution in ethyl alcohol was studied in terms of its effectiveness and compatibility with the stone structure. The treatment with nano-dispersive solution improved its physicochemical properties. The treatments did not affect the stone's water vapour permeability and thermal dilation characteristics showing compatibility of treated parts with the untreated parts of the stone. Formation of calcite crystals within the microstructure of the stone and their integration with its dolomite crystals were examined by SEM which showed the success of the treatments. Further studies with repeated treatments as well as treatments of deteriorated dolomites need to be done for the development of this method as a treatment for historical dolomitic structures.

5. Acknowledgement

In this study, financial support of The Scientific and Technological Research Council of Turkey (TUBİTAK) is gratefully acknowledged.

References

- Ambrossi, M., Dei, L., Giorgi, R., Neto, C., Baglioni, P., 2001, Colloidal Particles of Ca(OH)₂ Properties and Applications to Restoration of Frescoes, *Langmuir*, 17, 4251-4255.
- ASTM D5335-14: 2010 - Standard test method for linear coefficient of thermal expansion of rock using bonded electric resistance strain gauges, 7p. American Society for Testing and Materials.
- Bischoff, J.L., and Fyfe, W.S., 1968, Catalysis, imbibition and the calcite-aragonite problem, Part 1, The aragonite-calcite transformation, *Am. Jour. Sci.*, 266, 65-79.
- Caner, E.N., Demirci, Ş. and, Türkmenoğlu, A.G., 1985, Deterioration of Dolomite by Soluble Salts in Divriği Great Mosque-Turkey, V th. International Congress on Deterioration and Conservation of Stone, Ed. G.Felix, 1, 299-305, Ecole Polytechnique Federale de Lausanne, Lausanne, Lausanne,
- Caner, E., 2011, Limestone decay in historic monuments and consolidation with nanodispersive calcium hydroxide solutions, Middle East Technical University, Phd Thesis.
- Caner, E., Caner-Saltık, E.N., 2013, Deterioration mechanisms of historic limestone and development of its conservation treatments with nanodispersive Ca(OH)₂ solutions, 8th International Symposium on the conservation of Monuments in the Mediterranean Basin, 3, 54-72.
- Daehne, A., Herm, C., 2013, Calcium hydroxide nanosols for the consolidation of porous building materials, *Heritage Science*, 1(11).

- Daniele, V., Taglieri, G., Quaresima, R., 2008, The Nanolimes in cultural heritage conservation: characterization and analysis of the carbonation process, *Journal of cultural heritage*, 9, 294-301.
- Dei, L., Salvadori, B., 2006, *Journal of cultural heritage*, 7, 110-115.
- Giorgi, R., Dei, L., Baglioni, P., 2000, A new method for consolidating wall paintings based on dispersion, of lime in alcohol, *Studies in Conservation*, 45, 154- 161.
- Kitamura, M., Konno, H., Yasui, A., Masuoka, H. 2002, Controlling factors and mechanism of reactive crystallization of calcium carbonate polymorphs from calcium hydroxide solutions, *Journal of Crystal Growth*, 236, 323-332.
- Lippman, F., 1973, *Sedimentary Carbonate Minerals*, Springer Verlag, Berlin.
- Morrow, D.W., 1982, Diagenesis 1. Dolomite-Part 1. The chemistry of dolomitization and dolomite precipitation, *Geoscience Canada*, 9(1), 5-13.
- Morse, J. W., and Arvidson, R. S., 2002, The dissolution kinetics of major sedimentary carbonate minerals, *Earth Science Reviews*, 58, 51-84.
- RILEM, 1980, Tentative Recommendations, Comission-25-PEM, Recommended tests to measure the deterioration of stone and to assess the effectiveness of treatment methods, *Materiaux et Constructions*, 13(75):173-253.
- Teutonico, J.M., 1988, *A Laboratory Manual for Architectural Conservators*, ICCROM, Rome, p.32-122.
- Topal, T. and Doyuran V., 1995, Ultrasonic Testing of Artificially Weathered Cappadocian Tuff. *Preservation and Restoration of Cultural Heritage*, 205-211.

EUROPEAN PROJECT
“NANO-CATHEDRAL: NANOMATERIALS FOR CONSERVATION
OF EUROPEAN ARCHITECTURAL HERITAGE DEVELOPED BY
RESEARCH ON CHARACTERISTIC LITHOTYPES”

**A. Lazzeri¹, M.-B. Coltelli¹, V. Castelvetro², S. Bianchi², O. Chiantore²,
M. Lezzerini³, L. Niccolai⁴, J. Weber⁵, A. Rohatsch⁶,
F. Gherardi⁷ and L. Toniolo^{7*}**

Abstract

Europe has significant cultural and environmental diversity together with an exceptional ancient architecture and built environment. From the point of view of conservation, this architectural excellence and heritage may present degradation problems related to the variety of stone materials used for their construction. In the present project five different medieval cathedrals and a contemporary opera theatre were selected as they may be considered as representative of both different environmental conditions and types of stones (limestones, sandstones and marbles) in Western Europe. The project aims at developing new materials, technologies and procedures for the restoration and conservation of stone in ancient cathedrals and monumental buildings, with a particular emphasis on the preservation of the originality of the building materials and on the development of tailor-made approach to tackle the specific problems. The original materials will be analysed and classified, evaluating their connection with historical exploitation of quarries as a source of building materials. Nanomaterials suitable for the consolidation and protection of stones will be developed aiming at providing the best technological answer for the preservation of different types of stones, according to porosity and mineralogical and chemical features. The exploitation of the project will bring about the adoption of best practices for the preservation of the cathedrals and high quality buildings by selecting the most advanced nanotechnologies.

¹ A. Lazzeri and M.B. Coltelli
INSTM - Department of Civil and Industrial Engineering, University of Pisa, Italy

² V. Castelvetro, S. Bianchi and O. Chiantore
INSTM - Department of Chemistry and Industrial Chemistry, University of Pisa, Italy

³ M. Lezzerini
INSTM - Department of Geosciences, University of Pisa, Italy

⁴ L. Niccolai
Colorobbia Consulting S.r.l., Italy

⁵ J. Weber
University of Applied Arts Vienna, Austria

⁶ A. Rohatsch
Institut für Geotechnik, Technische Universität Wien, Austria

⁷ F. Gherardi and L. Toniolo*
INSTM - Department of Chemistry, Materials and Chemical Engineering, Politecnico di Milano,
Italy
lucia.toniolo@polimi.it

*corresponding author

Keywords: architectural heritage, nanomaterials, stone conservation, consolidation, protection

1. Introduction

1.1. Project “Nano-cathedral”

In the framework of the EC Horizon 2020 Nano-Cathedral project¹ launched in 2015, nanomaterials for the preservation of stone based monuments have been designed as a result of a collaborative effort of European research Centers, companies involved in the development and production of engineered inorganic nanoparticles, Conservation Institutions and Foundations managing monumental buildings. The general objective of the three-year project is the design, production and evaluation of different types of inorganic and polymeric nanoparticles as well as nanoparticles based formulations, to be applied as protective and/or consolidation treatments onto different lithotypes on European monuments characterized by a variety of environmental exposure conditions. In particular, the Cathedral of Pisa (Italy) and the Cathedral of Santa María of Vitoria-Gasteiz (Spain) are representative of south European “Mediterranean” climate in coastal and continental regions, respectively; the Sint-Baafs Cathedral of Ghent (Belgium), the Cathedral of St. Peter and Mary of Cologne (Germany) and the St. Stephen's Cathedral (Vienna), are included as representative of a Central-North European climate in continental regions. Moreover, the Oslo Opera House (Norway) was considered as an example of a contemporary building clad with white Carrara marble. The stones used for the construction of the buildings have been analysed and classified, evaluating their connection with historical exploitation of quarries as a source of building materials, thus improving the knowledge of the architectural and artistic heritage and the connections with the regional context. For this purpose a general protocol has been defined for the identification of the petrographic and mineralogical features of the stone materials, the evaluation of their state of conservation, the identification of correlations among the relevant state of decay, the material properties and the local macro and microclimatic exposure. The innovative nanomaterials, that will be developed, will be applied on stone materials taken from quarries representative of the selected lithotypes, and they will be tested before and after application of the consolidation and/or protection products to evaluate the effectiveness of the treatments, following a protocol of laboratory tests which include microscopic observations, colorimetry and spectroscopic analyses. Finally, the best formulations of consolidants and protective treatments will be applied on pilot-areas selected in each building and non-destructive tests will be carried out to monitor their effectiveness and durability.

1.2. Nanomaterials for stone conservation

Since ‘80s, the scientific research has been devoted to the development of nanomaterials to be applied in a wide range of fields, including the conservation of Architectural Heritage. Compared to traditional materials and methods, the innovative nanomaterials show enhanced effectiveness in their main properties as their higher surface area make them more reactive. Regarding the class of stone consolidants, one of the first synthesized

¹ H2020 Grant Agreement N.646178; NMP-2014-2015/H2020-NMP-2014-two-stage

nanomaterial is nanolime, that is a water or alcoholic dispersion of $\text{Ca}(\text{OH})_2$ nanoparticles. Nanolime has been used for the consolidation of calcareous stone and wall paintings, since it presents different advantages compared to traditional limewater: higher reactivity, deeper penetration in the substrate, reduction of carbonation time and higher stability (Chelazzi *et al.* 2013, Rodriguez-Navarro *et al.* 2013). Different commercial nanolime and dispersions of nano- SiO_2 are available on the market and their use is becoming more common among restorers, despite nowadays the most used consolidants are alkoxy-silane and oligomers. In order to overcome the drawback of alkoxy-silanes related to the formation of cracks of the silica gel, particle-modified consolidants, based on the introduction of different nanoparticles in pre-polymerized tetraethoxysilane, have been proposed (Miliani *et al.* 2007, Kim *et al.* 2009). Another interesting nano-consolidant is the one proposed by Verganelaki, which consists in the incorporation of nanoparticles of amorphous calcium oxalate monohydrate in TEOS to form a crack-free nanocomposite, with a good penetration depth inside the substrate, able to increase the strengthening properties of calcareous building stones and cement mortars (Verganelaki *et al.* 2015). Nanotechnology is also applied for the synthesis of protective treatments for stone materials, realized by adding different nanoparticles (SiO_2 , SnO_2 , Al_2O_3) inside polymeric media (poly(methyl methacrylate), functionalized perfluorinated polyether and polyalkylsiloxane) to increase the stone surface roughness (Manoudis *et al.* 2009, Facio and Mosquera 2013). These nanocomposites are able to confer super-hydrophobic (water contact angle $> 150^\circ$) and self-cleaning properties to the stone. Moreover, TiO_2 nanoparticles have been used for the synthesis of self-cleaning consolidants and protective treatments because of their photocatalytic property to promote the degradation of inorganic and organic pollutants and their ability to create superhydrophilic surfaces (Munafò *et al.* 2015). Among TiO_2 -based self-cleaning coatings for Cultural Heritage stone surfaces, two different categories can be identified. The first one includes hydrophilic nano- TiO_2 dispersions (Quagliarini *et al.* 2013), whereas the second one comprises hydrophobic and superhydrophobic nanocomposites (Kapridaki *et al.* 2014).

The results of the current and more recent literature demonstrates the potential of nanostructured consolidants and protective treatments for the conservation of architectural heritage, since they can overcome the open challenges related to durability, adhesion on the substrates, effectiveness and transparency issues.

2. Survey on commercial and research stone consolidants and protective coatings

One of the activities of the Project concerns the realization of a survey to setup a database of the most applied commercial products and the most relevant research products from the current scientific literature in Europe for the consolidation and the protection of natural decayed stones. The collected data are coming from the Project Partners on the basis of their professional and research experience and the elaborated data are strictly connected to this provenance; therefore, the database is not an exhaustive collection of all the commercial or research products available. Among commercial products, the total number of different consolidant materials is 37. They can be divided in three main chemical classes: alkoxy-silane and oligomers, acrylics and low molecular weight inorganics. 12 of them contain nanoparticles in the formulation, in particular $\text{Ca}(\text{OH})_2$, SiO_2 , ZrO_2 , Al_2O_3 (Fig. 1). Regarding the dispersing media, the most used ones are organic solvents. Among commercial products, the total number of different protective coatings is 21, 2 of which

have antifouling properties. They can be divided in 5 chemical classes: alkyl-alkoxy-silane oligomers, alkyl-aryl-polysiloxanes, fluorinated or partially fluorinated polymers, low molecular weight inorganics and vegetable polysaccharides. Among them 5 contain nanoparticles in the formulation, in particular Ag, SiO₂, TiO₂, ZnO nanoparticles (Fig. 1). Organic solvents are the most used in the formulations.

Among research products the total number of consolidants is 39, 2 of which have also antifouling properties. They can be divided in 4 main chemical classes: alkoxy-silane and oligomers, acrylics, low molecular weight inorganics and products of biomineralization. A wide range of nanoparticles have been used in the formulation but nano-SiO₂ is the most used one. Organic solvents are the most used in the formulations, which have been applied on different stone substrates, following different application methods. The total number of protective coatings is 27, 4 of which show antifouling properties and 2 of which show both properties. They can be divided in 4 main chemical classes: alkyl-alkoxy-silane oligomers, alkyl-aryl-polysiloxanes, acrylic polymers, fluorinated or partially fluorinated polymers, oxalates, low molecular weight inorganics and aliphatic polyesters. Also for research protective coatings, a wide range of nanoparticles have been used in the formulation among which nano-TiO₂ is the most used one. Organic solvents are the most used in the formulations, which have been applied on different stone substrates, following different application methods.

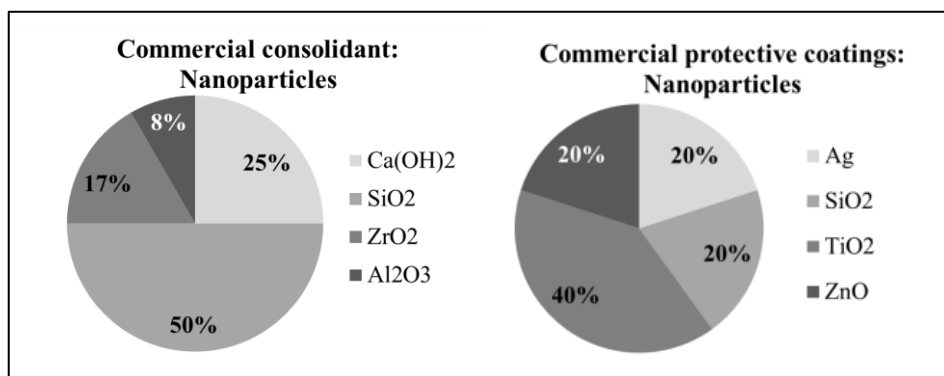


Fig. 1: Nanoparticles present in commercial consolidants (left) and protective coatings (right).

3. Selection of lithotypes

For each cathedral one lithotype has been selected (except for Cathedral of Cologne, for which two lithotypes have been selected) taking into account its petrographic properties and its representability for the building but also with respect to the European context, to grant a large scale application of the project results. The selected lithotypes are summarized in Tab. 1.

Tab. 1: Selected lithotypes for the full characterization and application of consolidation and protection formulations.

Building	Stone name	Lithotype
Cathedral of Vitoria-Gasteiz	Ajarte	Fossil limestone
Cathedral of Ghent	Balegem	Sandy limestone
Cathedral of Cologne	Obernkirchen	Sandstone
	Schlaitdorf	Sandstone
Cathedral of Vienna	St. Margarethen	Calcareous arenite
Cathedral of Pisa and Oslo Opera House	Carrara marble	Marble

4. Innovative consolidants and protective coatings

4.1. Aqueous Nanocalcite dispersions as consolidant

Nanoparticles of calcium carbonate are produced by a novel process involving colloidal particle stabilisation with either citrate or a block copolymer of poly(ethylene oxide) with poly(citrate). The optimisation of the synthetic procedure for the aqueous nanoparticle dispersions is targeting the smallest achievable particle size, since these nanocarbonates (calcite, vaterite which is a polymorph of calcium carbonate) are expected to penetrate to some extent into the porous network of degraded calcareous stones. The citrate anion plays a key role both as a nanoparticle stabiliser (it adsorbs efficiently onto the surface) and as a promoter of adhesion of the nanoparticle onto the calcareous stone surface (or inner pore surface) thanks to its ability to “chelate” the Ca^{2+} ion. Combinations of the obtained nanocalcite with conventional silane consolidants (e.g. based on TEOS) will also be explored, as it is expected that a “nanoparticle-modified consolidant” may improve the performance of simple TEOS-based treatments in terms of achieved stone cohesive strength and lower long-term damage (e.g. by shrinkage-induced micro-cracks in the silica-like material resulting from TEOS-based consolidation).

4.2. Water-borne polymeric and hybrid polymer/inorganic nanoparticle formulations

New self-stabilized amphiphilic or hydrophobic copolymers are being synthesized, as components of either consolidant or protective formulations, respectively. In particular, the composition and structure of the (acrylic) copolymers are designed to provide one or more of the following features:

- i) Enhanced stability to photo-oxidative aging, by inclusion of comonomer units bearing the 2,2,5,5-tetramethylpiperidine (or Hindered Amine Light Stabilizer, HALS) group in the side chain;
- ii) A combination of acrylic and methacrylic comonomers (e.g. methyl methacrylate, butyl acrylate) in a mole ratio providing the required balance of thermal and mechanical properties, while keeping the polymer photooxidative sensitivity at a minimum;
- iii) Side-chain semifluorinated comonomers for enhanced hydrophobicity and chemical stability;

- iv) One terminal hydrophilic short “block” of either poly(acrylic acid) (PAA) or poly(ethylene oxide) (PEO) to provide the polymer particle with the required colloidal and storage stability, without the addition of low molecular weight surfactants.

Depending on the expected performance and material requirements, the aqueous colloidal dispersions are synthesised according to one of the following two methods:

- a) Conventional free radical emulsion polymerisation, yielding a high molecular weight random copolymer with uncontrolled comonomer distribution and requiring addition of a molecular surfactant for colloidal stabilisation during and after synthesis;
- b) The so-called “ab initio” controlled RAFT (Reversible Addition Fragmentation Transfer) polymerisation, which may be performed in “soapless” conditions (without added surfactant) and leads to the formation of amphiphilic block copolymers, self-assembling into polymer nanoparticles of controlled size (typically within the 50-150 nm range). In this case the presence of a hydrophilic PAA or PEO block is mandatory, and may contrast the hydrophobic contribution of the remaining polymer structure. However, the PAA block may contribute to “anchoring” the polymer either to the stone surface, thus providing consolidation effectiveness, or to inorganic nanoparticle surface in hybrid formulations used as protectives. An advantage of the PEO block, on the other hand, is its inertness towards carbonatic stones and its photodegradation behaviour leading to fragmentation and eventually self-removal of this hydrophilic component from the polymer layer.

The specific contributions of these structural features to the ultimate polymer properties are assessed by a broad range of analytical techniques to fully characterize the relevant structural (by spectroscopies), morphological (by Dynamic Light Scattering and electron microscopy) and film surface (by contact angle, Zeta potential, and ATR-FTIR analyses) features.

5. Conclusions

The main objectives of this Project are: innovation in materials technology and rationalization of the conservation policy, affording a renewed knowledge of the complex system - treatment/stone substrate and of the durability threshold of these treatments.

The wide experience and literature on the nanostructured materials in the field, the multidisciplinary approach and the inclusion of industrial partners – Colorobbia Consulting Srl, Chem-Spec srl, Tecnologia Navarra de nanoproductos sl – will grant the possibility to set-up new affordable conservation treatments.

In the first semester of the Project, a decisive state of the art about the use of nanotechnologies for the consolidation of stone materials was carried out, assessing nano-SiO₂ and nanolime as the most used nanostructured materials. In the field of protection and water-repellent treatments for stone surfaces, TiO₂ and ZnO nanoparticles are the most employed in dispersions or formulations.

In the framework of this Project, some different new nanomaterials have been already designed and prepared. An important achievement is the set-up of the new synthetic procedure for nanocalcite which will be used and tested as simple dispersion, which can easily penetrate the porosity of calcareous stone materials, or will be used as an additive in particle modified consolidants (i.e. modified TEOS) and improve the adhesion of the system to the crystalline substrate. New self-stabilized amphiphilic or hydrophobic copolymers have been already synthesized to be used as protective treatments or in hybrid system covering nanoparticles of different nature.

A short testing protocol will be carried out in the following months to assess the most promising nanomaterials. Actually, the Technology Readiness Level of the project should be at least 5, as the developed technologies will be validated in lab and *in situ*, that is on the selected monuments.

Acknowledgements

The research project is supported by the European program Horizon 2020 Call NMP21- AC 646178.

References

- Chelazzi, D., Poggi, G., Jaidar, Y., Toccafondi, N., Giorgi, R., Baglioni, P., 2013, Hydroxide nanoparticles for cultural heritage: Consolidation and protection of wall paintings and carbonate materials, *Journal of Colloid and Interface Science*, 392(0), 42-49.
- Facio, D.S., Mosquera, M.J., 2013, Simple Strategy for Producing Superhydrophobic Nanocomposite Coatings In Situ on a Building Substrate, *ACS Applied Materials & Interfaces*, 5(15), 7517-7526.
- Kapridaki, C., Pinho, L., Mosquera, M.J., Maravelaki-Kalaitzaki, P., 2014, Producing photoactive, transparent and hydrophobic SiO₂-crystalline TiO₂ nanocomposites at ambient conditions with application as self-cleaning coatings, *Applied Catalysis B: Environmental*, 156-157(0), 416-427.
- Kim, E.K., Won, J., D,o J-y., Kim, S.D., Kang, Y.S., 2009, Effects of silica nanoparticle and GPTMS addition on TEOS-based stone consolidants, *Journal of Cultural Heritage*, 10(2), 214-221.
- Manoudis, P.N., Karapanagiotis, I., Tsakalof, A., Zuburtikudis, I., Kolinkeová, B., Panayiotou, C., 2009, Superhydrophobic films for the protection of outdoor cultural heritage assets, *Appl Phys A*, 97(2), 351-360.
- Miliani, C., Velo-Simpson, M.L., Scherer, G.W., 2007, Particle-modified consolidants: A study on the effect of particles on sol-gel properties and consolidation effectiveness, *Journal of Cultural Heritage*, 8(1), 1-6.
- Munafò, P., Goffredo, G.B., Quagliarini, E., 2015, TiO₂-based nanocoatings for preserving architectural stone surfaces: An overview, *Construction and Building Materials*, 84, 201-218.
- Quagliarini, E., Bondioli, F., Goffredo, G.B., Licciulli, A., Munafò, P., 2013, Self-cleaning materials on Architectural Heritage: Compatibility of photo-induced hydrophilicity of TiO₂ coatings on stone surfaces, *Journal of Cultural Heritage*, 14(1), 1-7.
- Rodriguez-Navarro, C., Suzuki, A., Ruiz-Agudo, E., 2013, Alcohol dispersions of calcium hydroxide nanoparticles for stone conservation, *Langmuir*, 29(36), 11457-11470.
- Verganelaki, A., Kapridaki, C., Maravelaki-Kalaitzaki, P., 2015, Modified Tetraethoxysilane with Nanocalcium Oxalate in One-Pot Synthesis for Protection of Building Materials, *Industrial & Engineering Chemistry Research*, 54(29), 7195-7206.

This page has been left intentionally blank.

NEW POLYMER ARCHITECTURES FOR ARCHITECTURAL STONE PRESERVATION

A. Lazzeri¹, S. Bianchi², V. Castelvetro^{2*}, O. Chiantore³, M.-B. Coltelli¹, F. Gherardi⁴, M. Lezzerini⁵, T. Poli³, F. Signori¹, D. Smacchia² and L. Toniolo⁴

Abstract

A series of multifunctional polymeric systems have been designed, synthesized and their effectiveness in modifying the surface properties of different stone types have been evaluated. Both the synthetic strategy and the design of the macromolecular structures are aimed at achieving maximum flexibility in the introduction of structural features that are required to provide the resulting polymers with a range of potential properties. For this purpose, the controlled free radical polymerization of acrylic monomers by the so-called RAFT (Reversible Addition Fragmentation Transfer) technique has been adopted to obtain amphiphilic block copolymers. These may be used either as such in the modification of aqueous dispersions of inorganic nanoparticles (silica, titania, zirconia, zinc oxide among others), resulting in hybrid nanocomposite treatment materials, or as self-assembling reactive precursors for *ab initio* emulsion polymerizations, leading to the formation of colloidal aqueous dispersions of nanostructured multifunctional polymer nanoparticles. Among the innovative features of the polymers under investigation, the self-stabilisation against photooxidative degradation is worth mentioning as the durability of organic polymers is a well-known open issue in conservation. To achieve enhanced stability, free radical scavenging groups such as Hindered Amine Light Stabilizers (HALS) are introduced in the polymer structure through copolymerization with HALS derivatives. In addition, combination of polymers and UV-blocking inorganic particles (ZnO, TiO₂) are also expected to greatly enhance durability. These polymeric materials, and other presently under development, are intended as components of either protective or consolidant treatments to be tested first at a lab scale on various stones (both carbonatic and silicatic), then in situ on 5 different cathedrals distributed throughout Europe and on a contemporary opera theatre.

Keywords: block copolymer, hybrid latex, self-stabilisation, protection, consolidation

¹ A. Lazzeri, M.B. Coltelli and F. Signori
INSTM - Department of Civil and Industrial Engineering, University of Pisa, Italy

² S. Bianchi, V. Castelvetro* and D. Smacchia
INSTM - Department of Chemistry and Industrial Chemistry, University of Pisa, Italy
valter.castelvetro@unipi.it

³ O. Chiantore and T. Poli
INSTM - Department of Chemistry, University of Turin, Italy

⁴ F. Gherardi and L. Toniolo
Department of Chemistry, Materials and Chemical Engineering, Politecnico di Milano, Italy

⁵ M. Lezzerini
INSTM - Department of Geosciences, University of Pisa, Italy

*corresponding author

1. Introduction

The stone materials undergo different kinds of alterations and degradation upon aging due to the different chemical, physical and mechanical characteristics of the stone and to the peculiar outdoor exposure. In the EU H2020 “NanoCathedral” project launched in 2015 five different medieval cathedrals and a contemporary opera theatre (Fig. 1) were selected as representative of both different macro- and micro-climatic conditions - continental vs. coastal; arid vs. humid - and different lithotypes - limestones, sandstones and marbles.

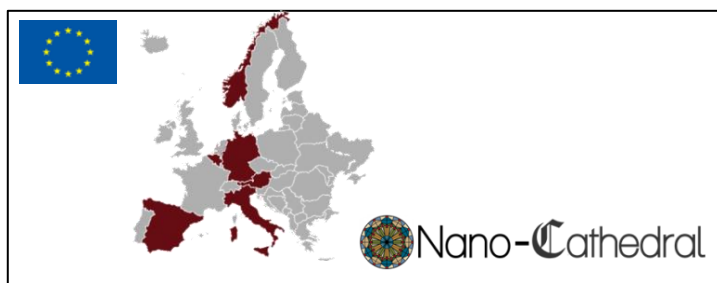


Fig. 1: Selected cathedrals within the Nanocathedral” H2020 project: Pisa (Italy) and Santa María of Vitoria-Gasteiz (Spain) exposed to south European climate in coastal and continental regions, respectively; Sint-Baafs (Ghent, Belgium), St. Peter and Mary (Cologne, Germany) and St. Stephen (Wien, Austria) exposed to North European climate in either coastal or continental regions. Oslo Opera House, dipping into the North Sea.

The project aims at providing innovative consolidant and protective products tailored for the specific stone-environment combination, while granting improved effectiveness and durability. In particular, a wide range of inorganic nanoparticles, innovative polymeric structures, and their hybrid combinations are being investigated. The best products and formulations, selected according to their performance and durability tests performed in three different laboratories and on stone specimens representative of those present in the different monumental buildings (fig. 1), will be applied during the second year of the three-year project on the participating Cathedrals for in situ evaluation.

A key requirement for *consolidants* is its effective penetration by capillarity into the stone porous network; this is often not achieved, as shown by the failure of many past consolidation treatments causing damage by formation of surface scales. Lack of chemical/physical compatibility or uncontrolled reactivity with the stone substrate is another reason of failure; poor durability of the consolidant a third one. Last but obviously not least, a consolidant material has to perform its main role of strengthening the micro-structure of the decayed stone by replacing lost original mineral bridges, partially recovering lost mechanical properties, and in some cases even converting unstable material into stable one (e.g. soluble into insoluble salts). Several reviews report on the state of art in stone consolidation (Clifton, 1980; Doehne and Price, 2010). Alkoxysilanes are currently the most commonly used consolidating materials, followed by acrylics. While the former may perform poorly due to bridging capacity limited to narrow fissures, long term shrinkage causing the formation of a secondary porosity, hydrolytic instability and poor chemical affinity with carbonatic stones, acrylics may develop better bridging properties but, as most organic polymers, their durability is poor and degradation products may be detrimental to the stone substrate.

Novel nano-materials may overcome penetration depth issues, while their extremely large surface area may promote the reactivity required to build up cohesive and adhesive forces. Nano-lime systems, also applied in combination with alkoxy silane treatments, have shown encouraging results, although the penetration and durability of such treatment has not been clearly demonstrated yet (Daehne and Herm, 2013). The so-called (nano)particle modified consolidant (PMC), typically based on tetraethoxysilane (TEOS) formulations with silica nanoparticles, can reduce the internal stone damages caused by the shrinkage and cracking during sol-gel condensation of TEOS (Ksinopoulou *et al.*, 2016). However, shortcomings are still related to the hydrolytic sensitivity and poor control of the time evolution of the consolidant nanophase during the sol-gel process. On the other hand other types of inorganic nanoparticles (e.g. Ti, Zn, Al, Si oxides or hydroxides) and hybrid organic-inorganic systems have been much less extensively investigated, although they may provide additional useful features such as biocidal (Gómez-Ortíz *et al.*, 2013) and self-cleaning properties, synergistic mechanical reinforcement, hydrophobicity, etc..

When dealing with hydrophobic protection the main open issues are durability inertness towards the stone substrate and lack of undesired aesthetic modifications upon and after application. Even in this case the limited durability of organic polymers is raising major objections, among conservators, against their application, although they are undoubtedly superior materials in providing hydrophobic and even self-cleaning surfaces. Even in this case, however, novel polymeric, hybrid or nanocomposite systems may provide solutions to overcome these drawbacks and even introduce additional useful features such as e.g. biocidal activity (van der Werf *et al.*, 2015). Among the various materials under development within the H2020 Nanocathedral project, here the design and synthetic approach to novel polymeric structures and their water based formulations will be presented, along with the preliminary results concerning their characterization and the evaluation of their performance and durability.

2. Approach and Results

2.1. Design of multifunctional polymer structures

The underlying criteria for the newly developed polymers are:

- a) A synthetic approach that may allow easy adaptation of the polymer structure according to the specific requirements of either consolidation or protection;
- b) Self-dispersibility in water (i.e. without added low molecular weight surfactants) in the form of nanoparticles with controllable (< 100 nm) size, for solvent-free application and effective penetration within the porous stone network;
- c) Functional groups for enhanced durability, water repellency, specific interaction and binding with inorganic nanoparticles (for nanocomposite treating materials) and with the stone substrate, respectively.

For such purposes, a synthetic scheme for multifunctional acrylic copolymers based on the controlled RAFT (Radical Addition–Fragmentation–Transfer) free radical polymerization is adopted. The relatively recent RAFT technique (Wang A.R. and Zhu S., 2003) has become very popular in recent years due to its tolerance towards most functional groups (thus allowing the synthesis of multifunctional polymers) and solvents (from hydrocarbon to water). Besides, the so-called “ab initio” RAFT emulsion polymerisation, may be

performed in “soapless” conditions (without added surfactant) by using amphiphilic RAFT mediators, leading to the formation of amphiphilic block copolymers self-assembled into nanoparticles of controlled size (typically 50-150 nm) (Chenal *et al.*, 2013).

With the above approach, water-based polymer dispersions with controlled composition and a range of functional groups have been prepared, for desirable properties such as:

- colloidal stability (for extended shelf life and easy application), by using a RAFT mediator leading to the formation of polymers with a short “block” of either poly(acrylic acid) (PAA) or poly(ethylene oxide) (PEO) at one chain end;
- adhesivity by incorporation of comonomers with either Ca²⁺ binding (e.g. carboxylate, for carbonatic stones) or sol-gel reactive (e.g. trialkoxysilyl groups for specific bonding to silicatic stones) functional groups;
- film cohesivity, by balancing the main copolymer composition (methyl methacrylate/butyl acrylate) for a polymer glass transition, T_g, slightly below room temperature, while keeping the polymer photooxidative sensitivity at a minimum;
- self-stabilisation against photo-oxidative aging, by incorporation of HALS group in the side chain (stabilisation against UV-induced photooxidation is based on a cyclic deactivation of photogenerated free radicals and peroxiradicals, followed by regeneration of the free-radical scavenging nitroxyl-amine active species).
- water repellency, by introduction of semifluorinated comonomers (in progress).

2.2. Polymer synthesis

The general synthetic scheme starts with an amphiphilic trithiocarbonate RAFT mediator extended with a short hydrophilic oligomer through controlled free radical polymerization. The obtained RAFT-active amphiphilic oligomers (Fig. 2) can then be used as block copolymer precursors of functional polymer nanoparticles (Fig. 3).

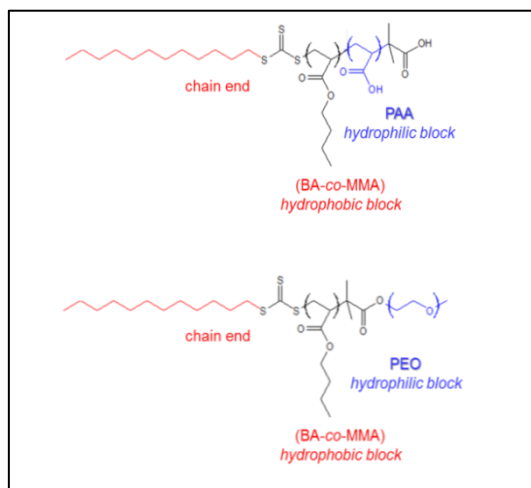


Fig. 2: RAFT-active amphiphilic block copolymer precursors.

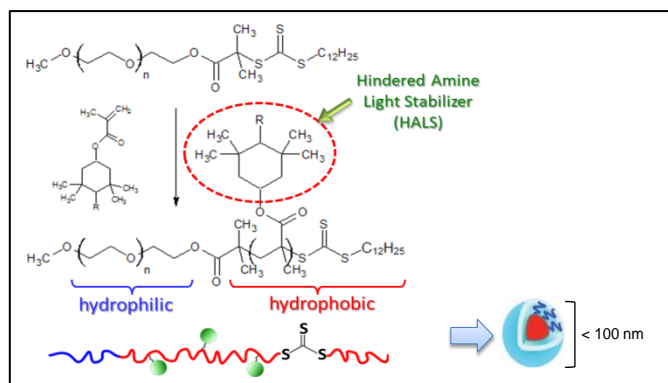


Fig. 3: synthetic scheme for self-stabilized multifunctional block copolymer nanoparticles by ab-initio RAFT emulsion polymerization of amphiphilic precursors.

3. Materials and characterizations

3.1. Latex Polymers

A selection of the functional polymer dispersions (polymer latexes) prepared during the first year of the project is listed in Tab. 1. Macro-RAFT is the alkyl-dithiocarbonate terminated oligo (acrylic acid) (PAA-TTC) or oligo(ethyleneglycol) (MPEG-TTC) of Fig. 2, used as a reactive surfactant and RAFT mediator in the ab initio emulsion polymerization of the butyl acrylate/methyl methacrylate (BM) mixture. The polymer latex acronyms indicate the amount of hydrophilic PAA or MPEG block (1 to 5 wt.-%) and of the HALS comonomer (1 and 3 wt.-% in H1 and H3 samples, respectively).

Tab. 1: Water borne polymer particles.

Polymer Latex		Macro-RAFT	PMPMA	Solids content	Particle size
		wt.-%	wt.-%	wt.-%	nm
BM-PAA5-H1	(DS4)	PAA-TTC	1	7.8	170
BM-PAA3-H1	(DS7)	PAA-TTC	1	9.0	143
BM-PAA1	(DS10)	PAA-TTC	//	9.1	188
BM-PAA1-H1	(DS11)	PAA-TTC	1	9.2	55
BM-PEG5	(DS9)	MPEG-TTC	//	8.0	79
BM-PEG5-H1	(DS12)	MPEG-TTC	1	7.9	181

The latexes were cast to clear films, and after dilution to 1 wt.% solids were applied by capillarity to Carrara marble and Schleitdorf sandstone (Cologne), respectively, to a nominal 1 μm -thick coating (actually thinner due to absorption into the porous stone). The

water contact angles (Tab. 2) and the surface Zeta potential data (Fig. 4) show that even at low concentration and without structure optimisation, these relatively hydrophilic materials are effective hydrophobic modifiers.

Tab. 2: Static water contact angle on polymer films and treated stones.

Polymer Latex		Smooth polymer film	Sandstone	Marble
		deg	deg	deg
Untreated stone			35.2 ± 2.3	35.2 ± 2.0
BM-PAA1	(DS10)	90.0 ± 2.0	105.3 ± 3.5	99.4 ± 5.4
BM-PAA1-H1	(DS11)	86.5 ± 0.8	104.5 ± 5.6	81.7 ± 7.0
BM-PEG5	(DS9)	91.6 ± 0.2	100.5 ± 8.6	67.7 ± 7.4
BM-PEG5-H1	(DS12)	97.2 ± 0.9	113.9 ± 5.8	99.8 ± 3.8

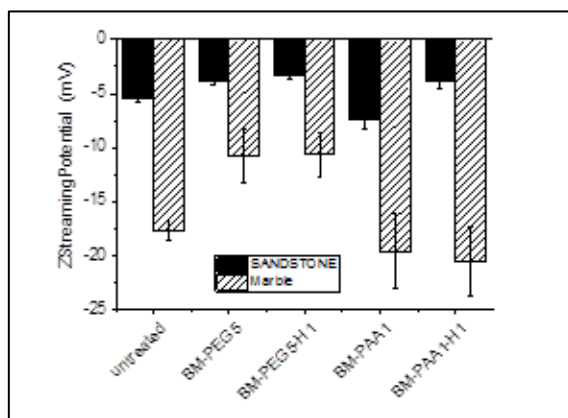


Fig. 4: ζ potential of uncoated and coated stone surfaces (measured with the Anton PAAR SurPASS® Electrokinetic Analyser).

3.2. Ageing tests

The FT-IR spectra of fig. 5 were recorded on cast films of selected polymers (DS#, as listed in Tab. 1) and of their nanocomposites with TiO₂ nanoparticles (DS#n), before and after the first 250 hours of simulated solar irradiation (Hereus Suntest CPS solar box, Xenon lamp, 300 nm cutoff filter, 750 W/m²). The preliminary results indicate that:

- After 250 hours of ageing only a slight oxidation is detected from the appearance of weak OH absorptions at 3220 cm⁻¹ and of a shoulder at 1640 cm⁻¹ due to chain-end double bonds (compare DS9 in Fig. 5a, and DS10 in Fig. 5b, before and after ageing).
- The HALS moiety inhibits the oxidation phenomena, as shown by the further reduction of the weak OH absorption at 3220 cm⁻¹ (compare DS12 with DS9 in Fig. 5a, and DS11 with DS10 in Fig. 5b)

- The photocatalytic action of TiO₂ promotes polymer oxidation phenomena (compare DS9 and DS9n in Fig. 5a) as shown by the growth of a broad absorption above cm⁻¹ due to formation of hydroxy groups, irrespective of the presence of HALS groups (compare DS12 and DS12n in Fig.5a).

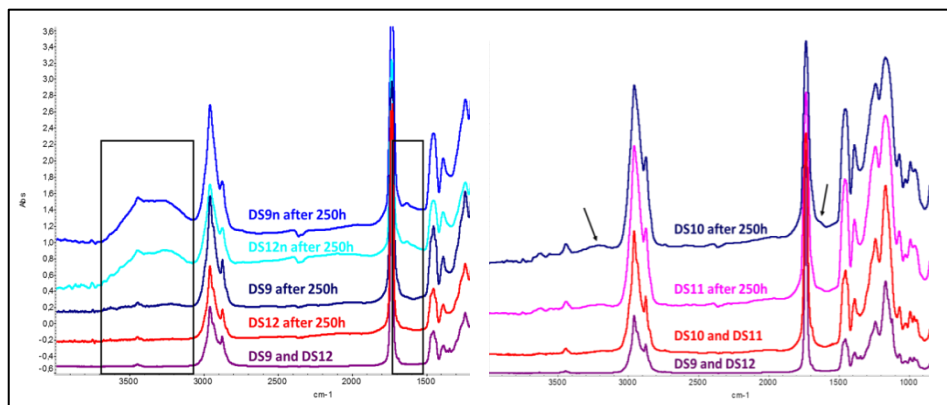


Fig. 5: FT-IR transmission spectra of films on silicon wafer.

4. Conclusions

A range of amphiphilic block copolymers and of self-stabilized, surfactant-free colloidal polymer dispersions (polymer latex) with small particle size (< 100 nm, for improved capillary absorption into the stone porous network) and reactive functional groups (carboxylate, for polymer anchoring onto stone substrates or inorganic nanoparticles) have been synthesized by means of the RAFT controlled polymerization method.

The amphiphilic block copolymers may be useful as modifiers of inorganic nanoparticles (ZnO and TiO₂ for protection, calcite, ZrO₂ and hydroxyapatite for consolidation) and as precursors of multifunctional latex particles or water-borne nanocomposite materials. Encouraging results have already been obtained from preliminary tests of application of the colloidal polymer dispersions onto sandstone and marble different stone samples (, respectively). In particular, very low amounts of applied polymer are sufficient to make the stone surface hydrophobic.

Aging tests have confirmed the foreseen stabilizing effectiveness of the HALS groups introduced by means of functional comonomers. On the other hand, the photocatalytic activity of embedded TiO₂ nanoparticles was shown to cause, as expected, accelerated degradation of the polymer matrix in nanocomposite films. Finally, a better understanding of the stone-polymer and stone-nanoparticle interaction and distribution at and within the porous stone surface may be achieved thanks to a combination standard (water absorption, water vapour permeability, contact angle) and less conventional techniques; among them, the Zeta potential may provide useful insights on the effectiveness of a treatment and on the evolution of the treated stone surface upon aging.

Aknowledgements

The research project is supported by the European program Horizon 2020 Call NMP21-AC 646178: “Nanomaterials for conservation of European architectural heritage developed by research on characteristic lithotypes (NANO-CATHEDRAL)”

References

- Chenal M., Bouteiller L. and Rieger J., 2013, Ab initio RAFT emulsion polymerization of butyl acrylate mediated by poly(acrylic acid) trithiocarbonate, *Polym. Chem.* 4, 752-762.
- Clifton J.R., 1980, Stone Consolidating Materials-A Status Report. U.S. National Bureau of Standards Technical Note 1118, Washington, D.C. (<http://cool.conservation-us.org/byauth/clifton/stone/>, accessed 30th June 2016).
- Daehne A. and Herm C., 2013, Calcium hydroxide nanosols for the consolidation of porous building materials - results from EU-STONECORE, *Herit. Sci.* 1, 11.
- Doehne E. and Price C., 2010, Stone Conservation – An Overview of Current Research, The Getty Conservation Institute, Los Angeles, 2nd ed. (<http://openarchive.icomos.org/1097/1/37730.pdf>, accessed 30th June 2016).
- Gómez-Ortíz N., De la Rosa-García S., González-Gómez W., Soria-Castro M., Quintana P., Oskam G. and Ortega-Morales B., 2013, Antifungal coatings based on Ca(OH)₂ mixed with ZnO/TiO₂ nanomaterials for protection of limestone monuments, *ACS Appl. Mater. Interfaces* 5, 1556–1565.
- Ksinopoulou E., Bakolas A. and Moropoulou A., 2016, Modifying Si-based consolidants through the addition of colloidal nano-particles, *Appl. Phys. A*, 122, 267
- van der Werf I.D, Ditaranto N., Picca R.N., Sportelli M.C. and Sabbatini L., 2015, Development of a novel conservation treatment of stone monuments with bioactive nanocomposites, *Herit. Sci.* 3, 29
- Wang A.R. and Zhu S., 2003, Modeling the reversible addition–fragmentation transfer polymerization process, *J. Pol. Sci.: Part A: Polym. Chem.*, 41, 1553-1566

TRIALS OF BIOCIDES CLEANING AGENTS ON ARGILLACEOUS SANDSTONE IN A TEMPERATE REGION

E. S. Long^{1*} and D.A. Young²

Abstract

Trials of biocide cleaning agents were carried out on an argillaceous sandstone to determine the efficacy of different application methods, to review any residual effect in the warm temperate conditions of Sydney, Australia and to compare products available on the local market. The trials were carried out on a significant public building which was designed in the Art Deco style and completed in 1952. The building does not have traditional detailing like cornices which discourage water from running down the façade. As a consequence, the upper courses of stone have become heavily marked by dark biological growths. Two commercial biocides containing benzalkonium chloride, but different co-formulants, were used in the trials. Following previous studies by others it was decided not to use any mechanical cleaning (scrubbing) in conjunction with the biocide treatment, but to trial a range of techniques including brush and poultice application and applying them to dry and to pre-wet surfaces. Monitoring the trials over two and a half years has demonstrated that effective biological control is attainable without scrubbing and that pre-wetting did not appear to make a significant difference in these conditions. Though initially it appeared that poultices performed better, it was found that run-off from untreated horizontal surfaces above the trial panels obscured the effects of different treatments.

Keywords: biological growth, biocide, benzalkonium chloride, poultice

1. Introduction

This investigation was prompted by cleaning the exterior of the building in 2012 and 2013. The work had been specified to include cleaning with water under low pressure, subject to site trials. During the works, despite repeated interventions by the conservation staff inspecting the cleaning, it became apparent that the pressure was too high for the surface, as evidenced by the amount of particles (from the stone surfaces) that washed off the façades.

The building had been cleaned previously in 2002 using water under high pressure. The specification said “nominally 2000 psi” (13,790 kPa), a pressure sufficient to cause considerable damage to this type of stone, even after the effects of pressure decrease from the pump to wall surface have been taken into account.

¹ E.S. Long*
Sydney Living Museums, Sydney, Australia
elishal@sydneylivingmuseums.com.au

² D.A. Young
Heritage Consultant, Melbourne, Australia

*corresponding author

A review of photographs from the time of construction until 2012 suggested a very slow build up in biological growth after the completion of the building in 1952, presumably as the stone weathered and the surface gradually became more open. Dark patches in areas of water run off first become noticeable in relatively small areas during the 1980s.

The review of photographs also suggested that the biological regrowth became more extensive, that is darker and over larger areas, *after* the cleaning programme in 2002 than it had been before. By 2012, the stone was again very dark on the upper wall surfaces and parapets, with growths more extensive on the southern, i.e. most-shaded, surfaces.

Concern about the rapid regrowth since 2002, the loss of surface grains when cleaned and the ongoing effect of cleaning at ever shorter intervals led to a review of the approach to cleaning sandstone and alternative methods of controlling micro-biological growths.

2. Climate

Sydney's warm temperate climatic conditions are favourable to micro-biological growth on stone: mild winters and warm humid summers. Summer highs average between 25-31° C (71-88° F) and winter highs average between 15-20° C (59-68° F). Winter lows are rarely below 5° C (41° F). Biological regrowth on porous surfaces can be rapid.



Fig. 1: View of the east face of the Museum of Contemporary Art building, Sydney. Trials were conducted on the inside faces of the parapets of the balcony at right.

3. The substrate

Much of the sandstone of the Sydney region is characterised by a warm golden colouring due to the presence of iron minerals in the matrix. The colouring makes them attractive building stones and characterises the architecture of historic Sydney. However, stones of the region typically have relatively high clay contents, where higher contents are linked to poor durability. Samples from the quarry from which this stone was taken have been shown to contain 15–22 % clay (Franklin, 2000).

Magnification of the surface using a field microscope showed that the surface of the stone was extremely open and porous. It is assumed that some of this loss of surface in such a young building may be due to past cleaning programs, and possibly to a post-construction wash down with acid, intended to remove mortar spills, and perhaps to intensify the yellow colour. Unfortunately, there are no records of such cleaning.

4. The biofilm

Before carrying out the trials, the biofilms on the building were reviewed in-situ by a botanist. It was found that the growths varied over the upper surfaces of the building. Red and green algae and various types of lichens, were identified (Archer, pers. comm.). As expected, lichens are more common on the horizontal surfaces and there are greater concentrations of algae on the shaded vertical surfaces.

5. Location of site trials

The trials were undertaken on the inside of the parapet walls of a roof-top balcony on the north-east corner of the building (Fig. 1 and Fig. 2). The choice was driven by the presence of significant levels of biological growth which were easily accessible for both application and monitoring, and which would not affect the outwards appearance of the building for the period that the trials were underway. The trials were applied to three parapet walls so that the effect of different orientations could be observed.



Fig. 2: The eastern wall of the balcony, 23 months after treatment. The dark area left of centre is the untreated control panel; to its left are panels treated by poultice application of biocide. Note the wide zones around the mortar joints showing a biocidal effect of the alkaline jointing material.

6. Biocides

Biocides, chemical compounds which kill or control micro-biological growth, are an accepted part of stone conservation. The most common active ingredient of biocidal agents for masonry is benzalkonium chloride, which is also a common ingredient in domestic disinfectants and swimming pool algacides. Benzalkonium chloride is a quaternary ammonium compound, which are also known as ‘quats’. They are used at very low dilution rates, e.g. 2% in water (Caneva, *et al.*, 2008; Nugari & Salvadori, 2003).

Two biocides that are common on the Australian market were trialled:

Biocide One: ‘Wet and Forget’

This product is supplied as a blue liquid concentrate in which the active ingredient is benzalkonium chloride. The concentrate was diluted on-site to produce a 2% solution (i.e. 20 grams per litre).

Biocide Two: ‘Boracol 100RH’

This product is supplied as an already diluted clear liquid. The active ingredients are benzalkonium chloride present at a rate of 22g/L, boron present at a rate of 23g/L and ethylene glycol at 109 g/L.

7. Methodology

Following the work of Charola *et al.* (2012) who found that pre-wetting improved the cleaning effect, the methodology provided for the application of both biocides by brush with three different surface conditions:

- dry surfaces;
- pre-wet with water on the day of application;
- double pre-wet with water: i.e. on the day before application and on the day of application.

One of the biocides was also applied within a commercially available absorbent poultice. The aim of testing the use of the poultice was to assess whether the longer contact time improved the effectiveness of the treatment. The same three surface conditions: dry, single pre-wet and double pre-wet were used with the poultice applications.

Ethylene glycol, a component of Biocide Two, was added to one trial of Biocide One to test whether the solvent improved the biocidal effect. Ethylene glycol is also used as a fungicide, particularly for treating rot in timber. Isopropyl alcohol was added to another of the Biocide One trials to test whether its presence improved penetration of the biofilm.

Tab. 1 sets out the different biocides, application methods and surface conditions. The complete scheme was applied three times, once each to the north and south walls in 0.5 metre wide panels, and once to the east wall in one metre wide panels. Untreated control panels were left at the end of each wall and were included in the middle of the range of trial panels. Poultices were covered with polyethylene film for five days and then allowed to dry naturally. All the trial panels were kept covered for 14 days to prevent them being affected by rain. The poultices were taken off when the coverings were removed.

Tab. 1: Biocide trials testing scheme.

No	Biocide	Application	Surface condition
1	Biocide One	brush	dry
2	Biocide One	brush	single pre-wet
3	Biocide One	brush	double pre-wet
4	Biocide One	Cocoon poultice	double pre-wet
5	Biocide One	Cocoon poultice	single pre-wet
6	Biocide One	Cocoon poultice	dry
7	Control	—	—
8	Biocide Two	brush	dry
9	Biocide Two	brush	single pre-wet
10	Biocide Two	brush	double pre-wet
11	Biocide One + 10% Ethylene Glycol	brush	double pre-wet
12	Biocide One + 10% Isopropyl Alcohol	brush	double pre-wet
13	Biocide One	brush	double pre-wet

8. Monitoring and recording of trials

The trials have now been monitored and reviewed for 2.5 years (30 months). Observations made at approximately six-monthly intervals have included visual inspections and digital photography. A field microscope has been used to assess whether there has been any regrowth.

9. Complicating factors

A range of factors have influenced the appearance of the trial panels and complicate assessment of the results. These include:

- orientation of the trial panels, which face north, west and south, leading to different micro-environmental conditions for the biological growths, and different photographic recording conditions, both making comparison between walls difficult;
- the influence of mortar joints — alkaline mortars have had a biocidal effect which extends some distance from the joints (Fig. 2);
- run-off from the uncleaned horizontal tops of the parapet which intensifies growths in some locations, and may be contributing to regrowth;
- previous cleaning — now visible as diffuse horizontal bands from high-pressure washing (Fig. 2);

- other treatments — which have left various marks on the stone surfaces, some of which have become apparent only after the cleaning trials have removed much of the biofilm;
- location of trial panels too close the walls of the main building — which has resulted in less-effective cleaning due to additional water run-off and splash from the wall surfaces;
- untreated control panels have continued to accumulate biological growths, increasing the contrast between treated and untreated panels, and so complicating assessment of the degree of cleaning achieved (Fig. 3).

10.Results

Bearing in mind the complicating factors, the following results have been found:

- both biocides were effective in controlling the biofilm, with little discernible difference between the two, and little or no loss of surface from the sandstone;
- separate additions of ethylene glycol and isopropyl alcohol to one of the biocides show no discernible differences;
- pre-wetting in this instance does not seem to have increased the efficacy of the biocides;
- the cleaning effect of the treatments continued to improve for at least eleven months after treatment, and is retained at 23 months;
- poultice applications left a residue which washed off most areas within one year, though some residue can still be seen with a field microscope after two years;
- untreated control panels have continued to accumulate biological growths.

11.Discussion

Following completion of the biocide applications, all treatments were left untouched so that any residual effects and changes over time would become apparent. As observed by Charola *et al.* (2012), the cleaning effect continued to improve for at least eleven months after treatment. Fig. 3 shows a sequence of images, which demonstrate improvement in panels treated by both poultice and brush applications until 11 months.

Also apparent in Fig. 3 is a white residue from the paper poultice, which is still visible after eleven months, but is almost gone at 23 months. Such a residue would not be acceptable in a full scale cleaning project, and so further trials should test different clean-up procedures and their timing.

The results of the different application methods were mixed, with some panels showing little difference between brush and poultice application (see Fig. 3), others suggesting benefits from poultices. A closer review of these results at 30 months showed that regrowth was concentrated where the horizontal surface of the parapets above the treated panels had not been cleaned, thus providing a source of further micro-organisms. Trial panels which had no microbiological growth in the catchment area above remained clean to a visual inspection after 30 months. This is an aspect that will be monitored during future inspections.

Pre-wetting was done with a hand-pumped sprayer which may not have delivered sufficient water to adequately ‘wet’ the biofilm in what can be a hot and windy environment. In future, multiple applications should be trialled.

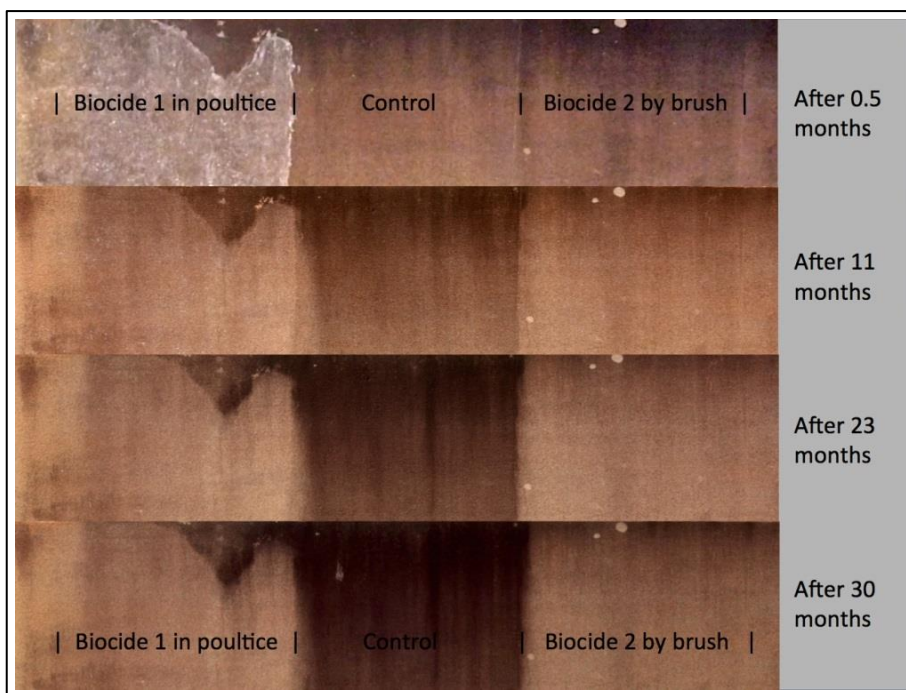


Fig. 3 Sequence of images taken 0.5, 11, 23 and 30 months after treatment, of a section of north-facing wall. The cleaning effect of the two treatments shown is similar, both improving until at least eleven months. Note the white residue from the paper poultice at left, which washes off with time; and the intensification of the dark biofilm in the untreated control panel.

12. Conclusions

The trials confirm that in these conditions:

- Effective biological control is attainable using biocides without scrubbing;
- There was no loss of surface material from the sandstone, unlike previous cleaning programmes;
- Biocide application must begin at the top of the building, or rain catchment surface, in order to prevent spores washing down and starting new growths;
- Effectiveness of the different methods of application were obscured by regrowth from the wash-down.

- Pre-wetting did not appear to improve the outcome in the particular circumstances of the trials.

The existing trials should continue to be monitored until the cleaning effect of the biocides declines. Future trials should:

- Ensure that trial panels are cleaned to the full height of their catchments;
- Test pre-wetting with greater quantities of water;
- Test methods of ‘opening-up’ the biofilm (e.g. light brushing with a stiff nylon bristled brush) prior to the main biocide application;
- Test a range of clean-up procedures and their timing for poultice applications.

Acknowledgements

Dr Alan Archer FRSC, Honorary Research Associate, National Herbarium of NSW, who investigated the biofilms. Niall Macken, Head of Heritage, Sydney Harbour Foreshore Authority, who sponsored the trials and their ongoing monitoring. NSW Public Works Centennial Stone Program, which funded the initial development of the biocide testing scheme.

References

- Caneva, G., Nugari, M.P. and Salvadori, O., (eds.) 2008, *Plant biology for cultural heritage: biodeterioration and conservation*, Getty Conservation Institute, Los Angeles, ISBN 9780892369393, 408pp.
- Charola, A.E., Wachowiak, M., Webb, E.K., Grissom, C.A., Vicenzi, E.P., Chong, W., Szczepanowska, H. and DePriest, P., 2012. Developing a methodology to evaluate the effectiveness of a biocide, in proceedings of the 12th International Congress on Deterioration and Conservation of Stone, Columbia University, New York.
- Franklin, B., 2000, Sydney dimension sandstone: the value of petrography in stone selection and assessing durability, in *Sandstone city: Sydney’s dimension stone and other sandstone geomaterials*, Proceedings of a symposium held on 7th July, 2000, McNally, G.H and Franklin, B.J. (eds) EEHSG Monograph 5, Geological Society of Australia, ISBN 1876315229, 98-116.
- Nugari, M.P. and Salvadori, O., 2003. Biocides and treatment of stone: limitations and future prospects, in *Art, biology and conservation: biodeterioration of works of art*, Koestler, R.J., Koestler, V.H., Charola, A.E. and Nieto-Fernandez, F.E., (eds) The Metropolitan Museum of Art, New York, ISBN 1588391078, 518-535.

DEVELOPMENT OF A METHODOLOGY FOR THE RESTORATION OF STONE SCULPTURES USING MAGNETS

X. Mas-Barberà^{1*}, M.A. Rodríguez¹, L. Pérez² and S. Ruiz²

Abstract

Nowadays, the structural joining of stone fragments of sculptures present, in some cases, reversibility problems. In this work, we present a new system based on the use of magnetic materials which is more reversible than present technologies. This technology is less invasive and, therefore, more respectful to the original artwork. We have used different materials normally used in sculpture (plaster gypsum, calcarenites from Novelda and marble from Macael). NdFeB magnets have been fixed to the different materials and the joints have been tested by different mechanical methods. From these experiments, a theoretical model based on Classical Mechanics has been proposed, a model that allows the prediction of the best choice of magnets and their optimal location in the piece to be restored. The external magnetic field created by the magnet has been calculated using finite elements simulations to minimize it, avoiding the contamination of the materials by magnetic particles suspended in the atmosphere. A system to separate the joint pieces in a reversible way has also been developed.

Keywords: magnets, fragments, unions, sculpture, magnetism

1. Introduction

Nowadays, the structural assistance in restoration of sculpture and ornaments are made with synthetic adhesives that, in some cases, are reinforced by rods of different materials (Ivorra *et al.*, 2013; Contrafatto and Cosenza, 2014; Raftery and Whelan, 2014), such as fiberglass (Polacek and Jancar, 2008), stainless steel (Rosewitz *et al.*, 2016), and other materials (Mas-Barberà, 2011; Quagliarini *et al.*, 2016). In most cases, when the piece has a complicated position or its weight is high, there is a conflict of interest in which the stability of the artwork is faced with the principle of minimal intervention and reversibility, as inserting rods is usually a fairly invasive work on the original artwork. The use of magnetic materials in this type of intervention could be an interesting alternative pathway, in order to have better reversibility being less invasive.

The use of magnetic materials in Conservation and Restoration is relatively recent. They are used as display system for paper and textile work (Spicer, 2010), as their use is non-

¹ X. Mas-Barberà and M.A. Rodríguez

Conservation and Restoration of Cultural Heritage Department, University Institute of Restoration of Heritage, Polytechnic University of Valencia, Spain
jamasbar@upvnet.upv.es

² L. Pérez and S. Ruiz

Departamento de Física de Materiales, Universidad Complutense de Madrid, Spain

*corresponding author

invasive and reversible. In addition the magnetic force can be controlled, which is essential to avoid distortions and brands. One good example of this application is the use of magnets by the Montreal Museum of Fine in the work of Betty Goodwin (Potje, 1988). Magnetic materials have also been used as a tool in the field of restoration such as sculpture and architecture (Watson, 2011), easel painting and archeology. In particular, they can be used as a straightening system to remove distortions (Bestetti, 2005), to remove cleansing gels in which metallic filler has been incorporated or to locate metallic cores or sediment.

Magnetic materials have also been proposed as a binding system for fragments and reconstructions, although not many works can be found in this direction. Probably, one of the most representative ones is the marble Christ from Andrea Sansovino (Oddy, 1999). The present paper provides a systematic study of these magnetic junctions, proposing a model to design this kind of systems for any artwork to be repaired and, therefore, opening an interesting path in the field of Conservation and Restoration (Rodríguez *et al.*, 2014, 2015).

2. Experimental methodology

2.1. Materials

In this work, we have used two different cylindrical NdFeB magnets supplied by Supermagnete, with 10mm (S-10-05-N) and 15mm (S-15-05-N) in diameter and 5 mm of height, magnetized parallel to the cylinder axis. The magnets were fixed to the different materials using Paraloid B-72 and Araldite epoxy resin.

We have used three different types of stone materials: calcarenite, marble and plaster gypsum. The Calcarenite, also called stone Novelda Bateig and supplied by Bateig Stone (Alicante), is a natural biocalcarene rock type, extracted from the Middle Vinalopó area with a high porosity (between 12.7% and 20.4%) (Fort *et al.*, 2002). The marble, supplied by Gonzalo Esteban Fernandez (Almería), is a white marble, mined in Macael (Almería). It has a total porosity of 2.5% and hardness 3 in the Mohs scale (Bello *et al.*, 1992; Sáez-Pérez and Rodríguez-Gordillo, 2009; Luque *et al.*, 2010). Finally, we have used the plaster gypsum "Alamo 70" supplied by AGM (Valencia), prepared by mold casting using a plaster/water ratio of 1/1.86.

2.2. Characterization of permanent magnets

Although the manufacturer provides us with a data sheet containing information about the magnetic force of the magnets, this force is normally measured between the magnet and a piece of iron. In this work we have used magnet-to-magnet junctions, so we need to characterize the maximum force between pairs of magnets i.e. the maximum force in each magnetic junction between the pieces to restore. We have determined the attraction force of the magnets by tensile experiments using a Lhomargy ADAMEL traction machine DY 30 model with the configuration presented in Fig. 1a. To determine the maximum operating temperature of the magnets we have slightly modified the measurement configuration by adding a thermocouple and a heating device, thus allowing for adjusting the temperature between 25°C and 140°C.

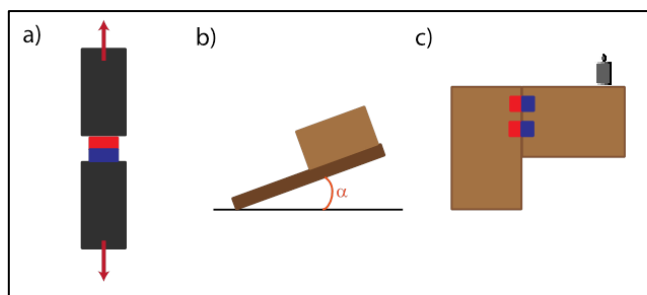


Fig. 1: Schematics of the different experimental set-ups: a) tensile experiment; b) determination of the static friction coefficient; c) static experiment.

We have also study the reversibility of the junction by measuring the minimum temperature necessary to separate it. For that, we have covered the different pieces with aluminum foil to protect them and homogenize the temperature and, afterwards, applied heating with a resistive belt. The internal (close to the magnets) and outside (on the edge of the piece) temperatures were monitored with thermocouples.

2.3. Measurement of static friction coefficients

The friction coefficient is a key parameter to understand the static behavior of materials. In general, it is tabulated for a wide range of materials. However, the different stone materials are generally included within a group called “stone”, without making differences among them. We have considered necessary to carry out experimental measurements of the friction coefficient for the three groups of stone materials under study. For this purpose, we placed together two pieces of the same material, tilting the pieces until the upper test piece slid on the lower piece (see Fig. 1b). The friction coefficient can be calculated as $\mu = \tan(\alpha)$, being α the angle at which the sliding begins.

2.4. Static studies

Before making a junction, it is compulsory to develop a model to predict the configuration of magnets required to make a connection between fragments. To establish the model, we performed various tests on model specimens. Different model configurations were selected, combining a rectangular block (10×10×15 cm) with two different suspended blocks (rectangular and truncated) of similar weight and dimensions (see Fig. 1c). The tests were performed using two magnets placed 3 cm from the top and 2 cm from each side of the rectangular block.

To perform the tests, we have been placed normalized weights on the suspended block, varying the distance between the test weights and the union, thus increasing the total mass supported by the junction as well as the distance from the center of mass of the assembly to the pivot axis. This is equivalent to add longer pieces to the junction, validating the joining for different geometries.

2.5. Magnetic field simulation

Considering that we are adding magnets to a sculpture, it is essential to guarantee that the magnetic field outside the artwork is low enough to prevent contamination by magnetic particles, which would lead to an aesthetic problem. For that, we have used a Finite

Element Calculation using Comsol Multiphysics software. Considering the stone is not ferromagnetic, the relative permeability of the stone materials could be approximated by the one of the air. The magnetic parameters to introduce in the input of the program have been extracted from the data-sheet of the magnets as well as from their characterization as described in section 2.2.

3. Results

3.1. Characterization of permanent magnets

The maximum value of strength obtained with the traction machine corresponds to the maximum force of attraction between the magnets before they separate. The mean value of this force is 33.6 ± 1.0 N for magnets 10 mm diameter and 5 mm in height, which is 43% greater than the data provided in the data sheet. For the rest of the magnets, we have obtained values similar or even higher than those of the date sheet. Therefore, we can use the values provided by the manufacturer in calculations and models because they guarantee enough strength to hold the fragments, providing a margin of safety.

To study the maximum working temperature, we have performed the same tensile tests in the traction machine, after heating the magnets in-situ at different temperatures. For heating treatments below 80°C, the magnets fully recover their magnetic properties when cooled. However, when the temperature increases above 100°C, magnets begin to lose their magnetic properties permanently. For example, after a treatment at 140°C, the maximum force is reduced by 52%. Therefore, we can consider that 80°C is the safety temperature for NdFeB magnets. This temperature is more than enough for applications in sculpture restoration in both outdoor and indoor environments.

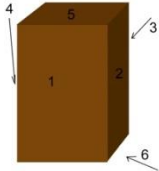
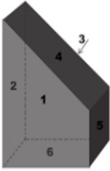
One of the most important features of the magnetic joints is the possibility of separating the pieces in a reversible way. In order to separate the magnetic junction making minimal mechanical force without damaging the original work, we apply heating while separating the pieces. We have already proved that, if the heating is below 80°C, the magnetic force is reduced without degrading the magnets.

Test specimen of plaster with magnets S-10-05-N and test specimen of marble with magnets S-15-05-N were heated. The temperature required to separate the pieces is, in all cases, close to 63°C outside the pieces. The temperature in the magnets is approximately 12°C lower. Once the pieces are cooled down, and therefore, the magnetic force is recovered, we repeated the tests. We observed that, after the third heating cycle, some loss of clamping force is appreciated. It is therefore recommended not recycle magnets more than twice after removing the junction. It should be noted that the stone material is unaffected by the heating. Therefore, this magnetic joint system is reversible and does not damage the artwork.

3.2. Measurement and calculation of static friction coefficients

Tab. 1 shows the value of the static friction coefficient measured in different faces of the studied materials. There is a clear dispersion between the different measurements, due to the fact that the friction coefficient depends greatly on the state of the surface. It is important to note this dispersion when defining the required values of strength in the union to use always a range of values of μ in the calculations that ensure a reasonable margin of safety.

Tab. 1: Friction coefficients measured in the different faces of the materials used in this work.

Block type	Material	Friction coefficient	Standard deviation
 <p>Block</p>	Calcarenite from Novelda	0.57	0.02
 <p>Truncated Block</p>	Plaster-gypsum	0.86	0.03
	Marble from Macael	0.78	0.04

3.3. Static studies

The static studies helps to model the behavior of the system and predict the best configuration of magnets to ensure a safe and reversible joining between the different pieces to restore in a sculpture. Fig. 2a shows a static study carried out in a joint made with Plaster-Gypsum. The test was repeated 5 times to ensure reproducibility.

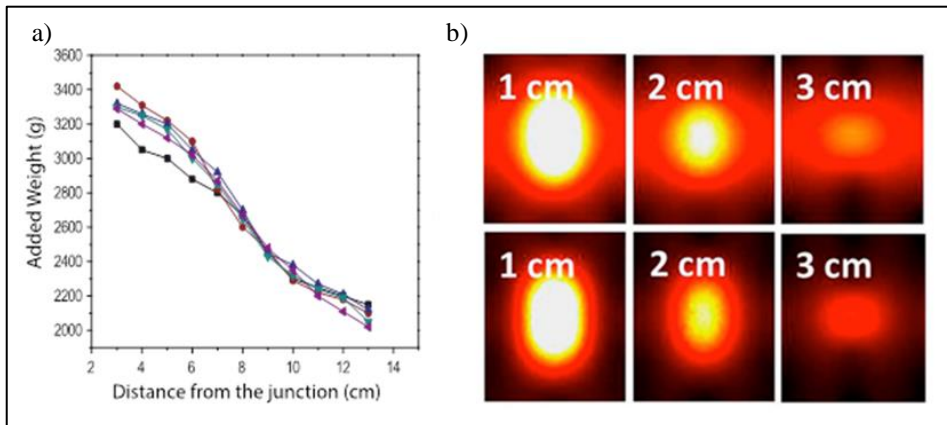


Fig. 2: a) Static study carried out in Plaster-Gypsum model probes; b) Simulated magnetic field at distances from the magnets for parallel (up) and antiparallel (down) magnet configurations.

Two interesting results can be extracted. First, there is a maximum weight supported by the union, which coincides with extra weight place in the closest position related to the

junction. Therefore, when the center of mass of the piece to be joined is close to the junction, the weight of the piece is the only parameter to consider developing a safe junction. Second, when the extra weight is placed far from the junction the weight supported is considerably lower. This configuration is equivalent to have longer suspended pieces in which the center of mass is more separated from the junction. In this case, it is also extremely important to consider the equilibrium of momenta.

3.4. Magnetic field simulation

By using Finite Element Simulations, we have calculated the magnetic field created by magnets placed in parallel and in antiparallel configurations. From the simulations, it is noted that the field in the antiparallel configuration attenuates much faster with distance (Fig. 2b). Considering that both configurations produce the same clamping force, the antiparallel configuration is more interesting for these applications because produces a smaller external field and therefore it reduces the potential for environmental contamination.

4. Theoretical model

We have developed a theoretical model that collects all the above exposes results. This model is based on the considerations of Statics, using the equilibrium of forces and momenta using the scheme shown in Fig. 3.

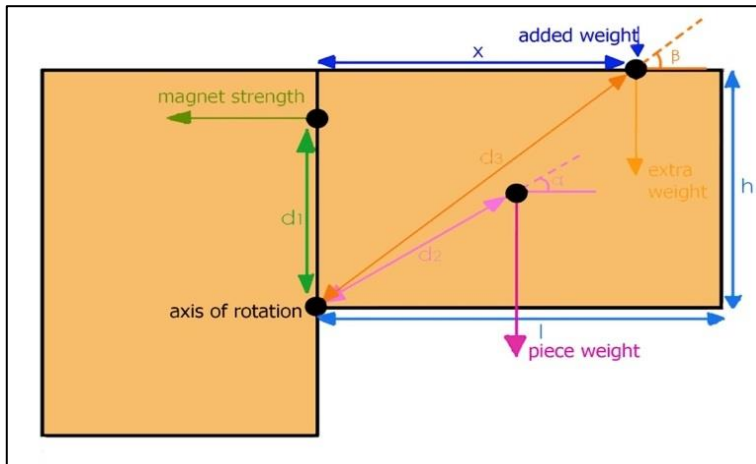


Fig. 3: Schematics of the model used to develop the theoretical calculations.

We start considering the balance of forces. The weight of the piece and the added weight are counteracted by the friction force:

$$\rightarrow \text{Piece weight} + \text{Added weight} = \text{Friction force} = \mu \text{ Magnet strength.}$$

In addition, the equilibrium of momenta should be also considered:

$$\rightarrow \text{Magnet strength } d_1 - \text{piece weight } l/2 = \text{Added weight } x.$$

This behavior corresponds to the hyperbolic behavior observed in the static tests.

5. Conclusions

To conclude, we have developed a reversible system based on magnets for restoration of stone sculpture. This model can be satisfactorily applied to real artwork. A theoretical model based on Classical Mechanics allows choosing the magnets and calculating their position to ensure a safety union. Simulations, carried out using a finite elements model, allow selecting a configuration that minimizes the magnetic field outside the artwork. We have also proved that the system is reversible under the application of moderate heating.

Acknowledgment

This work has been partially supported by Spanish Ministry of Economy and Competitiveness under grant HAR2011-29538.

References

- Bello, M. A., Martín, L. and Martín, A., 1992, Identificación microquímica de mármol blanco de Macael en varios monumentos españoles / Microchemical identification of Macael white marble in some Spanish monuments in *Materiales de construcción*, Vol. 42, n.º 225, 23-30.
- Bestetti, R., 2005, Ristrutturazione e trattamento delle lacune il caso del dipinto giardini romani di Giacomo Balla of the ICC Congreso Nazionale IGIIC lo stato dell'arte, Palermo, 336-343.
- Contrafatto, L. and Cosenza, R., 2014, Behaviour of post-installed adhesive anchors in natural Stone in *Construction and Building Materials* 68, 355–369.
- Fort, R., Bernabéu, A., García del Cura, M.A., López de Azcona, M. C., Ordóñez, S. and Mingarro, F., 2002, La Piedra de Novelda: una roca muy utilizada en el patrimonio arquitectónico / Novelda Stone: widely used within the Spanish architectural heritage in *Materiales de construcción*. Vol. 52. n.º 66, 19-32.
- Ivorra, S., García-Barba, J., Mateo, M., Pérez-Carramiñana, C. and Maciá, A., 2013, Partial collapse of a ventilated stone façade: Diagnosis and analysis of the anchorage system in *Engineering Failure Analysis* 31, 290–301.
- Luque, A., Cultrone, G., Mosch, S., Siegesmund, S., Sebastian, E. and Leiss, B., 2010, Anisotropic behaviour of White Macael marble used in the Alhambra of Granada (Spain). The role of thermohydric expansion in stone durability in *Engineering Geology* 115, 209–216.
- Mas-Barberà, X., (2011), *Conservación y restauración de materiales pétreos: diagnóstico y tratamientos*. Valencia, UPV. ISBN 978-8483635834, 190 pp.
- Oddy, A., and Carroll, S., (1999), *Reversibility – does it exist?* (British Museum Occasional Papers), London, British Museum Press, ISBN 978-0861591350, 179 pp.
- Polacek, P., Jancar, J., 2008, Effect of filler content on the adhesion strength between UD fiber reinforced and particulate filled composites in *Composites Science and Technology* 68, 251–259.

- Potje, K., 1988, A Traveling Exhibition of Oversized Drawings Montreal in The Book and Paper Group Annual. Volume seven (on line) <http://cool.conservation-us.org/coolaic/sg/bpg/annual/v07/bp07-09.html> consultation date 01/04/2016.
- Quagliarini, E., Monni, F., Bondioli, F. and Lenci, S., 2016, Basalt fiber ropes and rods: Durability tests for their use in building engineering in the Journal of Building Engineering 5, 142–150.
- Raftery, G.M. and Whenlan, C., 2014, Low-grade glued laminated timber beams reinforced using improved arrangements of bonded-in GFRP rods in Construction and Building Materials 52, 209–220.
- Rodríguez M.A., Mas-Barberà. X. and Pérez L., 2014, Optimización de sistemas magnéticos en la restauración de esculturas y elementos ornamentales of the XIII Congreso Nacional de Materiales, J. M. Guilemany (ed.), Barcelona, Sociemat, 75.
- Rodríguez, M.A., Mas-Barberà. X. and Pérez, L., 2014, Estudio para optimizar las uniones de fragmentos en escultura y ornamentos mediante sistemas magnéticos of the Jornadas Emerge 2014: Jornadas de Investigación Emergente en Conservación y Restauración de Patrimonio, M. V. Vivancos, M. T. Domenech, M. Sánchez and M. J. Osca (eds.), Valencia, UPV and IRP, 471-477.
- Rodríguez, M.A., Mas-Barberà. X., Pérez, L. and Ruiz-Gómez, S., 2015, Estudio de sistemas magnéticos a base de imanes para uniones de fragmentos y prótesis a la obra original escultórica of the La Ciencia y el Arte V. Ciencias y tecnologías aplicadas a la conservación del patrimonio, consejo editorial IPCE (eds.), Madrid, IPCE and Museo Centro de Arte Reina Sofía, 121-135.
- Rosewitz, J., Muir, C., Riccardelli, C., Rahbar, N. and Wheeler, G., 2016, A multimodal study of pinning selection for restoration of a historic statue in the Materials and Design 98, 294–304.
- Sáez-Pérez, M. P. and Rodríguez-Gordillo, J., 2009, Structural and compositional anisotropy in Macael marble (Spain) by ultrasonic, x-rd XRD and optical microscopy methods in Construction and Building Materials 23, 2121–2126.
- Spicer, G., 2010, Defying gravity with magnetism, in AIC News, volume 35, N° 6, 1-5
- Watson Adsit, K., 2011, An Attractive Alternative: The Use of Magnets to Conserve Homer by John Chamberlain in WAAC Newsletter. Volume 33. N° 2, 16-21.

THE ROCK RELIEFS “*STEINERNE ALBUM*” OF GROßJENA, GERMANY – PROBLEMS OF DETERIORATION AND APPROACHES FOR A LASTING PRESERVATION

J. Meinhardt^{1*}, T. Arnold² and K. Böhm²

Abstract

The baroque stone album consists of 12 reliefs of biblical motifs concerning viniculture, carved out of the bedrock. In their entirety these are the biggest stones reliefs of the European cultural area. The outcrop represents different varieties of Triassic sandstone. As a result of harmful environmental influences, especially during the GDR past, massive damage processes - caused by sulphur oxide emissions - began on the reliefs. The seriously affected stone album was restored between 1997-1999. After the restoration, a monitoring and care concept was established. Soon after restoration, strong sanding and flaking in combination with massive efflorescences were observed on some of the reliefs. The deterioration proceeds quite quickly, probably also because of unsuitable care measures. The monitoring care concept that has been agreed upon needs to be reviewed. Using wireless, minimally invasive sensors, the actual reservoir of soluble components in the depth profile and their migration depending on moisture penetration in the bedrock and the climate are currently being monitored. First data reflect significant fluctuations of humidity and impedance. On several sample areas different poultices for salt reduction measures were applied. The permanent covering of the endangered reliefs using poultices has been assessed as particularly promising. Initial results regarding the efficiency of the different materials are presented in the paper. A great challenge in this context is the forming of the poultices, considering the value of the monument.

Keywords: KSE, bedrock, salt reduction, poultices, monitoring and care concept

1. Introduction

The rock carvings of the “*Steinerne Album*” (Stone Album) are situated in central Germany, near Naumburg. It is about 25 km southwest of a major chemical site during the GDR past (Leuna, Buna and Bitterfeld). Due to the unprotected exposure, the carvings were contaminated with pollutants with an anthropogenic origin (sulphur oxide emissions). This contamination still has an impact today. During the restoration in the 1990s, no salt reduction measures were carried out. There were concerns that the theoretically constant supply of salts makes the reduction at the surface useless. On some stone reliefs the

¹ J. Meinhardt*

Institute for Diagnosis and Conservation of Monuments in Saxony and Saxony-Anhalt,
Halle/Saale, Germany
meinhardt@idk-denkmal.de

² T. Arnold and K. Böhm

State Office for Heritage Management and Archaeology Saxony-Anhalt, Halle/Saale, Germany

*corresponding author

weathering proceeds very quickly. Most likely, this is to be seen in the context of the salt content in the region near the surface and the direct connection to the bedrock. Despite periodic monitoring and care measures, the weathering progress cannot be slowed down significantly. Therefore the care concept needs to be modified, especially with regard to salt reduction measures.

The aim of the project is to find an appropriate approach for dealing with cultural heritage objects integrated in masonry (e.g. epitaphs) or directly connected to the bedrock, where the supply of moisture and salt is difficult to control. These objects are permanently exposed to these damage stimulating factors from their surroundings. The intention is to identify suitable compositions of salt storage mortars from the projects sample areas which have the potential of a long-term care measures. An important requirement of these mortars is their durability and their visual appeal. If the concept is successful, the outcomes of the current research project will be suitable for numerous other comparable objects.

2. The “Steinerne Album” of Großjena

2.1. History

In 1777, on the occasion of the 10th anniversary of the regency of Duke Christian, his court jeweler Johann Christian Steinauer had the Steinerne Album built on his vineyard by different stonemasons. The baroque stone album consists of 12 reliefs of biblical motifs concerning viniculture, carved out of the bedrock. The figures are partly larger than life size. In their entirety, these are the biggest stones reliefs of the European cultural area (see Fig. 1). Over time, the Steinerne Album fell slowly into oblivion and was only known among experts. More or less in the 1990s, the Stone Album was rediscovered and returned to the public awareness.



Fig. 1: Section of the Stone Album, located at the foot of the vineyard.

2.2. Geological conditions

The outcrop of the album represents three different varieties of Triassic sandstone - red and grey fine-grained and yellowish coarse-grained material. The reliefs represent the transition between Hardegsen- and Solling-Formation (Chirotheriensandstein) of the Middle Buntsandstein (Siedel 1998). The sandstone is clayey-siliceous bound with fluctuating decay stability. Hardegsen-Formation is clayey to poor siliceous and at the base also carbonatic bound (Rey 1975). Cement of the Chirotheriensandstone is also clayey to poor siliceous (Rey 1975). In some places lenses of clay occur. Clay-rich areas are accompanied by a worse weathering resistance of the material. Furthermore, an outflow of water (stratum water) can be observed in some parts of the outcrop.

The stone reliefs are situated close to the lower parts of the river Unstrut, about 10 to 12 metres above the river level. In the 1990s examinations regarding the origin of the salts in the Stone Album were carried out. Nearby, in the lower Unstrut valley, Permian salt springs are described where prehistoric salt-mining was carried out (Clasen & Sommerwerk 2003). In Großjena, the village in which the Steinerne Album is situated, hydrogeological investigations led to the conclusion that modern dewatering measures disrupted former saline-discharge in this area (Clasen & Sommerwerk 2003) thus, this salt spring discharge could have theoretically led to a contamination of parts of the stone reliefs. But isotope investigations had shown clearly that the sulphates stem from an urban environment and cannot be assigned to any Triassic rock formation (Siedel & Klemm 2001).

For several years now, the vineyard has been used as it was originally intended. In this context fertilisers have been applied which probably endanger the historic substance additionally.

2.3. Previous restorative and conservation measures

As a consequence of harmful environmental impacts, especially during the GDR past, massive damage processes caused by sulphur oxide emissions began. In the sulphuric acid environment, the dolomitic cement was transformed to the destructive salt Magnesium sulphate. Even though the stone reliefs are situated in a rural area, the proximity to one of the most popular chemical sites during the GDR past (Leuna, Buna and Bitterfeld) led to a massive contamination of the monuments in Central Germany by dry and wet deposition.

The strongly affected rock carvings were restored between 1997 and 1999 as a part of a project founded by the German Environmental Foundation (DBU) (Meinhardt 2013, 2015). The emphasis was placed on the conservation and protection of the historic substance. The 12 stone reliefs were strengthened using KSE almost entirely. In order to avoid an over-strengthening of the surface, the infusion method was applied in most areas. Using specially developed stone replacement mortars, the protection of detached parts was subsequently carried out. Furthermore, a plaster with high salt storage capacity was applied. This plaster acts as a storage container for the salts. When any moisture diffuses out through the render, it leaves the salts that were dissolved in it behind.

In the period between years 2008-2010, the Stone Album was part of the nationwide research project founded by the DBU: Stone monuments under the influence of anthropogenic environmental impacts - Development of methods and criteria for the long-term control of weathering and conservation. In this context the condition of the stone reliefs and in particular the durability of the applied conservation and restorative measures

were checked using a standardised methodology of natural stone monitoring (Auras *et al.* 2010).

At the time of these investigations, particularly in the lower parts of the endangered reliefs, strong sanding in combination with a massive salt load and flaking could be observed. In these areas mortar applications are often delaminated. Furthermore, efflorescences were covering areas with salt storage mortar, an indication of the depletion of the available pore space.

2.4. Monitoring and care concept

A monitoring and care concept was established right after restoration. The care concept comprises containing the adjoining vegetation, dry cleaning (brush) of the stone surfaces, removing efflorescences (brush), control and repair of the mortar applications using a stone replacement mortar (soft) on a pure mineral base (Remmers® Restoration Mortar), visual and haptic control of the surface strength and, if necessary, re-strengthening by using solvent-free stone strengthener on a silicic acid ethyl ester base (gel deposit rate: approx. 30 %) (Remmers®). Furthermore colour retouching was carried out in some parts (pigments dissolved in water). The same restorer who was already responsibly involved in the restoration carries out the monitoring and care measures every year. Because of the small amount of available money, only two or three stone reliefs can be inspected in closer detail each year.

Despite the improvement of the environmental conditions the stone reliefs are still permanently exposed to the environment due to their prominent position on the weather side of the vineyard and because of moisture transport in the slope.

2.5. Current state of damage

Regarding sustainability, some of the stone reliefs should be critically evaluated. Partly, the surfaces are overstrengthened. There is a thin crust, more like a skin, with burst pustules and flaking can be observed. The cohesion of the crust with the stone substrate is weak. The stone under this crust is weathered.

The status of the stone reliefs “Duke Christian” and “Marriage in Cana” is of particular concern. An explanation could be that the more endangered reliefs are in a completely vertical position and sheltered to some extent by a small overhang (see Fig. 2, left).



Fig. 2: Vertical relief “Duke Christian” (left) in comparison to inclined areas (right).

This could be associated with the fact that they stay dry longer during light showers. Thus, the salts cannot be reduced as in the case of reliefs with slight inclination (backwards) (see Fig. 2, right), which are obviously not in much danger. In both situations (vertical and inclined) the salts are already activated by a high relative humidity. But the reliefs in vertical position do not benefit from salt leaching as often as the inclined parts. Only in the case of a strong rain shower will they get completely wet. A further problem, especially in the context of recognisability, is the biological growth. The interested visitors are not allowed to get close to the Stone Album, it being located in a private section. The distance between the path and the reliefs is about 40-50 metres. Additionally to the different colours of the stone varieties, an intensive biological growth hinders the perceptibility significantly.

3. New approach to long term preservation

3.1. Modification of the care concept

During the comprehensive restoration in the 1990s no salt reduction measures were carried out. The main reason for the decision made at that time was the postulated ongoing transport of soluble components from the bedrock. Now, experience in the field of salt reduction measures on natural stone is so advanced that a renewed conservation approach on the basis of different salt reduction cycles is promising. Monitoring of the water transport and the salt content near the surfaces depending on environmental conditions was regarded as useful. Therefore sensors, working on the basis of electrical impedance measurements, were installed in one of the endangered stone reliefs. On the basis of the information about the real reservoir of soluble components and their transport - depending on moisture penetration in the bedrock and on the climate (precipitation) - a salt reduction concept can be established. In this context sample areas with different long-term poultices were prepared. The aim is to slow down the weathering process and to increase the sustainability of the conservation. Furthermore, the figures should become more easily recognised.

3.2. Electrical impedance measurement

In order to choose appropriate care measures for the stone reliefs and for a proper estimation of the effectiveness of the salt reduction measures, the salt content along the depth profile and the development of humidity in dependence on environmental conditions should be determined. To monitor the water transport and the accumulation of salts in historic structures continuously, a wireless impedance measurement system was developed by the MPA at the University of Stuttgart and TTI GmbH - TGU Smartmote (Krüger and Lehmann 2011). The electrical impedance of a porous material is influenced by both its moisture content and its salt concentration. High levels of moisture and high amounts of salt correspond to low impedances and vice versa. As both factors influence the impedance in a similar way, it may not be possible in situ to distinguish which parameter has changed. However, by observing the impedance over time continuously, it is possible to draw conclusions about the moisture source and, more importantly, the accumulation of salts (Krüger and Lehmann 2011). For the determination of the salt and water content, a representative area within a stone relief which is particularly endangered was chosen for the measurement. Because of recurring efflorescences or salt crystallisation, the surface of the relief is at risk. The devices were installed in a deteriorated and an un-deteriorated area in comparison directly next to each other. For the permanent investigations, two sets of six holes, each having a diameter of 6 mm, were drilled in each of the two areas (see Fig. 3)

with the aim of determining moisture and salt content at different depths. The available measuring devices unfortunately allow only data recording up to 10 cm. Furthermore, drill powder was taken for moisture and chemical analysis in depth profiles > 10 cm towards the interior. These results represent the starting point of data recording and they are helpful for a proper interpretation of the electrical impedance. These measurements strongly depend on temperature. Therefore it is logged additionally at all three depths. The measured values and climatic parameters can be collected remotely. Initially, measurements will be carried out on an annual cycle. First results, after four months, are shown in section 4 of this paper.

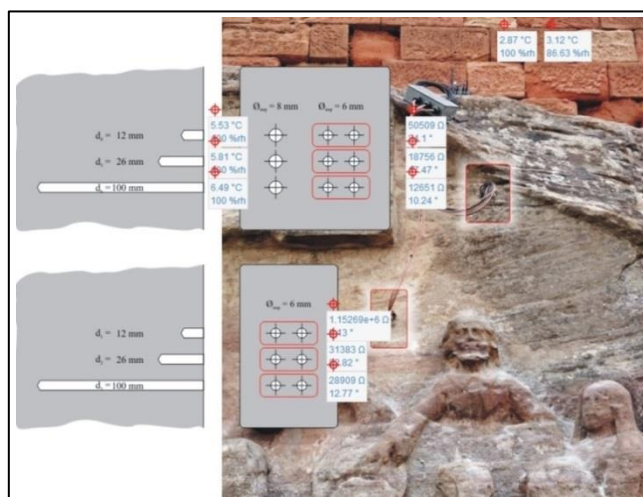


Fig. 3: Position of the boreholes for determining moisture, temperature and impedance (boreholes 1-3 below, left of the head and 4-6 above). Depth indicates the position of the sensors (graphic design by F. Lehmann, MPA Stuttgart).

3.3. Application of different long-term poultices

On the stone relief “Joshua and Kaleb”, in the inscription field in the lower part, where significant damage was already observed, sample areas with different poultice materials were applied (spray gun, multilayer) (see fig. 4, right). Previously, in adjacent areas without rock carvings the salt and moisture content along several depth profiles was determined. In order to get information about the general ability for fluid absorption, capillary water absorption tests were also carried out on the sample areas (w-values 0.8 - 1.8 kg/m²√h). Of course, a special focus is on the effectiveness regarding salt reduction. But furthermore the poultice application is also intended as a protective layer on the endangered surface and to enhance the recognisability of the reliefs (see Fig. 4, left) especially by an optical harmonisation of the different colours of the weathered surfaces (stone varieties, biological growth, replacement mortars).

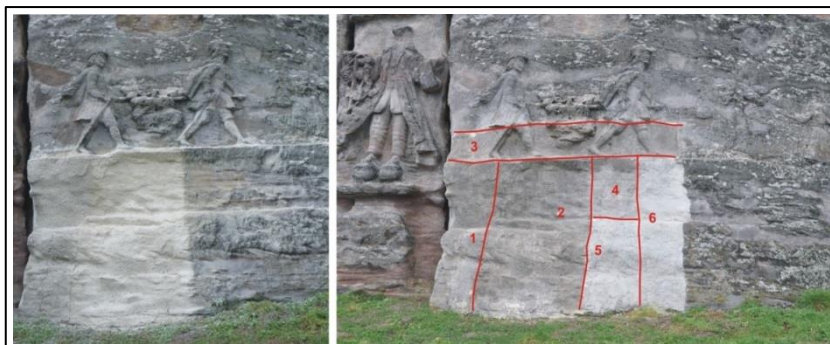


Fig. 4: Relief “Joshua and Kaleb” where different sample areas (right) were applied in the lower part. Recognisability is obviously enhanced by the poultices (left). Details of the relief underneath can be seen clearly.

By combination of protection (relocation of the reaction front out of the stone), permanent measures (salt reduction) and optimisation of the presentation, a promising long-term care concept can be achieved. By means of the different sample areas these parameters and the subsequent handling with the stone surface should be studied. The following poultice formulations were applied either using a funnel gun (8 mm) or with a trowel. Application with the funnel gun led to a smoother surface and therefore a better distinctness of the underlying relief. Whether the cohesion between poultice and stone surface is better than with trowel application will be derived from the results after the long-term exposition of the different poultices. By using a trowel, greater thickness of the material can be achieved.

- 1.) FEAD-poultice after FEAD GmbH Berlin: 1P (parts, weight) Bentonite; 4P fire-dried quartz sand 0-2 mm; 10P fire-dried quartz sand 0.1-0.5 mm; 2P quartz powder QM 1600 and 6P Arbocel®PWC500
- 2.) 0.5P Bentonite, 4P fire-dried quartz sand 0.1-0.5 mm, 2P Arbocel®PWC500
- 3.) 2P Kaolin, 1P fire-dried quartz sand 0-2 mm
- 4.) 2P sand 0-2 mm, 1,5P fire-dried quartz sand 0-0.7 mm, 0.3P Sepiolithe (after C. Pieper)
- 5.) 0.5P sand 0-2 mm, 1P fire-dried quartz sand 0-0.7 mm, 1P Poraver®foam glass 0.25 – 0.5 mm, 1,25P Poraver®foam glass 0.5-1 mm, 3P Arbocel® PWC500, 0.5P bentonite and 1P binder (slaked lime and NHL 5) (after lab E. Wendler)
- 6.) Remmers® desalination poultice Art.1070.

To ensure better sustainability of the poultices, all formulations are combined with slaked lime, except recipes 4 and 6. A covering slurry containing 2.5P fire-dried quartz sand 0-0.7 mm, 0.5P kaolin, 1P Otterbeiner® lime (NHL 5), 1P fire-dried quartz sand 0-2 mm and 1P slaked lime + methylcellulose was applied on sample areas 1-3 using a funnel gun (8 mm). Finally, Remmers®Silicone Resin paint LA, transparent (diluted with distilled water) was applied on all sample areas for a better weathering resistance and a colour adjustment.

4. First results

4.1. Poutlices

At the moment, a final statement regarding the effectiveness of the different poultice-mortars cannot be given. The samples should remain on the relief for about 12 months. But for a first orientation initial results were determined four months after application (see Tab. 1). Therefore two samples 10×10 cm were cut off the sample fields of every poultice formulation.

Tab. 1: First results regarding efficiency of the different poultice formulations (two samples per material type) (For all formulations the content of soluble components was determined on control samples. It was <0.12 M.-%).

Poultice (see section 3.3)	Content of soluble components after four months [M.-%]
1	0.16 and < 0.12
2	0.34 and < 0.12
3	0.26 and < 0.12
4	0.18 and < 0.12
5	0.30 and < 0.12
6	< 0.12

Tab. 1 indicates that efficiency of the poultices is different, even within one material type. Up to now in all sample fields, except material 6, a reduction of soluble components from the underground into the poultice can be determined. To get an idea of the real contamination in the adjacent areas of the sample fields, two depth profiles taking drill powder were set up. At a depth of 0-1 cm contents between 1.9-2.5 M.-% were detected. Between 1-2 cm contents of 0.8-1.4 M.-% were measured. Behind this superficial zone the content of soluble components decreases significantly. Between 2-5 cm 0.5 M.-% were determined. Obviously, a considerable contamination exists in the stone surface which can be reduced by appropriate poultices. Final evaluation of the different poultices should be drawn after one year. A statement regarding the quality of the connection to the stone surface comparing funnel gun and manual application cannot be given after this quite limited exposition time. For an objective conclusion regarding this matter, 12 months should first pass. The assessment of the visual impression showed that the application using the funnel gun led to much better surfaces than the manual application. The finer the components in the poultice, the smoother the surface of the mortar is, and details of the figuration are much more recognisable. Experience shows that in the case of a higher salt content in the object, better salt reduction can be achieved with thicker poultices. Proper relation between the thickness of the poultices and the recognisability of the 3D underground is required.

4.2. Electrical impedance measurement

After four months, first results of data recording can be given. Relative humidity at the different depths is very high during the logged period. A dependency from the ambience is not evident (see Fig. 5). In contrast, temperatures in the different depths follow the outside climate rather directly.

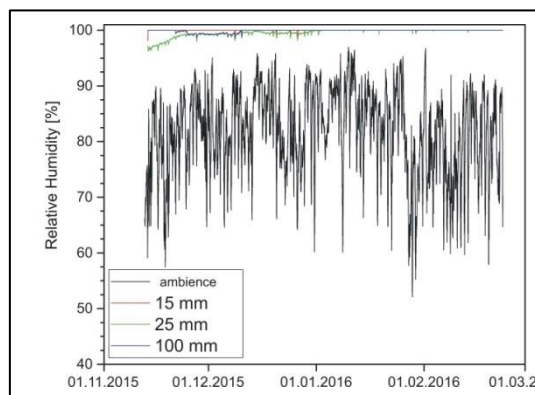


Fig. 5: Relative Humidity in the different bore holes and depths.

Furthermore, logged data reflect significant differences of the impedance in the different bore holes and depths (see fig. 6). In boreholes 1-3 (left) the impedance near the surface is much higher than in 25 and 100 mm. At the second measuring point (boreholes 4-6) the impedance is lower in all three boreholes and the difference between the depths is smaller (right).

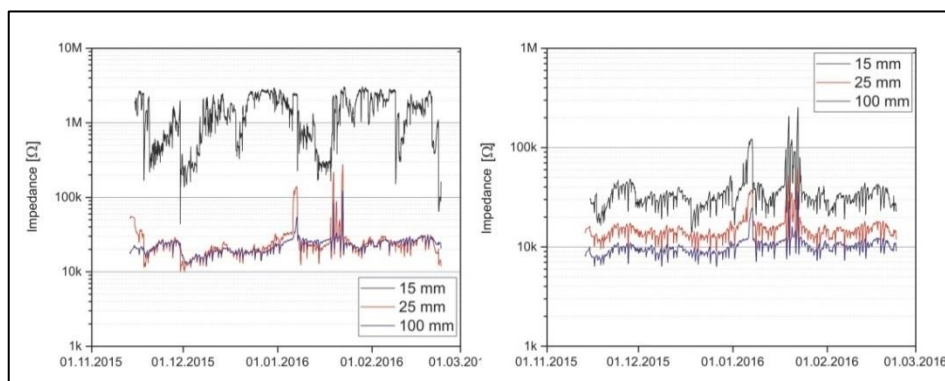


Fig. 6: Measured impedance at 10 kHz in the different boreholes (1-3 left and 4-6 right) and depths.

References

- Auras, M., Meinhardt, J. and Sneath, R., 2010, Leitfaden Naturstein-Monitoring, Nachkontrolle und Wartung als zukunftsweisende Erhaltungsstrategien, Fraunhofer IRB, Stuttgart, Germany.
- Clasen, S. and Sommerwerk, K., 2003, Die (hydro)geologischen Voraussetzungen für die prähistorische Salzgewinnung im Unteren Unstrut-Tal, Jahresbericht für Mitteldeutsche Vorgeschichte, Bd. 86,85-96.
- Krüger, M. and Lehmann, F., 2011, Wireless impedance measurements to monitor moisture and salt migration in natural stone, Proceedings of the European Workshop on Cultural Heritage Preservation, Berlin, September 2011, Fraunhofer IRB.
- Meinhardt, J. 2013, Das Steinerne Album in Großjena – Die Pflege eines barocken Kleinods in der Kulturlandschaft Saale-Unstrut. Denkmalpflege in Sachsen-Anhalt, Heft 1 (2013), ed. Landesamt für Denkmalpflege und Archäologie Sachsen-Anhalt.
- Meinhardt, J. 2015, Sicherung und Erhaltung der Felsreliefs des Steinernen Festbuchs bei Großjena – neue Ansätze der Restaurierung der barocken Sandsteinbilder, Abschlusskolloquium Modelhafte Konservierung der anthropogen umweltgeschädigten Felsenkapellen St. Salvator (Schwäbisch Gmünd), proceedings.
- Rey, S. 1975, Die Natursteinvorkommen im Bezirk Halle und ihre Eignung als Werk- und Dekorationsstein in Vergangenheit und Gegenwart, Dissertation, Martin-Luther-University Halle-Wittenberg: III + 139 pp, Halle (Saale), unpublished.
- Siedel, H. and Klemm, W. 2001, Salzausblühungen auf der Oberfläche von Sandsteindenkmalen und auf anstehenden Sandsteinen in Aufschlüssen – natürliche oder anthropogene Ursachen? Special Edition Geologica Saxonica, Proceedings of the Symposium in honour of Hanns Bruna Geinitz, Abhandlungen des Museums für Mineralogie und Geologie Dresden, Bd. 46/47, 203-208.
- Siedel, H. 1998, Petrographische Untersuchungen an Sandsteinproben vom „Steinernen Festbuch“ Großjena, internal report 10/98 Institute for Diagnosis and Conservation on monuments in Saxony and Saxony-Anhalt.

ETHYL-SILICATE CONSOLIDATION FOR POROUS LIMESTONE COATED WITH OIL PAINT – A COMPARISON OF APPLICATION METHODS

M. Milchin^{1*}, J. Weber², G. Krist², E. Ghaffari² and S. Karacsonyi¹

Abstract

Ethylsilicates (TEOS) are frequently used to consolidate porous limestones usually by full immersion in a consolidation bath or by run-off application *in situ*. For porous limestones with their high level of capillarity these methods are sufficient to achieve reasonable results as long as the surface is uncoated. However, when covered with oil-based paints or similar coatings stone surfaces effectively become impervious, which prevents consolidants from penetrating into the material, so alternative ways of application are required. This paper describes the case of a 19th century sculpture from Vienna, Austria. It was carved out of a porous calcareous arenite and originally painted with oil colour; over time several secondary layers of paint have been added. Some areas of the stone sculpture were in a very bad condition; the goal of the treatment was to consolidate the stone, but to preserve the original polychrome paint layer. Tests were conducted on dummies to achieve optimum penetration of the consolidant through the surface layers by three approaches, namely (1) total immersion, (2) run-off application, and (3) a patented low-pressure impregnation treatment known as VCP (Vacuum-Circling-Process) (Pummer 2007). The test specimens were coated with an oil-based paint prior to their laboratory treatment with TEOS in the mentioned ways. Penetration depth and drilling resistance were assessed and samples for polished thin sections were taken, on which polarizing light and scanning electron microscopy was performed. This latter group of analyses provided significant results in respect to the deposition of the silicate gel after consolidation. Based on the results, the sculpture itself was treated with the VCP-method and the effect was verified. It can be concluded that the VCP application is suitable for the consolidation of stone objects with a surface of inhomogeneous or reduced permeability.

Keywords: consolidation, TEOS, application, porous limestone, vacuum

¹ M. Milchin* and S. Karacsonyi
Institute of Conservation, University of Applied Arts Vienna, Austria
marija.milcin@uni-ak.ac.at

² J. Weber, G. Krist and E. Ghaffari
Section of Conservation Sciences, Institute of Art and Technology, University of Applied Arts
Vienna, Austria

*corresponding author

1. Introduction

For several decades ethylsilicates (TEOS), primarily developed and marketed to strengthen siliceous sandstones, have likewise been used for the consolidation of porous carbonate materials such as soft limestones from the Tertiary Leithakalk formation. These lithotypes play a predominant role for sculptural and architectural stonework in eastern Austria (see e.g. A. Kieslinger 1951, A. Török et al 2004, and A. Rohatsch 2005). TEOS is known to stabilize decohesive grain textures in these limestones and is thus widely used by conservators. However, its efficacy is frequently questioned by materials scientists (see e.g. C.A. Price&E. Doehne 2011 and G. Wheeler 2008); the chemical diversity between carbonate substrate and silicate consolidant is sometimes interpreted as a “chemical incompatibility” between both systems. This fact seems to account for the frequent observation by SEM that silica gel from TEOS treatments of limestones or mortars though precipitated in pores and cracks, show a rather poor contact with the calcitic mineral grains. Based on SEM observations alone, some scientists tend to doubt the ability of TEOS to consolidate limestones in general, notwithstanding the proven physico-mechanical effects of such treatments. Efforts have been made in the recent past to produce modified TEOS specialised for the consolidation of limestones. These specialised products were not part of the present study but have shown some problems on their own and should certainly be looked at more closely in future.

Some of the earlier applications of TEOS on façades in Vienna have caused problems in recent years. Strong delamination parallel to the surface can be observed. However, in most cases such failure is linked to either wrong application methods (e.g. spray or brush), or the application of TEOS on wet stones, or even the use of water (!) as a diluting agent.

In general the use of TEOS for the consolidation of porous Leithakalk limestones proved a good practice as long as the surfaces are permeable and the consolidant is not restricted from entering the structure. A critical situation emerges when porous limestone objects have their surfaces sealed such as when stones are covered with paint layers or coatings. In such situations the substrate is often very porous and in need of a consolidation, the coated surface however prevents the consolidant from penetrating. If the layer sealing the surface is of no historic or artistic value, its removal can be a possible solution, although the risk to damage the stone underneath may necessitate a number of additional measures on beforehand. In case the layer shall be kept e.g. because it represents an original paint, the problem becomes more difficult to handle. This is the case with the object presented in this paper, where a sculpture made out of a highly porous limestone, coated with layers of paint, most of which are oil bound was in great need of a structural consolidation.

2. The sculpture

The object of concern is a life-sized sculpture depicting the Madonna with Child (Fig. 1), carved out of a highly porous calcareous arenite. It is carved from Au Stone - named after the locality of extraction in the Southeast of Vienna – which is one of the softest lithotypes of the Tertiary Leithakalk formation. Formed in coastal areas of the shallow shelves of the Miocene Paratethys, this stone type was extracted from numerous quarries located in Eastern Austria, Southern Moravia and Western Hungary (Török *et al.* 2004). Rohatsch (2005) describes Au Stone as detrital limestone composed of fossil fragments (mainly Corallinaceae) and foraminifera at a grain size of below 2 mm. Feebly cemented by sparitic calcite, the average total porosity of the sound stone is well above 30% by volume, and its

water uptake amounts to about 17% by mass. From the 14th to the late 19th century, Au Stone was probably the most appreciated Leithakalk variety for sculptural stonework in Vienna and surroundings. The sculpture is dated to the middle of the 19th century, and was produced by the Viennese sculptor Joseph Käßman (1784-1856). It was originally painted with a linseed oil based paint containing lead white as pigment, accented with some gilded sections (crown and details of the dress). The sculpture was placed on a façade in the seventh district of Vienna where it remained on site until it was first moved for conservation in 2012; earlier interventions consisted in frequent repainting, according to the fashion of the time. While most of these secondary layers are also oil bound, the most recent ones are based on acrylic emulsion as binding medium.



Fig. 1: The sculpture of a Madonna with Child, 19th Cent., Vienna, by Joseph Käßman

During the recent campaign, the sculpture had to be removed from the façade because of its instability and the danger of losing pieces. When delivered to the atelier, the most exposed parts such as sections from the drapery and the feet were already heavily cracked or broken in many pieces. Initial analyses by light microscopy confirmed the presence of an original paint layer. Drilling resistance showed the poor condition of the stone underneath. It was therefore decided that the sculpture had to be consolidated. Based on the drilling resistance profiles, it was obvious that a deep penetration was essential. To this end, the consolidant had to penetrate through the craquele in the oil paint layer, or find its way through the few lacunae.

3. Methods

In view of the above, it was decided to perform a small laboratory program in order to test different application methods of TEOS consolidant on test specimens that were prepared in a way to imitate the presence of an impervious layer with just a few defects. Cubes of approx. 40×40×40 cm were cut out of a block of a Leithakalk limestone similar, though not identical to the original stone, since that exact type is no longer available. The cubes were coated with a commercial white oil paint. An area of 10×10 cm was left uncoated, simulating the usually unpainted underside. A split line was prepared on 4 sides before the paint layer was applied in order to facilitate the splitting of the cubes after consolidation. After the curing of the paint layer, different types of defects were produced in order to simulate those found on the object. Three drilling resistance profiles before consolidation were measured for all of the cubes on three different faces.

The blocks were then consolidated using different application methods. The test of the run-off method consisted of applying consolidant by means of a wash bottle in a way that it was left to freely flow over the surfaces until no more liquid was absorbed. In addition, the impregnation by total immersion in a bath was tested. With this test, the specimen was placed in the solution in such a way that first the consolidant was absorbed by capillarity before it was fully immersed until no more air bubbles were released. The final method was a patented method known as VCP or Vacuum-Circling-Process (Pummer 2007) and was employed by the patent holder. This procedure, frequently used *in situ*, is based on the airtight packing of the stone element, which is then subject to a regime of under-pressure to which the consolidant is injected. More details are given elsewhere in this volume (Pummer 2016). The TEOS product used in all three cases was Funcosil-300E[®] by Remmers, Germany, a concentrated elastified ethyl silicate with a gel precipitation rate of 300 g/L. For the VCP treatment this consolidant is modified to facilitate the process of hydrolysis.

Immediately after the application of the consolidant, the cubes were separated along a predetermined split line. The penetration depth was measured and photographically documented. Afterwards the fragments were reassembled to cubes using force loops and a tape, in order to re-establish as far as possible the initial conditions. After a period of 6 weeks, a time span commonly considered sufficient for the hydrolysis of TEOS, the drilling resistance was again measured and compared to the initial readings. Additionally small drill cores were taken for polished petrographic thin sections, which were produced after vacuum impregnation with a blue-dyed epoxy resin. These sections were analysed in a polarizing light microscope as well as by SEM under low vacuum. Based on the SEM-BSE images obtained in which the precipitated TEOS silica gel is revealed by a specific grey, its distribution in depth as well as its precise topographic position in the pore structure was visualized in pseudo colour. This not only allows for easier apprehension of the distribution of the consolidant in the micrographs, but would also enable digital image calculation of relevant parameters such as the degree of pore filling in selected areas of a depth profile, a procedure not followed however in frame of the present study.

In general, the information gained from the micrographs in combination with the readings from the drilling resistance and the penetration depth measured on the split planes all contributed to the final decision regarding the treatment of the sculpture.

4. Results

4.1. Test Series on Dummies

The first test results were based on the observation of the penetration depth along the split faces. The cubes that had been treated in a consolidation bath and by the VCP method, respectively, appeared fully soaked with the consolidant. On the contrary, the cube treated in the run-off test showed very low penetration depths of 0-7 cm (Fig. 2). In particular, the penetration was dependant on the condition of the paint layer in a specific area. Where the colour was scratched or lacunae were present, the consolidant could penetrate the stone fairly well. In areas with intact paint-layer the penetration depth was either very small or not determinable.



Fig. 2: Low and irregular penetration depth of the consolidant applied to the outer faces of the cube by run-off

The measurement of drilling resistance proved to be of limited use in the case of the dummies. This is probably due to the lack of strength profiles in the unweathered specimens before treatment. The cubes that were consolidated by total immersion and the VCP method had a uniform increase of the resistance after the treatment, while the cubes treated by the run-off method showed no relevant strength increase. On the contrary, drilling measurements yielded highly significant results for the sculpture with its obvious weathering profile (see 4.2).

Observations by optical microscopy and SEM revealed not only differences in the penetration depth of the consolidants for different modes of treatment (Fig. 3), but also showed that the specific places in the pore system where the silica gel preferentially precipitated or accumulated were likely governed by the method. As expected, virtually no silica gel could be detected in the sample from the cube that was treated by the run-off method, whilst the samples treated both by total immersion and by the VCP-method revealed significant amounts of silica gel in the full length of the drill core. In either case, however, the amounts of precipitate decreases with depth. In respect to the preferential position of gel precipitation, the consolidant was able to penetrate in smaller pores and thinner cracks when applied by the VCP method than in the case of total immersion, though the differences seem to be slight and further tests with more samples must be performed to clarify whether these observations are of relevance. Another observation relates to the deposition of the gel on the surface. While no silica could be detected on the surfaces of the sample consolidated by the VCP-method, the full immersion test left behind a surface coat

of gel even though the surface of the cube had been dried with a tissue after removal from the bath. It is likely that this layer had formed in the course of backwards migration of the consolidant during evaporation, a process that would have not taken place in the VCP test, either because the gel was preferentially trapped in smaller pores, or because of the reaction-facilitating additive.

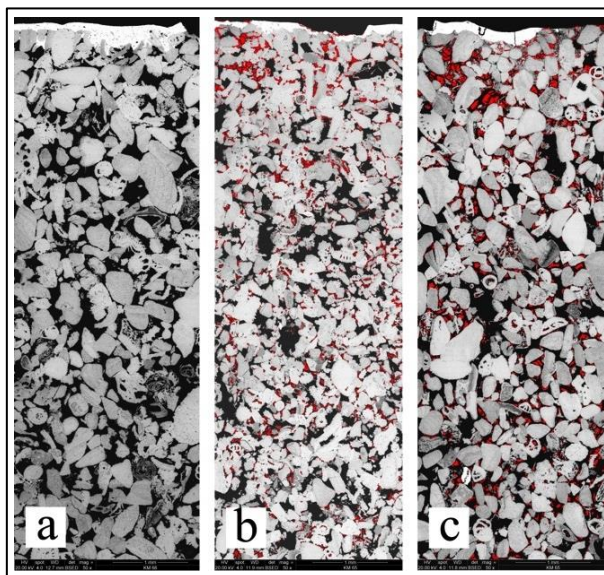


Fig. 3: In-depth distribution of silica gel (in pseudo colour) in the dummy stone subject to laboratory treatments (a) run-off, (b) immersion, and (c) VCP. SEM-BSE of polished thin sections, surface on top, depth of scanned area ca. 8 mm

4.2. Consolidation of the Sculpture

Following the results from the laboratory test series, the decision was made to consolidate the sculpture using the VCP method, which was performed by the company that holds the patent. After the curing period, drilling resistance measurements were conducted in six areas of the sculpture that had shown different degrees of decay, and were compared to drillings that had been made in the same areas before consolidation. Fig. 4 graphs this comparison and shows a significant increase in strength post-consolidation, with the greatest effect in the outermost 3 or 4 centimetres that had been in an extreme state of poor cohesion.

Just one core of 2 cm in diameter could be drilled out of the sculpture at its back side to check the consolidants precipitation in a polished thin section by polarizing light microscopy and SEM. Figures 5a and b illustrate the position of the gel at a depth of 2 cm from the surface. The findings support the drill resistance profile in that the VCP treatment of the sculpture has produced good results of consolidation.

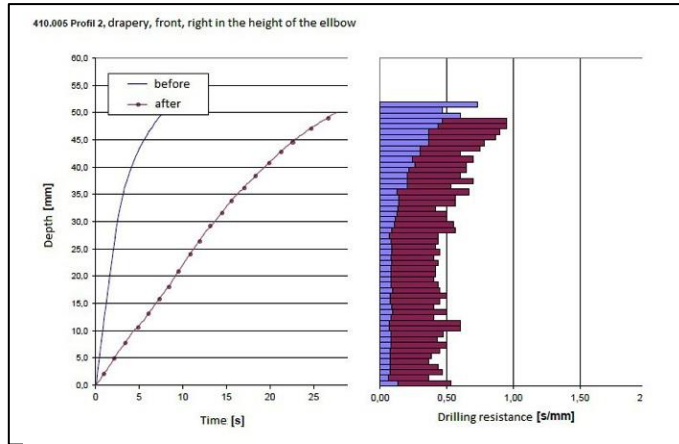


Fig. 4: Drilling resistance, before and after treatment, sculpture *Madonna with Child*. The graph shows an example representative of a total of six measurements taken in different places of the sculpture

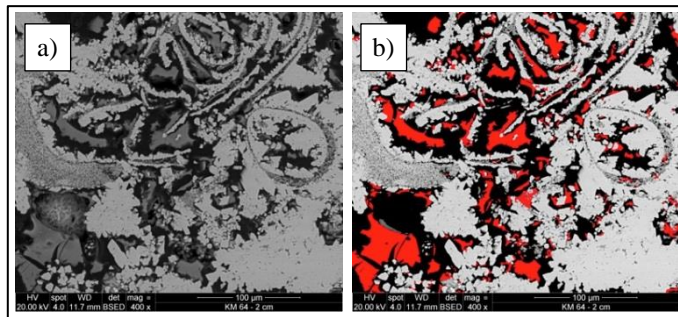


Fig. 5: Silica gel in the pores of the sculpture of *Madonna with Child* after the consolidation by the VCP method, approximate depth: 2 cm beneath the surface; (a) SEM image, (b) silica gel in pseudo colour

The amount of gel gradually decreases with the increase in depth. This finding, supported by the steady graph of the drilling resistance, correlates with the decreasing need for consolidant in the depth where the stone is in better condition. While quantitative values typically are not producible to establish the efficacy of a consolidation treatment along a gradient, one can try to estimate trends achieved by a treatment. The effect shown in our case was that the pronounced strength gradient before the consolidation has been partly flattened out, showing that the strength of the subsurface zone of the stone was significantly increased.

5. Conclusions

The results from the laboratory test series as well as from the treatment of the sculpture itself point to the fact that the consolidation with TEOS using the VCP-method is a very good possibility to consolidate porous limestone objects coated with layers of low permeability. The VCP-method offers one possibility to master these problems. In the

present case, the surface of the sculpture was covered with oil paint, but the results seem to be relevant to similar stones with different kinds of surface sealing coatings. The total immersion in a consolidant bath also proved to be a useful method when executed properly. The limitation of the size of the object is more relevant to the total immersion treatment than to the VCP-method. In recent years rather large objects have been treated with this method. Another advantage of VCP is that it can be done on site without dismantling any structures, as opposed to the full immersion technique that must be done in a studio, which can be difficult if not impossible for large structures.

Acknowledgements

Thanks are due to G. Fleischer from the Austrian Research Institute (ÖFI) for the measurements and data processing of drilling resistance on the sculpture as well as on the test cubes. Thanks go also to A. Baragona for editing the language of the text.

References

- Kieslinger, A., 1951, *Gesteinskunde für Hochbau und Plastik*, Österreichischer Gewerbeverlag, Vienna, Austria.
- Price, C. A., and Doehne, E. 2011. *Stone conservation: an overview of current research*. Getty Publications.
- Pummer, E., 2007, *Steinkonservierung; Die Kremser Dreifaltigkeitssäule*, Selfpublished, Rossatz, Austria.
- Pummer, E. 2007. European Patent no. 1295859 Vacuum Circular Consolidation Method. Owner Erich Pummer GmbH.
- Pummer, E., 2016, *Vacuum-Circling Process: Innovative Stone Conservation Method*. In: Proc. 13th International Congress on the Deterioration and Conservation of Stone, Glasgow, 6-10 September 2016 (this Volume)
- Rohatsch, A., 2005, *Neogene Bau- und Dekorgesteine Niederösterreichs und des Burgenlandes*, In: Mitt. IAG BOKU, Institut für Angewandte Geologie, Universität für Bodenkultur Wien, *Nutzbare Gesteine von Niederösterreich und Burgenland - „Junge Kalke, Sandsteine und Konglomerate – Neogen*, Vienna, Austria.
- Siedel, H., Wichert, J. and Frühwirt, T., 2016, *Application of ethyl silicate based consolidants on sandstone with negative pressure - a laboratory study*. In: Proc. 13th International Congress on the Deterioration and Conservation of Stone, Glasgow, 6-10 September 2016 (this Volume).
- Török, Á., Rozgonyi, N., Prikryl, R., and Prikrylová, J., 2004, *Leithakalk: the ornamental and building stone of Central Europe, an overview*. Dimension stone. Balkema, Rotterdam, 89-93.
- Wheeler, G., 2008, *Alkoxysilanes and the consolidation of stone: Where we are now*, - In: *Stone Consolidation in Cultural Heritage: Research and Practice; Proceedings of the International Symposium, Lisbon, 6–7 May 2008*, ed. J. Delgado Rodrigues and J. M. Mimoso, 41–52. Lisbon: LNEC (Laboratório Nacional de Engenharia Civil)

ELECTRO-DESALINATION OF SULFATE CONTAMINATED CARBONACEOUS SANDSTONE – RISK FOR SALT INDUCED DECAY DURING THE PROCESS

L.M. Ottosen^{1*}

Abstract

Sodium-sulphate is known to cause severe stone damage. This paper is focused on removal of this salt from carbonaceous sandstone by electro-desalination (ED). The research questions are related to possible stone damage during ED and subsequently suction cycles are made in distilled water before, during and after ED. During suction in water the salts are concentrated in the upper part of the sandstone. After 2 days of treatment the average water soluble SO_4^{2-} concentration was half the initial and for this sample corners were damaged as was the case for the reference stone. After 4 days of ED the average SO_4^{2-} concentration was 15% of the initial, and here no stone damage was seen from the suction cycles. This result shows that the damaging salts are removed and that no new harmful salts are formed during ED in the actual case. Acid is produced at the anode during ED. The acid is buffered in the poultice with carbonate. The acid would be highly damaging to the carbonaceous sandstone as the binder- CaCO_3 is soluble in acid. From *pH* measurements of the poultice it seems as if the acid is buffered well, as *pH* is still slightly alkaline after ED, but this is a measurement of the average *pH* and thus it was decided to measure the compressive strength of the stones after ED. The lowest compressive strength was measured for the reference stone, which had not been treated by ED (but had the highest salt content). Thus from this investigation there is an indication, that dissolution of carbonates in the stone did not happen, though the data material is too scarce to make a final conclusion. In summary, this investigation did support that ED removes the salts without new damaging side effects in the stone.

Keywords: electro-desalination, salt decay, sulphate, sandstone

1. Introduction

When water accesses the pore network of a stone, it may carry various salts in solution. Several mechanisms can subsequently cause crystal growth and crystallization-dissolution cycles, which can result in severe stone damage. The damaging effect varies between salts and salt mixtures, and not all salts are equally harmful, e.g. Rodriguez-Navarro & Doehne (1999) showed that evaporation from a saturated Na_2SO_4 solution caused more damage in limestone than evaporation from a saturated NaCl solution, because Na_2SO_4 easily forms supersaturated solutions, which is a mechanism for the generation of stress (Steiger & Asmussen 2008). According to Price and Brimblecombe (1994), at 20°C $\text{Na}_2\text{SO}_4 \cdot 10\text{H}_2\text{O}$ is

¹ L.M. Ottosen*

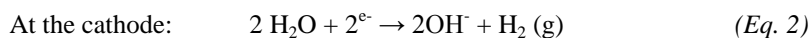
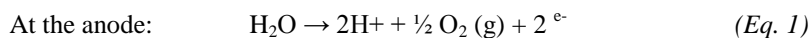
Department of Civil Engineering, Technical University of Denmark, Brovej, Building 118,
2800 Kgs. Lyngby, Denmark
LO@byg.dtu.dk

*corresponding author

the stable form of sodium-sulphate at relative humidity (*RH*) between 71 % and 93 %. $\text{Na}_2\text{SO}_4 \cdot 10\text{H}_2\text{O}$ occupies a 314 % larger volume than the anhydrous salt. Thus the volume of sodium-sulphate changes significantly with changes in *RH*, which is likely to be a major factor involved in the development of crystal pressure. The topic of the present paper is removal of Na_2SO_4 from carbonaceous sandstone by electro-desalination (ED).

The carbonaceous sandstone is Gotlandic sandstone, a soft, grey stone with approximately 20 % porosity and a fairly high degree of homogeneity, which makes it suitable for sculptures. The sandstone is sensitive to outdoor conditions due to the quite high porosity and the CaCO_3 bonding. The calcite can chemically be transformed to gypsum when exposed to acid-rain (Suneson 1942). Based on samplings from two monuments built of Gotlandic sandstone Nord and Tronner (1995) observed that rain dissolved calcite and decreased the Ca concentration in the stone. The dissolved Ca concentrated at the surface where a hard, thin gypsum crust was formed.

ED is based on application of an electric potential gradient and electromigration of the ions from the damaging salts out from the stone. During ED electrodes are placed externally on the surface of the salt infected stone. The electrodes are placed in a poultice in which the ions from the salts concentrate during the treatment. When the poultices are removed after the desalination, the ions of the salts are removed with them. At both electrodes there are *pH* changes due to electrolysis reactions:



As seen from (1) and (2) *pH* decreases at the anode and increases at the cathode. It is necessary to neutralize the *pH* changes to prevent severe *pH* changes of the stone. Herinckx *et al.* (2011) and Skibsted (2014) underlined the importance of avoiding stone acidification, as in experiments without *pH* neutralization; the stones were severely damaged next to the anode. Calcite rich clay poultice can be used for neutralization of the *pH* changes at the electrodes (Rörig-Dalgaard, 2009). The calcite buffers the *pH* changes and the clay gives workability, so the poultice can have optimal contact to the surface of the object to be desalinated. When the calcite buffers the acid from the anode, Ca^{2+} ions are released. If these ions do not precipitate with anions, they can be transported into the limestone by electromigration, and possibly precipitate with dissolved SO_4^{2-} . Should this happen, it may hamper the desalination and the formation of calcium- sulphates may even contribute to further salt weathering. In the present work it is investigated whether the stone is weakened during ED or at increased risk for salt decay during the process.

2. Materials and methods

2.1. Stone for the experiments

The Gotlandic stone pieces for the investigation were cut out of a former window frame from Kronborg Castle, Denmark. The original window frame had been removed and replaced during a renovation action. The outer parts of the stone were discharged, and the stone pieces for the experimental work (size 2.8×2.8×5.2 cm) were cut as seen in Fig. 1. The stone pieces were dried at 105°C. The pieces were vacuum saturated by 30 g/l Na_2SO_4 in a desiccator prior to the ED experiments.

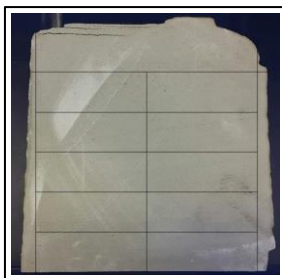


Fig. 1: The stone pieces were cut from a removed window frame.

2.2. Stone characterization

Two extra sandstone pieces were cut from the window frame ($4 \times 4 \times 5 \text{ cm}^3$) for measurement of capillarity, porosity and density. Capillarity: The samples were dried at 105°C . The dry samples were weighed and placed in a tray with distilled water with 5 mm height on the stone. The sandstones were weighed after 1, 2, 4, 6, 8, 16, 30, 60, 120, 180, 240 and 360 min. The samples were dried at 105°C again. They were vacuum saturated in a desiccator and the stones were weighed above and below water as it is required to calculate porosity and density.

2.3. ED experiments

Electrode compartments with the size $3 \times 3 \times 3 \text{ cm}^3$ were placed at each end of the sandstone piece (Fig. 2A). The frame of the electrode compartments were folded in thin plastic and jointed with tape to fit the ends of the stones. The frames were filled with poultice; a mixture of kaolinite and CaCO_3 (Rörig-Dalgaard, 2009). Inert electrode meshes (electrodes, which do not take part in the electrode processes themselves) were placed at the end of each electrode compartments, see Fig. 2a. The sandstone and electrode compartments were wrapped in plastic film to hinder evaporation. A constant current of 2 mA was applied. The durations of the ED experiments were 2, 4 or 7 days (denoted ED_2 , ED_4 and ED_7 respectively).

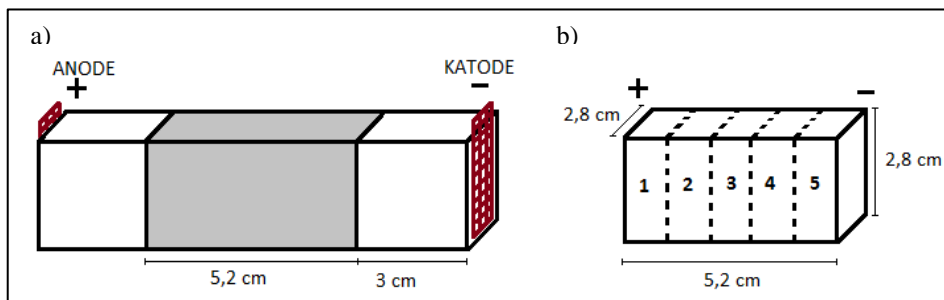


Fig. 2: a) ED setup with clay poultice and electrode mesh; b) segmentation of the stone after ED.

Each of the ED experiments was made in doublet. Concentration profiles were made on basis of one set of experiments, whereas suction cycles and compressive strength tests were made with the other set to evaluate the salt damage. See procedures below.

2.3.1. ED and concentration profiles

After ED the stones were segmented with hammer and chisel into five segments; numbered from the anode end (Fig. 2b). A reference stone (Ref.) was segmented directly after vacuum saturation by 30 g/l Na₂SO₄ to get the concentration profiles before ED. The water content in the five segments was measured and calculated as weight loss after drying at 105°C per dry weight. The dried segments were grinded in a mechanical mortar. Following 10 g powder was suspended in 25 ml distilled water and agitated for 24 h. The samples settled for 10 min and *pH* was measured. The samples were filtered through 0.45 µm filter. Na concentrations were analysed by ICP-OES. SO₄²⁻ (and for the reference sample also Cl) concentrations were analysed by ion chromatography (IC, Dionex DX-120). For each segment the concentrations were measured as double determinations.

2.3.2. ED and stone decay

The present experimental work focuses on stone decay caused by calcium sulfate formed during ED and since this salt has a low solubility it will not necessarily be seen in the concentration profiles measured in the suspension of powdered sandstone in water. Thus it is necessary to evaluate the ED process based also on the decay pattern. Two drying/wetting cycles were performed just after ED: the stone pieces were dried to constant weight at 50°C. They were placed in distilled water to a height of 1 cm (Fig. 3). The surface where the cathode poultice had been placed was placed in the water. The water level in the beaker was kept constant manually. When water had been sucked all the way through the stone piece, the stones were left for 1 day in the setup. The stones were dried again to constant weight at 50°C and the suction procedure was repeated. After the second suction was completed, the stone pieces were inspected visually and compressive strength tests were performed.



Fig. 3: Suction test after ED.

3. Results and discussion

3.1. Porosity, density and capillarity

The porosity of the experimental stone is 20.5% and the dry density 2120 kg/m³. In less than 2 hours water is sucked into the stone to full height (5 cm) and stable water content. The capillarity of the sandstone is high 5.98 kg/(m² s^{1/2}).

3.2. Removal of Na and SO₄²⁻ during ED

The Gotlandic stone for the investigation had been exposed to the outdoor environment at Kronborg Castle, which is situated just next to Øresund with salt water. As the stones thus potentially can be infected by Cl, the concentrations of Cl were measured in the five segments of the reference stone: 60.2 ± 7.2 mg Cl/kg. Thus the Cl concentration of the stone pieces for the ED experiments is low and thus the major salt is the Na₂SO₄ in which the stones were submerged.

Fig. 4 shows the concentration profiles of SO₄²⁻ and Na through the stone piece at the end of the ED experiments. It is seen, that SO₄²⁻ electromigrated towards the anode and Na towards the cathode, as it could be expected. The initial concentrations (Ref.) were 1950 ± 35 mg SO₄²⁻/kg and 940 ± 80 mg Na/kg. At the end of ED₇ the concentrations were decreased to 36 ± 4 mg SO₄²⁻/kg and 49 ± 5 mg Na/kg. This corresponds to removal percentages of 98% SO₄²⁻ and 95% Na during 7 days.

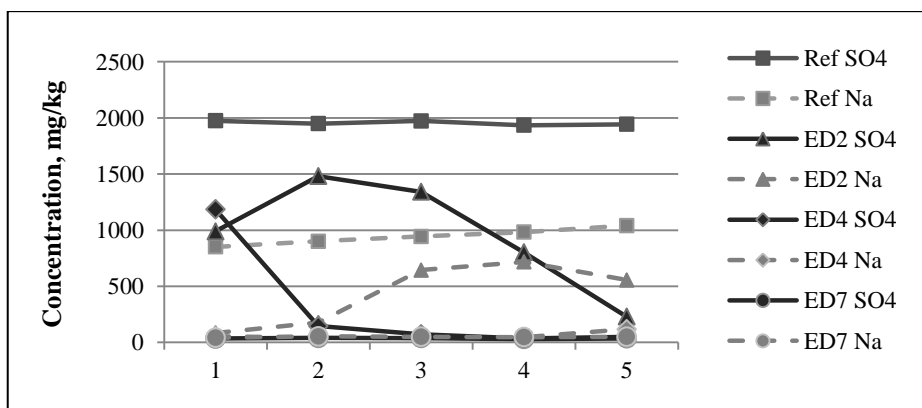


Fig. 4: SO₄²⁻ and Na concentration profiles of Ref and ED stones.

Skibsted *et al.* (2015) reported that the ED removal rate per valence for SO₄²⁻ was 75% of the ED removal rates for Cl⁻ and NO₃⁻ regardless the ionic mobility of SO₄²⁻ is slightly higher than that of the monovalent anions. The main reason for the lower removal rate for SO₄²⁻ was found to be the chemical interaction with Ca²⁺, which entered the brick from the poultice in the anode chamber. The concentrations of Ca²⁺ and SO₄²⁻ in the pore solution decreased after 5 days of ED and precipitation of gypsum was thus not considered as a permanent problem. Simulation results were congruent with those obtained experimentally. The present experimental work (Fig. 4) support this conclusion, however, in case calcium-sulfate salt with low solubility is formed during ED, it will not necessarily be seen in the concentration profiles of figure 4, because the concentrations shown here are measured in a suspension of powdered sandstone in water after filtration. The salt crystals will be removed from the sample during the filtration process if not dissolved. Thus it is necessary

to evaluate the ED process also on the decay pattern, which was done by suction cycles, see section 3.3 of this paper.

Electro neutrality is fulfilled all the time and thus during ED other anions than SO_4^{2-} ensures the electro neutrality in relation to the Na^+ concentration profile, as the concentration of this cation is high close to the cathode where the SO_4^{2-} concentration is low. In Paz-Garcia *et al.* (2013) it is suggested from numerical-chemical simulations that these are mainly OH^- ions (experimentally it is also often seen that *pH* increases slightly from the cathode side, which was also the case in the present work see section 3.4). There may thus be precipitation of $\text{Ca}(\text{OH})_2$ in the material if Ca^{2+} from the anode poultice and OH^- from the cathode meet inside the stone. Over time $\text{Ca}(\text{OH})_2$ may react with CO_2 from air and form CaCO_3 , but neither $\text{Ca}(\text{OH})_2$ nor CaCO_3 are considered damaging, because aqueous solutions of calcium hydroxide (limewater) have been used for many centuries to protect and consolidate limestone, and CaCO_3 is present in the original carbonaceous stone.

3.3. Decay of ED treated stone evaluated after suction cycles

Pictures of the stones Ref and ED's after two cycles of water suction are shown in Fig. 5. Some of the thin white layer on the upper horizontal surface originates from the poultice (see also Fig. 3). During the suction, the soluble salts are transported towards the top of the stone, which means a concentration of salt in this part and a lower concentration in the remaining stone. It is seen that the upper corners were damaged for the Ref and ED_2 experiments whereas similar damage was not seen for ED_4 and ED_7 revealing that the overall concentration was lowered sufficiently after 4 days.

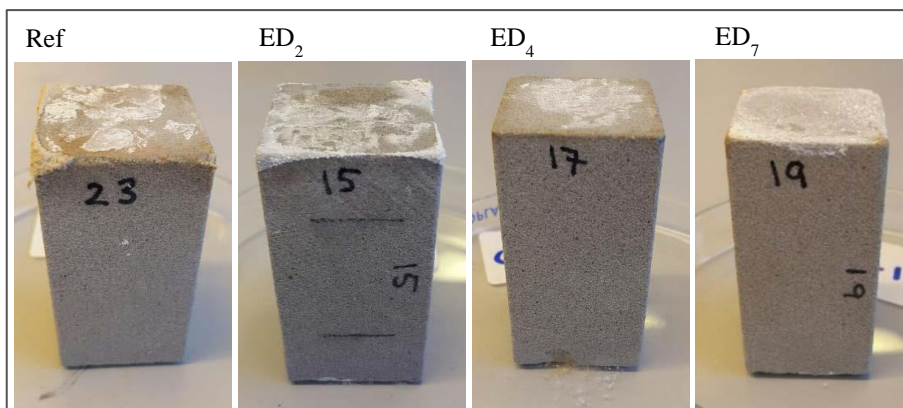


Fig. 5: Ref and ED stones after two water suction cycles.

It is noticed, that the soft material/crystals at the damaged corners of the Ref and ED_2 stone differs. At the Ref. it has the colour of the sandstone and at ED_2 the salt crystals are white. It might be different salts responsible to the decay in the two cases, but it is not determined in this investigation. In the Ref stone the Na_2SO_4 in which the stone was submerged is considered the major salt, whereas in ED_2 also Ca^{2+} may have been transported from the anode poultice into the stone. The calcium sulphate will dissolve again as long as Ca^{2+} and SO_4^{2-} are removed from the pore solution in the applied electric field as equilibrium supports the dissolution. The lack of crystals on ED_4 and ED_7 support this hypothesis.

3.4. Compressive strength of ED treated stone

The average pH in the segments from Ref. was 8.9 ± 0.05 and for ED₇ 9.0 ± 0.3 . The overall pH in the stone piece did thus not change significantly during ED. The pH remained the same in the anode end as initially, whereas the pH increase from the cathode was not buffered to the same extent, as pH in the segment closest to the cathode was increased to 9.5, which is though not considered a problematic level.

The fact that the pH did not change from the anode side is not a proof that H^+ did not electromigrate into the stone. Gotlandic sandstone has a buffering capacity towards acid as it is calcite bound, which was shown experimentally in Skibsted (2014). In case an acidification had occurred during the ED treatment, this would decrease the compressive strength of the stone as result of dissolution of calcite. Thus it was decided to make compressive test measurements. The compressive strength tests were conducted after the suction cycles, and the stone compressive strength could be influenced from both acidification and salt weathering. The result is shown in fig. 6 and 7. A quite large variation in compressive strength was observable between the four stones. The Ref. stone had the lowest compressive strength of all four stones, which may indicate that ED does not lower the strength significantly by dissolving the bonding calcite phases, but the data are too scarce to make a final conclusion on this point. Fig. 7 shows that the pattern with which the stones were broken during the compressive strength tests differed. The pattern was linked to the compressive strength in that for the Ref and ED₇ stones with the lowest compressive strength, the stones were damaged by flaking from the surface, whereas the two stronger stones ED₂ and ED₄ were broken in the expected pattern hourglass figure for a homogeneous sample.

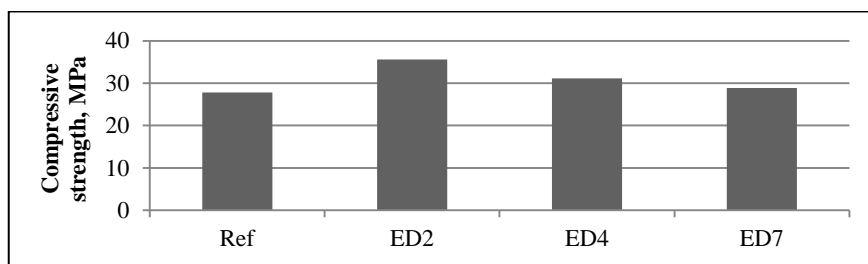


Fig. 6: compressive strength after ED and 2 suction cycles (single determinations).

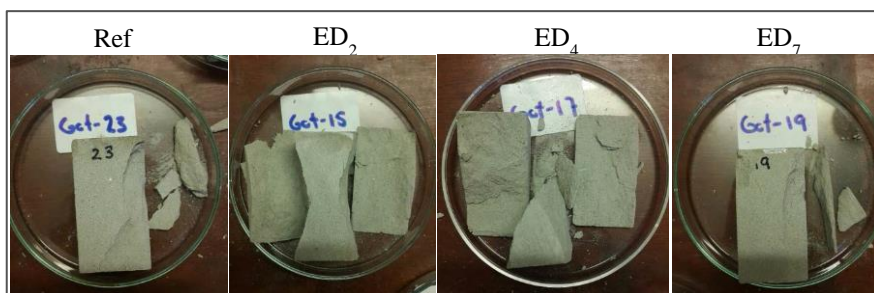


Fig. 7: The stones after compressive strength measurements.

4. Conclusions

Carbonate bound sandstones are weak and sodium-sulphate a highly damaging salt. ED was tested for removal of sodium-sulphate from Gotlandic sandstone, which is carbonate bound. The focus was on possible damaging side effects, such as dissolution of the carbonate phase or formation of new damaging salts, during the treatment. No indications of these side effects were seen. The compressive strength of the stones were measured and it was not decreased during ED, though this determination was only made in single determinations and the result must be taken with caution. The ED treatment followed by suction cycles did not show any stone damage after ED during 4 days, which was on the contrary to before treatment.

References

- Herinckx S, Vanhellefont Y, Hendrickx R, Roels S, De Clercq H., 2011, Salt removal from stone building materials using an electric field. In: I. Iannou & M. Theodoridou (eds.) Proceedings from the international conference on salt weathering on building and stone sculptures, Cyprus 19-22 October, 357-364.
- Nord, A.G., Tronner, K., 1995, Effect of acid rain on sandstone: The Royal palace and the Riddarholm Church, Stockholm. *Water, Air and Soil Pollution*, 85,2719-2724.
- Paz-Garcia, J.M.P.; Johannesson, B.; Ottosen, L.M.; Ribeiro, A.B.; Rodriguez-Maroto, M., 2013, Simulation-based Analysis of the Differences in the Removal Rate of Chlorides, Nitrates and Sulfates by Electrokinetic Desalination Treatments. *Electrochimica Acta*. 89, 436-444.
- Price, C.; Brimblecombe, P., 1994, Preventing salt damage in porous materials, In Eds A. Roy and P. Smith, Preventive conservation: Practice, theory and research" Ottawa Congress, 12-16 Sep., 90-93.
- Rodriguez-Navarro, C.; Doehne, E., 1999, Salt weathering: Influence of evaporation rate, supersaturation and crystallization pattern, *Earth Surf. Process. Landforms*, 24, 191-209.
- Rörig-Dalgaard, I., 2009, Preservation of masonry with electrokinetics – with focus on desalination of murals. PhD Thesis. Department of Civil Engineering, Technical University of Denmark.
- Skibsted, G., 2014, Matrix changes and side effects induced by electrokinetic treatment of porous and particulate materials, PhD Thesis, Department of Civil Engineering, Technical University of Denmark.
- Skibsted, G.; Ottosen, L.M.; Jensen, P.E.; Paz-Garcia, J.M., 2015, Electrochemical desalination of bricks - Experimental and modeling. *Electrochim. Acta*, 181, 24-30.
- Steiger, M.; Asmussen, S., 2008, Crystallization of sodium sulfate phases in porous materials: The phase diagram $\text{Na}_2\text{SO}_4 \cdot \text{H}_2\text{O}$ and the generation of stress, *Geochimica et Cosmochimica Acta*, 27, 4291-4306.
- Sunesson, E., 1942, *Bygningsmaterialer*, 3. Bind: Natursten. Jul. Gjellerups Forlag, 117-139.

PERMEABLE POSS-BASED HYBRIDS: NEW PROTECTIVE MATERIALS FOR HISTORICAL SANDSTONE

A. Pan¹, S. Yang¹ and L. He^{1*}

Abstract

Although much effort has been dedicated to the development of advanced materials and techniques, only a relatively small part of conservation science has focused on the production of innovative materials that can be applied to repair ancient stone. Because soft nanomaterials do not alter the original physical and chemical properties of artefacts, we report two kinds of well-designed polyhedral oligomeric silsesquioxanes (POSS)-based soft materials of ap-POSS-PMMA-b-P(MA-POSS) (P1) and PDMS-b-PMMA-b-P(MA-POSS) (P2) prepared for protecting historic stones. Their assembled soft nanoparticle, surface wettability, water adsorption and thermal properties are investigated. P1 gives lower water adsorption ($\Delta f=600$ Hz) and viscoelasticity ($\Delta D=75\times 10^{-6}$) but higher thermostability ($T_g=124$ C and $T_d=400$ C. P2 shows a silicon-rich surface, strong storage modulus (648-902 MPa), higher water adsorption amount ($\Delta f=2300$ Hz) and surface rigidity ($\Delta D=26\times 10^{-6}$). Therefore, two POSS-based hybrids are recommended to the protective performance of sandstone with different porosity as D1 (23.66%) and D2 (21.57%), evaluated by the colour variations, capillary water absorption, water vapour permeability, water static contact angles, salt-tolerance crystallization cycles and freeze-thaw cycles. All the results indicate that the colour variation of the treated stones is within the permitted range. Under the condition of invariable pore size distribution, the water resistance is obviously improved and the water permeability is slightly reduced, and P1 does better than P2. On the other hand, P2 is realized much better in salt-tolerance and freeze-thaw recycles than P1. The smaller pore size diameters (less than 2 μm) have been covered but the middle pore size is narrowed at 200-900 μm . The weathering behaviours also indicate good resistance to anti-salt and anti-freeze/thaw after 9 salt crystallization cycles and 50 freeze-thaw cycles. Therefore, P1 and P2 are suggested as protective materials to the historical stones.

Keywords: soft nanomaterials, POSS-based copolymer, permeability, film properties, protective performance

¹ A. Pan, S. Yang and L. He*,

Department of Chemistry, School of Science, Xi'an Jiaotong University, China
heling@mail.xjtu.edu.cn

*corresponding author

1. Introduction

Soft nanomaterials have been considered for protecting application of ancient stones (Baglioni *et al.* 2015, Son *et al.* 2009) based on their extraordinary surface properties, excellent film-forming properties (Zhang *et al.* 2013, Licchelli *et al.* 2013), high mechanical and anti-chemical properties (Cappelletti *et al.* 2015, Verganelaki *et al.* 2015, Xu *et al.* 2015), and undisturbed the original physical and chemical properties of artefacts. Actually, silica-based nanomaterials have been reported for sandstones protection with reinforcement and surface protective due to the better compatibility with the sandstones (Luo *et al.* 2015, Baglioni *et al.* 2013), such as “TEOS-SiO₂-ST-PDMS-OH” hybrid by combining TEOS, colloidal silica (200 nm) and polydimethylsiloxane (PDMS-OH) used for stone consolidation (Salazar-Hernández *et al.* 2010). The colloidal silica (200 nm) is favour of the micro-porous and mesoporous structures, and the organic segments of PDMS could improve the elasticity of the gel by chemical bonding with TEOS which could also improve the surface wettability. Recently, introduction of polyhedral oligomeric silsesquioxanes (POSS) particles, the smallest SiO₂, into organic matrix is used to improve properties of soft nanomaterials, based on that POSS with silsesquioxane cage ((SiO_{1.5})_n, n= 8-14) and organic functional groups (Kuo *et al.* 2011) could disperse in nanoscale and give higher reactivity in obtaining new nanomaterials (Tada *et al.* 2012). Actually, POSS-based nanomaterials present low surface energy surface and high mechanical properties without changing the surface structures and gas permeability (Kota *et al.* 2012).

Therefore, this work presents the well-designed two POSS-based block-structured nanomaterials and their protective application to historic stones. They are separately synthesized by aminopropylisobutyl POSS (ap-POSS, cages structure) and mono-carbinol terminated polymethylsiloxane (PDMS-OH, soft segments) initiating methylmethacrylate (MMA) and methacrylisobutyl polyhedral oligomeric silsesquioxane (MA-POSS) by ATRP technique to obtain ap-POSS-PMMA-b-P(MA-POSS) (named as P1; Yang *et al.* 2014) and PDMS-b-PMMA-b-P(MA-POSS) (named as P2; Yang *et al.* 2015). 1H,1H,2H,2H-heptadecafluoro-1-decanol (CF₂CH₂(CF₂)₈OH) is also used to initiate MMA and MA-POSS to gain F-PMMA-b-P(MA-POSS) (named as P3) for comparison (Pan *et al.* 2015). The differences of their self-assembly in solutions, surface morphology, wettability and thermo-stability are compared. Their protective efficiency onto two stones is evaluated by the colour variation, water absorption, permeability, surface contact angles, pore size distribution and salt/freeze/thaw decay behaviour.

2. Experimental section

2.1. Materials

Details of the used materials of (ap-POSS-PMMA-b-P(MA-POSS); Yang *et al.* 2014) and PDMS-b-PMMA-b-P(MA-POSS; Yang *et al.* 2015) are provided in Tab. 1. Their assembled nano-particle from molecular blocks prepared by casting 1 wt% homogeneous solutions in chloroform (CHCl₃) and the corresponding particle size distribution are investigated by TEM and DLS (Fig. 1). The ap-POSS-PMMA-b-P(MA-POSS) (Fig. 1a) behave 200 nm core-shell structured micelles (the inner dark core and out light shell) as the dark core of ap-POSS and P(MA-POSS), and the light shell of PMMA (Yang *et al.* 2014). The similar micelles are observed for F-PMMA-b-P(MA-POSS) in Fig. 1c. While, PDMS-b-PMMA-b-P(MA-POSS) in CHCl₃ solution form 200-500 nm opposite core-shell micelles Fig. 1b with the white PMMA core, and 50 nm thickness of the black shell formed by

PDMS and P(MAPOSS; Yang *et al.* 2015). However, the micelles (150 nm) are much smaller than ap-POSS-PMMA-b-P(MA-POSS) (200 nm), this is possible due to the poor solubility of F segments which could shrink the micelles. As we all know that the micellization behaviour is mainly controlled by the solvent and the interaction of solvent with the copolymer blocks. So another reason is that CHCl_3 solution has the smaller dielectric constant ($\epsilon = 4.81$) which could decrease the repulsive between the segments, and improve the affinity of PDMS and P(MA-POSS).

Tab. 1: The molecular weights of prepared samples by SEC.

Samples	Chemical composition	Mw/ Mn $\times 10^4$	Micelles size/nm TEM/DLS	Surface roughness, (nm)	Si element, (wt%)
P1	ap-POSS-PMMA ₁₅₂ -b-P(MA-POSS) _{8,4}	2.83/2.44	200-500/295	0.83	8.68
P2	PDMS-b-PMMA ₄₀₈ -b-P(MA-POSS) _{8,2}	5.36/4.41	100-300/283	2.48	14.62
P3	F-PMMA _{200,8} -b-P(MA-POSS) _{9,06}	3.02/2.74	100-300/135	1.69	6.34

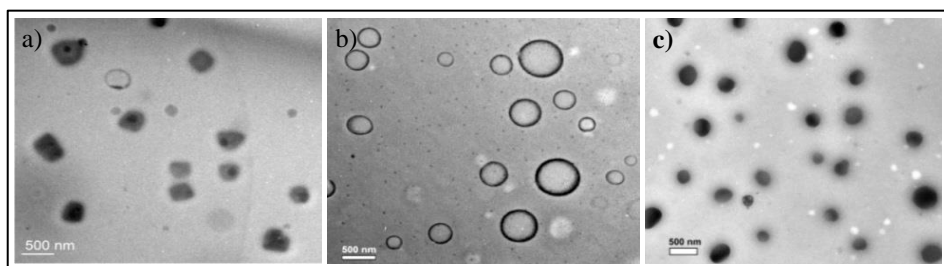


Fig. 1: TEM morphology of P1 (a), P2 (b) and P3 (c) in CHCl_3 solution.

2.2. Protection of historic sandstone

Sample preparations: The historic stone samples are collected from DaFoSi Grottoes (Red Stones) and Zhongshan Grottoes (Gray Stones) of Shaanxi province, famous Great Buddha Grotto in China. The stone samples are cut into $2 \times 2 \times 1 \text{ cm}^3$ (cube) and $4.2 \times 1.0 \text{ cm}^2$ (cylindrical) approximately, washed with deionized water, dried at 110°C up to constant weight (24 h), and then stored in silica gel desiccators before treatment. The historic stone samples are immersed in P1 or P2 solutions (1 wt%) until no air bubbles (about 1h). The treated stone samples are kept a 3-week interval for reaching constant weight.

Assessment method and process: The colour variation of stone surface is evaluated by colorimetric measurements using a Konica Minolta Colorimeter (CR-400). The measurements of water absorption are conducted by using the gravimetric method according to total completely immersion. Water capillary absorption is performed according to the Italian Standard UNI 10859. The capillary absorption coefficient is calculated at the end of the test for all the samples. The water vapour permeability is processed by the cylinder sandstone samples ($4.2 \times 1.0 \text{ cm}^2$). The surface morphology of treated stones is investigated by SEM. The surface contact angles measurements are

conducted on an OCA-20 DataPhysics Instruments GmbH with SCA 20 software at 25°C. The stone porosimetry is used to measure the pore size distribution of the macropores on an Autopore IV9500 Micromeritics Instrument. The anti-salt decay behaviour of stone samples is processed as total immersion into a saturated solution of Na₂SO₄ for 24 h and then drying at 105-110°C for 24 h. This cycle is repeated until obvious damage appeared. The freeze-thaw cycle is done as total immersion in deionized water at 20-25°C for 4 h and then freezing at -4°C for 4 h. This cycle is repeated up to twenty times. The weight loss percentage of the samples (measured at the end of cycle) is taken as a measure of the damage.

3. Results and discussion

3.1. The colour variation and surfaces wettability of protective stones

Table 2 shows the colour variation ΔE of the treated stone samples. P3-treated stone surface shows the biggest ΔE (3.57 for red stone and 3.74 for gray stone) due to the poor compatibility with the silicate-based stones. P1-treated surface presents the smallest colour variation ($\Delta E=1.69$ for red stone and 3.21 for gray stone). All of the stones treated by the materials are within acceptable limits (not larger than 5).

Tab. 2: Colour variation ΔE and water contact angle of the treated stone samples.

Samples	ΔE		Water contact angle in degrees	
	Red stone	Gray stone	Red stone	Gray stone
P1	1.69	3.21	128.6±3.6	122.9±2.1
P2	2.31	3.46	138.9±2.4	128.7±1.6
P3	3.57	3.74	127.2±3.1	120.2±1.7

The surface wettability is evaluated by water contact angles (WCA) in Table 2. All the stones samples treated provide the high-hydrophobic surface (WCA=120°-139°). When the water droplets contact the stone surface, the droplets are absorbed quickly for the untreated stones. However, the water droplets on the treated samples could keep for a long time. The WCA values show that P2 provide 138.9±2.4° for red stone (the biggest WCA) and 128.7±1.6° for gray stone, and P3-treated stones have the smallest WCA (127.2±3.1° for red stone and 120.2±1.7° for gray stone). All the results demonstrate markedly the surface wettability. As is well-known that surface wettability is controlled by the surface structure and morphology. Take red stone as example, POSS cages are able to grow into big crystals when they contact the silicate-based stones (regarded as the crystal-seed) (Fig. 2b), but P2 wearing PDMS chains with much better flexible and movement has better permeability and strong combination with the stones (Fig. 2c), while P3 do not influence the surface structures (Fig. 2d). All the results demonstrate that the stones surface keep un-changed and clear-outline surface without changing the surface structures after treated which could improve the surface wettability.

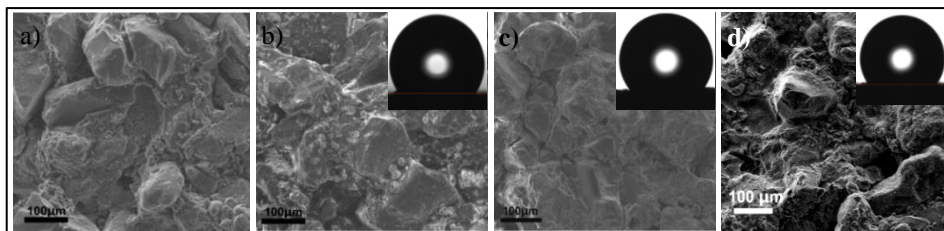


Fig.2. SEM images of untreated red stone (a) and treated by P1 (b), P2 (c) and P3 (d).

3.2. Water absorption and permeability

The water capillary absorption also reveals the water-resistant property of the treated stone samples. Figure 3 shows the water capillary absorption, and the capillary absorption coefficients calculated by the slope of initial 15 min of the capillary absorption curves. The untreated stones absorb rapidly a great amount of water, but this tendency is reduced by every treated sample, which indicates that the wettability has been improved after protective treatment. For red stones, all the samples show the similar capillary absorption coefficient of $7.89 \times 10^{-5} \text{ g}\cdot\text{cm}^{-2}\cdot\text{s}^{-1/2}$ for P1, $6.58 \times 10^{-5} \text{ g}\cdot\text{cm}^{-2}\cdot\text{s}^{-1/2}$ for P2 and $5.95 \times 10^{-5} \text{ g}\cdot\text{cm}^{-2}\cdot\text{s}^{-1/2}$ for P3, and similar water-absorption of 2.46% for P1, 2.22% for P2 and 2.72% for P3, which is much lower than the untreated samples ($1.53 \times 10^{-3} \text{ g}\cdot\text{cm}^{-2}\cdot\text{s}^{-1/2}$, 6.89% water-absorption). This is because that the red stones have much bigger interspaces which is in favour of the similar water-absorption. However, as for the gray stones, all the treated samples show the lower absorption speed (capillary absorption coefficient is $1.98 \times 10^{-3} \text{ g}\cdot\text{cm}^{-2}\cdot\text{s}^{-1/2}$ for P1-, $1.47 \times 10^{-4} \text{ g}\cdot\text{cm}^{-2}\cdot\text{s}^{-1/2}$ for P2 and $1.77 \times 10^{-3} \text{ g}\cdot\text{cm}^{-2}\cdot\text{s}^{-1/2}$ for P3) than the untreated samples ($2.50 \times 10^{-3} \text{ g}\cdot\text{cm}^{-2}\cdot\text{s}^{-1/2}$, 11.15% water-absorption). And P2-treated stone presents the lowest capillary absorption coefficient $1.47 \times 10^{-4} \text{ g}\cdot\text{cm}^{-2}\cdot\text{s}^{-1/2}$ and water absorption (5.95%). P1- and P3- treated stones have the similar tendency which is much lower than the untreated stone, but much higher than P2-treated samples. Actually, the gray stone have the smaller interspaces but the P2 could penetrate into the stones easier than other materials to decrease the water-absorption.

Furthermore, the water vapour permeability of treated stones is compared. For the red stones, all the treated red stones show the similar tendency and lower water vapour permeability ($1.03\text{-}1.53 \text{ g}\cdot\text{m}^{-2}$) than the untreated red stone ($2.52 \text{ g}\cdot\text{m}^{-2}$). P1 shows the highest water vapour permeability but P2 gives the poorest one. This is because P1 provide most POSS cages than P2 and P3 which is much better for water vapour permeability. As for gray stone, all the samples show the similar tendency with the red ones and P1 shows the highest water vapour permeability. Due to the compact structure of gray stones, its water vapour permeability ($0.206\text{-}0.274 \text{ g}\cdot\text{m}^{-2}$) is much lower than the red ones. The water vapour permeability results demonstrate that all the treated samples increase their wettability but decrease a little of water vapour permeability. It is concluded that much better water vapour permeability is supported by the more POSS cages in P1.

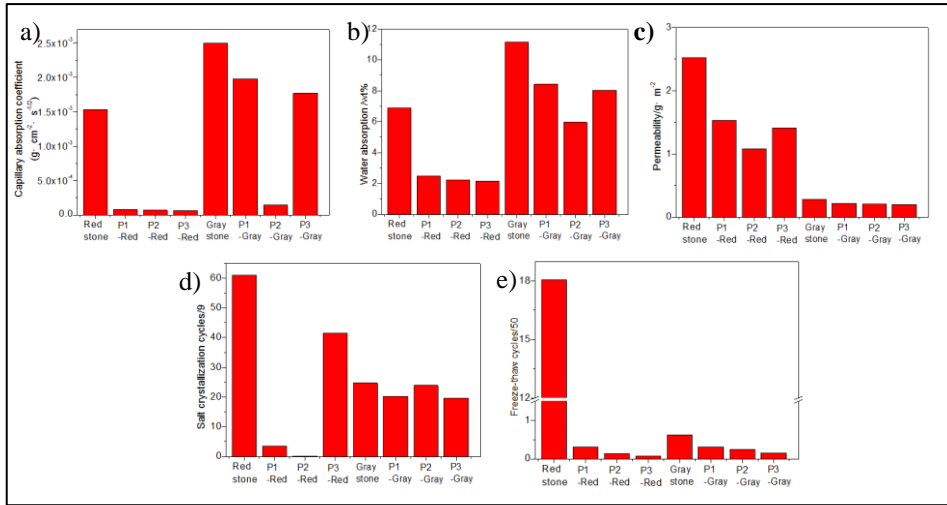


Fig. 3: a) Capillary absorption coefficient; b) Water absorption; c) Water vapour permeability, d) Weight loss percent after salt crystallization, e) Freeze-thaw cycles.

3.3. Pore size distribution

The pore size diameters of all treated stone samples are measured and are compared to the untreated one. For red stones, three different kinds of pore size diameters are observed: 200-900 μm , 3.5-40 μm and $<2 \mu\text{m}$ (Fig. 4). All the pore size diameters at 200-900 μm for three treated red stones have not changed, but the pore size diameters at less than 2 μm of P1-treated stone has disappeared and has become narrow as 10-30 μm compared to untreated one (3.5-40 μm ; Fig. 4a). The pore size diameters of P2-treated stone show the similar tendency (0.2-2 μm). But P3-treated stone gives a specific peak of pore size distribution appeared at 7-9 μm . All results demonstrate that after protective treatment, the smaller pore size diameters ($< 2 \mu\text{m}$) has been blocked and the middle pore size distribution become narrow but the pore size at 200-900 μm have never been changed.

As for gray stones, the untreated stones show three different pore size distributions at 20-900 μm , 0.3-20 μm and smaller than 300 nm in Fig. 4b. The pore size diameters of P1-treated stone at 200-900 μm has changed to 100-800 μm and the pore size diameters at 0.3-20 μm and less than 2 μm has been replaced by 0.2-10 μm . However, only one pore size diameter happened at 30-800 μm could be seen for P2- and P3-treated stones. Therefore, the smaller pore size diameters and the middle pore size distribution has been covered and the pore size at 200-900 μm have never been changed after treatment.

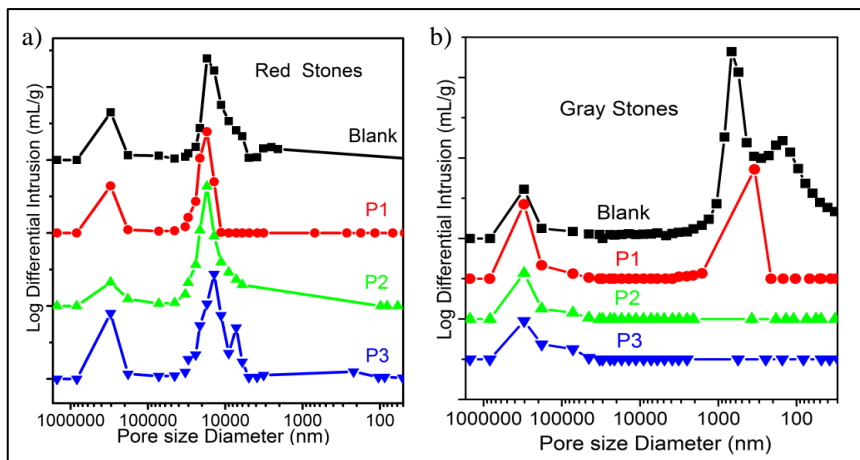


Fig. 4: Pore size distribution of red stone (a) and gray stone (b).

3.4. Salt and freeze/thaw cycles

Figure 5 shows the surface appearance of stone samples after salt crystallization cycles and freeze-thaw cycles. It is observed that the untreated red sample is damaged after one salt crystallization cycle. However, all the three treated samples are well preserved after the 6 salt crystallization cycles. After 9 salt crystallization cycles, the surface of both red and gray stone samples have the slightly damage in P3-treated red-stone (Fig. 5a, the last one), and the P-treated stone begins to be damaged. But P2-treated stone is still well preserved even after the continuing 9 salt crystallization cycles.

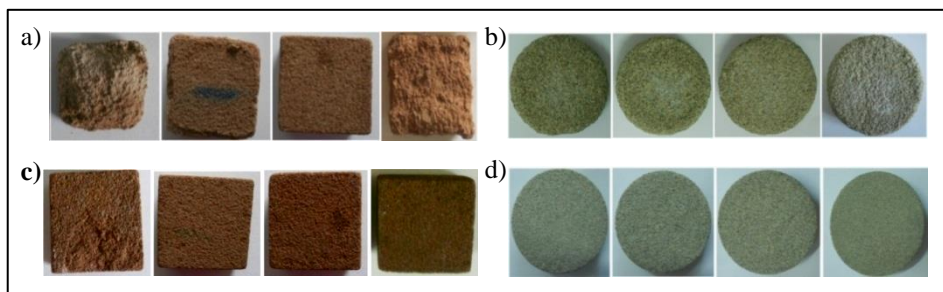


Fig. 5: The surface appearance of stone samples after 9 salt crystallization cycles (red-a and gray -b) and 50 freeze-thaw cycles (red-c and gray-d).

The weight loss percents of samples after 9 salt crystallization cycles are listed in Fig. 3. Compared with the big weight loss of the reference stones (60.94%), P2-treated stones provide the best resistance to salt crystallization (the weight loss is only 0.07%), and P3-treated samples has the poorest effect (the weight loss is 41.53%). On the other hand, all the gray stones show the similar resistance to salt crystallization (20.23% for P1, 23.88% for P2 and 19.67% for P3, respectively), which is a little better than the untreated-gray-stone (24.66%; Fig. 5b). While, after 50 freeze-thaw cycles, only some matrix powder in water

and some cracks happened in the surface of untreated stone sample with a higher weight loss percent (0.62%), while the other treated stone samples keep integrity with lower weight loss percents (0.13-0.31%) shown in Fig. 3 which indicate a good resistance to freeze-thaw.

4. Conclusion

Three well-designed POSS-based nanomaterials are prepared for the protection of historic stones, their properties and protective performance onto two stone specimens are evaluated. The protective efficiency demonstrates that all the colour variation of the treated stones is within acceptable limits ($\Delta E \leq 5$). P2-treated surface provide the biggest water-resistant property (WCA=138.9-128.7). After treated by three nanomaterials, the middle pore size distribution become narrow and the pore size at 200-900 μm has never been changed. The protective behaviour indicates a good resistance to anti-salt and anti-freeze/thaw after 9 salt crystallization cycles and 50 freeze-thaw cycles. Therefore, P1 and P2 are able to be suggested as protective materials to the historical stones.

Acknowledgment

This work has been financially supported by the National Basic Research Program of China (973 Program, No.2012CB720904), the National Natural Science Foundation of China (NSFC Grants 51373133, 51573145), and the International Cooperation Project of Shaanxi Province (No.2014KW11). The authors also wish to express their gratitude for the MOE Key Laboratory for Non-equilibrium Condensed Matter and Quantum Engineering of Xi'an Jiaotong University.

References

- Baglioni, P., Carretti, E., and Chelazzi, D., 2015, Nanomaterials in art conservation, *Nature Nanotechnol*, 10(4), 287-90.
- Son, S., Won, J., Kim, J.-J., Jang, Y. D., Kang, Y. S., and Kim, S. D., Son, S., 2009, Organic-inorganic hybrid compounds containing polyhedral oligomeric silsesquioxane for conservation of stone heritage, *ACS Appl Mater Interfaces*, 1(2), 393-401.
- Zhang, H., Liu, Q., Liu, T., Zhang, B., 2013, The preservation damage of hydrophobic polymer coating materials in conservation of stone relics, *Progress in Organic Coatings*, 76(7-8), 1127-1134.
- Licchelli, M., Malagodi, M., Weththimuni, M. L., Zanchi, C., 2013, Water-repellent properties of fluoroelastomers on a very porous stone: Effect of the application procedure, *Progress in Organic Coatings*, 76(2-3), 495-503.
- Cappelletti, G., Fermo, P., and Camiloni, M., 2015, Smart hybrid coatings for natural stones conservation, *Progress in Organic Coatings*, 78, 511-516.
- Verganelaki, A., Kapridaki, C., and Maravelaki-Kalaitzaki, P., 2015, Modified tetraethoxysilane with nanocalcium oxalate in one-pot synthesis for protection of building materials, *Industrial & Engineering Chemistry Research*, 54(29), 7195-7206.

- Xu, F., *et al.*, Xu, F., Wang, C., Li, D., Wang, M., Xu, F., Deng, X., 2015, Preparation of modified epoxy–SiO₂ hybrid materials and their application in the stone protection, *Progress in Organic Coatings*, 81, 58-65.
- Luo, Y., Xiao, L., and Zhang, X., 2015, Characterization of TEOS/PDMS/HA nanocomposites for application as consolidant/hydrophobic products on sandstones, *Journal of Cultural Heritage*, 16(4), 470-478.
- Baglioni, P., Chelazzi, D., Giorgi, R., and Poggi, G., 2013, Colloid and materials science for the conservation of cultural heritage: cleaning, consolidation, and deacidification, *Langmuir*, 29(17), 5110-5122.
- Salazar-Hernández, C., , María J. P. A., Patricia S., and Jorge C., 2010, TEOS-colloidal silica-PDMS-OH hybrid formulation used for stone consolidation, *Applied Organometallic Chemistry*, DOI 10.1002/aoc.1646
- Kuo, S.-W., and Chang, F.-C., 2011, POSS related polymer nanocomposites, *Progress in Polymer Science*, 36(12), 1649-1696.
- Tada, Y., Yoshida, H., Ishida, Y., T., Hirai, Bosworth, J. K., Dobisz, E., Ruiz, R., Takenaka, M., Hayakawa, T., and Hasegawa, H., 2012, Directed self-assembly of POSS containing block copolymer on lithographically defined chemical template with morphology control by solvent vapour, *Macromolecules*, 45(1), 292-304.
- Kota, A.K., Kwon, G., Choi, W., Mabry, J. M., and Tuteja, A., 2012, Hygro-responsive membranes for effective oil-water separation, *Nat Commun*, 3, 1025.
- Yang, S., Pan, A., and He, L., 2014, POSS end-capped diblock copolymers: synthesis, micelle self-assembly and properties, *J Colloid Interface Sci*, 425, 5-11.
- Yang, S., Pan, A., and He, L., 2015, Organic/inorganic hybrids by linear PDMS and caged MA-POSS for coating, *Materials Chemistry and Physics*, 153, 396-404.
- Pan, A., Yang, S., and He, L., 2015, POSS-tethered fluorinated diblock copolymers with linear- and star-shaped topologies: synthesis, self-assembled films and hydrophobic applications, *RSC Adv.*, 5(68), 55048-55058.

This page has been left intentionally blank.

DIFFERENTIAL EFFECTS OF TREATMENTS ON THE DYNAMICS OF BIOLOGICAL RECOLONISATION OF TRAVERTINE: CASE STUDY OF THE TIBER'S EMBANKMENTS (ROME, ITALY)

S. Pascucci¹, F. Bartoli¹, A. Casanova Municchia¹ and G. Caneva^{1*}

Abstract

Monuments exposed to the environment are subject to numerous causes of degradation, including the action of biological organisms forming patinas and crusts of various colour and different aggressiveness. However, these patinas can be used in contemporary art for the creation of drawings, as in William Kentridge's project, along the embankment of the Tiber River, illustrating the "Triumphs and Laments" of Rome history. More than eighty figures will be created through selective cleaning of the black biological patina on travertine, which is much used in Rome but little studied in biocide tests. The aim of this study is to understand which chemical treatments could delay the biological growth in the cleaned area, extending the lifetime of the images. Three commercial biocides (Algophase[®], Biotin R[®], Preventol R80[®]) and two water-repellents (Hydrophase superfici[®], Silo 111[®]) were chosen and tested *in situ* (30 tests areas, with three repetition) using different concentrations and mixtures, in accord with the safety of users and environment. In order to limit the re-colonization after treatments, colour measurements and portable optical microscope were conducted both on the bare surface of the stone (the control test) and on the stone after chemical treatments. The results show that each product has different biocidal efficacy and a different colorimetric response. The preventive treatment of Preventol R80[®] with subsequent application of biocides in mixture had the best results in preventing re-colonisation. The use of water repellents alone was revealed to be ineffective in preventing biological recolonization and also determined colorimetric alterations in terms of brightness. The experimental data has provided an improved understanding of the effects of chemical treatments on travertine and of the phenomena of biological recolonization dynamics.

Keywords: biocide, cyanobacteria, biodeterioration, travertine, water repellent

1. Introduction

Outdoor stone monuments are subject to many forms of alteration and degradation, among which is the biodeterioration that takes place when biological organisms forming patinas and crusts varying in colour and different aggressiveness (Tomaselli and Pietrini, 2008; Caneva *et al.*, 2008). These biological patinas have recently been used in contemporary art (Bio-art) as a basis for the creation of drawing and figures. During the late 90s some artists

¹ S. Pascucci, F. Bartoli, A. Casanova Municchia and G. Caneva*
Roma Tre University, Science Department, Rome, Italy
giulia.caneva@uniroma3.it

*corresponding author

became increasingly interested in the use of the tools of modern biology. There are several example of Bio-artist, such as Diego Scropo with his project involving the bioluminescent fungus *Panellus stipticus*, Jun Takita with many different bioluminescence project, or the bio-art created through bacteria design at the American Microbiology Society.

An interesting case study is represented by the embankment of the Tiber River (Rome), where the diffuse blackening of the surface is due by a biological colonization, and not to chemical cause (Bellinzoni *et al.*, 2003; Kumbaric *et al.*, 2012). In 2005 this biological patina present on the embankment was used in the creation of twelve figure representing Roman wolves. These figures, of about 8 meters high, were created by applying a stencil onto the surface and subsequently removing the biological patina through a pressure washer and sandblasting processes, forming the final figure in negative (see Fig. 1a). Unfortunately, three years later the figures had been obscured by biological re-colonization (see Fig. 1b).

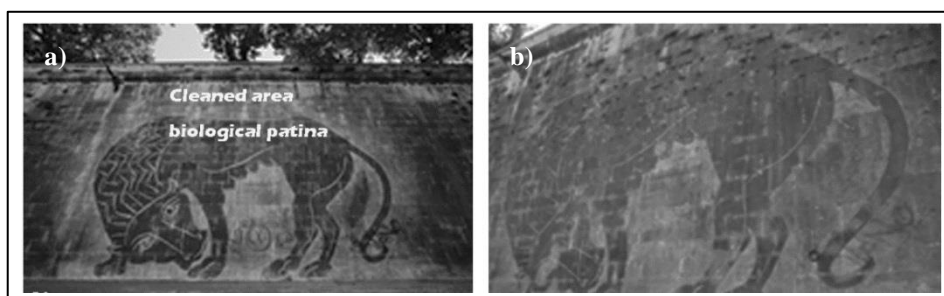


Fig. 1: a) The figure of a wolf on the Tiber embankment (2005);
b) The same figure three years later.

In April 2016 the artist William Kentridge together with TEVERETERNO foundation will realise a project for the city of Rome entitled “*Triumphs and Laments*”, a procession of eighty figures along the embankment of the Tiber River, between Ponte Sisto and Ponte Mazzini, using the same technique as the wolves. Based on previous experience, our research project is aimed to make long lasting in time this contemporary frieze by choosing the most suitable methodologies for preventing or slowing down the biological growth in the areas subjected to removal of the biological patina. There is an extensive literature on the effectiveness of water-repellents and biocides to prevent the re-colonization on the stone, tested overall in laboratory conditions (Nugari *et al.*, 1993; Tiano *et al.*, 1994; Urzì and De Leo, 2007; Bartolini and Ricci, 2009; Moreau *et al.*, 2008; Delgado and Charola, 2011; Pinna *et al.*, 2012). However, little has been reported on outdoor conditions, particularly with regard to travertine substrata.

Considering such lack in the literature, the aim of this study is to understand which chemical treatments could delay the biological growth in the cleaned area, extending the lifetime of the images, and the re-colonization dynamic process in different condition test.

2. Materials and Methods

2.1. Case study

The Tiber embankments are composed of load bearing walls, which are extremely deep and about 10 meters high, covered with travertine slabs of varying sizes. The travertine stone is

a sedimentary and limestone rock characterised by a low porosity but with a high number of macro-pores, which can increase the water content. Field tests were carried out in the stretch of the Margherita bridges.

The porosity combined with the inclination of the wall, along with input water, influence the amount of water contained in the substrate, contributing significantly to the rate of biological growth on the embankments. The blackish patina found on embankments walls is composed mainly of cyanobacteria and green algae species. In detail, *Chroococcus lithophilus*, *Myxosarcina spectabilis*, *Tolypothrix byssoidea* and *Synechocystis pevalekii*, occur frequently, while rarely *Synechococcus aeruginosus*, *Muriella terrestris*, *Chlorococcum sp.* and *Scytonema julianum*. *Nostoc punctiforme* and *Desmococcus vulgaris* appear rarely (Bellinzoni *et al.* 2003, Kumbaric *et al.* 2012). The maximum coverage of these patinas was found in the northern areas with no tree cover.

2.2. Tests with biocides and water repellents

The present study involves a series of tests using of mixtures of three chemical biocides and two water-repellents in various concentrations (Algophase[®] + Hydrophase superfici[®], Biotin R[®] + Silo 111[®] and with pre-treatments by Preventol R80[®]), and the application of water repellents alone. These biocides were selected according to the low toxicity and the safety for the users and environment (Caneva *et al.*, 2008). The mixtures of biocides with water repellents were selected according to their effectiveness against the biological recolonization on stone in outdoor conditions (Charola *et al.*, 2007; Urzì and De Leo, 2007; Pinna *et al.*, 2012) (Tab. 1).

Tab. 1: Features of products applied on test area.

<i>Biocides:</i>		
Product	Active principle	Concentration
Preventol R80 [®]	alkyl-dimethyl-benzylamine chloride	4% in distilled water
Algophase [®]	2,3,5,6-tetrachloro-4-methylsulfonyl-pyridine	5% and 3% of Algophase directly in Hydrophase Superfici
Biotin R [®]	OIT and Carbamate	4% and 3% of Biotin R directly in silo 111
<i>Water repellents:</i>		
Product	Active principle	Concentration
Silo 111 [®]	Methylethoxy polysiloxane	10% in white spirit
Hydrophase Superfici [®]	alkyl alcoxy silane	40% in isopropyl alcohol

One biocide (Preventol R80[®] (4% v/v)) was applied alone, while the other two biocides, Algophase[®] (5% v/v and 3% v/v) and Biotin R[®] (4% v/v and 3% v/v), were applied in different concentration in mixtures with water repellents, respectively in Hydrophase Superfici[®] (ready to use 40%) and Silo 111[®] (ready to use 10%).

In order to choose the best products, the appropriate mixture and the right concentration, 10 tests were performed in three series of repetitions on the embankments walls. For 4 tests (T1, T2, T3 and T4) a preventive treatment with Preventol R80[®] was applied, followed by the application of a biocides and water repellents mixture, for another 4 tests (T5, T6, T7 and T8) we applied the biocides and water repellents mixtures only and finally, 2 further tests (T9 and T10) looked at water repellents alone. All products were applied with a paintbrush until the entire surface was thoroughly saturated with the solutions.

2.3. Application of treatments

Close to Ponte Regina Margherita, 8 areas of cleaning of overall size of 64×64 cm were prepared. Each area consisted of a frame enclosing a circular or quadrangular cleaning test area, and the cleaning tests were carried out with a gently pressure washer (Fig. 2). For the purpose of the experiment, the cleaning tests areas were divided into 30 individual test areas (10.5×4 cm each) onto which the products were applied, and 4 areas were left untreated as a control.

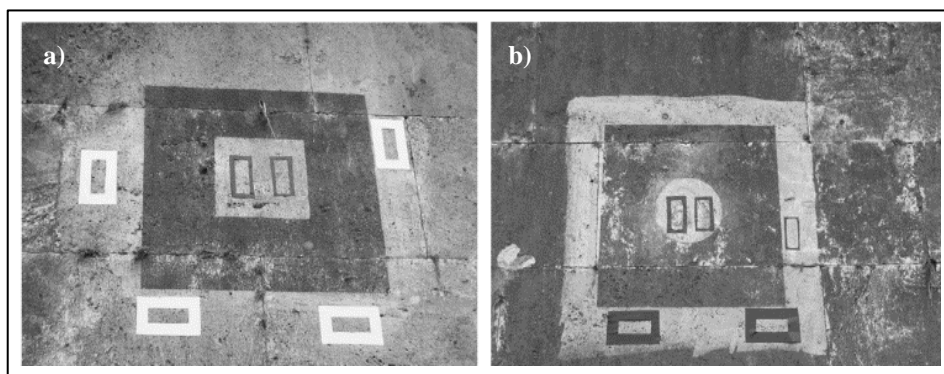


Fig. 2: Two examples of quadrangular (B) or circular (A) cleaning test area.

At the beginning: 3 tests areas were treated with Preventol R80[®] and Algophase[®] 5% v/v plus Hydrophase superfici[®] (T1); 3 tests areas were treated with Preventol R80[®] and Algophase[®] 3% v/v plus Hydrophase superfici[®] (T2); 3 tests areas were treated with Preventol R80[®] and Biotin R[®] 4% v/v plus Silo 111[®] (T3); 3 tests areas were treated with Preventol R80[®] and Biotin R[®] 3% v/v plus Silo 111[®] (T4); 3 tests areas were treated with Algophase[®] 5% v/v plus Hydrophase superfici[®] (T5); 3 tests areas were treated with Algophase[®] 3% v/v plus Hydrophase superfici[®] (T6); 3 tests areas were treated with Biotin R[®] 4% v/v plus Silo 111[®] (T7); 3 tests areas were treated with Biotin R[®] 3% v/v plus Silo 111[®] (T8); 3 tests areas were treated Silo 111[®] ready to use 10% (T9); 3 tests areas were treated Hydrophase superfici[®] ready to use 40% (T10); and 4 were left untreated as control areas (C).

2.4. Field analysis

The treated areas test and the untreated control areas were analysed using microphotos and colour measurements. The first measurements were taken one month after the application of the treatments, in April 2014, after which measurements were taken once every two months until February 2015. Re-colonization was evaluated using a photomicrograph coverage

analysis using through Image J software, and with a colorimetric analysis performed in situ during one year of observations comparing treated and untreated areas.

2.4.1. Stereomicroscope observations

In order to detect on site the biological re-colonization, a selection of treated and untreated areas selected were observed with a portable stereomicroscope (PCE-MM200 Microscope) using $\times 20$ and $\times 60$ magnifications. Micro-photos were taken at three separate points for each test due to the heterogeneity of travertine. The images obtained were then processed with ImageJ 3.0 software (Collins, 2007). This software allows for measuring the abundance of pixels pertaining to each colour class, quantifying the biological growth on the stone (as a percentage).

2.4.2. Colour measurements

Colour measurements were performed using a by Konica Chroma Meter CR 200 in accordance with the procedure described in European Standard EN15886:2010. Ten measurements were carried out for each test areas; results obtained on the test area with the same treatment have been averaged to obtain one single data point. Colour variation values are given using the *CIE-L*a*b** system (Uni EN15886:2010) and colour coordinates L^* , a^* and b^* determine the colour location in colour space: L^* indicates lightness; a^* (redness–greenness), and b^* (yellowness–blueness). The values of L^* , a^* and b^* were measured in selected treated areas, and in 4 untreated control tests. Total color variation (ΔE) was calculated from three colour parameters with the formula:

$$\Delta E = [(\Delta L^*)^2 + (\Delta a^*)^2 + (\Delta b^*)^2]^{1/2} \quad (\text{Eq. 1})$$

In this study, colour differences were measured between the data point on each treated tests areas and on the untreated areas “control test” areas obtained in April 2014, date of the first measurements (i.e. $L^* = L^*_{\text{treated}} - \Delta L^*_{\text{(untreated)}}$).

3. Results and discussions

For the tests subjected to pre-treatment with the Preventol R80[®] (T1, T2, T3 and T4), values of ΔE (see Fig. 3) show only minor colour changes ($\Delta E \sim 4$). In detail, a year after the application of the products, the treatments T1 and T2 did not significantly modify the colour of the surface, with a ΔE value of ~ 2 and therefore not detectable by the naked eye. The other 4 treatments (T5, T6, T7 and T8) with the sole application of biocides in mixture with water repellents caused significant colour variations with a value of ΔE of ~ 12 . The variations appear unvaried in time. On the other hand, a very strong variation was observed after the application with water repellents alone (T9, T10) characterised by a high ΔE value of ~ 18 . The variations of the parameters a and b are all close to zero, therefore the variation seems to be related mainly to a change in brightness (L^*) than to a change in the colour (a^* and b^*) of the surface. In detail, after one month from the application of all treatments the variation of brightness values (ΔL^*) shows a surface characterized by a general darkening (see Fig. 4). In the following months, tests with pre-treatment by Preventol R80[®] cause a surface whitening up to a value of $\Delta L \sim 3$ (February 2015, in test 3). In correspondence to these tests areas, the on-site observation and the biological coverage analysis by ImageJ software underline a reduction in the biological coverage, especially in test 3 (Preventol R80[®] and Biotin R[®] 4% v/v plus Silo 111[®]). In 4 tests

without Preventol R80[®] the surface became darker over time reaching values of $\Delta L \sim -11$, (February 2015). A re-colonisation of the surface could be the main factor responsible for the colour changes. Image analysis obtained in these tests confirms that, in the course of one year, there was an increase in colonization of almost 5%. In tests with the two water-repellents alone the colour of the surface changed markedly during the monitoring period, showing a clear decrease of ΔL with value of ~ -18 . It is interesting to note that the values of re-colonization in these tests are higher compared to the untreated area test. In accordance with previous study (Charola *et al.*, 2007) Preventol[®] shows to be more effective regarding the rate of re-colonization.

Our findings have shown that biological growth causes also colour changes in the untreated areas due to the re-colonization. The data obtained over time for the control test show a variation for ΔL of ~ -4 , detectable by the naked eye. The biological coverage analysis emphasizes an increase in the re-colonization of almost 8%.

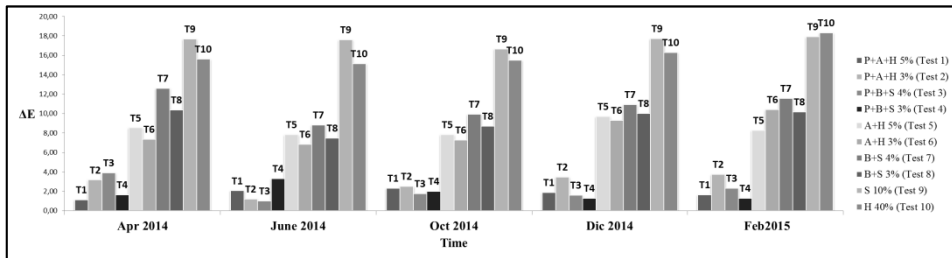


Fig. 3: Colour differences over time between treated and untreated area. The differences are reported as ΔE values.

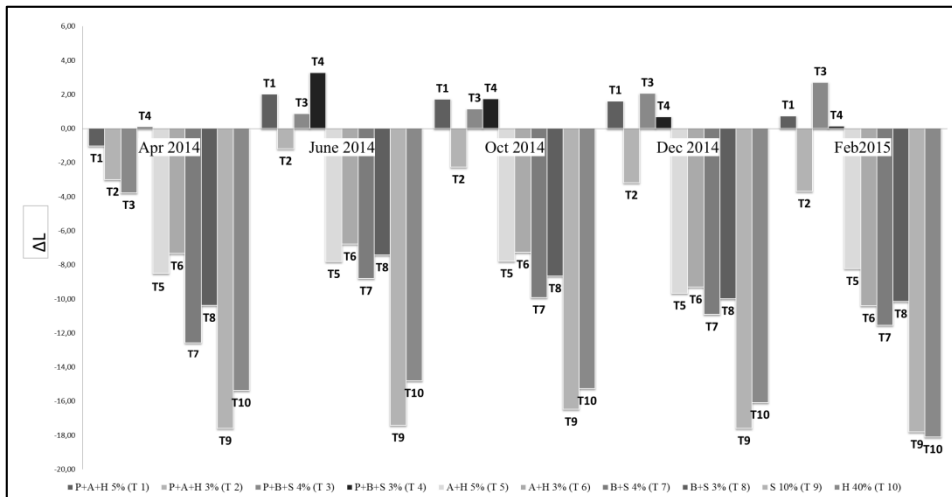


Fig. 4: Colour differences over time between treated and untreated area. The differences are reported as ΔL^* values.

4. Conclusion

Our results showed that tests with the preventive treatment with Preventol R80[®] followed by application of a mixture of biocides and water repellents were effective in preventing or delaying the biological growth. The colour measurements comparing treated tests area and the untreated control tests showed lower colour changes in the four tests characterised by the pre-treatment with Preventol R80[®]. In detail, test 3 (Preventol R80[®] and Biotin R[®] 4% v/v plus Silo 111[®]) gave the best results for the prevention of re-colonization, with a smaller biological coverage. This study provides an important contribution on effectiveness of biocide water-repellent mixtures for outdoor stone monuments, especially with regard to travertine stone, and in evaluating the dynamic of re-colonization processes. Future studies should therefore include follow-up work designed to continue performing tests over time and to identify the kind of re-colonization present on the stone.

References

- Bartolini, M., Pietrini, A.M., Ricci, S., 2007, Valutazione dell'efficacia di alcuni nuovi biocidi per il trattamento di microflora foto sintetica e di briofite su materiali lapidei. *Bollettino ICR*, 14, 101-111.
- Bellinzoni, A.M., Caneva, G., Ricci, S., 2003, Ecological trends in travertine colonisation by pioneer algae and plant communities, *International Biodeterioration & Biodegradation*, 51, 203-210.
- Caneva, G., Nugari, M.P., Salvadori, O. (Eds.), *Plant Biology for Cultural Heritage, Biodeterioration and Conservation*, The Getty Conservation Institute, Los Angeles, 2008.
- Charola, A.E., Anjos, M.V., Rodrigues, J.D., Barreiro, A., 2007, Developing a Maintenance Plan for the Stone Sculptures and Decorative Elements in the Gardens of the National Palace of Queluz, Portugal". *Restoration of Buildings and Monuments*, 13 (6), 377-387.
- Collins, T. J., 2007, ImageJ for microscopy, *BioTechniques*, 43, 25-30.
- Delgado, R., Charola, A.E., 2011, Conservation approach diversity to address the decorative elements in the Gardens of the National Palace of Queluz, Lisbon, Portugal. In: "Conservation of stone in Parks, Gardens and Cemeteries, International Conference", Paris pp. 22-24.
- Kumbaric, A., Ceschin, S., Zuccarello, V., Caneva, G., 2012, Main ecological parameters affecting the colonization of higher plants in the biodeterioration of stone embankments of Lungotevere (Rome), *International Biodeterioration & Biodegradation*, 72, 31-41.
- Moreau, C, Vergès-Belmin, V, Leroux, L, Oriol, G, Fronteau, G, Barbin, V., 2008, Water-repellent and biocide treatments: Assessment of the potential combinations. *J Cult Herit.* 9(4), 394-400.
- Nugari, M.P., Pallecchi, P., Pinna, D., 1993, Methodological evaluation of biocidal interference with stone materials –preliminary laboratory test. In: "Congress on Conservation of Stones and Other Materials". *Proceedings of International UNESCO/RILEM, Paris E & FN Spon, London*, pp. 295-302.

- Pinna, D., Salvadori, B., Galeotti, M., 2012, Monitoring the performance of innovative and traditional biocides mixed with consolidants and water-repellents for the prevention of biological growth on stone. *Science of the Total Environment*, 423, 132-141.
- Tiano, P., Accolla, P., Tomaselli, L., 1994, Biocidal treatments on algal biocoenosis control of lasting activity, *Science and Technology for Cultural Heritage*, 3, 89-94.
- Tomaselli, L., Pietrini, A.M., 2008, In: *Plant biology for cultural heritage: biodeterioration and conservation*. Caneva G., Nugari M.P., Salvadori O., (eds.), The Getty Conservation Institute, Los Angeles. 71-77.
- UNI-EN-15886:2010. Misura del colore delle superfici ICS: 97.195. Conservazione dei Beni Culturali, 2010.
- Urzi, C., De Leo, F., 2007, Evaluation of the efficiency of water-repellent and biocide compounds against microbial colonization of mortars. *International Biodeterioration & Biodegradation*, 60, 25-34.

STATISTICAL ANALYSIS AT THE SERVICE OF CONSERVATION PRACTICE: DOE FOR THE OPTIMISATION OF STONE CONSOLIDATION PROCEDURES

Y. Praticò^{1*}, F. Caruso¹, T. Wangler¹ and R.J. Flatt¹

Abstract

Ethyl silicates are extensively used in the field of conservation to treat various types of stones. It is common belief that the different conditions of temperature, humidity and techniques of application influence the resulting consolidation. In this study, a statistical Design of Experiments (DOE), that allows the exploration of the simultaneous effect of different factors in a limited number of experiments, is used to study this. It is applied to analyse the possible crossed effect of temperature, relative humidity, application procedure, concentration and pre-treatment with a swelling inhibitor on the consolidation of a swelling clay-bearing sandstone. The purpose is to obtain an optimization of the consolidation treatment under conditions that are both reliable in the laboratory and on site. The results obtained with our approach show that the consolidation is not affected by temperature, humidity or the application method. On the other hand, the curing time is strongly influenced by the above-mentioned factors. In particular, it is shown that higher initial moisture content is beneficial to the consolidation treatment as it significantly shortens the curing time.

Keywords: swelling clay-bearing sandstones, ethyl silicate, design of experiment (DoE), swelling inhibitor, consolidation

1. Introduction

The use of ethyl silicates as consolidants for the conservation of various types of stones is well established since the early 20th century (Wheeler, 2005a). The effectiveness and durability of such consolidation treatments is thought to be affected by factors such as temperature, humidity and technique of application, as well as by the chemistry of the product (Zha and Roggendorf, 1991). Most of these aspects are difficult to control on-site and, at the same time, their combined effect on the treatment cannot be characterised through standard laboratory tests, performed at fixed conditions.

As an example, some studies have explored the role of different application procedures on the effectiveness of consolidation treatments (Ferreira Pinto and Delgado Rodrigues, 2012; Franzoni *et al.*, 2014; Moropoulou *et al.*, 2003; Pinto and Rodrigues, 2008), yet without taking into consideration the potential concurrent influence of the environmental

¹ Y. Praticò*, F. Caruso, T. Wangler and R.J. Flatt
Physical Chemistry of Building Materials, Institute for Building Materials, ETH Zürich,
Stefano-Franscini-Platz 3, Zürich 8093, Switzerland
flattr@ethz.ch

*corresponding author

conditions. As a consequence, the information obtained through laboratory studies is not easily transferrable to application in the field.

From a more general point of view, the analysis of processes influenced simultaneously by many different parameters – as in the case of the consolidation with ethyl silicates – represents a challenge in many fields of science. The effort to isolate the effect of each variable makes these kinds of studies very time consuming, as the number of the experiments required increases exponentially with the number of factors involved. For this reason, systematic studies on the coupled effect of several parameters are rather uncommon in the field of conservation, where the time and resources available for research are often very limited.

The Design of Experiment (DOE) is a statistical method that allows for an efficient analysis of multiple factors, requiring only a limited number of experiments (Hoboken, 2008; Weissman and Anderson, 2015).

In this work, we use this methodology to optimize the consolidation strategy for a specific swelling clay-bearing sandstone, which was selected for its homogeneity and representativity of the Swiss molasses that we are studying for the restoration of the Cathedral of Lausanne. Based on preliminary experiments, discussion with conservators and literature review, we decided to examine the combined effects of temperature, humidity, application procedure, concentration and pre-treatment with a swelling inhibitor (Caruso *et al.*, 2012). The effect of the swelling inhibitor is studied only in relation to the initial consolidation. In further work, its influence on the durability of the treatment subjected to wetting/drying cycles in combination with the other factors will be explored. The efficiency of the treatment is assessed through the measurement of the final increase in dynamic elastic modulus (so called “total consolidation”) and the time necessary to reach this final value (“curing time”).

A sketch of the considered factors and responses is shown in Fig. 1:

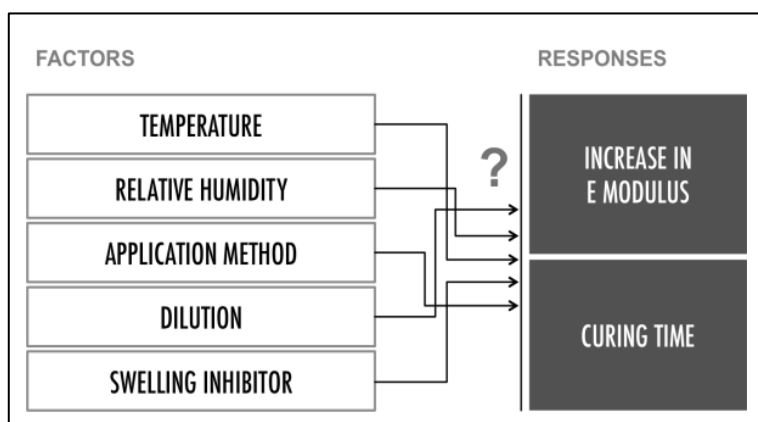


Fig. 1: Scheme of factors and responses in a consolidation treatment with ethyl silicate.

Dynamic elastic modulus measurements have the advantage of being non-destructive and therefore very useful for testing property evolution over time. While more extensive characterization would provide additional insights into differences of consolidation, the measured responses are sufficient to compare the efficiency of the application method as well as the other factors considered.

2. Experimental

2.1. Materials

The stone used is a Molasse Blue from Villarlod (Molasse de Villarlod.ch SA, Farvagny, FR, Switzerland). Stone samples were cut in cylinders of 5 cm of diameter and 5 cm of length from three different blocks, and randomized among the runs. The samples were cut so as to keep the bedding direction perpendicular to the cylinder axis. The consolidant used is SILRES® BS OH 100 (Wacker Chemie AG, Burghausen, Germany). This is a solvent-free, ready-to-use product of tetraethyl silicates (40-50%). Absolute ethyl alcohol ($\geq 99.8\%$) purchased from Sigma Aldrich (Sigma-Aldrich Chemie GmbH, Steinheim, Germany) was used for diluting the consolidant. The swelling inhibitor was 1,4-diaminobutane dihydrochloride ($\geq 99.0\%$), also purchased from Sigma Aldrich.

2.2. Methods

2.2.1. Design of Experiment (DOE)

The DOE was run on JMP 11.0 (SAS Institute Inc., Cary, NC, USA). The type of design employed was a fractional factorial with 2 replicates, and 5 two-level factors for a total number of 48 runs. The factors and their levels are shown in Tab. 1.

Tab. 1: Factors and levels chosen for the DOE study. Factors marked with a single asterisk (*) are continuous; factors marked with two asterisks (**) are categorical.

Factor	Low level	High level
Temperature *	10°C	30°C
Relative humidity *	50%	85%
Dilution *	Pure	1:3 (v/v) in ethanol
Application method **	Wet-on-wet	Sorptivity
Pre-treatment with swelling inhibitor**	No	Yes

The levels of temperature and relative humidity (*RH*) were chosen to maximize the difference between the levels, yet remaining in the range of plausible conditions for an on-site consolidation campaign (Wheeler, 2005b). Climate analysis was performed on local weather data (provided by IDAWEB Meteo Suisse) and by means of on-site measurements in the Swiss region.

The analysed responses were total consolidation and curing time. The curing time was estimated in terms of change in dynamic Young's modulus (E_{dyn}) computed from ultrasonic

pulse velocity (UPV) measurements. The curing time was defined as the necessary time for the ΔE_{dyn} to become lower than the uncertainty of the measurement ($\pm 10\%$).

The total consolidation was expressed in the form of final percentage increase of E_{dyn} . Since the dynamic elastic modulus depends on the RH at which the UPV measurement is performed, the initial and final E_{dyn} were recorded at the same conditions for every sample to obtain comparable results. More in detail, the initial E_{dyn} was measured on oven-dried, untreated stones; the final E_{dyn} was measured on fully consolidated samples, after equilibration at 20°C and 50% RH .

The UPV was measured with a Pundit Lab by Proceq SA (Schwarzenbach, Switzerland) with standard 54 kHz transducers mounted on a custom-modified optical rail by Geotron-Elektronik (Pirna, Germany). The customization of the device was developed to ensure a constant pressure between the transducers and the samples, by means of an air cylinder actuated by compressed air at 4 bars. Effective contact between the transducers and the specimens is achieved by means of a dry couplant of 2 mm thickness (Aqualene dry couplant, Olympus Scientific Solutions Americas Inc., MA, USA). A Mettler-Toledo PM4000 technical balance (Mettler-Toledo GmbH, Greifensee, Switzerland) was used to record the mass changes of the samples.

2.2.2. *Pre-treatment with swelling inhibitor*

Prior to the pre-treatment, all the samples were oven-dried for 72 hours at 105°C and then equilibrated at 20°C and 50% RH for one week. The samples were then immersed in a 0.3 mol/L aqueous solution of 1,4-diaminobutane dihydrochloride for 20 hours.

2.2.3. *Consolidant application*

All samples were pre-equilibrated at the target curing conditions before the consolidation treatment. Stable climatic conditions (maximum oscillations: $\pm 2^\circ\text{C}$ for the temperature and $\pm 8\%$ for the RH) were obtained in a Vötsch VC 4060 (Vötsch Industrietechnik GmbH, Balingen-Frommern, Germany) and in a Feutron KPK600 (Feutron Klimasimulation GmbH, Langenwetzendorf, Germany) climatic chambers.

Two different methods of application were used during this study: an application by sorptivity, and a cyclic “wet-on-wet” application. Both methods reproduce the effect of a consolidation treatment applied only on one side of a stone surface.

2.2.3.1. Sorptivity

The cylindrical samples were hung below a technical balance to monitor the mass increase, with one of the faces in contact with the consolidant. All the other surfaces of the sample were sealed with Parafilm to avoid evaporation. The treatment was stopped when the samples reached saturation.

2.2.3.2. Wet-on-wet applications

A cyclic wet-on-wet application was used to simulate on-site practice, such as the cyclic application with a brush. To control the quantity applied for each application, a pipette was used to spread the consolidant over the surface. The mass of consolidant absorbed at each application was measured with a technical balance. The procedure (quantity per application, as well as frequency of the applications) was designed according to the recommendations of the producers and case studies reports (Commission technique de la cathédrale de

Lausanne, 2012). The penetration of the consolidant (assessed by visual observation and mass uptake measurements) was always at least 4 cm. This depth of treatment would allow for the consolidation of severely damaged stones (swelling clay-bearing stones typically show scaling at up to a depth of 3 cm (Furlan and Girardet, 1996).

The application procedure was as follows: two cycles of applications were performed with an interval of 3 hours. Each cycle consisted of 3 applications of 0.4 g of consolidant every 5 minutes. Every 3 applications, an interval of 15 minutes was taken.

3. Results and discussion

Values of curing time across different combinations of factors varied from 7 to 98 days, whereas values of total consolidation varied from 0% to over 150%. The DOE analysis of the influence of the factors on total consolidation and curing time is presented in Fig. 2.

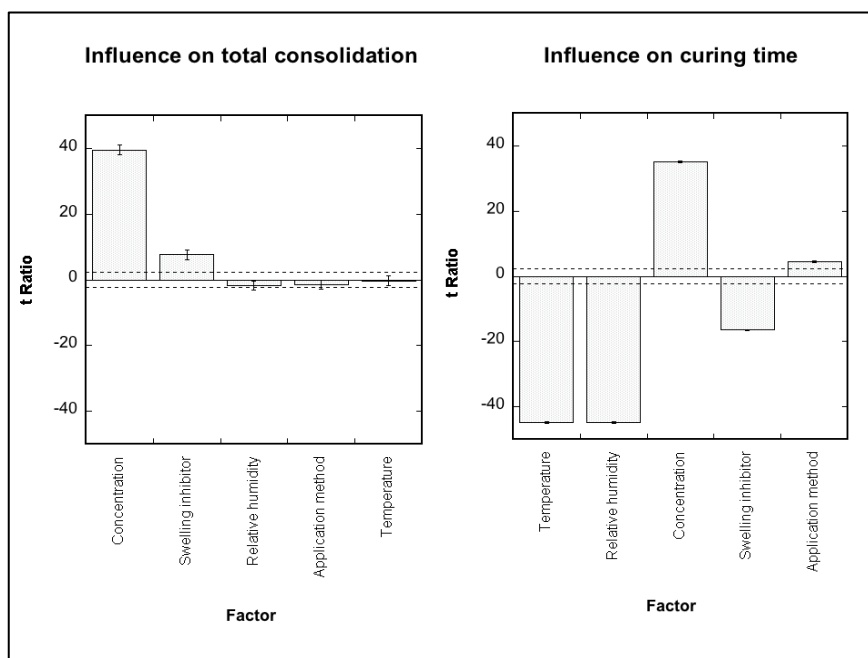


Fig. 2: *t*-Ratio plot 5 of the factors influence on the total consolidation (left) and on curing time (right). The *t*-Ratio is the ratio of the parameter estimated to its standard error and quantifies the influence of a factor. The effect of a factor is considered significant with a 95% confidence when the *t*-Ratio is higher than the critical value at 0.05 significance level (horizontal dashed line in Fig. 2). Positive numbers indicate a proportional influence of the factor on the response (i.e. higher concentration leads to a higher total consolidation), whereas negative numbers indicate a negatively proportional effect (i.e. high relative humidity decreases the curing time).

Fig. 2 (left) shows that the total consolidation is not affected by differences in the environmental condition or in the application procedure. On the contrary, the concentration of the consolidant seems to play a substantial role. In fact, despite what has been suggested in the literature (Scherer and Wheeler, 2009), under the conditions of our experiments, the dilution of the product leads to a dramatic decrease in the effectiveness of the consolidation (in some cases not showing any significant E_{dyn} increase), and – at the same time – does not show any positive effect on the penetration of the product (sorptivity data not shown).

The pre-treatment with the swelling inhibitor also causes an increase in the elastic modulus of the stone. This effect is known for this type of stone (Gonzalez and Scherer, 2004), and has been suggested to result from the ability of the swelling inhibitor to prevent the separation of the clay layers, but does not appear to be related to the consolidation process. In fact, the final positive effect recorded is equivalent to the initial E_{dyn} increase obtained on the unconsolidated stone.

On the other hand, most of the above mentioned factors show a significant effect on the curing time (Fig. 2, right). In particular, temperature and humidity have the strongest influence, drastically decreasing the time necessary for the curing when set on higher values. This is shown in Fig. 3, where the curves of samples treated with the same procedure but cured at different temperature and RH are compared.

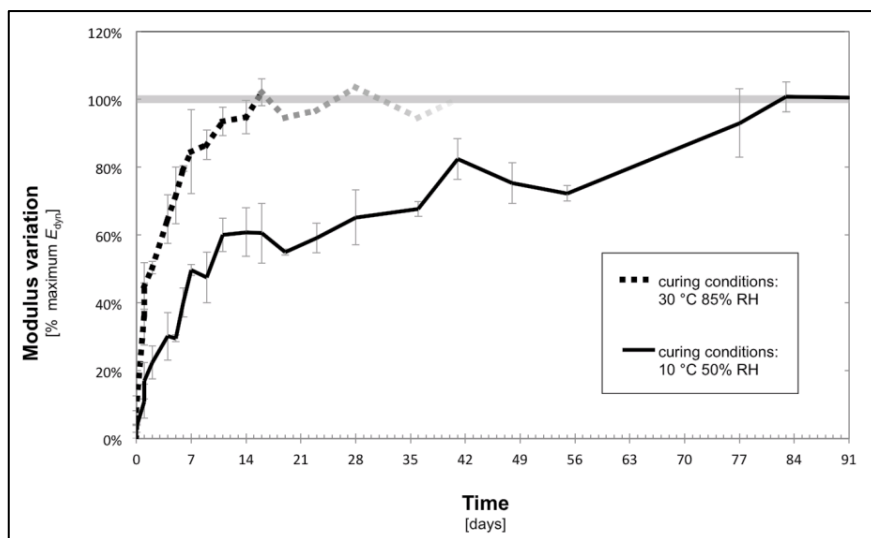


Fig. 3: Curing of samples consolidated with pure Wacker OH 100 by wet-on-wet applications, not pre-treated with swelling inhibitor. The curves are normalized to the highest total consolidation reached.

In this specific case, the samples treated at $T=30^{\circ}\text{C}$ and $RH=85\%$ showed a curing time as low as 14 days, whereas samples treated at $T=10^{\circ}\text{C}$ and $RH=50\%$ needed up to 85 days to reach a stable elastic modulus. With samples pre-treated with swelling inhibitor, this effect becomes even more evident, showing values of curing time of 7 days for samples cured at $T=30^{\circ}\text{C}$ and $RH=85\%$, and 98 days for samples cured at $T=10^{\circ}\text{C}$ and $RH=50\%$.

This seems to indicate that the consolidation depends on both the initial moisture content during a first phase and on the vapour pressure of water in the surrounding environment in a second phase, as suggested by the evolution of modulus in Fig. 3.

This can be explained assuming that the consolidation kinetics of the sample in the second phase is limited by the vapour diffusion and progressive uptake of water by the unreacted consolidant in the porous network. This must also be at stake in presence of the swelling inhibitor. However, the reason why this compound would accelerate the consolidation at high temperature and slow it down at a lower temperature is not obvious. Various processes, including a basic catalysis of the condensation may be involved, but we presently cannot advance a solid explanation for it.

4. Conclusions

This paper presents a study of the factors affecting the success of a stone consolidation treatment with ethyl silicates. The efficiency of the treatment on a clay-bearing sandstone was assessed by varying temperature, relative humidity, application procedure, concentration of the consolidant, and pre-treatment with a swelling inhibitor and by measuring the total consolidation and the time necessary to reach this final value.

One of the original aspects of this work was the use of the Design of Experiment for exploring the above factors and the way they dictate the effectiveness of the consolidation process. The results show that this kind of approach enables the study of such a multi-variable problem and for the extrapolation, from a relatively small number of experiments, of general principles useful for on-site practice.

The total consolidation (increase in dynamic modulus) only depends on the product used and remains the same regardless of the climatic conditions or the chosen procedure of application. This also implies that experimental results obtained through a controlled sorptivity procedure can be transferred to on-site “wet-on-wet” application.

Swelling inhibitors slightly increase the total consolidation, but in the same relative way they increase the elastic modulus of the untreated stone. This suggests that they do not directly interact with the consolidation process. On the other hand, a pre-treatment with swelling inhibitors decreases the curing time.

Finally, temperature and relative humidity strongly influence the curing time. In particular, curing time decreases drastically when the humidity “available” in the stone increases. This provides a completely new perspective with respect to what field experience claims about the factors affecting consolidation. Indeed, most of these reports probably refer to a fixed time period that can be expected to be shorter than what is needed to reach ultimate consolidation under detrimental conditions. Certainly this is relevant to practitioners, but not in terms of the monument being consolidated. We hope that this observation will stimulate critical thoughts on this important subject.

Acknowledgements

The authors would like to thank Mr Fred Girardet (Rino S.A.R.L.) for very useful discussions and Mr Christophe Amsler and Ms Olga Kirikova for their openness and support in discussing conservation issues in relation to the Cathedral of Lausanne.

References

- Caruso, F., Wangler, T.P., Aguilar Sanchez, A.M., Richner, H., Melchior, J., Flatt, R.J., 2012. Effect of swelling inhibitors and self restraint on the durability of ethyl-silicates consolidants applied to clay-bearing stones, in: 12th International Congress on the Deterioration and Conservation of Stone Columbia University. New York.
- Commission technique de la cathédrale de Lausanne, 2012. Déontologie de la pierre. Stratégies d'intervention pour la cathédrale de Lausanne. Actes Colloq. Pluridisciplin. 14 15 Juin 2012 hors-série 1.
- Ferreira Pinto, A.P., Delgado Rodrigues, J., 2012. Consolidation of carbonate stones: Influence of treatment procedures on the strengthening action of consolidants. *J. Cult. Herit.* 13, 154–166.
- Franzoni, E., Graziani, G., Sassoni, E., Bacilieri, G., Griffa, M., Lura, P., 2014. Solvent-based ethyl silicate for stone consolidation: influence of the application technique on penetration depth, efficacy and pore occlusion. *Mater. Struct.* 1–13.
- Furlan, V., Girardet, F., 1996. Pollution atmosphérique et dégradation de la molasse, in: *Matériaux de construction. Pierre. Pollution atmosphérique. Peinture murale.* Laboratoire de Conservation de la Pierre. Département des Matériaux., Lausanne.
- Gonzalez, I.J., Scherer, G.W., 2004. Effect of swelling inhibitors on the swelling and stress relaxation of clay bearing stones. *Environ. Geol.* 46, 364–377. Hoboken, N., 2008. *Design and Analysis of Experiments*, 7 edition. ed. Wiley.
- Moropoulou, A., Kouloumbi, N., Haralampopoulos, G., Konstanti, A., Michailidis, P., 2003. Criteria and methodology for the evaluation of conservation interventions on treated porous stone susceptible to salt decay. *Prog. Org. Coat.*, Athens 2002 48, 259–270.
- Pinto, A.P.F., Rodrigues, J.D., 2008. Stone consolidation: The role of treatment procedures. *J. Cult. Herit.* 9, 38–53.
- Scherer, G.W., Wheeler, G.S., 2009. Silicate Consolidants for Stone. *Key Eng. Mater.* 391, 1–25.
- Weissman, S.A., Anderson, N.G., 2015. Design of Experiments (DoE) and Process Optimization. A Review of Recent Publications. *Org. Process Res. Dev.* 19, 1605–1611.
- Wheeler, G., 2005a. Historical overview, in: *Alkoxysilanes and the Consolidation of Stone.* Getty Publications, pp. 1–11.
- Wheeler, G., 2005b. Practice, in: *Alkoxysilanes and the Consolidation of Stone.* Getty Publications, pp. 69–88.
- Zha, J., Roggendorf, H., 1991. Sol–gel science, the physics and chemistry of sol–gel processing, Ed. by C. J. Brinker and G. W. Scherer, Academic Press, Boston 1990, xiv, 908 pp., *Adv. Mater.* 3, 522–522.

VACUUM-CIRCLING PROCESS: A INNOVATIVE STONE CONSERVATION METHOD

E. Pummer^{1*}

Abstract

The vacuum-circling process (VCP) has been developed to minimise and avoid disadvantages associated with common surface treatments with silica acid ester (ESE). Shallow treatments with ESE using the “run-over application”, “brushing application” and “pad application” have been not able to achieve a profound penetration. The possible outcomes are the shedding of a few millimetres’ thickness, and spalling, which irretrievably destroys the original surface within a few years of treatment. The main problem of consolidation by plunging is that non-accelerated ESE may be leaking or sinking after treatment. Even objects with a highly damaged structure are often able to be treated with ESE using VCP because of the possibility of deep penetration when common ESE treatments fail. The method is also suitable for the consolidation of stone objects with surfaces showing varied or reduced permeability. The use of various strengthening agents is possible, and it is also possible to treat other materials, such as wood or concrete. Contamination of the environment, adjacent areas and users are eliminated using the process. Following restoration, intervals between treatments are increased due to the long-lasting conservation effects achieved by VCP treatment. The method of vacuum-circling has been successfully applied to a wide range of international monuments of various stone types. The effectiveness has been proven and documented by scientific methods via acknowledged institutes and also as part of promoted research projects by the EU and Deutsche Bundesstiftung Umwelt.

Keywords: vacuum, strengthening, consolidation, stone conservation, demineralisation

1. Vacuum-Circling Process (VCP) application

VCP (European patent No. 1 295 859/Austrian patent No. E 366.232, patents owned by Erich Pummer GmbH) offers a possibility for restoring monuments, stone sculptures, façades and other freestanding and weathered objects. A key advantage of applying the VCP is the high-level reliability observed due to the optimal penetration properties of the various strengthening agents in porous stone or other materials. This is an existentially important requirement, since a large number of listed monuments have suffered serious consequential damage in the last few decades as a result of pure surface treatment. This vacuum technology-based method is reliable and economic to apply *in situ* or in workshops. There are no superfluous chemicals that could build up or leak out, making this a user- and environment-friendly work method. With easy technical adaptations it is also

¹ E. Pummer*

Atelier Erich Pummer GmbH, Austria
office@atelier-pummer.at

*corresponding author

possible to use the treatment for demineralisation and drying. To create an airtight environment, the object in question—there are no limits to the size or form of the objects—is shrink-wrapped in solvent-resistant plastic film. A vacuum pump is used to draw the air out from the plastic film bag and also from the stone object’s pore volume. Once a relative vacuum has been achieved, a precise dosing system allows the injection of an appropriate strengthening agent which immediately distributes itself evenly in the vacuum and deep into the stone, even when the surface is predominantly covered with impenetrable coatings, as investigations have shown. The whole process is completely odourless, without any overspill.

The equipment is easily moveable and offers the possibility to conserve objects in any position or situation, on buildings or freestanding (Fig. 1 and Fig. 2). The principle of VCP is shown in Fig. 2.



Fig. 1: Mobile VCP equipment, vacuum pump (in the back of the van), balance tank (middle), tank A&B combination (left; see Fig. 2 for further details).

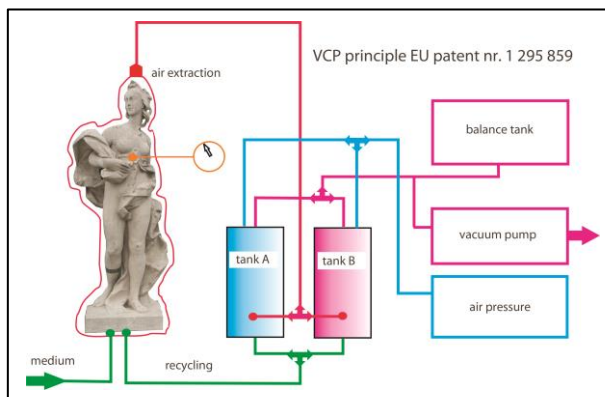


Fig. 2: Principle of the vacuum circling process.

2. Operation, utilisation and results by object examples

2.1. Demounted Madonna by Austrian sculptor Joseph Käßmann (1845)

2.1.1. Processing

The sculpture was situated on a façade in the 7th district of Vienna. It is sculptured in a very porous calcareous Arenite with an original polychromic executed using an oil technique. The sculpture was demounted and was transported to the restoration laboratory of the University of Applied Art. The conservation and restoration of this statue are the subject of a diploma thesis with the task of strengthening the inner structure of the Madonna, which is covered by several layers of oil paint (2, see Paper for the 13th International Congress on the deterioration and Conservation of Stone 2016; M. Milchin *et al.* 2015). As a first step, the whole statue was wrapped in polypropylene fleece material (Fig. 3). This material had the function of protecting the surface of the statue but also to avoid leaking of the polyethylene foil used to create the airtight environment. On the highest points of the statue, purging valves were fixed with the foil. At the lowest position, inflow valves were mounted. A manometer for controlling the negative pressure inside the foil was also connected (Fig. 3).



Fig. 3: VCP treatment of the 160-cm-high statue.

After evacuating the air, the inflow of the strengthened medium silica acid ester (ESE) 300E/accelerated began. The negative pressure inside the foil went up to 800 mb and lasted for the whole process of 6 hours. When no more medium was absorbed by the stone the degree of saturation was reached, controlled by measuring the backflow in the circular flow. As a result, 61 kg ESE was absorbed, despite the fact that the surface of the stone was covered by oil paint up to nearly 95 percent. The deep penetration took place through the cracks and small defects in the coating and also through the uncoated base. At the end of the treatment the excess medium was extracted by the lowest inflow valve. The surface was not left with any oversaturation because the fleece had the function of blotting paper and absorbed all surplus liquid. The reaction of the accelerated ESE usually requires a temperature-dependent time of 4–6 weeks. Because of the prompt start of the reaction, the ESE neither drained out nor sunk inside the stone.

2.1.2. Results by drilling resistance

Drilling resistance profiles report the solidity in the different steps of depths. Figures 4 and 5 show examples for drilling resistance profiles. The analysis was done in steps of 1 mm; blue curve – before strengthening, red curve – after strengthening. The results report the successful VCP treatment with ESE 300E. The increase in solidity has been achieved uniformly from the surface right into the depths.

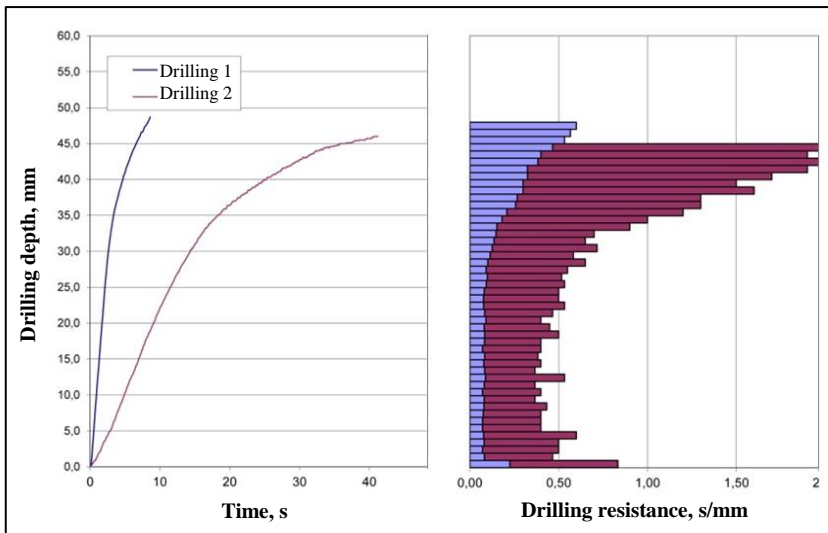


Fig. 4: Profile 1 - Garment fold right, thigh height, covered by several layers of oil paint.

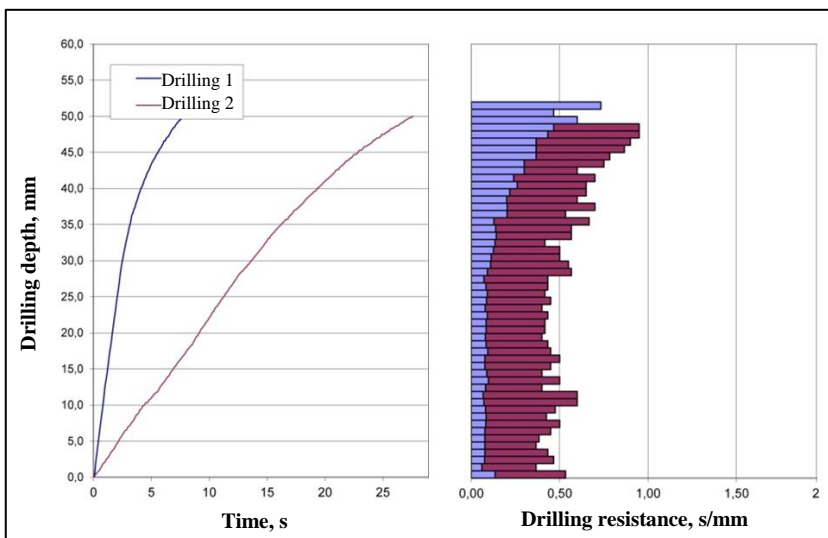


Fig. 5: Profile 2 - Garment fold right, elbow height, covered by several layers of oil paint.

2.1.3. Principle of drilling resistance measurements

The following figures (Fig. 6 and Fig. 7) show the working principle of the device used for measuring the drilling resistance prior and after the treatment by VCP.

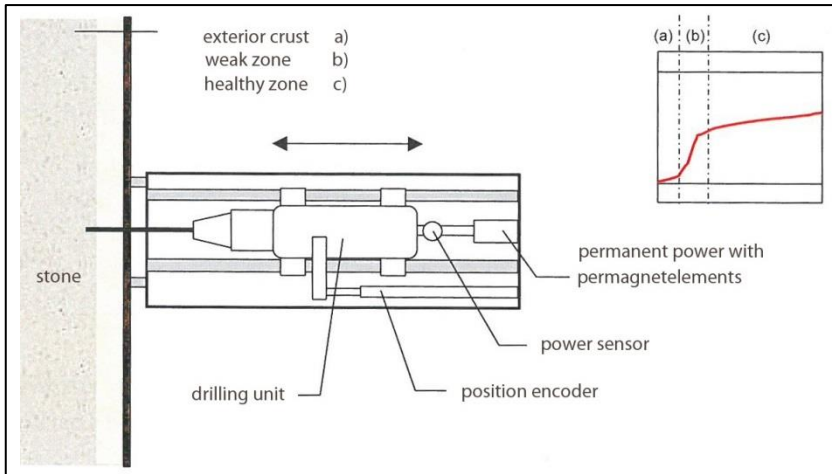


Fig. 6: Principle drilling resistance.

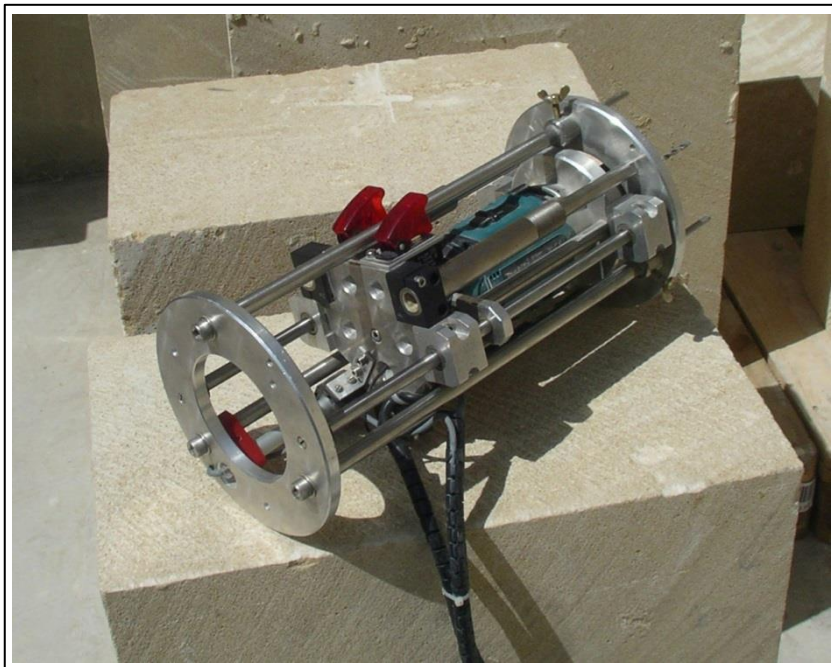


Fig. 7: Device for measuring the drilling resistance device, developed by Dr Günther Fleischer, OFI Technologie & Innovation GmbH, Vienna, Austria.

2.2. *In-situ treatment: Saint Michael's Church in Munich, Germany*

VCP conservation was implemented on four sovereign statues made of Euville limestone. These were: Theovalda, Duke Albrecht V, Duke Wilhelm V and Imperator Maximilian I. The conservation was carried out in situ without any movement of the statues, which had a height of 250 cm. The strengthened media were ESE 300E accelerated and 500E accelerated, applied in succession.

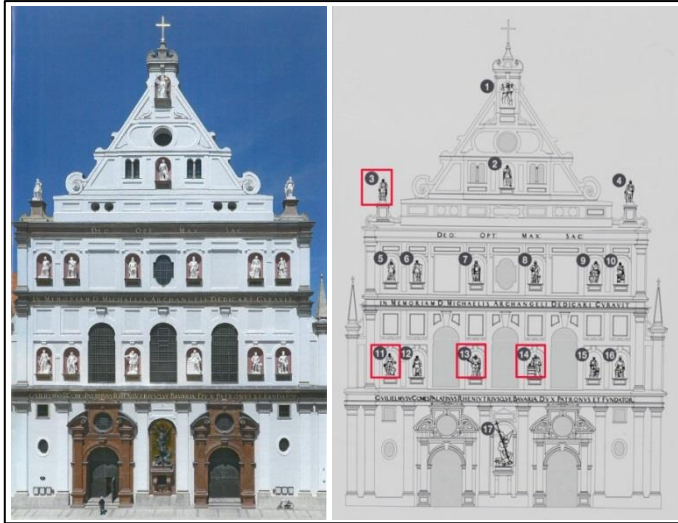
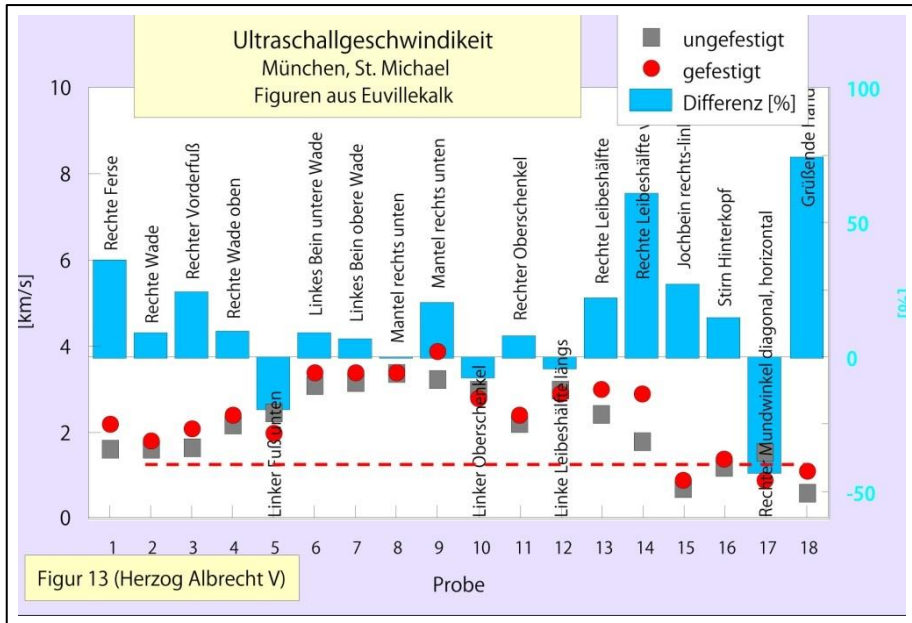


Fig. 8: VCP conservation of four sovereign statues.



*Fig. 9: In situ VCP conservation of Duke Albrecht V; Duration of treatment: 10 hours;
Absorption of ESE: 50 kg.*



*Fig. 10: Ultrasonic measurement report
(grey – not consolidated, red – consolidated, blue – difference)
by Dr Eberhard Wendler, Munich (Germany).*

3. Result of a surface treatment from 20 years ago

VCP conservation was implemented on four sovereign statues made of Euville limestone. These were: Theovalda, Duke Albrecht V, Duke Wilhelm V and Emperor Maximilian I. The conservation was carried out in situ without any movement of the statues, which had a height of 250 cm. The strengthened media were ESE 300E (accelerated) and 500E (accelerated), applied in succession. Up to a depth of 10 mm the outside section is still conserved, but because of the different physical characteristics of treated and untreated stone, the outside section has lost coherence to the inner structure. Therefore the harder outside section shows spalling.



Fig. 11: Photograph of a limestone statue surface-treated with ESE 300 20 years ago.

4. Conclusion

New conservation methods are existentially important, as a large number of listed monuments have suffered serious consequential damage in the last few decades because of pure surface treatment. Most negative effects have been identified on fine-grained limestones and sandstones. Treatments with ESE are having different effects on different types of stone. The common surface treatments use methods including run-over application, brushing application and pad application. By using these treatments, more often than not, the natural capillary absorption is not sufficient to penetrate deep enough inside the stone to permeate the corroded zone to the inner, healthy core of a stone object. Using negative pressure to apply ESE enables the medium to penetrate very deep inside the stone. It is even possible to penetrate the entire already-strengthened outside zone to reach the weak inside zones below. The VCP application is also suitable for the consolidation of stone objects with surfaces demonstrating varied or reduced permeability (M. Milchin *et al.*, 2015). Contamination of the environment, adjacent areas and of users is avoided due to the process.

References

Milchin, M., Weber, J, Krist, G., Ghaffari, and S. Karacsonyi E., 2015, 2, Ethyl-silicate consolidation for porous limestone coated with oil paint – a comparison of application methods / 2016 paper for the 13th International Congress on the Deterioration and Conservation of Stone.

SUSTAINABLE CONSERVATION IN A MONUMENTAL CEMETERY

S. Salvini^{1*}

Abstract

The 'Foce' monumental cemetery in Sanremo (Liguria, Italy), founded in 1838 and used until 1948, was central in a study that the Author carried out since January 2013: it is a site rich in stone artefacts and seriously deteriorated due to the absence of a plan for weed control and conservation, the lack of heirs and the marine environment. In this study, the attention is especially focused on sustainable conservation: the paper describes the specific-drawn maintenance plan for the conservation of the site, it also underlines the importance of using products and techniques with a low environmental impact and finally, it briefly presents the possibilities of socio-economic sustainability of valorisation and management considering the cemetery characteristics. The design of maintenance plan is a key step in modern conservation that is more and more oriented to preventive restoration and continuous care techniques in spite of sporadic and extraordinary restoration interventions. In this work, a lot of effort has been put into the design of an inspection form that needs to be strongly efficient in saving time and economic resources and in the research of low impact activities of maintenance.

Keywords: stone conservation, sustainability, cemetery conservation, green conservation.

1. Introduction: sustainability in conservation

Since the meaning had been defined by Gro Harlem Brundtland in the *UN report Our Common Future* (1987), the term 'sustainability' has been connected with the wish of not to compromise a common heritage in order to permit the future generations respond to their needs. This term has soon become a central key – word of the technical debates of the last decades in many fields, including the Cultural Heritage conservation and management.

Sustainability can be applied at various levels: environmental, social, economic. In this perspective the goals of the conservation discipline are intrinsically sustainable: from a socio-cultural point of view, cultural heritage is a common asset, because it is the inheritance of past generations and a container of the collective identity. The reuse of existing heritage also avoids the consumption of economic and environmental resources caused by the activity of rebuilding and moreover the construction bubble had led to more activities on the BH and there could be still a lot of work (Cinieri and Zamperini 2014)

¹ S. Salvini*

Built Heritage & Landscape (SSBAP) in-Genova, Italy and
Department of Geosciences, Via Gradenigo 6, 35131, Padua, Italy
silvia.salvini@gmail.com

*corresponding author

Unfortunately, in the majority of restoration activities carried out on cultural heritage chemical products are usually employed. These substances can have harmful effects both on workers and on environment and so they are unsustainable: moreover, the product selection is often affected by economic interests or sectorial advertising (Macchia *et al*, 2014). In addition to the toxicity, in the long run these products can produce unexpected negative effects (e.g. interactions with atmosphere and pollutants) and so they could cause a pejorative transformation of the material. Regarding the environmental sustainability there is more attention on the quality design of interventions and on the choice of products and techniques safer for the environment and the operators. Renewable and natural resources are more and more recommended.

Moreover a correct conservation also lead to a conservation of the intangible heritage constituted by the traditional techniques, which were generally more durable than actual ones and which unfortunately are put down less and less. In addition, the energy rehabilitations often do not consider the incorporate energy of a building and constructive characteristics of a specific climate and territory are destroying our heritage. In the past, the non-sustainability of the restoration, against the recognized value of a cultural asset, has often been considered acceptable. While this reasoning may still be acceptable for certain outstanding heritage property, it cannot be extended to the widespread heritage, sometimes not declared of cultural interest and rarely object of public funding.

It is evident that the ideal aim is a condition of balance, which minimizes the development of the decay phenomena. Although it is acknowledged that there is not a ‘perfect recipe’ that could stop perpetually a natural and inevitable phenomenon as the degradation of the cultural heritage, strategies for slowing deterioration phenomena based on the techniques of preventive restoration and maintenance plan are widely recognized in academic debates. It is well established that the successful use of these techniques in spite of isolated emergency restoration activities leads to definitely lower costs in the long run, a condition extremely important, especially for the critical case of the immense and widespread Italian Cultural Heritage, cemetery or not, in need of protection (Salvini and Cinieri, 2014).

2. A monumental cemetery: Issues of conservation

Historic Cemetery Heritage in Europe includes a large number of monuments often dated to the period between the XIX and the XX century, when the funerary sculpture reach its climax. Cemetery heritage, mostly marble, has complex issues of conservation.

Actually, in a cemetery a variety of materials can be observed: different types of stone, metals, Liberty decorations (concrete, glass, ceramic tiles, etc.) and so on. Moreover, in some sites there are high numbers of monuments and complex artefacts like funerary chapels. However, the major problems are related to the lack of care. In fact, even if the uncontrolled presence of heirs could signify wrong procedures in most cases they are beneficial. A consequence of abandonment is the boost of the weed control related issues that in some contexts encouraged by particular climatic conditions can became a thorny question.

2.1. Case study: The ‘Foce’ monumental cemetery

2.1.1. History of the ‘Foce’ monumental cemetery of Sanremo, Italy

The ‘Foce’ monumental cemetery was founded in 1838, soon after a cholera epidemic in 1837, and now counts about 2500 graves, one third of which belongs to foreigners,

evidences of the city as outstanding tourist destination of the international upper class during the Belle Epoque (1880-1915). In fact, thanks to its good climate the city was renowned for the recovery from the diseases of chest by many people, even by Maria Alessandrovna, Czarina of Russia. Since the end of XIX century many important people came to Sanremo from all over the world and sometimes here they passed by and were buried: people like the painter Edward Lear, the anatomist Arthur Hill Hassal, the lady in waiting of Victoria Queen Lady Caroline Giffard Phillipson, Prussian nobles, a good number of Russian aristocrats, and many others...

This cemetery is located near the shore in the Western section of the city of Sanremo between the Foce and San Bernardo streams because the previous and nearer Vallotto cemetery, had become insane for the city of Sanremo due to the development of the hygienist theories which culminated in the Napoleonic edict of Saint Cloud (1806). The present city cemetery is the "Armea" in the Eastern limit of the city, a new site that has been inaugurated in 1948 causing the partial abandonment of the 'Foce' cemetery. In 1980 the cemetery was declared "Monumental Cemetery" in order to protect the area from building speculation and now, even if some graves had been moved to the new cemetery the visit of the Foce cemetery is a true dip in the past, in the golden age of the city of Sanremo.

2.1.2. Specific site issues

Unfortunately, this cemetery is seriously deteriorated. The causes are numerous, the most important being the lack of heirs and the absence of a plan for weed control and conservation. The coastal environment also greatly contributes to the acceleration of the degradation of the building materials, especially metallic ones.

The major part of the graves date back before 1915 and the lack of heirs and of general care in the past decades had led to the present critical situation made of statically unstable graves and arcades, weedy plants and typical local shrubs growing wild. Due to the land occupation of the surrounding area, the cemetery cannot expand and so there is little space left for new burials that they would be a convenient economic income for the Municipality. Finally, economic resources do not exist or they are minimal and it is evident that the site needs the best resource optimization possible.

3. Methodological approach

The solutions proposed in the following paragraphs are based on the main and established principles of the academic debates of contemporary restoration, i.e.:

- Minimal intervention: Elimination of unnecessary jobs directly or un-directly related to the perpetuation of the good. The creations of pure embellishment or modernization are severely limited since the sign of the time is an historical and an aesthetic value, extraordinarily evocative.
- Reversible and identifiable (to the trained eye) intervention.
- Compatibility of restoration materials with the original ones.
- Non-destructive and possible no-invasive diagnostic investigations.
- Preventive conservation and restoration.

4. The conservation project: from urgent activities to continuous care

4.1. Urgent conservation activities

It is evident that the site needs urgent conservation activities. In the preliminary research grave materials and infesting plants have been mapped in order to facilitate the subsequent inspections and the design of the maintenance plans. It is worth noting a widespread presence of canker of cypress, a fungal infection pervasive in Mediterranean area.

Treatment of *Seiridium cardinal* (the pathogenic fungus of cypress canker) with *Pseudomonas* (Raio *et al.* 2011) require a specialized labour and exceptional precautionary measures for the operator, which are objectively not available in the case study site. The diseased cypresses must be cut down and then the tools should be disinfected with ethanol and the cut plants burnt (Giunti and Lorenzini, 2013). In order to avoid damage to the surrounding graves the activities must be carried out by skilled workers who can install proper protection for underlying gravestones during the operations; moreover, in order to optimize the resources, they should also secure the graves with static instability and remove the other weedy and invasive plants (especially *Chamerops sp.*).

Another critical situation is represented by the roof coverings of the vaulted arcades where there is often a discontinuity in the earthenware coverings frequently associated with decay of woody secondary structures and disconnection of almost all the gutters and drainpipes. The roofs will be disassembled and cleaned from weeds; the underlying vaults must be consolidated on the extrados with carbon fibres if they are made of brick or with a fibre-reinforced net together with gypsum mortar if they are made of *arelle* (typical wooden strips); secondary wooden structures should be replaced or restored according to their conditions (Musso, 2013). The roof surface seems to rest directly on the rafters and joists so I recommend the use of a waterproof and transpiring sheath or of a tarred sheet on the replaced/restored joists (the roof planking is optional since we could not find it). Finally, the drainage channels of the paths must be rearranged and new gutters and drainpipes made of copper, a material compatible with the building historic and more durable of the current aluminium one, should be installed (Salvini, 2014).

The shaft tombs were common in the English colony burials: they often have structural failure of the inside vault and then instability can be observed on the exterior. Due to the fact that they are graves with a strong historical value they cannot be re-granted, in some critical cases the quickest and most sustainable solution (economically and environmentally) is the complete filling of the burial chamber with gravel and sand in order to eliminate the instability due to the cavity below.

After these early interventions of paramount importance some restoration work had to be exceptionally carried off on many artifacts. The choice of the restoration techniques, as well as that of the maintenance activities, is not immediate. It should be made according to the material and then the most appropriate methodology is further selected by the state of conservation of the material, its frailty and its historical and artistic value. Experience from the past taught us to be careful when choosing product and methodology since it became clear that there no 'perfect product' available yet, probably never will be, which stops the decay forever. In conclusion this means that conservation is a process of constant care and attention.

This study underlines the better sustainability of some conservation methods for the stone materials (Musso, 2013; Salvini, 2014). For example regarding the cleaning physical methods, like soft brushing with deionized water and micro sandblasting and Dry-Ice systems, or natural products, like gel agar-based and xi-xi of the Mexican tradition (Segarra Lagunes, 2006), should be preferred. For the removal of weeds the methods based on microwaves or flaming are very promising and minimally invasive (Olmí *et al.* 2011, Frasconi *et al.* 2015). For the stone consolidation a widespread method is the ethyl silicate but nano-silica based formulations or injections of lime mortar with local hydraulic aggregates are more sustainable. The re-adhesion must be performed only when necessary using a resin inside the fracture and micro-stuccoes made of lime and powder of the stone of interest to its outer. The necessary replacements must be performed with materials compatible with the originals (similar properties, colour, porosity, grain, ...) and also having similar properties. For the integrations, injections of lime and stone paste are suggested. Regarding the final protection, the methods are controversial and further studies are needed: the most used method in conservation is the periodic application of microcrystalline waxes with high melting point (thanks to stability, minimal color changes or interactions with the substrate). However, these waxes are not very efficient and they also have the defect of being soluble only in aromatic compounds at room temperature (this characteristic makes the periodic replacement difficult and not fully sustainable).

4.2. The maintenance plan: design of the inspection form

It is evident that the site firstly needs emergency restoration but with the goal of never reach any more a critical situation such as the current, a maintenance plan has also been drafted. The maintenance programme should provide inspections that, in absence of specific anomalies or exceptional events (weather events, earthquakes, vandalism, etc.), must always be done at a fixed time rate, possibly in relation to the critical environmental issues (present degradation, distance from the sea and from pollution source, estimate of future degradation, ...) where the artefact is placed. In a cemetery context, it is impossible to think of an 'item based' monitoring (Cecchi and Gasparoli, 2011) since the compilation of all the reports would require too much time and economic and skilled resources that almost always could not be found (taking also into account the vastness of the cultural heritage, cemetery and not, in needs of protection). Moreover, too many reports would distract from the most important issues if there was a presence of degradation phenomena that affect more than one grave. So, in this contribution is presented the designed inspection form (or technical schedule) structured for cemetery areas (see Fig. 1).

The 'Foce' cemetery (area: 20000 m² and about 2500 gravestones) has been divided into 47 monitoring areas. For a quicker scheduling of maintenance, gravestones had been renumbered in a more logical way than that used in burial records, sometimes missing. The form has been designed in order to optimize the execution of the monitoring: it presents a spatial orientation part and another one related to the inspection itself. In the first part the items constituent the area under investigation are shown as a list of codes together with a planimetry (of course with indication of codes). In the second part, it has been made a list of alterations of the lexicon ICOMOS (or UNI EN 1182:2006) to be monitored: the deterioration patterns that are more unstable or have a tendency to evolve more rapidly than others have been selected because these alterations are also those that generally require a timely intervention and/or could lead to a rescheduling of the maintenance plan.

drafted case by case, as it is working in other monumental cemeteries (es. Genova, Paris). Another source of income can be the cultural activities staged at the cemetery (es. Poblenu cemetery, Barcelona), given the presence of an area suitable for the purpose.

The cemetery valorisation is required in order to obtain funds for its preservation. The historical importance of the site, evidence of the importance of the city of Sanremo during the *Belle Epoque*, must be preserved: different routes connecting the cemetery with the artistic surrounding assets were created and in the future they will be enhanced through Internet and mobile Apps (Salvini, 2014). The site management must consider the participation of the local workforce like custodians and gardeners and grave caretakers properly formed (Nagaoka, 2011) and supervised.

Dealer/Caretaker	always	Limit the use of candles and flowers, check the seal of the vases
	From 1 to 4 times a year	Soft brushing
Gardener	Once a month	Maintaining the lawn with the mower and sweeping of calcestre avenue
	2-4 times a year	Contrasting the weeds on free surfaces
	Twice a year	Cleaning of gutters and drainage channels Herbicide treatment (spot) of calcestre avenues, gutters and drainage channels
Skilled worker	Once a year and if necessary	Interventions for balancing the foliage of cypresses Removal of ivy and dry vegetation Repair broken and deteriorated elements of roofs and gutter
	Every two years	Patching up of drainage channels (every 2 years)
	If necessary	Replacement of elements (roof, gutter, drainage ch.)
Conservator	Twice a year	Removal of weeds from the stone surface by chemical means and /or manuals ones (preferred)
	Once a year	Re-bonding of the broken elements
	Every 3 years	Wraps or sandblasting (spot) to clean new stains
	Every 7 years	Removal and re-application of protection (microcr. wax)
Spec. technician	Only when necessary	Total cleaning up
	Minimum twice a year and after extreme events	Technical survey for monitoring areas
	Max. every 2 years	Technical control of tree C-FRC category
	Every 2-3 years	Technical control of tree B-FRC category
	Every 5 years	Technical control of tree A-FRC category
WHO?	WHEN?	WHAT?

Fig. 2: Timetable of the maintenance activities.

5. Conclusions

The 'Foce' cemetery is a hidden pearl of the city of Sanremo that by now has not received the attention it deserves, but there are the presuppositions to make it a practical example of sustainable conservation and continuous care. The interest of local associations has enabled a first small restoration in accord with local institutions: on 9th July 2015 ended the restoration of the anatomist A.H. Hassall's grave (thanks to the sponsor Rotary Club Sanremo) and in November 2015 have begun sporadic volunteer days where local people perform routine maintenance activities supervised by experts according to the Superintendency.

References

- Cecchi, R., Gasparoli, P., 2011, La manutenzione programmata dei beni culturali edificati: procedimenti scientifici per lo sviluppo di piani programmati di manutenzione, Alinea, Firenze.
- Cinieri, V., Zamperini, E., 2014, Approccio lifecycle alla gestione e conservazione sostenibile del patrimonio costruito, in Proceedings of XXXth Scienza e Beni Culturali, Biscontin, G. and Driussi, G. (Eds.), Arcadia R., Venezia, 723-732.
- Frasconi, C., Fontanelli, M., Martelloni, L., Pirchio, M., Raffaelli, M. and Peruzzi, A., 2015, Thermal weed control in archaeological sites as an alternative to herbicides application, in Book of Abstracts, Green Conservation Workshop, October 27th-28th, Roma.
- Giunti, M. and Lorenzini, G. (Eds.), 2013, Un archivio di pietra: l'antico cimitero degli inglesi di Livorno – Note storiche e progetti di restauro, Pacini, Pisa.
- Macchia, A., Sacco, F., Morello, S., Prestileo, F., La Russa F.M., Ruffolo, S., Luvidi, L., Settimo, G., Rivaroli L., Laurenzi Tabasso, M. and Campanella, L., 2014, Chemical exposure in Cultural Heritage restoration: questionnaire to define the state of art, in Proceedings of XXXth Scienza e Beni Culturali, Biscontin, G. and Driussi, G. (Eds.), Arcadia R., Venezia, 723-732.
- Musso, S.F., 2013, Tecniche di restauro, UTET, Torino.
- Nagaoka M., 2011, Revitalization of Borobudur. Heritage Tourism Promotion and Local Community Empowerment in Cultural Industries, In AA.VV. Actes du Symposium scientifique de la 17ème Assemblée générale de l'Icomos. Icomos, Paris, pg. 658-671.
- Olmi, R., Bini, M., Cuzman, O.A., Ignesti, A., Frediani, P., Priori, S., Riminesi, C. and Tiano, P., 2011, Investigation of the microwave heating method for the control of biodeteriogens on cultural heritage assets. Proceedings of Art11 - 10th International Conference on non-destructive investigations and microanalysis for diagnostic and conservation, Firenze.
- Raio, A., Puopolo, G., Cimmino, A., Danti, R., Della Rocca, G. and Evidente, A., 2011 Biocontrol of cypress canker by the Phenazine producer *Pseudomonas Chlororaphis* subsp. *Aureofaciens* strain M71, *Biological Control*, 58(2), 133-138.
- Salvini, S., 2014, Cimitero monumentale della Foce di Sanremo: percorsi di valorizzazione e linee guida per la conservazione preventiva e la manutenzione programmata, Final relation of the Post graduate School in Built Heritage and Landscape, SSBAP-University of Genova, Relator: Musso, Co-relators: Arcolao, De Cupis.
- Salvini, S. and Cinieri, V., 2016, La conservazione del patrimonio ecclesiastico diffuso in Italia, in Proceedings Precomos Conference 2014, Nardini, Firenze, pg.169-178.
- Segarra Lagunes, S., 2007, Conservazione e restauro: il caso del cimitero storico del Tepeyac a Città del Messico, in Proceedings of MO06, Aracne, Roma.
- United Nations, 1987, Report of the World Commission on Environment and Development: Our Common Future.

CONSOLIDATION OF SUGARING MARBLE BY HYDROXYAPATITE: SOME RECENT DEVELOPMENTS IN PRODUCING AND TREATING DECAYED SAMPLES

E. Sassoni^{1,2*}, G. Graziani¹, E. Franzoni¹ and G.W. Scherer²

Abstract

Consolidation of sugaring marble (i.e., marble affected by granular disaggregation) still lacks fully effective solutions. Consequently, the use of an innovative phosphate-based treatment, aimed at bonding calcite grains by formation of hydroxyapatite at grain boundaries, has recently been proposed. In this paper, firstly a novel method for producing artificially decayed marble samples, by contact with a heating plate, is proposed. Then, some results are presented about the effectiveness and the compatibility of two different formulations of the phosphate treatment, differing in terms of concentration of the phosphate precursor (3.0 M or 0.1 M aqueous solutions of diammonium hydrogen phosphate, DAP), possible ethanol addition to the DAP solution and number of DAP solution applications (1 or 2). The results of the study point out that the new weathering method produces specimens with a gradient in microstructural and mechanical properties with thickness, just like naturally weathered samples. Both phosphate treatments were able to significantly improve marble cohesion, without causing significant changes in thermal behaviour and aesthetic appearance after treatment. The addition of small quantities of ethanol to the DAP solution seems to be a very promising method for favouring HAP formation and improving the treatment performance.

Keywords: grain loss; thermal ageing; thermal diffusivity; calcium phosphate; ethanol

1. Introduction

The so-called "sugaring" of marble is a degradation phenomenon that consists in grain detachment and loss, leading to severe alteration of the original morphology of architectural elements and sculptures. As an example, sugaring affecting carved marble decorations in the Monumental Cemetery in Bologna (Italy, XIX century) is illustrated in Fig. 1.

Sugaring originates from cyclical thermal excursions that outdoor marble elements experience. Daily temperature variations cause anisotropic deformation of calcite grains of which marble is composed, with the result that micro-cracks open at grain boundaries and grains start to detach (Siegsmund *et al.*, 2000).

¹ E. Sassoni*, G. Graziani and E. Franzoni,
Dept. Civil, Chemical, Environmental and Materials Engineering (DICAM), University of Bologna,
Italy
enrico.sassoni2@unibo.it

² E. Sassoni* and G.W. Scherer
Dept. Civil and Environmental Engineering (CEE), Princeton University, United States of America
esassoni@princeton.edu

*corresponding author



Fig. 1: Sugaring marble in the Monumental Cemetery in Bologna, Italy (XIX century).

In spite of the wide diffusion of this weathering phenomenon, no fully satisfactory treatment for effectively and durably stopping marble sugaring has been developed yet. Organic polymers exhibit limited compatibility and durability, alkoxysilanes give modest mechanical improvement and long-term performance, lime-based treatments (also at the nano-scale) are affected by low penetration depth and effectiveness, ammonium oxalate provides insufficient consolidation and long-term protection (Sassoni and Franzoni, 2014b).

For this reason, an innovative inorganic phosphate treatment has recently been proposed for sugaring marble consolidation (Sassoni *et al.*, 2015). The phosphate treatment, originally proposed for limestone consolidation (Sassoni *et al.*, 2011) and marble protection (Naidu and Scherer, 2014), is based on the reaction between the calcitic substrate and an aqueous solution of di-ammonium hydrogen phosphate (DAP) to form hydroxyapatite (HAP).

Results obtained so far on the use of HAP for consolidation of sugaring marble are extremely promising, in terms of both effectiveness and compatibility of the new treatment (Sassoni *et al.*, 2015). However, further research is still needed, because:

- (i) Experimental tests on the HAP-treatment have been mainly carried out on marble samples artificially weathered by heating at 400°C for 1 hour in oven, according to a procedure previously developed by the authors (Sassoni *et al.*, 2011; Franzoni *et al.*, 2013; Sassoni and Franzoni, 2014). This procedure proved to be effective in producing samples with characteristics very similar to those of naturally sugaring samples, namely with increased open porosity and coarsening of the pore size, with respect to the unweathered condition. However, samples produced in that way are *entirely* decayed, whereas naturally weathered samples exhibit a *gradient* in microstructural and mechanical properties, the superficial part being highly damaged and the inner part being basically undamaged. As one of the goals of consolidation is to restore cohesion in the decayed part of a stone, so as to bring it back to the condition before weathering, the use of artificially weathered samples with a gradient in properties is a very important aspect for studying new consolidants (Lubelli *et al.*, 2015).
- (ii) A recent study by the Authors has shown that the addition of ethanol (EtOH) to the aqueous DAP solution, used to react marble to form HAP, is able to significantly improve HAP formation (Graziani *et al.*, *in press*). EtOH addition resulted in better coverage of marble surface by HAP and a reduction in cracking

of the HAP layer, as well as a reduction in the DAP concentration, hence a beneficial effect is expected also in the case of sugaring marble consolidation.

Therefore, in the present study some preliminary results are presented about:

- (i) a new methodology to produce artificially weathered marble samples with a gradient in microstructural and mechanical properties;
- (ii) the effects of adding ethanol to the aqueous DAP solution, in terms of consolidating efficacy and compatibility with the substrate.

2. Materials and Methods

2.1. Marble

Carrara marble was used for the tests, considering its wide diffusion in historic architecture and sculpture. For tests on artificial weathering, samples with $2.5 \times 2.5 \times 5$ cm³ dimensions (provided by BasketweaveMosaics.com, USA) were used. For tests on the phosphate treatments effects, samples with $2 \times 2 \times 3$ cm³ dimensions (provided by Imbellone Michelangelo s.a.s., Italy) were used.

2.2. Artificial weathering of marble samples

For producing a gradient in marble properties, samples were put in contact with a heating plate already at 350°C, as illustrated in Fig. 2. Four thermocouples, put in contact with sample surface at various distances from the heating plate (0, 10, 25 and 50 mm) and connected to a pc, were used to continuously record the temperature reached by the sample at different heights from the plate. To identify the most suitable time of heating, the method described in the following was used.

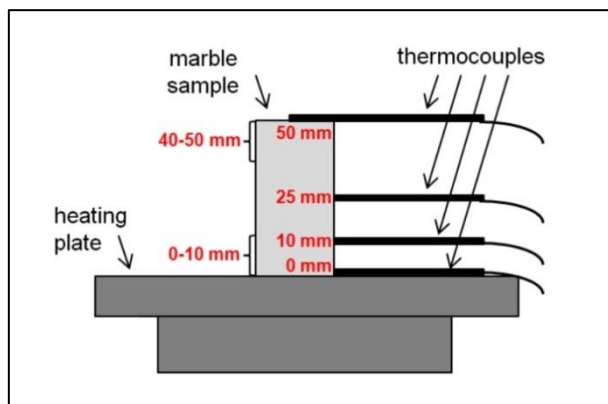


Fig. 2: Experimental set-up for accelerated ageing of marble samples.

Assuming that the heat flow from the heating plate is one-dimensional (which is the case if sample sides are covered with an insulator, so that heat losses are prevented), the equation governing the heat flow is:

$$\frac{\partial T}{\partial t} = \frac{\partial}{\partial x} \left(k(x, t) \frac{\partial T}{\partial x} \right) \quad (\text{Eq. 1})$$

where T is the temperature, t is the time, x is the distance from the heating plate and k is marble thermal diffusivity. It can be demonstrated, for the case of constant k , that the sample top at 50 mm from the heating plate is not subject to warming (and hence a gradient in sample properties can be expected) if the time of heating is limited to:

$$t \leq \frac{0.1H^2}{k} \quad (\text{Eq. 2})$$

where H is the sample height. To estimate the time of heating, preliminary tests were carried out to determine the thermal diffusivity of Carrara marble (no reference value was found in the literature). A 5 cm side cubic sample was placed in contact with the heating plate (initially cold) and then heated from 24°C to 270°C, heat losses being prevented insulating sample's lateral sides with a porous stone and top with a glass fibre board. Temperature variations at different heights from the heating plate (0, 10, 20, 30, 40 and 50 mm) were measured as a function of time, by means of six thermocouples inserted inside purposely drilled holes. By fitting the $T(x,t)$ curves measured at different heights from the plate to a numerical solution of Eq. (1), $k(x,t)$ was found to vary parabolically with temperature, decreasing from $1.6 \times 10^{-6} \text{ m}^2/\text{s}$ at 24°C to $4.0 \times 10^{-7} \text{ m}^2/\text{s}$ at 270°C. A very good fit was obtained to $T(x,t)$ measured at each of the thermocouples, so this model can be used in the future to simulate arbitrary heating procedures. The details of these calculations will be presented in a future publication. The decrease in k with T is thought to be a consequence of microcracks opening as temperature increases. Using Equation (2), with $H=5$ cm, the times of heating corresponding to the limiting values of k were calculated and times of about 2.5 and 10 minutes were obtained.

The effects of heating samples by contact with the heating plate at 350°C for 5 and 10 minutes were evaluated by comparing the two parts of the sample at 0-10 mm and at 40-50 mm from the plate (hence, respectively, directly in contact with the plate and at the opposite side, Fig. 2). This comparison was performed in terms of ultrasonic pulse velocity (UPV) and elastic modulus (E) determined by nanoindentation test. UPV was measured, before and after heating, by transmission method, using a PUNDIT commercial instrument with 54 kHz transducers and a rubber couplant between the sample and the transducers. E was calculated as the slope of the unloading part of the force-displacement curve obtained by subjecting the marble sample to the following loading cycle: loading to 400 μN , holding, unloading. The loading cycle was performed using a Digital Instruments AFM with integrated nanoindentation capability.

2.3. Consolidation of marble samples

As optimization of the novel weathering procedure is still in progress (cf. § 3.1), samples to be treated with the phosphate consolidants and untreated references were preliminarily artificially weathered by heating at 400°C for 1 h in oven, according to a procedure previously developed by the Authors (Sassoni *et al.*, 2011; Franzoni *et al.*, 2013). Two treatment conditions were considered:

- (i) "3.0 M DAP". These samples were firstly treated with a 3.0 M solution of DAP (Sigma-Aldrich, reagent grade) and de-ionized water, applied by brushing 15 times. At the end of brushing application, the samples were wrapped in a plastic film to prevent solution evaporation and left to react for 48 hours. Then, they were unwrapped, rinsed with water and left to dry. Finally, they were treated with a

saturated solution of calcium hydroxide (Sigma-Aldrich, reagent grade) in de-ionized water (so-called limewater), applied by poultice. The poultice was prepared using limewater and dry cellulose pulp (MH300 Phase, Italy) with a weight ratio 6:1. After wrapping in a plastic film for 24 hours and then drying, samples were ready for characterization tests.

- (ii) "0.1 M DAP with 0.5 wt% EtOH + 0.1 M DAP". These samples were treated according to the method recently proposed by Graziani *et al.*, *in press*. As a first step, samples were treated by immersion in a 0.1 M DAP solution with addition of 0.5 wt% EtOH for 24 hours. After rinsing with water and drying, samples were then subjected to a second treatment with a 0.1 M DAP solution, again applied by immersion. After drying, samples were ready for tests.

The consolidating efficacy of the two treatments was evaluated in terms of increase in *UPV*, with respect to the untreated references. *UPV* was selected as it is very sensitive to healing of microcracks and is hence frequently adopted to assess the efficacy of stone consolidants (Weiss *et al.*, 2002). *UPV* was measured with a Matest commercial instrument with 55 kHz transducers, using a rubber couplant between the samples and the transducers.

The compatibility of the two treatments was evaluated in terms of alterations in thermal behaviour and aesthetic appearance. As marble decay is mainly induced by thermal excursions, the evaluation of the thermal behaviour of consolidated marble is very important (Ruedrich *et al.*, 2002). Untreated and treated samples (30×9×7 mm³) were subjected to the following thermal cycle, using a push-rod dilatometer Netzsch mod. 402 E (Netzsch-Gerätebau GmbH, Selb, Germany): (i) heating from room temperature to 80°C at 1°C/min, (ii) isothermal dwell for 1 hour at 80°C, (iii) cooling to room temperature at 1°C/min. The maximum heating temperature was chosen to simulate environmental conditions experienced in the field (Siegesmund *et al.*, 2000). The residual strain after cooling to room temperature (ϵ_r) was considered. The aesthetic alteration was evaluated in terms of colour change, defined as $\Delta E = (\Delta L^{*2} + \Delta a^{*2} + \Delta b^{*2})^{1/2}$. The colour parameters $L^*a^*b^*$ (L^* = black÷white, a^* = red÷green, b^* = yellow÷blue) were measured using a Spectrophotometer cm-2600d, Konica Minolta Sensing, Inc.

3. Results and Discussion

3.1. Artificial weathering

For marble samples put in contact with the heating plate initially at 350°C for 5 and 10 minutes, a remarkable temperature gradient is present inside the samples, as illustrated in Fig. 3 (left). The thermocouple in contact with the sample and the plate registers a temperature of 312-335°C after 5 and 10 minutes, respectively (both temperatures being lower than the initial one because contact with the sample lowers the plate temperature). At a height of 10 mm from the plate the temperature is sensibly lower (106-117°C, respectively). At the top of the sample (50 mm height) the temperature is still quite close to ambient temperature after 5 minutes (42°C) and a little higher after 10 minutes (53°C).

Correspondingly to this temperature gradient, a significant gradient in mechanical properties was registered. In terms of *UPV*, decreases with respect to the initial condition are reported in Fig. 3 (right). In the sample part close to the plate (0-10 mm), a strong *UPV* decrease is registered after 5 minutes (-58%). When contact with the plate is increased up to 10 minutes, a similar *UPV* decrease is recorded in this sample part (-56%). However, the

situation is quite different at the top of the sample (40-50 mm from the plate). While after 5 minutes only a minor *UPV* decrease is registered (-5%), in agreement with the limited temperature reached in this layer (42°C), after 10 minutes a non-negligible *UPV* decrease (-21%) is registered also in this layer, in agreement with the higher temperature reached (53°C).

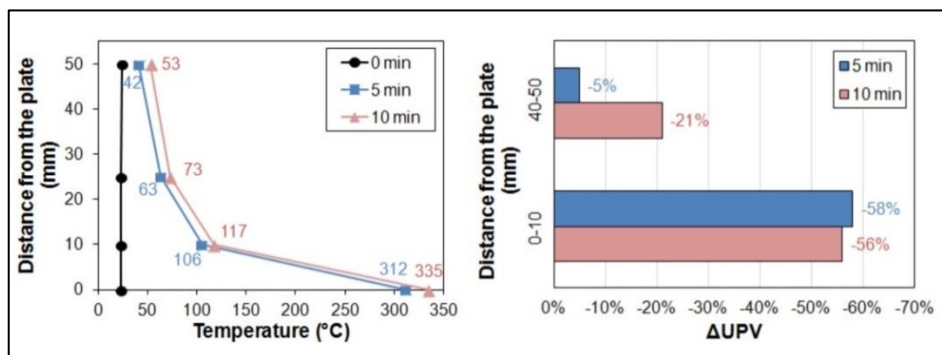


Fig. 3: Effects of accelerated ageing: temperature (left) and *UPV* variation (right) at different heights from the heating plate after 5 and 10 minutes.

Based on these results, a time of heating of 5 minutes seems to be the most suitable, as it allows to obtain a marked gradient in *UPV* across sample thickness, without significantly altering properties at the extremity of the sample far from the plate. Accordingly, in the sample heated for 5 minutes a marked difference (-75%) was registered also in terms of elastic modulus, *E*, determined by nanoindentation, between parts at 0-10 mm and 40-50 mm from the heating plate.

However, results reported above were obtained for a sample that had been heated over the plate without insulating the sides and the top, so that some heat loss was experienced. Consequently, conditions for calculating the time of heating using Equations (1) and (2) were not strictly respected. For samples subjected to artificial weathering with thermal insulation, an even more pronounced gradient in temperature and hence in microstructural-mechanical properties is expected. Tests involving insulated samples are currently in progress. On these samples, a systematic evaluation of mechanical property alteration as a function of the distance from the heating plate will be carried out by nanoindentation. Being a non-destructive technique (causing only nanometric damage to calcite grains), it will be possible to derive profiles of sample elastic modulus *E* after artificial weathering and after consolidation by the phosphate treatment.

3.2. Consolidation

The effects of the two consolidating treatments are summarized in Tab. 1. Both treatments proved to be highly effective in restoring marble mechanical cohesion, being able to bring *UPV* almost back to the value before artificial weathering (3.2 km/s). Between the two treatments, that involving a higher DAP concentration allowed to achieve a higher *UPV* increase. However, it is remarkable that the treatment involving EtOH addition allowed to achieve a comparable increase in *UPV*, notwithstanding the much lower (30 times) concentration of DAP used. This can be ascribed to the beneficial effect of: (i) adding EtOH, that according to some studies favours HAP formation (Lerner *et al.*, 1989); (ii)

applying double treatments, that allow to achieve a better coverage of calcite grains, without causing excessive growth of the HAP film (Graziani *et al.*, in press).

In terms of thermal behaviour after consolidation, both treatments gave good results, causing a residual strain after the heating-cooling cycle less than or equal to that of the untreated reference (Tab. 1). This is very important, because if an increase in residual strain were found, an increase in sensitivity to thermal cycles should be expected (Ruedrich *et al.*, 2002). Notably, the residual strain of the sample treated with EtOH addition is very close to the value exhibited by marble before artificial weathering (0.15 mm/m). This is a positive feature, as stone consolidants should ideally modify the properties of decayed stone so as to bring them back to the condition before decay.

In terms of aesthetic appearance, the two consolidating treatments exhibited a good compatibility (Tab. 1), in both cases leading to a colour change ΔE^* lower than the threshold commonly accepted for stone consolidants ($\Delta E^* = 5$) and even lower than the human eye detection limit ($\Delta E^* = 3$). The ΔE^* caused by the treatment with EtOH addition was actually lower than the other treatment, which can be ascribed to the lower DAP concentration involved by this treatment condition.

Tab. 1: Effects of the two consolidating treatments.

Specimen	UPV (km/s)	ϵ_r (mm/m)	ΔE^*
Untreated	0.6	0.24	-
3.0 M DAP	2.9	0.23	1.5
0.1 M DAP with 5 wt% EtOH + 0.1 M DAP	2.2	0.16	1.1

4. Conclusions

In the present paper, some recent developments were reported on the production of artificially weathered samples for testing of consolidants and on the effects of two different formulations of the hydroxyapatite-based treatment for consolidation of sugaring marble. Heating marble samples by contact with a heating plate at 350°C for 5 minutes proved to be an effective way to produce samples with a marked gradient in mechanical properties (just like naturally weathered marble), namely an UPV decrease of -58% at a distance of 10-20 mm from the plate and basically no damage at a distance of 40-50 mm. As for consolidation, the double treatment involving the addition of a very small quantity of ethanol to a DAP solution with low concentration (0.1 M DAP) produced a significant mechanical improvement, with only minor alterations in thermal behaviour and aesthetic appearance. This suggests that ethanol additions to the DAP solution are a very promising method for favouring HAP formation and improving the treatment performance.

Acknowledgments

This project has received funding from the European Union's Horizon 2020 research and innovation programme under the Marie Skłodowska-Curie grant agreement No 655239 (HAP4MARBLE project, "Multi-functionalization of hydroxyapatite for restoration and preventive conservation of marble artworks"). Prof. Winston Soboyejo and M.Eng. Emre Turkoz (Dept. Mechanical and Aerospace Engineering, Princeton University, USA) are gratefully acknowledged for collaboration on nano-indentation tests. Prof. Maria Chiara Bignozzi and Dr. Giovanni Ridolfi (Centro Ceramico Bologna, Italy) are gratefully acknowledged for collaboration on thermal behaviour tests.

References

- Franzoni, E., Sassoni, E., Scherer, G.W., Naidu, S., 2013, Artificial weathering of stone by heating, *J Cult Herit*, 14S, 85-93.
- Graziani, G., Sassoni, E., Franzoni, E., Scherer, G.W., Hydroxyapatite coatings for marble protection: optimization of calcite covering and acid resistance, *Appl Surf Sci* (in press).
- Lerner, E., Aoury, R., Sarig, S., 1989, Rapid precipitation of apatite from ethanol-water solution, *J Cryst Growth*, 97, 725-730.
- Lubelli, B., van Hees, R.P.J., Nijland, T.G., Bolhuis, J., 2015, A new method for making artificially weathered stone specimens for testing of conservation treatments, *J Cult Herit*, DOI: 10.1016/j.culher.2015.01.002.
- Naidu, S., Scherer, G.W., 2014, Nucleation, growth and evolution of calcium phosphate films on calcite, *J Colloid Interf Sci*, 435, 128-137.
- Ruedrich, J., Weiss, T., Siegesmund, S., 2002, Thermal behavior of weathered and consolidated marbles, in *Natural stone, weathering phenomena, conservation strategies and case studies*, Siegesmund, S., Weiss, T., Vollbrecht, A. (Eds), Geological Society, London, Special Publications, 205, 255-271.
- Sassoni, E., Naidu, S., Scherer, G.W., 2011, The use of hydroxyapatite as a new inorganic consolidant for damaged carbonate stones, *J Cult Herit*, 12, 346-355.
- Sassoni, E., Franzoni, E., 2014a, Influence of porosity on artificial deterioration of marble and limestone by heating, *Appl Phys A-Mater* 115, 809-816.
- Sassoni, E., Franzoni, E., 2014b, Sugaring marble in the Monumental Cemetery in Bologna (Italy): characterization of naturally and artificially weathered samples and first results of consolidation by hydroxyapatite, *Appl Phys A-Mater*, 117, 1893-1906
- Siegesmund, S., Ullemeyer, K., Weiss, T., Tschegg, E.K., 2000, Physical weathering of marbles caused by anisotropic thermal expansion, *Int J Earth Sci*, 89, 170-182.
- Weiss, T., Rasolofosaon, P.N.J., Siegesmund, S., 2002, Ultrasonic wave velocities as a diagnostic tool for the quality assessment of marble, in *Natural stone, weathering phenomena, conservation strategies and case studies*, Siegesmund, S., Weiss, T., Vollbrecht, A. (Eds), Geological Society, London, Special Publications, 205, 149-164.

APPLICATION OF ETHYL SILICATE BASED CONSOLIDANTS ON SANDSTONE WITH PARTIAL VACUUM: A LABORATORY STUDY

H. Siedel^{1*}, J. Wichert² and T. Frühwirt²

Abstract

To improve the penetration depth of a TEOS consolidant on Cotta sandstone with high amount of small voids and clay mineral content, the so-called “Vacuum Circulation Process” (VCP) was applied to test cubes of fresh sandstone. Changes of mechanical and hydric properties were determined on drill core profiles across the test cubes after a 4 month reaction time. Especially for Remmers Funcosil 300E, the results show a significantly higher penetration depth compared to a reference cube brushed by hand with the same agent. Moreover, biaxial flexural strength and Young’s modulus profiles for Funcosil 300E / VCP are acceptable in terms of the relation of both properties and their change along the profile line from surface to the interior. Hydric properties show a still slightly hydrophobic reaction of the penetrated outermost zone. Although these results encourage the use of VCP also for building stones with a high amount of smaller voids, the role of the partial vacuum during the process remains unclear, since similar penetration depths were reached by total immersion of a sandstone cube under atmospheric pressure.

Keywords: consolidation, hydric and mechanical properties, sandstone, penetration depth, vacuum circulation process

1. Introduction

Inappropriate penetration depths of stone consolidants are a common problem especially for the treatment of building sandstones with a higher amount of smaller voids and clay mineral contents. In restoration practice, the so-called “vacuum circulation process” (VCP, Pummer 2008) has been occasionally used for consolidation treatments of small objects like sculptures to reach better penetration of the consolidant. For this treatment, the entire stone object is sealed in a tight plastic foil bag which is “evacuated” by partial vacuum down to -900 mbar (g). Maintaining the partial vacuum, fluid tetra ethyl ester of the orthosilicic acid (TEOS) is subsequently sucked in the bag with the object via valves in the foil skin. Although there are only few systematic investigations on the change of physical properties after VCP treatment, it seems to work well in practice with respect to the penetration depth especially for stone varieties with coarse voids. However, conservation issues often concern sandstones with higher amounts of smaller voids and clay contents which are on one hand

¹ H. Siedel*

Institute of Geotechnical Engineering, Chair of Applied Geology, TU Dresden, Germany
Heiner.Siedel@tu-dresden.de

² J. Wichert and T. Frühwirt

Geotechnical Institute, Chair of Rock Mechanics, TU Bergakademie Freiberg, Germany

*corresponding author

susceptible to weathering and on the other hand hard to penetrate for liquids. The study aimed at testing the VCP treatment for clay mineral bearing building sandstone with low average pore diameter. For the tests Elbe Sandstone (Cotta type) from the region of Saxony (Germany) with median pore diameter D50 of 1.4 μm was chosen (see Fig. 1 and Fig. 2). The problem of low penetration depths of consolidants is well known from several conservation measures on this material.

2. Materials and methods

2.1. Cotta sandstone

Cotta sandstone is a building stone from the Upper Cretaceous (Turonian) quarried in the Elbe Valley some 20 km south of the city of Dresden since the 15th century. The fine to medium grained quartz arenite (Fig. 1) contains clay minerals like kaolinite and illite and has a broad pore size distribution shown in Fig. 2.

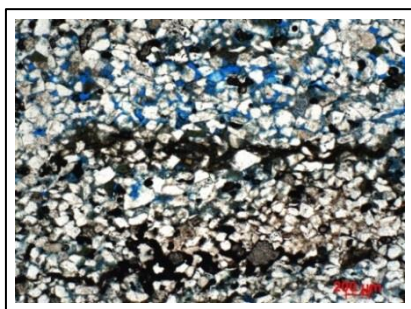


Fig. 1: Thin section image of Cotta sandstone (Nicols II) with light quartz grains and dark clay mineral layers

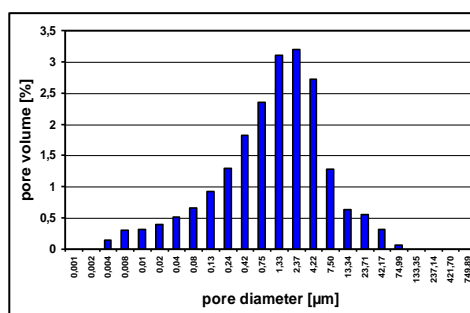


Fig. 2: Pore size distribution of Cotta sandstone used for the tests (U), according to MIP. Total porosity of this sample is 20.6 %.

2.2. Samples and treatment with VCP

Test cubes of 20×20×20 cm were cut from Cotta type sandstone from the quarry Lohmgrund II, Sächsische Sandsteinwerke GmbH. The chosen format represents the thickness of smaller objects such as tombstones or parts of sculptures. In the restorer's workshop (Erich Pummer, Rossatz / Wachau, Austria) the cubes were air dried, sealed in foil bags and treated with TEOS systems with "soft segments" (polyether chains, Snelthage 2014) and different SiO₂ gel "content" (Remmers Funcosil 300E, pre-condensed Remmers Funcosil 500E) applying the VCP. The TEOS systems contained an (unknown) reaction accelerator designed by Remmers for the use in VCP. Treatment duration was 6-7 hours for Funcosil 500E and 8 hours for Funcosil 300E; with a TEOS consumption of 5.2 and 3.4-5.2 litres, respectively. As reference additional test cubes were treated in a conventional way by brushing the liquid (Funcosil 300E without reaction accelerator) several times "wet-in-wet" on the surface until the stone surface was visibly saturated. To compare the penetration depth reached by applying partial vacuum to that reached by embedding the same stone in the liquid under atmospheric pressure, another cube was stored in Funcosil 300E for 6 hours (TEOS consumption 2.7 litres) and cut immediately afterwards.

After the treatment, all sample cubes were stored 4 months at 65 % *RH* / 21°C. Subsequently, 8 drill cores were taken from every cube normal and parallel to bedding planes of the sandstone, respectively.

2.3. Investigation of physical properties

Drill cores taken from the test cubes were cut into 5 mm thick discs normal to the cylinder axis to obtain profiles from the surface to the depth. Before cutting the cores, measurements of the ultrasonic wave velocity (UWV, air-dried condition) had been performed stepwise, in two orthogonal directions normal to the cylinder axis, with a GEOTRON system. In a first step, hydric properties (total water uptake, hydric swelling, and water vapour diffusion) of the discs were determined by non-destructive measurements, followed by destructive measurements in order to obtain mechanical properties (Siedel and Siegesmund 2014).

2.3.1. Hydric swelling and total water uptake

The air dry samples were fixed in a sample holder (Invar) combined with dilatometer (precision 0.01 mm) and immersed in demineralised water for 96 h. The maximum swelling value [mm/m] was registered. Before immersion and after water storing, the samples were weighed and the mass difference was compared with the dry sample mass [wt.-%].

2.3.2. Water vapour diffusion resistance

Water vapour diffusion was measured following EN-ISO 12572 in the “wet cup” conditioning (96 vs. 50 % *RH*, 21°C). From the mass difference over time, the water vapour resistance value (μ) was calculated. This parameter indicates how many times the resistance of a material against streaming water vapour is higher compared to a layer of pure air of the same thickness.

2.3.3. Biaxial flexural strength and Young’s modulus

Biaxial flexural strength (BFS) and Young’s modulus (YM) were determined on each disc, with the circular disc resting upon a larger ring while pressure is being applied centrically by a second smaller ring, according to the method described by Kozub (2008).

3. Results and discussion

3.1. Penetration depth

The penetration depth of the liquid consolidant was assessed by cutting two control cubes immediately after treatment with VCP and Funcosil 300E. Moreover, another test cube was cut after full immersion in Funcosil 300E under atmospheric pressure. The results are displayed in Fig. 3 and Fig. 4. They show, that the maximum penetration depths vary between 2.5 and 5 cm for two different cubes of Cotta sandstone treated with VCP under the same conditions (-200 to -500 mbar (g)) and do not differ significantly from those observed on the cube immersed in Funcosil 300E under atmospheric pressure (maximum 3 cm). As can be seen in Fig. 4 (below), penetration depth along bedding planes of the sandstone is slightly higher than normal to bedding.



Fig. 3: Test cubes penetrated by Funcosil 300E with VCP and cut parallel to bedding immediately after the procedure (photos: E. Pummer).

Fig. 4: Test cube penetrated by Funcosil 300E with total immersion under atmospheric pressure and cut parallel (above) and normal to bedding (below) immediately after the procedure (photos: M. Eilenberger).

3.2. Ultrasonic wave velocity

Fig. 5 displays the average values of all UWV profiles measured for the differently treated samples as well as for the untreated cube after 4 month of storage. The differences of UWV in the cores of the different sample cubes (deeper than 50-60 mm from surface) give the range of natural scattering in Cotta sandstone. As can be seen from the graphs, the hand-

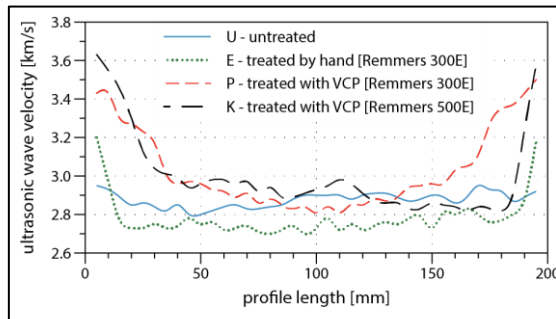


Fig. 5: Ultrasonic wave velocity profiles across the test cubes (average values for all measurements on drill cores).

treated cube (E) shows the lowest change of UWV of all samples with effects limited to the first 10 mm from surface. Samples treated with VCP clearly show deeper and stronger effects (up to about 50 mm in case of Funcosil 300E (P) and about 30 mm in case of Funcosil 500E (K)). In contrast to the steep slope of the profiles of E and K in the outermost zone, the cube P treated with VCP and Funcosil 300E shows a more smooth profile. The profiles obtained from measurements in two different directions, both normal to the axis of the cores, are highly consistent.

3.3. Biaxial flexural strength and Young's modulus

Changes in BFS and YM profiles for all samples after the treatment displayed in Fig. 6 and Fig. 7 reflect the changes in UWV (cf. Fig. 5).

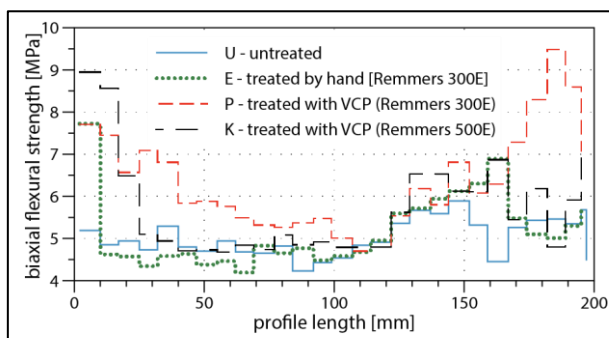


Fig. 6: Biaxial flexural strength profiles across the test cubes (average values for all measurements on 5 mm discs cut from drill cores).

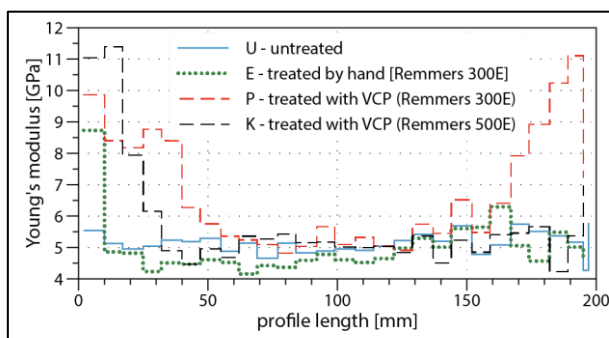


Fig. 7: Young's modulus profiles across the test cubes (average values for all measurements on 5 mm slices cut from drill cores).

The profiles show steep slopes of BFS and YM from the surface to the interior in case of the hand-treated cube E and the cube K treated with VCP and the pre-condensed consolidant Funcosil 500E, respectively, whereas cube P treated with Remmers 300E and VCP shows a more gradual decrease of the values for both parameters. According to Snethlage (2014), the evolution of YM and BFS values per distance from the surface in a profile, the relative increase in YM and BFS achieved through treatment as well as the relation between YM and BFS are crucial criteria to avoid delamination of the stone surface

by “over-strengthening” the surface layer. Regarding the change of YM (≤ 1 GPa/mm) and BFS (≤ 0.2 MPa/mm) from surface to the interior, the changes observed in the profile after treatment with Fungosil 300E and VCP are within the limits established by Sneathlge 2014 (cf. Fig. 6 and Fig. 7). Although the changes in YM and BFS for cube P, compared to YM and BFS of its untreated inner core, are slightly over the limit in the outermost zone (changes must be $\leq 50\%$ according to Sneathlge 2015), the results are generally satisfying with that respect. Discussing these parameters, one has to keep in mind that, in contrast to the hand-treated cube E, the impregnation depth reached by VCP in case of cube P is much higher. Mechanical stresses affecting the stone material e.g. due to moisture load from the surface will not reach deeper than a few millimetres, as indicated by the relatively low capillary water uptake coefficient of fresh Cotta sandstone ($1.5\text{-}2\text{ kg/m}^2\text{h}^{0.5}$). The relation between YM and BFS displayed in Fig. 8 shows a slight increase towards the surface penetrated by the consolidant for the VCP-treated samples. Due to the strong scattering of this coefficient even in untreated stone material this has to be discussed with some care. All in all, however, the results obtained for mechanical parameters are acceptable in case of VCP with Fungosil 300E.

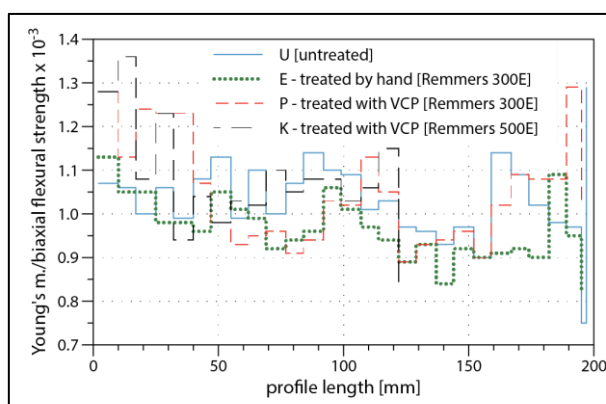


Fig. 8: Relation between Young's modulus and biaxial flexural strength along profiles across the test cubes (average values for all measurements on 5 mm discs cut from drill cores).

3.4. Hydric properties

The results obtained for total water uptake and hydric swelling are displayed in Fig. 9 and Fig. 10. The results for water vapour diffusion resistance can be found in Fig. 11. As can be seen from Fig. 9 and Fig. 11, water uptake is reduced in the impregnated zones, whereas diffusion resistance has increased. The investigation of the pore size distribution of the impregnated and the non-impregnated zones by mercury intrusion porosimetry (Wichert *et al.* 2015) has shown that there is no significant change in pore volumes in the diameter range between 0.1 and 100 μm , which is responsible for capillary transport. Thus, the decreased water uptake and the increased diffusion resistance might be explained by a slightly hydrophobic state of the outermost impregnated zones (i.e. the reaction of TEOS to silica gel is still incomplete after 4 months because the humidity during setting the gel obviously was too low). Testing with water droplets on the surface of the cubes confirmed

this assumption. Although changes are higher than demanded by Snethlage 2014 ($\leq 20\%$), they should be reduced in future with further reaction of the consolidant. Measurements of hydric dilatation (Fig. 10) did not show significant changes due to the impregnation.

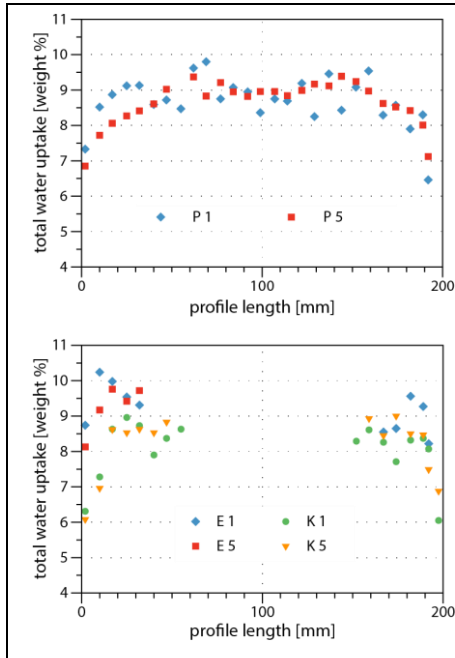


Fig. 9: Total water uptake profiles across the test cubes (measurements on 5 mm discs cut from drill cores; the discs from the inner core were not measured for cubes E and K).

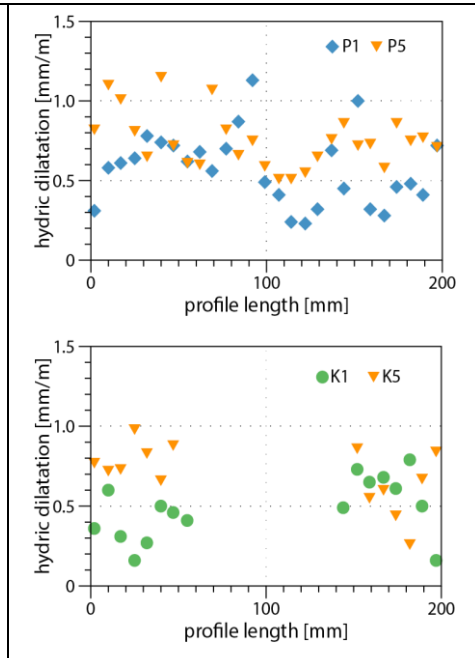


Fig. 10: Hydric dilatation profiles across the test cubes P and K (measurements on 5 mm discs cut from drill cores; 1 parallel, 5 normal to bedding). Discs from the inner core were not measured for cube K.

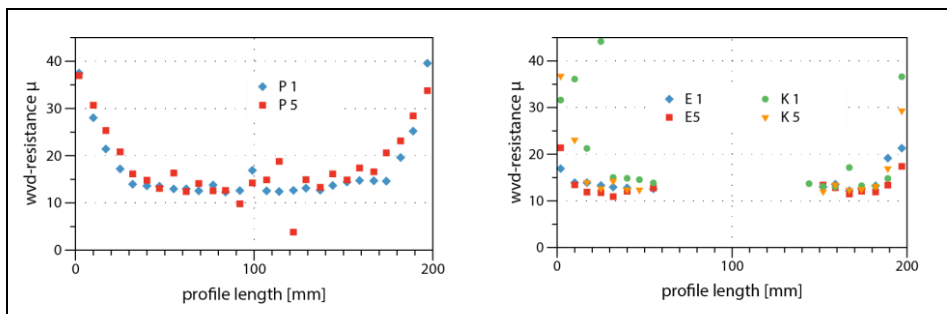


Fig. 11: Water vapour diffusion resistance profiles across the test cubes (measurements on 5 mm discs cut from drill cores; 1 normal, 5 parallel to bedding). The discs from the inner core were not measured for cubes E and K.

4. Conclusions

Treatments of test cubes made of Cotta sandstone with TEOS Funcosil 300E by hand and with Funcosil 300E and 500E by VCP showed significantly higher penetration depths for the VCP impregnated cubes. According to measurements of mechanical and hydric properties on drill core profiles taken from the test cubes, the obtained spatial distribution of BFS and YM are satisfying in case of Funcosil 300E and VCP, whereas the cubes treated with Funcosil 500E (VCP) and 300E (by hand) show steep decreases of both values from surface to the interior, which might be harmful with respect to delamination due to over-strengthening. However, the impregnated zones of all cubes are slightly hydrophobic, indicating a still incomplete reaction of TEOS after more than 4 months. Although these results in principle encourage the use of VCP in practice also for building stones with a high amount of smaller voids, the role of partial vacuum during the process still remains unclear, since similar penetration depths were reached by total immersion of a sandstone cube under atmospheric pressure only by capillary suction. Due to the expectable wide range of physical properties in geologically different stones, the results obtained cannot be easily applied to similar sandstones. The decision for appropriate conservation techniques needs detailed investigations of the stone properties and the weathering state in every case.

Acknowledgements

Thanks to Erich Pummer for the good cooperation within the common project and to K. Bretschneider, W. Lange and M. Eilenberger for technical help. The project funding by the German Federal Foundation for the Environment (Az 30408) is gratefully acknowledged.

References

- Kozub, P., 2008, To the determination of the Young's modulus from the biaxial flexural strength, Proceedings of the 11th Int. Congress on Deterioration and Conservation of Stone, Lukaszewicz, J.W. and Niemcewicz, P. (eds.), Torun, University of Torun, 407-413.
- Pummer, E., 2008, Vacuum circulation process, innovative stone conservation, in Proceedings of the 11th Int. Congress on Deterioration and Conservation of Stone, Lukaszewicz, J.W. and Niemcewicz, P. (eds.), Torun, University of Torun, 481-488.
- Snethlage, R., 2014: Stone conservation, in Siegesmund, S. and Snethlage, R. (eds.), Stone in Architecture, Springer, Heidelberg, New York, Dordrecht, London, ISBN 978-3-642-45154-6, 415-550.
- Siedel, H. and Siegesmund, S., 2014, Characterization of Stone Deterioration on Buildings, in Siegesmund, S. and Snethlage, R. (eds.), Stone in Architecture, Springer, Heidelberg, New York, Dordrecht, London, ISBN 978-3-642-45154-6, 349-414.
- Wichert, J., Siedel, H. Frühwirt, T. and Konietzky, H., 2015, Innovatives Verfahren zur Festigung von schwer konservierbaren umweltgeschädigten Sandsteindenkmalen und numerische geomechanische Simulation der Risiken, Report for the German Federal Foundation for the Environment, TU Bergakademie Freiberg and TU Dresden, 117 pp (in German).

MOULD ATTACKS! A PRACTICAL AND EFFECTIVE METHOD OF TREATING MOULD CONTAMINATED STONEMWORK

B. Stanley^{1*}, N. Luxford¹ and S. Downes²

Abstract

Almost one third of English Heritage's archaeological collections are stored in several areas of Fort Brockhurst, Gosport. For the last decade an adequate environment was maintained in these areas but during the summer of 2014 a combination of extreme moisture ingress from heavy rainfall patterns, coupled with the catastrophic failure of the industrial dehumidification units resulted in a widespread mould outbreak in one of these spaces. This paper will discuss certain assumptions; including the 'safe' environmental range of below 65% relative humidity (not applicable to this *Aspergillus* strain) and suitable treatment methods, following research carried out at Birkbeck College indicating alcohol based treatment was also ineffective against *Aspergillus*. With relatively little literature available regarding the efficacy and risks of alternative methods we will discuss several treatments considered and the UVC method trialled and approved in more detail. Finally it will discuss certain logistical and practical considerations relating to a large scale treatment of approximately 36 metric tons of stonework.

Keywords: limestone, mould, hydrogen peroxide, ultra-violet, smart ventilation

1. Introduction

A large proportion of English Heritage's reserve archaeological collections have been stored at Fort Brockhurst, Gosport for the last decade. The spaces are turf-roof, brick-built casemates, which although not typical storage spaces have maintained adequate environmental conditions for robust collections, including stonework. During summer 2014, a combination of extreme moisture ingress from heavy rainfall and catastrophic failure of the industrial dehumidification units resulted in a mould outbreak at Fort Brockhurst. The rapid speed of events led to the contamination of a large number of stone items; approximately 1,400 items, which were stored on wooden pallets but not crated due to their size. The majority of the stonework was limestone, although sandstone and granite were also present.

The risk of damage to collections from mould, including stonework is well documented, with staining of stone commonly reported, Rodrigues & Valero (2003). Literature also

¹ B. Stanley* and N. Luxford
English Heritage Trust, United Kingdom
bethan.stanley@english-heritage.org.uk

² S. Downes
University of London, United Kingdom

*corresponding author

describes how hyphal penetration of the porous spaces within stone, leads to bio-pitting, particularly on marble and limestone, Warscheid et al (2000). In addition there are a wide range of MVOCs that could also cause damage produced during the metabolic process of fungi that may cause damage in high concentrations, Korpi *et al.* (2009). The risks from damage due to germination in an environment with high *RH* levels meant the necessity to remove the spores was paramount.

The most prevalent species were isolated from the environmental swabs and morphologically sorted. *Aspergillus* was found to be the primary species and those with varying colony morphologies were genetically analysed using the internal transcribed spacer regions of the fungal rDNA. This was achieved by DNA extraction, PCR using the primer pair of ITS4 and ITS5. The resulting products were screened for purity by gel electrophoresis and then column cleaned and sent for Sanger sequencing. The sequences produced were then base called, aligned and compared against published fungal sequenced held by GenBank. Readings indicated a CFU count of over 10 times the recommended limit. This posed a particular concern as this *Aspergillus* strain can have severe health risks, Englehart et al (2002). As xerophilic fungi, this strain can grow at a reduced rate, below 65% *RH*, the ‘safe’ figure often quoted for environmental control. In-vitro, this species also germinated within 24 hours of inoculation at 20°C so is incredibly fast growing.

Location	Av CFU per m ³	% <i>Aspergillus</i>	% Penicillin	% <i>Claosporium</i>	% Yeast
Bay 9	1850	10	10	15	4
Bay 2	4383	57	18	18	3
Bay 4	4600	46	2	10	2
Bay 6	2550	35	2	12	2
Bay 8	6650	80	2	2	0
Wood Store	2600	40	3	5	2
Object Store	5367	26	7	3	0
Av Museum	3467	38	8	3	2
Outside	883	36	11	6	0

Fig. 1: Air test results, October 2014.

2. Previous Research

Knowledge that the mould strain present at Fort Brockhurst would need considerably lower *RH* levels than previously anticipated, highlighted that it might not be possible, or practical, to achieve this throughout the year. This was of particular concern as analysis of weather patterns indicated that 2104 was the fourth wettest year in the UK rainfall series from 1910, behind 2012, 2000 and 1954, Kendon, McCarthy & Jevrejava (2015). The rainfall amount in SE England during 2014 was 135% of the 1981-2010 average rainfall. This follows approximately 30 years (1961-1990) of lower than the 1981-2010 average rainfall. Should the increased rainfall seen during the last decade continue, it may be possible that previous environmental control methods would be inadequate to maintain the environment conditions in this store.

It was also important to know that should any collections be moved to another location and stored with other objects no cross contamination might occur. Research carried out at Birkbeck indicated alcohol based treatment was ineffective against this strain of *Aspergillus* and there was little literature on the efficacy and risks of alternative methods. In-vivo,

although alcohols can have an inhibitory effect (70% methanol and ethanol) after two weeks of incubation at 20°C, the effect on the growth of the fungi was no longer evident. The ethanol was however more effective than the methanol. Other solvent treatments have been trialled by this lab in the past (on organic materials) which resulted in both propan-2-ol and IMS increasing the rate and intensity of re-colonisation after cleaning.

Sterflinger and Piñar (2013) have described the limited number of biocides tested for cultural heritage use and outlined some of the risks, such as treatment with quaternary ammonium compounds leading to a more resistant community, including melanised fungi. Their work also describes the use of gamma radiation, which has both PPE and object risks associated with it. Shirakawa et al (2004) described the disinfection followed by repainting with or without a biocide included, whilst the biocide reduced the recolonization up to 10 months after treatment, after 12 months there was no statistical difference.

A common problem found was that papers either focussed on identifying the species present without commenting on their removal (Ciferri (1999), Jurado et al (2008), Montanari et al (2012)), or on possible treatments (Rodrigues and Valero (2003) Gatenby (1990) Severson (2010)) without having identified the species. Little information was available on successful treatment methods for specific species. Only recently have assessments of the efficacy of a treatment started to appear in the conservation literature (Mason and Scheerer 2014).

3. Treatment Criteria

The resilience of the mould species and quantity of collection needing treatment meant that clearly any system had to be effective. Due to the scale of collection requiring treatment it would also need to be practical to administer so therefore as quick and efficient as possible. This would include the drying time necessary with wet treatments; a particular concern as alcohol treatments had been discounted. The spaces available for storage and treatment were unheated and therefore evaporation rate was likely to be slow. From Florian's (2002) paper it was clear a thorough misting was necessary to ensure the effectiveness of the surface treatment but from tests this would result in a saturated surface.

With the quantity of stonework needing to be treated, cost was also a consideration. The industrial treatment used for all non-collection items could be bought in bulk as a powder and mixed as required, with minimal PPE. The grade of hydrogen peroxide required for stonework treatment (silver filtered, rather than the commercial grade hydrogen peroxide, which has acid added and therefore a lower pH, posing a risk to limestone) gave a cost of over £200 per 5 litres. From spray tests, this would only be sufficient for several pallets worth of stonework, so to treat approximately 450 pallets could potentially cost £20-30,000.

From the swab results, it was apparent that although the culture rate on the underside was lower, it was still significant. Therefore all sides of the stonework would need to be treated, in some instances the stone items weighed in excess of 200kg with an average weight of at least 80kg. As we would need to buy in expertise to enable this work, the project was treated as an opportunity to undertake any other outstanding issues at the time such as weighing pallets and dealing with outstanding documentation or labelling of items.

4. Analysis and Trialled Treatments

Smaller items such as bulk pottery, tiles and stone fragments are stored in plastic crates or boxes. The contents were checked and the majority of objects were not found to have mould growth. Surface swabs were randomly taken on a number of items and the results confirmed that the spore count was low for these items. In the small number of instances where active mould was observed, these crates were labelled and separated and all contents were dry dusted and repacked (this work is on-going).

The exterior of all crates were sterilised, regardless of the visual or swab results of the contents. Diluted hydrogen peroxide was suggested as a safer alternative to domestic chloride bleach and this was tested at a concentration of 1.3% and 2.5% (to avoid lowering the *pH*). A concentration of 4% was also trialled on the plastics. Commercial treatments Steri7™, Steri7 plus™ and Virkon™, which had previously been used at other properties were also tested for effectiveness. The solutions were tested ‘in situ’ on a variety of plastic crates and boxes and also in-vitro testing was conducted using an *Aspergillus* biofilm on PDA plates. Results from both swab and culture tests indicated that the Virkon™ was the most effective treatment, although Steri7™ products also performed well. Hydrogen peroxide, even at 4% concentration was not effective without multiple applications, hindered by the drying time needed between each cleaning and spraying application.

The Virkon™ and Steri7™, although very effective on the plastic containers, would not be suitable for treating stonework. As well as the pink colouration from the Virkon™, both solutions contain ammonium salts which would have the potential to cause harmful salts in the structure of limestone, calcareous sandstones and marble stonework. Similarly diluted domestic bleach could cause chloride salts to form. Hydrogen peroxide was initially trialled, but at safe concentrations for limestone (1.2%) was found to be ineffective without multiple applications and long drying times. The solution would potentially fizz when in the presence of biological factors (mould) but also if the limestone was reacting with the solution. This made it very difficult to visually check for signs of damage whilst carrying out the treatment.

Thorough cleaning using natural bristle brushes into a HEPA filter vacuum without further surface treatment was also trialled. This is used extensively as a treatment for localised mould, such as on a small area on the underside of a piece of furniture for example. It was also considered that dry dusting might be the most practical treatment for collections that were not robust enough to be treated by any of the systems tested and particularly where the display or storage environment is likely to be more controlled. Interestingly it was found that this method showed a significant improvement, with a 50-60% reduction of spore germination on the lab cultures. Regular cleaning would also help to reduce the likelihood of dust or organic matter depositing on the surface of collections on open display (including stonework), which might encourage mould growth.

Previous work on UVC treatment had noted the appearance of a salt bloom due to salt efflorescence as a result of heating and drying, Stewart et al (2008) and there was sparse information regarding light sources, methodology and treatment times. Product literature for UVC lights (Phillips UV Disinfection) gave values of the rate constant and required dose for different bacteria, yeasts, mould spores, viruses, protozoa and algae, along with calculations to determine the required dose for different UVC lights and treatment parameters. Variables include the effective irradiance (lamp dependent) and the survival

rate. Calculations during the UVC trial demonstrated that reducing the survival rate for *Aspergillus niger* from 10% to 1% required a doubling of the treatment time (from 57 min to 114 min for the selected lights). As stonework would need to be treated and then turned to treat the other side, the length of treatment time to be effective had a significant effect on the schedule. For example a treatment time of 24 hours, Stewart et al (2008) would effectively require a treatment schedule of 2.5 days per batch whereas a treatment time of 2 hours (calculated from the UVC lights selected) could potentially allow a batch of stonework to be treated each day.

Location	Treatment	Colony count (approx)	% improvement from control
SO 1	UV 2	0	-
SO 2	UV 2	0	-
SO 3	UV 3	2	-
OS 1	No Cleaning	166	-
OS 1	Dry Dusting	36	78.3%
OS 1	UV 1 Top	8	95.2%
OS 1	UV 1 Bottom	0	100.0%
OS 2	No Cleaning	439	-
OS 2	Dry Dusting	152	65.4%
OS 2	UV 1 Top	3	99.3%
OS 3	No Cleaning	127	-
OS 3	Dry Dusting	89	29.9%
OS 3	UV 1 Top	0	100.0%

Fig. 2: Table of results for cleaning methods.

To test the UVC treatment a pallet of stonework with mould contamination was identified to give a spread of differing stone types (limestone, chalky limestone, limestone with extensive pitting and moss and lichen growth, sandstone, granite). Each item of stonework was thoroughly dry dusted and placed on a plastic pallet. The test area was set up using existing pallet racking shelving to support the light source, a metre above the pallet containing the stonework. Three light fittings with Osram UVC 51V, 15W, G13 (T8) light bulbs were selected and attached to the underside of the pallet racking shelf and the whole area tented around with aluminium film to reflect the light inside the tent and black stage curtain fabric to prevent possible light leakage. The lights were left on for 24 hours and then the stonework was turned over and the process repeated. This was repeated with a second pallet with a 2 hour UVC light exposure (calculations had indicated this would be sufficient time to be effective). The difference in performance between treatment times was negligible, with preliminary tests on individual pieces of stone showing 94% to 100% effectiveness for both timescales.

5. Practical Treatments

With a suitable treatment tested and showing good results it was agreed to set up a room space for large scale treatments to optimise the process. A sturdy garden marquee frame measuring four metres square was purchased and lengths of battening cut to size to affix florescent light fixings with Osram UVC 51V, 15W, G13 (T8) bulbs fitted. A total of 35 lights were dispersed around the frame. The windows were all covered with black stage curtain fabric to prevent any light bleed and signage displayed on all doors leading to the space. A risk assessment was prepared and shared with all staff, to prevent accidental

exposure; including PPE, locking up procedure and operational safety. This space allowed an optimum average of 25 Pallets to be treated each time. It would be possible to fit more into the space but this then made the process of turning the stonework on pallets very difficult and time consuming.

All stonework has now been treated; a total of 486 pallets, at just under 36 metric tonnes of stonework. Swabs were taken at different points during the treatment, on different collections and types of stone and other than one sample (which has been retreated and it is assumed that human error was to blame, with the failure to turn the piece over) all readings give a reassuringly low result. This is particularly relevant, as, in hindsight, the increased distance between the pallets and the gazebo versus the trial racking increased from approximately one to two meters should have merited a recalculation of treatment times.

6. Smart Ventilation and Environmental Improvements

With the removal of all objects from the storage spaces, all organic storage materials were removed from the space (including shelving inserts). The area was completely cleaned and decontaminated by a professional company (Rentokil) and the results were checked using air samples gathered before and after cleaning. Once the spore levels were reduced to an acceptable level consideration was given to the most effective way to control the environment. Dehumidifiers were initially installed into the affected spaces to help reduce high *RH* levels. Calculations had shown that for the volume of spaces, the number and capacity of the dehumidifiers, should reduce the *RH* levels within a few hours. However the environment failed to improve. This highlighted that water ingress was a current rather than a historic problem resulting from heavy rainfall in 2014.

In some spaces there were fans built into the external wall of the casemate. These were utilised to provide ventilation, however there were concerns that these would bring in damp air from outside, exacerbating the problem. As a result a trial of smart ventilation was set up. One of the key controls is to calculate the absolute humidity internally and externally and switch on the fan when it is drier outside and turn it off when outside is damper. The trial is continuing in one space, however the high moisture level inside means it is rarely wetter outside and as a result other internal fans now run continuously. Additional internal fans provide further air movement around the spaces to prevent the formation of damp microclimates. The project has highlighted possible building failures leading to the ongoing water ingress. As a result investigations will shortly begin to determine the causes of water ingress and identify possible solutions. This work will determine whether the spaces are reused in the future or if alternative storage spaces will be required in the long term.

7. Conclusions

The treatment of such a quantity of collection has been a logistical challenge and has taken substantial resources. It has also challenged the perceived wisdoms regarding mould, without identifying the mould species it might have been assumed that maintaining an environment of around 65% *RH* for robust stonework would be suitable for long term storage. Similarly, many existing treatment methods in the available literature are not as effective as initially thought and has challenged us to re-examine our methods.

Many positives have come from such an unfortunate situation. It has created an opportunity to investigate more effective ways to deal with mould on robust collections and

to quantify their effectiveness on real objects as well as in the lab. A more effective solution has also been trialled and identified for non-collection materials such as crates and boxes. It is also reassuring to know that good housekeeping can add *reducing the potential of mould germination*, to its list of virtues. This information will be used to formulate guidance on mould treatment and form the basis for any further research on treatments. Discussion has begun about the merits of using this system on robust fired items such as pottery and tiles, although further investigation will be required to confirm any glazes or colorants will not be damaged and that thermal response will not cause an adverse reaction.

The existing equipment is still available and discussion has begun regarding setting up a 'quick response' system that could be used at different sites when appropriate. It has also give an opportunity to reassess other protocols, for instance the collections team will revise storage procedures to avoid substrates attractive to mould whenever possible, such as wooden pallets in aggressive environments, and include mould outbreaks in Integrated Emergency Planning. The stonework which has been treated has improved storage as it has all now been thoroughly cleaned and treated and repacked. All documentation has been checked and the new barcoding system used on all pallets to improve the tracking and identification of objects. Although this not how we would wish to begin a storage project, the works undertaken have resulted in improved conditions for all the objects involved.

Acknowledgments

A number of individuals have assisted during this project to bring the treatments to a successful conclusion, but particular thanks must go to Timothy Hill and Adrian Braddock who carried out the works on site. Also to the following English Heritage Trust staff; Andrew More, Paul Lankester, Dave Thickett, Amber Xavier-Rowe, Kirsty Huggett, Emma Hallums, Ann Katrin Koester, Pam Braddock, Cameron Moffett and Martin Allfrey. Thanks also to Jane Nicklin and Krystina Merka-Richards from Birkbeck College.

References

- Stavroudis, C., (compiled by), 2012, Superstorm Sandy: Frontline Advice for Dealing with Mold and Salvaging Electronic Devices, WAAC Newsletter 34 (3)
- Ciferri, O., 1999, Microbial Degradation of Paintings, Applied and Environmental Microbiology, 65, 879-885
- Engelhart *et al.*, 2002, Occurrence of Toxigenic *Aspergillus versicolor* Isolates and Sterigmatocystin in Carpet Dust from Damp Indoor Environments, Applied and Environmental Microbiology, 3886–3890
- Florian, M.L., 2002, Fungal Facts: Solving fungal problems in heritage. London, Archetype Publications
- Gatenby, S., 1990, An Investigation into Cleaning Procedures for Mould Stained Australian Aboriginal Objects Painted with Modern Media, in 9th ICOM-CC Triennial Meeting, Dresden (26-31 August 1990), Grimstad, K. (ed.), Los Angeles, ICOM Committee for Conservation, 157-162

- Gadd, G. M., 2007, Geomycology: Biogeochemical Transformations of Rocks, Minerals, Metal and Radionuclides by Fungi, Bioweathering and Bioremediation, *Mycological Research*, 111, 3-49
- Jurado, V., Sanchez-Moral, S. and Saiz-Jimenez, C., 2008, Entomogenous Fungi and the Conservation of the Cultural Heritage: A Review, *International Biodeterioration and Biodegradation*, 62, 325-330
- Kendon, M., McCarthy, M., and S. Jevrejeva (2015): State of the UK Climate 2014, Met Office, Exeter, UK http://www.metoffice.gov.uk/media/pdf/0/a/State_of_the_UK_climate_2014.pdf
- Korpi *et al.*, 2009, Microbial Volatile Organic Compounds, *Critical Reviews in Toxicology*, 39, 139–193
- Mason, L. and Scheerer, S. 2014, Mould Attack! – Assessment of Dry-Cleaning Methods for the Decontamination of Leather, In *ICOM-CC 17th Triennial Conference Preprints*, Melbourne, 15-19 September 2014, Bridgland, J. (ed.), Paris, International Council of Museums, flash drive 0702_259
- Montanari, M., Melloni, V., Pinzari, F. and Innocenti, G., 2012, Fungal Biodeterioration of Historical Library Materials Stored in Compactus Movable Shelves, *International Biodeterioration and Biodegradation*, 75, 83-88
- Philips, n.d., UV Disinfection – Application Information: Perfection Preserved by the purest of light
- Rodrigues, J. D. and Valero, J., 2003, A Brief Note on the Elimination of Dark Stains of Biological Origin, *Studies in Conservation*, 48 (1), 17-22
- Severson, K., 2010, Formulating Programs for Long-Term Care of Excavated Marble: Removing & Suppressing Biological Growth, in *Proceedings of Conservation and the Eastern Mediterranean: Contributions to 2010 IIC Congress*, Istanbul, Rozeik, C., Roy, A. & Saunders, D. (eds.), London, Archetype Publications, 172-177
- Shirakawa, M. A., John, V. M., Gaylarde, C. C., Gaylarde, P. and Gambale, W. 2004. Mould and Phototroph Growth on Masonry Facades After Repainting, *Materials and Structures*, 37, 472-479
- Sterflinger, K., 2000, Fungi as Geologic Agents, *Geomicrobiology Journal*, 17, 97-124
- Sterflinger, K. and Piñar, G., 2013, Microbial Deterioration of Cultural Heritage and Works of Art – Tilting at Windmills?, *Applied Microbiology and Biotechnology*, 97, 9637-9646
- Stewart, J., More, A. and Simpson, P., 2008, The Use of Ultraviolet Irradiation to Control Microbiological Growth on Mosaic Pavements: A Preliminary Assessment at Newport Roman Villa, in *Conservation: An Act of Discovery*, 10th Conference of the International Committee for the Conservation of Mosaics, Palermo, October 20-26 2008, Michaelides, D. (ed.), Palermo, Centro Regionale per la Progettazione e il Restauro, 296-305
- Warscheid, Th. and Braams, J., 2000, Biodeterioration of Stone: A Review, *International Biodeterioration and Biodegradation*, 46, 343-368.

INJECTION GROUTS BASED ON LITHIUM SILICATE BINDER: A REVIEW OF INJECTABILITY AND COHESIVE INTEGRITY

A. Thorn¹

Abstract

The bonding of detached sandstone in outdoor exposure remains a challenge where long term stability must combine with sufficient durability to withstand exposure to severe environmental stresses. Grouts that form or are comprised of minerals not identical to the original surface run the risk of creating hydrothermal differentiation, altered permeability, or chemical incompatibility that may lead to rapid future decohesion or the enhanced growth of micro-flora that become more disfiguring than a poorly matched initial grout. Following successful development of lithium silicate bound mortars, this paper focusses on the development and performance of injectable grades that can be applied to closed voids through 2-3 millimetre openings that set to form a substantial bond between detachment and parent stone. Following these evaluations the best performing formulation has been applied to a test site with satisfactory initial results. The visualization provided by the test method allows the application to be far better informed about the need for consolidation and injection grouting as symbiotic procedures.

Keywords: lithium silicate injectable grout, ethyl silicate, sandstone

1. Introduction

Previous studies have evaluated the potential for lithium silicate to consolidate sandstone and calcitic stones (Thorn 2011a) including in wet conditions (Thorn 2011b) and to act as a binder for bulk mortars (Thorn 2010) the final chapter in developing an all-round repair material is in the capacity of lithium silicate as an injectable grout, applied by syringe to closed spaces where it will provide adhesive reattachment of detaching stone. Ethyl silicate has been trialled as a mortar (Leissen 2004, Thorn 2010) but found to be too weak and lacking in both cohesion and adhesion when injected through a small opening. Ethyl silicate rapidly loses strength when grain size is reduced to catheter dimensions and excess silicate becomes a negative factor. Overall ethyl silicate is unsuited to the high adhesion demands of an injectable grout. Lithium silicate by contrast has very high bond strength and is capable, for example, of binding individual sand grains to a glass substrate at high strength.

This paper considers whether lithium silicate can be successfully formulated, pass through a 2 mm opening into a larger cavity, and form a cohesive and adhesive cured mass capable of securing a detachment to its parent stone. The test methods have been influenced by the very useful GCI manual - *Evaluation of Lime-Based Hydraulic Injection Grouts for the Conservation of Architectural Surfaces: A Manual of Laboratory and Field Test Methods*

¹ A. Thorn

Fine art and heritage site conservator, PO Box 333, Carlton North, Victoria 3054, Australia
Andrew.Thorn@artcare.cc

*corresponding author

(Bicer Simsir B. and Rainer L. 2011). While this manual (referred to henceforth as the GCI methodology) is focussed on the evaluation of grouts appropriate for calcitic plaster attachment, its framework provides a useful starting point for the assessment of all injectable grouts.

The focus on injectable lithium silicate has resulted in a stable material that can be injected through a catheter or 2 mm opening to completely fill an enclosed void and secure a 10 mm thick detachment to its matching parent stone. There are separation and shrinkage issues that remain concerns but the testing has shown how these are not such an issue in real world application or not as damaging as some test methods might indicate.

2. Grout formulation

The aim of this paper is not to give batching formulations, for which the research is not complete enough, but to outline the parameters by which a successful injectable grout can be designed. The limiting factors are that the material must be able to enter an enclosed void through a two millimetre opening, flow to completely fill all parts of the void below the hole and to set in a reasonable time to hold the outer detached surface in place with sufficient adhesive strength. The applied grout must be absorbed into the cavity walls in such a manner that both initial lubrication and final bond is achieved. The final set grout should allow moisture to pass through at levels relevant to its location within the stone, as opposed to how it might respond to direct surface flooding, and ensure that no staining of the surface will develop through nutrient minerals migrating to the surface and thus supporting differential bio-colonies. This latter condition is considered critical as mortars and grouts of both lime and Portland cement have been observed to induce substantial dark bio-staining on the surface even when placed at depth.

In earlier studies using ethyl silicate as binder, it was found that once the grain size was reduced below 500 microns the cohesion strength reduced dramatically. Even with grain size greater than this the strength of non-injectable ethyl silicate mortars was barely satisfactory in terms of cohesive and adhesive strength. Lithium silicate mortars have much higher adhesive and cohesive properties to the extent that where they were used to fill surface cavities in a polished marble sculpture isolated sand grains from the mortar became strongly attached to the polished surface surrounding the cavity.

Early experimental formulations reduced the lithium silicate content from its original 22% solids content to as low as 2%. It has been found over the course of several years that undiluted product will produce a readily water absorbent cured mortar and this is equally the case with finer grained grouts. One of the advantages over ethyl silicate mortars is that the material is water absorbent from the outset whereas ethyl silicate passes through a strongly hydrophobic gel phase, remaining water repellent for several weeks. The downside of water permeability is that the lithium grout or mortar is readily disturbed by rain and must remain covered until complete set, as discussed further on.

Lithium silicate binder can be added in its supplied form or diluted 1:1 with water to make a more porous grout with lower strength. Dilution with solvents is very limited with no more than 20% ethanol being compatible in the liquid phase. Lime grouts contain large quantities of free water and this has been considered deleterious. To minimize this, conservators have for many years reduced the water content while maintaining fluidity by substituting solvents such as isopropanol. This is only possible to a limited extent with

lithium silicate and the current testing has shown that this is not an essential requirement of the grout.

The addition of phosphoric acid has been discussed elsewhere (Thorn 2012) as a means of converting the bi-product lithium carbonate into the less soluble and more usefully binding lithium phosphate. This reduces the *pH* of the applied liquid, producing a more durable cured mortar. For this study the modification of the end product has not been addressed in detail but phosphoric acid additions certainly produce a more durable material, especially in wet conditions. This paper is focussed exclusively on the mechanics of injection, cure and bond rather than the formulation of the optimal product, which will be discussed in time.

In preliminary trials mortar shrinkage was assessed by placing a coarse mix containing river sand and gravel up to 5 mm into a straight sided glass culture dish. The curing mortar expanded progressively over several weeks to finally shatter the dish. By contrast the finest filler used in the mortar formulation was a trass (pozzolanic ash) incorporated solely for colour matching purposes. The trass ranges up to 50 microns in size and when placed in the same dish displayed extensive shrinkage cracking. Fig. 1 shows both results side by side.



Fig. 1: Two preliminary studies of the interaction between lithium silicate and silicate fillers. On the left a coarse river sand expanded to the point where the glass container was cracked. On the right a very fine Trass (pozzolana) shrank excessively.

Quartz flour sieved to 100 microns showed no internal shrinkage cracks but some peripheral shrinkage. Increasing the grain size to 300 microns did not alter the shrinkage pattern to any substantial degree. Fig. 2 gives the particle size distribution of the chosen quartz flour (Sibelco 100WQ) in comparison with other grades.

Grouts applied to enclosed cavities do not need to match surface colour and those applied to open pockets can be capped with an appropriately matched mortar optimized for exposure. Hence the current trials have focussed only on granulometry and not aesthetic considerations. It is important to note however that injectable lithium grouts will, like other materials, adhere to the opening, which itself needs to be capped to complete the treatment.

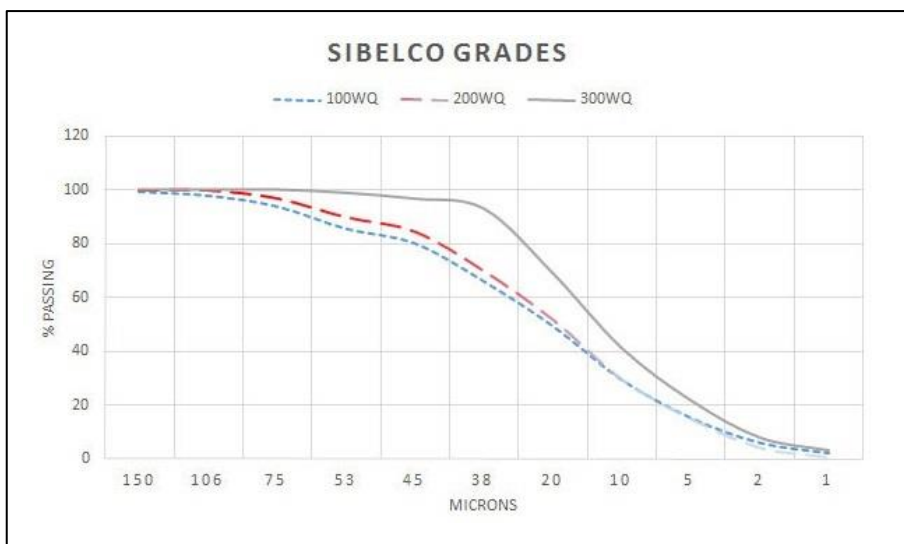


Fig. 2: Particle size distribution of the selected filler 100WQ compared to two other grades of Sibelco quartz flour.

3. Test methods

3.1. Shrinkage

The GCI methodology measures shrinkage by placing a quantity of fresh grout into an open cup made from either an impervious material or, in another method, from a plaster cup, which better emulates the natural placement conditions, particularly with reference to absorption during set. In the current development lithium silicate at 20% and 10% solids (the latter diluted with water 1:1) were mixed with quartz flour 100 WQ to a viscosity that could be drawn into a 1 mm diameter catheter. The quartz to lithium silicate ratio was established intuitively to give the desired pick up viscosity than confirmed as 100:55 filler to binder ratio.

Adopting the GCI methodology created a difficult result. The upper surface shrank dramatically after about 2 weeks (Fig. 3), but exposed a very stable cured grout beneath. This anisotropic cure was clearly the result of surface effects of evaporation and reverse migration depositing excess lithium silicate in the outer crust. A similar crust had been seen on some of the previous test mortars prepared in glass dishes, although this has never been an issue with many site trials where the cured mortar remains very close to the texture of the surrounding stone, largely due to the constant working of the surface to achieve a level and suitably textured finish.

Under the GCI methodology the grout would not pass the shrinkage test, however it was recognized that an open cup does not represent the true placement conditions. An enclosed cavity does not have a broad surface exposed to the atmosphere but rather two broad surfaces in contact with the stone, a lower depth of ever decreasing dimensions to a point where an homogenous grout will cease to flow, and an upper thin surface exposed to a wide

opening or small drill hole of no more than 4 mm. A series of modified test procedures were adopted to better reflect the real life dimensional configuration that could also observe the flow and cure behaviour over time. Time lapse photography was employed to record the behaviour of each test.



Fig. 3: Excessive shrinkage from the 100:55 quartz flour : lithium silicate formulation when poured into an open impervious cup. This result led to the alternative test methods relying on more replicative applications to vertically oriented cavities.

The series consisted of combinations of stone surfaces and 1.5 mm thick transparent plastic sheet (polyethylene phthalate glycol - PETG). The configurations were as follows and as illustrated in Fig. 4:

- Two sheets held vertically and spaced 2 mm apart. All edges were sealed except the top access surface. The top surface could be temporarily sealed to emulate the access hole dimensions and natural evaporation conditions.
- Two sheets, as above but clamped along the bottom edge to provide a wedge shaped cavity of decreasing width down to less than 0.1 mm.
- One PETG sheet spaced 2mm off a sawn sandstone surface and sealed as above
- A 10 mm thick sawn sheet of stone spaced with 2mm wooden spacers off a larger sawn parent stone, the detachment held against the spacers and removed at timed intervals. The 10 mm detachment was considered to be heavier than most detachments that are more typically no more than 3 mm in thickness with proportionally less mass.

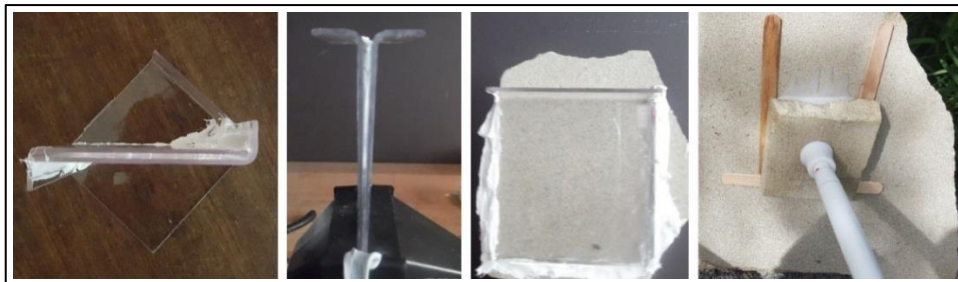


Fig. 4: The four cavity configurations. From the left; two PETG sheets spaced 2mm apart (top view), the same sheets formed into a tapered cavity closed but not sealed at the bottom (side view), a PETG sheet spaced off a sawn sandstone block, and a 10 mm thick block pressed dry onto spacers and then filled with grout. The 10 mm detachment fell after 2 hours but remained firmly in place after 14 hours.

Applying grout to the spaced parallel sheets resulted in an homogenous grout showing initial shrinkage but eventually, bleed liquid above the initial settlement mark. There was an initial shrinkage of 10.5%, but upon release of the bleed liquid the final level showed a net expansion of 6.7%, all of which was lithium silicate solids with no quartz flour filler (Fig. 5). Further grout applied to the system, emulating a sequential application such as those necessary to fill large voids, settled onto the top of what had seemed to be bleed liquid but was in fact solidified lithium silicate. This was undesirable to have a thin band of solid lithium silicate creating a differential band in the void but also most likely continuing to a point where it became a brittle non-adhesive rubble in the fill. The final product showed no signs of cracking, with the shrinkage along the top edge being the only defect. Expansion of more than 6% may present issues in a closed system, however this only occurred in the wholly PETG wall scenario. Once stone surfaces were introduced into the system all bleed liquid was absorbed and no expansion was noted. The PETG on stone configuration produced an almost perfectly stable dimensional material.

Two sheets of plastic are far from an accurate model for a detachment void in stone. The next test applied the grout between a plastic sheet spaced off a sawn stone surface. In this case there was no bleed liquid as it was absorbed into the stone surface as it formed, or was sufficiently absorbed not to form at the upper surface of the grout. In all tests involving stone surfaces the stone was saturated with lithium silicate to emulate a normal treatment protocol. The cured grout appeared stable and in this case did not develop a transparent lithium silicate upper edge.

The same 100:55 grout was applied to the two stone surfaces following saturation with liquid lithium silicate. The 10 mm detachment was considered far heavier than a typical delamination but an appropriate measure of the ability of the grout to form bonds sufficiently strong to hold such weight. Stone detachments were spaced 2 mm from the surface and held in place by a single telescopic prop typically used in practice. Once the dry system was secured in position the internal stone walls were pre-wet with lithium silicate and the void filled with grout. No topping up was attempted but any leakage through the spacers was plugged and the void filled to near the top. The prop was removed after 2 hours with immediate failure. The prop from the second sample was removed after 14 hours (replicating overnight curing) and in this case the 10mm thick detachment remained

perfectly positioned and secured to the parent rock. At this stage no intermediate setting times have been established and it is reasonable to propose a 24 hour propping period for normal field practice.

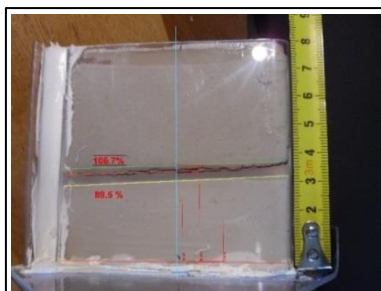


Fig. 5: Grout applied to parallel PETG sheets shrank initially by 10.5% but the bleed liquid formed a transparent solid block that showed a final expansion of 6.7%. A further grout application has been applied over the first to indicate the final level of the lower application. Expansion and bleed liquid were only apparent where two plastic sheets formed the walls of the cavity. Once sandstone walls were introduced they absorbed all bleed liquid and showed shrinkage only.

The stone on stone sample was further exposed to outdoor conditions for 45 days where it received rain, incidental watering and ambient temperatures of up to 40°C. After the 45 days the detachment was separated from the parent rock to empirically assess its bond strength and, more importantly, the consistency of the cured grout. It was seen that the grout displayed a network of shrinkage cracks not seen in the test configurations involving plastic sheet (see figure 6). There was no evidence of bleed water related transparent lithium silicate but some evidence of shrinkage to the open top surface but not away from the three enclosed sides. The test, as with all those previously described, relied on the bond strength of pure lithium silicate without the additions, previously indicated, that improve the strength and rheological properties of cured product. At this stage the research is concentrating on the performance of pure lithium silicate knowing that it can be strengthened with proven additions.



Fig. 6: Grout applied to two sandstone surfaces remained secure for 45 days at which point it was separated. The bond was adequate but lower than ideal. The inner surface showed a network of cracks that no doubt contributed to this. The shrinkage is considered to be the result of the stone sucking liquid from the grout too quickly, emphasizing the need for adequate pre-wetting of the inner surfaces.

The final grout was adequate for reattachment of a heavy detachment but less than achieved with the plastic sheet trials containing all of the grout with no absorption into adjacent porous material. The grout formed between two stone surfaces was also substantially weaker than lithium silicate mortars applied directly to stone surfaces. From this a couple of points of consideration emerge. The first is that wetting of the inner stone surfaces must be thorough; a critical consideration when applying grouts to closed voids. The second is that further improvement is desirable. While the lithium silicate was adequate it was not ideal. Both the addition of silica sol and especially phosphoric acid has shown a marked improvement in cohesive strength of lithium silicate mortars and these refinements will be evaluated in ongoing trials. The additive performance is already well understood from previous mortar trials and thus the transfer of knowledge presents reasonably well defined parameters.

3.2. Bleed liquid

Bleed water has been discussed already but it is worth highlighting the issues specific to lithium silicate grout. The GCI methodology for lime grouts defines limits of 0.4% bleed water. This may be significant for lime grouts as the excess water contributes little to the final product but substantially to shrinkage cracking and other defects. Recent field research on the stabilisation of clay renders for Himalayan mural paintings by Nicolaescu (2016), in which this author assisted, it was found that the bleed water content of the ideal clay based grout was almost 9%. In that research the amount of water required to pre-wet the clay walls, using industry standard pre-wetting procedures, exceeded the bleed water content of the clay based grouts. Hence bleed water was considered less threatening to the stability of the mural than the accepted pre-wetting regime. The 9% bleed water is that achieved in a glass cylinder and, as in the lithium silicate experiments described above, does not translate to conditions encountered inside a clay void where suction into the render on one side and the mass of adobe blocks on the other determines that no amount of bleed water will neutralize suction.

Bleed liquid measured in a sealed container reached approximately 10% after 24 hours. This was less than the solid transparent lithium silicate zone formed in the vertical cavity trials (figure5), which indicated a 16% expansion from the maximum shrinkage to final expansion states.

The current view of bleeding, both in clay stabilisation and the current research, is that its contribution to the grouting process needs to be clearly understood and not assumed to be negative without firm evidence. In the current research bleed liquid is considered positive, as illustrated by grouts flowing into the plastic sheet wedge aimed at measuring unimpeded flow properties. In this test the standard 100:55 grout was deposited into a plastic wedge with both sides sealed, the bottom clamped tightly together and the top open to a width of approximately 5mm. The side view of this configuration, any point of which could be precisely measured from photographs, can be seen second from the left in figure 4. The grout flowed quickly initially to where it stopped flowing at around 0.9mm width. Over the following 24 hours the grout continued to flow into finer voids, eventually arriving at the bottom of the wedge where the width was less than 0.2 mm. During this delayed flow, and perhaps because of it, bleed liquid emerged at the bottom of the void rather than at the top of the grout. Two phases developed, one a transparent phase of presumably pure lithium silicate and a second milky phase that contained some quartz flour. Fig. 7 shows after 5 days that the grout has separated into three phases. The bulk of the grout remains in the

zone 0.2-0.9 mm with a milky phase flowing into available spaces. The clear areas in the lower section are all solid lithium silicate, indicating that the grout is self-filling through the release of bleed liquid. While the intended 100 micron grout formulation does not flow much below 200 microns the subsequent bleed phases do allow further penetration. Torraca (1981) has articulated the importance of securing a detachment at its crack propagation point and the bleed liquid can achieve this better than the bulk grout alone. It has to be borne in mind however that lithium silicate bleed liquid is not observed once a porous wall is introduced into the system. Lithium silicate will be deposited into the finest pore spacings through the pre-wetting treatment and the treatment does not rely on bleed liquid performing this function.

Where the 100:55 grout was applied to two stones surfaces the pull-off resistance was lower than desired. This combined with the crazed inner surface (Fig. 6) suggests that rather than excessive bleed liquid, the system suffers too much from suction into the stone surfaces, leaving the grout depleted of binder. This means that no further reduction of lithium silicate is currently contemplated and that a more thorough pre-wetting regime is necessary.

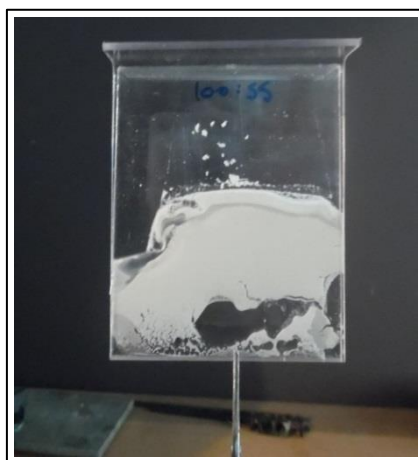


Fig. 7: Lithium silicate grout applied to a tapered cavity ranging from 5 mm at the top to less than 0.2 mm at the bottom. The grout sat initially at cavities greater than 0.9 mm then in time began to flow into the finer dimensions down to 0.2 mm. This only began once the bleed liquid provided additional lubrication and some separation of the particles began. The clear areas at the bottom are transparent lithium silicate solids while a zone of milky grout can be seen along the left edge in two places.

3.3. Flow

The GCI protocol describes two means of assessing flow. The first is flow down an open grooved tile where 10mL of an ideal grout should travel at least 200 mm, and the second is a rubble filled syringe through which the grout should flow and depart through the open hole at the bottom.

These tests were performed using the lithium silicate grouts. The open tile test achieved a high score and the rubble filled flow test showed grout flowing through the rubble

adequately, provided it was sufficiently wet prior to grout application. The grout, due to its broad viscosity tolerance (pure lithium silicate Li 22 will set into a solid transparent film that maintains structural stability for years) can have controlled flow depending on the application. What would be considered too wet in a lime based grout will form a solid stable lithium silicate grout. Films of lithium silicate and quartz flour that formed on the sides of the plastic sheet could be removed as thin sheets of less than 50 microns and retain their cohesive structure and yet these would have been very liquid films when applied.

4. Conclusion

While the work described here remains experimental the final grout, using several modifications not yet discussed, will be applied to a controlled field trial at a site that has received extensive ethyl silicate grouts over 20 years. It has been established that the lithium silicate mortar variant is far superior to those achieved with ethyl silicate. Injection grouts were not possible using ethyl silicate with the injected product lacking cohesive and adhesive properties when applied to porous surfaces.

The lithium silicate grouts described here have proven themselves capable of attaching an oversized delamination to parent rock with minimal pre-wetting and preparation. Earlier mortar development with modifications of silica sol and phosphoric acid, while not complete enough when incorporated into injectable grouts to describe here, increase the cohesive strength. This combined with a more thorough pre-wetting regime should ensure that a lithium silicate based injectable grout is capable of reattaching stone in the short term. Controlled trials will establish the longevity of such treatments.

References

- Leisen, H., von Plehwe-Leisen, E., Warrak, S. 2004. Success and limits for stone repair mortars based on tetra ethyl silicate-conservation of the reliefs at Angkor Wat Temple, Cambodia. In Proceedings of the 10th International congress on Deterioration and Conservation of Stone; ICOMOS Sweden, Stockholm. 331-338.
- Nicolaescu, A.C. 2016. Conservation of Buddhist wall paintings with traditional materials. In XII World Congress on Earthen Architecture, Lyon. In press.
- Thorn, A. 2010. Two siliceous grouts for the preservation of stone. In Proceedings of the 2nd conference and of the Final Workshop of RILEM TC203-RHM: Pro 78; Historic Mortars. 1199-1208.
- Thorn, A. 2011a The consolidation and bonding of water-saturated siliceous stone with lithium silicate —A preliminary evaluation. In Proceedings of the Canadian Conservation Institute Symposium 2011: Adhesives and Consolidants for Conservation. Accessed on 05/02/16 at <https://www.cci-icc.gc.ca/discovercci-decouvriricc/PDFs/Paper%2028%20-%20Thorn%20-%20English.pdf>.
- Thorn, A. 2011b. Preliminary evaluation of lithium silicate for consolidation and grouting of stone in wet locations. In Wall Paintings in Crypts, Grottoes and Catacombs. Strategies for the Conservation of Coated Surfaces in Damp Environments. ICOMOS Germany.
- Torraca, G., 1981, Porous Building Materials: Materials Science for Architectural Conservation. ICCROM Rome.

INNOVATIVE TREATMENTS AND MATERIALS FOR THE CONSERVATION OF THE STRONGLY SALT- CONTAMINATED MICHAELIS CHURCH IN ZEITZ, GERMANY

W. Wedekind^{1*}, R.A. López-Doncel², J. Rüdrieh³ and Y. Rieffel⁴

Abstract

The sandstone of the Michaelis Church in Zeitz shows a strong decay in form of relief and alveolar weathering. The main cause for the deterioration is an extreme salt attack by magnesium sulfate. The stone as well as the weathering forms were investigated. The alveoles were desalinated by using a sprinkling method and filled by a developed hot-lime mortar. Consequently, a concept of conservation could be formulated from all the investigations and the results obtained from the treatments that could be successfully applied in a test case.

Keywords: alveolar weathering, salt, desalination, conservation

1. Introduction

The Michaelis Church in Zeitz represents a 10th century building, which has consistently undergone modifications to its façade over time. The church was constructed out of dolomite cemented sandstone that often shows alveolar weathering as a result of salt weathering (Ruedrieh *et al.* 2006).

2. Preliminary investigations

2.1. Geological setting, rock material and weathering agents

2.1.1. Geological setting and rock material

The walls are constructed from the regional sandstone (Buntsandstein Formation). Hirschwald (1910) mentions quarries near Kretschau and Kuhndorf. Other large rock formations are located in the north-eastern region around the Zeitz as is shown in (Fig. 1b).

¹ W. Wedekind*

Geoscience Centre of the University Göttingen and
Applied conservation Science (ACS), Göttingen, Germany
wwedekind@gmx.de

² R.A. López-Doncel

Geological Institute, Autonomous University of San Luis Potosi, Mexico

³ J. Rüdrieh

Geoscience Centre of the University Göttingen, Germany

⁴ Y. Rieffel

Berlin Monument Authority, Berlin, Germany

*corresponding author

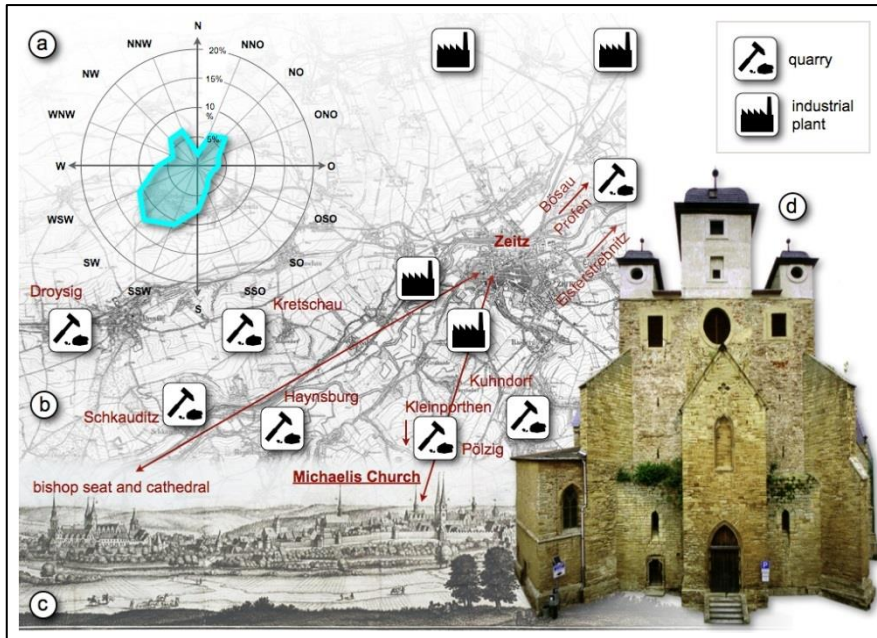


Fig. 1: a) The main wind and rain directions in percent (www.windfinder.com). b) Zeitz and its environs around 1912 with location of quarries and industrial areas. c) Lithograph of the medieval city of Zeitz from the “*Topographia Germaniae*” by Matthäus Merian (1593-1650), showing the outstanding historical buildings and topography. d) The western façade of the church in 2005.

2.1.2. Environmental impacts and geographical setting

During the industrial revolution Zeitz became one of the main centers for charcoal extraction and coal briquette production, starting in 1800 and continuing up into the 1990s. The briquette production factories, that produce a high content of sulfur from industrial pollution, were located near the mining areas west of the town. The church is located on a hill at the southwest of the historical city. The main wind and rain direction is from the southwest with 13.4 %, followed by a west-southwest direction with 11.6 %, and the south-southwest with 10.9 % (Fig 1a). Consequently, sulfur pollutants were transported continuously in the direction of the historical city over a period of nearly two hundred years. The impact can be seen today on the Michaelis Church, which exhibits dramatic forms of alveolar weathering on the western and southwestern side of the building (Fig. 1d, Fig. 2b).

2.1.3. Salt and weathering forms

In the case of historical buildings in Zeitz, industrial pollution in combination with the binding material of the sandstone creates a salt with a high potential for damage: magnesium sulfate. This salt results in extensive salt weathering in historical monuments as well, if dolomite-cemented stone or mortar and gypsum mortars are present (Siedel 2003, 2013, Wedekind 2014). The system of magnesium sulfate consists of three stable

crystalline phases in the atmosphere with a different number of water molecules bound within the crystalline structure: epsomite ($\text{MgSO}_4 \cdot 7\text{H}_2\text{O}$), hexahydrate ($\text{MgSO}_4 \cdot 6\text{H}_2\text{O}$) and kieserite ($\text{MgSO}_4 \cdot \text{H}_2\text{O}$). The damage potential of magnesium sulfate can be traced back to the stress generated by crystallization and hydration (Steiger *et al.* 2008). The main stress is induced by salt crystallization (Balboni *et al.* 2011). Salt weathering in Zeitz is characterized by contour scaling associated with alveolar weathering (Fig. 2).

2.2. Methods of Investigations and applied conservation

2.2.1. Petrographic and petrophysical properties of the rock

Porosity and the matrix- and bulk density were measured using hydrostatic weighting (DIN 52 102). The capillary water absorption or water uptake was measured on cubes (65 mm) with respect to the X, Y and Z directions. For the compressive strength tests, standard cylindrical specimens of 50 mm in diameter and 50 mm in length with co-planar end-faces were used and tested by a servo-hydraulic testing machine. To assess the salt weathering sensitivity of the investigated sandstone in this study, a salt-weathering test according to the standard DIN EN 12370 was performed. Polarisation and cathodoluminescence microscopy on standard thin sections were used for the petrographic analyses (e.g. mineralogical composition, grain boundary geometry, average grain size and sorting).

2.2.2. Onsite investigations

To register and evaluate the weathering damages, mappings of intensity and forms were done for selected sub-areas at the main façade of the building. Samples were taken by drill cores (Fig. 5 b). The amount of soluble salts was measured by ion chromatography and photo-spectrometry. In order to identify the crystalline salt phases, x-ray diffraction was carried out.

2.2.3. Desalination and evaluation

Salt reduction is a basic prerequisite for a sustainable restoration. The most suitable desalination method is dependent on a number of factors. Factors that need to be taken into account are the rock material, the degree of contamination and depth and type of salt responsible for the damage. It becomes clear that the contamination detected at depth can not be reached by the poultice method (Fig. 4b) and the drying rate of the material is quite small. In general, immobilization of the salt by chemical ionic exchange and subsequent precipitation would be possible but in this case difficult to control. For this reason the sprinkling method was chosen as the most effective technique in terms of function, time and costs. To evaluate a suitable conservation treatment a strongly weathered pillar was chosen as a test case. The surface of the pillar was divided into different treatment sections (Fig. 2). The development of weathering was documented by using historical photos (Fig. 2a to 2c).

The sprinkling method was developed for the desalination of salt contaminated tafoni of the rock cut façade in Petra/Jordan (Wedekind, Rüdrieh 2006). The method was already used successfully for the desalination of architectural elements at the Franciscan Church in Zeitz (Wedekind, Rieffel 2014). Through spray nozzles, connected within a raster-like pipe system, water was sprayed on the different sections. The water running down the pillar was collected and measured by electrical conductivity. At the beginning of the procedure the water is predominantly absorbed by the porous stone surface through capillary forces. Water absorption is dependent upon the transport properties of the material. These are

controlled by the pore space properties, such as porosity and pore radii distribution, and are a time-dependent process (Wittmann 1996).

At the lower end of the treated area a drain gutter was constructed from clay, so that the eluate can be funneled into a sample container. Excess water not absorbed by the stone was collected in five liter amounts and measured for electrical conductivity (mS/cm). Fifty liters of eluate were collected and tested in five liter amounts per cycle. The sprinkling was terminated after a treatment of about 10 minutes. After every sprinkling cycle, a break of one week was observed in order to initiate the drying procedure, which leads to the concentration of salts in the near-surface area of the stone.

Five cycles were done over a period of three months. The correlation between the electrical conductivity and the real content of soluble substances within the eluate was calculated by evaporation of different samples consisting of one liter eluate in a drying oven and weighing. Consolidation was not necessary because all the unstable material was removed by the smooth washing process of desalination.

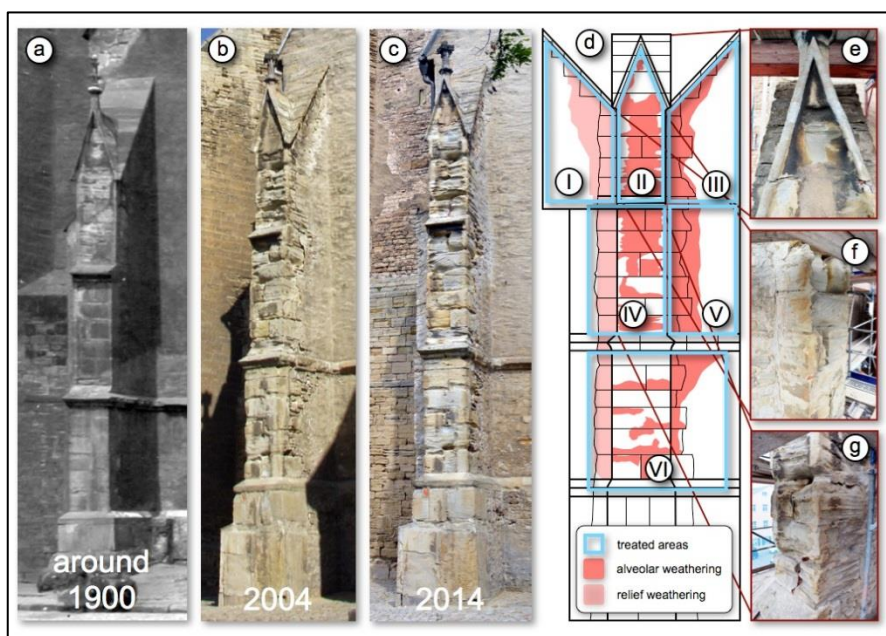


Fig. 2: a-c) The chosen pillar during different years. d) Architectural drawing with weathering conditions and treatment areas and e-g) alveolar weathering forms in detail.

2.2.4. Material physics of the restoration mortar

As a finishing mortar for restoration a modified hot-lime mortar was configured. To reduce and to control the speed of thermal reaction as well as to enhance the workability, an additive of a hydraulic binder was added to the dry mortar mix. The change in reaction could be measured by thermal expansion and temperature. Crushed and sieved sand made from the local sandstone with a grain size distribution ranging 0.1-0.5 mm was used as

aggregate to create compatibility with the stone material. Specimens after DIN EN 196-1 (4×4×16 cm) of different mortar mixes were made: The binder/aggregate composition of the hot lime mortar was 1:3. Main binding material of the specimens for the hot lime mortar was unhydrated lime C1 80 Q modified with white Portland cement (WC) in different ratios. During the process of hardening, the surface temperature as well as the dilatation was measured on the specimen top to evaluate the intensity of the exothermic reaction and the process of expansion and shrinking. After 28 days of drying under the same conditions, porosity, density and flexural (FS) and uniaxial compressive strength (UCS) were measured.

3. Results

3.1. The sandstone

3.1.1. Petrography

The sandstone of Zeitz mostly has a yellow color. Besides these varieties, which clearly dominate the stone architecture of the town, grayish to greenish types are also present. The medium sandstones show a good parallel or obliquely layered structure. Many sedimentary structures like cross bedding and wavy lamination, mudcracks and ripple marks are observable. The sandstones show grain sizes ranging 0.2 to 0.5 mm, are poorly rounded to angular, well-sorted grains of polycrystalline and monocrystalline quartz (50 - 60% vol.), feldspars (35 - 40%) and lithoclasts (<10%) and are embedded in dolomitic cement. The rather coarse cement proportion (40%) is dolomitic and shows a clearly oolitic texture (Fig. 3 a), causing a very strong reduction in porosity. The secondary porosity is caused by a local, minor dissolution of the cement and its values range 1 - 3% of the whole rock (very poor porosity) (López-Doncel et al, 2002).

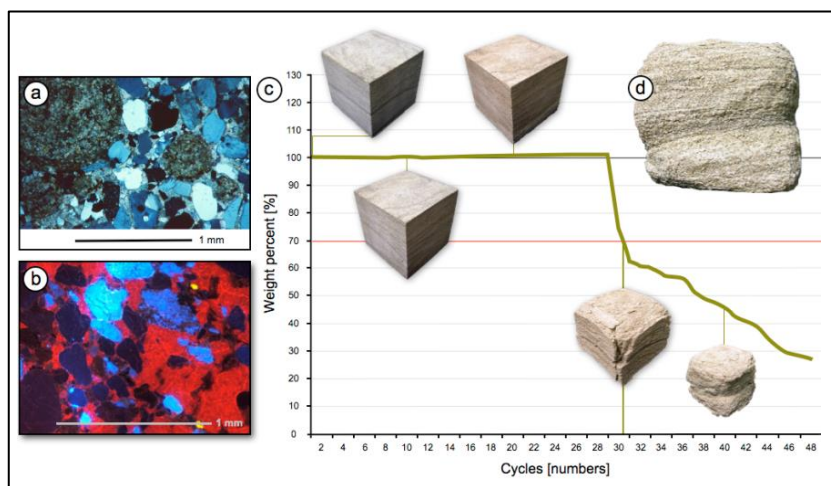


Fig. 3: a) Thin section of the Zeitz sandstone (Rounded oolites are visible in grains of mono- and polycrystalline quartz) and feldspars, which are embedded in a dolomitic matrix. b) Thin section under cathodoluminescence. c) Salt bursting test and d) weathering related to the bedding.

The color of the stone is due to high concentrations of feldspar, mica and clayish substances clearly identified by CL-microscopy (Fig. 3b). The dolomite cement could be determined by cathodoluminescence microscopy (red), clay is blue and feldspar shows a light blue color (Fig. 3b).

3.1.2. Petrophysics

The rock material has a low porosity that varies between 3 and 15 % with a dominance of macropores, and contains a homogeneous fine to medium grain size with a clearly visible layered structure. The dolomite cementation varies between 13 and 76 % by volume, and therefore reaches a density of 2.72 g/cm³. The stone has a low water uptake rate (averaged 0.8 kg/m² that varies as much as 46 % with the bedding direction. Compressive strength with 100 N/cm² is quite high as compared to other sandstones. This may be the reason why the stone shows a good resistance to salt bursting, which was performed on cubic samples 6.5 by 6.5 cm in size and submersed in a 10 % NaSO₄ solution (DIN EN 12370). A material loss of 30 % after 30 cycles could be determined (Fig. 3c). After discoloration due to iron oxidation, a massive contour scaling starts at the 20th cycle and continues with further material loss (Fig. 3c). In the last stage a weathering related to the bedding is observable, which can also be found at the church building (Fig. 3d).

3.2. Weathering forms and agents

3.2.1. Weathering forms

The sandstone blocks show severe deterioration with weathering depths up to 30 cm (Fig. 4a to Fig. 4c). The main decay phenomena are two different types of weathering, relief and alveolar (Fig. 4a). Dark crusts and discolorations are of only subordinate importance. Weathering is characterized by heterogeneous back-weathering, which depends on the bedding of the sandstone. The relief "weathering type I" represents a modified alveolar weathering, which is characterized by deep gouges. The material loss is dominated by granular disintegration. For "relief weathering type II" the weathering intensity is slight with up to 3 cm. Strong back-weathering also follows the bedding of the sandstone. This weathering form achieves back-weathering rates up to 30 cm. The material loss in the gouges is dominated by flaking and contour scaling. Relief weathering type II is located at areas of direct water action, whereas relief weathering type I and strong back-weathering occurs in expositions protected by water run-off but effected by moisture penetration.

3.2.2. Salt-weathering

The x-ray diffraction shows that different magnesium sulphate hydrate phases are detectable. Next to epsomite (MgSO · 7H₂O) and hexahydrate (MgSO · 6H₂O) kieserite (MgSO · H₂O) also occurs (Fig. 5a). The quantitative salt analyses show that the salt content of magnesium sulphate from samples of relief type II is much higher than those of relief type I (Fig. 5b). Some samples taken out of the alveolar weathered areas show a contamination that reaches a profile depth of more than 10 cm (Fig. 4b and Fig. 5).

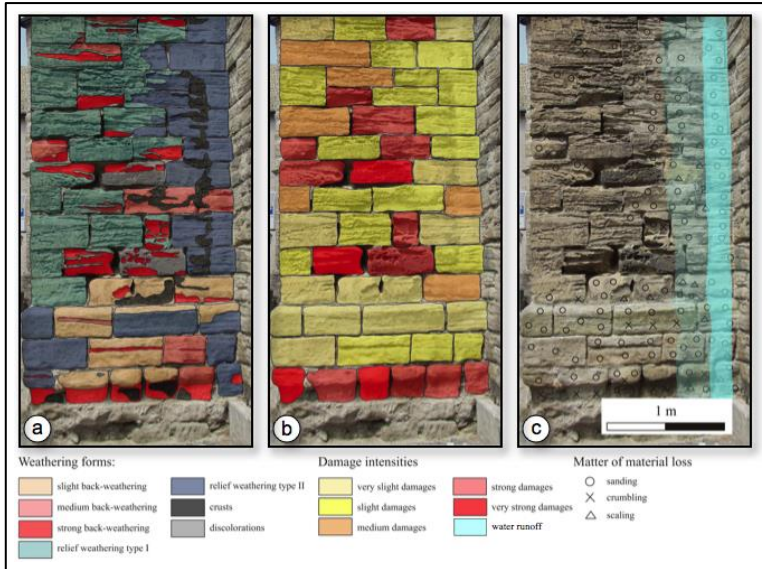


Fig. 4: a) Weathering forms, b) damage intensity and c) reasons for material loss at the testing area.

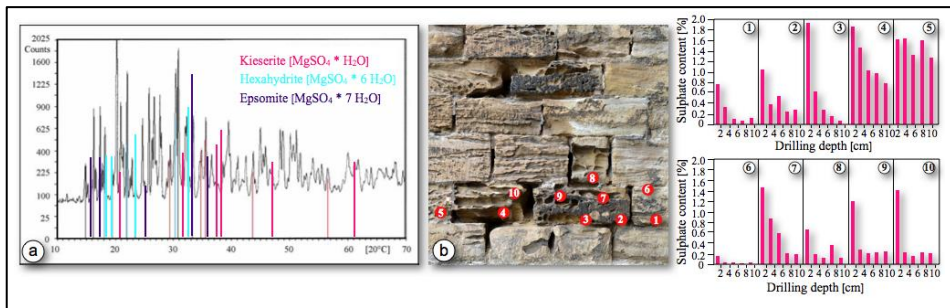


Fig. 5: a) X-ray diffraction of the salt efflorescences shows different MgSO₄-phases. b) Quantitative salt analyses in the depth profile taken from different weathering zones.

3.3. Conservation/restoration

3.3.1. Desalination

Around 1100 g of soluble material could be extracted, while the desalination rate of the different sections differs between 21 g/m² and 71 g/m² according to the intensity of weathering (Tab. 1). The effect of desalination was also tested by drill dust samples that show a significant decrease of salt load after treatment.

Tab. 1: Summary of results from the desalination.

Sprinkling area	Sum of electrical conductivity	Total salt content	Rate of desalination
	[mS/cm]	[g]	[g/m ²]
I	61.68	88	22
II	121.32	173.3	69.3
III	187.66	286	67
IV	86.91	124	31
V	201.46	288	71
VI	97.76	140	21
Total / Ø	757.78	1099	44 Ø

3.3.2. Restoration

During the hardening of the pure hot lime mortar (Cl 80 Q), the temperature rose from 21°C to 45.7°C in a period of 10 minutes (Fig. 6a). The expansion reached 0.8 mm, a percentage of 2 % and exhibits a low shrinking tendency (Fig. 5b). The specimens modified with the white cement (WC) attained temperatures of 29.6°C/8min to 37.3°C/18min (Fig. 7a). No shrinking took place but a moderate expansion ranged between 0.1 mm and 0.5 mm (Fig. 6b). The mortars modified with white cement reach up to two times higher values of compressive strength (USC) and flexural strength (FS) than the pure hot lime mortar (Fig. 6c). The different amounts of the hydraulic additive result in an increase from 1.42 MPa to 2.05 MPa in the case of USC and from 0.58 MPa to 0.98 MPa for FC as shown in Fig. 6c.

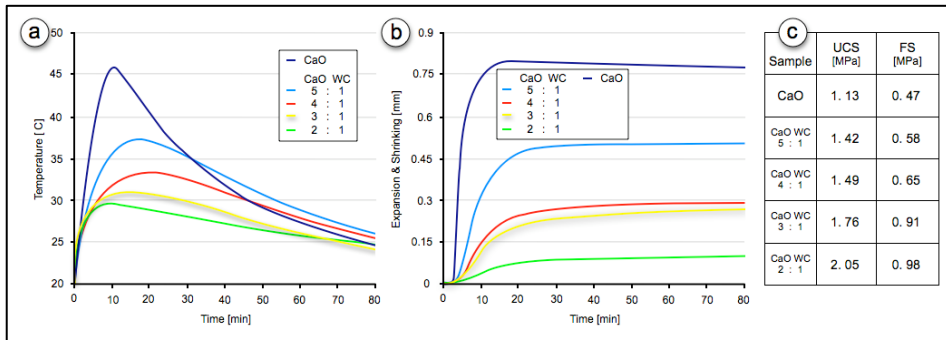


Fig. 6: a) Exothermic reaction of the different mortar mixes and b) expansion/shrinking of the different mortar mixes. c) Compressive and flexural strength of the different mortars.

4. Final Conclusions

The results of these investigations lead to an understanding of the weathering process and the development of a suitable conservation strategy. By using the described sprinkling technique for desalination, a control of the process was immediately possible by electric conductivity measurements. This allows a calculation of the contamination as well as the planning and application of the whole desalination process. The hot lime mortars show interesting properties for stone conservation and restoration. According to the results, a fractional amount of white-cement improves the mechanical properties as well as the workability of the material. For restoration the variety with a CaO:WC ratio of 3:1 was chosen. Structural interventions can be prevented in the historical building by the desalination and mortar filling method, thus costs can be reduced by around 30%. Furthermore, by conservation instead of traditional restoration the church can be restored close to the international regulations of conservation as defined in the "Charta of Venice" and other regulations of ICOMOS (International Council on Monuments and Sites).

Acknowledgments

We would like to thank master sculptor Christian Spaete and architect Regina Hartkopf for their friendly cooperation.

References

- Balboni, E., Espinosa-Marzal, R.M., Doehne, E., Scherer, G.W., 2011, Can drying and re-wetting of magnesium sulfate salts lead damage of stone?, *Environ Earth Sci*, (63, Issue 7-8), 1463-1473.
- Hirschwald, J., 1910, Die bautechnisch verwertbaren Gesteins-Vorkommnisse des Preussischen Staates und einiger Nachbargebiete. Bornträger, Berlin.
- Ruedrich, J., Seidel, M., Wedekind, W., Siegesmund, S., 2006 Damage Phenomenon and Salt Deterioration at the Michaelis Church in Zeitz (Germany). Poster-presentation at the *EGU General Assembly 2006* Vienna, Austria.
- López-Doncel, R.A., Heise, G., Kulke H., 2002, Kirche Breunsdorf - Charakterisierung und Kartierung der Bausteinarten in den Bauphasen von der Romanik bis zur Neugotik, Untersuchungen zu ihrer Herkunft. In: OEXLE, J. (Ed): Kirche und Friedhof von Breunsdorf - Beiträge zu Sakralarchitektur und Totenbrauchtum in einer ländlichen Siedlung südlich von Leipzig. Band 35: 125-146.
- Siedel, H., 2003, Dolomitmalkmörtel und Salzbildung an historischer Bausubstanz, in *Mauersalze und Architekturoberfläche in proceedings Salze im Mauerwerk*, Leitner H., Laue S., Siedel H. (eds.), Hochschule für bildende Künste, Dresden, 57-64.
- Siedel, H., 2013, Magnesium sulphate salts on monuments in Saxony (Germany): regional geological and environmental causes. *Environmental Earth Sciences*, Vol. 69, Issue 4, 1249-1261.
- Steiger, M., Linnow, K., Juling, H., Gülke, G., El Jarad, A. Brüggerhoff, S., Kirchner, D., 2008, Hydration of $MgSO_4 \cdot H_2O$ and Generation of Stress in Porous Materials, *Crystal Growth and Design* 1 (8), 336-343.

- Wedekind W., 2014, Schwierige Ruinen - Zur Erhaltung der Ruinen an der Unstrut, in Natur - Stein - Kultur - Wein - zwischen Saale und Unstrut, Siegesmund S., Hoppert M., Epperlein K. (eds.), Leipzig, Mitteldeutscher Verlag, 289-316.
- Wedekind W., Rüdlich, J., 2006 Salt-weathering, conservation techniques and strategies to protect the rock cut facades in Petra/Jordan, proceedings of Heritage, Weathering and Conservation, Fort R., Álvarez de Buergo M., Gomez-Heras M. and Vazquez-Calvo C. eds., London, Taylor & Francis, 261-268.
- Wedekind, W., Rieffel, Y. 2014, Desalination of the painted vault ribs of the Franciscan monastery Church of Zeitz. In proceedings SWBSS 2014 Third International Conference on Salt Weathering of Buildings and Stone Sculptures Brussels, De Clercq, H. (ed.) Royal Institute for Cultural Heritage (KIK/IRPA): 469-480.
- Wittmann, F.H., 1996, Feuchtigkeitstransport in porösen Werkstoffen des Bauwesens, in Verfahren zum Entsalzen von Naturstein, Mauerwerk und Putz, Goretzki, L. (ed.), Freiburg, Aedificatio-Verlag, 6-16.

FIELD TRIALS OF DESALINATION BY CAPTIVE-HEAD WASHING

D. Young¹

Abstract

Captive-head washing is a system designed for cleaning dirt and grime from building façades in which the dirty wash water is retained within a close-fitting head and captured by a wet vacuum cleaner, thus minimising clean-up and waste disposal issues. The system's potential for reducing excessive salt loads in masonry has been recognised for some years and anecdotal evidence suggests that it works well enough to justify its on-going use, yet there is little data to support this. Trials were conducted in 2014 on an internal face of an exterior wall of an 1820s brick blacksmith's shop at the World Heritage listed Woolmers Estate in Tasmania, Australia. The 350 mm thick brickwork suffers from rising and penetrating dampness carrying salts through the wall to the interior surface where the low-fired bricks are severely decayed by salt attack. Samples of the wash water from two cycles of captive-head washing were analysed for soluble salts (total dissolved solids) by electrical conductivity. The results show that a significant quantity of salt was removed from the wall: depending on assumptions made about the depth of penetration/extraction and the density of the brickwork, salt extraction was in the range 0.2–0.6% by weight (for the two cycles combined). The second cycle removed about one third the amount of salt of the first cycle, which raised the question of whether additional cycles may be beneficial. Further trials were conducted in 2015 with four cycles of captive-head washing. Although these were simple field trials, they confirm that the technique has considerable potential for use in desalinating masonry walls.

Keywords: desalination, captive-head washing, salt attack, salt weathering

1. Introduction

Captive-head washing is a system designed for cleaning dirt and grime from building façades in which the dirty wash water is captured by a wet vacuum cleaner, thus minimising clean-up and waste disposal issues. Figure 1 shows the head in use, cleaning dust and dirt from a brick wall prior to render repairs. The head contains a low-pressure spray nozzle which is connected to a water supply at normal pressures. A flexible rubber 'skirt' encloses the head and seals the unit against the wall surface so that the attached wet vacuum-cleaner recovers almost all of the wash water. The system's potential for reducing salt loads has been recognised for some years (Young, 2008) and anecdotal evidence suggests that it works well enough to justify its on-going use, yet there is little data to supports this. Trials were conducted during the 2014 and 2015 sessions of the Longford

¹ D. Young*

Heritage Consultant, Melbourne, Australia
david.young@netspeed.com.au

*corresponding author

Academy, a combined training and fieldwork program organised by the Australasian Chapter of the Association for Preservation Technology International (APTI) and located at the Brickendon and Woolmers World Heritage properties at Longford, Tasmania, Australia.



Fig. 1: Captive-head washing system being used by Walter Heim to remove dust and dirt from brickwork prior to render repairs at Brickendon, Longford, Tasmania.

2. Woolmers Blacksmith's Shop

The 1820s blacksmith's shop on the Woolmers estate (Fig. 2) is a brick building with a harled or roughcast-rendered exterior and limewash finishes on the interior. The 350 mm thick brickwork suffers from rising and penetrating dampness which carry salts through the walls to the interior surfaces. The northwest wall is the worst-affected, the low-fired bricks are severely decayed by salt attack (salt weathering) across much of the interior surface (Fig. 3). Moisture transport through the walls towards the interior would have been increased when the smithy was in operation, producing warm evaporative conditions inside the building.

The weak, powdery surface of the decaying brickwork was consolidated by multiple applications of limewater in May 2013. The surface hardening was sufficient to allow desalination treatment without significant further loss of material. The 2014 and 2015 campaigns included trials of the captive-head washing system, which was kindly supplied and operated by Walter Heim of Heim Surface Technologies, Sydney.



Fig. 2: Woolmers Estate blacksmith's shop from the north. Failed rendering (harling) on the northwest wall (to the right) is allowing penetrating dampness to carry salts through the 350 mm brickwork to the interior (see Figure 3).



Figure 3: Interior of northwest wall showing extensive decay of low-fired bricks due to salt attack. Early limewash finishes remain on undamaged parts of the wall.

3. 2014 trials

In 2014 trials were conducted on the interior of the northwest wall (Fig. 3) and covered an area of 8.8 square metres. The captive-head unit was drawn slowly across the surface to allow time for the wash water to dissolve readily-soluble salt lying on and in the surface of the brickwork. Two separate passes were made across the whole surface of the wall.

The amount of wash water retained by the vacuum system was recorded and samples of each batch were collected and analyses for soluble salts (total dissolved solids) by electrical conductivity. This technique uses a portable conductivity meter and is a quick and simple way of determining the total concentration of salt present, though it cannot distinguish between different types of salt. The salt concentrations are multiplied by the volume of wash water to obtain the total amount of salt extracted.

4. 2014 results

The first pass extracted 81.6 g, the second 27.8 g making a total of 109.4 g of salt extracted from a wall area of 8.8 m², at an average of 12.4 g/m².

Deriving a weight per cent salt extraction depends on two assumptions:

- Depth of effective extraction in mm;
- Density of the brickwork, which, for this purpose, is assumed to be 2.0 g/cm³ (kg/L) though given the very porous bricks, it could be much lower.

Assuming that the depth of effective extraction is one mm into the brickwork, the average salt extraction is around 0.6% by weight. This is a high figure; it is more than the commonly used 0.5% threshold above which salt extraction is warranted. Alternatively, if the effective depth of extraction is two mm, then the salt extracted is 0.3% by weight, and if the extraction depth is three mm, the figure becomes 0.2% by weight of the brickwork. Any of these results is a good outcome; substantial salt has been removed from the wall.

The amount of salt extracted in the second pass was about one third that of the first pass. However, less water was used in the second pass (15 L instead of 25 L in the first pass), which indicates that the second pass was faster (assuming the water supply rate remains constant). Ignoring the differences in the amount of water used, and considering only the concentration of the salty wash water, the second pass extracted about 60% of the salt extracted in the first pass. These results suggest that a third, or even fourth, pass should be effective at salt extraction, and that slower passes extract more salt.

5. 2015 trials and results

In 2015 an additional area of 1.2 m² was treated, but this time using four passes of captive-head washing, with the aim of testing the observations from the previous year's work. The four passes extracted a total of 22.7 g salt at an average of 18.9 g/m². Significantly, the third and fourth passes continued to extract salt, as shown in Tab. 1.

Table 1: Results of 2015 trials

Passes	Concentration	Water used	Salt extracted
	ppm	L	g
1 & 2 (combined)	512	25	12.8
3	320	15	4.8
4	512	10	5.1

These results show a decline in salt concentration from the first and second to the third pass, which is expected as the salt load in the wall is reduced. However, the concentration of the fourth pass increases to the previous level, which may suggest that salts deeper in the wall are being mobilised and brought to the surface. In turn, this suggests that additional passes are warranted to maximise salt extraction.

6. Discussion

There are a range of variables and factors that should be considered in designing future trials. These include the solubility of the various salts and whether pre-wetting of the wall is warranted to initiate dissolution of the salts. The walls should not dry out between passes, and between any pre-wetting and the first pass. This is to ensure that the salts remain in solution so that (a) they can be removed in subsequent passes, and importantly, (b) that they do not recrystallize and cause more damage to the masonry. This is particularly important in hot dry places like Australia. In turn this means arranging the work flow so that, once commenced, the treatment of a section of wall can be completed without it drying out. This does not necessarily mean passing the captive head at a fast rate over the wall surface, nor that the interval between passes should be as short as possible. Rather, a slower rate of passing across the surface should extract more salt (per pass) and maximising the total time of wetting (i.e. passes plus the intervals between them) should maximise the chances of (a) less-soluble salts dissolving, and (b) deeper salts migrating towards the surface.

7. Conclusions

Field trials have demonstrated that captive-head washing is effective at desalinating porous masonry walls with high salt loads. Multiple passes may be required to reduce salt loads to acceptable levels. Slower passes across the wall surface will extract more salt per pass. A combination of multiple passes and adjusting the rate of passing across the surface should be trialled in order to optimise the technique. Other factors which should be considered include pre-wetting to initiate dissolution, and the effect of different nozzle flow rates.

Future trials should test:

- Pre-wetting to initiate dissolution;
- Multiple passes across the surface;
- Varying speeds of passing across the surface;
- Different substrates and salt loads, and
- Different nozzle flow rates, in order to optimise the technique.

Reference

Young, D., 2008, Salt attack and rising damp: a guide to salt damp in historic and older buildings. Heritage Council of NSW, South Australian Department for Environment and Heritage, Adelaide City Council, Heritage Victoria, Melbourne, Australia, ISBN 978-0-9805126-5-6, 80pp.

DIGITISATION

This page has been left intentionally blank.

DIGITAL MAPPING AS A TOOL FOR ASSESSING THE CONSERVATION STATE OF THE ROMANESQUE PORTALS OF THE CATHEDRAL OF OUR LADY IN TOURNAI, BELGIUM

J. De Roy^{1*}, S. Huysmans¹, L. Hoornaert¹, L. Fontaine² and N. Verhulst¹

Abstract

In the framework of the conservation of the Cathedral of Our Lady in Tournai (Belgium), the Royal Institute for Cultural Heritage (KIK-IRPA, Brussels) was called upon in 2012 to carry out a preliminary study of two Romanesque portals called the *Mantile* and *Capitole* portals. The aim of this study was to understand the deterioration mechanisms of the stone and to propose a conservation strategy. Both portals are constructed from the local black Tournai stone, with the exception of the 19th century restoration in Belgian bluestone. Due to the strongly deteriorated state and the large size of the portals, a detailed visual inspection survey of each stone block was necessary to obtain an overview of the actual state of conservation and to develop an adapted conservation strategy. The deterioration patterns were digitally mapped with the Metigo *MAP* software (fokus GmbH), using rectified photographs as a template. These mappings present a visual clarification of the location, extent and degree of the different deterioration patterns. They also enable us to evaluate and compare the deterioration patterns of both portals and can be linked to the results of the laboratory analyses.

Keywords: Tournai stone, deterioration mapping, Tournai cathedral, Romanesque portals, Metigo *MAP*, delamination, black crust

1. Introduction

Construction of the Cathedral of Our Lady in Tournai (Belgium) started in the first half of the 12th century. The nave and transept date back to the Romanesque period and are topped with five towers, all predating the Gothic choir. Its important artistic and historical value was recognised by UNESCO in 2000 with their acknowledgement of the Cathedral as a World Heritage Site. Despite successive architectural changes to the Romanesque construction, two original side portals dating from around 1125 (Deléhouzée 2013) have been spared: the *Mantile* and *Capitole* portals, located respectively at the northeast and southwest side of the nave. In spite of their strongly deteriorated state, these finely sculpted portals in Tournai limestone are unique examples of Romanesque monumental sculpture in Western Europe (Fig. 1). Both portals consist of multiple round arches embodied in a trefoil arch with a drip moulding. The arches are supported by jambs and jamb columns. Each

¹ J. De Roy*, S. Huysmans, L. Hoornaert, L. Fontaine and N. Verhulst
Stone sculpture studio, Royal Institute for Cultural Heritage, KIK-IRPA, Brussels, Belgium
judy.de.roy@kikirpa.be

² L. Fontaine
Monuments and monumental decoration lab, KIK-IRPA, Brussels, Belgium

*corresponding author

block is decorated with a Romanesque sculpted relief and the entire surface was probably polychromed (for further details see De Roy J. *et al.*, in press).

In 1999, a new restoration campaign of the Cathedral was considered crucial. In this framework, a preliminary study of the Romanesque side portals was commissioned to the KIK-IRPA in 2012. The aim was to understand the deterioration mechanisms of the black Tournai stone in an urban environment and to work out a conservation strategy for these portals.



Fig. 1: Mantile portal (left), picture dating from 1899 © KIK-IRPA, Brussels, B3188. Capitole portal (centre) © KIK-IRPA, Brussels, A126815. Relief of inner arch of Mantile portal (upper-right) © KIK-IRPA, Brussels, X049701. Relief of trefoil arch of Capitole portal (bottom-right) © KIK-IRPA, Brussels, X057496.

2. Characterization of the stone

Both the architecture and the sculptures of the *Mantile* and *Capitole* portals were executed in black Tournai stone, a local “black marble” (sedimentary limestone that allows for fine polishing) also known as Noir de Tournai, which was widely used in the Low Countries from the 11th to the 15th century (Groessens 2008). Tournai stone is a local stone exploited on the right bank of the Scheldt river near the city of Tournai. Geologically, the black Tournai stone is a compact, fine-grained, silicified and clay-bearing limestone from the Lower Carboniferous (Tournaisian) age (Camerman 1944; Hennebert and Doremus 1997). The stone can be described as a bioclastic wackestone according to Dunham’s classification (Dunham 1962) and as a biomicroite according to Folk’s classification (Folk 1965).

Petrographic analysis of loose samples from the portals revealed that the silicified matrix of the stone mainly consists of calcite, sometimes with grains of dolomite. While the compact stone core has coarser bioclasts ($\leq 250 \mu\text{m}$) than the outer edges ($\leq 100 \mu\text{m}$), careful examination reveals a more prominent presence of small clay laminae in the outer edges which are almost absent in the stone core. The clay laminae form a laminated structure on

the outer edges of the stone. As further research revealed, this distribution of clay minerals in the stone, in combination with extrinsic factors, is the most important reason for the deteriorated state of the portals (for further details see Fontaine *et al.*, 2015).

3. Material history

Already in the mid-18th century the ruinous state of the portals was mentioned (Van Den Noortgaete, 1995) and in the second quarter of the 19th century it was argued that there would soon be nothing left of the original sculptures (Scaff, 1971). This poor condition led to the restoration of the two Romanesque portals by architect Bruyenne between 1848 and 1871. The restoration mainly consisted of replacing strongly degraded stone volumes by Belgian bluestone or Petit Granit. The fact that the *Capitole* portal contains far more replaced stone volumes than the *Mantile* portal suggests that the former was much more deteriorated in the 19th century. Since the replacement stone is still in good condition, it was not included in this preliminary study.

Despite this restoration, the poor condition of the remaining original Tournai stone was still mentioned throughout the 20th century (Van Den Noortgaete, 1995). Photographs from different archives confirm this ruinous state, but a detailed inventory of the condition has never been made.

A precious source of information for evaluating the progression of the degradation are the photographs from 1943 made by the KIK-IRPA in the context of a major inventory campaign during the Second World War. Comparison with the current state of conservation leads to conclude that the general condition of the portals did not undergo major changes. Large lacunae did not expand and the current deterioration patterns were already present.

4. Digital mappings

To obtain an overview of the state of conservation two kind of mappings were carried out by visual inspection from scaffoldings:

- Detailed mappings of each different deterioration pattern of each single block of Tournai stone: 78 blocks for the *Mantile* portal and 57 for the *Capitole* portal (Fig. 2)
- General mappings for each portal with the main deterioration patterns, the positioning of the stone blocks, the readability of the sculpted reliefs and an inventory of the 19th-century restoration

Rectified, accurate photographs on true scale were used as templates for these mappings, carried out using the Metigo *MAP* software by Fokus GmbH. The true scale gave us the opportunity to document each deterioration pattern in detail but also to calculate very precisely the damage of each deterioration pattern. Nevertheless it has to be taken into account that it concerns reliefs mapped in two dimensions and thus sculptural undercuts are not included. The mappings of the portals are a combination of line- and area-mappings. The mapping terminology and colour scheme of the weathering phenomena was based on the classification of the ICOMOS-ISCS *Illustrated glossary on stone deterioration patterns* (ICOMOS-ISCS, 2008).

The following deterioration patterns were observed on both portals: detachment/delamination, cracks, black crusts in various thicknesses, soiling, biological colonization, blistering and efflorescence.

For quantitatively important deterioration patterns, namely black crusts and delamination, sub-categories were made to indicate the degree of the deterioration.

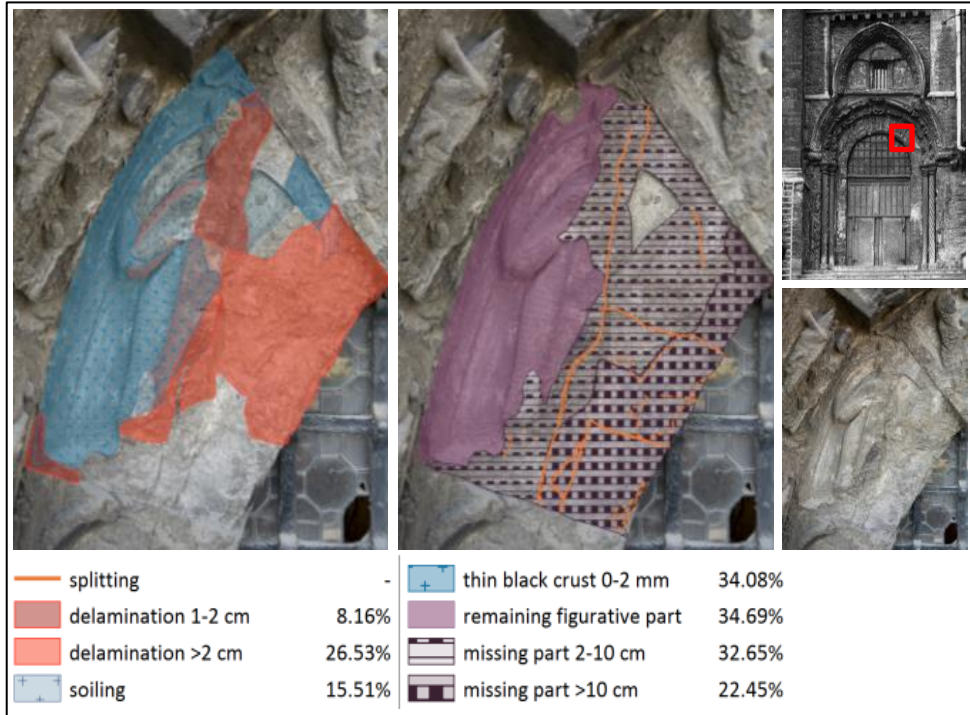


Fig. 2: Detailed mapping of block BC2 (Bandeau Cintré 2) of the Mantile portal. © KIK-IRPA, Brussels.

The mapping of the bedding planes of the Tournai stone proves that the construction of both portals is similar. Although the positioning of each block was not random (Fig. 3), the bedding planes were not taken into account during the construction of the portals. The blocks were positioned in three different directions, namely natural-bedded, edge-bedded and face-bedded. The latter blocks suffer from material loss due to their weaker and fragmented schist-like outer edge positioned parallel to the surface. This loss continues to a few centimeters depth, making a lot of sculpted reliefs hardly readable or even leading to their total loss.

From the identical positioning of the stone blocks in both portals we can derive that the lower part of the *Capitole* portal was very likely face-bedded. This would explain why that part would have suffered substantial material loss and was replaced with Belgian bluestone in the 19th century.



Fig. 3: Mapping of the bedding planes of the original stone blocks in the Mantile (left) and Capitole portal (right). Hatchings underlines the bedding planes, while crosshatching is used for face-bedded blocks. Blue-coloured zones correspond to the 19th century restoration with Belgian bluestone ©KIK-IRPA, Brussels.

5. Results

From the detailed mappings an overview can be deduced of the different degradation phenomena and their distribution on the portals (Fig. 4). Detachment is a common phenomenon of the original Tournai stone and was found on 51% of the original surface of the *Mantile* portal and on 39% of the *Capitole* portal. Black crusts were omnipresent as well: on 62% of the *Mantile* portal and on 79% of the *Capitole* portal. These phenomena are divided in different subcategories according to their degree of degradation. Other deterioration patterns such as biological colonisation, blistering and efflorescence were less common and will thus have less impact on the conservation treatment.

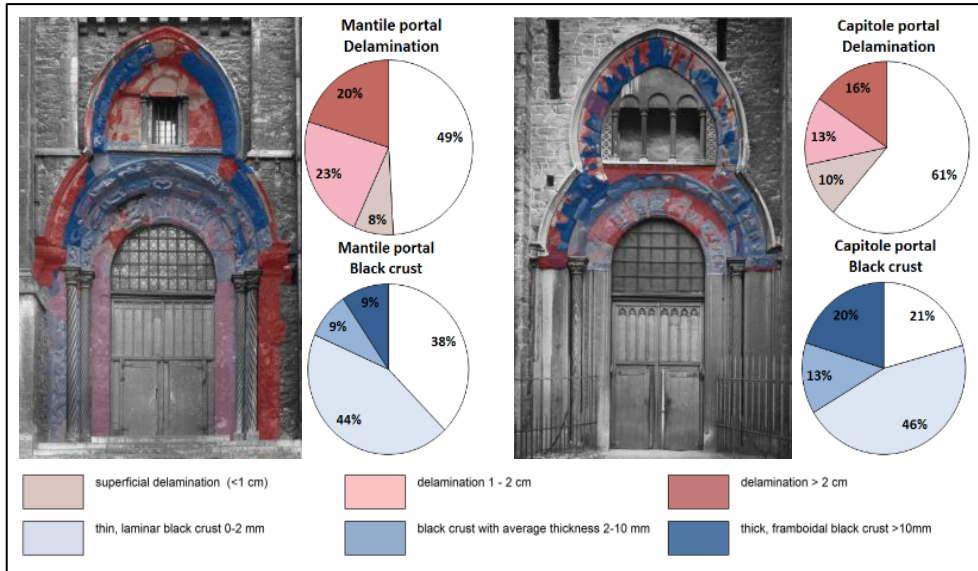


Fig. 4: Mappings and diagrams of the delamination and black crusts on the Mantile (left) and Capitoile portal (right) © KIK-IRPA, Brussels.

A general mapping describing the state of the sculpted surface comprises four different categories: first of all sculptures with an original surface in good condition, secondly stone blocks with an original surface that is hardly readable, thirdly original stone surfaces that have completely disappeared and lastly 19th-century replacements (Fig. 5).



Fig. 5: General mapping and diagrams of the state of conservation of the sculpted surface. Mantile portal (left) and Capitoile portal (right) © KIK-IRPA, Brussels.

Unfortunately hardly 5% of the finely detailed Romanesque sculptures remains for the *Capitole* portal and 21% for the *Mantile* portal. In total 66% of the *Capitole* portal and 15% of the *Mantile* portal was replaced by Belgian bluestone in the 19th century, leaving only around a third of the original stone of the *Capitole* portal while the *Mantile* portal still contains 85% of its original stone volumes.

From the mappings it became furthermore clear that orientation of a portal has an influence on its conservation state. Due to its southwest orientation, corresponding to the direction of prevailing winds and ample exposure to the sun, the *Capitole* portal is more deteriorated than the *Mantile* portal, as we can read out of the mappings.

Stone volumes in the deeper parts of the archivolts of both portals are better protected from meteorological phenomena such as rain and direct sunlight and are thus better preserved. These sheltered areas, however, contain more black crusts.

6. Practical use of the mappings for the conservation treatment.

The detailed mappings were used as a guideline for further scientific research in order to understand the mechanisms of the deterioration. Furthermore they were used to select representative locations for sampling and allow an informed choice of on site test-areas for micro-drilling resistance, ultrasonic pulse velocity and water absorption measurements (for further details see Fontaine L. *et al.*, 2015).

The results of these measurements in combination with additional scientific research and the data from the mappings revealed that the specific degradation of the Tournai stone is caused by intrinsic as well as extrinsic factors. These were studied by the monuments and monumental decoration lab of the KIK-IRPA. The presence of numerous clay laminae in the schist-like outer edges of each stone block constitutes an intrinsic factor for the degradation of the stone. This schist-like ‘crust’ makes the stone unsuitable for use as a building stone and must ideally be removed before use in an outdoor context. The core of these blocks is, however, in good condition. The cracks in the outer edges follow the bedding plane of the stone block. This leads to a high amount of material loss by detachment when the blocks are face-bedded.

Furthermore also extrinsic factors such as climatic conditions (temperature, humidity, precipitation) and a malfunctioning of the rainwater drainage system are significant for the degradation of the portals. Hydric dilatation is the main driving force of this degradation but hygric and thermic dilatation also play an important role (for further details see Fontaine L. *et al.*, 2015).

The principal aim of the study of the two Romanesque portals was to develop a conservation treatment based on a representative test area. The area chosen for this pilot conservation had to include all the different deterioration phenomena. A representative area was selected on the basis of the mappings. Furthermore the main focus of the conservation, namely the stabilization of the detachment, could be deduced from the mappings. With this in mind, an injection mortar was designed and tested in the lab. During the pilot conservation all the different steps of the treatment were executed onsite, starting with injecting an ethyl silicate-based mortar and followed by the removal of the soiling and the black crusts. The latter was carried out with compresses in combination with micro-abrasion for the crusts with a thickness of more than 2 mm and by a mechanical elimination followed by a soft micro-abrasion cleaning for the thinner films (for further details see De

Roy J. *et al.*, in press). During the removal of the crusts thicker than 2 mm, additional injections turned out to be necessary due to the thicker transition zone of the outer stone layer with very limited cohesion (Fontaine L. *et al.*, 2015). This is in contrast with the thin film-like crusts where the underlying stone support appears in relatively good condition.

The mappings were also used to estimate the cost and time required for the future conservation project as all the deterioration patterns had been linked to a specific conservation method.

7. Conclusion

The digital mappings proved to be extremely useful for this complex case of the *Mantile* and *Capital* portals in Tournai stone. Apart from the general mappings, a total of 135 blocks of stone were individually mapped on site using the Metigo *MAP* software. These information confirmed the need for a conservation treatment, revealing that most attention should be paid to stabilizing the delamination. This deterioration pattern is caused by a combination of both intrinsic and extrinsic factors and led to a study of suitable conservation methods. The different orientation of both portals is clearly visible in the state of conservation. Besides a conservation treatment, preventive measures should be taken into account. The digital mappings can be reused and completed as at the time of our inspection some cracks and losses were still covered by thick black crusts. We conclude that such digital mappings are also the perfect tool for monitoring the condition of the portals in the future.

Acknowledgments

This research is part of the preliminary study of the Romanesque side portals, commissioned in 2012 by the Walloon cultural heritage agency (DGO4/Département du Patrimoine), the Province of Hainaut and the City of Tournai. The study has been carried out in collaboration with the monuments and monumental decoration lab of the Royal Institute for Cultural Heritage (KIK-IRPA, Brussels). The authors would like to thank the following colleagues at the KIK-IRPA for their contribution to the preliminary study: R. Hendrickx, C. De Clercq and H. De Clercq.

References

- Camerman, C., 1944, La pierre de Tournai : son gisement, sa structure et ses propriétés, son emploi actuel, Mémoires de la Société belge de Géologie, de Paléontologie et d'Hydrologie, Nouvelle série in-4°, 1-86.
- Deléhouzée L., 2013, La place des portails dans la chronologie du chantier roman, Book of abstracts Les portails romans de la Cathédrale Notre-Dame de Tournai: Contextualisation et restauration (international conference), Tournai (Belgium), January 31-February 1, p 1.
- De Roy J., Fontaine L., Hoornaert L., Hendrickx R., De Clercq C., Huysmans S., De Clercq H., in press, Les portails romans de la cathédrale Notre-Dame de Tournai (Belgique). Résultats de l'étude matérielle et technique en vue de la conservation, Archéovision .
- Ecclesiology Today 29:3-11 (www.ecclsoc.org/ET.29.pdf)

- Dunham R.J., 1962, Classification of carbonate rocks according to depositional texture. In: Ham WE (ed) Classification of carbonate rocks, Am Assoc Pet Geol Mem 1, 108-121.
- Folk R.L., 1965, Petrology of Sedimentary Rocks. Hemphill Publishing Company, Austin (USA), 182.
- Fontaine, L., Hendrickx R. et De Clercq H., 2015, Deterioration mechanisms of the compact clay-bearing limestone of Tournai used in the Romanesque portals of the Tournai Cathedral, Environmental Earth Sciences, 74, 3207-3221.
- Groessens, E., 2008, La pierre de Tournai, un matériau de choix depuis la période romaine et un des fleurons parmi les autres marbres belges, Revue trimestrielle de la Société tournaisienne de géologie, préhistoire et archéologie, X (7), 197-216.
- Hennebert M, Doremus P., 1997, Notice explicative de la carte géologique Hertain-Tournai 37/5-6 à l'échelle 1:25000. Direction Générale des Ressources Naturelles et de l'Environnement, Ministère de la Région Wallonne, Jambes, Belgium, 66.
- ICOMOS-ISCS, 2008. Illustrated glossary on stone deterioration patterns – Glossaire illustré sur les formes d'altération de la pierre. Monuments and Sites XV, 78 p.
- Scaff, V., 1971, La sculpture romane de la cathédrale Notre-Dame de Tournai, Tournai, Casterman.
- Van Den Noortgaete, T., 1995, Étude préliminaire à la restauration de la cathédrale de Tournai. Porte Mantile et Porte du Capitole. Rapport archéologique préalable à la restauration des sculptures romanes, 2 vol., rapport inédit.

This page has been left intentionally blank.

DIGITAL FIELD DOCUMENTATION: THE CENTRAL PARK OBELISK

C. Gembinski ^{1*}

Abstract

The digital field documentation of the existing conditions and application of the conservation treatments at the Central Park Obelisk performed in 2014 created challenges for conservators, historians and those studying or working on the monument in the field. New and constantly changing technologies can make gathering and sharing information, as well as planning interventions, faster and easier. Today, we anticipate increasingly more applications that will allow the opportunity to explore, discuss, and fine-tune options for digitally generating and storing information suggesting that our documentation efforts no longer desire the creation of static models; rather we seek an interactive solution. Our experience to date translating hand-drawn field notes into digital formats has shown a potential for the loss of information, or the inclusion of incorrect data. While digital documentation in the field cannot replace the artistry of hand-draw sketches, it can reduce, if not eliminate potential transcription errors. The digital application ultimately selected for the documentation of the work at the Obelisk came after researching and testing three applications on several conservation projects. This paper illustrates discussions specific to the Obelisk project, including how users favoured the methods they knew, and how conservators entering information on handheld devices often returned to paper and pencil, thereby adding to the continuing discussion of how field documentation for conservation can advance together with technology and our ever changing expectations.

Keywords: digital documentation, mobile applications, field recording, existing conditions, conservation treatment, Central Park Obelisk

1. Introduction

Two goals were identified for the conservation work at the Central Park Obelisk: 1) Archival information, and 2) Data Analysis. The need for accurate archival information was important in order to create a baseline document for use in analysing the patterns and factors involved in the development of the existing conditions, and develop a proposed treatment campaign. Documentation of the treatment applications was desired to provide future conservators with the locations of previous conditions and applied treatments, and to help them monitor the success of the treatments as well as predict potential future deterioration. With on-going observation, the documentation should also assist in the identification of a rate of change.

¹ C. Gembinski*

Building Conservation Associates, Inc., United States of America
cgembinski@bcausa.com

*corresponding author

An iterative documentation process utilized multiple digital applications to collect and record the data in multiple formats, analyse the efficiency and effectiveness of the recording methods, and modify the approach and/or application to meet the requirements of the Project.

2. Examination of the Obelisk

The Central Park Obelisk is a solid pink granite shaft approximately 21 meters high and tapered 2 ¼ meters to 1 ¼ meters, set on a base of the same stone, originally quarried in Aswan and erected in Heliopolis to honour Pharaoh Thutmose III and later Ramses II (Central Park Conservancy 2016). It is thought to have been originally erected approximately 3,500 years ago and was brought to New York City and erected in its present location on Greywacke Knoll, behind the Metropolitan Museum of Art in 1881.

The project team: The Central Park Conservancy (CPC), a Conservancy Consulting Scientist (CCS), Building Conservation Associates, Inc. (BCA), and SAT, Inc. (SAT)¹ completed conservation work on October 31, 2014. The work addressed the previously untreated weathered conditions on the granite obelisk shaft and its supporting plinth. Using existing Computer Aided Design (CAD) survey documents provided by the CPC, the team also examined the monument to confirm locations of previously documented conditions of deterioration and previously applied temporary stabilization treatments. The conservators performed and documented conservation work on over 6,000 conditions, thus proving the need for a documentation method that could record and deliver a large amount of information.

Using the International Council on Monuments and Sites “Glossary of Stone Deterioration Patterns” as the basis for identifying the conditions, the team recorded locations of atmospheric soiling, biological growth, cracks, disaggregation, and spalls. The conservators implemented and documented treatments developed by the team onsite. Areas of granular disintegration were treated with a polymer consolidant (Paraloid B-48N in solution with acetone). Some very isolated areas of disintegration warranted a treatment with an ethyl silicate consolidant (Conservare OH100). An adhesive injection repair for the treatment of cracks and microfissures included the application of a chemical adhesive (Paraloid B-48N in solution with acetone, ethanol and xylene and the addition of Cab-o-sil M5 fumed silica). Isolated spalls required the application of an injectable proprietary mortar grout (Edison X53i grout) where injection of adhesive could not adequately fill cracks or allow water to shed from treated areas. All locations exhibiting obvious biological growth were treated with a proprietary biocide before the application of any adhesive repairs (D/2 Biological Solution).

3. Documentation

3.1. Previous Documentation

A previous project in 2013 included cleaning and stabilising the Obelisk surface. At that time, the CPC took advantage of the opportunity to thoroughly document the monument and create a reference point for future study and conservation. That previous documentation included the use of laser scanning, photography, and hands-on surveys.

¹ Maria Warsh, Matthew Rielly, and John Harrigan, CPC; Dr. George Wheeler, CSS; Raymond Pepi, Christopher Gembinski, John Glavan, Zach Tatti and Steve Johnson, BCA; Steve Tatti, SAT.

A High Definition Survey phased-based 3D Laser Scan of the Obelisk was created in March 2013, which provided the team with a data point cloud that could be used in conjunction with other imaging applications. However, it did not provide a consistent and suitably detailed level of data to be useful to the conservators (Central Park Conservancy 2016). The 3D laser scan did not provide sufficient detail to comprehensively document the condition of the surface therefore high-resolution digital photographs were taken by the Metropolitan Museum of Art for this purpose in August 2013. Each face of the Obelisk was divided into 63 rectified digital images, which were tiled together to create a composite Portable Document File (PDF) of each elevation of the monument. Conditions were recorded as overlays on these images in a CAD program (Central Park Conservancy 2014). The photographs proved useful in two ways. First, they assisted in documenting a baseline condition of the monument. Second, they provided the graphic documents on which new information could be traced during subsequent surveys and treatment campaigns.

3.2. Goals of the Present Documentation

CPC required that the documentation for the treatments applied to the Obelisk “be recorded in detail on the survey documentation provided, and this documentation of treatments incorporated into a final report on the conservation,” (Central Park Conservancy 2014). In addition to creating a record of the work performed in 2014, it was the conservators’ desire to provide new documentation that, among other goals, could be digitally archived, used as an analysis tool and be updated in the future. Other goals included the elimination of the need to print and transport physical drawings between the site and office; the elimination of potential for transcription errors; and the creation of readily available information in a flexible format. Ultimately, the best solution would consider the project budget, along with the accuracy and detail of the documentation.

3.3. Field Documentation Application Comparison

This study looks at three digital applications for collecting data in the field to document the as-applied treatments at the Obelisk. Note that none of these programs were evaluated for the collection of data into a database management program for this project.

3.4. Computer Aided Design (CAD) Computer Program

Initially, the conservators found that using a CAD program (AutoCAD 2013 by AutoDesk, Inc.) to record the as-applied treatments on site on a laptop computer proved cumbersome and the equipment required a portable power source due to the limitation of the batteries in the device at the time. The laptop did provide a touch screen function with stylus feature. Although this feature allowed the conservators to document the applied treatments directly into the CPC CAD file, it proved to have limited accuracy in sketching actual conditions and the documentation progress was slow. At the time, files were stored directly on the laptop hard drive, requiring hard wired transfers to a server at a different time and location. In addition, multiple expensive devices, as well as users with proficient knowledge of the programs, were required. If the team had chosen to continue with this method it also would have required additional time to train the hands-on conservators who did not know the program, or it would have required additional CAD trained staff. Therefore, the first alternate digital solution was considered for efficiency.

3.5. 2D PDF Mark Up Application

The second digital documentation application used was a proprietary tablet application ReVu 2014 by Bluebeam Software, Inc. using a mark up overlay system layered on the PDF files of the existing documentation. This application was considered and tested for its ability to mark up 2D PDF documents with customisable tools such as text, lines, highlighting, and hatch patterns. The expectations were that this application would help annotate the existing project documentation files and illustrate the new as-built conditions. The digitisation of the information was intended to save time, and the application purported to improve the sharing of information as well as keep the information organised and conveniently stored in a central location.

Using a stylus in the field, the conservators could mark up PDF files on user defined layers with components such as lines or polygons, and highlight selected areas. An icon-based toolbar could be customised to create an efficient workflow by making “rubber stamps” for specific treatments. The application allowed for the manipulation of components using a “one-click” process for changing the appearance (colour, fill, line type, etc.). A calibrated scale feature could resize the components automatically with different scales within zoom viewports during the recording process. The components included customisable attributes that could record the date, conservator, application issues, measurements, quantities, etc. The information contained within the components was stored in a database within the digital file in customisable cells and columns, containing formulae and other information accessible from dropdown menus or manually entered. The information could be managed in a list format within the application, filtered, or searched, and exported to CSV, XML or PDF formats.

The project files could be stored and accessed from either the local tablet drive on site or a cloud based storage system from both the field tablets via Wi-Fi, or an office desktop computer connected to the Internet. Information stored directly on a tablet required uploading to a server for access by others. Real time editing and multi-users in one file was not available for this application at the time of the project. At times the upload/download process resulted in the loss of information due to the overwriting of data stored in one or more devices during offline editing. Reportedly, the newest version of the software allows for real time collaboration of mark ups and comments with shared users. This feature, not available at the time of the Obelisk project, was available in the third solution considered.

3.6. CAD File Reader and Editor Tablet Application for Files in DWG Format

As third solution AutoCAD 360 2014 by Autodesk, Inc. a proprietary portable CAD file reader and editor for files in DWG format was investigated. It was considered because it could connect directly to the existing project CAD files via Wi-Fi access if available. If Internet connectivity was not possible, the files could be stored locally on mobile devices and the information uploaded/downloaded when Internet access became available. The extent of the real-time link to the files between desktop, web and mobile device applications surpassed the other applications tried.

Although advertised as simple and easy to use, the program required some knowledge of the features available in the proprietary desktop program. The drafting of lines, polygons and other components was similar to the first program considered. However, it was limited to the tools available within the application. The CAD application, at the time of the project, allowed for very little customisation, particularly in the field. The creation of

components with customisable attributes did exist, but it was only a feature available on the desktop version of the program.

The real-time cloud collaboration sharing tools allowing work with other users in multiple locations, albeit remarkable at first, did not end up being utilised in the actual documentation process. The ability of the application to use password protection of files and set user permissions could be set up to prevent the overwriting of data thereby reducing the risk of lost or incorrect records. Files used and shared in this application were stored on a third-party web-based server and accessible on both portable devices and desktops with Internet connectivity. Files created in this application could be exported to other DWG file compatible programs. However the information contained in attributes of the components drafted in the application could not be accessed from the tablet.

3.7. Observations and Comparison

The assessment of the digital documentation solutions evaluated for the Obelisk project considered, among the features available: the level of accuracy and detail; the level of efficiency; and the risk of recording inaccurate data and the potential for lost data. The features for all digital solutions continue to develop and increase. All of the applications evaluated maintained a similar amount of customisation at the time. All provided the ability to sketch onto the two types of digital files using a stylus. The tablet applications offered Wi-Fi connectivity to a remote server.

The level of accuracy of the information recorded tended to be more detailed in the CAD program and CAD application. The PDF application consisted of documentation that appeared more “cartoonish” and relied more on notes and comments. The rubber-stamp feature was a quick method of documentation, although it recorded generic information that required edits. Not surprisingly, the conservators were able to document a higher level of detail by hand with pencil on paper.

The efficiency of all three programs was disputable. While the field collection of data in digital format appeared to be faster, this was not always the case. What was gained in efficiency in the field tended to be balanced by the amount of work interpreting the data in the office. For all applications evaluated the documentation on digital devices removed the conservators from the hands on conservation work to perform the digital documentation. In the case of the PDF application, the time saved by the effective functions of the application in the field required additional time in the office to transfer the information into the CAD files as required by the Project. Sketching directly in the CAD files in the field proved more time consuming for the conservators, albeit this process eliminated the potential for transcription errors, which was one of the Project goals. Again, sketching with pencil on paper was the fastest method of documenting the locations of the applied treatments at the Obelisk.

The CAD program and application required the conservators in the field either to already know the program or take time to learn it. When the conservators applying the treatments did not know the CAD application, additional staff required to perform the documentation increased the number of field personnel and the cost.

All digital hand held devices collecting data in the field over a Wi-Fi Internet connection have an increased risk of data loss. The connectivity of the CAD editing program was attractive, but proved to be more of an amusement (watching people on a desktop computer

sketch in the field miles from the office) and was not used to any further possibility. However, the information was directly linked to a remote server, which reduced the potential for the loss of data once it was input into the file.

The volume of the data files was limited to that of the hand held device in the case of the tablet applications or laptop computer when connection to a remote server was not possible. In the case of the PDF application, this was an issue because the PDF files were too large to store more than a few at a time on the tablets. Therefore, the information needed regular transfer between the field devices and the office computers. The PDF application performed with undesirable results and after several events when data was lost, the CAD tablet application became the preferred tool. Working on a laptop computer increased the amount of storage available.

4. Conclusions

For the documentation at the Obelisk, the conservators began using one program and, based on their experience in the field continued to seek either customisation of that program or an alternate application, changed to another application, and ultimately, to a more traditional method of hand drawing with the expectation of digitising the information off-site at a later time. Our experience showed that a few factors continually lead us back to the use of paper and pencil. First, the conservators found it distracting to document the treatments as they were applying them. It distracted them from the execution of the repairs in that once a repair was complete, the documentation process obliged them to look away from the repair site potentially missing for example the migration of excess materials requiring clean up. Using digital media continued to be slow and the conservators reported that at times, it was difficult to record multiple treatment locations as applied since the treatments used at the Obelisk were by design virtually invisible. However, this situation is not solely a problem of the digital solutions.

The sequencing of the documentation was considered. Documentation of the treatments before application did not prove useful nor was it an efficient procedure because the treatments when applied did not always conform to the graphic recorded before application. This was the case for both digital applications and hand drawn documentation. Documentation immediately after the application of treatments proved to be the most efficient recording method and the most accurate in identifying the repair locations. Ultimately, the conservators chose to trace the applied treatments by hand on the printed photographs to save time and to provide more accurate records of the applied repairs. This highly accurate documentation, however, left open the possibility for transcription errors when entering the data at a later time.

The potential for transcription errors was discussed after the conservators decided that using paper and pencil was the most efficient and accurate recording method for them. It was determined that since a record hard copy of the documentation existed, any future discrepancies in the digital files could be checked against the original documentation. Essentially, this process created a redundancy in the data that could prove valuable.

Additionally, the loss of data recorded on paper was a concern. Digital technology does not alleviate this fear; in fact one could suggest that it increases it. When using pencil and paper, one could argue that a torn or water damaged piece of paper or smeared ink still can

convey information, even if partial, potentially triggering the memory of a detail or condition. The lost of digital data presents no peripheral opportunities.

Why do we keep going back to paper and pencil? Does the existence of technology create anticipation that there will be a paradigm shift to all digital solutions? Why do we continue to pursue digital solutions for traditional methods of documentation? We do learn something, however esoterically or intrinsically defined, when measuring by hand and drawing details with pencil on paper. What is lost when the process is digitised? Sketching on a tablet is still sketching by hand. The options for hundreds of colour and textures in a digital sketch are attractive, but not necessary. A pencil has comparatively limited options, however, it still gets the job done, inexpensively and so far comparably quickly. Digital technology has the ability to transform the way we work, and hand held device applications can replace paper, but there should be an effort to continue to keep the tactile form of documentation among the tools used for collecting data. That documentation is important in the conservation process is not a question. Proper and accurate documentation can assess value, inform the efforts of conservators, and manage risk.

David Woodcock, guest editor of the APT Bulletin listed several concerns regarding digital documentation in 2010: transferability, the size of files, the lack of standards for collection, transmission and integration, as well as the demand of clients to provide greater access to information (Woodcock 2010). Today, in 2016, these same issues remain in the forefront of our discussions regarding the use of digital technology for the recoding of heritage assets. The goals of digital documentation vary widely, whether it is, as in the case of the Obelisk, the recording of existing conditions and applied treatments, the gathering of a large volume of data related to heritage assets, or the development of public access to previously unavailable information on art and archives. The complexity of each of these goals requires different approaches to the collection and management of the data. The solutions available need to be specifically tailored to each project. A single digital solution is not possible, however the view of digital documentation as a tool that can assist in the management of data is correct, but only so far as it is designed on a case-by-case basis, making the linking of application and data between disparate projects difficult. The expectation that one solution can be used across many projects becomes difficult as technology continues to rapidly develop; they become obsolete or are replaced with new versions with enhanced features.

Acknowledgements

The author would like to thank Maria Warsh, Matthew Rielly, and John Harrigan of The Central Park Conservancy, and Dr. George Wheeler, the Conservancy Consulting Scientist, their extensive time and generous support during this Project.

References

- Building Conservation Associates, Inc., 2014, “Central Park Conservancy Central Park Obelisk, New York, NY: Conservation treatment Report”, Building Conservation Associates, Inc., 1-6.
- Central Park Conservancy, 2014, “Request for Proposals: The Conservation of the Obelisk in Central Park, New York, New York”, Central Park Conservancy, 3-4.

- Central Park Conservancy, 2014, "Conservation Treatment Proposal: The Obelisk, Near 80th Street and the East Drive in Central Park, New York, New York", Central Park Conservancy 1, 3, 7, 10.
- Central Park Conservancy, 2016, "Final Report of the Conservation of The Obelisk, Near 80th Street and the East Drive in Central Park, New York, New York", Central Park Conservancy, 11.
- Clark, Kate, 2010, "Informed Conservation The Place of Research and Documentation in Preservation", APT Bulletin, 41 (4), 5-10.
- Letellier, Robin, and Rand Eppich, eds., 2015, "Recording, documentation and information management for the conservation of heritage places".
- Roy, Ashok, Foister, Susan, and Rudenstine, Angelica., 2007, "Conservation Documentation in Digital Form: A continuing Dialogue About the Issues", Studies in Conservation, 52 (4), 315-317.
- Woodcock, David, G., 2010, "Guest Editor's Note", APT Bulletin, 41 (4), 3.

COMPUTATIONAL IMAGING TECHNIQUES FOR DOCUMENTATION AND CONSERVATION OF GRAVESTONES AT JEWISH CEMETERIES IN GERMANY

C.A. Graham^{1*} and S. Simon¹

Abstract

The following study focuses on the application of computational imaging techniques to enhance legibility, enable dissemination and aid conservation of eroding gravestone inscriptions. This methodology comprises the use of reflectance transformation imaging (RTI) in order to create dynamic visualizations and 3D models. RTI is an extremely powerful method of digitization that brings specific analytical attributes to a project as the generation of digital surrogates and their realization in visualization software allow for an unprecedented degree of user interaction and investigation.

Keywords: gravestones, RTI, interactive re-lighting, 3D surface geometry, conservation practice

1. Introduction

1.1. Aim

A major aim of this project is to use computational imaging techniques and new viewing tools to create and disseminate digital documentation of gravestones that are susceptible to deterioration and weathering in Jewish cemeteries. This on-going and evolving endeavor seeks to bring together students and specialists alike to advance didactic and conservation objectives associated with these gravestones in order to shine a light on the once vibrant Jewish communities of Lower Franconia in the German state of Bavaria.

1.2. Cultural relevance

Vanishing inscriptions on undocumented gravestones tell the stories of Jewish communities that resided in the Bavarian countryside before the Second World War. These communities were disturbed greatly by the war as Jewish families were uprooted and expelled from their villages. Funerary symbols and inscriptions hold some of the last remaining information after the holocaust pertaining to the social structure of these communities, rich with demographic details about vocation, gender, kinship, and interconnectedness of village inhabitants. As time passes, agents of erosion render these engravings more difficult to decipher and, as such, the history they hold falls in greater peril of being lost forever.

1.3. Previous work

In recent years, vulnerable Jewish cemeteries in Lower Franconia have served as the focus of a documentation enterprise carried out by two high schools: Rhön Gymnasium (Bad

¹ C.A. Graham* and S. Simon

Institute for the Preservation of Cultural Heritage, Yale University, United States of America
c.graham@yale.edu

*corresponding author

Neustadt an der Saale, Germany) and Mikve Israel (Holon, Israel). This project, comprising fieldwork and classroom seminars, is carried out under the auspices of their long-standing partnership. Since 1992, the schools have hosted cultural exchanges in their home country every second year. In 2013 and 2015, German and Israeli students worked together closely to map Jewish cemeteries in Lower Franconia and record information about past inhabitants. From the onset, their work fostered a real sense of collaboration, as they drew from multiple sources in order to form a complete picture of the lost Jewish communities.

The students' efforts have been complimented by technical support in the form of documentarians, historians, archivists, conservators and imaging specialists, who help to give context to their work. The project unites people from different countries, backgrounds, religions and ages to explore a joint or intersecting past. Documentarians provide the framework for the students' work, which extends beyond documentation in the cemetery to historical societies, archives and the homes of local villagers and ex-pat survivors. When possible, students collect oral histories in person and via electronic correspondence. As gravestone inscriptions are connected with historical records and first-hand accounts, the character and dynamics of the community emerge.

As a major consideration for this project is to provide universal access to and promote preservation of eroding gravestones, a project website was established (Caine 2014). This site presents the results of the work carried out in the Jewish cemetery in Bad Neustadt an der Saale during the 2013 exchange. The newly established record of the cemetery is publically available in English and German to visitors from around the world. The collaborative efforts and outstanding dedication that were necessary to achieve these results were acknowledged when the project received the second honor in the prestigious Simon-Snopkowski award ceremony held in Munich in 2014. This prize, awarded by the Bavarian State Ministry of Education and Culture, was established to recognize research projects that study Jewish history and culture in Bavaria and the holocaust.

1.4. Current focus

In the autumn of 2015, the documentation project was continued with a renewed focus on a cemetery in the nearby village of Unsleben. This cemetery is located atop a steep hill about a kilometer outside of heart of the village, where a Jewish community originally began to burgeon under the patronage of a nobleman in the mid 1500s. In this cemetery stand the gravestones of locals of Jewish faith, 229 of whom were interred from 1856 through 1942 (Hesselbach nd, Main Post 2008). The mostly sandstone memorials are currently badly weathered and were desecrated during the Second World War. After the war, dedicated villagers attempted to restore the cemetery as best they could, but many ambiguities remain as to the gravestone inscriptions and identities of those buried (Hesselbach *pers. comm.*). This project strives to resolve some of those uncertainties. While the fieldwork in the cemetery focused on student-driven transcription of symbols and inscriptions, it also featured the application of computational photography techniques.

2. Digitization

2.1. Methodology

The primary form of digitization employed, reflectance transformation imaging (RTI), is a non-contact method of capturing how the surface of an object interacts with light. RTI has long been lauded for its ability to aid in visualization and inspection of cultural heritage

objects (Malzbender *et al.*, 2001). The acquisition process encompasses the capture of a sequence of images of an object illuminated by a light source set at different positions. Standard field documentation is traditionally photography with uniform lighting and static shadows, which poses problems for legibility and enquiry, especially for researchers at a distance. RTI differs in that the change in the angle of illumination between each capture is visible in the varying highlights and shadows that are present in images. Data captured during an RTI acquisition can be post-processed into visualizations that convey the detail and dimension of the surface of an object. These visualizations allow for examination of the surface morphology by allowing a user to manipulate the direction of light sources and promote the virtual investigation of the geometry of surface in three dimensions.

2.2. Applications

Through RTI, reflectance values for the surface of the object are captured per pixel, as a stationary camera takes a series of images of an object under changing light conditions. Since the camera and the object remain stationary, each pixel corresponds to the same feature on the surface of an object in each image in the series. This pixel-specific information is processed through a mathematical algorithm, which renders a texture map that allows for dynamic simulation of how each pixel will interact with light under varying conditions.

This technique yields visualizations that allow users to interactively manipulate the direction of virtual light sources in real time. In doing so, users may illuminate an object and change the appearance of highlights and shadows. Software for viewing RTI visualization files is free, intuitive and embeddable on the web (Palma *et al.*, 2012). This software allows for user interaction with the manner in which light falls across the surface of an object, thus accentuating the fine-grained geometry of low relief surface features, such as inscriptions, tool marks, veins and fracture lines.

The reflectance values captured corresponding to the surface of an object further allow for a per-pixel approximation of the direction of normals on the surface of an object (Malzbender *et al.*, 2006; Palma *et al.*, 2010). Surface normals are the directional vectors perpendicular to the surface plane of an object at specific points. Since RTI data contains detailed information about surface normals, it can be used to generate fine-grained 3D information for surface geometry of an object. The scale of this data can exceed the detail yielded through laser scanning and does not require any additional acquisition time.

It is of great interest to generate 3D data for individual features from RTI, especially in the context of this project, where more importance is placed on surface morphology and geometric detail of the inscriptions than the holistic geometry of the gravestone. The rapidity of acquisition and post-processing for 3D data generated from RTI far surpasses laser scanning. 3D models have significant applications in research, dissemination and educational outreach (Dellepiane *et al.*, 2012).

3. Reflectance transformation imaging of gravestones in Unsleben

3.1. Data acquisition

During the first week of October 2015, RTI capture was carried out for 13 gravestones in the Jewish cemetery in Unsleben. The acquisition campaign was led by a digital imaging specialist from the Institute for the Preservation of Cultural Heritage at Yale University and performed by German and Israeli students who worked together in mixed groups of three.

Before the start of this project, *in-situ* RTI acquisition strategies for gravestone inscriptions were established and refined during a project in the historic crypt of the Center Church on the Green in New Haven, Connecticut. Development of this local pilot project enabled an optimized approach to student training and allowed for an organized focus on gravestone selection in Unsleben.

Criteria for selection of gravestones for imaging were guided by three main factors – legibility of inscription, degree of deterioration of inscription and stability of stone structure. Illegible, visibly eroded and particularly unstable gravestones were given priority for RTI. Imaging was also impacted by other factors, however, including student schedules, additional documentation activities in the cemetery and position of sun in the sky. The cemetery is located atop a hill with the inscribed faces of gravestones facing westward with little cover from the sun. During the project, the cemetery was abuzz with activity, as approximately 40 students carried out documentation work.

These factors allowed for creativity in problem solving during RTI acquisitions using the highlight method (Duffy 2013). For this method of imaging, the team used a standard DSLR camera and synched flash. The flash was manually situated at equidistant locations and moved between shots in an arc around the surface of the inscription, creating a virtual umbrella of light around the face of the gravestone. A string was affixed to the flash to ensure the distance of the flash to the center of the inscription remained consistent for all images. Team members were assigned distinctive responsibilities – orientation of flash, maintenance of consistent distance, and remote camera control via computer (Fig. 1).



Fig. 1: A group prepares to capture a photograph of a gravestone in the Jewish cemetery in Unsleben in an RTI sequence using the highlight method.

A color checker and two reflective spheres were set in the frame of each image for the purpose of reliability in future data generation. The purpose of the reflective spheres is to capture the flash location in each image. Since they remain immobile throughout the capture sequence, they may be individually isolated during post-processing and sampled in order to create a comprehensive map of the coordinates of all light directions captured during the acquisition.

3.2. Data processing

Thirteen unique sets of captures were taken of gravestones at the Jewish cemetery in Unleben in order to support an RTI workflow. For each gravestone, between 30 and 60 images were processed in order to yield RTI visualization files and 3D models. Due to time constraints, data was solely collected and assessed in the cemetery and then post-processed after fieldwork.

The first step in processing the data was to thoroughly examine the data sets to validate the quality and consistency of images. Corrupted images, due to human or mechanical error were rejected. Coordinates of reference spheres were closely analyzed and compared. Two reference spheres were placed in the composition of each frame in case one was unintentionally moved. This happened often due to the high volume of activity in the cemetery. Moving forward with the approved image set, processing commenced.

For the purposes of creation of high fidelity data, minimal image editing and no image enhancement took place. Lens and color corrections were carried out consistently to all of the images in a sequence from the capture of an individual gravestone. Free and open-source software, RTIBuilder, was used to process images into RTI visualization files.

In order to extract the 3D data from the image sets, masks were produced. A mask is a black and white image created in order to guide the software. First, the gravestone was outlined, and then erased so that white substitutes the silhouette. Next, the background was deleted and filled in with black. The creation of this high contrast image focuses the software for creation of 3D geometry from surface normals corresponding to the pixels in the white region. Software created by Yale University's Department of Computer Science, RTI23D, was used to generate this data. These 3D models may be viewed and manipulated in free, open-source software, MeshLab (Cignoni 2008).

3.3. Interpretation and dissemination

RTI allows for visualization and interaction with the manner in which light falls across the surface of an object, opening new possibilities for examination (Fig. 2). Visualization of low-relief geometry has benefitted greatly from RTI, with results that address the needs of historians, scientists and conservators alike (Fig. 3). Conservators have added RTI to their arsenal of diagnostic and documentary tools. Historians and researchers are able to view and accentuate surface properties to enhance the appearance of features of interest. Interactive visualizations can be enhanced to bring crumbling inscriptions into focus. These visualizations can lead to important discoveries, guide practices and allow access and collaboration across the distances.

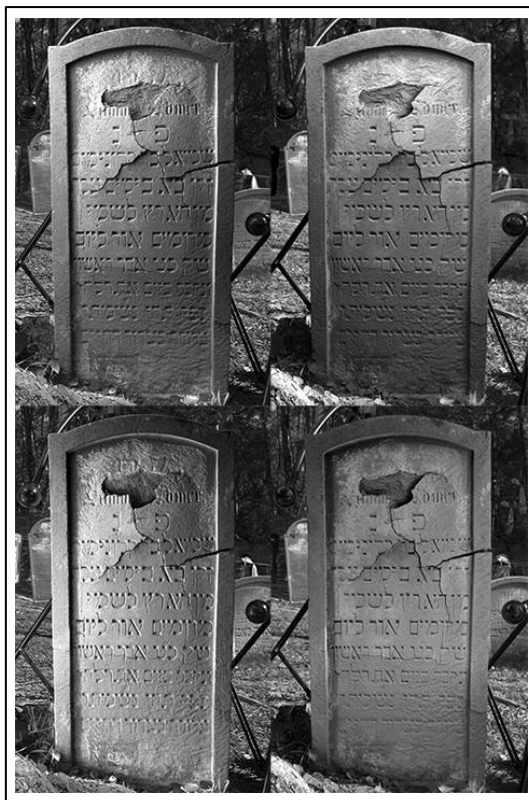


Fig. 2: Snapshots of an RTI visualization of an inscription on a gravestone in the Jewish cemetery in Unsleben with lighting from different directions.



Fig. 3: A side-by-side comparison of a standard image (left) and a snapshot of an enhanced RTI visualization (right) of an inscription on a gravestone in the Jewish cemetery in Unsleben.

The by-products of the RTI campaign in Unsleben will be applied to meet different goals, including research, preservation and public education. Interactive visualizations of inscriptions from the gravestones in Unsleben cemetery will be featured on a website sponsored by the town council. This form of exhibition can be used to engage viewers and garner public interest and support for the care of cemeteries.

While RTI is an effective way to connect an audience with the past, it is also a powerful way to ensure the trajectory of the gravestones in an endangered cemetery into the future. RTI is a diagnostic tool, which can help to guide both assessment and preservation. 3D data can be applied in stress modelling for evaluation of structural integrity and formation of a conservation plan for gravestones at risk.

RTI also has quantitative applications in conservation and conditions monitoring (Manfredi *et al.*, 2013, 2014). Imaging can be used as a benchmark of the current state of an object. The data can then be compared to future conditions via deviation analysis. This is a way to track the effect of weathering and erosion. The clear, customizable visualizations that RTI generates give an enhanced perception of surface morphology and have the ability to inform and extend research and conservation methods.

4. Conclusion

Digitization allows for enhanced perception of the inscriptions on the surface of gravestones that agents of erosion and damage have garnered less prominent over the years. Through computational imaging, inscriptions that have long eluded visitors may be digitally illuminated, accentuated and disseminated to allow for interaction and interpretation by a wide audience in a manner that has previously been impossible. This kind of access aims to bring viewers closer to the identities of those interred, despite long distances or the passing of time, to reveal relatable stories that are rooted in the rich culture of the past Jewish communities of Bavaria.

This digitization project serves as a manner of applying computer vision to quickly eroding historical records. It offers a means to document, preserve and make accessible culturally rich funerary engravings. This has proven essential in that through digitization, enduring intangible, yet interactive results have been yielded. These kinds of digital visualizations serve a didactic purpose as active agents of public education. The results, which are still very much in development, will be incorporated into an accessible website for virtual investigation well into the future.

Acknowledgements

Many thanks to the teachers and students of Rhön Gymnasium and Mikve Israel, the exchange leaders: Günter Henneberger, David Avshalom and Judith Tal, the documentation team: Eyal Tagar and Nadav Madanes, and Unsleben town council. Much appreciation and admiration are also due Prof. Dr. Josef Hesselbach.

References

- Caine, M., 2014, Wiederentdeckte Gemeinden: Die verlorenen Juden von Bad Neustadt. (<http://www.judaica-badneustadt.de/>, accessed 20 November 2015).
- Cignoni, P., Callieri, M., Corsini, M., Dellepiane, M., Ganovelli, F., and Ranzuglia, G., 2008, MeshLab: an open-source mesh processing tool, in the Proceedings of the Eurographics Italian Chapter Conference, 129 - 136.
- Dellepiane, M., Callieri, M., Corsini, M. and Scopigno, R., 2012, Using digital 3d models for study and restoration of cultural heritage artifacts, in Digital Imaging for Cultural Heritage Preservation: Analysis, Restoration, and Reconstruction of Ancient Artworks, Stanco, F., Battiato, S., and Gallo, G. (eds.), CRC Press, 1439821739, 37 -67.
- Duffy, S. M., 2013, Multi-light imaging techniques for heritage application, English Heritage, 1 - 23.
- Hesselbach, J., nd Geschichte der Juden in Unsleben. (<http://www.unsleben.rhoensaale.net/Unser-Dorf/Geschichte/Juedische-Geschichte>, accessed 20 November 2015).
- Main Post, 2008. Miteinander wird großgeschrieben (<http://www.mainpost.de/regional/rhoengrabfeld/Miteinander-wird-grossgeschrieben;art765,4813309>, accessed 20 November 2015).
- Malzbender, T., Geld, D. and Wolters, H., 2001, Polynomial texture maps, in the proceedings of *the 28th annual conference of the Association for Computing Machinery's Special Interest Group on Computer Graphics and Interactive Techniques (ACMSIGGRAPH)*, 519 - 528.
- Malzbender, T. Wilburn, B., Gelb, D. and Ambrisco, B., 2006, Surface enhancement using real-time photometric stereo and reflectance transformation, in the proceedings of the Eurographics Symposium on Rendering, 245 - 250.
- Manfredi, M., Williamson, G., Kronkright, D., Doehne, E., Jacobs, M., Marengo, E. and Bearman, G., 2013, Measuring changes in cultural heritage objects with reflectance transformation imaging, in the proceedings of Digital Heritage International Congress, Volume 1, 189 - 192.
- Manfredi, M., Bearman, G., Williamson, G., Kronkright, D., Doehne, E., Jacobs, M. and Marengo, E., 2014, A new quantitative method for the non-invasive documentation of morphological damage in paintings using RTI surface normals, *Sensors*, 14 (7), 12271 - 12284.
- Palma, G., Corsini, M., Cignoni, P., Scopigno, R. and Mudge, M., 2010, Dynamic shading enhancement for reflectance transformation imaging, *Journal on Computing and Cultural Heritage*, 3 (2), 6:1 - 20.
- Palma, G., Siotto, E., Proesmans, M., Baldassarri, M., Baracchini, C., Batino, S., Scopigno, R., 2012, in the proceedings of the 40th Computer Applications and Quantitative Methods in Archaeology (CAA) Conference, 177-185.

A METADATA-SUPPORTED DATABASE SCHEMA FOR STONE CONSERVATION PROJECTS

E. Kardara^{1*} and T. Pomonis¹

Abstract

The aim of this work is to help stone conservators benefit from the ease of use of modern cultural databases. We introduce an approach for a database schema that not only constitutes a complete, typical digital cataloguing system for monuments and artefacts, but is also used to log and provide additional conservation-oriented information for each one of them. The whole database schema is focused on the process of stone conservation and contains all the information needed by conservators during the treatment of a monument or artefact. In addition, the whole data structure is supported by a custom metadata schema, originating from the Dublin Core Metadata Initiative. Stone conservators can exploit this information architecture to manage and support all of their activities while facing a monument.

Keywords: database schema, metadata, stone conservation, projects

1. Introduction

Nowadays we witness a really broad use of computer technology and software products in all aspects of cultural information management, especially in terms of digital archiving of cultural heritage and culture-specific databases. The main incentive behind this broad spreading of cultural databases came from museums and cultural institutions all over the world, as there was a great need for cataloguing and supporting the documentation of its collections, in an efficient and cost effective way. That's why they started developing their own in-house solutions in order to support their specific needs. All this effort led to really interesting and innovative implementations, but also to a complex and greatly fragmented reality of DBMS solutions and usage. In museums and conservation centres, as well as in conservation and restoration sites, the need for a Database Management System arises for the purpose of efficient object-related information storage and retrieval. The use of such a DBMS for archiving is a reasonable choice. With the aid of an ordinary DBMS it is possible to store, modify, display specific records as well as find records that satisfy certain search criteria. Although there are several database products that offer this level of functionality, either they are not specialized to cultural heritage objects archiving, or they lack seriously in conservation specific functionality.

¹ E. Kardara* and T. Pomonis

Conservation of Cultural Heritage Department, Technological Educational Institution of Ionian Islands, Greece

kardaraeva@gmail.com

*corresponding author

2. A conservation-oriented database

2.1. Background

There are many such DBMS implementations all over the world, from institution-oriented databases as CDS/ISIS¹ and Museum Plus², to more complete and solid solutions like the European Union research project NARCISSE, which provided a solid framework for the digital representation of art-related information (European Commission, 1993). The thing is that all these DBMS solutions were developed to support cataloguing of collections and, more or less, lack in describing the aspect of conservation and restoration process in an efficient and thorough way. The need for conservation-specific solutions led to the development of such databases and modules that could support the required processes. Because of the complexity of this issue, most of them are limited in certain aspects of the conservation process (Basir *et al.*, 2014), (Pedeli, 2013) or stay focused on a single domain (Pappas *et al.*, 1999), (Velios and Pickwood, 2005). There are also more complete and solid approaches that vary from holistic management ideas (Yen *et al.*, 2011) and documentation-oriented systems (Naoumidou *et al.*, 2008), to even more complex and powerful solutions like the EROS database (Aitken *et al.*, 2005). Although the latter are potent and sufficient in covering the conservation process, they lack greatly in simplicity, mainly because they are mostly based in CIDOC-CRM (Doerr, 2002) which sacrifices ease of use to provide greater completeness.

2.2. Our approach

To overcome the above handicaps we decided to design a custom database for stone conservation cataloguing, utilised in stone conservation projects, but also for in-house use in stone conservation courses at Conservation of Cultural Heritage Department (<http://conservation.teiion.gr>) of Technological Educational Institute of Ionian Islands.

2.2.1. Design

During the design process the desired characteristics were:

- I. Our database would be operated mainly by conservators so its metadata schema has to be focused on conservation processes.
- II. It had to be easy to operate as it will be used by conservation students during their lessons and practice, and visited by inexperienced users.
- III. It had to be as object-agnostic as possible, meaning that it had to be able to handle any kind and size of stone artefacts under conservation.
- IV. If possible, it had to interoperate with other pre-existing artefact cataloguing systems and cultural databases.

2.2.2. Structure

To make our database able to interoperate with pre-existing cataloguing schemas, we decided to divide it in two discrete modules, an Object Description Module and a Conservation Module. The first one contains only the cataloguing information about an object, while the latter comprises all the conservation specific data and documentation. These two modules are interconnected only on foreign key basis, so it is possible to put

¹ http://portal.unesco.org/ci/en/ev.php-URL_ID=2071&URL_DO=DO_TOPIC&URL_SECTION=201.html

² <http://www.zetcom.com/en/products/museumplus/>

aside the Object Description one and use the Conservation Module with any convenient cataloguing schema.

3. Metadata schema

As we decided to divide our database into two modules, we had to provide a suitable metadata schema for each one. For the Object Description Module we decided to keep in line with all the current cultural database trends, and design a trivial schema mainly based on Dublin Core metadata standard (France and Toth, 2006) while also incorporating the Object ID guidelines (Thornes, 1999). The result was a typical cultural documenting schema that can be used even as a separate solution (Fig. 2). The really challenging part was to design a suitable schema for the Conservation Module. For this we had to track the exact process used on stone conservation tasks and try to deduce the discrete steps and their requirements. The result was a highly abstractive schema that can be used on almost all cases of stone conservation and restoration (Fig. 1).

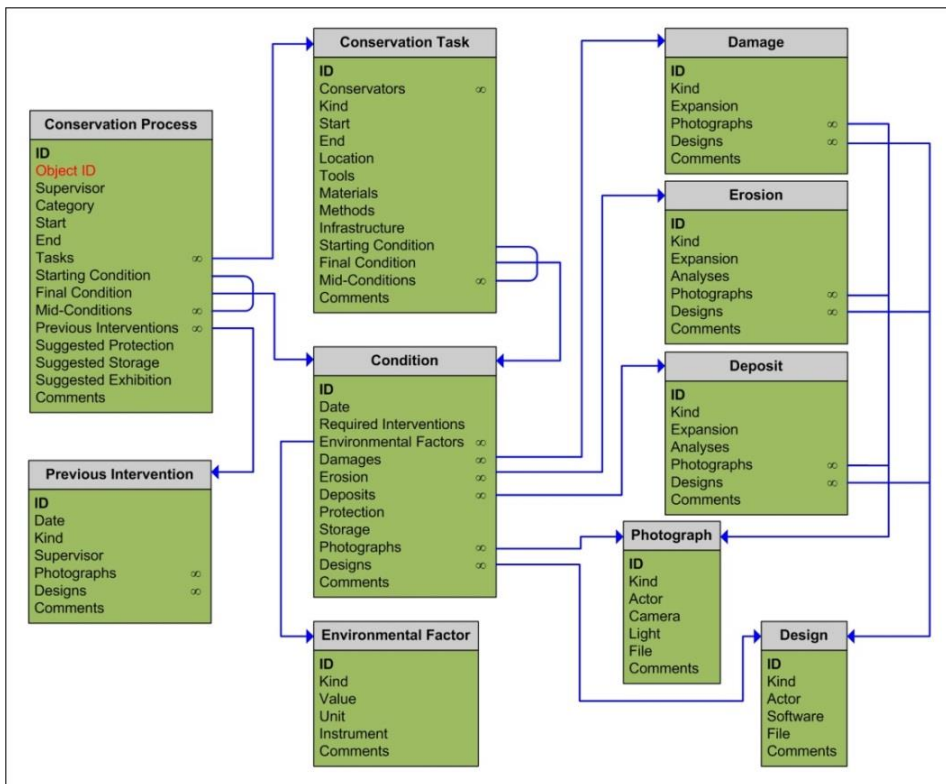


Fig. 1: Conservation Metadata Schema.

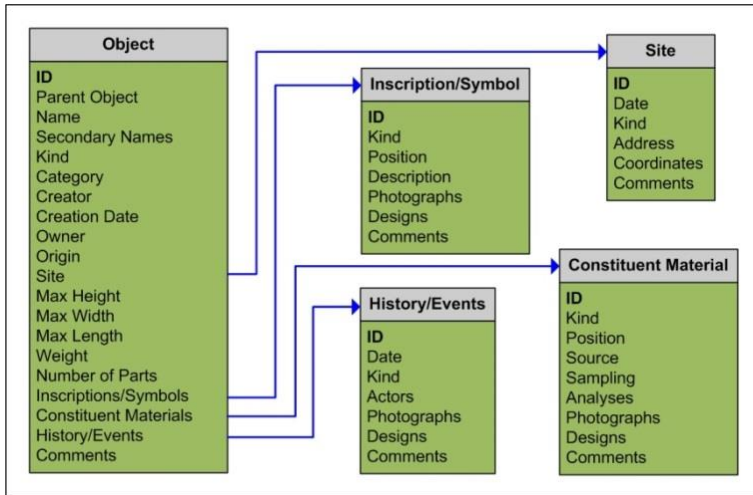


Fig. 2: Object Description Metadata Schema.

The fundamental entities in this schema are Conservation Process, Conservation Task and Condition, which are used to describe the main steps and instances of conserving an artefact.

3.1. Main entities

Their main entities are:

- Conservation Process
 - Supervisor: The conservator responsible for the whole conservation process.
 - Category: Preventive or Interventive conservation.
 - Start: Date and time that the process started.
 - End: Date and time that the process ended.
 - Tasks: The sub-tasks of this process.
 - Starting Condition: The object's condition at the beginning of the conservation.
 - Final Condition: The object's condition at the end of the conservation.
 - Mid-Conditions: Object's condition instances during the conservation.
 - Previous Interventions: Everything that happened due to human interference.
- Conservation Task
 - Conservators: All the persons involved in this task.
 - Kind: What kind of conservation act is performed, e.g. cleaning, fill etc.
 - Location: Where it is taking place, e.g. dig site, laboratory etc.
 - Tools: Which tools were used.
 - Materials: Which materials were used.
 - Methods: Which methods were used.
 - Infrastructure: Any required conservation infrastructure, e.g. scaffolding.

➤ Condition

- Date: Date and time of the object's condition instance.
- Required Interventions: What has to be done.
- Environmental Factors: Environmental conditions in this instance.
- Damages: e.g. cracks, deformation, etc.
- Erosion: e.g. loss, rounding, etc.
- Deposits: e.g. dust, biological, etc.
- Protection: Temporal protection in this instance.
- Storage: Temporal storage in this instance.
- Photographs: Photographic material of this instance.
- Designs: Designs of this instance.

3.2. Secondary entities

In addition, there are some secondary entities that conclude the above ones:

- Damage: Kind, Expansion.
- Erosion: Kind, Expansion, Analyses.
- Deposit: Kind, Expansion, Analyses.
- Environmental Factor: Kind, Value, Unit, Instrument.
- Photograph: Kind, Actor, Camera, Light, File.
- Design: Kind, Actor, Software, File.

3.3. Thesaurus

To support the above metadata fields, we had to create a corresponding Greek thesaurus of conservation terms, which conservators keep in mind while filling the respective fields. This thesaurus was based on ICOMOS-ISCS: *Illustrated glossary on stone deterioration pattern* (http://www.icomos.org/publications/monuments_and_sites/15/pdf/Monuments_and_Sites_15_ISCS_Glossary_Stone.pdf) and *A Glossary of Historic Masonry Deterioration Problems and Preservation Treatments* (Grimmer, 1984).

4. Conclusions

In this paper we presented a proposed metadata schema for a conservation-oriented database that can be used during stone conservation projects, while being as simple and easy to operate as possible. The specific schema was used in developing a primary version of an in-house database solution for the Conservation of Cultural Heritage Department of Technological Education Institution of Ionian Islands. This database was then utilized by students of stone conservation lessons in their laboratory practice, where they handled objects of various complexity and materials. In addition our database was used in cataloguing the real-time conservation process of several stone parts and also of some mid-scale monuments in Zakynthos island. All these examples resulted in a really useful stress test for our database and proved its usefulness in supporting the conservation process. From now on we intend to continue developing and testing our database in ever more complicated and different conservation cases, to fine-tune it where needed, while trying to extend it towards supporting the conservation process of artefacts made of different materials other than stone. Finally, we aim in developing an international (English) version of our implementation and have it open-accessed in order to be used by other conservators.

References

- Aitken G., Lahanier C., Pillay R. and Pitzalis D., 2005, EROS: An Open Source Database For Museum Conservation Restoration. In Preprints de la 14eme reunion triennale du Comite International pour la Conservation ICOM-CC, pp. 15–23.
- Basir W.N.F.W.A., Setan H., Majid Z. and Chong A., 2014, Geospatial database for heritage building conservation. ISDE, International Symposium of the Digital Earth, 8 - IOP Conference Series: Earth and Environmental Science (Online).
- Doerr M., 2002, "The CIDOC CRM - an Ontological Approach to Semantic Interoperability of Metadata". AI Magazine - Special Issue on Ontologies, March.
- European Commission, 1993, NARCISSE: Network of Art Research Computer Images Systems in Europe, Arquivos Nacionais/Torre Do Tombo, Lisbonne.
- France F.G. and Toth M.B., 2006, Developing cultural heritage preservation databases based on Dublin Core data elements. In Proceedings of the 2006 international conference on Dublin Core and Metadata Applications: metadata for knowledge and learning (DCMI '06). Dublin Core Metadata Initiative 233-243.
- Grimmer E.A., 1984, A Glossary of Historic Masonry Deterioration Problems and Preservation Treatments, Department of the Interior National Park Service Preservation Assistance Division.
- Naoumidou N., Chatzidaki M. and Alexopoulou A., 2008, "ARIADNE" Conservation Documentation System: Conceptual design and projection on the CIDOC CRM framework and limits, 2008 Annual Conference of CIDOC Athens.
- Pappas M., Angelopoulos G., Kadoglou A. and Pitas I., 1999, "A Database management System for Digital Archiving of Paintings and Works of Art", The Gordon and Breach Publishing Group, (15-35).
- Pedeli C., 2013, An Interdisciplinary Conservation Module for Condition Survey on Cultural Heritages with a 3D Information System In: Recording, Documentation and Cooperation for Cultural heritage, XXIV International CIPA 2013 Symposium, Strasbourg.
- Thornes R., 1999, Introduction to Object ID: Guidelines for Making Records that Describe Art, Antiques and Antiquities. Getty Information Institute.
- Velios A. and Pickwoad N., 2005, Current use and future development of the database of the St. Catherine's Library conservation project. The Paper Conservator, 29. pp. 39-53.
- Yen Yaning, Weng Kuo Hua, Cheng Hung Ming and Hsu Wei Shan, 2011, The standard of management and application of cultural heritage documentation. Proceeding of CIPA 23rd symposium.

3D PHOTO MONITORING AS A LONG-TERM MONUMENT MAPPING METHOD FOR STONE SCULPTURES

B. Kozub¹ and P. Kozub^{1*}

Abstract

This 3D monument mapping method is a non-destructive procedure which allows scientists to see even the smallest changes on the stone sculpture. Until now it has been common method to use 2D- mapping. The biggest problem is, the information must be transferred from the 3D- dimensional object to a two dimensional image. This paper describes preliminary results from a novel optical-based system for three-dimensional damage mapping used on different stone sculptures, the Moai of Easter Island and a late baroque tombstone and shows the advantages of 3D photo monitoring as a non-destructive documentation tool.

Keywords: cultural heritage, 3D photo monitoring, monument mapping, point cloud

The results, which are presented here, pertain to the appraisal of climate-induced deterioration of the stone sculpture Moai of Ahu Hanua Nua Mea on the Easter Island. The appraisal was done as part of the expert activity of Prof. Dr. Peter Kozub during the German Archaeological (DAI) project. Another object is a late baroque tombstone (ca.1725 AD, Wolkenburger quarry) which is now located in the restoration atelier of the University of Applied Sciences in Cologne.

¹ B. Kozub and P. Kozub*

TH Köln - University of Applied Sciences, Cologne Institute for Conservation Sciences (CICS),
Ubierring 40, 50678 Köln, Germany
peter.kozub@th-koeln.de

*corresponding author

1. Stone sculptures on Easter Island

Easter Island lies in the Southeast Pacific, approximately 3800 km off the Chilean coast and is known for its stone sculptures, the so-called Moai. There are about 900 Moai on the island, most of which are made of lapilli tuff. They were sculpted in the period between the 10th and the 16th century and, since 1995, are enlisted as a UNESCO World Heritage Site. Their cultish significance has faded from collective memory. However, scientific research leads to the conclusion that they formed an integral part of the cult of ancestors. They were most likely knocked over in the 18th century, when rivaling tribes on the island engaged in altercations. Many of the stone sculptures are damaged and lie facedown.



Fig. 1: Monumental stone sculpture: Moai on the Easter Island, Rano Raraku quarry.

2. Object of research

The volcanic island is made up entirely of volcanic rocks. It comprises three principal volcanoes and over 70 subsidiary eruptive centers. Each of the main volcanoes has a different structure - Poike, to the east, is a simple strato-volcano; Rano Kau, to the southwest, has a well-developed central caldera; Terevaka, to the north, is a complex fissure volcano. The volcanic rocks on Easter Island belong to the alkaline suite and have a wide petrographical and geochemical range, from basalt to trachyte and tuff.

Almost all of the Moai stone sculpture which are presently found on the Island were carved from the Rano Raraku lapilli tuff. Most of them were built by using a Tuff outcropping in the southern part of the Rano Raraku volcano, where ancient quarries are still visible. From the volcano, hundreds of Moai were obtained and erected on the Island. Also, the object of this research: Moai of Ahu Hanua Nua Mea was carved quite likely from Rano Raraku lapilli tuff.



Fig. 2: 3D point cloud: Moai of Ahu Hanua Nua Mea lies facedown, with surroundings.

2.1. Material used for the Moai

The material used for the Moai may be described as a stratified tuff, with very frequent variations in grain size within the single layers. It is made up of a yellowish-brownish pumiceous and ashy matrix with embedded lapilli, scoriae, pumices and black lava fragments of a size ranging from a few mm to several cm. The tuff coherence varies from level to level, but generally it is not very strong: frequently, just by manual pressure, pulverisation or fragment detachment occurs on the surfaces. Weakness is particularly evident on the junction plane of different-grain-sized levels. The overall colours varies from light brown to yellowish with greenish shades.

2.1.1. Stone deterioration

Since 1956, several Moai have been re-erected and detailed research has been done by specialists as pertains to morphology and deterioration mechanisms. The first research concerning the morphology and the nature of the damage of the rocks, was done at the request of UNESCO in 1973 by Hyvert and in 1981 by Domasłowski.

The main damage phenomenon was rainfall followed by wind erosion, biological growth mainly due to lichens and algae and salt decay connected with marine spray. These deterioration mechanisms were confirmed in 1988 by Charola and Lazzarini, adding a further factor: the effects of temperature changes on the surface of tuff. When the surface of the Moai is overheated by the sun, and then cooled down by a sudden shower, the rock undergoes thermal fatigue, which produces superficial scaling and exfoliation over time. They are all influenced by the mode of cutting of the Moai from the tuff beds. Those cut along the strata are better preserved than those cut at an angle or perpendicularly. The Moai

carved out of finer-grained pyroclastics are generally better preserved than those with coarse to medium grain size lapilli and other components.

As pertains to the Moai of Ahu Hanua Nua Mea which is the object of this research, its scaling is neither vertical nor horizontal but rather diagonal through the stone sculpture. The grain size varies widely, ranging from coarse to fine.

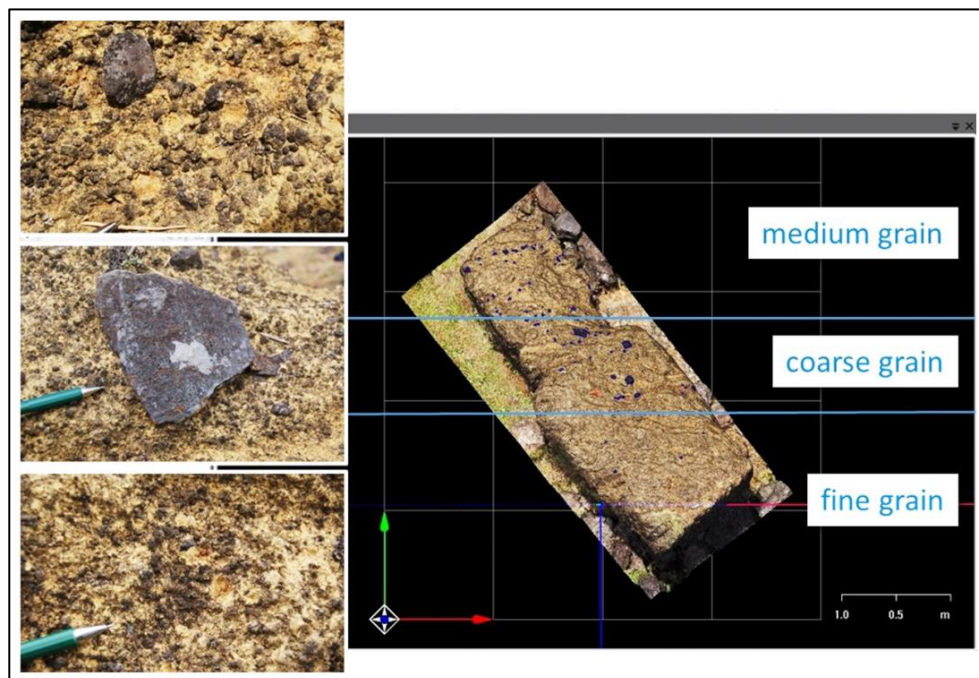


Fig. 3: Differences in the composition of the individual layers

2.1.2. Stone deterioration of Moai from Ahu Hanua Nua Mea

The weathering of stone sculptures means the long-term loss of cultural heritage. When mapping the damage, the terminology from the ICOMOS (International Scientific Committee for Stone) - ISCS glossary was used in order to prevent misunderstandings concerning the interpretation of damage and to build the basis for a scientific discussion.

The visible main damage of the stone sculpture Moai of Ahu Hanua Nua Mea:

- *Differential erosion.* As a result, the stone deteriorates irregularly. This feature is found on heterogeneous stones containing harder and less porous zones.
- *Detachment – Bursting.* Local loss of the stone surface from internal pressure usually manifesting in the form of an irregularly sided crater.
- *Encrustation.* Compact, hard, mineral outer layer adhering to the stone. Encrustations are frequently depositions of materials mobilized by water percolation and thus coming from the object itself. Carbonates, sulphates, metallic oxides and silica are frequently found.

- *Crack*. Individual fissure, clearly visible by the naked eye, resulting from separation of one part from another. Fracturing of a stone along planes of weakness.
- *Biological colonization – Lichen*. Colonization of the stone by micro-organisms. Lichen is a common feature on outdoor stone and is generally best developed under clean air.
- *Soiling*. Deposit of a very thin layer of exogenous particles giving a dirty appearance to the stone surface. With increasing adhesion and cohesion, soiling can transform into a crust.

2.2. *Non-destructive method for damage diagnosis*

Stone sculptures, like the Moai, are an important part of our cultural heritage. While doing research on the Easter Island, it was important to choose a method of diagnosing the damage of the sculptures that would not, itself, damage the sculptures further. As is widely known, the damage mapping method is a good method for documenting the current condition of the stone and to thus make later changes visible. In this case, the acquisition of the data concerning the weathering damage to the lapilli tuffs was a suitable possibility to do long-term research and to control the change processes of the stone sculpture.

2.2.1. *Non-destructive damage documentation on the Moai stone sculpture*

The damage mapping of this particular Moai statue lasted from 2012 until 2015. This long term method allows scientists to see even the changes on the sculpture. Until now it has been common method use 2D mapping. Using this method, damages of the object are entered into the image processing software manually. The biggest problem is that information has to be transferred from a 3D object onto a 2D image.

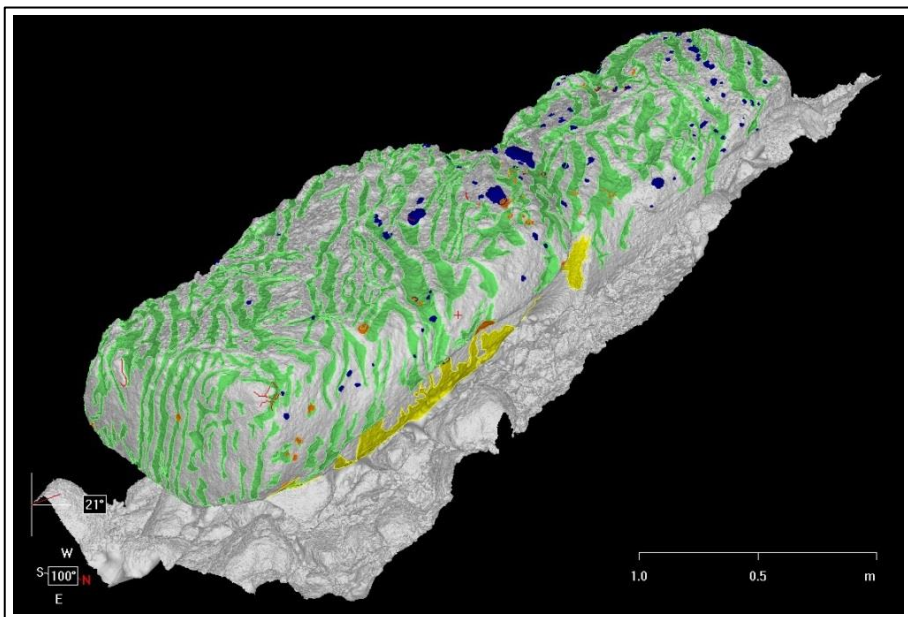


Fig. 4: 3D monument damage mapping. Surface of object is rendered shaded.

2.2.2. 3D model of the Moai of Ahu Hanua Nua

In 2015 we decided to create a 3D model of the Moai of Ahu Hanua Nua Mea and to map damage on this model. We used the software aSPECT3D. With this program it is possible to generate 3D models from digital image sequences, which can be recorded using commercially available digital cameras. We used Olympus OM-D E-M1. The model was very precise and of high graphic quality so that it was possible to transfer the damage directly onto the model.

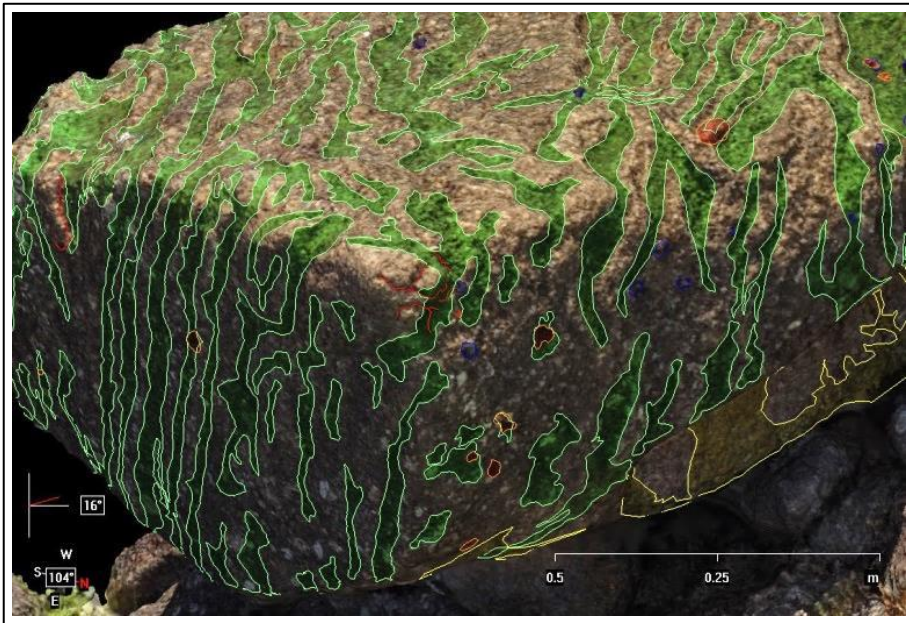


Fig. 5: 3D monument damage mapping detail: Differential erosion and cracks.

2.2.3. 3D model of a late baroque tombstone

The advantage of 3D-mapping are now going to be presented by example of another object. The object is a late baroque tombstone (ca. 1725 AD, Wolkenburger quarry) which is now located in the restoration atelier of the University of Applied Sciences in Cologne.

Despite the relatively flat, relief-like nature of the tombstone, using the classical 2D-mapping would render difficult any precise damage mapping. Especially the location of the damage on the Christ figure and on the sides are often not accurately definable in 2D-mapping. In most cases it is the appraisal of the different recorded damage from all angles that allows for a correct interpretation.

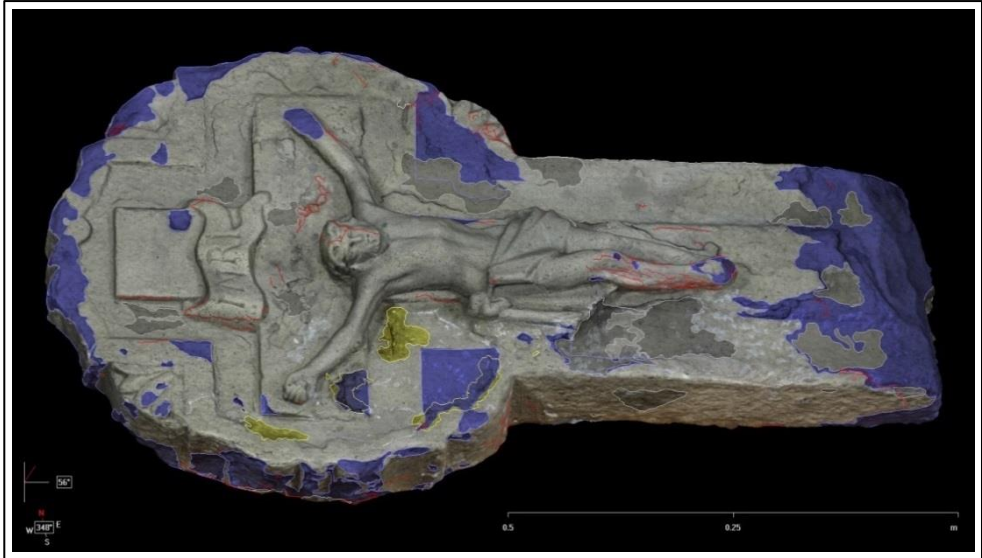


Fig. 6: 3D monument damage mapping of late baroque tombstone: All recorded damage.



Fig. 7: 3D monument damage mapping of late baroque tombstone: Detail.

2.3. Advantage of 3D-damage mapping

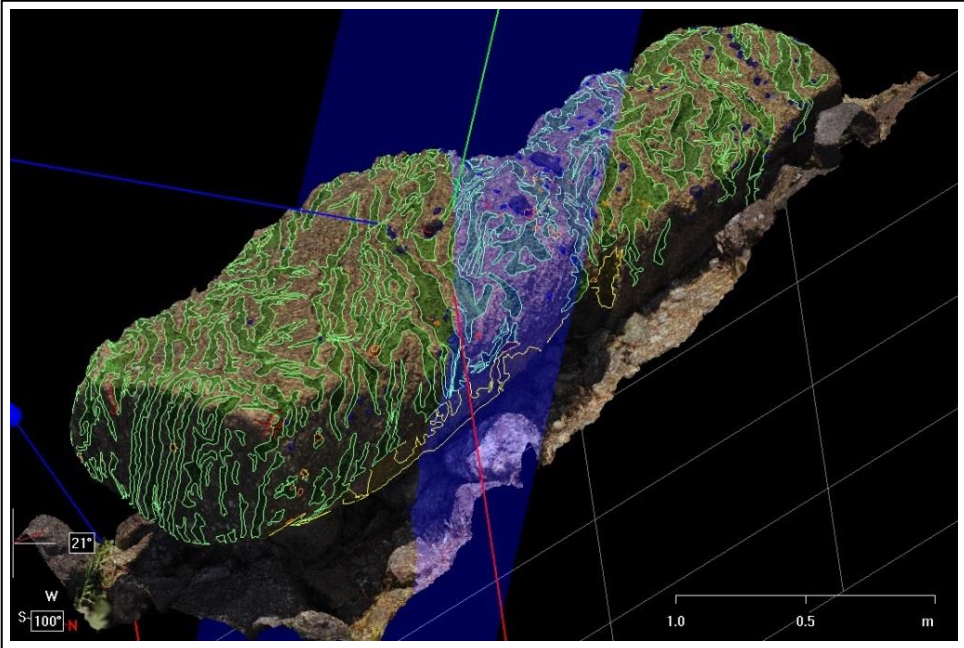


Fig. 8: 3D monument damage mapping: differences in the composition of the individual layers

The advantages of this new system for 3D-damage mapping are:

- The entire surface of the sculpture is visible. With 2D mapping, certain zones can be distorted.

In the case of the Moai of Ahu Hanua Nua Mea:

- one can see the course of the water damage very clearly.
- The damage mechanism such as differential erosion can be precisely documented.
- Damage on the surface of the Moai can be calculated. The differential erosion affected area is 2-5 square meters, which accounts for about 25% of the total registered area.
- The exact dimensions of the object can be registered without distortion. The exact height of the Moai is 3.34 m.
- The different layers with the varying composition of rocks can be easily discerned.
- The inclination of the base of the stone sculpture is visible.

3D monument damage mapping has the advantage that damage can be traced a lot more precisely than with conventional 2D mapping, especially as pertains to 3D objects. Hence, a diagnosis that rests upon 3D damage mapping is of much higher quality. Another recommendation for damage free long-term documentation in the case of the Moai is 3D photo monitoring.

References

- Domasłowski, W., 1981, Les statues en pierre de l'Île de Pâques. UNESCO, Paris, 54pp.
- Fitzner, B., Heinrichs, K., 2005, Kartierung und Bewertung von Verwitterungsschäden an Natursteinbauwerken. [Mapping and evaluation of weathering damage on stone monuments] – Z. dt. Ges. Geowiss., Schweizerbart'sche Verlagsbuchhandlung, Stuttgart, 7-24.
- Internationalen Rat für Denkmalpflege (ICOMOS) (eds.), 2011, Illustrated glossary on Stone deterioration patterns /Illustriertes Glossar der Verwitterungsformen von Naturstein, Imhof, Petersberg, ISBN: 978-3-86568-667-1, 80pp.
- Kersten, Th., Lindstaedt, M., Vogt, B., 2009, Preserve the Past for the Future - Terrestrial Laser Scanning for the Documentation and Deformation Analysis of Easter Island's Moai, Proceedings of the International Archives of the Photogrammetry, Remote Sensing and Spatial Information Sciences. Vol. XXXVII. Part B5. Beijing, 271-277.
- Kozub, B., Kozub, P., 2015, 3D photo monitoring of tuff surface alterations of the moai of Ahu Hanua Nua Mea, 9th International Conference on Easter Island and the Pacific (EIPC 2015) CULTURAL AND ENVIRONMENTAL DYNAMICS. Ethnological Museum Dahlem, Berlin, article in press.
- Kozub, B., 2014, Konservatorische Erhaltung von Objekten mit Mahnfunktion. Über ein internationales Online-Projekt, in International Council of Museums (ICOM, Internationaler Museumsrat Deutschland) (eds.), Zur Ethik des Bewahrens: Konzepte, Praxis, Perspektiven, Tagungsband zur Jahrestagung von ICOM Deutschland 2013, ICOM Deutschland – Beiträge zur Museologie 4, Berlin, ISBN 978-3-00-045736-4. 69-74.
- Kozub, B., 2011, Konservierung und Restaurierung von „negativem Kulturgut“, scripvaz-Verlag, Schöneiche bei Berlin, ISBN 978-3-931278-58-8. 167pp.
- Kozub, P., 2006, Anwendung von 3D-Modellen für die Visualisierung der tomographischen Ultraschallmessungen am Beispiel der Königinnenstatue aus Tell Basta, in Tell Basta, Archäologie in Ägypten. Ein Forschungsüberblick über die Grabung bis 2005, Tietze Chr. (eds.), DVD. Potsdam, Universität Potsdam.
- Lazzarini, L., Lombardi, G., Marconi, F., Meucci, C., 1996, New data on the characterization and conservation of the easter island's pyroclastics used for the moais, in Proceedings of the 8th International Congress on Deterioration and Conservation of Stone, Riederer, J. (eds.), Berlin, 1147-1158.
- Schaich, M., 2012, Mit digitalen Fotoserien zum 3-D-Modell. Anwendungsmöglichkeiten einer Software, in RESTAURO / Zeitschrift für Kunsttechniken, Restaurierung und Museumsfragen 5, Callway, München, 26-30.
- Seipt, H., Simon, S., Kozub, P., 2008, Ultrasonic Tomography - Correlation of Ultrasonic Velocity with Strength Parameters and Exemplary Application on Historical Stone Objects using Virtual 3D-Models, Proceedings of the 11th International Congress on Deterioration and Conservation of Stone, Łukaszewicz J.W., Niemcewicz P. (eds.), Toruń, Nicolaus Copernicus University Press, 505-512.

This page has been left intentionally blank.

EMERGING DIGITISATION TRENDS IN STONEMASONRY PRACTICE

S. McGibbon¹ and M. Abdel-Wahab^{1*}

Abstract

Stone forms a major component of Scotland's pre-1919 building stock. Current governmental policy and conservation guidelines stipulate that high quality repair and maintenance should be carried-out without compromising the building's historical features whilst minimising the impact on the natural environment and providing value for money. Addressing these challenges requires investment in new technologies and calls for innovative practice. Therefore, this paper examines digitisation trends in the heritage sector, which includes: Terrestrial Laser Scanning (TLS), Infra-Red Thermography (IRT), and Historic Building Information Modelling (HBIM). Such trends have the potential to revolutionise stonemasonry practice of historic buildings by providing accurate site-surveying and diagnosis of the building condition for informing the development of appropriate method statements for repairs. Moreover, these technologies can provide Quality Assurance to ensure that the repairs have been carried-out to the required standards. Raising awareness of the current digitisation trends is essential for shaping and informing curriculum development in Further Education (FE) colleges. Demonstration projects thus become paramount for showcasing the application of digital technologies in a live project environment along with its accrued benefits.

Keywords: digitisation, laser scanning, stonemasonry, repair, maintenance, skills development

1. Introduction

Scotland has over 450,000 pre-1919 building stock, and stone is an integral part of the construction of these buildings. Almost £400 million was estimated to have been spent on repair and maintenance of these buildings in 2013/14 (Historic Scotland, 2014). Yet, disrepair levels to the residential and non-residential stock of pre-1919 buildings of 90%, present a critical period for Scotland's uniquely diverse stone built heritage; (Scottish House Condition Survey, 2014; Historic Scotland, 2012). Moreover, a combination of neglect and poor practice, particularly for stonework repair, further endangers historic building stability and functionality. Particularly, the methods used for selection and application of replacement stone and mortar, which have not always resulted in the most appropriate repair being used resulting in damage to adjacent masonry (Torney et al 2014; Lott, 2013; Hughes, 2012). This is not solely a common problem for historic buildings; there is lack of understanding of building physics across the wider R&M sector (The Royal

¹ S. McGibbon and M. Abdel-Wahab*

School of Energy, Geoscience, Infrastructure and Society (EGIS), Heriot Watt University, Edinburgh, United Kingdom
m.abdel-wahab@hw.ac.uk

*corresponding author

Academy of Engineering, 2010). Yet, the Scottish Historic Environment Policy calls for appropriate material selection, methods of working and skills to retain historic character and future performance of older buildings, in line with the British Standard *70913:2013 Guide to the conservation of historic buildings*. Furthermore, government legislation requires that climate change, energy efficiency and sustainability are embedded in the R&M practice of historic buildings (Scottish Government, 2014). With the move to a low carbon economy, the up-skilling of the workforce in the use of new technologies and processes in the repair and maintenance (R&M), of historic buildings becomes essential (Abdel-Wahab and Bennadji, 2013).

The historic building R&M sector therefore has the dual-challenge of addressing current performance shortcomings as well as incorporating the sustainability agenda in existing stonemasonry practice. Research suggests that there is a perennial problem of a stonemasonry skills shortage and deficiency at both craft and professional level when it comes to R&M of historic buildings (Pye Tait, 2013). The problem is further complicated due to the substantial errors in the way that traditional buildings are treated in building standards, regulations and assessment systems (Sustainable Traditional Buildings Alliance (STBA), 2012). Recent research found that it is far more likely to observe poor quality surrounding standards of workmanship and knowledge of masonry practices and that the number of incidences of previous poor practice and neglect coupled with the challenge of hidden defects, such as loss of structural integrity had led to an increase in project budget/planning/programming and difficulty in recruitment (McGibbon and Abdel-Wahab, 2014). This becomes unsurprising when considering that stonemasonry apprenticeship training and assessment programme (TAP) at Scottish Vocational Qualification (SVQ) level 3, only covers 13% of R&M industry requirements although 20% is more a realistic figure now that sustainability has been embedded across the course however it is in generic form and not directly related to building standards.

Clearly, there is a significant gap between current training provision and industry requirements. As such, there is a need for the provision of an up to date technical handbook for the R&M of historic buildings to meet current/future quality and performance standards and thereby attempting to address the current gaps in training provision (McGibbon and Abdel-Wahab, 2014). Moreover, adopting new technologies and innovative practice to historic building R&M throughout a project lifecycle (from planning to completion), will be fundamental to repair specification to inform practice and generate viable method statements for on-site operations. Therefore, the aim of this paper is to examine the current digitisation trends in the R&M of historic buildings by showcasing exemplar projects and along with its potential impact on the training provision and practice of stonemasonry. Digitisation refers to the process of converting information into a digital format which enables capturing an accurate record of the current condition of a historic building. COTAC (2014) suggested that digitisation could enhance work prioritisation, project scheduling/programming and monitoring work progress. Digitisation technologies includes: Terrestrial Laser Scanning (TLS) and Historic Building Information Modelling (HBIM) (Fig. 1) – which are subsequently discussed.



Fig. 1: 3D Laser Scanner and Historic Building Information Modelling (HBIM).

2. Exemplars of digitisation in the Heritage sector

2.1. Terrestrial Laser Scanning (TLS)

TLS is increasingly used for surveying and digitally recording historic buildings (Chalal and Balbo, 2014) as the TLS data capture not only provides accurate representation of complex buildings and structures containing important yet irregular surfaces both externally and internally, but also the sculptural features and other intricate architectural elements which make up these unique buildings (Fig. 2). As such, TLS offers numerous possibilities such as highly accurate measured surveys, structural and condition monitoring as well as the production of 2D elevation and plan drawings in AutoCAD (Laing *et al.*, 2014).

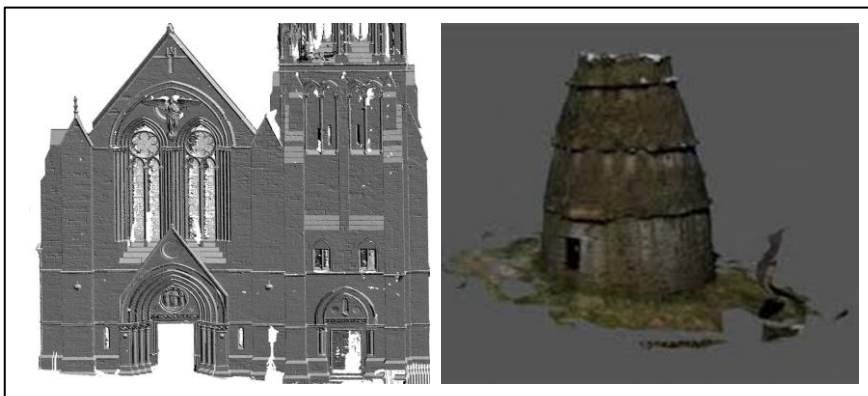


Fig. 2: TLS capture of a diverse variety of buildings.

Although, when collecting survey data, the level of detail of data required will inform the type of TLS method to be employed, as each technique provides differing levels of accuracy based on survey requirements (Smits, 2011) (Tab. 1). Yet laser scanning is not without its limitations as generating and manipulating point clouds, meshes, and models can be extremely complicated, time consuming, and can be very expensive (Scott, Laing & Hogg, 2013). Nonetheless with today's increasing pace in technological change, the use of 3D laser scanners are becoming increasingly more affordable and user-friendly, this in turn will make 3D-modelling faster, easier, and widely accessible (Sabrina and Wärmländer, 2013). For example, recent research has begun exploring the possibilities of combining a cheap line laser and a smart-phone into a fully portable laser scanning device (Kolev *et al.*, 2014) which, as long as it was capable of delivering the required level of accuracy as outlined in Tab. 1, could provide both professionals and contractors the ability to capture relevant on-site activity.

Tab. 1: Terrestrial Laser Scanner Types Source: Adapted from Smits (2011).

Laser Scanner	Accuracy @ operating range	Operating Range	Stone Element
Triangulation	0.05mm-1mm @ 0.1m - 25m	Close-range	Intricate architectural details
Terrestrial Phase Comparison	5mm @ 2-50m Mid- range	Mid-range	Façade surveying
Terrestrial Time of Flight	3-12mm @ 2-100m	Mid to long-range	General surveying

Therefore, for historic building stone conservation and repair work the uptake of this rapidly developing technology with its non-destructive nature will provide new approaches to the traditional practices of stonemasonry, particularly stone replacement and stone carving. For example, the production of highly accurate 2D section drawings of individual stones from the TLS data will allow the creation of profile templates of the decayed stonework without the need to cut into the façade. In addition, McGibbon and Abdel-Wahab, (2014) highlighted that for historic stone re-construction (recording, removing and re-positioning stones in the exact previous position) laser scanning was instrumental for visualising the required scale of maintenance (material and skill requirements) but it was not used for the development of a method statement and Quality Assurance (QA) for on-site operations. Recently, the Glasgow School of Art's Mackintosh building was laser scanned in the aftermath of a fire outbreak. A 3D plan was created of what survived after the fire, allowing stones to be marked up corresponding to the data in the plan, and the damaged wall to be deconstructed and sections of stonework laid aside for conservation. As such the 3D Models derived from the scan data will allow comparison of project specifications with as-built data as part of an objective quality assurance approach as opposed to a subjective quality check, which currently relies on the skill, knowledge and experience of both the craftsman and the professional (González *et al.*, 2010).

2.2. Historic Building Information Modelling (HBIM)

BIM is defined by international standards as “shared digital representation of physical and functional characteristics of any built object, which forms a reliable basis for decisions” (Volk *et al.*, 2014). In considering the use of BIM for historic buildings, the concept is absolutely relevant for R&M (Murphy, McGovern and Pavia 2013) (Fig. 3).

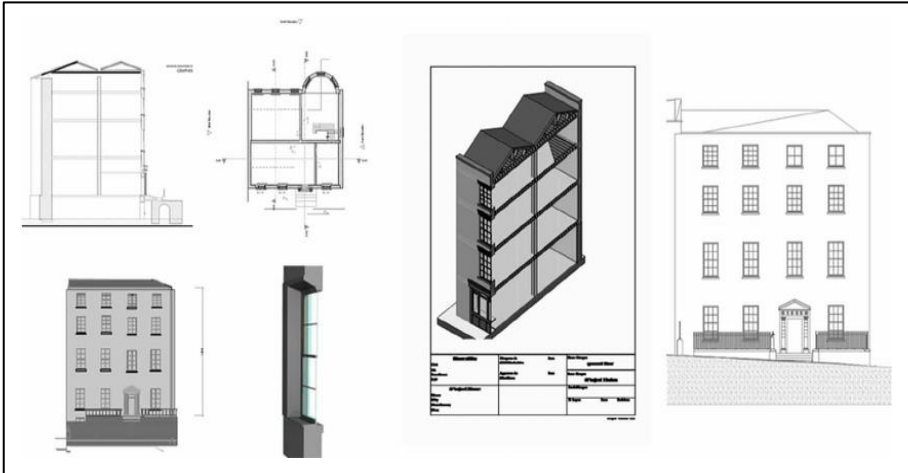


Figure 3: HBIM including automated documentation (Murphy *et al.*, 2013).

HBIM allows the metric surveying process to produce high resolution reality-based digital models capable of being linked with different historic building repair documentations (Cheng *et al.* 2015); from full engineering drawings and schedules (programme, cost, inspection, etc) including intelligence to point cloud data, such as detail behind the object’s surface concerning its methods of construction and material makeup to developing the HBIM model to simulate structural and energy behaviour for virtual analysis (Logothetis *et al.*, 2015). CyArk in collaboration with Fresenius University of Applied Sciences, Cologne and Heriot-Watt University, Edinburgh are currently 3D laser scanning Cologne Cathedral to develop highly detailed 2D and 3D BIM conservation documents as well as build a dimensionally accurate photorealistic 3D model for interpretation purposes (Fig. 4). The data will be used to analyse the structure of the Cathedral, comparing the older sections of the Cathedral with later construction. For example, the 3D model could be augmented with any historical drawings/records, if available, to generate a time-lapsed digital representation of the deterioration of the building. Not only will this provide more accurate historical record, but also it can inform the development of an effective R&M programme. While this ability to provide an even more accurate representation of the original form of the building is essential for historic building conservation work, yet the current trend in digitisation tends to be focused on documentation with virtually no application for on-site practice. In fact HBIM like TLS is absolutely relevant for on-site activity as significantly; the very detailed data collected could act as a benchmark to precisely monitor the future level of stone erosion of historic buildings elements, in particular intricate stone carved architectural details such as cornices, statues and pillars, allowing accurate diagnosis of the building condition for informing the development of

appropriate method statements, as well as QA key performance indicators such as conformance to standards, construction time and cost etc. for stonework repairs.

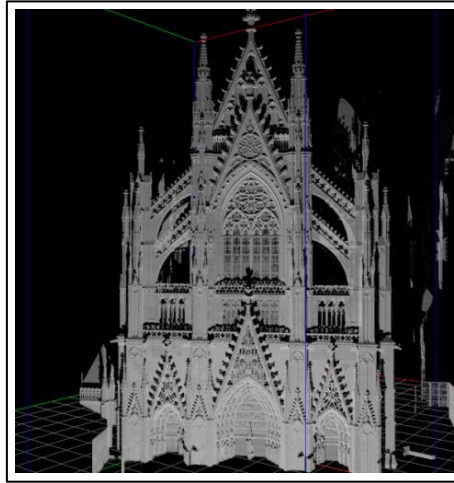


Fig. 4: 3D Laser Scanning of Cologne Cathedral (Zoller + Fröhlich, 2015).

2.3. Piloting a Digital Workflow

Currently there is no defined process available for quality stone replacement in historic buildings, unsurprising given the majority of techniques and methods used at the specification and application phases for stonemasonry are still deeply rooted in traditional practices. Moreover, stone replacement relies on a visual and subjective assessment of the stonemason resulting in inadequate performance such as inaccuracies in stone replacement measurements, excessive waste removal, and damage to stones when removing mortar as well as when on-site variations are required, in part due to inadequate use of modern power tools. Therefore, developing a holistic process for stone replacement is paramount for supporting delivering high quality R&M of historic buildings and adopting new technologies and innovative practice will be fundamental to repair specification to inform practice. As such, current research by McGibbon and Abdel-Wahab (2016) proposes the introduction of a digital workflow as a viable framework for on-site operations (Fig. 5).

The project will pilot a new process for stone replacement to historic stonework that involves the application of laser scanning as well as a demonstration of emerging digital technology adopted during the surveying, installation and in-use phase, which is low cost, off-the-shelf and user friendly. The process is disruptively innovative and seeks to change the landscape of stonework repairs in the historic building R&M sector, shifting the paradigm for the provision of high quality repair from traditionally subjective appraisals towards highly objective assessments gained from modern technology application whilst improving communication both on and off-site, not only between management and operatives but also improve the flow of information across the supply chain and its logistics.

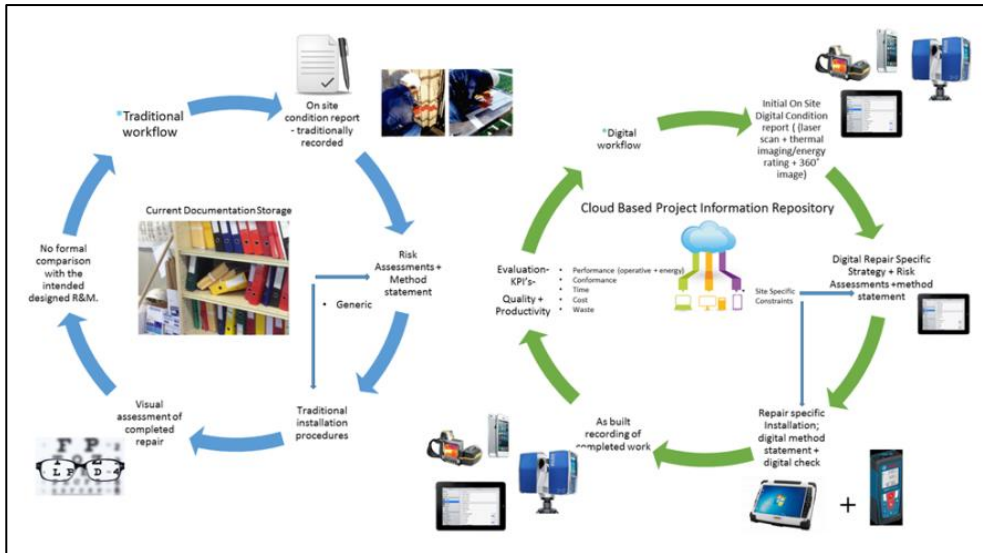


Fig. 5: Innovative Digital Workflow (McGibbon and Abdel-Wahab, 2016).

The aim of the project is to examine how historic building stonework repair can be enhanced by incorporating innovative/modern technologies (3D laser scanning; Photogrammetry; Digital documentation) into construction practice by providing an on-site tool for repair specification in historic stonework. The project will examine current difficulties in the process for stone replacement surveying, procurement and quality assurance process through the use of case studies of best practice of natural stone replacement (indenting) to answer questions such as: What do these difficulties mean for emerging technologies and processes to aid repair specification and on-site activities? What does the adoption of emerging technology mean for workforce quality, health and safety, performance and skills policy development in historic building repair and maintenance (R&M)? What types of skills development (technical, functional, management) underpin this proposed innovative process for stonemasonry practice?

It is the belief that this project has the capability to revolutionise the industry and is a fantastic opportunity for showcasing the latest innovations for stone replacement. It could lead the way for modernising practice in the R&M of historic buildings by yielding new empirical data that can contribute to the use of emerging technologies and processes to improve workforce performance by providing an on-site tool for repair specification in historic stonework, whilst developing recommendations for addressing the training needs of the workforce for appropriate use of emerging technologies for historic building R&M. as well as informing stakeholders (training providers, policy makers, funders, SMEs, etc.) on areas for skills policy development and implementation, such as quality and standards for training.

3. Conclusion

With the increasing demand for delivering high quality R&M, stonemasonry practice still faces the challenges of: poor skills, skills shortages, application of complex materials and techniques such as lime mortar, addressing climate change, energy efficiency and sustainability whilst providing value for money. For practitioners, the embracing of digitisation trends (3D laser scanning, HBIM, and IRT), and innovative practice (combining of new technologies tailored to specific project challenges), has the potential to revolutionise R&M practice of historic buildings by providing accurate site-surveying and diagnosis of the building condition for informing the development of appropriate method statements for repairs. Moreover, these technologies can provide Quality Assurance to ensure that the repairs have been carried-out to the required standards and in turn provide a level of protection for both the client and contractor vis-à-vis the defects liability period. With the unprecedented pace of technological change, FE colleges need to keep-up with modernising their curriculum and demonstrating that digitisation has its place in the industry which can only attract the digital natives – Generation Y. Digitisation in the R&M of historic buildings can enhance and promote the image of the heritage sector as being innovative, high-tech and not for underachievers (Abdel-Wahab, *et al.*, 2012). Therefore, raising awareness of the current digitisation trends is essential for shaping and informing curriculum development in FE colleges. Demonstration projects thus become instrumental for showcasing digitisation technologies in a live project environment, which will require an in-depth understanding of industry practice as well as a good understanding of the capabilities and limitations of digitisation technologies.

References

- Abdel-Wahab, MS (2012). 'Rethinking apprenticeship training in the British construction industry' *Journal of Vocational Education and Training*, vol 64, no. 2, pp. 145-154., 10.1080/13636820.2011.622450
- Abdel-Wahab, M., & Bennadji, A. (2013). Skills development for retrofitting a historic listed building in Scotland. *International Journal of Low-Carbon Technologies*, ctt043.
- Armesto-González, J., Riveiro-Rodríguez, B., González-Aguilera, D., & Rivas-Brea, M. T. (2010). Terrestrial laser scanning intensity data applied to damage detection for historical buildings. *Journal of Archaeological Science*, 37(12), 3037-3047.
- British Standards Institution (2013) BS 70913:2013 Guide to the conservation of historic buildings. *British Standards Institution*, London, UK, BSI
- Chalal, M. L., and Balbo, R. (2014) Framing Digital Tools and Techniques in Built Heritage 3D Modelling: The Problem of Level of Detail in a Simplified Environment. *International Journal of the Constructed Environment*, 4(2).
- Cheng, H. M., Yang, W. B., and Yen, Y. N. (2015). BIM applied in historical building documentation and refurbishing. *ISPRS-International Archives of the Photogrammetry, Remote Sensing and Spatial Information Sciences*, 1, 85-90.

- Conference on Training in Architectural Conservation (COTAC) (2014) Integrating Digital Technologies in Support of Historic Building Information Modelling: BIM 4 Conservation(HBIM) <http://www.cotac.org.uk/docs/COTAC-HBIM-Report-Final-A-21-April-2014-2-small.pdf>
- Heritage Innovation Preservation (HIP) Institute (2015) ABOUT“SCANPYRAMIDS” http://www.scanpyramids.org/layout/spm/press/About_ScanPyramids-en.pdf
- Historic Scotland (2012) Establishing the Need for Traditional Skills. Historic Scotland. Edinburgh
- Historic Scotland (2014) Scotland’s Historic Environment Audit (SHEA). APS Group Scotland
- Hughes J.J. (2012), RILEM TC 203-RHM: Repair mortars for historic masonry. The role of mortar in masonry: an introduction to requirements for the design of repair mortars. *Materials and Structures*, 45, pp.1287–1294.
- Kolev, K., Tanskanen, P., Speciale, P., & Pollefeys, M. (2014) Turning mobile phones into 3D scanners. In *Computer Vision and Pattern Recognition (CVPR), 2014 IEEE Conference on* (pp. 3946-3953). IEEE.
- Laing, R., Leon, M., Mahdjoubi, L. and J. Scott (2014) Integrating Rapid 3D Data Collection Techniques to Support BIM Design Decision Making, *Procedia Environmental Sciences*, 22, 120-130.
- Logothetis, S., Delinasiou, A., and Stylianidis, E. (2015). Building Information Modelling for Cultural Heritage; A review. *ISPRS Annals of Photogrammetry, Remote Sensing and Spatial Information Sciences*, 1, 177-183.
- Lott, G. (2013) The Sands of Time, Britain’s Building Sandstones, The Building Conservation Directory <http://www.buildingconservation.com/articles>
- McGibbon, S., and Abdel-Wahab, M. (2014) Skills development for stonemasonry: Two case studies of historic buildings in Scotland, *Heritage Research Showcase event* (18-19th February 2014), Surgeons’ Hall, Edinburgh, UK.
- Murphy, M., McGovern, E., & Pavia, S. (2013). Historic Building Information Modelling– Adding intelligence to laser and image based surveys of European classical architecture. *ISPRS journal of photogrammetry and remote sensing*, 76, 89-102.
- National Heritage Training Group (2007) Traditional building Skills-assessing the Need. Meeting the Challenge. Scotland. *NHTG*, London
- Pye Tait Consulting Limited, (Firm) (2013). Skills Needs Analysis 2013 Repair, Maintenance and Energy Efficiency Retrofit of Traditional (pre-1919) Buildings in England and Scotland. *English Heritage, Historic Scotland and CITB*
- Robertson, S (2005) Structural Inspection: Duntarvie Castle. Robertson *Eadie Consulting Engineers*, Edinburgh
- Sabrina, B., & Wärmländer, S. K. (2013). 3D laser scanning as a tool for Viking Age studies. *The First International Conference held at the State Hermitage Museum*; 4–6 June 2012; St. Petersburg, Russia (pp. 170-184).

- Scottish Government (2014) Historic Environment (Amendment) (Scotland) Act 2014
<http://www.legislation.gov.uk/asp/2014/19/contents/enacted>
- Scottish House Condition Survey (2013) Key Findings.
www.scotland.gov.uk/Publications/2011/11/23172215/7 accessed 20/06/2015
- Smits, J. (2011) Application of 3D Terrestrial Laser Scanning to Map Building Surfaces, *Journal of Architectural Conservation*, 17:1, 81-94
- Snow, J. and Torney, C. (2015), Lime Mortars in Traditional Buildings, Short Guide. Edinburgh: Historic Scotland.
- Sustainable Traditional Buildings Alliance (STBA) (2012) Responsible Retrofit of Traditional Buildings
http://www.sdfoundation.org.uk/downloads/RESPONSIBLERETROFIT_FINAL_20_SEPT_2012.pdf
- The Royal Academy of Engineering (2010) Engineering a low carbon built environment the discipline of Building Engineering Physics. *The Royal Academy of Engineering, London*
- Torney, C, Forster, A.M, Szadurski, E.M. (2014), "Specialist 'restoration mortars' for stone elements: a comparison of the physical properties of two stone repair materials ", *Heritage Science* 2014, 2:1
- Volk, R., Stengel, J., & Schultmann, F. (2014). Building Information Modeling (BIM) for existing buildings—Literature review and future needs. *Automation in Construction*, 38, 109-127.
- Zoller & Fröhlich (2015) How we build reality; Student project "3Dom"
http://www.zflaser.com/fileadmin/editor/Press_Releases/3Dom_press_release_en.

DIGITALISATION AND DOCUMENTATION OF STONE DETERIORATION, USING CLOSE-RANGE DIGITAL PHOTOGRAMMETRY

M.Á. Soto-Zamora¹, R.A. López-Doncel², G. Araiza-Garaygordobil¹ and I.E. Vizcaino-Hernández³

Abstract

The digitalisation of the deterioration in stone elements is a complex problem due mainly to the difficulty in accurate geometrical definition of the volumetric losses of the studied element. Despite the existence of methodologies for geometrical documentation and digitalisation of the deterioration of stone in the market, such as laser scanners, these methodologies have a limited application, especially in developing countries, where the cost of the required equipment as well as the training for application, precludes the massive application of these techniques. Because of this, it was decided to evaluate the application of a very economical and easy-to-apply technique, close-range digital photogrammetry; this technique consists in taking photographs from different angles of the object to be modelled, and by applying photogrammetry software, a model is constructed. This model represents a good precision in the representation of the geometry, colour and textures of the modelling object. This paper presents the results of the evaluation of the photogrammetric method in the geometric modelling of stone specimens damaged artificially. The volumetric loss of the specimens for each cycle of degradation was evaluated by comparing the results of the volume calculated with photogrammetric method and the volume of the specimens obtained through direct measurement in laboratory testing. It has been found that the correlation between the volumes calculated and measured in the laboratory for these specimens is very good, which leads us to conclude that close-range digital photogrammetry is a very inexpensive and easy-to-apply tool for the digitalisation in the documentation of the deterioration processes in stone elements, allowing for the massification of its application.

Keywords: digitalisation, Close-Range Digital Photogrammetry (CRDP), 3D-modelling, stone deterioration

¹ M.Á. Soto-Zamora* and G. Araiza-Garaygordobil
Universidad Autónoma de Aguascalientes, México
miguelsoic86@gmail.com

² R.A. López-Doncel
Universidad Autónoma de San Luis Potosí, México

³ I.E. Vizcaino-Hernández
Instituto Tecnológico del Grullo, México

*corresponding author

1. Introduction

Close-range digital photogrammetry (CRDP) is a technique that allows one to obtain information on the geometric properties of any object through obtaining stereoscopic photographs of the objects by computer processing the characteristics of these images, minimising physical interaction with the analysed object. This technique has long been used as a technique for the three-dimensional topographic representation of certain regions of the Earth's surface and for measuring the elements in the photographs, mainly through the use of aerial or satellite photographs using stereoscopic pairs of photos by using an optical or digital stereoscope. In our days, thanks to the power of the existing computer equipment, and the enormous availability of quality cameras that have appeared, various software have the ability to overlay hundreds and even thousands of stereoscopic photographs to create high-resolution three-dimensional models. This is of great importance when very accurate representations of the dimensions and the geometrical characteristics of objects of complex geometry are required, as is the case of deterioration in architectural stone by anthropogenic or natural effects.

The main advantages of CRDP over other remote measurement methods, such as laser scanners, lie in four fundamental aspects:

- a) CRDP is an inexpensive technique since it does not require the use of specialised equipment, cameras used can be of any kind, including the ones integrated in mobile phones as long as their resolution is of good quality, preferably over 5MPX.
- b) Specialised training is not required for the implementation of the technique. Anyone who can operate a camera can gather information in the field, which makes this technique accessible to anyone with minimal training regardless of their academic or practical background.
- c) This technique allows a better control of the density of vectorial meshes, because the amount of spatial points can be defined during the process step, according to the needs of the research and computational capacity of equipment employed.
- d) The final modelled object, further contains surface colour and texture making it optimal for carrying out stone mapping, as well as the present pathologies.

The main objective of this study was to verify the applicability of the technique to record the volumetric deterioration of the stones in architecture, verifying the volume of various specimens modelled with CRDP; these results were contrasted with the results to volumetric measurements in laboratory of the same specimens using a digital scale yielding very encouraging results, for the application of this technique.

2. Methodology

The methodology consisted in obtaining stone specimens, which were subjected to degradation cycles. In each specimen and for each cycle of degradation a number of stereoscopic photographs was performed; with these photographs, a photogrammetric model was generated; also, the volume of the specimen was measured in the laboratory by implementing a digital balance.

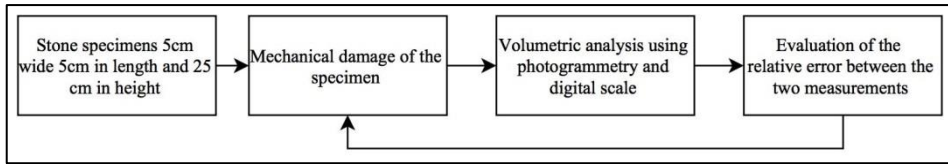


Fig. 1: Flowchart demonstrating the cycles of deterioration, modelling and measurement.

These flowcharts illustrate the methodological process that is followed in order to evaluate CRDP to the deterioration of the stone. The first (Fig. 1) represents the general cycle for the experimental campaign presented in this paper; the second (Fig. 2) one shows the detailed process for obtaining the relative error in the calculated volumes using both methods.

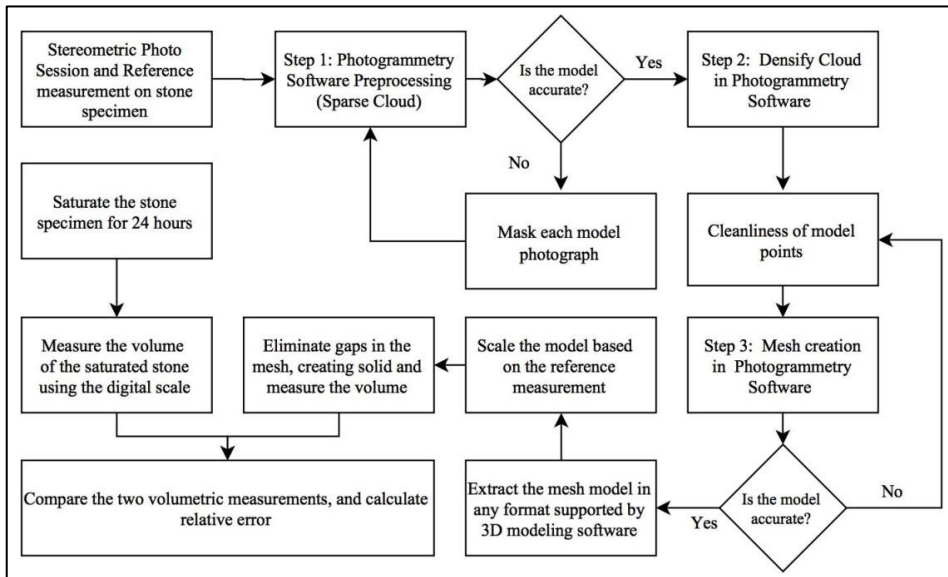


Fig. 2: Flowchart demonstrating the volumetric measurement processes for each deteriorating cycle.

2.1. Materials and Equipment

2.1.1. Stone specimens

To perform the experimental campaign, four specimens, including three natural stone specimens 5cm wide, 5cm long and 15 cm in height, were prepared. For each specimen, natural stone of a specific colour and texture was used in order to evaluate the effect of these characteristics on the quality of the generated models with CRDP. Stone 'A' - Black to grayish pyroclastic igneous rock with a porphyritic to serial texture made of non collapsed black pumice fragments, white pumice fragments, lithics and phenocrystals of sanidine, quartz and plagioclase. The matrix has a glassy texture. The ratio between components and matrix is (65%-35%). This rock is locally called Cantera Negra (Black Tuff) from Escolasticas (Querétaro) and is classified after Fisher (1966) as Lapilli tuff /

Tuff breccia. Stone 'B' - Pink to reddish pyroclastic igneous rock with a porphyritic texture composed out of lithic fragments, fiammes, collapsed pumice and quartz and sanidine phenocrystals hosted on a microcrystalline, devitrified reddish matrix with eutaxitic texture. Contains about 40% of components and 60% matrix. This rock is locally called as Cantera Melón from Galindo, (Querétaro) and it is classified after Fisher (1966) as Lapilli tuff. Stone 'C' - Gray to pale-gray pyroclastic igneous rock with a porphyritic-seriate texture composed out of lithic fragments, few fiammes, non-collapsed pumice, quartz, alkali feldspar and many lithic clasts (phenocrystals) embedded in a glassy / microcrystalline matrix (hypocrystalline texture). This volcanic tuff rock contains around 40% crystals and grains and 60% matrix. This tuff rock is locally called as Cantera Blanca de Huichápan (Hidalgo) and it is classified after Fisher (1966) as Lapilli tuff. The fourth specimen used was a concrete cylinder 7.5cm in diameter and 15cm in height.

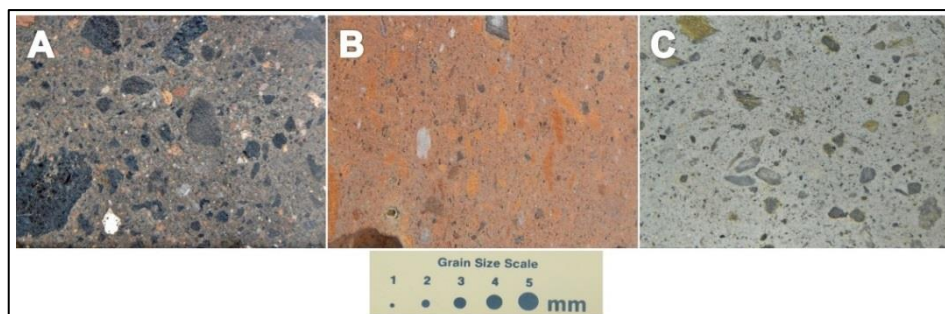


Fig. 3: Stone Specimens used in the experimental campaign.

In order to facilitate the photogrammetric process, photogrammetry markers were placed, which, thanks to its colour and distinctive patterns, can improve the detection of match points, increasing the quality of the generated models.

2.1.2. Equipment

In order to obtain the photographs of the models analysed in this investigation, the following photographic equipment was used:

- a) Nikon COOLPIX® L820 Digital Camera 16.0 million Effective pixels Image sensor 1/2.3-in. type CMOS.

An assembled computer was used to perform the process; this computer has the following hardware:

- b) AMD FX 8-Core Black Edition FX-8350, S-AM3+, 4.00GHz, 8MB L2 cache
- c) RAM Memory Kingston HyperX Savage DDR3, 2400MHz, 32GB (4 x 8GB)
- d) Graphic Nvidia MSI GeForce GTX 970 Gaming 4 GB
- e) Motherboard ASUS Crosshair V Formula-Z AM3
- f) Ventilation Corsair Cooling Hydro Series H80i + 6 Air Ventilators

For determining the volume of the specimens in laboratory:

- g) Digital scale with capacity of 1000 g and precision $e = 0.1$ g

2.1.3. Software

The photogrammetric process was carried out using a Student Version License Software Agisoft PhotoScan® a stand-alone software product that performs photogrammetric

processing of digital images and generates 3D spatial data to be used in cultural heritage documentation as well as for indirect measurements of objects of various scales. The 3D rendering and volume calculation was performed using SketchUp Pro 2015 Teacher Version®.

2.2. Techniques and Procedures

2.2.1. Stone Deterioration

In the early stages of this project, we considered using a technique of artificial damage based on salts, specifically Magnesium Sulphate ($MgSO_4$); however, once the degradation cycles were initiated, it became clear that for the stones most resistant to chemical weathering, the volumetric changes between one cycle and another were less than 0.50%, making it impossible to determine if the measured volumetric change is significant because the change is very close to the relative error of the method used. Given this situation, we decided to use random mechanical wear on the specimens, in order to generate geometries as complex as possible. Such wear was performed using metal hammers of different dimensions and progressively removing random sections of material specimens.

2.2.2. Photogrammetric Models

The application of CRDP method requires taking photographs of the object or surface to model; the number of photographs used depends on the size of the element to model, as does the distance from the camera to the object, in this case were used between 50 and 60 photographs at an approximate distance of one meter, such photographs must be taken from different angles to achieve the stereoscopic effect; in addition to this, the photographs must meet two basic conditions to be aligned in the model:

- a) The photographs must have an effective connection between them so the software can be able to detect the commonalities between these pictures and make a calculation based on the depth of the gap between them.
- b) They should cover the whole object or surface as much as possible to avoid gaps in the mesh.

After taking the photographic sequences (regardless of the equipment and instruments used), there are two options for building the model: the first is to conduct a pre-processing of the pictures by using masks, selecting only the areas of each photo that are required for the photogrammetric model, which concentrates all the connection points in defined areas, improving the quality of the generated model thanks to the densification of points made by the software; however, it is possible to generate models without the use of masks, but this reduces the quality of the generated model. Once the pre-processing of the information is done and applying one or more software, a process of four stages, which contribute to the final integration of photogrammetric model, is performed:

- a) Once the photographs of the model are selected and pre-processed, the first phase involves the orientation of photographs, a process by which the software defines a number of points (sparse cloud) in common between the photographs, by which it then calculates the position of each photo and by a digital parallax technique, calculates the depth of those points in the entire set of the scene. During this process, it is necessary to define a reference measurement whereby we may scale

- the photogrammetric model; the measure must be easily recognisable between two points in the mesh, to facilitate the modelling. If during this stage of modelling, the model has deficiencies, such as discontinuities, incorrect overlaps, or not modelled faces, the photographic sequence must be repeated to increase the number of photographs and the overlap between them.
- b) The second process consists of densifying the dispersed cloud of points, adding points interpolated between points already detected in the first procedure; each of these points possesses information concerning both its spatial position and a defined colour according to the pictures that have been obtained. After completing this process, it is quite possible to faithfully observe the model with all of its elements as a dense cloud of points. During this stage, it is possible to eliminate the points that should not be interpolated to create the mesh, this in order to clean the model of all points not required for the modelling.
 - c) The third stage creates the mesh of the model. At this stage, a series of triangles defined by the points of the dense or sparse cloud, are generated leading to a triangle mesh. Usually, as the mesh density is defined by the density of the cloud of points to be used, it is necessary to limit the number of mesh elements created in order to avoid creating too heavy a model.
 - d) Generally, the mesh created by photogrammetry software presents gaps and has no defined scale, so it is essential to import them into software that repairs the mesh errors and scales the model according to the reference measurement initially obtained. After this is done, convert the mesh into a solid bounded by a closed surface which can be measured in order to obtain the volume. Almost any three-dimensional modelling software has these characteristics; however, it is important to consider that given the number of polygons of the mesh generated by the photogrammetry process, a computer system with high capacity and speed is required for the processing.

The laboratory measurement of the volumes of specimens for each cycle of degradation was performed using a digital scale weighing each of these specimens "in the air", and then the specimen gained weight while the specimen was immersed in double distilled water. For each measurement cycle, the water temperature for the determination of density was recorded; given the purity of the water, no variations were considered in the density of water due to dissolved solids. The formula used to calculate the volume was as follows:

$$V_{Lab} = \frac{W_a - W_s}{\rho_{w^{\circ}C}} \quad (Eq. 1)$$

where V_{Lab} is the volume of the specimen measured in laboratory, W_a is the weight of the specimen in the air, W_s is the weight of the specimen submerged in water and $\rho_{w^{\circ}C}$ is the density of the water for a certain temperature (West 1989).

3. Results

Tab. 1 shows the results of the volumetric measurements performed in the laboratory and from the CRDP model, the initial state (Cycle 0) and two cycles of mechanical wear is shown. The relative error was calculated as follows:

$$E_r\% = \frac{|V_{Lab} - V_{CRDP}|}{V_{Lab}} * 100 \quad (Eq. 2)$$

where V_{Lab} is the volume of the specimen measured in laboratory and V_{CRDP} is the volume of the specimen measured in the 3D modelling software.

Tab. 1: Summary of results in measurement of the volumes by both methods.

Specimen	Measurement Methodology	Degradation Cycle		
		Cycle 0	Cycle 1	Cycle 2
Stone A	V_{Lab} (dm ³)	0.3784	0.3555	0.2132
	V_{CRDP} (dm ³)	0.3824	0.3519	0.2177
	$E_r\%$	1.0571 %	1.0127%	2.1107%
Stone B	V_{Lab} (dm ³)	0.3957	0.2028	0.1666
	V_{CRDP} (dm ³)	0.3942	0.2011	0.1659
	$E_r\%$	0.3791%	0.8383%	0.4202%
Stone C	V_{Lab} (dm ³)	0.3968	0.3735	0.3328
	V_{CRDP} (dm ³)	0.3934	0.3730	0.3339
	$E_r\%$	0.8569%	0.1339%	0.3305%
Concrete A	V_{Lab} (dm ³)	0.6510	0.5880	0.5070
	V_{CRDP} (dm ³)	0.6490	0.5870	0.5020
	$E_r\%$	0.3070%	0.1700%	0.9860%

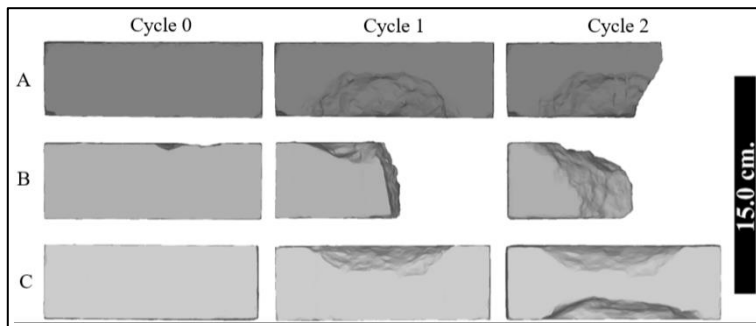


Fig. 4: Models of the stages of deterioration of the stone specimens.

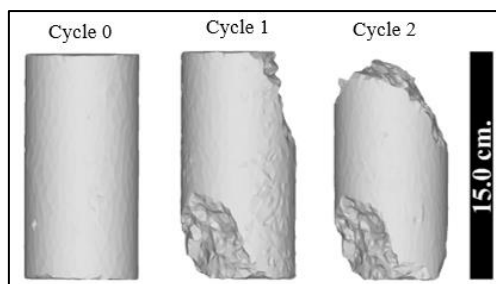


Fig. 5: Models of the stages of deterioration of the concrete cylinder.

4. Conclusions

The implementation of the CRDP method for the Measuring and registering of the deterioration of stone and architectural elements built from these is widely recommended, especially for its low cost, high precision and little training required for its implementation in the field. This allows almost anyone with minimal training to gather information in the field, after which the information is properly processed by specialised 3D modelling staff, allowing one to obtain models of high precision using everyday equipment like common photo cameras and even those present in modern mobile phones. In most of the cases analysed, the relative error generated by the modelling was less than 2.2%, which justifies the conclusion that the method is accurate enough to model the mechanical wear caused by natural or anthropogenic factors. However, these levels of precision are not sufficient for the documentation of chemical weathering, as this occurs in a very long time and therefore the volumetric losses (in most cases) are too small to distinguish from the probable error of the method. Likewise, there is no evidence that the colour of the specimen material affects the precision of the CRDP method, but it is preferable to work with objects that have distinctive elements, which allow the photogrammetry software to align and calculate the depth of the elements on the scene; however, if the element to model does not possess these characteristics, one can apply photogrammetric markers that serve as points of alignment between photographs. The time required for the implementation of this method represents a significant advance compared to other methods, mainly in the field information recording and generation of meshes for geometric modelling, but the demands of the software make it necessary to have a computational equipment with high RAM capacity and processor speed.

References

- Fisher, R.V. 1966, Rocks composed of volcanic fragments. In: *Earth Sci. Rev.*, 1: 287- 298; Amsterdam.
- West, R.C., 1989, *CRC Handbook of Chemistry and Physics 69TH Edition*, CRC Press, Inc., 978-0849304699, F4.

RECORDING, MONITORING AND MANAGING THE CONSERVATION OF HISTORIC SITES: A NEW APPLICATION FOR BGS SIGMA

E.A. Tracey^{1*}, N. Smith¹ and K. Lawrie¹

Abstract

Historic Environment Scotland (HES), a non-departmental public body of the Scottish Government charged with safeguarding the nation's historic environment, is directly responsible for 335 sites of national significance, most of which are built from stone. Similar to other heritage organisations, HES needs a system that can store and present conservation and maintenance information for historic sites; ideally, the same system could be used to plan effective programmes of maintenance and repair. To meet this need, the British Geological Survey (BGS) has worked with HES to develop an integrated digital site assessment system that provides a refined survey process for stone-built (and other) historic sites. Based on the BGS System for Integrated Geoscience Mapping (BGS•SIGMA)—an integrated workflow underpinned by a geo-spatial platform for data capture and interpretation—the system is built on top of ESRI's ArcGIS software, and underpinned by a relational database. Users can populate custom-built data entry forms to record maintenance issues and repair specifications for architectural elements ranging from individual blocks of stone to entire building elevations. Photographs, sketches, and digital documents can be linked to architectural elements to enhance the usability of the data. Predetermined data fields and supporting dictionaries constrain the input parameters to ensure a high degree of consistency and facilitate data extraction and querying. Presenting the data within a GIS provides a versatile planning tool for scheduling works, specifying materials, identifying skills needed for repairs, and allocating resources. The overall condition of a site can be monitored accurately over time by repeating the survey at regular intervals (e.g. every 5 years). Other datasets can be linked to the database and other geospatially referenced datasets can be superimposed in GIS, adding considerably to the scope and utility of the system. The system can be applied to any geospatially referenced object in a wide range of situations thus providing many potential applications in conservation, archaeology and related fields.

Keywords: heritage management, conservation, maintenance and repair,
geospatial data capture

1. Introduction

Many heritage organisations are responsible for conserving and maintaining historic built sites. In Scotland, under the “Historic Environment Scotland Act” (2014), Historic

¹ E.A. Tracey*, N. Smith and K. Lawrie
British Geological Survey, United Kingdom
emiace@bgs.ac.uk

*corresponding author

Environment Scotland (HES; a new non-departmental public body) was established to take over the functions of Historic Scotland and the Royal Commission on the Ancient and Historic Monuments of Scotland. Under the Act, the new organisation is required to monitor and report on the condition of properties in the care of Scottish Ministers (referred to as the ‘HES Estate’ in this paper). The HES Estate comprises 335 sites of national significance, most of which are built from stone.

Historically, HES architects undertook detailed analogue condition assessments for each historic site across the HES Estate. The aim of the condition assessment was to inform and prioritise the conservation work at individual historic sites and across the entire HES Estate. The output format was typically a Microsoft Word document. This method of data capture and delivery has made any subsequent interrogation of the data captured for individual or multiple sites extremely difficult and time consuming, both in terms of condition or conservation work done and by whom or when. Today, HES needs a system that can store and present conservation and maintenance information for historic sites; ideally, the same system could be used to make the process of recording data more efficient and more consistent, and plan effective programmes of maintenance and repair.

Property asset management systems with monitoring schemes and planning tools have been in existence for decades. However, these systems are most suitable for the management of non-historic assets and are generally based on ‘obsolescence’ (i.e. repairs and replacement based on fashion and usefulness rather than perpetuity (Historic Environment Scotland 2015)). Some heritage asset management systems do exist. For example, ‘The Museum System’ was designed for museum collections and archives management, but was not intended for use with built sites; and ‘Tribal’ was recently specified by Historic England for managing its historic estate. However, none of the available asset management systems (for heritage assets or otherwise) seem to provide a means of interrogating the data recorded at a particular site on a particular date, or comparing the data amassed over a period of time. It is also apparent that it is challenging to keep many asset management systems up to date, mainly due to complexities of data entry.

To address these issues, the British Geological Survey (BGS) has worked with HES to research and develop an integrated digital site assessment system that provides a refined survey process for stone-built (and other) historic sites. Based on the BGS System for Integrated Geoscience Mapping (BGS•SIGMA) - an integrated workflow underpinned by a geo-spatial platform for data capture and interpretation - the system is built on top of ESRI’s ArcGIS software, and is underpinned by a relational database. The system is capable of generating indicators of urgency and risk for conservation and maintenance issues across the HES Estate and is currently assisting with the preparation of a methodology for monitoring and reporting the condition of the Estate to Scottish Ministers.

2. Historic Environment Scotland SIGMA application

The System for Integrated Geoscience Mapping (BGS•SIGMA) is a digital tool that was initially developed by BGS to facilitate the collection of digital data during geological field surveys and the interpretation of this data once back in the office. BGS•SIGMA is a suite of fully customised ArcGIS tools and data entry forms that store data in a fully relational geodatabase. Within BGS it is the default toolkit for projects requiring geological data acquisition in the field. Data are currently captured using ‘ruggedized’ Panasonic Toughbooks and Toughpads. BGS•SIGMA is designed to allow a wide range of geological and other data to be captured quickly and consistently. Separate modules are tailored to different types of survey (e.g. geological mapping and borehole logging activities).

Building on the existing BGS•SIGMA toolkit, a prototype field-based site assessment system has been developed recently by BGS to store and present conservation and maintenance information for the historic sites within the HES Estate. Data capture modules specific to HES requirements are included in the prototype, which currently is referred to as ‘HES•SIGMA’. HES•SIGMA has been developed using ESRI ArcGIS 10.1 software with an underlying Microsoft Access personal geodatabase.

BGS implemented the following to develop HES•SIGMA:

1. Unique GIS layers (feature classes), attributes and dictionaries within the personal geodatabase.
2. Modifications to existing BGS•SIGMA forms and modules to facilitate HES data entry.
3. New custom forms for capturing condition survey items and associated maintenance actions data which are stored in the personal geodatabase.
4. Report output tool for exporting all recorded data.

The application module consists of a database of hierarchically arranged attribute fields, many of which are supported by dictionaries of defined terms that guide and constrain the way they can be populated. A simplified representation of the hierarchical structure of HES•SIGMA is shown in Fig.1 and screenshots of the HES•SIGMA forms with predetermined data fields and supporting dictionaries are presented in Fig.2. Further explanation of these is provided by means of the case study presented in the following section.

Capturing accurate survey data for historic sites in a concise, consistent way is made difficult due to the fact that built sites vary enormously in many ways, including their physical attributes, materials and construction history. For example, an effective data capture system needs to be able to accommodate any type of built structure (e.g. buildings, monuments, bridges, paved areas) and, for buildings alone, it needs to be able to deal with any number of façades, roof pitches and corresponding architectural elements (walling, dressings, chimneys, carvings, etc.).

The key features of HES•SIGMA are:

- Individual architectural elements are recorded as separate entities associated to individual sites (e.g. buildings) and are fully linked to the site which they belong by means of a unique identifier, GPS location and data fields with supporting ‘site hierarchy’ dictionaries.

- Predetermined data fields and supporting dictionaries guide and restrict the range of conservation and maintenance properties that can be recorded, ensuring a high degree of consistency in the dataset.
- Conservation and maintenance properties can be recorded for the different architectural elements of an individual site.
- Once the survey is complete, the recorded data can be interrogated directly in the database or visualized within a Geographic Information System (GIS).
- A report generator tool enables the data to be output in the form of tailored Microsoft Word documents, thus suiting any project requirement.

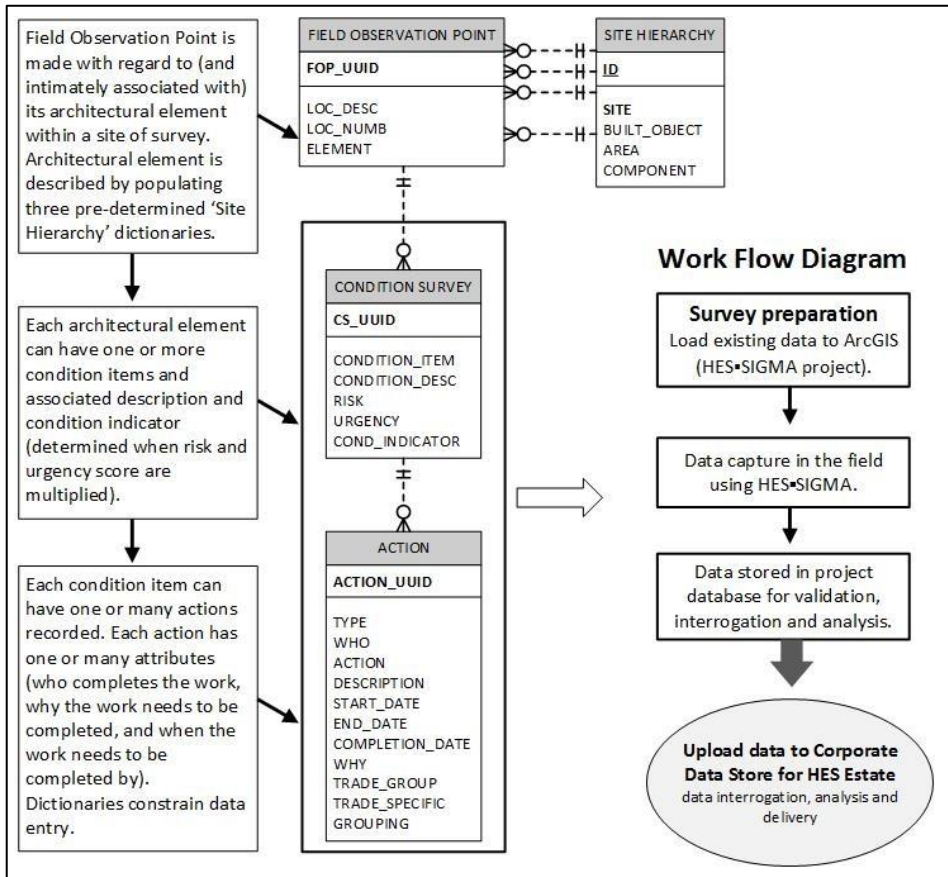


Fig. 1: 'Integrated Logical' and 'Work Flow' diagrams for HES •SIGMA. The former defines the relationship of the data elements in HES •SIGMA and their underlying structures, while the latter sets out the process of population and data delivery.

The combined database-GIS approach provides a convenient means of systematically recording, storing, updating, interrogating and displaying a wide range of spatially referenced data. In its GIS form the dataset can be presented as tabulations, statistical results, or on a map. Queries can be used to quickly select, organise and view subsets of data, or to compare and contrast different aspects of the data, thereby providing a powerful and versatile planning tool.

The digital, hierarchical method of data capture and storage has two important advantages over traditional ‘analogue’ methods: (i) the predetermined hierarchy of fields and the supporting dictionaries ensure a high degree of consistency in the dataset; (ii) data recorded for single attributes or combinations of attributes can be selected and manipulated easily, allowing statistical and/or geospatial patterns to be drawn from the data.

3. Craigmillar Castle case study

Craigmillar Castle (part of the HES Estate) provides a useful case study to demonstrate the utility and GIS output of HES•SIGMA. The castle, which now lies within the city of Edinburgh, is an early 15th century L-plan towerhouse with later extensions, curtain walls and ancillary buildings, and is constructed mainly of local stone from the Carboniferous Kinnesswood Formation. BGS has hosted workshops with future users of the new system at Craigmillar Castle to ensure the application modules fulfil the needs of HES. Data captured as part of a survey must inform and help prioritise conservation work at individual sites, and also across the whole of the HES Estate. HES•SIGMA generates a form for the user to record the condition and maintenance issues for a historic site and the actions that must be taken to remedy each issue. Once the survey is complete, it is followed by a process of interrogation and interpretation from which the user is able to plan effective programmes of maintenance and repair.

3.1. The survey

The HES•SIGMA data capture modules were designed to accommodate a wide range of historic site types (e.g. roofed and unroofed structures, standing stones, carved stones, field monuments). Prior to survey, ‘baseline data’ are collated and loaded to a HES•SIGMA project for the site. This includes any 2-dimensional data that can be used in GIS (e.g. site boundaries, plans, national topographic survey maps (past and present), aerial photographs, past survey documentation). Incorporation of baseline data allows the user to take any additional information into the field that may assist them with the survey.

For each site, observations relating to condition and maintenance issues are recorded against architectural elements and stored in the project database. Prior to recording observations, the location of the architectural element is identified by clicking on the desired position within the site polygon (in this case Craigmillar Castle) to create a new ‘field observation point’ (FOP). Once the FOP has been created, the ‘Switchboard’ form (Fig. 2a) automatically opens allowing the user to enter additional location information using ‘site hierarchy dictionaries’.

The figure displays three screenshots of the HES SIGMA software interface, arranged clockwise from left to right.

a) 'Switchboard' form: This form is used for recording detailed data within the system. It includes fields for:

- Locality No: CRMC_PRAN_18 (08/03/2016 10:)
- Easting: 328825.5677
- Northing: 670882.6643
- Built Object: Craigmillar Castle
- Area: Preston Range Interior, East Leg
- Component: Ground Storey, Kitchen
- Element Information: Element (Floor), Overall Description (Stone slabbed floor), Summary Label.
- Buttons: PRECIS, SAVE, ADD DATA (CONDITION SURVEY, OPEN 3D MODEL, PHOTO, SKETCH, SAMPLE, COMMENT).

b) 'Condition Survey' form: This form is used for recording condition and maintenance issues. It includes:

- Condition: CRMC_PRAN_18
- Condition Item: Cracked slabs
- Description of Condition: cracked and uneven slabs in NW corner of flooring - trip hazard
- Condition Indicator: Risk (3), Urgency (3), Condition Indicator (9)
- Action: WORKS
- Action Description: Replace slabs
- Action completed on: []
- Table with columns: Item, Description, Risk, Urgency, Condition Indicator, Hide.

c) 'Condition Actions' form: This form is used for recording maintenance issues. It includes:

- Action: WORKS
- Details: WHO, TRADE, WHY, INSPECT
- Dates for the Action: Start date, Finish date, Date completed
- Description: Replace slabs. Work must be done before site re-opens to visitors.
- Table with columns: Grouping, Type, Action, Who, Why, Trade Group, Trade Specific, Description.

Fig. 2: HES SIGMA forms (clockwise from left to right): a) 'Switchboard' form; b) 'Condition Survey' form; c) 'Condition Actions' form.

'Site hierarchy dictionaries' are prepared for each historic site to ensure consistency across the dataset and between users, and to provide the ability to monitor maintenance issues on the same architectural element over a period of time. This also allows for data sorting, querying and statistical analysis upon survey completion.

The 'Switchboard' form (Fig. 2a) is the primary access point for recording detailed data within the system. On this form location information and architectural element descriptions are entered; photographs, sketches and samples (e.g. stone, mortar) can be attributed to the architectural element described; and access to the more detailed data entry forms for recording condition and maintenance 'issues' is provided.

'Description', 'Risk', 'Urgency' and 'Condition Indicator' observations on condition and maintenance issues are attributed to each architectural element in the 'Condition Survey' form (Fig. 2b). More than one condition can be captured if necessary.

'Actions' can also be recorded against each observation on the 'Condition Survey' form. A dictionary of pre-defined terms constrains the actions required based on what stage in the repair process the work is in (i.e. monitor and review, develop proposals, works, obtain budget costs). The action can be further described, and a date can be assigned upon completion of the action. Details of who will complete the action, what specialist skills are required and why the action needs to be completed (e.g. routine conservation, maintenance) are entered in the 'Condition Actions' form (Fig. 2c). A timescale for inspection of works may also be attributed to the observation in this form. These data can be entered either in the field or back in the office.

HES•SIGMA has no limitation on the number of architectural elements that can be recorded or observation data that can be attributed to specific architectural elements. All entered data are displayed in a 'data grid' on the bottom of the Condition Survey form and Condition Actions form for easy viewing.

3.2. Data outputs and uses

Data entered in the field can be immediately viewed in GIS for interpretation. Once field work is complete, the captured data can be utilised in the office for site-wide interpretation, then validated and loaded to a corporate database for estate-wide analysis and data delivery. With data in the corporate database, analysis on one, many, or all historic site(s) can be undertaken. The conceptual work flow diagram for HES•SIGMA is presented in Fig. 1.

If the data are uploaded to a central database it is easy to quantify the number of observations at any given site, and identify what the risk and urgency associated with any of these observations are, what actions are required, who needs to complete the actions and within what time scale. Data gathered using HES•SIGMA provide crucial information that can be used by architects, for example, when planning work on a historic site. The data allow users to assess and plan programmes of works for a single site and across an entire estate. In GIS, users are able to use baseline data in conjunction with collected data relevant to the site to assist in data interrogation and to produce useful datasets for architects and tradesmen. Another key functionality within HES•SIGMA is the 'Report Generator' tool. This tool creates a formatted Microsoft Word document containing all entered data for a single site or multiple sites. The output can be adapted to suit project requirements.

4. Conclusion

A system that can store and present conservation and maintenance information for historic sites is being developed for Historic Environment Scotland (based on the BGS System for Integrated GeoScience Mapping [BGS•SIGMA]). The system, referred to as HES•SIGMA, allows for a wide range of attributes describing condition to be linked to individual architectural elements within single geospatially referenced sites, rapidly and consistently, in a digital, hierarchical form, in the field. The system is designed to facilitate more effective planning of programmes of maintenance and repair.

The fully relational capability of HES•SIGMA, with data fields and predetermined dictionaries, allows subsets of the data to be queried and analysed. The results can be presented in either statistical or map form in GIS, thereby providing a powerful and versatile planning tool.

This approach provides the flexibility required for surveying historic sites. The resulting datasets provide crucial information that can be used by architects for planning programmes of conservation works for single sites or entire estates. A range of expertise is needed to fully populate the module; however, the data can be presented in a user-friendly visual manner as a GIS map or in the form of a Microsoft Word document using the built-in Report Generator tool. Additionally, the spatially referenced digital data can easily be interrogated through queries and converted into statistical form due to the use of pre-determined, hierarchical fields and supporting dictionaries, which ensure a high degree of accuracy and consistency in the dataset. Other spatially referenced data can be imported into a GIS for comparison and further analysis.

HES will use this newly developed survey methodology to ensure a consistency of approach and provide a means to store and present conservation information for historic sites included in the HES Estate. The system will allow HES to plan effective programmes of maintenance and repair works, and to monitor the condition of the Estate over an extended period of time. HES•SIGMA will provide a means of reporting on the condition of the Estate to the Scottish Government and to its members. With further development, HES•SIGMA could be applied across the heritage sector as a planning and management tool for the wider historic built environment.

Acknowledgements

This paper is published with the permission of the Executive Director of the British Geological Survey (NERC).

References

- Historic Environment Scotland Act 2014, asp 19 (http://www.legislation.gov.uk/asp/2014/19/pdfs/asp_20140019_en.pdf, accessed 1 November 2015).
- Historic Environment Scotland, 2015, Condition monitoring system for properties in the care of Scottish Ministers and associated collections (<http://www.historic-scotland.gov.uk/hes-condition-monitoring-system.pdf>, accessed 1 November 2015).

CASE STUDIES

This page has been left intentionally blank.

CONDITION SURVEY OF AQUIA CREEK SANDSTONE COLUMNS FROM THE U.S. CAPITOL RE-ERECTED AT THE U.S. NATIONAL ARBORETUM

E. Aloiz^{1*}, C. Grissom², R.A. Livingston³ and A.E. Charola²

Abstract

Aquia Creek sandstone was the preeminent stone used in the architecture of early federal buildings in Washington, D.C., including the U.S. Capitol and White House. In 1826, a portico with 10-meter-high monolithic columns made of the sandstone was completed on the east front of the Capitol. In 1958, columns from the portico were put into outdoor storage and replaced with marble replicas. Thirty years later, 22 of the 24 original columns were re-erected free-standing as a “ruined classical temple” at the U.S. National Arboretum. Since then this site has become the Arboretum’s most prominent visitor attraction. Visible evidence of stone deterioration by delamination and concern about falling pieces from the columns’ Corinthian capitals led to a systematic survey of damage. Each of the columns was documented visually by a series of photographs that were stitched together. Different types of damage and past repairs were defined and mapped digitally. Nondestructive methods included sounding with a handheld tool to detect delaminations or voids. Limited areas were also scanned for delamination using passive thermal IR imaging. A major type of distress is the loss of the original smooth surface layer on the column shafts. This layer is indurated, apparently by evaporation of quarry sap, and it tends to spall, mostly from the bottom of column shafts upwards. Another type of damage is associated with the corrosion of wrought-iron rings, which were embedded into the tops of column shafts. Corrosion of the rings has led to cracking and loss of stone from astragals at the top of the column shafts. Evidence of human intervention is also apparent, including original patches, paint traces, dutchmen, and eight broken shafts that were reconstructed. Treatments to retard deterioration were tested, and consolidation was undertaken on one astragal. Recommendations were made for future stabilization.

Keywords: sandstone, delamination

1. Introduction

Many of the earliest buildings in Washington, D.C., made use of Aquia Creek sandstone, including the Bullfinch Gateposts and Gatehouses, U.S. Patent Office (now the

¹ E. Aloiz*

John Milner Associates Preservation, United States of America
emilya@jmapreservation.com

² C. Grissom and A.E. Charola

Museum Conservation Institute (MCI), Smithsonian Institution, United States of America

³ R.A. Livingston

Materials Science and Engineering Department, University of Maryland, United States of America

*corresponding author

Smithsonian Museum of American Art/National Portrait Gallery), White House and the U.S. Capitol. Twenty-two of the 24 Aquia Creek sandstone columns from the east central portico of the U.S. Capitol currently stand in the Ellipse Meadow of the U.S. National Arboretum in Washington, D.C. (Fig. 1), where the ensemble is known as the Capitol Columns. Each column is 10 meters high and composed of five blocks. A Corinthian capital was modeled after a design in Sir William Chambers' *Treatise* (1791), carved in two parts, and placed above an un-fluted, monolithic shaft finished with an astragal at top and fillet at bottom. Below the shaft is a single block composed of a circular base and rectangular plinth. A square pedestal supports each column.

Since the Capitol Columns are the Arboretum's most prominent visitor attraction, concern about falling pieces and other deterioration prompted this study of the columns, carried out on site and at the Smithsonian Museum Conservation Institute from March through September 2013. For a systematic survey of damage, each column was inspected and photographed; using AutoCAD software, conditions were mapped on photographs, which had been stitched together. To assess surface detachments and voids behind them, a combination of sounding and thermal imaging was used. Sounding was conducted on all of the lowest portions of column shafts, as well as many upper portions reachable from a lift. A large flat-head screw driver was gently glided over the surface of the stone; a tone change identified the presence of voids. Thermal imaging, conducted by Gary Johanssen of the Smithsonian's National Museum of Natural History, confirmed the location of voids using a FLIR T640 Thermal Imaging Camera. Air heats at a different rate than stone, and distinct infrared radiation of voids was revealed as columns began to heat in the morning.

2. The journey of the columns

The columns are in remarkably good condition considering their nearly 200-year exposure since quarrying on an island in Virginia and placement on the east portico of the U.S. Capitol (1826 to 1958), storage at two locations for 27 years and re-erection at the Arboretum in 1988. Evidence of repairs from their initial carving and their time on the Capitol Building can still be found on the columns. Examples include patching material found to contain white lead and paint remnants in the decorative crevices of the capitals. The columns were regularly painted white, and in 2001 a study by Blythe McCarthy and William Ginell identified 16 layers of paint on them. Gouges also remain where a railing was attached between pedestals on the Capitol building.

In 1958, the columns were removed in separate pieces from the Capitol along with the rest of the portico for replacement there with marble replicas. The shafts were lifted using two bands around their girth, revealing circular lead sheets that were installed beneath them while they were on the Capitol. Once removed, each shaft was covered with slats and stored horizontally, as documented by photographs in the archives of the Architect of the Capitol. The capitals were crated, but the pedestals and base/plinths were left exposed. Without a home or purpose, column pieces were moved multiple times. Eight shafts were broken during that time, and much of the paint was lost.



Fig. 1: Twenty-two Aquia Creek Sandstone columns from the U.S. Capitol are seen here at their present location in the National Arboretum in Washington D.C.

After many false starts, the columns were physically transferred to the Arboretum in 1984 to be erected in a classical temple plan with central fountain as envisioned by the noted English landscape architect, Russell Page (1906–1985). The installation process at the Arboretum, which required moving the columns a seventh time, involved considerable planning and diverse voices, including landscape architects, the Friends of the Arboretum non-profit organization, structural engineers, mechanical and electrical engineers, architects and multiple contractors (EDAWinc. *et al.* 1987). A concrete foundation and footer were created for each column, and all column parts were connected with stainless steel dowels epoxied into newly drilled holes. The capital tops, which had never been directly exposed to rain before, were covered with flashing, and a damp-proof metal course was installed beneath the pedestals. In addition, the columns were stripped of remaining paint, and a consolidant with a water repellent, Conservare H (comparable to Wacker H), was applied to two columns.

3. Ongoing deterioration

Aquia Creek sandstone itself has inherent vice: it is not optimal as a building stone in terms of durability, as was already recognized at the time of its selection; rather, it was chosen because it was locally available and easily worked. Aquia Creek is an arkosic sandstone formed by deposition of sediments during the Lower Cretaceous period over 100 million years ago, part of the Potomac Group (Nelson 1992, McGee and Woodruff 1992). The sediments were compacted along the Potomac River near Aquia, Virginia (Fig. 2). Major components of the sandstone include quartz, which gives the stone strength and acid resistance, and smaller amount of feldspars, which give the stone warm coloration. Small amounts of iron averaging about 1% according to XRF and ICP analyses (McCarthy and Ginell 2001, p 27) provide red coloration to the stone, appearing in the form of uniform “stains,” lines or dots. Grains are bound with secondary amorphous silica (Hockman and Kessler 1957), but the stone is considered weakly cemented.

Pervasive surface delamination was identified during the condition survey. Contour loss, where the delaminated surface has completely detached, was found on 18 of the 22 shafts during this study, mostly around the bases of the shafts, but also around shaft repairs and isolated areas higher up on the shafts. Fig. 3 shows an area of detachment, and Fig. 4 shows an example of contour loss at the base of a shaft. The detached crusts range up to 13 mm in thickness. The same type of deterioration was found on many of the pedestals,

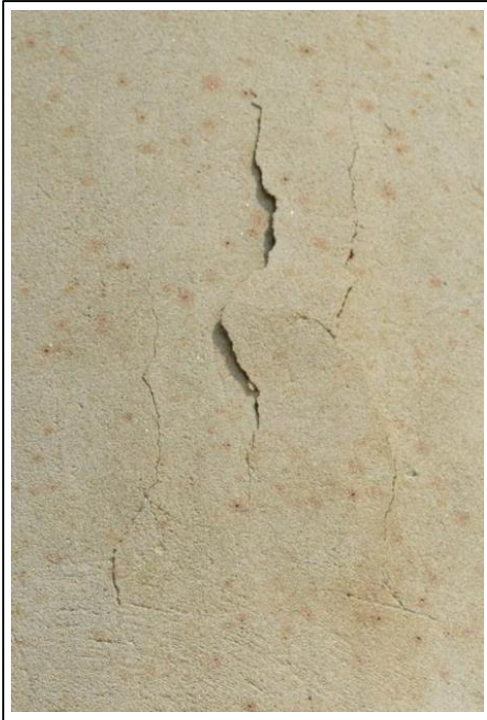


Fig. 3: A detachment on the shaft of column L20, which is has not progressed to contour loss.



Fig. 4: The lower shaft of column L20 has the highest contour loss, extending more than six feet; a detached area reaches even higher. The area of detachment can be seen on the left.

Washington D.C. has a humid, subtropical climate with multiple wet/dry and freeze/thaw cycles that would continually stress weaker areas, eventually leading to contour loss, although the exact driving mechanism remains a matter of discussion. Detachment was likely occurring early in the columns' existence while still on the U.S. Capitol or in subsequent storage, since significant contour losses were documented by the architectural firm Oehrlein and Associates just before the columns were erected in the Arboretum (EDAWinc. *et al.* 1987, A2-A7). The earliest photographs that could be obtained showing contour losses were taken by the second author in 1988: comparison to current condition suggests about 10-15% additional loss over the 25 years since then (Fig. 5 and Fig. 6).

Wrought-iron rings set in lead at the top of each shaft present a second instance of inherent vice. Since the rings are covered by the capitals, it is almost certain that they were installed at the time of original construction, although their purpose remains unclear. Corrosion of the iron has resulted in cracking or loss at 13 of the 22 astragals, as seen in Fig. 7.

Deterioration at the tops of the shafts is particularly concerning because of their height from the ground, which could harm visitors when pieces fall. Loose pieces of one astragal were removed from column L7 during the survey to prevent this from occurring. The area from

which they were taken was disaggregating; in order to strengthen the newly exposed surface, Prosoco's Conservare OH 100 was applied according to the manufacturer's specifications. The same treatment was also applied to the pieces removed from the deteriorated astragal. Comparison of thin sections made before and after treatment showed that the consolidant provides reinforcement along the tangential surfaces of the grains without substantially filling the pores.

Multiple repairs to the columns, including various patches, reattachment of broken pieces with adhesives and dutchmen, appear to have occurred through multiple phases of the columns' existence. The majority of old repairs are in stable condition. Additional deterioration can be linked to joints made during installation of the shafts at the Arboretum; the joints appear stable, but impermeable epoxy adhesive is likely causing stone at exterior edges to deteriorate and shallow mortar applied to the outside of the epoxy joint to detach.

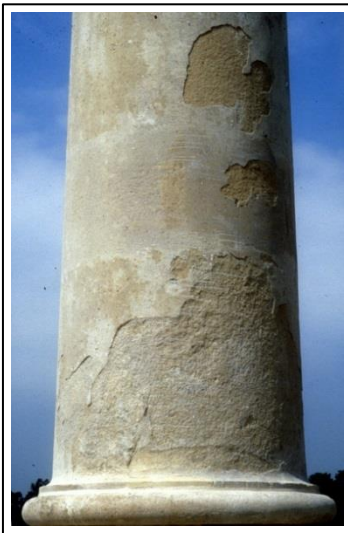


Fig. 5: Contour losses on column L5 in 1988.



Fig. 6: Same location as the previous in 2013, showing an estimated 10-15% additional contour losses after 25 years.

4. Recommended treatments

Not all damage to the columns requires immediate or any treatment. Many alterations are evidence of the long history of the columns. However, maintenance of old patches is required to prevent moisture from pooling in vulnerable areas, such as where mortar repairs are detaching at the bases of the shafts. Use of epoxy adhesive and a polyester adhesive previously employed to reattach broken fragments is not recommended, because their strength and porosity are not compatible with the stone, and durability is limited in UV light. However, where old repairs are stable and not causing damage to the surrounding stone, it is recommended that they be left in place instead of risking further damage in their removal.



Fig. 7: Detail of stone loss from L13's astragal, revealing its iron ring directly below the bottom edge of the capital.

The astragals present the most complex and difficult problems for the columns, since the lead-bedded iron rings set into the top of column shafts are covered by the capitals. The only means of completely halting deterioration would be to remove the rings. This would be nearly impossible to do without harming the stone, since the capitals are fixed to the shafts with epoxied steel dowels and mortar. In lieu of removal, a method to slow water entry is required such as flashing to top surface of the astragals.

The breakdown and redeposition of minerals on the surface of Aquia Creek sandstone is inevitable outdoors, but loss of surface crusts may be hindered. Grouting is recommended in voids behind detached crusts to reestablish adhesion and stop water from pooling. Where the crusts have already been lost, consolidation can strengthen the fragile surface. Voids were filled on two columns behind detached surface layers. Use of a pozzolanic lime-based grout is recommended as it sets with moisture and chemical reactions to form vapor-permeable solids that have properties similar to Aquia Creek sandstone. Voidspan's CG-70 was tested in four areas of detachment; a year and a half later the surfaces are still intact. Monitoring will determine the long-term effectiveness of the treatment. Applying a surface coating such as paint would not stop void formation and might even encourage it by making the surface layer less permeable. Furthermore, the application of Conservare H in 1988 does not appear to have stopped contour loss on the two columns to which it was applied, but left visible glossy streaking that is still visible today.

5. Conclusions

The case study of the twenty-two Aquia Creek sandstone columns at the National Arboretum demonstrates the complexity of stone heritage preservation. To understand the condition of the stone, its geology is an essential factor, and indeed the inherent vice of the Aquia Creek sandstone has led to delamination of indurated surface crusts; however, additional factors, such as storage, transportation and previous repairs play a role in the monument's durability. Conservation treatment is recommended on a limited basis to areas where patches have failed and in areas of water retention such as in voids behind delaminating surfaces or at top of the shafts where water can reach the iron rings. Where surface crusts have already been lost, consolidation may be a viable option to protect weakened areas newly exposed to the weather. As this popular monument adds new layers

to its already multifaceted history, the condition documentation completed during this study will be essential in determining the rate and occurrence of change.

Acknowledgements

Funding for this project was made available by the National Arboretum of the U.S. Department of Agriculture. Additional staff time and research was provided by the Smithsonian's Museum Conservation Institute (MCI# 6542). The authors would also like to thank Ramon Jordan, Nancy Luria, John Blunt and Christine Moore of the Arboretum as well as MCI staff Robert J. Koestler, Paula DePriest, Harriet F. Beaubien, Mel Wachowiak and E. Keats Webb. Norman Weiss and Irving Slavid provided valued time, expertise and their research into hydraulic lime grouts. Finally, Blythe McCarthy was generous in bringing this project to the attention of the authors as well as providing copies of all documents related to the Capitol Columns in her possession; this report is indebted to the report that she and William Ginell completed in 2001.

References

- Chambers, W., Gwilt, J., Leeds, W.H., and Hardwick, T., 1791, *A Treatise on the Decorative Part of Civil Architecture*, Lockwood, London, 167.
- EDAWinc., Cutts and Associates, Glassman LeReche and Associates, and Oehrlein and Associates, 1987 (September 1), *National Capitol Columns at the National Arboretum*, unpublished construction documents, 34 pp.
- McCarthy, B.E., and Ginell, W.S., 2001, *Deterioration of the U.S. Capitol Building Aquia Creek sandstone columns at the National Arboretum, Washington D.C.*, unpublished report, The Getty Conservation Institute, Los Angeles, 45 pp.
- Nelson, L., 1992, *White House Stone Carving: Builders and Restorers*, U.S. Government Printing Office, Washington, D.C., ISBN 9780160380143.
- McGee, E.S. and Woodruff, M.E., 1992, *Characteristics and weathering features of sandstone quoins at Fort McHenry, Baltimore Maryland*, Department of the Interior. U.S. Geological Survey, Open-File report 92-541, Washington, D.C., 10 pp.
- Hockman, A. and Kessler, D.W., January 8, 1957, *A study of the properties of the U.S. Capitol sandstone*, National Bureau of Standards Report 4998, Gaithersburg, MD, 29 pp.
- Stumm, W. and Morgan, J.L., 1981, *Aquatic Chemistry*, Wiley Interscience, New York, ISBN 9780471048312.

THE BLACK SURFACES OF THE PORTA NIGRA IN TRIER (GERMANY) AND THE QUESTION OF CLEANING

M. Auras^{1*}, H. Ettl², W. Hartleitner³ and T. Meier⁴

Abstract

Many monuments and buildings made of natural stone are or have been covered by black crusts or - more generally speaking - by black surface alterations. Various detrimental effects are reported for these black crusts and similar surface alterations and therefore in most cases the crusts are removed or are at least reduced by various cleaning techniques. However, in the case of the Porta Nigra at Trier - belonging to the UNESCO world heritage - the black surface is a characteristic feature of the entire building and thus the decision about stone cleaning is not trivial. In preparation to future conservation work it was necessary to distinguish various types of blackened surfaces and to evaluate the role of different damage processes. Preferentially non-destructive techniques, like ultrasonic Rayleigh wave propagation, or low-destructive methods such as drilling resistance measurements and microscopic studies on small samples were applied to quantify stone properties and alterations by black films and crusts. Various cleaning techniques were tested and it is shown that laser-induced cleaning of low intensity is sufficient to open the sealed surface and to allow for the successful application of a consolidant while the dark colour of the surface is only changed to a minimum extent.

Keywords: conservation of stone, black crust, cleaning, laser cleaning

1. Introduction

The Porta Nigra (Fig. 1, left) is regarded as the largest city gate from Roman times north of the Alps. It was built at the end of the 2nd century AD. The construction work stopped in the 3rd century. The gate endured for many centuries because it was transformed into a Christian church in the 11th century. At the beginning of the 19th century it was retransformed into a Roman gate and only one medieval element of the church, the Romanesque apsis attached to the eastern tower, was conserved.

The building material of the Porta Nigra is a fine-grained, muscovite-bearing sandstone of a light grey colour. Today the sandstone is called Kordeler Sandstein and stratigraphically it

¹ M. Auras*

Institut für Steinkonservierung e.V., Mainz, Germany
auras@ifs-mainz.de

² H. Ettl

Labor für Erforschung und Begutachtung umweltbedingter Gebäudeschäden, München, Germany

³ W. Hartleitner

Planungsbüro für Naturstein und Denkmalpflege, Hofheim-Rügheim, Germany

⁴ T. Meier

Institut für Geowissenschaften, Christian-Albrechts-Universität, Kiel, Germany

*corresponding author

belongs to the Upper Buntsandstein. The name Porta Nigra, meaning „The Black Gate“, is known since medieval times. It provides evidence that the darkening of the stone surface has been characteristic for the monument for very long times.

Scientific investigations on the origin of black crusts and related kinds of darkened surfaces have been carried out on many historic stone buildings. In many studies the compounds of those black crusts have been analysed and always the role of air pollution was pointed out (amongst others Honeybourne 1990, Camuffo 1996, Becker *et al.* 2005). The most important factor is the deposition of sulphur dioxide and its secondary products which finally leads to the formation and enrichment of gypsum on the surface of buildings. Those gypsum-rich crusts attracted much interest because they are obviously connected to stone damage. They are confined to building parts sheltered from direct run-off rain water. Besides gypsum, compounds of iron and other metals have been deposited from air on the surfaces of buildings. Soot, dust, particulate matter, soluble salts, microorganisms, and their decomposition products have been identified (Wilimzig *et al.* 1993, Nijland *et al.* 2003, Warscheid 2005, Brimblecombe 2011, Graue *et al.* 2013).

Besides air pollution the oxidation and mobilization of iron and manganese compounds from within the stone and their precipitation at the surface can lead to intensive blackening of sandstones (Nord & Ericson 1993, Neumann 1994, Steger & Mehnert 1998, Thomachot and Jeannette 2000). This process leads to the formation of thin black films particularly at building parts exposed to the run-off rain water.

Several detrimental processes and their complex interactions have been discussed as causes for stone deterioration by black crusts and other kinds of surface alterations. For example, the delay of drying may lead to higher moisture contents behind the crusts, the increase of strength and brittleness, the enrichment of gypsum and other soluble salts, the increased heating by insolation, the enhancement of microbiological growth, and further aspects have been considered (Camuffo 1996, Thomachot and Jeannette 2000, Charola and Ware 2002, Warscheid 2005, Snethlage and Sterflinger 2011, Sterflinger 2011).

Therefore, black crusts on stone surfaces are usually seen as detrimental to the stone and as unaesthetic to the building. In most cases they are removed or at least reduced during conservation work.

Stone cleaning is problematic in the case of the Porta Nigra because the characteristic blackening should be conserved. Thus several topics were to be investigated, before a decision is possible. Within the framework of a research project the following questions had to be answered:

- Which processes led to the blackening of the stone's surface?
- Is it possible and necessary to distinguish different kinds of black surfaces?
- Is it possible to identify the various damaging mechanisms suggested in the literature and to evaluate their damage potential for the Porta Nigra?
- Should the stones of the Porta Nigra be cleaned for reasons of preservation?

2. Methods

A precise survey and mapping of the building materials and their damage forms provided the base for a detailed classification of surface alterations associated with colour changes.

A light-optical microscope (Zeiss Axioplan) and two scanning electron microscopes (FEI ESEM Quanta 200 FEG at the Technical University Darmstadt and Zeiss DSM 960 A at the Ludwig-Maximilians-Universität München) were used for the analysis of the black surfaces and for the evaluation of cleaning tests.

The chemistry of black surfaces was examined onsite by means of portable XRF (Tracer IV-SD, Bruker) with friendly assistance by the Römisch-Germanisches Zentralmuseum Archaeological Research Institute. Based on this survey, 10 samples of black surfaces were taken and analysed by ICP-OES at Bauhaus-Universität Weimar. Organic compounds were analysed by GC/MS and HRGC/LRMS by the Gesellschaft für Umweltchemie, Munich.

Ultrasonic measurements were performed in a frequency range between 10 kHz and 300 kHz using piezoelectric broad-band transducers and receivers (Geotron Elektronik, Pirna). Rayleigh waves were recorded by measuring profiles using a coupling device with a fixed source and movable receiver. The measurements were performed without any coupling medium. Details are given by Meier *et al.* (in press).

The results of additional tests to determine capillary water adsorption, drilling resistance and thermal properties will be reported elsewhere.

Micro-sandblasting was applied for cleaning tests using slag tap granulate, calcite powder, and garnet powder as blasting materials. Cleaning tests with laser were carried out with fiber-coupled laser cleaning devices based on diode pumped solid-state lasers with 20 W or 100 W power and a duration of the laser pulses of about 100 ns (CL 20 and CL 100 devices, Clean-Lasersysteme, Herzogenrath).

3. Results

To ensure the conciseness of this publication, only aspects regarding black surfaces are reported here. Other topics, such as stone conservation require their own discussion.

3.1. Classification of discolouration, pollution, and crusts

A detailed macroscopic survey of the darkened stone surfaces of the Porta Nigra led to the following classification:

- A) Brownish discolouration due to the enrichment of Fe-(hydr-)oxides
- B) Grey pollution due to deposition of dust and soot
- C) Black films, thin and strongly adherent to the stone, covering the surface partially or completely
("Patina" after ISCS glossary, but here the term "black film" is used, see 3.2)
- D) Black crusts, a few millimetres thick, characterized by irregular formed surfaces and showing a tendency to detach from stone with increasing thickness
- E) Microbiological growth, predominately by algae, fungi and moss
- F) Colour paint, of dark greyish colour, applied during the restoration work in 1969-1972

Manifold small-scale transitions and overlaps were observed between these types.

The types A, C, and D are characterized by the enrichment of Fe-(hydr-)oxides on the stone surface. Drill cores taken from a weathered sandstone block with a slightly discoloured surface (Type A-B) displayed an intensive brownish discolouration after testing the capillary water adsorption and subsequent drying (Fig. 1, right). This indicates that the enrichment is mainly due to the mobilization of some compounds in the interior of stone and their transport to the surface with pore fluids.



Fig. 1: The Porta Nigra in Trier and drill cores showing brown discolouration after testing for capillary water absorption.

The deposition of particulate matter is a relevant factor for the formation of types B, C and D. The occurrence of typical black crusts (D) is confined to narrow zones being periodically moistened but sheltered from direct wetting by run-off rain water. These are the undersides of cornices and capitals or areas behind corners where turbulences occur. Compared to the large areas covered by type C, the type D crusts occur in small and confined zones only, because they were removed during former conservation work in 1968-1973 and the formation of new crusts was rather limited. Microbiological growth (E) is confined to areas of increased moisture content. These are protruding parts, water run-off zones, and areas exposed to splash water. Dark grey colour paints (F) were applied during former restoration work on replaced stones and on restoration mortars. In the surrounding of those newly added parts the colour paint also was applied on historical stone surfaces. Aesthetically the colour paint tries to imitate black films but it shows differing physical and chemical properties.

3.2. Properties of the blackened surfaces

Qualitative analysis by mobile XRF, by EDX at SEM investigations and the results of quantitative analysis by ICP-OES showed enrichments of Ca, S, Fe, P, Ti, Pb, and Sr in both black films and black crusts (Fig. 2). These results are consistent with the results of SEM-studies (Fig. 2) and with literature data on the chemistry of black films and black crusts from other monuments (amongst others Neumann 1994, Thomachot and Jeannette 2000, Nijland *et al.* 2003, Graue *et al.* 2013).

Regarding the use of the term black films, it should be pointed out that several previous studies stated an origin of the black films or black layers on sandstone mainly by mobilization of iron oxide compounds in the stone, their subsequent transport by pore fluids and their enrichment at the stone's surface. (Nord and Ericson 1993, Neumann 1994;

Steeger and Mehnert 1998; Thomachot and Jeannette 2000). Because this process might be seen as a “natural” response of the sandstone to the impact of precipitation, sometimes the term “patina” is used for this type of blackening, *e.g.* in the ISCS glossary (ISCS 2008).

In the case of the Porta Nigra chemical data and SEM observations (Fig. 2) provide evidence that the enrichment of iron oxide compounds from the stone’s interior is superimposed by the deposition of airborne particulate matter. Thus the formation of black films is not only of intrinsic, but also of environmental origin. Therefore the term “black film” is preferred in this paper instead of “patina”.

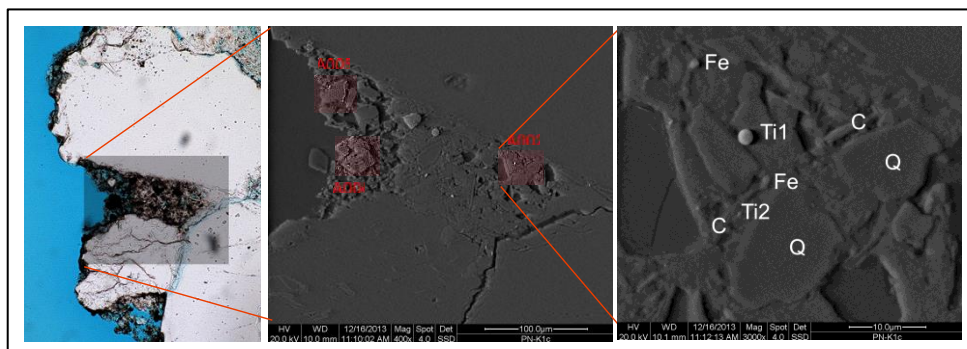


Fig. 2: Polished thin section of a sample with black film under optical and scanning electron microscope: An interstice between quartz grains (Q) filled with Ti-rich fly ash (Ti1) and other Ti- (Ti2) and Fe-rich (Fe) particles embedded in gypsum and between clay minerals (C) and small quartz grains.

Organic compounds were analysed in two steps. Screening tests detected various alkanes and other substances in two of six samples, that are probably related to diesel and biodiesel fuel from nearby road traffic. In another sample DEHP, a common plasticizer, and *n*-Nonacosan, a long-chain alkane, were detected. Furthermore 23 representative polycyclic aromatic hydrocarbons (PAH) were analysed. In 5 of 6 samples the PAH concentrations exceeded the detection threshold. The highest concentrations were found in a sample taken close to a heavy-trafficked bus stop.

Ultrasonic surface measurements show a broad range of Rayleigh wave velocities between 0.6 and 1.9 km/s. Variations of stone properties and different degrees of deterioration are the causes of this spread. Rayleigh wave velocities from different measuring profiles show varying dependencies on frequency. Since the frequency comprises also information about the depth of the surface wave sensitivity, different forms of damage can be recognized by the variation of velocity with frequency. Examples are given in Fig. 3, whereupon every curve represents an average of 10 to 15 measurements at one profile. Results of wave form inversion showed that in the case of the Porta Nigra sandstone the analysed frequency band corresponds to depths up to 2 cm (Meier *et al.* 2014).

Fig. 3 shows curves from thin black films (Fig. 3a) and thick black crusts (Fig. 3c) where Rayleigh wave velocity increases with frequency, indicating an increase in density at or just below the stone's surface. Microscopic studies on a few samples show that this corresponds to the part of the pore space commonly filled with gypsum, clay minerals and iron oxides (Fig. 4). Based on waveform inversions, the thickness of the crusts is estimated to vary between a few millimetres and nearly a centimetre (Meier *et al.* 2014). However, between film and crust the stone is characterized by a bright and sanding surface (Fig. 3b) and accordingly the velocities decrease with frequency. These negative slopes point to a loss of strength in the outermost millimetres.

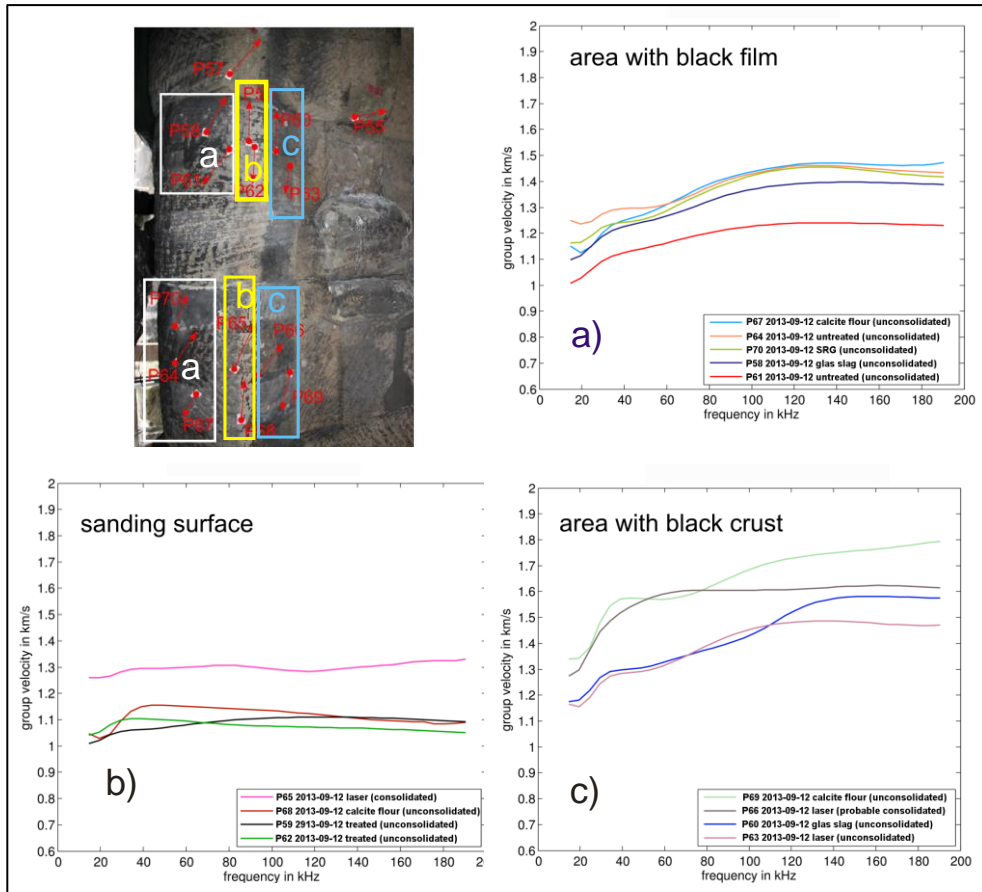


Fig. 3: Rayleigh waves showing an increase or decrease of velocity with increasing frequency (Meier 2016).

Microscopic studies proved the occurrence of gypsum and Fe-(hydr-)oxides in the pore space below black films and black crusts. The zone of gypsum enrichment underneath black crusts is about 1–10 mm thick, whereas underneath black films it is confined to a few grain layers (0.2–2 mm).

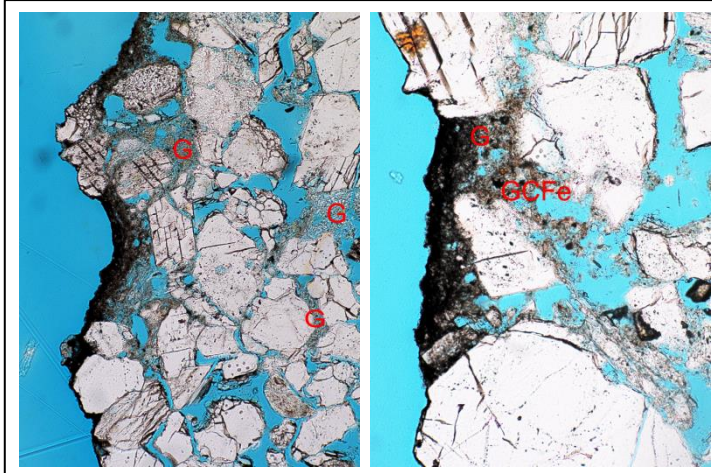


Fig. 4: Thin section images showing gypsum (G), and agglomerates of gypsum, clay minerals and Fe-compounds (GCFe) in the pore space below very thin black films.

3.3. Evaluation of cleaning tests

Cleaning tests were carried out using micro-sandblasting and laser ablation, shifting the intensities gradationally. The efficiency of the cleaning was evaluated by the optical appearance and SEM studies, as well as by measurements of capillary water adsorption (Karsten tubes), permeability, and colour changes. In Tab. 1 some results of the Karsten measurements are compiled. They show a very effective increase of capillary water adsorption after cleaning at low intensities.

Tab. 1: Coefficient of capillary water adsorption coefficient [in $\text{kg}/\text{m}^2\cdot\text{h}^{0.5}$] of black films before and after cleaning

Black Film	Untreated	After micro-sandblasting	After laser cleaning
On Roman Stone	0.15	5 - 10	5 - 8
On Romanesque Stone	4	10	13

Applying low-intensity laser cleaning only achieved minor colour changes, but thermal heating by insolation and capillary water adsorption were restored to values corresponding approximately to the unspoiled stone. Furthermore air permeability showed a distinct increase after cleaning. SEM studies verify the partial removal of black films from the mineral surfaces by laser cleaning, while gypsum remained in the pore space.

4. Conclusions

The darkened stone surface of the Porta Nigra, the famous Roman city gate in Trier, Germany, has been the subject of comprehensive scientific research. Various types of discolouration, pollution and colour paint were classified and analysed. The weathering forms and intensities of deterioration were mapped and examined. This paper focusses on the sensitive aspect of stone cleaning and therefore other parts of the research are omitted. The stone surfaces of the Porta Nigra show different types of discolouration and pollution related to their exposure to weather and air pollution. The main feature is the coverage by thin black films adhering firmly to the stone. It could be shown that moisture transport, strength profiles and thermal properties vary between the different types of surface alterations. These factors are compiled in Tab. 2, giving a basis for an evaluation of the risk estimation of each of those alterations.

Tab. 2: Changes of physical and chemical properties due to the different type of surface alteration

Type	A	B	C1	C2	D	E	F
Enrichment of soluble salts	-	-	+—	+—	++	-	-
Sealed surface, decrease of capillarity and drying	-	-	o	++	?	?	++
Reduction of air permeability	-	-	o	++	+—?	-	++
Hardening of the surface	o	o	+	++	++	?	++
Deterioration of the stone's surface	o	o	+—	+—	++	+—	o
Increased heating by insolation	-	-	-	++	-	-	++
Increased thermal dilatation	-	-	+	+	-	-	++
Increased hygric dilatation	-	-	-	-	-	-	-
Increased moisture content	-	-	-	-	-	+	-
Risk estimation	low	low	low	medium	high	low	high

-	not determined
o	no or negligible effect
+—	Effect sometimes verifiably
+	Effect definitely verifiably
++	Obviously combined with damage

The following recommendations can be deduced from Tab. 2:

- Types A and B: Brownish discoloration and grey staining have a low risk potential and do not need any treatment.
- Type C: Thin black films require further classification:
 - o C1: When they cover the surface only partially, their effects on the physical properties of stone are not detrimental.
 - o C2a: When they cover the surface completely, their effects are conflicting: capillary water absorption is reduced, but on the other hand air permeability is also strongly reduced and heating by insolation is considerably increased. This stage can be tolerated as long as there is no visible damage or massive enrichment of gypsum below the black films.
 - o C2b: At construction parts particularly exposed to rainfall or run-off the black films and the outermost grain layers often are detached from the stone and the light stone is visible. In the majority of these cases a strengthening treatment with silicic acid ester will be necessary and a thinning of the black films in adjacent areas is recommended.
 - o C2c: If there is an additional enrichment of gypsum below the surface, it will be beneficial to reduce the content of gypsum. Otherwise the frequent recrystallization of gypsum in the pore space will have detrimental effects as it is the case for thick gypsum crusts. The data of ultrasonic surface wave measurements showed that in most cases ultrasonic velocities are enhanced below the surface, providing evidence for a densification in the first 3–10 mm of the surface which is due to the enrichment of gypsum. Reduction of gypsum in the pore space needs an opening of the sealed surface, which can be achieved by cleaning.
- Type D: Thick black crusts rich in gypsum have a serious detrimental effect as reported by Charola and Ware (2002), Brimblecombe (2011), and others. The frequent recrystallization of gypsum in response to changing conditions of moisture and temperature obviously causes alternating stresses to the stone, leading to the formation of micro-cracks in the stone's surface and finally to visible damage. These crusts have to be removed by cleaning in order to prevent further damage.
- Type E: The growth of algae, lichen and moss develop mostly at construction parts with increased moisture content. Instead of using biocides it is recommended to check the possibilities of constructive methods to reduce the run-off of rain water in order to diminish the moisture content in these parts.
- Type F: A removal or at least a thinning of the silicate-bound colour paint is recommended, because microscopic studies, measurements of capillary water absorption, Rayleigh waves and air permeability show, that they seal the stone surface almost completely and strengthen the outermost grain layers of the surface intensively. Both factors are known to be detrimental on a long term scale.

Besides the question of cleaning several other aspects of conservation work were examined. But yet the removal of gypsum from the pore space is not yet solved. This issue needs further tests and examinations of the building.

Acknowledgements

Thanks to Marion Basten, Ercan Erkul, Moritz Fehr, Lothar Goretzki, Janina Haus, Kalle Jepsen, Thomas Kessler, Karin Kraus, Esther Klinkner, Daniel Köhn, Klaus Rapp, Helmut Santl, Dirk Scheuven, Eric Spangenberg, Florian Ströbele and others for experimental assistance and organizational support. Funding by the German Federal Environmental Foundation is gratefully acknowledged.

References

- Becker, K.-H., Brüggerhoff, S., Steiger, M., Warscheid, T., 2005, Luftschadstoffe und Natursteinschäden. In: Siegesmund, S., Auras, M., Snethlage, R. (eds), *Stein Zerfall und Konservierung*, Edition Leipzig, 36-45.
- Brimblecombe, P., 1987, *The Big Smoke*. Methuen, London
- Brimblecombe, P., 2011, Environment and Architectural Stone. In: Siegesmund, S., Snethlage, R. (eds.): *Stone in Architecture*, Springer-Verlag, Berlin, S. 317-346.
- Camuffo, D., 1996, Perspectives on Risks to Architectural Heritage, In: Baer, N.S. and Snethlage, R., (eds), *Saving Our Architectural Heritage*, Dahlem Workshop Report, John Wiley and Sons, New York, S. 63-92.
- Charola, A.E., and Ware, R., 2002, Acid deposition and the deterioration of Stone: A brief review of a broad topic. In: Siegesmund, S., Weiss, T., and Vollbrecht, A. (eds), *Natural stone, weathering phenomena, conservation strategies and case studies*. *Geol Soc Spec Publ* 205: 393-406.
- Graue, B., Siegesmund, S., Oyhantcabal, P., Naumann, R., Licha, T., Simon, K., 2013, The effect of air pollution on stone decay: the decay of the Drachenfels trachyte in industrial, urban, and rural environments—a case study of the Cologne, Altenberg and Xanten cathedrals. *Environmental Earth Science*, 69, 1095-1124.
- Honeybourne, D.B., 1990, Weathering and decay of masonry. In: Ashurst, J. and Dimes, F.G. (eds.): *Conservation of Building and Decorative Stone*, Butterworth-Heinemann, London, Vol. 1: 153-178.
- ISCS, 2008, *Illustrated glossary on stone deterioration patterns*. ICOMOS International Scientific Committee for Stone (ISCS), *Monuments & Sites XV*, 86 pp.
- Meier, T., Auras, M., Erkul, E., Fehr, M., Jepsen, K., Milde, C., Schulte-Kortnack, D., Spangenberg, E., Steinkraus, T., Wilken, D., 2014, *Physikalische Untersuchungen an der Porta Nigra - Ultraschall-Oberflächen-Messungen und thermische Untersuchungen*, IFS-Bericht Nr. 47, Institut für Steinkonservierung e. V., Mainz, 50-62.
- Meier, T., Auras, M., Fehr, M., Köhn, D., Cristiano, L., Sobott, R., Mosca, I., Ettl, H., Eckel, F., Steinkraus, T., Erkul, E., Schulte-Kortnack, D., Sigloch, K., Bilgili, F., Di Gioia, E., Parisi-Presicce, C., in press, *Investigating surficial alterations of natural stone by ultrasonic surface measurements*. In: Masini, N. and Soldovieri, F. (eds.): *Sensing the Past*. Springer International Publishing AG.

- Neumann, H.-H., 1994, Aufbau, Ausbildung und Verbreitung schwarzer Gipskrusten, dünner schwarzer Schichten und Schalen sowie damit zusammenhängender Gefügeschäden an Bauwerken aus Naturstein. Dissertation, Universität Hamburg.
- Nijland, T.G., C.W. Dubelaar, van Hees R.P.J., van der Linden, T.J.M., 2003, Black weathering of Bentheim and Oberkirchen sandstone. *HERON*, 48, No. 3 (Special Issue), 179-195.
- Nord, A.-G., Ericson, T., 1993, Chemical analysis of thin black layers on building stone. *Studies in Conservation*, 38., 1/1993, S. 25-35.
- Snethlage, R., and Sterflinger, K., 2011, Stone conservation. In: Siegesmund, S., Snethlage, R. (eds.): *Stone in Architecture*. Springer, Berlin, 411-544.
- Steger, W. E., Mehner, H., 1998, The iron in black weathering crusts on saxonian sandstones investigated by Mössbauer spectroscopy. *Studies in Conservation*, 43, Heft 1, S. 49-58.
- Sterflinger, K., 2011, Biodeterioration of Stone. In: Siegesmund, S., Snethlage, R. (eds.): *Stone in Architecture*. Springer, Berlin, 291-316.
- Thomachot, C., Jeannette, D., 2000, Petrophysical properties modifications of Strasbourg's Cathedral Sandstone by black crusts. *Proceedings of the 9th International Congress on Deterioration and Conservation of Stone, Venice*, 265-273.
- Warscheid, T., 2005, Mikrobieller Befall und Schädigung von Natursteinen und Möglichkeiten einer praxisgerechten Beseitigung. In: *Grabsteinerhaltung*. Institut für Steinkonservierung e.V., Mainz, IFS-Bericht Nr. 20: 57-62.
- Wilimzig, M., Fahrig, N., Meyer, C., Bock, E., 1993, Biogene Schwarze Krusten auf Gesteinen. *Bautenschutz + Bausanierung*, 16, 2/93, S. (22-25).

This page has been left intentionally blank.

THE CONSERVATION OF GIOVANNI LABUS'S SCULPTURE OF BONAVENTURA BAVALLIERI (1844) AND ANTONIO GALLI'S SCULPTURE OF CARLO OTTAVIO CASTIGLIONE (1855)

I. Ruiz Bazán¹, V. Bresciani², A. Balloi³, A. Quarto⁴,
I. Marelli⁴, M. Colella^{5*}, C. Sotgia⁶ and F. Arosio⁷

Abstract

In this project a cleaning intervention of the neoclassical statues in the Brera Academy courtyard was performed with the use of living microbial cells. These living organisms, belonging to the species *Desulfovibrio vulgaris*, were able to remove chemical alterations, mainly caused by sulfates, from the stone surface of the statues. The method has been chosen because it is highly efficient, respectful to the original material, the environment and the restorer operating it. Thanks to the microorganism's selectiveness, it was possible to remove only the harmful alteration of the stones, respecting the so-called "noble patina" a key element in art pieces. Considering the precarious state of conservation of the hands belonging to the statue of Carlo Ottavio Castiglione, a 3D (Rilievo 3D) survey was taken.

Keywords: 3D survey, convergent photogrammetry, bio-restoration, sculpture, marble, cleaning

¹ I. Ruiz Bazán
Architect, Milan, Italy and Zaragoza, Spain

² V. Bresciani
Bresciani s.r.l., Milan, Italy

³ A. Balloi
Micro4yoU s.r.l., Milan, Italy

⁴ A. Quarto and I. Marelli⁴
Soprintendenza Belle Arti e Paesaggio, Milan (Italy)

⁵ M. Colella*
Servabo Conservation Studio, Milan, Italy
servabo.colella@gmail.com

⁶ C. Sotgia
C.S.G. Palladio s.r.l., Vicenza, Italy

⁷ F. Arosio
Amici di Brera, Milan, Italy

*corresponding author

1. Introduction and historical background

Designed by Francesco Maria Richini (1584-1658) for the Jesuit College, the Brera Academy courtyard (1615) hosts in its arcades stone busts and statues figuring the most illustrious Milanese artists, scientists and philosophers. Thanks to the coworking of: Associazione Amici di Brera, Musei Milanesi, the Milanese superintendence BSAE and the generous contribution of Pirelli it was possible to restore the statues of Bonaventura Cavallieri and Carlo Ottavio Castiglione.

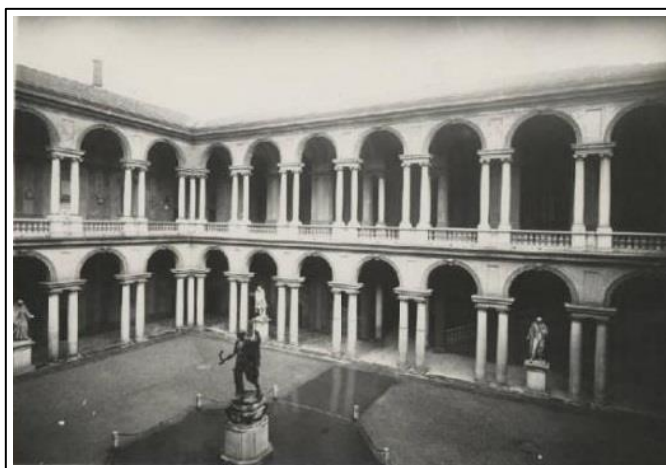


Fig. 1: Brera courtyard (Silver Bromide fixed on paper (1920-1940) from: Raccolte Grafiche e Fotografiche del Castello Sforzesco, Civico Archivio Fotografico, RI 14344).

Of Milanese birth Bonaventura Cavallieri (1598-1647) studied mathematics at the University of Pisa where he was student of Galileo Galilei. Bonaventura's fame is due to his approach to the method of the indivisibles, useful to determine areas and volumes. His studies were of fundamental importance for the future development of infinitesimal calculus. The statue representing this great mathematician was created by Giovanni Antonio Labus (1806-1857) who was a teacher at the Brera Academy and operated in the most outstanding construction sites of his times like the Duomo of Milan and the Arco della Pace. This extremely eloquent statue is one of his greatest achievements.

Carlo Ottavio Castiglione (1784-1849) was a numismatist and a scholar of Semitic and Indo-European languages. In 1819 he published a detailed description of Kufic coins, minted by the Normans and kept in the Brera cabinet. His main work regard the study of oriental languages and researching the origins and history of the city of Barbary (Tripoli) whose name can still be found on ancient Arab coins. Sculptor Antonio Galli (1812-1862) studied at the Brera Academy and moved to Rome to work in Thorvaldsen's studio. After this Roman stay he returned to Milan to work in the Duomo construction site. Galli presents Castiglione purposely seen from below with an intense look pointing his finger directly to a coin held in his hand.



Fig. 2: Initial phases of the conservation of Antonio Galli's sculpture of Carlo Ottavio Castiglione (1855). Height of statue plus the pedestal 503 cm (198 inches), Just the statue 305 cm (120 inches). The original surface appears hidden by a layer of aged protective varnish.

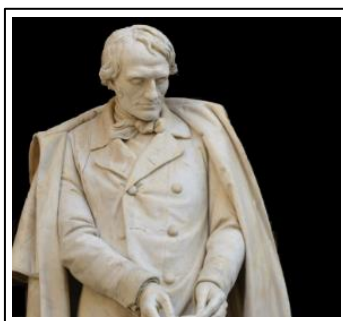


Fig. 3: Final phase of the conservation - Cleaning by sulphate reducing bacteria has given back the surface's original smoothness caused by the use of fine chisel for surface finishing and reveal a compact saccharoidal white limestone that is very similar in appearance to Venato Apuano marble.

2. 3D Survey by convergent photogrammetry

Since the hands are probably the most fragile parts on the sculpture a 3D model of the hands of the statue has been created as a preventive measure before the restoration to allow for future reproduction of those pieces. Due the difficult morphology of this area of the statue, we chose the convergent photogrammetry technique, which is one of the most used methods on sculpture. The basis of this method is the reinterpretation of the conic perspective through the use of an assemblage of pictures taken of the sculpture. Unlike lasers, this method does not reflect light back to the camera which makes it very useful for mapping complex surfaces. Another advantage of this method is that we obtain a map of the real texture of the surface which can then be incorporated in the 3D model thus significantly improving the accuracy documentation. With this high degree of accuracy it is possible to create an exact replica of the object.

3. Diagnostic phase

Two samples were taken: the first from the sculpture of Carlo Ottavio Castiglione in a yellowed area, the second from the sculpture of Bonaventura Francesco Cavalieri in a blackened area. Sample 1 was embedded in polyester resin to prepare a specimen of the cross section. First the cross section was examined by optical microscopy before proceeding with investigations including the use of an electron microscope (ESEM) and a FTIR spectrophotometer. Especially, the latter was used to determine inorganic and organic compounds, for example products due to previous conservation work, which might be responsible for surface alteration. For the characterization of the composition of sample 2, which consisted of powder, XRD and EDS analyses were carried out.

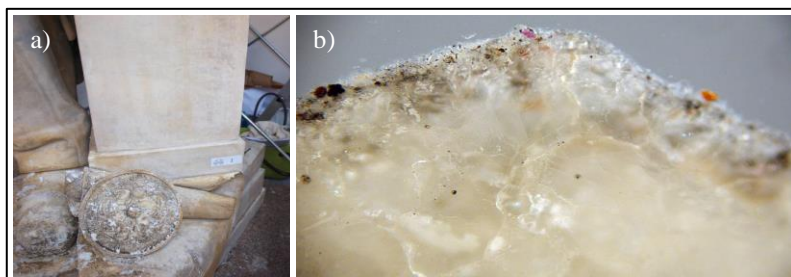


Fig. 4: a) Sampling point for sample 1; b) Micrograph of the cross section of sample 1 (magnification: $\times 240$).

In both samples analysed it has been revealed the presence of gypsum and specific air pollution: this is related to a widespread surface sulfation. In particular in sample 1 the electron microscope images show an advanced state of decohesion of the stone material. The spectrophotometric FTIR analysis has revealed calcium carbonate, gypsum and silicate but also very weak absorptions of probably synthetic resin and/or oxalates. The oxalates are usually referred to the organic substances degraded. In sample 2 both XRD analysis and EDS measurements could confirm the presence of sulfates in the form of gypsum (calcium sulfate dihydrate) and of bassanite (calcium sulfate hemihydrate). The EDS analysis has revealed silicates and also fluorine: these can be linked to conservation attempts based on fluorinated compounds or fluorosilicates undertaken in the 1970s and 1980s.

4. Conservation

The conservation work took place in the months of June, July and August 2015 in the Brera Academy courtyard. In the case of Antonio Galli's sculpture of Carlo Ottavio Castiglione Castiglione the cleaning effort has given back the surface's original smoothness produced by a fine chisel. The Bonaventura statue surface is rougher, with intentionally visible circular furrows made by the chisel. The statues in which we intervened are made of white compact saccharoidal marble, which is thought to be an apuano marble in between the common white Carrara marble and the so called Venato Apuano marble. It is a white marble with intense grey veins which the sculptor has let fall obliquely on the drapery.

During these conservation interventions there was no access to first hand data specifying the quarries from which these marbles came from. Judging by the aesthetic appearance of these marbles it can be assumed that this type of sculpting stone comes from Tuscany more specifically from the zones between Minucciano (Lucca), Cantonaccio and Fivizzano

(Massa Carrara). The tone is compact and of a medium fine grain, with a light greyish colour with abundant dark grey veins. These dark grey veins intersect each other, creating an intense dense superficial weave. There are also rare small (not more than a couple of millimetres) grey spots on the surface. A large part of the surface is covered by deposits of atmospheric particles and a conspicuous sulfation. Thin section analysis has revealed sulfation to measure circa 5 mm deep. In particular the ESEM images have revealed a remarked decohesion in the intergranular spaces of the calcite crystals (Fig. 5).

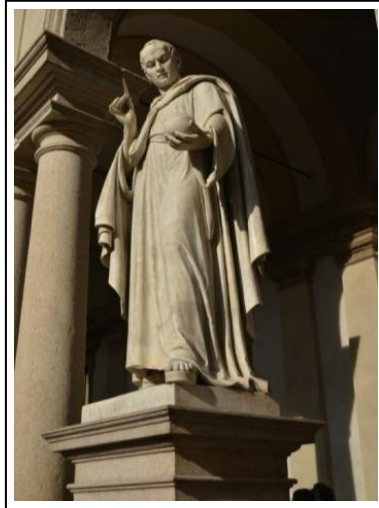


Fig. 6: The removal of aged yellowed protective layer and dirt has revealed the original surface texture the statue of Bonaventura which presents signs of scratches and abrasion related to the use of a fine but large chisel (circular furrows) for the surface finish.

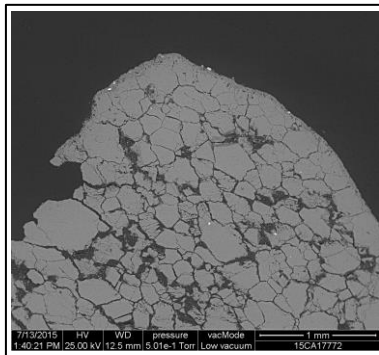


Fig. 5: SEM-BS image (low vacuum mode) of sample 1 showing the intergranular decohesion is apparent throughout the thickness of the sample.

Since the statue hands had reached such a critical state it was opted for consolidation by submerging them in a low viscos acrylic dispersion with either Primal[™] B60 or Primal[™] WS-24 (by Rohm & Haas) and water (dip coating, Fig. 7). The web of acrylic dispersion which is generated inside the pores increases the mechanical properties of the treated

surface, reducing its porosity though not obstructing the pores and respecting the surface's qualities. The consolidation resulted in the creation of bridges in the spaces in between the grains of the degraded stone.

Sulfation caused by smog is a widespread problem in all major urban centres. Sulfur dioxide in the presence of humidity, is transformed into sulfite ions, these in contact with oxidants such as oxygen become sulfate ions. Sulfate ions, once in contact with the stone, cause a consequent chemical transformation of the calcium carbonate (CaCO_3) into calcium sulfate dihydrate or gypsum ($\text{CaSO}_4 \cdot 2\text{H}_2\text{O}$). During the crystallization of gypsum, airborne pollutants, such as carbonaceous particles (soot), are embedded in the mineral matrix and cause the formation of black crusts in sheltered areas. Sulfate-reducing bacteria belonging to the species *Desulfovibrio vulgaris*, thanks to their metabolism are able to dissociate gypsum into Ca^{2+} and SO_4^{2-} ions. SO_4^{2-} ions are then reduced by the bacteria into H_2S , while the Ca^{2+} ions react with carbon dioxide to form new calcite. The commercial name of the microbial product used in this work is Micro4Art, made by Micro4yoU Srl and distributed by Bresciani Srl.

With the help of Dr. Annalisa Balloi sulfate-reducing bacteria through a gelatinous medium were applied on sulfated areas that appeared altered. The gelatinous medium was left overnight on the stone surface until the desired result where obtained. The bacteria contained in the gel attack and eliminate the sulfate. Local interventions of traditional cleaning were limited to the removal of varnish drops that had fallen from above. These interventions have been performed by swabbing soluble non-polar solvents. The conservation intervention was then concluded with a mild application (4% micro-dispersed acrylic in water) with a protective patina on all the surfaces, to reduce the absorption of meteoric and condensation water (albeit for a limited time).



Fig. 7: a) Scheme of the consolidation system adopted (dip coating); b) Dr. Annalisa Balloi during the application of sulfate-reducing bacteria through a gelatinous medium on the areas that were altered and covered by sulfates.



Fig. 8: Signature of Antonio Galli on the statue of Carlo Ottavio Castiglione (1855) before the application of sulfate-reducing bacteria by a gelatinous medium.



Fig. 9: Signature of Carlo Ottavio Castiglione's statue (1855) during the cleaning using sulfate-reducing bacteria applied to the surface with the aid of a gelatinous medium. The cleaning has brought to light (for example in the right area of the cartouche) some punctual spots along the surface. FTIR analysis carried out by Palladio Analisi s.r.l. laboratories identified calcium carbonate, gypsum, silicates, and very feeble traces fluorosilicate absorptions, which are most probably left by residues of protective and polishing products used in the past.

5. Conclusion

The use of sulfur-reducing bacteria was found to be much more effective when removing sulphate from stone surfaces than the traditional solvents, which sometimes can cause harm to both the art piece and the operator. Other advantages of Bio-Restoration are:

- Growing bacteria on large scale does not require great disbursements are easily applied on surfaces.
- Using bacteria does not imply any ethical conflict, since these microbes are not genetically modified.
- Bacteria represent no harm for sculptures and people working with them.

References:

- Bacci M., F. Baldini, R. Carlà, and R. Linari: "A Color Analysis of the Brancacci Chapel Frescoes. Part I" *Applied Spectroscopy* 45 (1991), 26-30.
- Bacci M., S. Baronti, A. Casini, F. Lotti, M. Picollo and O. Casazza: "Nondestructive spectroscopic investigations on paintings using optical fibers", *Mat. Res. Soc. Symp. Proc.*, 267 (1992) pp. 265-283.
- Bacci M., M. Picollo, B. Radicati and R. Bellucci: "Spectroscopic Imaging and non-destructive reflectance investigations using fiber optics", 4th Intern. Conf. Non-Destructive Testing of Works of Art Proc., Berlino (1994), pp. 162-174.
- Bacci M. and M. Picollo: "Non-destructive detection of Co(II) in paintings and glasses", *Studies in Conservation* 41 (1996), 136-144.
- Chiari R., Picollo M., Porcinai S. and Radicati B.: "Non Destructive Reflectance Spectroscopy in the discrimination of two authigenic minerals: gypsum and weddellite" 1996, 2nd Intern. Symp. The Oxalate films in the conservation of works of art Proc., Milano (1996), 379-389.
- Bacci M., M. Picollo, S. Porcinai and B. Radicati: "Spectrophotometry and colour measurements" *Techne* 5 (1997), 28-33.
- Cappitelli, F. *et al.*, 2007. Advantages of using microbial technology over traditional chemical technology in removal of black crust from stone surfaces of historical monuments. *Applied and Environmental Microbiology*. 73: 5671-5675.
- Polo, A. *et al.*, 2010. Feasibility of removing surface deposits on stone using biological and chemical remediation methods. *Microbial Ecology*. 60: 1-14.
- Gioventù E. 2010. Comparing the bioremoval of black crusts on colored artistic lithotypes of the Cathedral of Florence with chemical and laser treatment. *International Biodeterioration & Biodegradation*. 65: 832-839
- Jazayeri I., Fraser C.S., Cronk S., Automated 3D object reconstruction via multi-image close-range photogrammetry. *International Archives of Photogrammetry, Remote Sensing and Spatial Information Sciences*, Vol. XXXVIII, Part 5 Commission V Symposium, Newcastle upon Tyne, UK. 2010, 305-310.
- Remondino, F. Heritage Recording and 3D Modeling with Photogrammetry and 3D Scanning. *Remote Sens.* 2011, 3, 1104-1138.
- McCarthy, J. Multi-image photogrammetry as a practical tool for cultural heritage survey and community engagement. *Journal of Archaeological Science*. Volume 43, March 2014, pages 175-185.

RESTORATION OFF-SET BY THE PUBLIC EXHIBITION OF DECORATED STONE ELEMENTS RESCUED FROM THE DEMOLISHED VĂCĂREȘTI MONASTERY, ROMANIA

C. Bîrzu^{1*}

Abstract

The present paper reports a project aiming to recover the image of a now disappeared monument – the Văcărești Monastery Church. Since the reconstruction of the Văcărești Monastery Church was not an option, it was decided to conserve the decorated stone parts, which could be saved during the demolition of the building, and place them in the "Memorial - Lapidarium". In this cultural space the remaining stone columns are most spectacularly placed in their vertical orientation to restore, at least partially, the greatness of the old ecclesiastical edifice of the Văcărești Monastery. Such approach aims to combine today's cultural act with the Brâncoveanu style and art of the 18th century.

Keywords: stone conservation, stone restauration, decorated stone elements, exhibition

1. Văcărești Monastery - Brief history

An achievement of great value, which falls in the cultural landscape of the time, the Văcărești ensemble benefited from the specific cultural accumulations of the era of Ruler Constantin Brâncoveanu. Founded by Nicolae Mavrocordat between the years 1716-1722 (1st Phanariot ruler of Wallachia) and continued by his son between the years 1732-1736 the Văcărești ensemble represents one of the most important ensembles in the Byzantine world at its time (Fig. 1a).

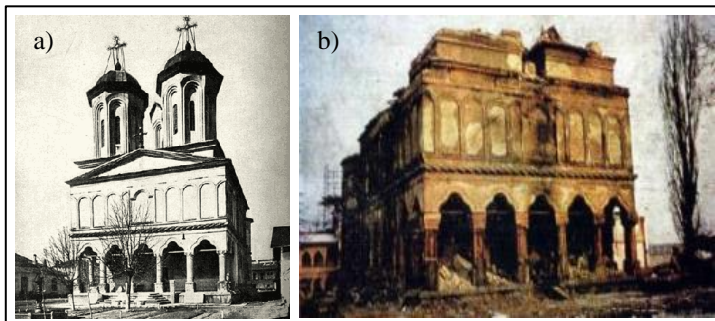


Fig. 1: Văcărești Monastery Church before (a) and during the demolition (b).

¹ C. Bîrzu
National University of Arts, Bucharest, Romania

*corresponding author

However, in the 19th century Văcărești Monastery had been abandoned for a long time and was subsequently turned into a prison for the Romanian revolutionaries of Wallachian Revolution in 1848. This event probably marks the starting point for the irreversible deterioration of the Văcărești ensemble, which eventually ended with its demolition in 1985-1986 (Fig. 1b).

2. Removal of the decorated stone elements and fresco fragments prior and during the demolition of the Văcărești Monastery Church

Regarding the removal or saving of the stone elements, the undertaken actions at the time of the demolition were hasty and as far as known without any intention of preserving anything for future use in an attempt to rebuilt of the church. For example, cracks in the preserved columns from both the porch and of the narthex show that these elements were not carefully removed, but had been simply hit from the side to destroy the structural integrity of the building. After demolition, the stone blocks were transported to various locations, with most of them (324 pieces) reaching Mogoșoaia Palace (near Bucharest). In this case the remaining stone fragments were stored under a covered outdoor space at the eastern edge of lake (Fig. 2). Some other parts arrived at Brâncoveni Monastery, the National Museum of Art, and the Cotroceni Museum.



Fig. 2: Storage space of the decorated stones.

3. The beginning of the Memorial - Lapidarium project

Ideas for conservation/restoration of these stone elements with their decorations arrived very soon after the demolition of Văcărești Monastery. Some of these ideas included the rebuilding of the monastery while other only considered a placement of selected stone pieces in a museum. Fortunately, following the intervention by historian Mrs Doina Mândru (cultural director of the ensemble Mogoșoaia Palace) a project for a museum, which combines memorial and cultural purposes, was initiated, thus allowing at least for the display of the most spectacular stone pieces. At the moment, the project is coming to an end as the building is approaching its completion. After the completion of a long study plan the stone pieces have already been installed in the building. Specifically, in the periphery areas of the Memorial (terrace), 16 assembled stone objects are on display as vertical columns (similar to their position in the original building).

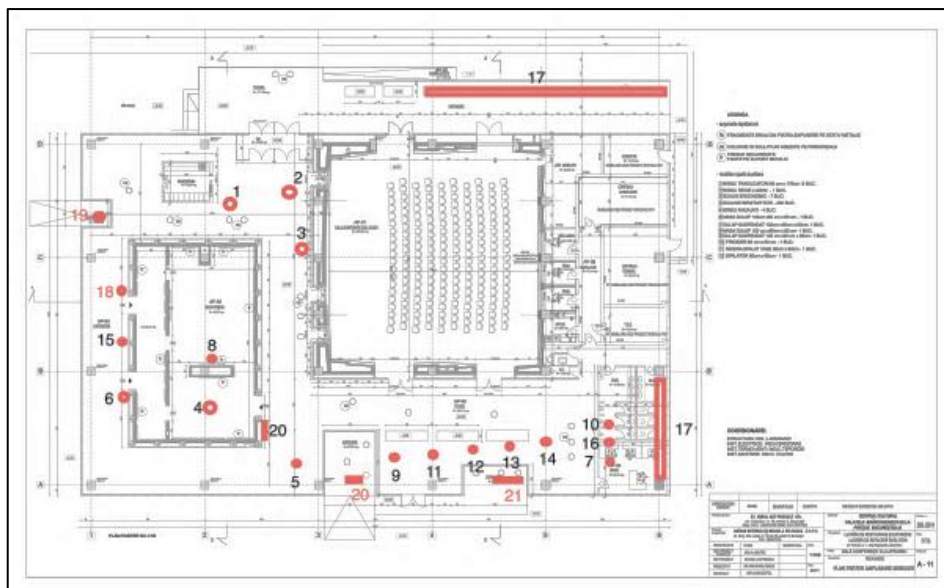


Fig. 3: Plan of the Memorial - Lapidarium. The red circles or squares mark the future position of the decorated stones

4. Conservation, restoration and enhancement activities

4.1. Description of the conservation status and decay factors

From the mineralogical analysis it became clear that the rubble stones of the stone components of Văcărești Architectural Ensemble were carved in biogene limestone with nummulites from the Eocene age quarried in the area of Albești, Câmpulung Muscel-România.

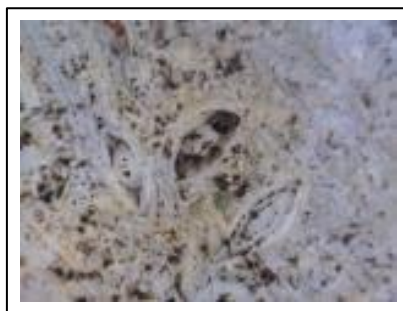


Fig. 4: Structure of the stone at a magnification of $\times 50$.

Two chronological stages of the damages are observed. The *first phase* was the period before the demolition of Văcărești Monastery Church in 1986.

On the inside:

- Considering the church had only been in little use for religious services, the specific decay and deposits on the stone surface were found to be insignificant.
- Certain repair attempts were undertaken in the past. With respect to the three layers of paint being found on the stone surface: white, green and ochre (and in chronological order also cement mortars) it appears as first repair work as dates probably back to the 19th century. Traces of cement mortar seem to indicate a repair attempt in the second-half of the 20th century.

On the outside

- Girdle fragments showed deposits/crust probably caused by tars from air pollution. After a closer examination of the girdle fragments, we could conclude that the damage level of the girdles was in a 10-15% range. The black crusts were especially concentrated on the decorated areas of the stone (which are the most exposed from a geometrical point of view) and areas formerly protected from wind and rain.

The *second phase* of damage is the time after the demolition, including transport and storage in the current shelter.

- Deposition of fine particulate (dust), different plant debris originated from the storage environment reached a level of 100%.
- Rust stains (small patches of about 10/4 cm) were observable on certain stone pieces in some areas can be related to the iron support structure of the storage shelter.
- Biological attack by of several species of lichens was discovered at closer investigation of the surface crust/biofilm.

4.2. Cleaning and Conservation of the stone fragments

Selection of stone pieces and their future location in the newly build Memorial was done under the aspect of creating a visual and iconographic spaces within the Memorial. The narthex columns (large columns and associated bases and capitels) were considered to be the most spectacular pieces, followed by the porch columns and several other secondary items (gird, framing of the window, etc.).

In preparation for their future display the selected stone fragments underwent an extended restoration and conservation process. Surface cleaning started with the removal of the remainders of soil and of vegetation inflicted by the years of outdoor storage as well as paint and cementitious repair materials from the previous conservation and repair attempts. Subsequently, wet removal of the superficially adherent deposits was carried out using water, sponges, a steamer (steam machine) and different types of brushes, suitable for the surface geometry of the stone fragments. Additionally, in cases of tougher surface contaminations paper pulp poultices of ammonium bicarbonate were repeatedly applied at

different exposure times. In several cases (fragments belonging to the girdle in the torsade of the church) the removal of deposits (black crusts produced by pollution) from the stone surface required microsanding, using silicate powder (120 or 150 mesh, 1-1.5 bar pressure). However, only a reduction of the crust was attempted to maintain an appropriate looking patina on the surface. The occasionally present biofilm was treated with a biocide. If required a consolidation with ethyl silicate was performed. Epoxy resin was used for the reattachment of fragments to the fractured stone elements. In order to prevent corrosion issues after the assembling of the columns at their new location all metal elements were removed from the stone blocks.

Straight from the beginning it was considered that especially the surviving columns have to be installed similar to their original constellation within in the ecclesiastical space of Văcărești monastery church to create a place of similar meaningfulness at the new location. Based on the statically requirements it was concluded that an additional support/reinforcement system, which consists of 3 epoxy resin embedded fiberglass rods (with a maximum diameter of 2 cm), has to be installed between the different elements of each column (Fig. 5d). Depending on the mechanical requirements holes with a depth of 20 or 30 cm were drilled into the stone blocks to accommodate the fibreglass rods. Additionally, all columns were also anchored in the concrete floor by 4 fiberglass rods (Fig. 5a to 5c) with each anchor point reaching 22 cm into the floor. Epoxy resin EPO 120 (or EPO 150) distributed by CTS, Italy was used for the embedding of the fibreglass rod.



Fig. 5: Installation of the columns: a and b) Bottom pin structure, c to e) Assembly of the decorated stone block to columns in the Royal House; f) Columns of the veranda.

5. Conclusion

Surviving stone parts of the in 1986 demolished Văcărești Monastery Church were successfully restored to their old beauty and placed in the newly created Memorial – Lapidarium. In this cultural space the remaining stone fragments are put on display in a manner the aims to restore at least partially the greatness of the old ecclesiastical edifice of the Văcărești Monastery.

References

- Dragut, V., 1974, Short historical and architectural documentation of the former monastic ensemble Vacaresti from Bucharest, BCMI, no. 2 –p1
- Ioan, A., What is it and how it looks the architecture with national specific? Conference NEC –p3
- Leahu, G., 1996, Destruction of Văcărești Monastery, Publisher Arta Grafică, Bucharest, 1996, 25-27
- si Laura Mora, P., Philippot P., 1986, The conservation of the mural paintings, Publisher Meridiane, Bucharest, 252- p6
- Panaiteescu, A., 2008, Remember Văcărești Monastery, Publisher Simetria, Bucharest, 44–p1

ROSSLYN CHAPEL - A REVIEW OF THE CONSERVATION & ACCESS PROJECT

N. Boyes^{1*}

Abstract

Rosslyn Chapel is a building of exceptional significance, with national and international architectural and historical importance. Due to the vulnerable condition that the building was in the 1990's, an action plan was developed to ensure its long term integrity. The Chapel was subject to major water ingress problems, combined with poor environmental conditions, the consequence of which was a cold, damp internal environment within the building with significant organic growth on the internal roof and wall surfaces. In the late 1990's a steel canopy was erected over the Chapel to protect it from the worst of the weather and allow an extended natural drying out process, which significantly changed the situation. The works on the Chapel commenced in 2005 as part of a conservation, presentation and accessibility plan. Due to the exposure of the building to the elements, the masonry suffered from natural physical decay, such as disaggregation, delamination and contour scaling. Furthermore, one of the most significant decays affecting the building was the sulphation layer (environmental pollution crust) that was covering the external stonework. This paper presents a detailed statement of the methodology that was used to conserve this extraordinary historic building by means of traditional stone masonry skills and the newest conservation technologies, such as the use of conservation lasers to reduce the level of environmental pollution products affecting the Rosslyn Chapel stonework.

Keywords: scheduled monument, survey, environmental pollution soiling, laser ablation, efflorescence

1. Introduction

Rosslyn Chapel is a Category A listed building and Scheduled Ancient Monument located 7 miles South West of Edinburgh in the village of Roslin, Scotland. It is a building of exceptional national and international significance because of the quality, quantity, and breadth of the stone carving which covers the building, both internally and externally. The carvings not only feature traditional Christian iconography but also a variety of plant and animal life and mythical creatures. The chapel was founded in 1446 by William St. Clair, 3rd Earl of Orkney, as the Collegiate Church of St. Matthew. The building was originally intended to be cruciform in plan, featuring a nave, side aisles, transepts, choir and tower. However, the building was not completed, and only the Lady Chapel, ambulatory, choir and sacristy were completed before St. Clair's death in 1484, at which point, work on the building stopped. The St. Clair family used the completed section of the church until its altars were destroyed

¹ N. Boyes*

Nicolas Boyes Stone Conservation, Scotland, United Kingdom
nic@nb-sc.co.uk

*corresponding author

in 1592 during the Scottish Reformation. No longer a functioning church, the building gradually fell into disrepair. Conservation efforts have been a part of Rosslyn Chapel's over 500-year history. The earliest known efforts took place in 1736 when the roof was repaired, the flagstones in the floor were replaced, and the windows were glazed for the first time. Architect William Burn conducted remedial works during the first half of the 19th Century. In 1862, restoration work was undertaken after Queen Victoria visited the chapel and expressed a desire to see it preserved. These works were completed by Architect David Bryce and allowed the chapel to once again function as a working church. As a result of those restorations, the chapel held Sunday services for the first time in 200 years. In 1950, repair works were carried out by the Ministry of Works, during which a multi-media, multi-layered surface treatment was painted onto the interior stone surfaces. Despite these well-intentioned though often misguided, conservation attempts, Rosslyn Chapel was in a serious state of deterioration by the 1990's, suffering from damage to the original stone fabric due to stone decay, previous conservation treatments and other interventions. This paper will give a brief description of Rosslyn Chapel's condition when conservation work began in 2005 and the efforts undertaken by Nicolas Boyes Stone Conservation (NBSC) that have significantly improved the chapel's condition since then, including a mixture of traditional stone masonry skills and new technology such as conservation lasers.

2. Conservation works

2.1. Treatment of stone decay

Rosslyn Chapel is constructed of carboniferous sandstone from two nearby quarries. Over time, the original stone fabric has suffered from several processes of decay, resulting from the exposed position of the Chapel, the ingress of water through the roof and the subsequently high level of moisture throughout the building. Many other factors contributed, as well, including a range of misguided previous repairs. As a result, Rosslyn Chapel exhibited several types of stone decay, including cracks, pits, scaling, disaggregation, delamination, and loose or lost fragments. The first step in addressing these problems was the erection of a steel canopy over the entire structure in the 1990's to allow for the chapel to dry out for an extended period of time. Once the building had sufficiently dried out, NBSC began careful consolidation works on the deteriorated stone. Areas of scaling, disaggregation and cracking were treated by first using soft brushes and air 'puffers' to remove all loose material from the affected areas. Areas were then treated by injecting a solution of 10% (w/v) Paraloid B72 acrylic resin in acetone into or over affected areas, using a syringe and hypodermic needle. Where cracks, pits or areas of scaling were identified as requiring consolidating fills, an acrylic resin based repair mortar was applied. Repair mortars were designed, according to each individual fill required, to be sympathetic to the host stone in terms of colour, texture and durability. In order to do this, aggregates were selected from a prepared range to closely match the host stone. This was achieved by collecting a range of sandstones recovered from remedial masonry works to the nearby ex-visitor's reception building. These were crushed and divided into groups according to their colour. The crushed stone was then sieved to achieve coarse and fine fractions of aggregates. Subsequently, to avoid any introduction of salts into masonry, aggregates were desalinated by washing in still water. Aggregates were left in containers filled with deionised water, and water was changed every day for a week. This caused the water soluble salts to diffuse out of the aggregates into the water. Finally, all aggregates were dried properly and stored, ready to mix with Paraloid B72 solution to create repair mortars.

In addition, if the correct colour could not quite be achieved, some earth pigments were added to repair mortar to properly match the stone colour. Earth pigments like sienna, ochre, umber and natural iron oxides were used because of their natural appearance and their compatibility with mineral composition of sandstones. The ultimate function of these repair mortars is to be less durable than the host stone and thus work as a renewable sacrificial element in order to protect the vulnerable host stone against effects of preferential weathering.

2.1.1. Response to previous treatments

Previous conservation efforts, although well-intentioned, also contributed to the deterioration of the building over time and needed to be reversed. These included the application of a layer of asphalt over the roof, use of Ordinary Portland Cement (OPC) mortar in construction joints and installation of ferrous clamps.

2.1.2. Asphalt roof removal

A thick, hard, brittle layer of asphalt had been applied to the barrel roof, Lady Chapel, and North and South Aisle Clerestory level roofs as a protective measure during conservation works in 1954, in line with current thinking at the time. Works were undertaken to carefully remove this asphalt layer. This was a delicate process and was conducted using hand tools to minimize any damage to the original stonework beneath, whether through vibration or direct contact with the tools. A range of sharp tungsten tipped chisels and nylon mallets were used for this purpose. Similarly the number of conservators conducting these works at any one time was kept to a minimum; only one worked on the barrel and Lady Chapel roofs at one time. All construction joints on the external barrel roof pointed with OPC mortar were carefully raked out and re-pointed in a traditional lime mortar. The asphalt removed from the North and South Aisle roofs took a slightly different form from the other areas. They were found to have a similar thick, hard top layer of asphalt, which was carefully removed using the same methods as in the previous areas. Beneath this top layer, however, the stone surface was found to be covered with a very sticky and soft asphalt residue, firmly adhering to the stone surface. This residue was removed from the stone surface by gently “pecking” with sharp chisels. In this way small parts of asphalt residue were chipped revealing a striped tooled stone surface. The surface of the stone laying on the north aisle roof was largely in good condition. The surface of the stone laying on the south aisle roof was in contrast often quite friable and delaminated. Fragments lost due to such delamination were re-attached where possible using strategic quantities of thixotropic polyester resin. Friable areas were consolidated where necessary using acrylic B72 solution in acetone.

2.1.3. Asphalt run-off cleaning

A number of asphalt runoffs were visible, and it was decided to conduct a series of cleaning trials to determine the most appropriate and sympathetic method of removing them. These trials included the use of chemical solvents, laser treatment and mechanical tools. Ultimately, it was decided that mechanical tools alone (including scalpels and sharp chisels) were the best method for the removal of asphalt run offs, assuming that the utmost care was given at all times to ensure no damage to the stone surfaces. This gave the same result as the chemical method but without any smearing effect caused by the solvents. The remaining asphalt run offs were removed in this manner.

2.1.4. Portland cement removal & Lime mortar repointing

Significant portions of the chapel's construction joints had been repointed with OPC mortar during an earlier intervention. OPC is harder and less breathable than traditional lime mortar, causing sacrificial erosion of the surrounding stone as it deteriorates due to the excess moisture. Because of this, it was important to remove all OPC from the joints at Rosslyn Chapel and repoint them with traditional lime mortar. All construction joints identified as requiring re-pointing were carefully raked out using sharp tungsten tipped chisels and mallets to a sufficient depth to accept lime mortar repair (*Fig. 1*). Any loose material within the joint that could decrease the adhesion of the mortar was removed in a scooping action using a tool of appropriate width to ensure no marking of the dressed stone surface occurred. The joints were next washed out with water to remove any remaining debris or dust.



Fig. 1: Raking out vault joints.

Construction joints were then re-pointed using an appropriate lime mortar mix. Immediately prior to re-pointing, the joints were sprayed with water to prevent the lime mortar from drying too quickly. This was applied to the joint using hand tools of appropriate width to prevent marking the dressed surface, pushed deep into the joint and filled until the mortar was slightly full of the joint. In the cases where the joints were very deep or wide they were packed also with slate or porous sandstone pieces, terracotta tiles or oyster shells, all soaked first in water, to prevent shrinkage and improve the setting characteristics and durability of the lime mortar. The mortar was then pressed back using steel hand tools, covered with damp hessian and protected from the wind by tarpaulins, so as to prevent premature drying out and left to carbonate for 2-3 days. During this period of carbonation the lime mortar pointing and hessian was repeatedly sprayed with water. The surface of the lime mortar was scraped with a wooden scraper and "stippled" with a fibre bristle brush as the mortar stiffened. Care was taken to ensure the style of pointing matched the original as much as possible. A number of small lime mortar repairs were also conducted at various locations on the Chapel; these were conducted in much the same manner as the lime mortar pointing. Where necessary, grooves were cut into the stone surface using tungsten tipped chisels and mallet, to provide a key on to which the mortar would adhere more easily. Immediately prior to the application of this mortar, the surface

was sprayed with water to prevent the lime mortar from drying too quickly. Mortar was then applied to the surface using spatulas to model the repair into the correct shape. A conservative approach was adopted to fills so only the necessary repairs were made – no speculative remodelling was completed. Where repairs were particularly deep, they were completed in layers, to prevent excessive shrinkage causing cracking and failing of the repair. Each layer was given a new ‘key’ on to which the next layer might more easily adhere. The rest of the process was completed in a manner similar to that used in the re-pointing of construction joint previously described.

2.1.5. Ferrous cramp replacement

Approximately 150 ferrous dog cramps were identified in the ground level plinth course of each of the Chapel bays, at the North, South and East and West elevations. These were causing significant damage to stonework as a direct result of their expansion and the subsequent pressure causing cracking and fragmentation of the stonework. In some areas the damage had already been done and fragments of stone as well as the original iron cramps had long since been lost. A trial was conducted to remove one such cramp and insert a more sympathetic stainless steel replacement. The original ferrous cramp was removed very easily due to its advanced state of decay, using simple hand tools. The resulting gap was then measured in order to cut a replacement cramp to the appropriate size. For this, a 12mm threaded rod stainless steel cramp was used. The resulting gap was cleaned out thoroughly using soft bristle brushes and the cramp was inserted. This was adhered into place using strategic quantities of thixotropic polyester resin. The construction joints directly above and below were pointed using traditional lime mortar as follows, using the method described in section 2. On the success of the initial trial, works commenced to replace the remainder of the cramps using the same method as outlined above.

2.2. Rebuilding works and replacements

2.2.1. Pinnacles, finials and ribs

All pinnacles, the East gable finials and a number flying buttresses were identified as unstable to varying degrees and requiring careful deconstruction or partial deconstruction to remove all ferrous dowels causing oxide jacking and movement within the structures, as well as failed bedding mortar, debris and any vegetation/roots growing within joints). Careful reconstruction could then be conducted. This process was conducted as follows. Construction joints filled with OPC mortar were raked out using sharp tungsten tipped chisels and mallets. Any loose material within the joints was removed in a scooping action. A chain hoist was set up directly above the identified pinnacle, finial or rib and each course slung with lifting slings one by one and lifted carefully onto nearby softening. Stones were marked to ensure replacement in the correct order and directions. At this point any identified ferrous fixings were removed using hand tools and electric drills where required. The beds of each dismantled stone were cleaned thoroughly of mortar and debris using chisels and a mallet and brushed clean with soft bristle brushes, prior to inserting new stainless steel 12mm threaded rod dowels to replace the original fixings or as additional fixings where required. These were fixed into position using strategic quantities of thixotropic polyester resin. In some cases further stainless steel or phosphor bronze cramps were inserted due to cracks or other failures within the stones. Beds were then thoroughly wetted with clean water to remove any surplus dust/debris, and once again prior to applying the bedding mortar to prevent it from drying out too quickly. Lime mortar was laid across

the beds using a hand trowel and the stones lifted back into place, using slings and a chain hoist. The resulting construction joints were re-pointed using a traditional lime based mortar.

2.2.2. *Indents*

Following a detailed survey of the building, a number of items were identified as requiring new stone indents. These were only specified when deemed absolutely necessary to the structural integrity of the building. For example, where structural components such as window arches and tracery were failing and it was no longer possible to simply consolidate existing stone, new stone indents were specified to prevent the surrounding historic stone fabric from falling into disrepair (Fig. 2).

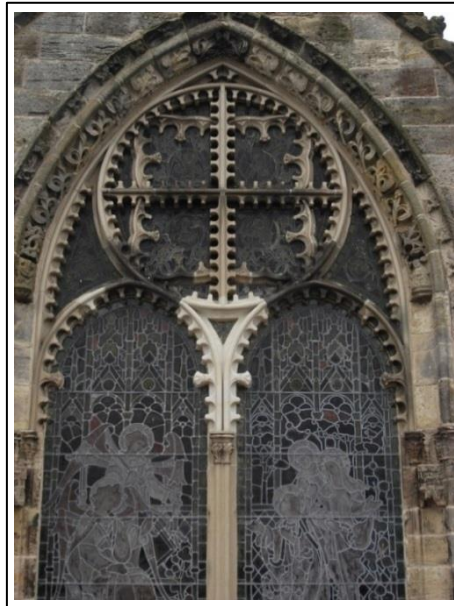


Fig. 2: Indent in East window tracery.

It was vital that the stone used for indents matched the original stones in terms of general appearance, texture, porosity, micro properties and mineral composition. This was to ensure that the new stone performed in a similar manner to the original stone under the influence of various conditions and thus ensure long term compatibility. In order to select the most appropriate stone for indents, two Building Stone Assessments (Geo Reports) were conducted by British Geological Survey.

2.3. *Response to other alterations*

2.3.1. *Biological growth removal*

Due to the exposed location of the Chapel, the external stonework is affected by a range of biological growth, including lichen, algae and moss. The South elevation suffered to a lesser degree than the North, but upper exposed features such as the pinnacles, finials and ribs were still affected. This biological growth was reduced in a number of locations to improve visibility of the stonework beneath and allow an accurate assessment of the

condition of the stonework. Lichens and moss were largely removed dry with the aid of scalpels, dental tools and brushes. Algae and the more stubborn lichen was further reduced using water from typical hand held sprayers and brushes. The run-off was removed using a sponge to prevent transportation of spores down the masonry.

2.3.2. *Salt efflorescence*

Salt efflorescence was identified all over the chapel. This salt efflorescence phenomena is produced in this area due to an increase of moisture produced by the water dispersal system, which was designed to shed water from the building at height. This system does not appear to have functioned successfully due to the exposed position of the chapel, and much of the dispersed water would have been directed back onto the walls at a lower level. This increase in water residence on the masonry resulted in an enhanced flux of moisture to the surface by evaporation resulting in cryptofluorescence and the subsequent blistering. Salt efflorescence was treated at the most advanced areas where salts were further contributing to other decay mechanisms. All loose material on the surface was carefully removed using scalpels, dental tools, soft brushes and a vacuum cleaner to prevent reintegration into the stone. At this stage any blistering identified in combination with salt efflorescence was also removed using the same method. Salts were then removed by applying poultice applications of acid-free tissue paper pulp and clean de-ionised water, in order to draw the identified salts from the surface of the stone into the poultice. Repeat applications were applied as necessary.

2.3.3. *Desoiling*

The Nd:Yag Conservation Laser was employed throughout this project to reduce the level of environmental pollution products affecting the Rosslyn Chapel stonework (*Fig. 3*). The level of soiling to be removed was determined after much discussion and a number of trial areas. Soiling was initially identified as heavy, medium and light, and a distinction was made between soiling visibly causing 'preferential erosion,' or the visible accelerated decay of adjacent stonework, and that causing no apparent immediate harm.



Fig. 3: Desoiling using Nd:Yag Conservation Laser System.

In line with the conservative approach of all conservation works, soiling identified as requiring removal was restricted to the 'heavy' or 'medium' soiling (the thickest, most homogenous) at carved detail that was visually disfiguring or causing accelerated decay to adjacent or underlying valuable carved stonework. Similarly, the 'heavy' or 'medium' soiling was not entirely removed but reduced to a 'medium' or 'light' level where appropriate. In this way the stonework suffering from decay related to this soiling was safeguarded against further decay but no unnecessary work was conducted. Aesthetically, soiling was reduced in a manner to promote a consistent view of the stonework, and importantly to improve the visibility of carved stonework previously concealed from view.

3. Conclusions

Since 2005, Nicolas Boyes Stone Conservation has conducted a series of conservation works at Rosslyn Chapel to slow the deterioration of the historic stone fabric caused by natural stone decay, previous misguided interventions and other transformative alterations. These works included the use of traditional masonry techniques as well as new technologies and chemical treatments. The conditions of the chapel have improved significantly thanks to these efforts. In the future, it is hoped that work will continue with the removal of the cement layer covering the chapel's interior surfaces.

References

- Cameron, S., *et al.* (1997). *Biological Growths on Sandstone Buildings: Control and Treatment*, Edinburgh, Historic Scotland.
- Forbes, R., (1761). An account of the CHAPEL or ROSLIN, &c. Most respectfully inscribed to WILLIAM ST. CLARE of ROSLIN, Esq; Representative of the Princely Founder and Endower, *The Edinburgh magazine*, v-xii.
- Historic Environment Scotland, "Roslin, Roslin Chapel," (<https://canmore.org.uk/site/51812/roslin-roslin-chapel>, accessed 25th November 2015).
- ICOMOS-ISCS, (2008). *Illustrated glossary on stone deterioration patterns, Monuments and Sites*, XV, Verges-Belmin V. (ed.), Champigny/Marne, France.
- MacGibbon, D. and Ross, T., 1896. *The ecclesiastical architecture of Scotland: from the earliest Christian times to the seventeenth century*, Edinburgh, D. Douglas.
- Maxwell, I., (2007), *Inform Guide: Cleaning Sandstone - Risks and Consequences*, Edinburgh, Historic Scotland.
- Parker, J. H., ed., *Restoration of Roslin Chapel, The Gentleman's Magazine: and historical review*, July 1856-May 1868, 212 (May 1862), 599.
- Urquhart, D., (2007), *Stonemasonry Skills and Materials: A methodology to survey sandstone building facades*, Edinburgh, Historic Scotland.
- Snow, J. and Torney, C., (2014), *Short Guide: Lime Mortars in Traditional Buildings*, Edinburgh. Historic Scotland.

LABORATORY AND IN SITU EVALUATION OF RESTORATION TREATMENTS IN TWO IMPORTANT MONUMENTS IN PADUA: “LOGGIA CORNARO” AND “STELE OF MINERVA”

V. Fassina^{1*}, S. Benchiarin² and G. Molin²

Abstract

In the present study, an evaluation of the durability of consolidation products, commonly used on historical buildings of Padua in the last four decades, was carried out on two significant monuments. Non-destructive and micro invasive tests were performed *in situ* as well as in the laboratory. In the Loggia Cornaro, *in situ* water absorption tests (EN 16302) showed a higher moisture absorption uptake in the lower parts of the monument than those carried out on the upper parts. This suggests that surfaces close to the basement are more susceptible to environmental decay than the upper ones. The different deterioration patterns observable seem to support this suggestion. Stone blocks of the basement and of the lower parts are characterized by significant amounts of clay minerals as detected by SEM investigations on cross-sections of the extracted samples. Clay minerals occur near cracks and microcracks and are also extensively found in the inner parts of the stone far from the external surface. Surface observations of bulk samples revealed different situations. In the Loggia Cornaro, some areas show a widespread resin coating, visible on SEM images, which present a smooth skin with occasional cracks and microcracks. On the contrary, other areas show coating layers recognisable by the smooth appearance of calcite crystals. The latter situation also occurs in the Minerva Stele surfaces, although the layer is less evident. No appreciable traces of resin, except in some isolated cases, were observed on this monument. The depth of penetration of the resin into the stone and its internal distribution was investigated by SEM mapping of silicon, which is assumed as a marker of the consolidant material used. Cross-sections of treated specimens proved to be particularly good in detecting and discriminating polymer distribution from the inorganic matrix and are very useful in observing polymer and substrate relationships.

Keywords: deterioration patterns, durability, siloxane polymers, ethyl silicate

¹ V. Fassina*

Honorary Inspector of Superintendency to Cultural Heritage of Veneto, Italy,
vasco.fassina@gmail.com

² S. Benchiarin and G. Molin

Dipartimento dei Beni Culturali, Università degli studi di Padova, Italy

*corresponding author

1. Introduction

In Padova, between 1975 and today, a lot of restoration interventions have been performed on external stone surfaces using silicone polymers (Fassina et al, 1985). While there are many reports on the performance of water repellents and consolidants in laboratory based situations (Apollonia *et al.*, 2001; Alvarez *et al.*, 2001, D'orazio *et al.*, 2001; Cardiano *et al.*, 2002; Favaro *et al.*, 2006, 2007), conservation scientists should be aware that results from stone samples treated in the laboratory are not necessarily representative of those which would be obtained on real buildings. In the laboratory, samples can be effectively impregnated. However, on building surfaces it is seldom possible to achieve the same level of control. Laboratory based applications therefore produce more reproducible results than the ones that can generally be expected in the field. Despite these difficulties, laboratory based tests can provide a useful indication of the potential performance of a treatment where the volume of sample and its situation are a good simulation of the building façade. More recently, comprehensive studies on chemical deterioration of these synthetic polymers have been performed with particular emphasis to their behaviour when applied on stone surfaces, especially taking into consideration the deterioration of building materials treated with polymers (Fassina *et al.*, 2004, Favaro *et al.*, 2005). To know the condition of the treated stones it is of great relevance to identify and characterize the polymer applied on previous treatments and the related decay by-products, in order to understand the deterioration pathways they undergo after a long term exposure to outside atmospheric environment. The polymer deterioration in outdoor conditions can modify both their chemical composition and physical properties: chemical decay leads primarily to the formation of oxidized species, which quite often produce yellowing of the treated stone surfaces; on the other side physical changes induce a stiffening and brittleness of polymers which often result in polymer fissures, detachments from the stone substrate and worsening of mechanical properties (Melo, 1999).

In the present study the evaluation of the durability of restoration products, commonly used on historical buildings of Padua in the last four decades, was carried out on two significant monuments. Loggia Cornaro, made in Nanto stone, is an important example of Renaissance architectural building, underwent to restoration works in this period (Fig. 1). After twenty years from the first intervention and four from the latest, a survey on the condition and the residual efficiency of treatments was carried out by means of *in situ* tests and analytical laboratory techniques. Another important artwork restored two decades ago is "The Stele of Minerva", made in Yellow San Germano Stone. The presence of significant deterioration patterns on the monument façade like strong differential decay, white and black features, surface deposits, etc. were observed (Fig. 2). Two main types of products were used for restoration. The first is Rhodorsil RC70 (from Rhodia), ethyl silicate, at a concentration of 70% and a density of 0.9 kg/dm³, in the form of a transparent liquid, diluted in white spirit and designed for pre- and post-consolidation operations. After consolidation, a final application of methylsiloxane as water repellent was applied to the Minerva Stele. The second type of restoration product, a methylphenyl-polysiloxane resin, Rhodorsil RC 90, designed for consolidation and protective operations, was applied to the Loggia Cornaro.



Fig. 1: a) Loggia Cornaro; b) Minerva stele.

2. Experimental part

The evaluation of treatments was carried out using a non-destructive technique, as well as laboratory methods that require sampling from treated parts.

- a) The in situ water absorption test EN 16302 provides a simple method for measuring the volume of water absorbed by a material within a specified time period and represent a measure of the susceptibility of the stone to take up water through the exposed surface. This test is one of the specific measurements carried out to evaluate the efficacy of water repellent treatments applied to stone materials. An effective treatment should substantially reduce permeability of the stone material to water. By doing so, the treatment will reduce the material's vulnerability to water-related deterioration. The field areas to be tested were selected to ensure that the site equipment can conveniently be used in each position. Typically, four points along the perpendicular, at different height from the ground, were selected. For the test to be effective, a relatively smooth surface, free from dust, debris and organic growth, is required. At least three sets of readings were taken at each test area.
- b) Optical microscopy. Observations by U-polarisation microscope at different magnification, on thin sections, were carried out to define the textural parameters and obtain a detailed petrographic characterization of the stones employed. Also reflected light microscopy observations on cross sections were performed.
- c) Scanning Electron Microscope (SEM). Texture, distribution and penetration depth of the polymer of treated samples have been observed by Camscan MX2500 scanning electron microscope equipped with an energy dispersive micro-analyser (SEM-EDS). Both stone surfaces (SE images) and sections perpendicular to the exposed surface (BS images) were analysed. All specimens were coated with a graphite film before SEM-EDS investigations.

3. Discussion of the results

3.1. In field evaluation of consolidation treatments

In situ water absorption tests (EN 16302) for the Loggia Cornaro, showed that moisture absorption uptake of the lower part of the monument was higher than the one measured on the upper parts. This suggests that surfaces close to the basement are more susceptible to environmental decay than the upper ones, and, indeed, different deterioration patterns were found. The basement and lower parts have a strong marly component ascribed to significant amounts of clay minerals (Fig. 2). Clay minerals occur near cracks and microcracks and are also extensively distributed in the internal part far from the façade surface.

The stone of the upper part of the façade belongs to a stratigraphic horizon with lower contents of clay minerals, thus explaining the good condition and probably lower moisture uptake. Measurements made vertically at various points showed moisture uptake values between 0 and 0.04 ml/cm². In general, these values are still quite low compared with those of the untreated limestone (110 ml/cm²). The lower values in most of the vertical locations indicate that, after four years, the treated surfaces are still sufficiently water-repellent. However, water is clearly able to penetrate into the various parts of the building, albeit slowly. The build-up of small amounts of water behind some surface areas probably indicates that the effectiveness of the treatment is deteriorating in these areas, and they may need attention in the near future. The surfaces of Stele di Minerva could not be examined, owing to the fact that the pipe tube could not be used on its vertical surfaces.

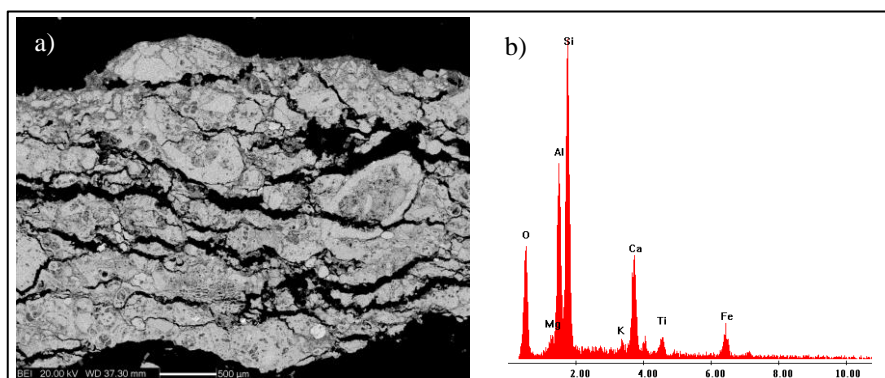


Fig. 2: a) Typical appearance of stone of lower part of the façade with deep microcracks parallel to the external surface are visible; b) Microanalysis of clay minerals.

3.2. Evaluation of penetration depth of consolidation treatments

In order to study the stone behaviour, small specimens from the surfaces of the two monuments were taken and analysed in laboratory. The depth of penetration of the resin into the stone and its internal distribution were studied by SEM. Cross-sections of treated specimens proved to be particularly good in detecting polymers and their interaction with the substrate. The technique was capable of discriminating polymer distribution from the inorganic matrix.

Surface observations of bulk samples revealed different situations. In the Loggia Cornaro, some areas show a widespread resin coating, visible in SEM-BS images, which present a smooth skin with occasional cracks and microcracks. On the contrary, other areas show coating layers recognisable by the smooth appearance of calcite crystals, visible in SEM-SE images. The latter situation also occurs in the Minerva Stele surfaces, although in the latter case the layer is less evident and no appreciable traces of resin were observed, except in some isolated cases. SEM observations show that ethyl silicate precipitates as an amorphous SiO_2 layer, which covers some portions of the stone surface while in the inner part of the stone pore and capillary walls were partially coated by amorphous silica, which does not always seal them. In the Loggia Cornaro, the substrate is covered by a very compact external layer of silicon-based composition ascribable to polysiloxane polymer with thickness ranging from 10 to 100 μm . However, this covering layer was not observed in all samples, and often it is irregular in thickness and continuity on the surface. (Fig. 3).

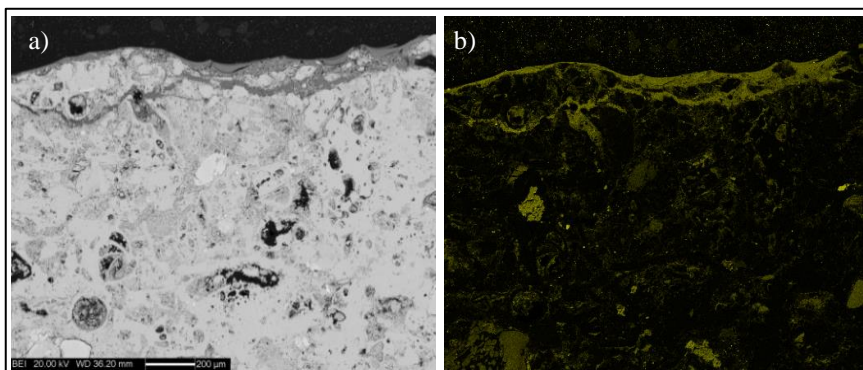


Fig. 3: Loggia Cornaro, sample LC 18: a) SEM-BS image of mapped area; b) Si- K_{α} X-ray map showing the resin distribution and a Si rich layer on the surface.

Evidence of penetration of polymer inside the stone are frequent in several samples, even if only some cracks are filled with siloxane compared to the totality of fissures. In some samples penetration path can be visualised by means of X-ray maps on cross sections of calcium and silicon as markers respectively of calcium carbonate substrate and silicon-based consolidant. These images show a higher content of Si component on the external layers of stone surface (Fig. 3b). The in depth penetration of polymeric product inside cracks is clearly visible in Fig. 4.

The situation for the Minerva Stele samples was quite different. Here, only some samples had external coatings, due to the protective substance being not very adhering to the substrate thus showing pores and voids between coating and substrate. The presence of this fill substance, was ascertain for little thickness, in general to a depth of 800 μm . It seems in general loose from the substrate but incorporate a lot of carbonate particles.

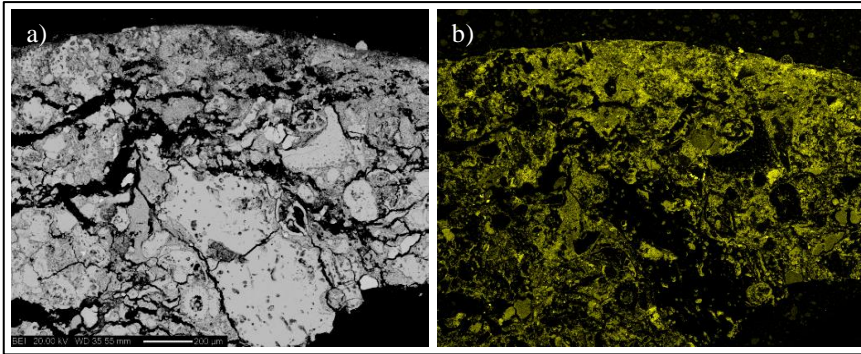


Fig. 4: Loggia Cornaro, sample LC 24: a) SEM-BS image of mapped area; b) Si- K_{α} X-ray map showing the resin distribution.

X-ray maps of calcium (calcium carbonate) and silicon (silicone products) markers made on cross sections show a certain deposition of silicon polymer inside the pores and a higher concentration on the surface (Fig. 5).

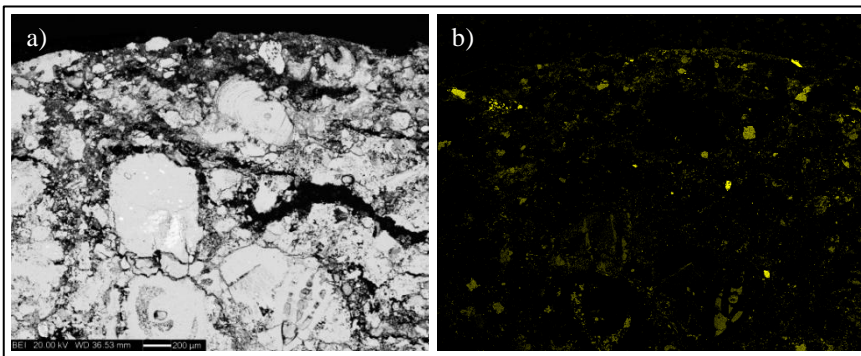


Fig. 5: Minerva Stele, sample SM 18: a) SEM-BS image of the cross section of sample SM 18; b) Si- K_{α} X-ray map showing the sparse resin distribution and numerous grains of silica minerals

In the Loggia Cornaro, the samples do not exhibit the typical external deposition layer of carbonaceous particles and gypsum crystals due to the accumulation of pollutants. In the Minerva Stele, the extensive presence of gypsum as both lenticular crystals and compact crusts was evident. The former occur in areas where the polymer has probably disappeared and consequently the decay process is starting again. X-ray silicon distribution maps indicate a silicon-based treatment. Silicon distribution is very different in the two monuments. All samples show that silicon is homogeneously distributed to a depth of 1 mm, but the Loggia Cornaro samples have 5 to 10 times higher amount of silicon than those ones of the Minerva Stele. In both monuments, however, many cracks in depth (to 3 mm) are empty. In particular, in the Loggia Cornaro, a series of microcracks parallel to the surface is not filled by the resin, although others at a greater depth are filled. The depth of penetration of newly formed decay products was also quantitatively studied by means of a thin drilling core micro-sampling system. Various locations were investigated by

considering samples every 2.5 mm of thickness up to a depth of 10 mm. In the Minerva Stele sulphates amount, representing the gypsum presence, is decreasing from a maximum of 17% in external layer from 0 to 2.5 to a minimum of 0.5% for the 7.5-10 mm. depth. In the Loggia Cornaro, the sulphate amount is decreasing from 2% to 0.2% from the external to the internal layer, probably due to incomplete cleaning operations; in the Minerva Stele there is evidence of decay ascribable to atmospheric pollutants.

4. Conclusions

Performance evaluation of treatments on two monuments in the city of Padova was performed, respectively four and twelve years after restoration operations, and it was aimed at verifying their effectiveness and durability. Cross-sections of treated samples proved to be particularly useful in detecting synthetic products applied. Distribution and changes in structure and adherence to the substrate were ascertained with good precision. Applying the test results, it is possible to make initial evaluation of the effectiveness of a surface treatment or if a previously treated surface has become ineffective. A shift in pore size distribution towards smaller pore radii, as well as the percentage reduction of larger pores, was observed in our treated stone samples, and it is attributed to the deposition mechanism of the consolidant on the pore surfaces (formation of films or precipitation as amorphous SiO₂).

Penetration depth of the consolidant and new formation of decay products show that silicon concentration generally decreases from the external surface inwards in both monuments. SEM-EDS analysis of the cross sections showed large quantities of silicon on the surface down to a depth of 300 µm.

As regards the new decay formation products, the deposition of sulphur-based compounds has slightly influenced further gypsum formation in the Loggia Cornaro. In fact, no very important decay was observed, and cross-section analyses showed the widespread presence of residual amounts of still active consolidant and protective coating. The salts currently present were probably insufficiently removed before consolidation. In the Minerva Stele a significant amount of gypsum was detected thus enhancing more marked decay phenomena with respect to the Loggia Cornaro. Residual traces of treatments, but not very abundant were found.

Polymer application has certainly slowed down, but not completely halted, the deterioration processes of the stone materials examined here. Decay due to atmospheric pollutants has been greatly reduced, but it has rarely been possible to prevent the penetration of salt solutions or mitigate the effects of moisture and temperature changes, which undoubtedly cause disruption within the pore structure as a consequence of mechanical stresses.

These results indicate that certain treatments applied to the monuments have already deteriorated to such an extent that a re-treatment needs to be considered soon. Data obtained in the case of Loggia Cornaro are still generally within acceptable values. We suggest that maintenance should be carried out in the near future by renewing the protective coating on the whole surface and by consolidating the stone in some areas which are not in a good state of conservation. In both cases, however, this type of stone may need a maintenance gentle surface re-treatment approximately every five years.

References

- Alvarez de Buergo Ballester M., Fort Gonzalez R., 2001, Basic methodology for the assessment and selection of water-repellent treatments applied on carbonatic materials. *Progress in Organic Coatings*, 43, 258-266.
- Apollonia L., Borgia G.C., Bortolotti V., Brown R.J.S., Fantazzini P., Rezzaro G., 2001, Effects of hydrophobic treatments of stone in pore water studied by continuous distribution analysis of NMR relaxation times. *Magnetic Resonance Imaging*, 19, 509-512.
- Cardiano P., Sergia S., Lazzari M., Piraino P., 2002, Epoxy-silica polymers as restoration materials. *Polymer* 43, 6635-6640.
- D'Orazio L., Gentile G., Mancarella C., Martuscelli E., Massa V., 2001, Water-dispersed polymers for the conservation and restoration of Cultural Heritage: A molecular, thermal, structural and mechanical characterization. *Polymer Testing* 20, 227-240.
- EN 16302, many authors, Conservation of cultural heritage-test methods-Measurement of water absorption by pipe method. CEN TC 346, European Committee for Standardization.
- Fassina V., Cherido M., 1985, The Nanto stone deterioration and restoration of Loggia Cornaro in Padova, *Proceedings of 5th Int. Congress Deterioration and Conservation of Stone*, Felix G. (eds.), Lausanne, Polytechniques Romandes, 313-324.
- Fassina V., Pezzetta E., Cherido M., Naccari A., Melica D., 2004, A survey on the behaviour of restoration materials of the Loggia Cornaro in Padova after fifteen years, *Proceedings of the 10th Int. Congress on Deterioration and Conservation of Stone*, Kwiatkowski D., Lovendahl R. (eds.), Stockholm, 415-422.
- Favaro M., Mendichi R., Ossola F., Russo U., Simon S., Tomasin P., Vigato P.A., 2006, Evaluation of polymers for conservation treatments of outdoor exposed stone monuments. Part I: Photo-oxidative weathering. *Polymer Degradation and Stability*, 91, 3083-3096.
- Favaro M., Mendichi R., Ossola F., Simon S., Tomasin P., Vigato P.A., 2007, Evaluation of polymers for conservation treatments of outdoor exposed stone monuments. Part II: Photo-oxidative and salt-induced weathering of acrylic-silicone mixtures". *Polymer Degradation and Stability*, 92, 335-351.
- Favaro M., Simon S., Menichelli C., Fassina V., Vigato P.A., 2005, The four virtues of the Porta della Carta, Venice-Assessment of the state of preservation and re-evaluation of the 1979 restoration, *Studies in Conservation*, London, 50, 109-127.
- Melo M.J., Bracci S., Camaiti M., Chiantore O., Piacenti F., Photodegradation of acrylic resins used in the conservation of stone", *Polymer Degradation and Stability*; 66, 23- 30.

INVESTIGATIONS GUIDING THE STONE RESTORATION OF THE “SCHÖNER ERKER” IN TORGAU, GERMANY

C. Franzen^{1*}, H. Siedel², S. Pfefferkorn³, A. Kiesewetter⁴ and S. Weise⁵

Abstract

As part of the planning for the restoration of the Schöner Erker, a sandstone oriel in Schloss Hartenfels in Torgau, Germany, extensive preparatory investigations were undertaken. Several questions about the construction and the material properties had to be addressed. Investigation techniques included: metal detection, drilling resistance, thermography, climate measurements, salt and mortar analysis. The results were an important basis for the restoration work including dismantling, transport, desalination, consolidation, rebuilding and formulating protective treatment. The now-completed measure makes a striking new impression in the courtyard of the castle due to the spirited colours of the surface finish. The paper recounts how the measurement results determined the stone restoration decisions on the various parts of the oriel.

Keywords: Elbe sandstone, pre-investigation, salt deterioration, stone conservation

¹ C. Franzen*

Institut für Diagnostik und Konservierung an Denkmälern in Sachsen und Sachsen-Anhalt e.V.
(IDK), Dresden, Germany
franzen@idk-denkmal.de

² H. Siedel,

Technische Universität Dresden, Institut für Geotechnik, Dresden, Germany

³ S. Pfefferkorn

HTW Dresden, FB Bauingenieurwesen / Architektur, Dresden, Germany

⁴ A. Kiesewetter

Landesamt für Denkmalpflege Sachsen, Dresden, Germany

⁵ S. Weise

Heidelmann&Klingebiel Planungsgesellschaft mbH, Dresden, Germany

*corresponding author

1. Introduction

The architectural building element "Schöner Erker", which could be translated: the Beautiful Oriel Window, was built in 1544 in Schloss Hartenfels. It is one of the most important achievements of sculptural art from the Early Renaissance in Central Germany. Within the ensemble of the Hartenfels castle in Torgau it is - in its unity of filigree architecture, ornamentation and figured reliefs - in artistic balance with and complementary to the Großer Wendelstein (Grand Spiral Staircase) in the courtyard.

The Hartenfels castle in Torgau was founded in the 10th century. Extensive construction work was started after 1470 when its status was raised to a Saxon Electoral castle. The central building with the Grand Spiral Staircase was built in 1536. The staircase is one of the boldest and most important staircase structures of the Renaissance in Central Europe. The stairs led to the room of the Elector of Saxony. - Building of the castle church started in 1540. It was consecrated by Martin Luther in 1544 as the very first Protestant church. The "Schöner Erker" (Beautiful Oriel) was built directly beside the castle church in the same year. Its carved decorations are ascribed to the Leipzig sculptor Stephan Hermsdorf. Hartenfels Castle developed into one of the most important seats of the Saxon Electors in the 16th and 17th centuries. The castle came into the possession of Prussia in the middle of the 18th century and became dilapidated by unsuitable usage. It was used as barracks from 1815 until the end of the 19th century. First restoration work on the Schöner Erker, which was in danger of collapse, was started in 1836. The whole oriel was pulled down and rebuilt and clamped together using a great part of the historic stones. The originally three storeys were reduced by one in order to minimise the load. Moreover, it was completely covered with oil paint. In 1927/1928 a new roof was added, the oil paint was removed by means of caustic soda and the stones were partially repaired. In the beginning of the 21st century preparation for a sustainable restoration took several years, not only due to financial causes but also for technical challenges in stone conservation. Finally the restoration was carried out in 2009-11. Some aspects of the investigations for restoration of the oriel window are presented in the paper.

2. Methodology

The history of the oriel was compiled based on archive research. One main focus was the gathering of information about previous damage reports and restoration actions on the oriel. The existence and distribution of iron anchors in the oriel construction was investigated with a metal detector, Elcometer Protovale 331 "CoverMaster". Metal search was undertaken from outside and inside the rooms of the oriel.

Salt analyses were carried out at several stages of the restoration and in different ways. During the pre-investigations efflorescences were sampled and subsequently investigated by XRD, by Siemens D5000, DIFFRAC plus EVA/AUTOQUAN at TU-Dresden. For the investigation on distribution of soluble salt contents in the sandstone material sampling of material profiles by drilling was undertaken. Soluble salts were extracted with deionized water from the drill powder samples and also from poultice material. The total salt content of the samples was determined by evaporating the solution and weighing the remaining dry solid matter. Mg, Ca, K, SO₄, Cl, and NO₃ were quantitatively analysed in the aqueous solution by means of a HACH spectrophotometer using standardized reagents. Na was determined with an ion selective electrode. The results were related to the dry sample mass [wt.-%]. Also poultice application for desalination was analysed. Samples in size of

10×10 cm were taken to laboratory. The correct dimensions of the sample is important for the evaluation of the desalination effectiveness, as this is based on a reference to the area (Franzen 2006). Results of poultice analysis are expressed in g/m^2 following the recommendations of WTA (2005). The 100 cm^2 samples were diluted in 400 ml H_2O and the filtered eluates were used for further analysis. The electrical conductivity, pH (by HANNA HI 991300) and dry residue at 105°C were measured in line with normal practice in building conservation.

Near-surface weathering profiles were investigated by microdrilling resistance. For the in-situ measurement of hardness profiles of historic (building) material like stone, brick and mortar drilling resistance is a well established technique (Pamplona *et al.* 2007). The Durabo drilling systems used here and the procedure are described in Siedel & Siegesmund (2014). Drill bits (Fa. Porzner) with an aperture of $\text{Ø}=3\text{ mm}$ came into use. Drill velocity was stage 2, hammering function, pressure load 1 kg or 2 kg. Due to differences in heat conduction of building parts the temperature distribution of an object gives insight in the construction. Infrared thermography measurements were conducted by VARIOSCAN 3021 ST-camera (InfraTec). The camera detects radiation between 8 and $12\ \mu\text{m}$ wavelengths. Data processing was conducted with IRBIS-professional 2.2.

3. Damage

By the late 1990s the oriel was in a highly problematic state. Irregular visible inspection from the ground and with telescope or also cumbersome out of the windows indicated serious damages and an ongoing damage progression on the sandstone parts. Figures 1a and 1b show the significant damage progress within ten years.

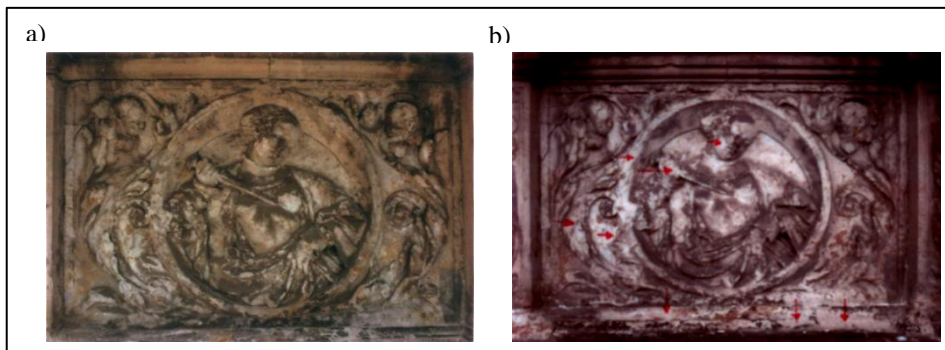


Fig. 1: a) Relief of Lucretia at 1991; b) Relief at 2000 (red arrows point out additional losses compared to 1991).

In 2000 and 2004 more detailed inspection was proceeded by means of a portable hoisting platform. Serious losses in the artistic highly precious reliefs by sanding, soiling and a conspicuous peeling (terms as recommended by Vergès-Belmin *et al.* 2008) was observed pointing out the alarming state. Looking at the total construction losses of joints in many positions and several cracks were detected. Due to risks of falling parts the bottom periphery had to be roped in. A first investigation on the structural conditions raised several questions about the bonding of the oriel into the building and possible anchoring between the sandstone parts. Some cracking seemed to originate from corrosive expansion of iron anchors.

Because many details of the damages and their causes were not clear and the risks of ongoing damage had to be reduced much more understanding was needed. The main decision that had to be made was whether the weathered parts of the oriel could be treated in-situ, or the whole construction dismantled for a more thorough conservation in the restorer's workshop. An international expert panel, meeting in 2004 recommended detailed conservation scientific research on the oriel to address a series of questions.

4. Sandstone

The oriel is built from Cretaceous sandstone quarried about 100 km SE upstream the river Elbe. All artistic parts are carved in the Cotta type Elbe sandstone which is a fine to medium grained, clay-bearing quartz sandstone. This relatively weak sandstone has been widely used for centuries, particularly for sculptures in Saxony (Götze *et al.* 2007). Siliceous bonding is dominant and the grainsize lies in the range of 63 to 200 μm . Along the bedding planes pore filling cements consisting of the clay minerals illite and kaolinite can be found occasionally. The median pore diameter is approximately 1 μm . Petrophysical properties of the material, which are strongly dependent on the clay mineral content, are given in Tab. 1.

Tab. 1: Petrophysical properties of Cotta type Elbe Sandstone.

Compressive strength¹	Flexural strength¹	Porosity	Capillary water uptake	Water vapour diffusion, μ	Hydric dilatation
MPa	MPa	vol.-%	$\text{kg}/\text{m}^2\text{h}^{0.5}$		mm/m
33.5–37.4	4.1–5.4	22.8	1.3–5.5	11–21	0.3–0.9

¹ tested by MPA Dresden

5. Construction

To understand the bonding of the oriel into the castle building the interior plaster was partially removed. Prior to that a conservator inspection of the wall paints made sure that in and near to the oriel no original plaster and colours could be found. With a metal detector several anchors clamping oriel parts to the building masonry could be traced. These inner anchors showed a good state in terms of corrosion. A different picture was gained from the external inspection. All the reliefs were fixed into the construction by iron anchors (Fig. 2) which showed serious corrosion in places. Moreover it became obvious, that neither the cramps nor single reliefs could be taken out of the construction without severe damage to the sandstone masterpieces.

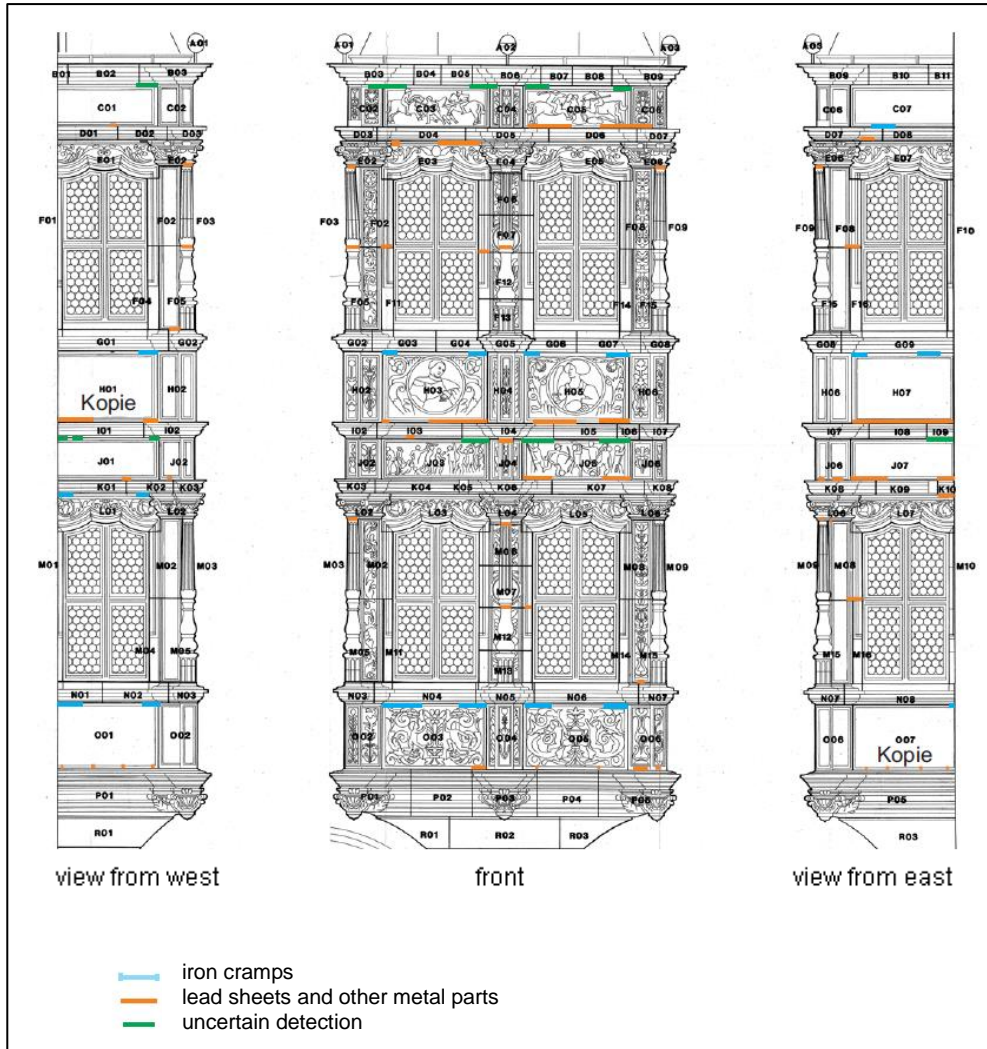


Fig. 2: Distribution of iron cramps and anchors shown on a base plan which identifies all stone pieces. "Kopie" indicates pieces replaced in 1928.

6. Salt

6.1. Salt content

Salt content of the sandstone was investigated by sampling of powder from the drilling profiles. Samples were taken at 5 mm intervals for the first 2 cm, and after that at 1 cm intervals to a total depth of 5 cm. All profiles showed a similar trend with respect to the salt concentrations. In the first 5 mm interval, and partially also in the second until 1 cm depth, soluble salts were present in amounts higher than 2 wt.-%. Sulphate contents were rated as "extreme" taking into account the scheme of WTA (2005). To the next steps there is a

remarkably reduction of soluble salt contents to values lower than 1 wt.-% (Fig. 3a and 3b). Near the surface sodium, as well as some nitrate was detected, besides abundant calcium. Those concentrations vanish in greater depth. Sulphate is the dominant anion in all steps, but in the depth the concentrations are rated as “low” with respect to their damaging potential (WTA 2005). Also salt efflorescences were sampled and analysed. Those salt crystals were easily visible on the damaged sandstone surface. Moreover, short time after undertaking a Karsten tube test a white salt rim generated around the tested area. All XRD measurements showed thenardite (Na_2SO_4) and gypsum ($\text{CaSO}_4 \cdot 2\text{H}_2\text{O}$) as crystallised soluble salts. The remarkable sodium contents are related referred to the earlier restoration action when the oil paint was removed by caustic soda (Hoferick & Siedel 1999). Thus, desalination was needed for all original sandstone pieces, and was undertaken by poultice desalination of the contaminated surfaces.

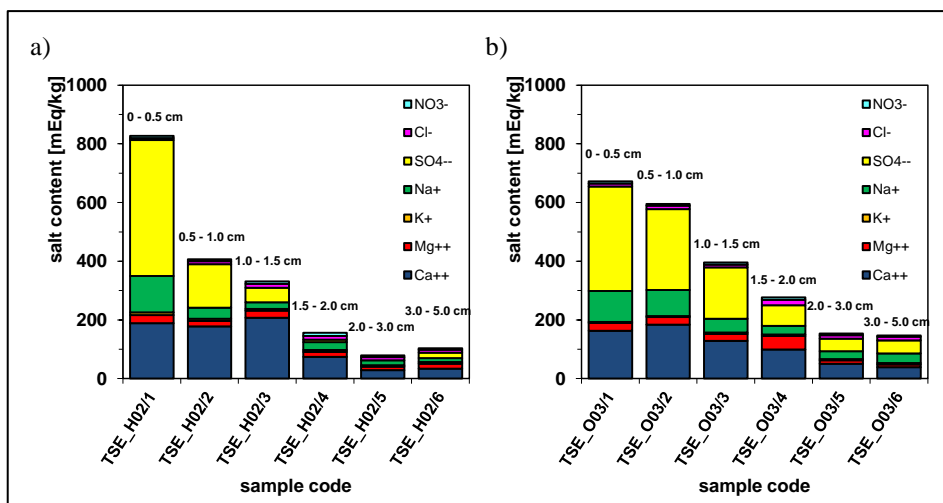


Fig. 3: Salt contents into depth, profile for stone H02 (a) and profile for stone O03(b).

6.2. Poulticing

Desalination proved to be a key step in the conservation action restorative action. In the workshops the reliefs were treated with wet poultices applications (Vergès-Belmin & Siedel 2005, Heritage *et al.* 2013) in two cycles. The surface was pre-wetted with deionised water (electrical conductivity $< 10 \mu\text{S}/\text{cm}$), and the aqueous cellulose poultice was attached to the stone surface. After the migration of dissolved ions into the drying poultice, the dry, salt laden poultice was removed. Several poultice samples were analysed for their salt content to monitor and evaluate the desalination progress (Franzen 2006, WTA 2005). In the laboratory some of the poultices produced a yellow staining to the eluate, probably caused by the transport of humic material (Franzen *et al.* 2015). Most poultices absorbed up to $50 \text{ g}/\text{m}^2$ soluble salts. In one case more than $200 \text{ g}/\text{m}^2$ salts was analysed. Areas which were identified as highly salt loaded were subsequently treated several times. The ion mixture in the poultices contained much more sodium, compared to the ionic composition detected in the material itself. More soluble salts such as thenardite are well extracted by the poultices while hardly soluble gypsum is not reduced significantly.

7. Drilling resistance

To gain an insight in the weathering profile of the sandstone, drilling resistance was measured on damaged and intact surfaces (Fig. 4a and 4b). Fig. 4b compares the profile of a damaged area (BW1.1) with that of an area, where no damage was observed (BW1.4). The absolute height of the profiles is not comparable, as the pressure applied to BW1.4 was double than for BW1.1, but the development with depth is revealing. The damaged area starts with low strength near the surface, which increases until 2 cm depth. Higher values in depths > 2 cm can be attributed to increasing side effects by material transport during drilling (Siedel & Siegesmund 2014). The visibly intact area has a more or less continuous drilling resistance profile. The damaged area of the surface had to be consolidated, and the consolidant needed to reach a depth until 2 cm, with decreasing degree of intensity to replace the lost strength.

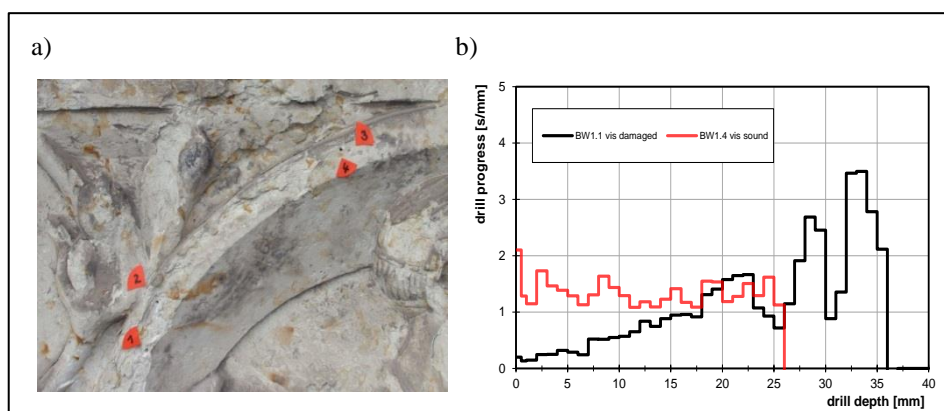


Fig. 4: a) Position of drilling profiles shown in Fig. 4b (left: damaged; right: intact);
b) Drilling profiles of visibly damaged and intact areas.

8. Infrared thermography

Inspection by infrared thermography was intended to locate the iron components in the construction. Although the measurement circumstances were good (the first storage room was heated up to 18°C, outer temperature was about -6.5°C) the testing was not successful. As revealed by the metal detector tests, the metal parts are hidden in geometrically complex positions, and in those parts they do not significantly contribute to heat transfer. However, it was observed that very steep temperature profiles occur in winter situations in the thin sandstone reliefs. While the thicker structural sandstone parts have surface temperatures of about -4.6°C to -2.1°C, which is close to the outside temperatures, the thin relief panels show outer surface temperatures of up to 0.9°C.

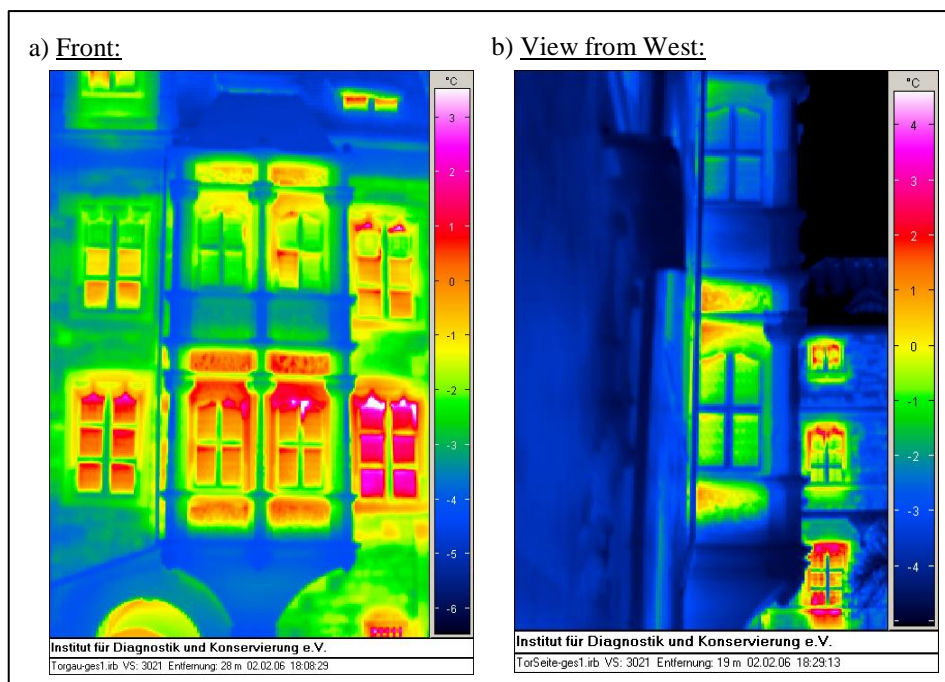
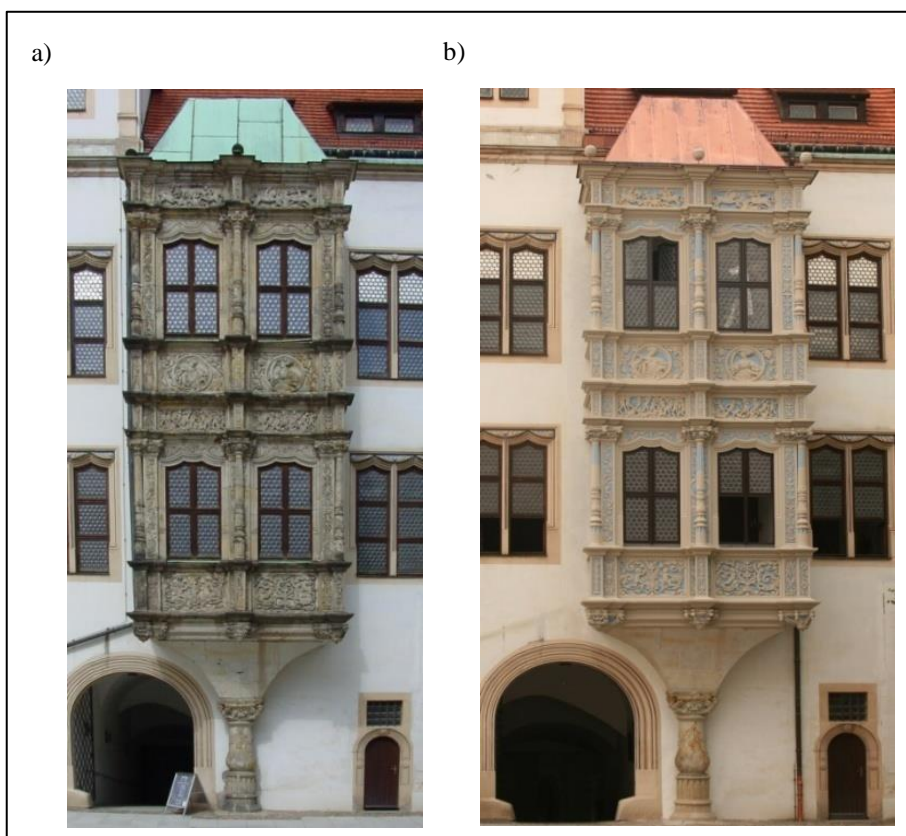


Fig. 5: IR-Thermography 'Schöner Erker'.

9. Conclusion

The sandstone monument 'Schöner Erker' in Torgau, one of the most important achievements of the art of sculpture from the Early Renaissance in Central Germany, was rescued by a thorough stone restoration approach including structural and climatic measures. Extensive investigations were an indispensable basis for sound planning and realisation of the works. An initially favoured in-situ restoration of all or the most parts of the oriel window was suspended for several reasons. Due to severe damage, demonstrated by mapping of weathering forms, salt analyses and measurements of drilling resistance, and resulting in very fragile stones, all reliefs had to be treated in a workshop. But they could not be removed without serious damage and risks to the overall structure. Moreover the corroding iron clamps had to be replaced, which also could not be reached without massive intervention. Dismantling and reconstruction, which was justified as a last resort decision, required higher efforts in logistics. The monument had already been dismantled once before in its lifetime, and so there was neither a concern about originality nor loss of related decoration like interior wall paintings. The detection of iron parts within the construction by metal detector and mapping of their positions provided valuable information for the practical interventions. To further avoid loads on material due to steep temperature profiles in the thin sandstone panels (as demonstrated by infrared thermography) it was recommended that the use of the rooms be adapted towards a climatic situation better coupled to that of the exterior. As could be shown by archive research and salt investigations, the sandstone had a history of painting, chemical removal of paint and

posure to environmental pollution, which lead to serious salt loads and consequent decay. As desalination is better approached as a reduction of salt contents rather than total removal, residual contents have to be acknowledged. As demonstrated by chemical analyses, very large amounts of the active and damaging sodium sulphates were extracted by poulticing. The deteriorated softened surface parts were consolidated with TEOS and in parts with Paraloid B72. Its application from the most damaged direction -the outer surface-enabled reinstatement of a continuous strength profile. For aesthetic reasons related to the overall concept of renewed coloured surfaces on the Castle of Hartenfels, a decision was made on a colour finish based on the original colour composition of the oriel. The coating, based on a silicon resin binder system, should avoid further massive rain and salt attack. This case study demonstrates the essential contribution of scientific investigations to successful planning and undertaking of restoration measures on high-value architectural stone objects.



*Fig. 10: a) “Schöner Erker” prior its restoration in 2004;
b) Restored “Schöner Erker” in 2011.*

Acknowledgements

The restoration and most parts of the investigative study were made possible due to cooperative grants of the World Monument Fund (WMF) and the Ostdeutsche Sparkassenstiftung (OSS). Additional investigation work and publication presentation was supported by the Ministerium des Innern, Sachsen, Germany.

References

- Franzen, C., 2006, Analytische Begleitung von Salzreduzierungsmaßnahmen, in, Praxisorientierte Forschung in der Denkmalpflege –10 Jahre IDK-, Hrsg., Institut für Diagnostik und Konservierung an Denkmalen in Sachsen und Sachsen-Anhalt e.V. 2006, 31 – 40.
- Franzen, C., Kretschmar, J., Franzen, C. and Weiss, S., 2015, Staining on heritage building stone identified by NMR spectroscopy, *Environmental Earth Science*, Volume 74/ 6, 5275-5282, DOI, 10.1007/s12665-015-4538-9.
- Götze, J. and Siedel H., 2007, A complex investigation of building sandstones from Saxony Germany. – *Materials Characterization* 58 11-12, 1082-1084.
- Heritage, A., Heritage, A. and Zezza, F., 2013, *Desalination of Historic Structures and Objects*, Archetype Publications, London
- Hoferick, F. and Siedel, H., 1999, Die Ablaugung von Ölfarbanstrichen am Dresdner Zwinger – Geschichte und Folgeschäden. - *Mitteilungen des Landesamtes für Denkmalpflege Sachsen*, 80-88. in German
- Pamplona M., Kocher M., Snethlage R. and Aires-Barros, L., 2007, Drilling resistance: overview and outlook. *Z. dt. Ges. Geowiss.*, 158 (3), 665–676.
- Siedel, H. and Siegesmund, S., 2014, Characterization of stone deterioration on buildings. In Siegesmund, S. & Snethlage, R. (eds.) *Stone in Architecture*, Springer, Berlin and Heidelberg, 349-414.
- Vergès-Belmin V., Anson-Cartwright, T., Bourguignon, E., Bromblet, P., Cassar J., Charola, E., DeWitte, E., Delgado-Rodriguez, J., Fassina, V., Fitzner, B., Fortier, L., Franzen, C., Garcia de Miguel, J.M., Hyslop, E., Klingspor-Rotstein, M., Kwiatkowski, D., Krumbein, W.E., Lefèvre, R.A., Maxwell, I., McMillan, A., Michoinova, D., Nishiura, T., Queisser, A., Pallot-Frossard, I., Scherrer, G.W., Simon, S., Snethlage, R., Tourneur, F., Van Hees, R., Varti-Matarangas, M., Warscheid, T., Winterhalter, K., Young, D., 2008, *Illustrated glossary on stone deterioration patterns*, ISBN, 978-2-918068-00-0, 78 p.
- Vergès-Belmin, V. and Siedel, H., 2005, Desalination of masonries and monumental sculptures by poulticing, a review. *International Journal for Restoration of Buildings and Monuments*, 11 6, 391-407.
- WTA Guideline 3-13-01/E, 2005, *Non-destructive desalination of natural stones and other porous materials with poultices*. WTA Publications, Munich.

AN ANALYSIS AND TREATMENT OF THE FIRE-DAMAGED MARBLE PLAQUE FROM THOMAS JEFFERSON'S GRAVE MARKER

C. Grissom^{1*}, E. Vicenzi¹, J. Giaccai², N.C. Little¹, C. France¹,
A.E. Charola¹ and R.A. Livingston³

Abstract

The original grave marker for Thomas Jefferson (1743-1826), third U.S. President, consists of a granite cube and obelisk, into which was set a white marble plaque inscribed with his epitaph. After damage led to replacement with a copy in the cemetery at Monticello, the original grave marker was given to the University of Missouri. Granite portions were installed in front of the university's main building, while the plaque was placed inside for safekeeping. The building burned down in 1892, and the plaque fragmented, portions disaggregated and were lost, and fire-related materials accreted on its face. Soon afterward, the plaque was reassembled atop a new marble block with hydraulic lime plaster. When examined more than a century later, the pieces were found to be misaligned, and areas on the face had deteriorated, with further loss of lettering and some instability. Instrumental analyses were done prior to conservation treatment. Stable isotope analysis sourced the stone to Vermont marble quarries. Other analytical techniques indicated that the marble had calcined and to some extent recarbonated, and they identified elemental constituents in the surface accretions deposited during the fire, including copper, tin, lead, and sulfur. Treatment included disassembly and reassembly of the plaque using Paraloid B48N, reconstruction of missing areas using a Paraloid B72/ground alabaster mixture for surface fills and a filled epoxy to support the fill material where there was a large loss, surface cleaning, and consolidation. Two reproductions were made using photogrammetry, and one was installed on original granite portions of the grave marker on the University of Missouri's David R. Francis Quadrangle.

Keywords: fire, Vermont marble, calcination, recarbonation, photogrammetry

¹ C. Grissom*, E. Vicenzi, N.C. Little, C. France and A.E. Charola
Museum Conservation Institute (MCI), Smithsonian Institution, United States of America
grissomc@si.edu.

² J. Giaccai
Freer/Sackler Galleries, Smithsonian Institution, United States of America

³ R.A. Livingston
Materials Science and Engineering Department, University of Maryland, United States of America

*corresponding author

1. Introduction

The original grave marker for Thomas Jefferson (1743-1826), third U.S. President, was made according to his instructions and erected in 1833 in the graveyard at Monticello, his Virginia home (Peden 1953). It consists of a granite obelisk resting on a granite cube, with the epitaph carved in a white marble plaque set into the obelisk (Jefferson famously omits that he had been president in his epitaph). After the grave marker was damaged by souvenir hunters and replaced by a copy at Monticello in 1883, the original was given to the University of Missouri. Granite portions were displayed in front of Academic Hall, the university's main building, while the plaque was placed inside it for safekeeping. Academic Hall burned down in 1892, and the "sacred relic ... cracked and burned" (Peden 1953, p 13). In 2012, the university requested examination and possible treatment of the plaque by the principal author, and the following year it was sent to the Smithsonian for treatment. At that time the plaque was enclosed in the same display case and exhibited essentially the same fragments and fills as in an historic photograph from the 1890s (Fig. 1). Moreover, it was photographed on the granite structure of the tombstone in front of the ruins of the fire-damaged building, suggesting repair soon after the fire. After the display case was removed in 2013, discarded printed matter from the 1880s and 1890s was found used as shims, confirming this hypothesis.



Fig. 1: Thomas Jefferson's grave marker displaying the repaired plaque in a frame following the 1892 fire, on the grounds of the University of Missouri. Courtesy, University of Missouri Archives.

2. Examination and analyses

2.1. The marble

Marble grains on the plaque range from 0.25 to 0.6 mm; accessory feldspar and quartz are found at grain boundaries. In the absence of documents sourcing the marble, it was hypothesized that its small grain size limited possibilities to marble imported from Carrara, Italy, or quarried in Vermont. Carbon and oxygen isotopes for samples from the plaque were compared to reference isotope datasets from Carrara and quarries in the northeast U.S. (Dooley and Herz 1995) and found to best match those of Dorset, Proctor, West Rutland, or Pittsford, Vermont (Fig. 2).

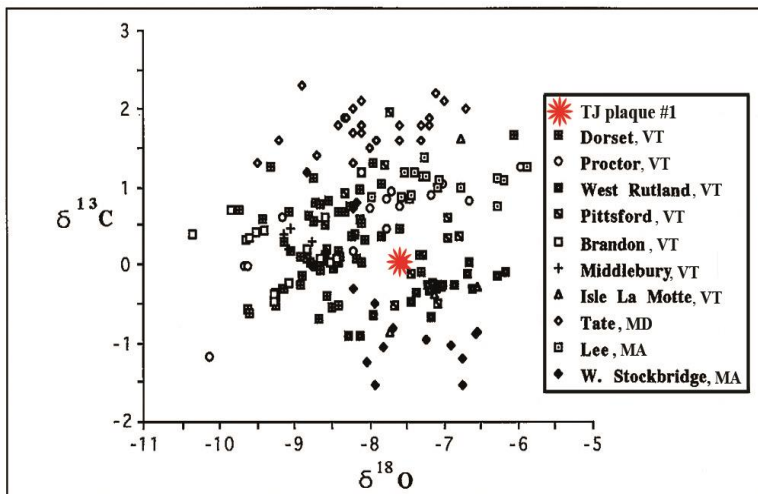


Fig. 2: The stable isotope average for TJ #1 is plotted on a graph showing averages for marble samples mainly from Vermont and Massachusetts, after Dooley and Herz (1995).

2.2. Condition of the plaque before treatment

Examination of the plaque at the Smithsonian revealed considerable fire-induced damage, including breakage into five pieces, numbered in Fig. 3. After disassembly, break edges were found to have the convex shapes characteristic of fire damage, known as conchoidal fracture (Steiger *et al.* 2014, p 227-228). Disaggregation along broken edges suggested that fragmentation occurred from simultaneous expansion and contraction of anisotropic calcite crystals, which can induce strain in marble at temperatures as low as 60° C (Siegesmund and Dürrast 2014, p 149-150). The rate of transmission of heat through the 5-cm-thick block would have been highest at corners, consistent with detachment of the small triangular pieces designated 1 and 4, as well as the formation of oblique cracks across the lower left corner visible in Fig. 4. Losses can also be readily seen in Fig. 4 because of the irregular surfaces of fills that replaced them. They are significant along broken edges, particularly at the left edge, where as much as 3 cm of the plaque is missing (apart from small areas at top and bottom corners) and may indicate the direction of the fire. Adjacent to this loss, a layer about 1-cm thick is missing on the back face, suggesting that the plaque may have been in a wooden case that burned in the fire. The plaque is slightly convex on

the back, probably from residual expansion caused by greater exposure to the fire; concomitantly, it is slightly concave on the front. Front surfaces at the left and bottom are partially calcined, distinguishable by whitening (Fig. 3). Expansion of these areas can be felt where they intersect sound stone. Partially delaminated areas with voids below were also found to have expanded, preventing readhesion; during treatment, the voids were filled instead. Since the historic photograph was taken in the 1890s, lettering has been lost at the left edge, visible as bright areas, e.g., where the first letter of “AMERICAN” is missing.

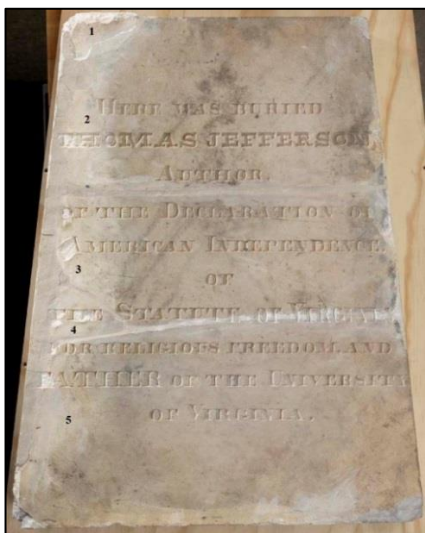


Fig. 3: The tombstone plaque before treatment; fragments are numbered at left. Height = 74cm. Photo by Don Hurlbert

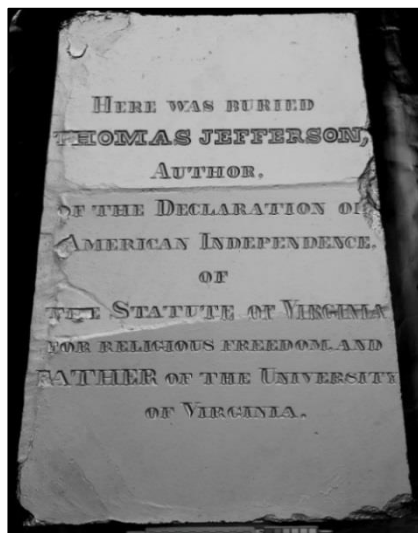


Fig. 4: RTIViewer screenshot in the specular enhancement mode shows surface irregularity of the plaque before treatment. Photo by E. Keats Webb

2.3. Deterioration of the marble

Decomposition of calcite (CaCO_3), or calcination, occurs at temperatures above 700°C ; carbon dioxide (CO_2) evolves, leaving calcium oxide (CaO) behind. The CaO can subsequently recarbonate in air to form poorly cohesive calcite. The calcined upper part of a marble sample from the plaque appears chalky white to the naked eye (Fig. 5), and a thin section shows that the marble's granular texture there has been replaced with an opaque material (Fig. 6), which is very fine. Micro-X-ray diffraction analysis of samples from such areas found both calcite and calcium hydroxide [$\text{Ca}(\text{OH})_2$], and preliminary thermogravimetric analysis (TGA) indicates about 95% calcite and 5% $\text{Ca}(\text{OH})_2$. In the intermediate zone between calcined marble and smoke-darkened marble grains below (Fig. 7), hyperspectral energy dispersive analysis using the SEM indicated that rims of grains had calcined and recarbonated. Below this zone, smoke-darkened marble retains its structure but is disaggregating (Fig. 5 and Fig. 6), presumably because of the heat-induced residual stresses in calcite grains.

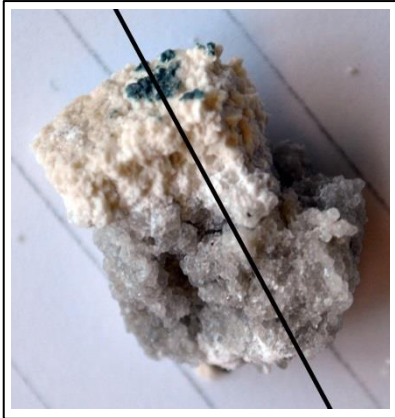


Fig. 5: Damaged sample from the plaque. The calcined surface is opaque and white, with a dark blue spot on top; below, smoke-darkened marble grains are disaggregating. The black line marks the plane of the thin section in the next image.

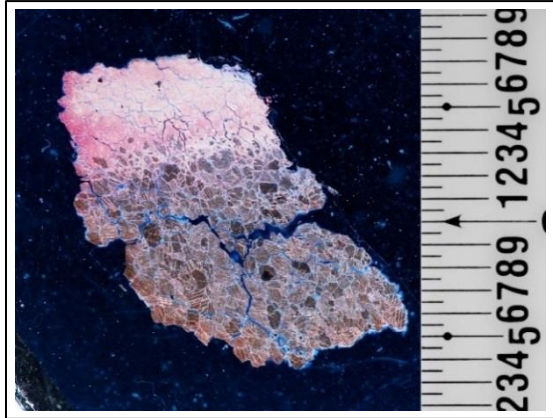


Fig. 6: Thin section made from the previous sample in darkfield illumination, with mm scale at right; stained red for calcite. The calcined upper surface has lost its marble texture, while grains and cleavage planes can still be seen in the smoke-damaged disaggregating marble below. The partially calcined zone in between is shown at higher magnification in the following figure.

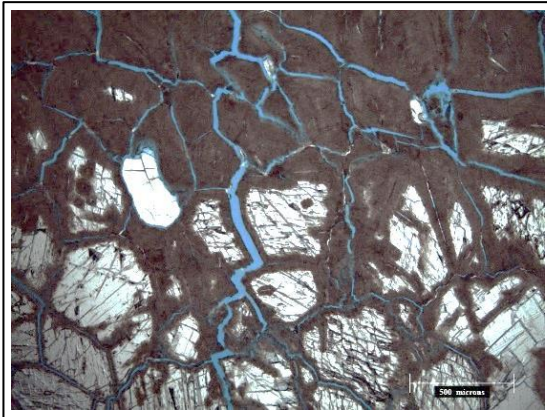


Fig. 7: An area in the intermediate zone of the previous thin section, at higher magnification in plain polarized light. Completely calcined marble (above) is dark. Calcite grains (below) are bright, except where calcined at rims and at cleavage planes. The brightest particle at center left is quartz. Blue epoxy medium can be seen in cracks, which to some extent follow grain boundaries. Bar = 500 μ m.

2.4. Surface accretions

A light cleaning using a surfactant and water revealed several materials disfiguring the front surface of the plaque. Constituents were analysed to determine which should be removed, and cleaning tests were done to determine removal feasibility. Micro-scanning X-ray fluorescence (XRF) analysis using a Bruker AXS Artax proved valuable for suggesting extraneous materials related to the fire by identifying elements in them compared to adjacent stone. Dark veins appeared to follow a diagonal pattern across the plaque from

upper right to lower left (Fig. 3) but were sometimes difficult to differentiate from surfaces soiled by smoke. Scanning XRF confirmed locations of veins by finding silicon and potassium in them, consistent with quartz and feldspars. No elements, other than calcium, were found in areas that appeared more likely to be darkened by smoke. This finding does not rule out the presence of carbon deposited from smoke, however, since this element is

not detectable by the XRF instrument. Cleaning tests found reduction but not elimination of soiling from smoke, apparently because smoke had penetrated the disaggregating stone. Disfiguring black spots and streaks of a type seen in Fig. 8 were found to contain copper, tin, lead, and sulfur as the main elements, confirmed by SEM EDS; they are probably metal sulfides derived from plumbing or other building materials burned in the fire. Microscopic examination of these accretions indicated that they were so intimately mixed with the stone that they could not be removed mechanically or by laser ablation without damaging the stone. Scanning XRF identified mainly sulfur and calcium in dark blue spots atop calcined areas (Fig. 5) but also small amounts of lead, confirmed by X-ray micro-analysis of a dark blue spot on both the thin section (Fig. 6) and a second fragment; this result suggests that lead sulphide may have provided the blue color. A sticky material on the surface of the plaque was analysed by Fourier transform infrared spectroscopy (FTIR) and found to have a spectrum similar to parchment. This would be consistent with application of a material such as animal glue during the 1890s restoration and its removal with an aqueous solution during the 2013 treatment.



Fig. 8: Copper, tin, lead, and sulfur were the main elements found in the black spot using scanning XRF and SEM EDS analyses. Bar = 0.5 mm.

3. Treatment of the plaque

Treatment included disassembly and reassembly of the plaque, reconstruction of missing areas, surface cleaning, and consolidation. During the restoration after the fire, the five fragments had been reassembled on a nearly 3-cm-thick marble block with hydraulic lime plaster, also used to fill losses. Individual fragments were not in the same plane, the composite was heavy, and fills were deteriorating and unattractive. It was decided to remove the original fragments from the newer marble support block, which would reduce the weight significantly, allow for improved reassembly, and provide an opportunity for replacing deteriorating fills. Disassembly was time consuming but more easily done than expected. The plaster was found to be poorly adhered to both the original and new marble, and it was often cracked, allowing relatively easy separation near edges. Toward the center, the plaster was sawn through to separate the original and new marble blocks.

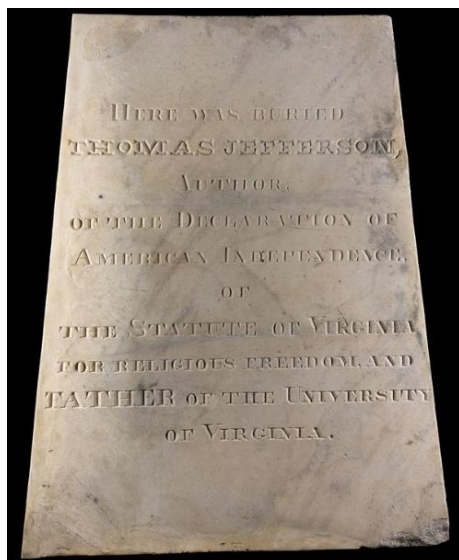


Fig. 9: Plaque front after treatment. Lighting is even; hence, lighter areas at left and bottom reflect calcination. Photo by Brittany Hance.



Fig. 10 Back of plaque after treatment. At the right, a structural fill completes the edge; next to it is an area missing a cm-thick layer of stone. In the light-colored central area, a thick layer on the surface has been calcined but remains. At the left, the marble is smoke damaged but more or less intact. Photo by Brittany Hance.

Fragments were separated from each other mechanically, and old fill material was removed. The five pieces were reassembled using the acrylic resin Paraloid B48N dissolved in acetone as adhesive. Small compromises had to be made in joining fragments, attributed to distortion by the fire. Reattachment of detached surfaces and consolidation of weakened stone was done with a second acrylic resin, Paraloid B72 in acetone. Fills were also made with that resin heavily bulked with alabaster ground to pass a sieve with 500 μm openings (Wolfe 2009). On the front, fills were made smooth and level with the stone (Fig. 9), but on the back they were recessed slightly and textured (Fig. 10). To begin recreation of the missing area on the left edge, a structural fill was made on the back using filled epoxy putty (Aves' Fixit) isolated from the stone with the acrylic fill material; the latter was also used to complete the left edge and cover the filled epoxy.

The front surface of the plaque was initially cleaned using mineral spirits, acetone, and an aqueous solution with a surfactant. Areas in good condition were further cleaned with methyl cellulose poultices; to prevent detachment of calcite grains, the poultices were bulked with silica and calcium carbonate powders and removed before dryness. Cleaning was limited on calcined areas at left and bottom edges because of their fragility. Treatment was completed with retouching of fills using watercolor and gouache paints to match the stone on the front (Fig. 9). Fills on the back were left lighter in color than the stone (Fig. 10).

Staff at the Smithsonian's Office of Exhibits Central made two replicas of the plaque using photogrammetry. Digital photographs of the conserved tombstone were taken, and files were manipulated using Autodesk's Recap (freeware) and Geomagic. From those results, a copy was milled in hard foam using a CNC (computer numerical control) machining center. After the copy was touched up, a silicone rubber mold was made. One copy was cast in glass fiber-reinforced gypsum (GFRC) for exterior display and a second in fiberglass. The replicas were painted with acrylic paints to imitate the plaque when it was new and coated with a flat automotive polyurethane paint for protection.

The conserved plaque was returned to the University of Missouri, where it is now displayed in a case indoors. The GFRC copy is displayed outdoors on the original granite portions of the tombstone, forming a "complete" grave marker for the first time in many years.

4. Conclusions

The study and treatment of the tombstone plaque is a rare contribution to the literature on burned marble artifacts. In addition, a sacred relic has been preserved representing the thoughts of a U.S. President as to his important contributions: the Declaration of Independence, the Virginia statute for religious freedom, and founding of the University of Virginia – but not his role as president.

Acknowledgements

Staff time for research and treatment of the Jefferson plaque was underwritten by the Museum Conservation Institute (MCI #6526). Thanks especially to Marianne and Bob Marti for facilitating the project and Miriam Hiebert for XRD analyses.

References

- Dooley, K. and Herz, N., 1995, Provenance determination of early American marbles, in *The Study of Marble and Other Stones Used in Antiquity*, Y. Maniatis, N. Herz, and Y. Basiakos (eds.), Archetype, ISBN 1 873132 0 18, 243-252.
- France, C.A.M. and Grissom, C.A., 2015, Carbon and oxygen isotopes as indicators of provenance in cultural artefacts: A case study of Thomas Jefferson's tombstone plaque, Abstract for Seventh MaSC (mass spectrometry and chromatography) Meeting, Chicago, 17-22 May 2015.
- Peden, W., 1953, The Jefferson Monument, *University of Missouri Bulletin*, 54 (32), 1-18.
- Siegesmund, S. and Dürrast, H., 2014, Physical and mechanical properties of rocks, in *Stone in Architecture: Properties, Durability*, S. Siegesmund and R. Snethlage (eds.), Springer, ISBN 9 783642451 5 46, 97-224.
- Steiger, M., Charola, A.E., and Sterflinger, K., Weathering and degradation, in *Stone in Architecture: Properties, Durability*, S. Siegesmund and R. Snethlage (eds.), Springer, ISBN 9 783642451 5 46, 225-316.
- Wolfe, J., 2009, Effects of bulking Paraloid B-72 for marble fills, *Journal of the American Institute for Conservation*, 48, 121-140.

THE DIAGNOSTIC AND MONITORING APPROACH FOR THE PREVENTIVE CONSERVATION OF THE FAÇADE OF THE MILAN CATHEDRAL

D. Gulotta¹, P. Fermo², A. Bonazza³ and L. Toniolo^{1*}

Abstract

The importance of preventive conservation strategies for the built heritage has been debated in the last years, but there still is a limited number of applied research involving complex architectural sites. The identification and monitoring of the decay processes after the restoration activities can provide valuable information on the degradation rate and extent, thus supporting the future planned conservation. In the present work the methodology and some selected results of the post-treatment diagnostic and monitoring of the façade of the Milan Cathedral are presented. The main conservation issues have been identified and studied. A non-invasive colorimetric monitoring of selected areas of the façade has been carried out during a two-year period in order to evaluate the soiling effect. Fragments of stone and samples of the particulate matter deposits have been collected and characterized in laboratory according to a multi-analytical approach. As the early stages of deposition and erosion at the end of the intervention are particularly relevant for the evaluation of the degradation rate, several set of stone specimens have been also exposed on the façade in different conditions. The results of the in situ monitoring, supported by the study of the specimens, confirmed that soiling is the main and most rapidly-evolving deterioration effect and it is therefore expected to have a significant impact in the next future. Moreover, beside the carbonaceous fraction responsible for the surface blackening, the deposits composition showed high content of potentially harmful soluble compounds which can react with the stone matrix and therefore needs to be monitored over time.

Keywords: monitoring, marble decay, deposition, surface erosion, stone blackening, preventive conservation

1. Introduction

The importance of preventive conservation strategies for the built heritage has been debated in the last years. Despite the theoretical studies available so far (Della Torre 2003), there is still a limited number of applied researches conducted in the field and involving complex

¹ D. Gulotta and L. Toniolo*
Politecnico di Milano, Dipartimento di Chimica,
Materiali e Ingegneria Chimica “Giulio Natta”, Italy
lucia.toniolo@polimi.it

² P. Fermo
Università degli Studi di Milano, Dipartimento di Chimica, Italy

³ A. Bonazza
Nazionale delle Ricerche - Istituto di Scienze dell’Atmosfera e del Clima, Italy

*corresponding author

architectural buildings and sites (Brimblecombe & Grossi 2005; Price 2007; Ghedini *et al.* 2011; Bortolotto *et al.* 2013). As far as the stone surfaces exposed outdoor are concerned, the identification and the monitoring of the decay processes after the restoration activities can provide valuable information on the degradation rate and extent. Indications for preventive conservation able to delay and possibly reduce the occurrence of the damage can be provided accordingly. In the present work, the diagnostic and monitoring strategy for the preventive conservation of the façade of the Milan Cathedral is presented. The Duomo is a major landmark of the city, a remarkable example of the late gothic architecture and a primary touristic resource. The continuous exposition to the highly polluted atmosphere of Milan city centre progressively damaged the Candoglia marble of the façade according to well-known deterioration mechanisms (Watt *et al.* 2009), so that extensive conservative interventions had to be performed during the last century in 1935-39 and 1972-74. More recently, due to the worrying state of conservation of the surfaces, particularly affected by soiling and black crust formation (Toniolo *et al.* 2009), a new and complex restoration project was carried out in 2003-2009. The post-intervention monitoring and diagnostic activity started two years later. The main conservation issues to be monitored have been identified and included: i) soiling and blackening effects due to the deposition of atmospheric pollutants and soil dust in sheltered areas; ii) surface erosion of the elements exposed to direct rain-wash. A non-invasive colorimetric monitoring of selected areas of the façade has been carried out during a 18-month period in order to evaluate the soiling and blackening effect. Fragments of stone and samples of the particulate matter deposits have been collected and characterized in laboratory according to a multi-analytical approach. As the early stages of deposition and erosion at the end of the intervention are particularly relevant for the evaluation of the degradation rate, several set of Candoglia marble reference specimens have been exposed on the façade in different conditions (height, orientation, superficial finishing, sheltered/non-sheltered condition) and monitored every 6 months.

2. Materials and methods

Colorimetric measurements have been performed by a Konica Minolta CM-600D instrument equipped with a D65 illuminant at 8° (400-700 nm range). Measurements were elaborated according to the CIE $L^*a^*b^*$ standard colour system; FTIR analyses were carried out with a Nicolet 6700 spectrophotometer with a DTGS (4000-400 cm^{-1} range) on powder samples in KBr pellets; XRD analyses were performed using a Philips PW1830 diffractometer with Bragg-Brentano geometry using a Cu anticathode and $K\alpha$ radiation ($\lambda = 1,54058 \text{ \AA}$). ESEM-EDX analyses were performed using a Zeiss EVO 50 EP environmental scanning electron microscope, with an Oxford INCA 200-Pentafet LZ4 spectrometer. Anions analysis was carried out by means of a Ion Pac AS14A (Dionex) column and a detection conductivity system equipped with a ASRS-ULTRA suppression mode (Dionex). Cations determination was performed by means of a CS12A (Dionex) and a detection conductivity system equipped with a CSRS-ULTRA suppression mode (Dionex). Laser profilometry was performed by a UBM Microfocus instrument, with a 150 pts/mm density.

3. Results and discussion

3.1. Soiling and blackening effects

3.1.1. Deposits characterization

After few years from the last cleaning operations most of the marble surface of the bas-relief, of the sculptures and of all the areas sheltered from direct rainfall show slight to significant accumulation of deposit. Samples of the dark deposits have been collected from seven different locations which varied in height from the ground level to almost 20 meters. The XRD characterization of the deposit highlighted the presence of quartz, feldspar, gypsum and calcite as the main mineralogical phases, together with clay minerals in minor amount. Sodium chloride, as halite, has also been found in some of the samples collected from the lowest locations. The deposit has also been studied by SEM-EDX (Fig. 1). Metallic particles containing iron and titanium are the most diffused within the deposited material, with an average diameter which decreases with height: in the highest sampling site (almost 20 m), where the prevalent transport mechanism is the wind-driven deposition, the particles diameter ranges from 2 to 20 μm ; in the lowest location (2 m), where anthropogenic and vehicular re-suspension of soil dust and particulate matter from the ground is also effective, their diameter rises to a range of 20 to 50 μm . Aluminosilicate particles have been traced as well, but their size distribution seems to be less effectively related to height. Only rare carbonaceous particles containing sulphur and vanadium have been found in the upper sampling sites.

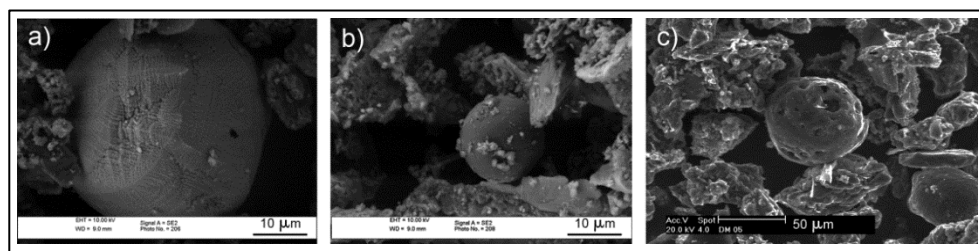


Fig. 1: ESEM micrographs of metallic (a), aluminosilicate (b) and carbonaceous (c) particles from the façade surface deposits.

The compositional characterization after FTIR analysis (Fig. 2) confirmed the prevailing presence of gypsum as the major component of the deposit (characteristic absorption doublets at 3532-3405, 1680-1622, 1140-1116 and 670-600 cm^{-1}). The sharp intense peak at 1385 cm^{-1} indicates the presence of high amount of nitrates and the smaller one located at 1323 cm^{-1} is related to the presence of calcium oxalate (most probably as weddellite). The calcite contribution is evidenced by the peaks around 1430, 875 and 715 cm^{-1} , present in minor amount together with silicates (Si-O characteristic peak around 1030 cm^{-1}) and quartz (779-799 cm^{-1}). The comparison between the deposits formed over the real sculpted surfaces (Fig. 2, grey line) as a result of the outdoor post-restoration exposition and the deposited material collected from the Candoglia marble specimens after six months of sheltered exposing condition on the façade (Fig. 2, black line) shows that no significant differences in the general composition are present.

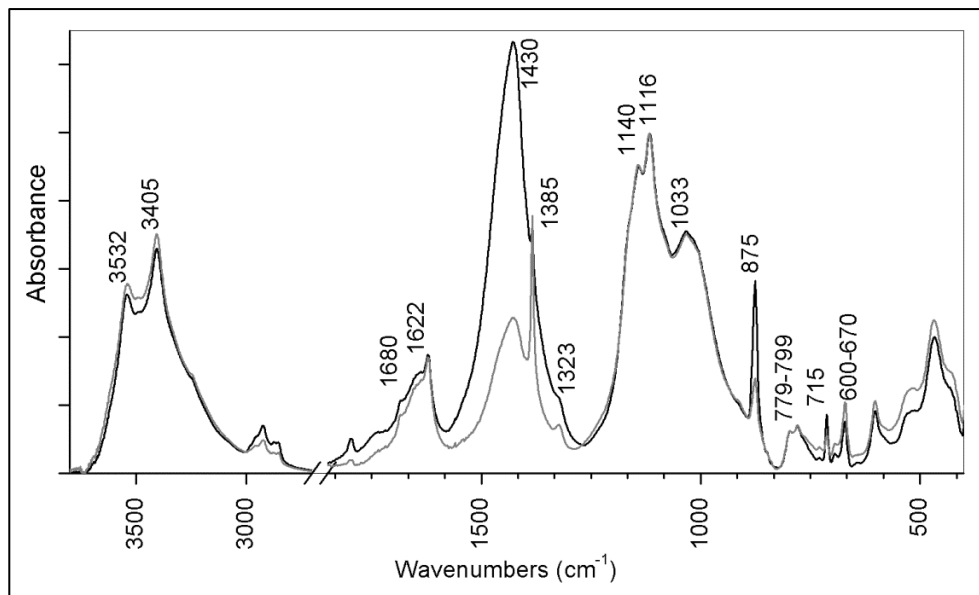


Fig. 2: FTIR spectra of samples of deposit from real façade surfaces (grey line) and collected from exposed Candoglia marble sample (black line).

The natural deposition over the sculpted surfaces is enriched in soluble compounds due to the longer exposition to the atmospheric pollutants and, as for gypsum, to the contribution provided by the partially sulfated substrate. It is worth noting that the overall composition of the latter deposits shows similar characteristics respect to the results of black layers and black crust characterization of samples of previous studies of the façade (Toniolo *et al.* 2009; Barca *et al.* 2014).

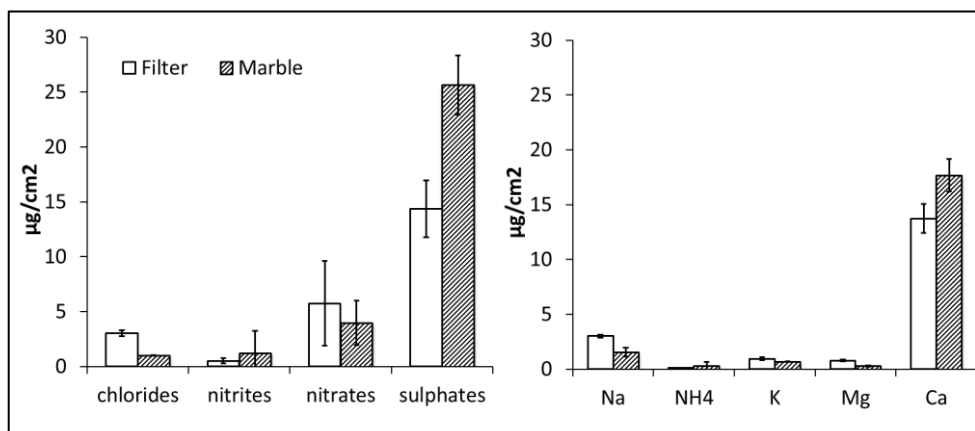


Fig. 3: Anions and cations content of deposit on quartz filter (white bars) and Candoglia marble specimens (grey bars) after six months of sheltered-condition exposition on the façade.

The evaluation of the soluble salts content of deposits collected on stone specimens and quartz filter after a six-month exposition period is reported in Fig. 3. The main ions concentrations determined in the two different cases are characterized by a comparable trend, thus confirming that the quartz filter represents a valid supporting material to collect the atmospheric particulate matter affecting the surfaces. Marble shows slightly higher concentrations of sulfate, nitrate and calcium. These differences could be partly due to early stage of sulfation process of the stone material.

3.1.2. Blackening

Surface blackening has been evaluated by colorimetric monitoring of fifty selected areas of the façade. The main parameter related to the blackening effect is the variation of L^* which effectively describe the darkening of the surface as a result of the deposit accumulation. The real façade surfaces have shown a high dispersion of the initial values of this parameter due to the very different conditions of the substrate respect to: orientation, finishing, material heterogeneity and, most of all, presence of substituted elements as a result of the conservative interventions and of the regular maintenance activity of the building. The initial value of L^* of the “original” surfaces (those belonging to elements not recently substituted) ranges from 50 to 75 units, whereas the values of the substituted elements is always above 85. A general trend for such diverse situations therefore cannot be traced. In Fig. 4 is reported, as an example, the evaluation of two surfaces characterized by the same orientation, location and overall geometry but with significantly different exposition period. The “original” horizontal sheltered upper surface of the sculpted element shows an initial L^* value of 51, which decrease of about 5 units at the end of the first year of monitoring. The substituted element shows a similar trend but with a lower variation in the same period (3 units), which can be related to the different surface condition of the marble characterized by a less weathered surfaces (as confirmed by on-site qualitative microscopic observation). Such surface can be considered as less prone to deposit accumulation due to its lower surface roughness.

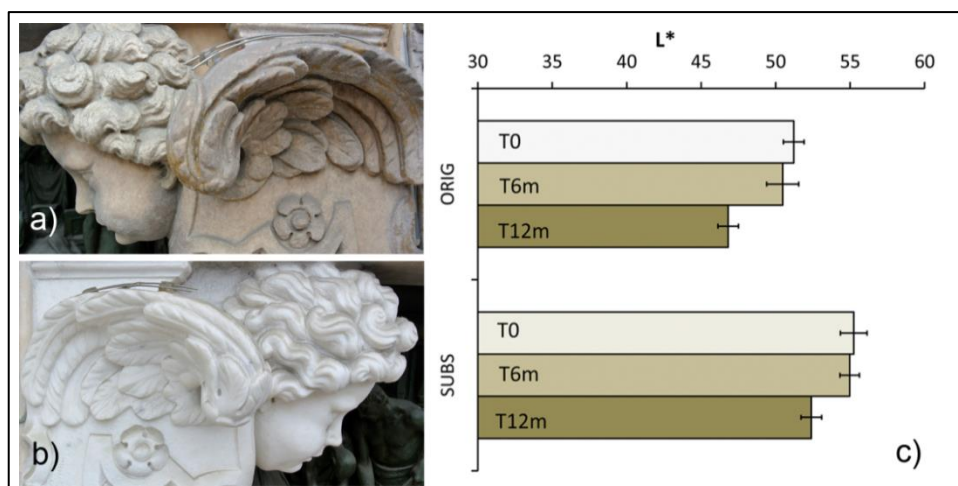


Fig. 4: Photographic documentation of two areas of the colorimetric monitoring characterized by the presence of “original” (a) and more recently substituted (b) marble elements; b) variation of the L^* parameter within the first year of monitoring.

The generally limited L^* variations of the real areas have been compared to those of marble reference specimens, to properly take into account the non-linear trend of surface blackening (Brimblecombe & Grossi 2005). The results of the reference specimens exposed in the central area of the façade indicate a more significant and progressive reduction of the superficial lightness (Fig. 5, left). After the first exposition interval (6 months), the variation of L^* is around 4 units, thus being already barely detectable by the naked eye, and it reaches a final decrease of 14 units after 18 months. The b^* variations follow an opposite trend (Fig. 5, right) indicating that the deposit accumulation is characterized by a saturation of the yellow colorimetric coordinate, even though to a minor extent respect to the most relevant blackening effect. The final increase of the b^* value is limited to almost 4 units.

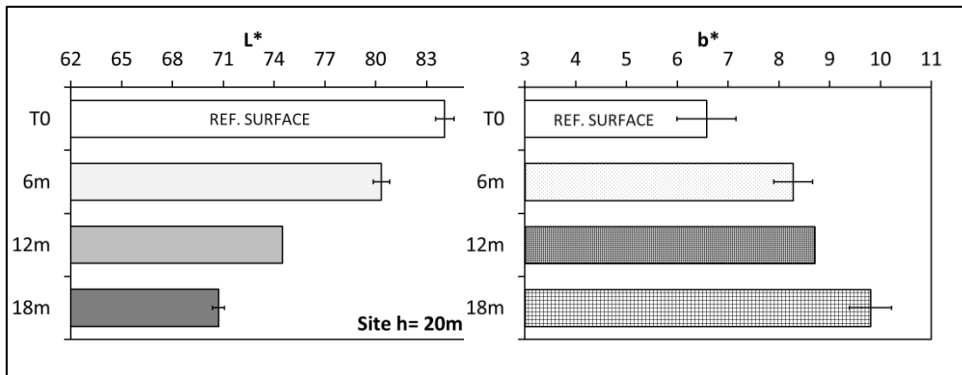


Fig. 5: variation of the L^* (left) and b^* (right) parameters of Candoglia marble reference specimens within 18-month exposition in sheltered condition.

3.2. Surface erosion

The surface erosion of marble due to the effect of direct rain wash and of run-off water flowing over the flat cladding slabs represents a major conservation issue that all the previous interventions had to deal with. Such mechanism is particularly efficient on the elements located on the top of the façade, such as the spires, and on the prominent sculpted figures of the lower register. The progressive erosive effects on the Candoglia microstructure are visible in Fig. 6, where the reference non-exposed material (Fig. 6a) is compared to fragments coming from a recently substituted element (Fig. 6b) and an “original” one (Fig. 6c). The grain morphology of the freshly sculpted marble is characterized by a very compact appearance, where the single grains show well defined regular borders and no discontinuities are present.

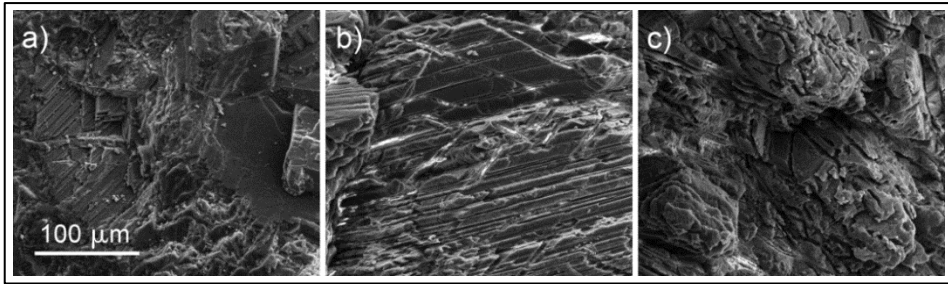


Fig. 6: ESEM documentation of the marble microstructure of a reference non-exposed material (a), compared to fragments from a recently substituted element (b) and from an “original” one (c).

As a result of the outdoor exposition, the erosive effect can be identified in the rounding of the grain edges and in the typical accentuated cleavage planes (Weber *et al.* 2007), which can be observed as parallel fissures. The prolonged exposition further enhances this deterioration pattern, leading to dramatic rounding of the grain and loss of material even on a macroscopic scale. The erosion extent has been monitored by laser profilometry on polished marble reference specimen exposed to the most severe non-sheltered façade condition.

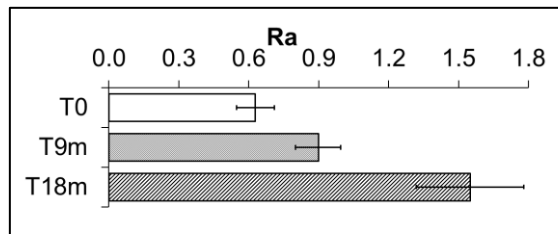


Fig. 7: Average surface roughness (R_a) of marble reference specimens evaluated after laser profilometry.

The decay effect has been evaluated respect to the variation of the surface roughness, as an indicator of the state of conservation of the superficial microstructure. The results show an increment of the average roughness as a result of the exposition, which is more than twice the initial one after 18 months of exposition (Fig. 7). Moreover, the higher standard deviation calculated for the final measurements is related to the increased surface irregularity (loss of material, formation of fissures, rounding effects) which is confirmed by the ESEM observations.

4. Conclusions

The diagnostic and monitoring approach for the real surfaces, supported by the study of the marble reference specimens, indicates that soiling is the main and most rapidly-evolving deterioration effect and is therefore expected to have a significant impact in the next future. Beside the carbonaceous fraction responsible for the surface soiling and blackening, the deposits composition showed high content of potentially harmful soluble compounds, which can react with the stone matrix leading to crystallization damages and crust

formation. It therefore needs to be monitored over time. The deposition rate is confirmed to be particularly effective during the first stage of the exposition of the cleaned surfaces and tend to slow down over time. This suggests the importance of a proper planning of the monitoring activity, which should start at the very beginning of the post-restoration period. The enhancement of the surface roughness potentially leading to loss of material at a macroscopic scale is the main effect of the erosion mechanism in the non-sheltered areas. With respect to preventive conservation indications, the results point the attention to the need for further research to set-up sustainable methodologies for the periodic removal of the deposits and for surface protection to mitigate the marble corrosion effects.

Acknowledgements

Authors wish to acknowledge the “Veneranda Fabbrica del Duomo di Milano” and Ing. Benigno Mörlin for the assistance and technical support during the project.

References

- Barca, D. *et al.*, 2014, Impact of air pollution in deterioration of carbonate building materials in Italian urban environments, *Applied Geochemistry*, 48, 122-131
- Bortolotto, S., Gulotta, D. and Toniolo, L., 2013, La cultura della manutenzione, in *Il Cortile del Richini. Un monumento da salvare*, Negri, A., and Tucci, P. (eds.), Skira, ISBN 8857222141, 239-259
- Brimblecombe, P. and Grossi, C.M., 2005, Aesthetic thresholds and blackening of stone buildings, *Science of The Total Environment*, 349 (1–3), 175-189
- Ghedini, N. *et al.*, 2011, Atmospheric aerosol monitoring as a strategy for the preventive conservation of urban monumental heritage: The Florence Baptistery, *Atmospheric Environment*, 45 (33), 5979-5987
- Price, C., 2007, Predicting environmental conditions to minimise salt damage at the Tower of London: a comparison of two approaches, *Environmental Geology*, 52 (2), 369-374
- Toniolo, L., Zerbi, C. and Bugini, R., 2009, Black layers on historical architecture, *Environmental Science and Pollution Research*, 16 (2), 218-226
- Della Torre, S., 2003, *La conservazione programmata del patrimonio storico architettonico. Linee guida per il piano di manutenzione e consuntivo scientifico*, Guerini e Associati, ISBN 8883353595
- Watt, J. *et al.*, 2009. *The Effects of Air Pollution on Cultural Heritage*, Springer Science & Business Media, ISBN 9780387848938
- Weber, J., Beseler, S. and Sterflinger, K., 2007, Thin-section microscopy of decayed crystalline marble from the garden sculptures of Schoenbrunn Palace in Vienna, *Materials Characterization*, 58(11-12), 1042-1051

ENVIRONMENTAL MONITORING AND SURFACE TREATMENT TESTS FOR CONSERVATION OF THE ROCK-HEWN CHURCH OF ÜZÜMLÜ, CAPPADOCIA

C. Iba^{1*}, Y. Taniguchi², K. Koizumi³, K. Watanabe⁴, K. Sano⁵,
C. Piao⁶ and M. Yoshioka¹

Abstract

A project at Üzümlü Church (St. Nichita's church: the end of the seventh century AD) in the Red Valley in Cappadocia, Turkey, has been launched to establish a suitable method for conservation of the extremely soft and fragile tuff structure of the church through geo- and environmental-engineering techniques. This project aims to find a method for prolonging the life of the tuff structures of Cappadocia using material that allows retreatment and is chemically compatible with the original tuff. To understand the cause and factors of rock weathering, *in situ* environmental monitoring was conducted, particularly focusing on heat and moisture flow in the rock structure and underground. From the results, it seemed that freeze-thaw cycles would not occur frequently and would not severely damage the structure. Erosion by water infiltration derived from rain or melting snow appeared to be more harmful to the rock structure; therefore, prevention of infiltration by liquid water is emphasised in our project. An outdoor exposure test was launched to evaluate the effectiveness and aging characteristics of a water-repellent consolidant. To quantify the degree of weathering, stainless steel nails were anchored to the rock surface and their lengths were measured by local collaborators every few months using a digital calliper. The water repellents had the effect of at least delaying deterioration. This case in Üzümlü is certainly a most technically difficult challenge and could serve as a model case for new approaches to integrating, presenting and advancing ethical conservation in Cappadocia.

Keywords: rock weathering, fragile tuff, environmental monitoring, surface treatment, water repellent

¹ C. Iba* and M. Yoshioka

Department of Architecture and Architectural Engineering, Kyoto University, Japan
iba@archi.kyoto-u.ac.jp

² Y. Taniguchi

Faculty of Humanities and Social Sciences, University of Tsukuba, Japan

³ K. Koizumi

Department of Global Architecture, Graduate School of Engineering, Osaka University, Japan

⁴ K. Watanabe

Department of Environmental Science and Technology, Mie University, Japan

⁵ K. Sano

D&D Corporation, Japan

⁶ C. Piao

Hytec Inc., Japan

*corresponding author

1. Introduction

In 1985, Cappadocia was selected as a UNESCO World Natural and Cultural Heritage Site under the name ‘Göreme Natural and Historical National Park’ (UNESCO 1985). In this region, there are many rock-hewn churches, which often contain reliefs and wall paintings dating from Byzantine and later periods that constitute part of their historical value. However, the fabric of these churches, which acts as bodies and supports of wall paintings, is severely damaged and collapses occur due to weathering and seismic activity every year. The unique landscape of Cappadocia is composed of soft, fragile tuff. The structure of this rock suffers from stone powdering, spalling and other types of deterioration caused or exacerbated by wind and rain erosion and insolation stresses. Particularly during winter, the region receives fairly high levels of rainfall and snowfall, which may cause freezing and thawing and other severe surface problems, resulting in rapid weathering at a rate of 0.4–2.5 mm/a (Erguler 2009).

Earlier, the problems of acute cracking and erosion were commonly addressed by applying a lime-cement-based render over the tuff surface as a tentative measure, since no proposed water repellents seemed to be convincing for realistic application (Idil 1995). Although trials were conducted using an iron mesh at the capping-tuff rock interface, detachment between them always occurs because of possible water infiltration and thermal impact by intense solar radiation (Yorulmaz et.al 1995). None of the surface treatment and capping have not been effective at reducing the rate of tuff erosion. Often, intense intervention does not allow future treatments and fails to provide continuous preservation.

This project aims to find a suitable method for prolonging the life of Cappadocia’s fragile tuff structures to preserve these valuable sites. This method is expected to slow the speed of erosion by application of material that is chemically compatible with the original tuff and does not involve covering the tuff with foreign material. We also aim to allow ‘retreatability’ in at least 10-yr intervals.

The Üzümlü Church (Fig. 1) in the Red Valley, a stand-alone rock-hewn church, was selected for this case study. The church shows deterioration phenomena such as severe cracking, surface disintegration and exfoliation caused by the environment, rock composition and tectonic activity as well as biological and human activities including continuous vandalism. The church structures have not been treated in the past, providing a unique opportunity for this type of study.

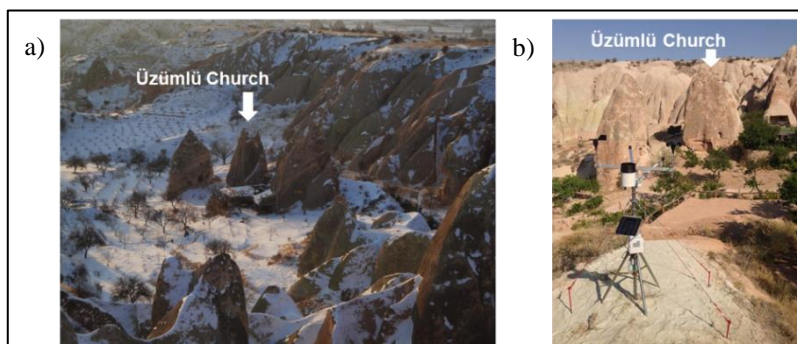


Fig. 1: Üzümlü Church (a) Appearance in winter (b) Environmental monitoring stations.

To consider the mechanism of rock weathering and preservation of rock structures, water and heat flows in the rock should be measured. Temperature and moisture behaviour in the soil and rocks were monitored at the base of Üzümlü Church. The micro-environment of the church interior and surroundings was also monitored. Based on the monitoring data obtained over 12 months, some types of alkoxy-silane-based water repellents with consolidation properties (Permeate® HS-360) were selected for *in situ* tests to evaluate their effectiveness and aging characteristics.

2. Environmental monitoring

To understand the environment around the church, meteorological data, indoor temperature and humidity, soil water content, soil water potential and temperature were measured throughout the year.

2.1. Measurement outline

A set of environmental monitoring stations (Onset HOBO U30-NRC) for monitoring air temperature (T), relative humidity (RH), rainfall, wind speed/direction and solar radiation were installed near Üzümlü Church (Fig. 1b). Additionally, two sets of data loggers, HOBO U23 for RH/T , were placed in the church to monitor the indoor thermal environment. One logger was placed in the alcove near the entrance (Fig. 2 (Entrance)), and the other was set in Room 3 (Fig. 2 (Interior)). Two small pits ($15 \times 15 \text{ cm}^2$) were trenched on the south (sunny) and north (shady) sides of Üzümlü Church. As shown in Fig. 2, soil water (5TE) and potential (MPS2) sensors were horizontally inserted into the rock wall at three different depths (50, 100 and 300 mm) in each pit. The pits were refilled with the original soil. All data were recorded every 10 min.

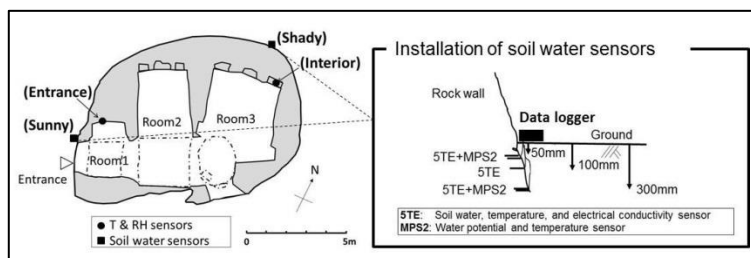


Fig. 2: Installation of environmental sensors.

2.2. Outdoor/Indoor/Ground temperatures

Fig. 3 shows the outdoor and indoor temperatures and global solar radiation (including direct and diffuse sky radiation) and the underground temperature (shady side, 300 mm depth). There are large diurnal temperature variations in the outdoor air. The temperature fluctuations in the church are smaller than those outside. The temperature near the entrance is notably affected by the outdoor air due to ventilation, whereas in Room 3, it slightly fluctuates owing to the heat capacity of the thick rock. Furthermore, the outer wall in Room 1, located on the southwest side of the church, is exposed to more solar radiation than Room 3, located on the northern side. We considered that the critical temperature associated with frost damage to soil or rock is approximately -4°C based on previous studies (Fukuda 1974, 1983). Such situations were observed only four times in the 2014–2015 season, significantly less often than that assumed.

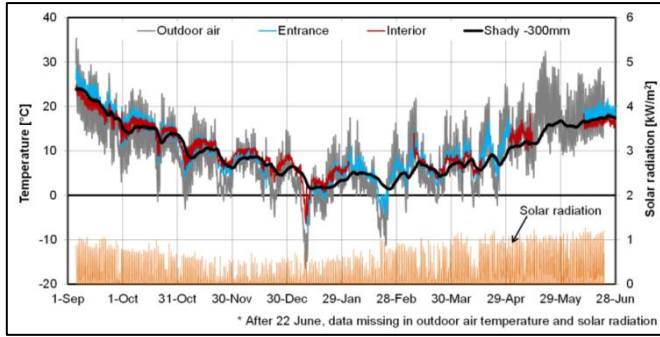


Fig. 3: Outdoor/indoor temperatures and solar radiation (September 2014–June 2015).

The underground temperatures on both the sunny and shady sides of the church are shown in Fig. 4, focusing on the winter season (December–February 2014). On the sunny side, diurnal temperature fluctuations were observed in the soil near the ground surface (50 and 100 mm depth), which may result from the effect of direct solar radiation. The temperature at 300 mm depth was on average a few degrees centigrade higher than that on the shady side. The underground temperature deeper than 50 mm below the ground surface did not fall below zero even in the coldest season. From these results, freezing appears to not penetrate the ground.

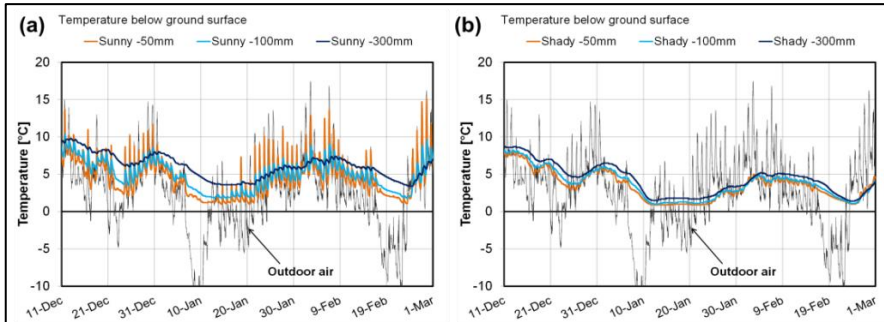


Fig. 4: Underground temperature during winter (December 2014–February 2015)
(a) Sunny side (b) Shady side.

2.3. Wind speed and direction

The upper part of Fig. 5 shows wind roses, which indicate the wind direction frequency in each direction in each season (except for summer) for both daytime and night time. Particularly in autumn and spring, there is a clear difference in the wind rose between daytime and night time. Interestingly, since its installation, the weather station has consistently shown the prevailing wind direction to be north–south around Üzümlü Church (September 2014–May 2015) probably owing to the geological setting of the Red Valley. One of the reasons for the daily wind direction change might be caused by the surface temperature change of the slope behind (north of) the church. An updraft can occur near the back slope, producing a south wind. The lower part of Fig. 5 shows the cumulative

frequencies of wind speeds for daytime and night time. In this area, moderate wind speeds were usually recorded, although relatively strong winds blew, mainly in the daytime, from the south. When there was slightly heavy rain (over 2.0 mm/10 min.), the wind speed was generally less than 1.5 m/s from autumn to spring. Therefore, apparently, the influence of wind direction and speed on moisture transfer in the soil or rock can be ignored in the analysis of erosion and frost damage.

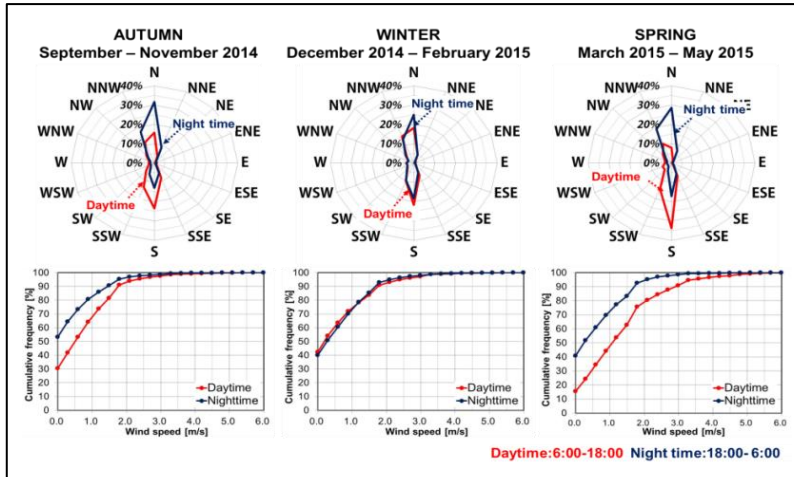


Fig. 5: Wind direction and speed near Üzümlü Church (September 2014–May 2015).

2.4. Soil water content, potential and temperature

Fig. 6a shows the soil water potential (depth: 50 and 300 mm) at the sunny and shady sides of the church and the precipitation measured at the weather station. When the soil is dry, the water potential has a large negative value. Soil water flows because of a potential gradient (Fig. 6b); therefore, the direction of water flow under the ground surface can be determined from the potential difference between depths of 50 and 300 mm.

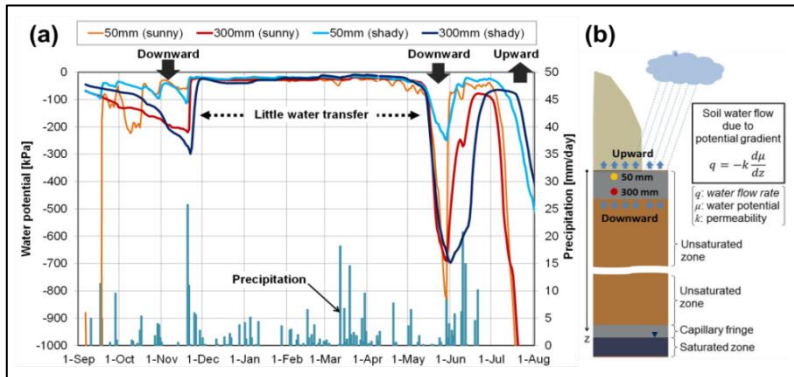


Fig. 6: Underground water potential (a) Time profile from September 2014 to July 2015 (b) Schematic of moisture flow due to water potential gradient.

Until the end of November 2014, water appeared to flow downward on both the sunny and shady sides. After heavy rain at the end of November, the water potential at all measured points rapidly increased. During winter (December–April), the water potential at each depth remained high due to periodic small precipitation, and the potential gradient became nearly zero. After April, the potential in the deeper area decreased, leading to downward water flow. In June, heavy rain appeared to occur and the potential at 50 mm depth steeply increased, then gradually increased at 300 mm depth. During summer, the moisture in the area near the ground surface was prone to evaporate and upward water flow was observed. Similar tendencies were observed in both sunny and shady sides. Based on these conditions, we can infer that the church structure did not continuously suck up significant amounts of groundwater in this area regardless of the solar radiation intensity.

In contrast, a few intervals of heavy rainfall were observed in this area, which could cause severe erosion of the fragile tuff structure. Therefore, coating with a consolidant/water repellent and reducing water infiltration to the structure are considered to be very effective for preventing degradation.

3. Rock consolidation/water repellent test on small rock masses

Based on the environmental monitoring results, an outdoor exposure test was launched to evaluate the effectiveness and durability of consolidation by surface treatment agents for tuff rocks.

3.1. Characteristics of water repellent/consolidant

In this trial, Permeate® HS-360 (D&D Corp.) was selected as a surface treatment agent after laboratory tests to identify possible consolidants and protective materials for tuff substrates (Sano and Mizukoshi 2015).

Permeate® is based on alkoxy silane containing a methyl or phenyl group, and an alkoxy group is polymerised by hydrolysis with atmospheric moisture. After polymerisation, the 3D Si–O–Si structure improves bulk strength by firmly hardening in the gaps within the object. Moreover, after polymerisation, a methyl or phenyl group is left. As these groups are hydrophobic, the substance becomes water-repellent after curing. This alkoxy silane-based consolidant does not form a film on the porous surface but penetrates and hardens at a few millimetres depth. Vapour can permeate through the consolidant layer although liquid water cannot infiltrate the layer. In practice, hydrolysis takes over 24 h.

3.2. Test rocks and testing method

Two small-scale tuff masses near Üzümlü Church were chosen for the test. Fig. 7 shows the one (b) that was splayed with the Permeate® HS-360 and the other (a) that was left untreated as a control. To quantify the degree of weathering of the tuff masses, stainless steel nails were anchored to the rock surface (Fig. 8a). Two nails were set in each direction (upper and lower parts) and on the top; i.e. each test rock contained nine nails. The nail length appearing outside the rock was measured with a digital calliper (Fig. 8b) on both right and left sides. After anchoring, the measurement error of four different measurements was checked because the rock surface was considerably uneven. The relative error for the average value was mostly within 10%. The nail length was measured by local collaborators every few months. In the ‘control’ mass, weathered tuff powder accumulated below the rock, and four out of the nine nails fell off the mass in the four months after anchoring. In contrast, in the ‘treated’ mass, the weathered deposits were generally small and only one

nail fell off. As flakes of a particular suitable thickness appeared to exfoliate in some places in the 'treated' mass in winter, deterioration might occur if moisture could accumulate in local areas of the mass. A follow-up examination will consider the possibility of frost damage.

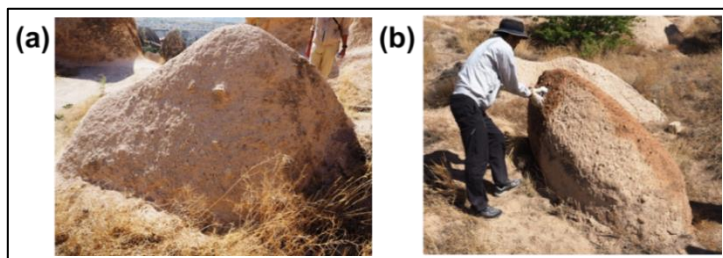


Fig. 7: Outdoor exposure test rocks: (a) Control (b) Treated mass.

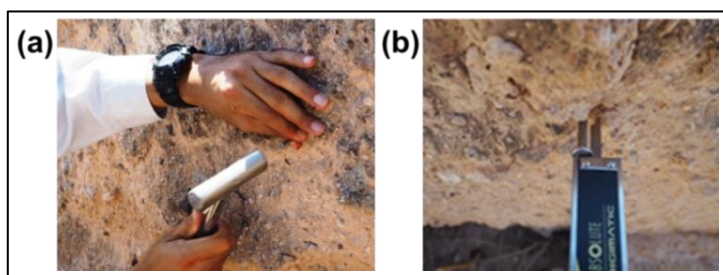


Fig. 8: Quantification of the degree of weathering
(a) Anchoring of a nail (b) Measurement of nail length.

4. Conclusions

To understand the causes and factors of rapid weathering of extremely friable tuff rock structures in Cappadocia, *in situ* environmental monitoring has been ongoing since 2014, focusing particularly on heat and moisture flow in the rock structure and underground. Freeze–thaw cycles occur infrequently and do not appear to cause severe damage to the structure. Furthermore, upward moisture flow from underground to the above-ground rock structure scarcely appeared in winter, i.e. groundwater would not be sucked up and supplied to the structure. From the results, we concluded that prevention of rainwater and infiltration water from melting snow from outside are the most appropriate measures to be taken in the project.

For that purpose, some outdoor exposure tests were carried out beforehand in Japan to assess the efficiency of the water repellent/consolidant. The test sample without water repellent broke in two weeks and collapsed in four weeks, whereas the sample with water repellent retained its shape for three months (Sano and Mizukoshi 2015). Following the results, an outdoor exposure test has been started in Cappadocia to evaluate the effectiveness and aging characteristics of the consolidant. The water repellents had the effect of at least delaying deterioration. The degree of weathering will be quantitatively evaluated through the project.

Both method and materials must be compatible with the original materials and implemented on a minimal scale to avoid excess and unnecessary treatments. Moreover, it is necessary to carefully verify whether a surface treatment might cause different damage or exacerbate deterioration of the rock structure. Although infrequent, frost damage could occur in this region. Detailed investigation of heat and moisture flow will be performed using computational analysis in future.

Due to similarities in the original technique and deterioration with other sites in Cappadocia, this study will have relevance for a wider region. The case in Üzümlü is certainly a technically difficult challenge and could serve as a model for new approaches to integrating, presenting and advancing ethical conservation in the Cappadocia region.

Acknowledgements

The authors would like to express their appreciation to MEXT/JSPS KAKENHI (24101014) and the Kajima Foundation for their financial support on this project. The Üzümlü project has been supported by numerous individuals in both Turkey and Japan, especially staff members of the Nevşehir Restoration and Conservation Regional Laboratory Directorate: Hatice Temur, Ayça Baştürkmen, Uğur Yalçınkaya, Alev Elçin Cankur, Merve Aziz Işın, Mustafa Toptepe, Tuğba Eryaşar. Director of the Nevşehir Museum: Murat Ertuğrul Gülyaz. Director of the Niğde Museum: Fazıl Açıkgöz and Ibrahim Sakınan and family.

References

- Erguler, Z.A., 2009, Field-based experimental determination of the weathering rates of the Cappadocian tuffs, *Engineering Geology*, 105, 186-199.
- Fukuda, M., 1974, Rock weathering by freezing-thawing cycles, low temperature science (in Japanese), *Low temperature science. Series A, Physical Sciences*, 32, 243-249.
- Fukuda, M. 1983, An experiment of freeze-thaw cycles of rock specimens (in Japanese), *Low temperature science. Series A, Physical Sciences*, 42, 163-169.
- Sano, K. and Mizukoshi, S., 2015, II-5 Preliminary aging tests (outdoor environment) of consolidants for tuff rock samples, in *Scientific Studies on Conservation for Üzümlü Church and its Wall Paintings in Cappadocia, Turkey*, Taniguchi, (ed.), Annual report on the activities in 2014, University of Tsukuba, 37-41.
- UNESCO, 1985, Structural conservation of Göreme. Göreme, land of fairy chimneys. Ministry of Culture and Tourism, Turkey. General Directorate of Antiquities and Museums.
- Yorulmaz, M., Ahunbay, Z. 1995, Structural Consolidation of El Nazar Church, In *The Safeguard of the Rock-Hewn Churches of the Göreme Valley (Proceedings of an International Seminar, Ürgüp, Cappadocia, Turkey, 5–10 September 1993)*, 135–142. Rome: ICCROM, 1995.
- İdil, A, Ç., 1995, Testing three products in Göreme valley, Cappadocia, In *The Safeguard of the Rock-Hewn Churches of the Göreme Valley (Proceedings of an International Seminar, Ürgüp, Cappadocia, Turkey, 5–10 September 1993)*, 143–149. Rome: ICCROM, 1995.

TIME TESTED REPAIRS: A REVIEW OF 11 YEARS OF CEMETERY STONE REPAIR

M. Jablonski^{1*}

Abstract

We have completed the stone repairs. We have finished the job and walked away. However, how long will our repairs last? Rarely is there an opportunity to answer this question. Published information on the durability of outdoor stone treatments over time is minimal as there is little or no monitoring of exterior stone repairs. There is often little chance to evaluate the work five or ten years later. Stone repairs in cemeteries offer an opportunity for evaluation if it is known what materials were used and how they were applied. Many treatments and repairs made to cemetery markers are used on stone buildings and cemeteries are relatively easy to access. While stone cemetery markers are smaller and more exposed than many stones on buildings, they still provide insight into the durability of repairs over time. This paper examines pinning and grouting repairs made in four cemeteries in the Mid-Atlantic region of the United States.

Keywords: cemetery, pinning repairs, grouting repairs, sandstone, marble

1. Introduction

The idea for this paper evolved out of a project my company; Jablonski Building Conservation (JBC) has been working on for three years, Prospect Cemetery in Jamaica, Queens New York City. JBC has repaired 43 markers. As our firm returns each year for the next phase of work, it is possible to see what repairs are successful and which are failing. Everyone talks about reviewing their past work but it is difficult to find the time and permission to do so. I decided it was time to look back at work that I was involved in over the last 11 years. There are of course lessons to be learned. This paper will examine two important types of repairs, pinning and grouting as they are repairs that can have the most impact on historic fabric.

For an architectural conservator, the goal of our work is to stabilize and slow the rate of deterioration. We follow the ethic of “Do no harm”. Cemetery repairs strive for a minimalist treatment that will have the least impact on the historic stone of the marker. The ideal repair is minimally invasive and retreatable. Interventions should be removable if necessary with the minimal amount of damage should they fail. However, in order to do no harm, we need to know the efficacy of our treatments and the failures of treatments that have occurred.

¹ M. Jablonski*

Jablonski Building Conservation and Columbia University, United States of America
mjablonski@jbconservation.com

*corresponding author

The two treatments discussed in this paper were selected for review because they can be damaging. Mechanical pinning requires drilling holes into the stone to receive the pins. Even if the pins are later removed, original fabric is still lost. Injecting grout into voids or cracks does not always allow for the removal of failed grout without seriously damaging the marker.

2. Cemeteries Included in this Study

2.1. Bottle Hill Cemetery Main Street Madison, NJ

Bottle Hill Cemetery has grave markers dating from the mid-eighteenth century to the early twentieth century. It contains almost 2,000. The cemetery is owned and administered by the Presbyterian Church of Madison, NJ and is made up of two historically separate cemeteries, the burial ground of the Presbyterian Church of Madison and the Hillside Cemetery. Over a three year period, from 2005 to 2007 JBC provided conservation treatments to 97 markers. The conservation treatments were extensive and included pinning as well as grout repairs. The markers conserved were a mix of zinc, sandstone and marble with the majority of them, 67, being sandstone.

2.2. Whippany Burying Ground, Whippany, NJ

The Whippany Burying Ground is located in Hanover Township in New Jersey. It has graves dating back to at least 1718 making it one of the oldest cemeteries in New Jersey. There are approximately 450 graves at the site. Jablonski Building Conservation worked on 25 markers between 2005 and 2008. Most of these markers were sandstone markers and the treatments included both pinning and grouting repairs.

2.3. Orient Cemetery, Orient, NY

The Orient cemetery, located at the northern tip of Long Island dates to the early nineteenth century. In August of 2006, a car crashed into an Orient cemetery and mowed a path through the cemetery damaging 16 markers; 14 marble and 2 sandstone. JBC was retained in 2007 to conserve and stabilize the damaged markers. Four of the marble markers were smashed into 20 to 30 pieces each, and the two oldest brownstone markers in the cemetery were shattered into approximately 10 pieces each. After the cemetery was searched, various pieces were carefully matched and the markers were pinned together and conserved. The pinning was extensive and complicated due to the number of fragments.

2.4. Prospect Cemetery, Queens, NY (New York City)

Prospect Cemetery is in the Jamaica section of the borough of Queens in New York City and was established in 1668. Markers to be conserved were selected by the Prospect Cemetery Association and repair specifications were completed by another conservator. Many of the repairs were made to early sandstone markers, particularly those in danger of losing the face of the marker due to delamination of the sandstone. In addition to grouting, an alternative treatment to pinning, the installation of stainless steel armatures, was undertaken.

3. Pinning

3.1. Pinning Criteria

The basic criteria for architectural pinning repairs are: pins should not corrode, the adhesive should not stain the stone, the repairs should be aesthetically pleasing, and none of the materials should cause harm.

Conservation pinning repairs must be kept simple. In order to retain as much historic fabric as possible, the drilling of holes should be kept to a minimum. The size and number of pins used should be based upon the shear and tensile strength requirements of the stone being repaired. While it would be ideal to test the materials for each application, this is frequently not viable so judgements are made by each conservator. Many of the tests carried out and reported on in the journals and in thesis work have all been performed in the laboratory (Glavan 2004 and Wheeler *et al.* 2010).

Stones have been repaired with pins since ancient times. Traditionally, pins were wrought iron or bronze. In the later part of the 20th century, threaded nylon pins threaded stainless steel and ceramic pins came into use. A consideration when selecting pins is that cemetery markers often sustain impact damage. Traditionally lime mortar or lead were used to hold pins in place. By the end of the twentieth century epoxy resin adhesive was extensively used for exterior repairs.

3.2. Pinning Methodology

All of the pinning repairs examined for this study are concealed, blind pinning repairs made using stainless steel threaded pins. The pins are made by cutting stainless steel rods to the size of pin required. When making a blind pin repair, holes of equal depth are drilled into each of the two surfaces. Adhesive is placed in each hole, then pins are inserted into the holes and the two pieces are adhered with an adhesive at the joined surfaces. For the cemeteries in this study, either Akimi Akepox 2040 or 5000 were used as the adhesive. Both of Akepox 2040 and Akepox 5000 are designed for use with damp stones. The Akepox 5000 is designed to be more stable in ultra violet light. Once the adhesive has cured, the joint at the break is patched to keep the adhesive from contact with ultraviolet light and to match the stone surface. The pins are threaded to increase the bond between the pin and the adhesive. The adhesive then holds the pin in place ensuring lateral stability of the repair. There has also been testing of adhesives in the laboratory but little examination of exterior stone adhesives in situ over time (Muir 2008).

3.3. Pinning Failures

Pinning treatments generally fail by breakage of the pin, breakage of stone around the pin, or pullout of the pin. Failure of the pin will depend on the size of the pin and the type of pin material. Tensile failure is often assumed to be unlikely as the expected stresses associated with differential movement are far less than the tensile strength of the pins. However, impact damage can create tensile forces greater than those of low strength pins.

Stone is also susceptible to cracking and breaking from the pins. This can be caused by placing pins too close to an exterior surface or spacing the pins too close together. This type of failure can also occur in cases where the properties of the pin, such as modulus of elasticity and thermal expansion coefficient, are not compatible with the stone. Research undertaken by George Wheeler (Wheeler 2010) has noted when pins are installed and touch the marble, micro-cracking at the pin hole can occur.

Most of the failures found in older repairs occurred in the marble markers. However, due to what appears to be human interaction with these failures, it is not possible to evaluate how much the pin itself has impacted the failure in the cemeteries reviewed.

Pinning failures were found in thin marble markers in the Orient cemetery which was the only cemetery where pinning repairs were made to thin markers. Marble markers are more likely to have surface disintegration and intergranular disaggregation than granite or sandstone. This makes drilling the holes more difficult and the adhesion of the broken sections more challenging as there is little sound surface to adhere the broken components. Cracking and breakouts are common characteristics found in pinning failures where there has been impact damage by vehicles, mowers, and vandalism. Thicker sandstone or marble markers are more durable and able to take impact damage better than the thin stones.

Two of the marble pinned markers in the Orient cemetery failed 8 years after treatment. As with many failed pinning treatments, these markers were thin marble, one marker was 2 inches in depth and the other 2 ½ inches. When the cemetery was examined two years ago, both markers were intact. Currently the two markers are lying on the ground, each in a different direction, and they are broken again along some of the pinned breaks. It is not clear exactly what happened but it appears some human factor was involved. A pin was bent on one marker and stone is still attached to top of the pin in a pattern similar to failure in a pull- out test.

Another mode of failure found during the survey, is failure of the adhesive. The bond between the adhesive and the stone was either weak to begin with or the bond to the stone never occurred. An examination of the breaks in the Orient failure may be a failure of the epoxy adhesive in the repair. Some of the epoxy adhered to the stone and it was well adhered to one pin in each stone. The epoxy did not adhere to the top hole in one stone and the bottom hole in another. In addition, the adhesive along the break minimally adhered to the bottom stone, and not to the top. Also the epoxy had yellowed on all surfaces including where it nominally adhered to the stone. It is supposed to be colorless. The cross-section of the epoxy was examined under the microscope and is not yellowed. It was also noted during the microscopic examination by Helen Thomas, a conservator at Jablonski Building Conservation, that the surface of the epoxy has the imprint of the stone, even if there was no adhesion. This is the same epoxy, Akepox 2040, that was used in all other cemeteries included in this study. However, conservators have recently been discussing the issue of this epoxy yellowing when used for sculpture repair in New York City. In one example, a stone patch repair on a fountain yellowed within months of its application.

It would appear that the markers may have been “bumped” and the failure of the epoxy contributed to the failure of the repair. Luckily the stone was minimally damaged except where it was pulled apart at the one pin. There was no cracking of the stone and the adhesive failed before the stone cracked.

3.4. Successful Pinning Repairs in Sandstone and Marble

Stones with a depth of more than three inches have successful pinning repairs whether the stone is marble or brownstone. The 10 year pin repairs to sandstone and marble markers in Bottle Hill Cemetery, exhibited no failures. Three sandstone and the 7 pinned marble markers including a large obelisk were in excellent condition. There was one very complex sandstone repair of a horizontal 4 inch slab in that had been broken into 10 pieces remains

completely intact 10 years later (Fig. 1). In addition, a pinned brownstone marker that was found toppled in the cemetery survived intact. All pinning repairs in the Whippany cemetery are also intact, for the marble and brownstone. The marble markers at Whippany were all thick marble greater than 3 inches in depth. Eight marble markers were pinned at the Orient cemetery as part of their treatment and 6 are still in good condition are both of the sandstone pinning repairs.



Fig. 1: Vault Slab with Pinning Repair 10 years later.

3.5. Alternate Solutions to Pinning Thin Marble Markers

Our firm remains wary of pinning thin marble markers and is trying a new solution: a stainless steel armature (Fig. 2). Stephanie Hoagland, a conservator at Jablonski Building Conservation saw a similar armature in a cemetery and modified the design. We have only been using these armatures for three years but to-date, they appear to be working well. The armature supports markers externally by holding them intact. There is no drilling or adhesives used. This type of armature is used for any marker that is less than 2 inches in depth as these are impossible to pin.

4. Grouting

4.1. Grouting Criteria

Injection grouting is a typical method for reattaching delaminating stone layers and filling voids and small cracks in historic masonry. It has been used for cemetery repairs for many years. The conservation requirements for grout are: it be injectable, stable, able to mechanically bond with the stone and be chemically compatible with the stone. There must also be minimal, if any, shrinkage of the grout.

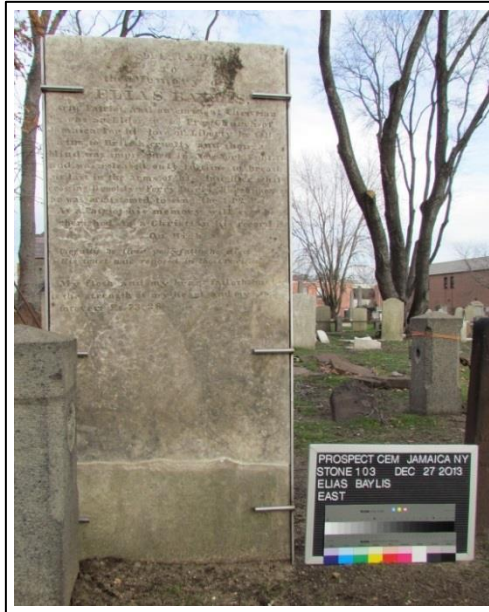


Fig. 2: Armature supporting thin marble marker in Prospect Cemetery.

4.2. Grouting Methodology

Many of the earliest extant markers in the Northeastern United States are a form of brown sandstone called “brownstone”. The face of the sandstone markers is carved and can be quite elaborate in their decoration. In addition to giving information about the deceased, these stones can be masterpieces of folk art with occasionally the name or initials of the carver. At the Bottle Hill cemetery, there were a number of stones signed by a very prominent carver in New Jersey, Ebenezer Price and his workshop. Price was born 1728 and was one of the most skilled and prolific gravestone carvers in colonial America, Price's work began to appear in the burial grounds of northern New Jersey in 1757 (Sarapin 1994).

One of the major deterioration problems with sandstone is delamination or separation along the bedding plane of the stone. Sandstones are sedimentary stones formed in layers through deposits of mineral or organic particles. Weakly joined sedimentary planes when exposed to weather, have a tendency to separate along the planes. If the stones are placed so that they are faced bedded, the bedding planes are at right angles to the position they had in the ground. Weathering can deteriorated the less compacted sedimentary layers causing the

stone to delaminate. Delaminating sandstone markers faces pose serious conservation challenges. It has even been suggested that the service life for some of these stones is only 100-125 years (McGinley Kalsow 2012).

Removing deteriorated stone from the delaminating layers and voids is the most difficult process. It must be removed or consolidated in order to ensure proper adhesion with the rest of the stone. Deteriorated stone is flushed from the voids out through port holes as best possible. An attempt is made to keep the port holes as small but they have to be large enough for debris to be flushed out of them. It can be difficult to remove all the deteriorated stone. Also these holes can be visually intrusive.

After cleaning the void is grouted. The grout needs to be as low viscosity as possible in order to flow into the void. Too much water though will result in shrinkage of the grout as it cures. The port holes are made into the stone at the void to clean it are used to grout it from the bottom up with syringes. Many of the grouts are difficult to keep at a low viscosity in the syringe. Where deteriorated stone is left, the bond between the grout and sound stone is not very good. Where the face of the stone had come off either before or during the treatment of a marker, and the deteriorated stone can be almost completely removed, the repairs are quite solid 10 years later.

4.3. Grouting Failures

Bottle Hill Cemetery in New Jersey has 10 year old repairs. Sixty-seven stones were grouted with Jahn M40 (manufactured by Cathedral Stone Products, Inc.). It is a non-shrinking grout formulated to repair cracks and voids approximately 5 mm to 15mm and is completely mineral based. In 2015, 35 or 52% have failed where the grout has debonded from the stone, cracked, crumbled or all three (Fig. 3 is one example). 22 or 33% are seriously deteriorated where it sounds hollow behind the repairs and the patching over the grout has failed. 10 repairs or 15% appear to still in good sound condition. It should be noted that the mortar caps failures over the grout repairs were approximately 90% but these mortar repairs did not fail when they were used on stone without the grout. The grout repairs at the Whippany Burying Ground had similar failures and a 90% failure rate.

Because the success of grouting repairs is dependent on the stone, markers with substantial friable layers of deterioration may not be treatable. Conservators aim for minimal treatments which limits aggressive treatments. When the faces delaminate, they can be cleaned and most of the deteriorated stone can be removed and the faces reattached. Where these treatments were performed in Whippany and Prospect Cemeteries they have so far been successful. However, it remains exceedingly difficult to predict which stones can be successfully grouted. The voids vary for each marker in size and location. Each marker collects debris as well as the grains of disaggregating stone in varying amounts and size. Flushing this debris out of small openings is not always effective. One stone in Prospect Cemetery had snails living in a void. They did not wish to remove themselves and it was not until the grout failure caused the face of the stone to delaminate that they were removed. There is also the questions of whether washing the voids may also be contributing to further deterioration of the already disaggregated stone.

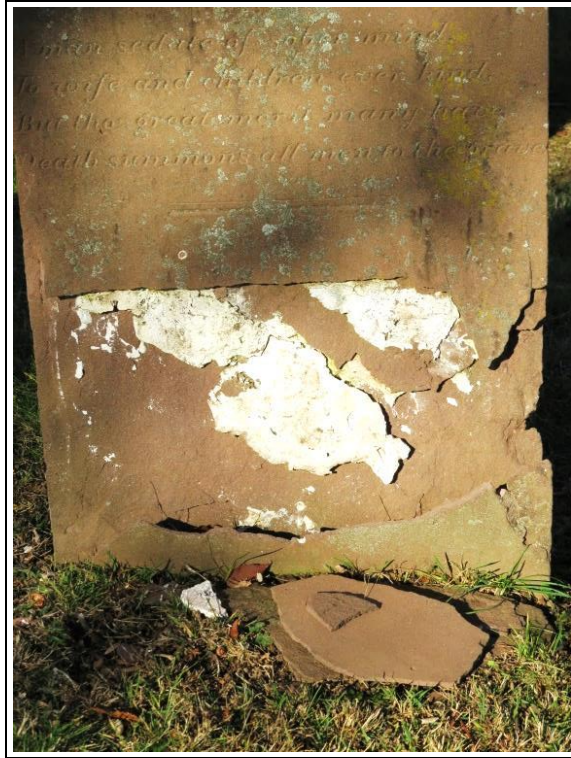


Fig. 3: Grouting Failure at Bottle Hill Cemetery.

Injecting grouts into a hidden void does not allow for control over the flow and location of flow. It is difficult if not impossible to determine if the entire void has been grouted, if the void is only in one layer, or if there are more voids behind the one closest to the surface. There are serious concerns about whether grouting may cause more damage to the stone by accelerating the delamination rather than leaving them to deteriorate. Mortar caps on the grout deteriorate at a much quicker rate than the caps over stone. Often the mortar caps are gone or cracked which raises concerns. Is the grout contributing to further deterioration of the already deteriorating stone?

Grouting may be the last resort treatment for some stones. Grouting treatments will continue for delaminating sandstone markers when there is no other solution and only where the treatments can be monitored over time. Therefore, monitoring will continue for the Void Span repairs yearly to see if this product lives up to its promise.

4.4. Grouting Successes

In 2013 at Prospect cemetery, 10 stones were grouted. A working sample or mockup was made using a mix of St. Atier's natural hydraulic lime (NHL) 3.5, sieved through a #50 mesh and added casein powder as needed. The grout failed as areas that had been filled sounded hollow several days later. Next, a mocked up was made using a lime sand and micro-balloon mixture. Again, the grout treatment failed. The following year, a new commercially available product, Void Span PHLc Grout, produced by VoidSpan

Technologies, LLC, was tested. This grout is a breathable, ultra- low shrinkage, flowable, self-consolidating grout for use in filling cracks and voids in older masonry structures. Based on a pozzolanic hydraulic lime as per ASTM C1707, it is a low- to-moderate strength adhesive, filler and mortar replacement material. One year later the grout appears to be working well in the 10 markers grouted with the Void Span PHLc.

Earlier grouting success appeared to occur where there was more control over removal of deteriorated stone, mainly when the faces or portions of the faces of the stone were separated from the stone. In addition, there were two stones at Bottle Hill Cemetery that appeared to have a different mineralogy and the grouting repairs on these stones is still solid.

4.5. Alternatives to Grouting

As it is difficult to predict the success of a grout treatment, it is therefore necessary to examine other solutions to treating delaminating parallel layers of stones. One treatment is to install a lead cap over the top of the stone. We have been using these for the last two years and as long as the squirrels do not eat the lead, they work very effectively.



Fig. 4: Lead cap over delaminating sandstone marker.

5. Conclusion

It must be recognized that a repair may eventually fail or be detrimental to the marker. We should also consider that we might want to wait to treat stones when we are not sure of the outcome as there is the possibility that future materials, methods, and technologies may offer better treatment choices. Ultimately, the effectiveness of treatments performed on cemetery markers relies on quality of the stone, as well as the quality of the work, repair techniques, and performance of materials used to make the repairs.

Examining old treatments has shown that pinning repairs do appear to work in many instances although pinning thin marble markers is not necessarily a good idea. Grouting repairs have not had a very good track record. It may be that new products coming out on the market will assist in making these more durable repairs. Time and monitoring of treatments will tell.

When we leave the cemetery, we need to leave a monitoring and a maintenance plan behind. Too often there is the belief by the owner that the conservation treatments do not need any further attention. We know products fail; the execution of the repairs can be faulty; and common techniques may be damaging. It is only through monitoring we will truly understand what treatments have withstood the test of time.

References

- Bradley, Susan. "Strength testing of adhesives and consolidants for conservation purposes." Adhesives and consolidants. N.S. Brommelle *et al.*, eds. London: International Institute for Conservation of Historic and Artistic Works, 1984. 22-25.
- Glavan, J. 2004. An evaluation of mechanical pinning treatments for the repair of marble at the Second Bank of the United States. Master's Thesis. University of Pennsylvania, Philadelphia.
- Grimmer, Anne E. Glossary of historic masonry deterioration problems and preservation treatments. Washington, DC: National Park Service, Preservation Assistance Division, 1984.
- McGinley Kalsow & Associates. Brownstone & Masonry Repairs and Exterior Historic Structures Report: Concord Town House. 22 Monument Square, Concord, MA 01742. November 8, 2012.
- Muir, Christina. 2008. Evaluation of Pinning Materials for Marble Repair. Master's Thesis. Columbia University, New York, NY.
- Riccardelli, Carolyn, George Wheeler, Christina Muir, George Scherer and Joe Vocaturo. An examination of pinning materials for marble sculpture. *Objects Specialty Group Postprints, Volume Seventeen, 2010.* 95-112.
- Sarapin, Janice Kohl. Old Burial Grounds of New Jersey: A guide. Rutgers University Press, 1994. 26.
- Wheeler, George "New Insights on Pinning Fractured Marble". Talk presented at APTI Conference: Layers Across Time. Denver 2010.
- Zinsmeister, H, etal, 'Laboratory Evaluation of Consolidation Treatment of Massillon (Ohio) Sandstone', *Association for Preservation Technology Bulletin*, 20:3, 1988

THE CURRENT STATE AND FACTORS OF SALT DETERIORATION OF THE BUDDHA STATUE CARVED ONTO A CLIFF AT MOTOMACHI IN OITA PREFECTURE OF JAPAN

K. Kiriyama^{1*}, S. Wakiya², N. Takatori³, D. Ogura³,
M. Abuku⁴ and Y. Kohdzuma⁵

Abstract

The Motomachi stone-cliff Buddha is located in Oita prefecture, Japan. It was engraved onto a soft-welded tuff cliff around the 11th to 12th centuries. At this site, salt crystallisation is a major factor causing deterioration of sediments, especially during winter. This paper attempts to discuss the relationship between the behaviour of salt and environmental factors at the Motomachi stone-cliff Buddha site. We conducted four seasons of environmental research, analysis of dissolved ions in the groundwater, and salt analysis. Results suggest that a drop in temperature and vapour pressure due to the opening of the doors, combined with water intrusion within the high-water-content stone could be causes for salt crystallisation at this site.

Keywords: salt deterioration, Sodium sulphate, Calcium sulphate, environmental research, solubility, shelter

1. Introduction

Salt crystallisation is one of the most common causes for the occurrence of stone deterioration. Recent studies have investigated the effect of temperature and relative humidity on in-situ salt crystallisation (Bionda 2004, Zehnder and Schoch 2009). However, the behaviour of salt, especially in-situ salt crystallisation, remains controversial. In Japan, major methods to prevent salt crystallisation include using polymers to strengthen the stone surface and lowering of groundwater levels. However, the issue of an ideal environment to restrain salt deterioration awaits further investigation. This paper attempts to investigate the

¹ K. Kiriyama*
Graduate School of Advanced Integrated Studies in Human Survivability,
Kyoto University, Japan
kiriyama.kyoko.24n@st.kyoto-u.ac.jp

² S. Wakiya
Nara National Research Institute for Cultural Properties, Japan

³ N. Takatori and D. Ogura
Graduate School of Engineering, Kyoto University, Japan

⁴ M. Abuku
Faculty of Architecture, Kinki University, Japan

⁵ Y. Kohdzuma
Nara National Research Institute for Cultural Properties, Japan

*corresponding author

relationship between salt behaviour and environment at the Motomachi stone-cliff Buddha and aims to consider measures to prevent salt deterioration.

2. Background of the Motomachi stone-cliff Buddha

The Motomachi stone-cliff Buddha is located in Oita prefecture, Japan. It was engraved onto a cliff of soft welded tuff around the 11th to 12th centuries and was covered by a shelter which was built during later periods (figure 1). The entrance of the shelter faces east. At this site, salt crystallisation especially in winter (figure 2) is a major factor causing deterioration. Powdering and scaling occur on the surface of the stone. A previous investigation identified thenardite and mirabilite by X-ray diffractometry (XRD) (Oita city board of education 1996). Although a drainage tunnel and drainage well were built in order to lower the groundwater levels as a conservation measure, an increase in the amount of salt was reported after this construction.

3. Methods

To investigate the environmental effects on salt crystallisation, environmental research, analysis of dissolved ions in the groundwater and analysis of the salt deposit were carried out over several seasons (1 August 2014, 8 November 2014, 8 February 2015, 18 April 2015, 2 August 2015).

3.1. Environmental research

To investigate the interior environment of the shelter, the interior temperature, relative humidity, and ventilator frequency were measured, in addition to meteorological observations. Fig. 3 indicates the locations of door-opening/closing sensors, temperature and relative humidity data loggers, and the weather station. Temperature and relative humidity were measured inside and outside the shelter from November 2014. The counts of door-opening/closing were measured from February 2015. Local meteorological data was measured from February 2015 at the weather station.



Fig. 1: View of the site from distance.



Fig. 2: Seasonal changes in salt deposit.

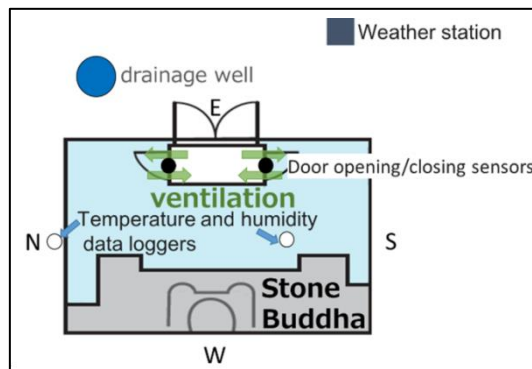


Fig. 3: Measurement points.

3.2. Dissolved component analysis of the groundwater

To evaluate the effect of groundwater on salt crystallisation, dissolved ions of groundwater were analysed quantitatively by ion chromatography during each season as noted above. Water-sampling was conducted at the drainage well and observation hole (Fig. 4a). The drainage well is located in front of the shelter and the observation hole is located behind the stone-cliff Buddha. The sampled water was transported in a cold state and filtered with 0.45 µm nuclepore filters for analysis. Further, data of annual changes in groundwater tables were provided by Oita City records.

3.3. Salt analysis

Salt was observed during all field surveys. The salts were identified by X-ray diffraction during each season. The sampling points are shown in Fig. 4b. These points were selected in order to compare the salts between different horizontal points, where they appeared to be in different forms, and different vertical points in which the water content ratio appeared differs.

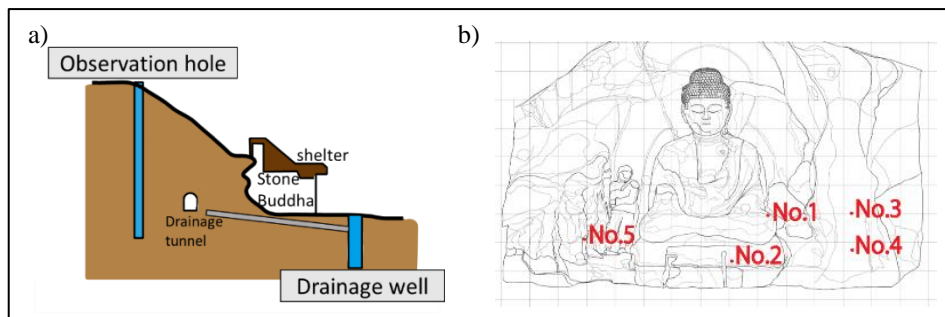


Fig. 4: a) Water sampling points (drainage well and observation hole);
b) Salt sampling points.

4. Results and Discussion

4.1. Observation

According to these observations, it appears that salt crystallisation was concentrated in the lower part of the surface of the stone. The distribution of crystallised salt could be affected by water movements. The elevation of the bottom of the stone Buddha and the drainage tunnel is around the same. Therefore, water may have flowed from the ground into the stone. Since salt crystallisation was observed in areas that have deteriorated on the surface of the stone (along a joint or on an exposed surface by scaling), it is suggested that salt was concentrated here owing to high permeability.

4.2. The interior environment of the shelter

Fig. 5 shows the exterior and interior temperature and absolute humidity throughout the year. The annual and diurnal fluctuations of the interior temperature and absolute humidity (Fig. 5) reveal that the shelter has a low degree of airtightness. Figures 6 show temperature and absolute humidity both inside and outside the shelter during summer and winter period. The door-closing periods are shaded. During summer and winter, when the doors were opened, the interior absolute humidity exhibited the same behaviour as that noted in the exterior. On the other hand, when the doors were closed, the interior absolute humidity was higher than that of the exterior. If absolute humidity decreases the amount of water evaporation from stone will increase. Water evaporation promotes salt crystallisation. Therefore, the opening of the doors may be a factor in salt crystallisation.

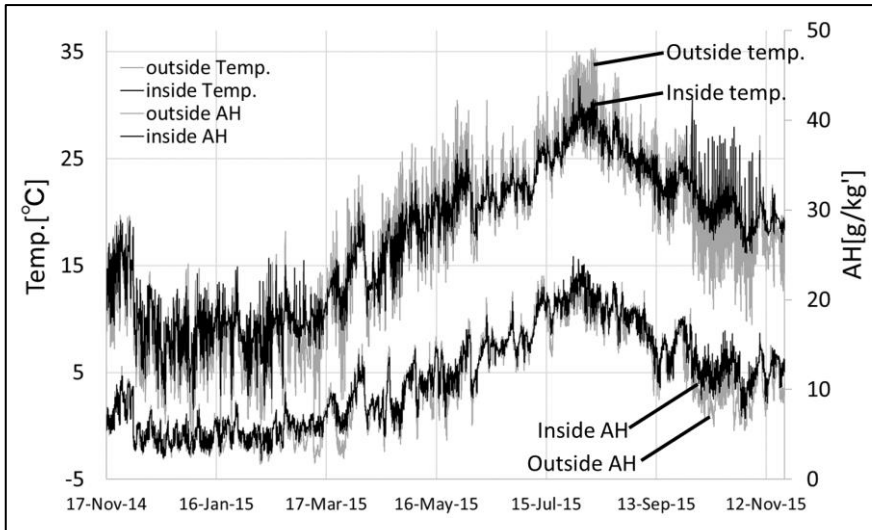


Fig. 5: Inside and outside temperature and absolute humidity.

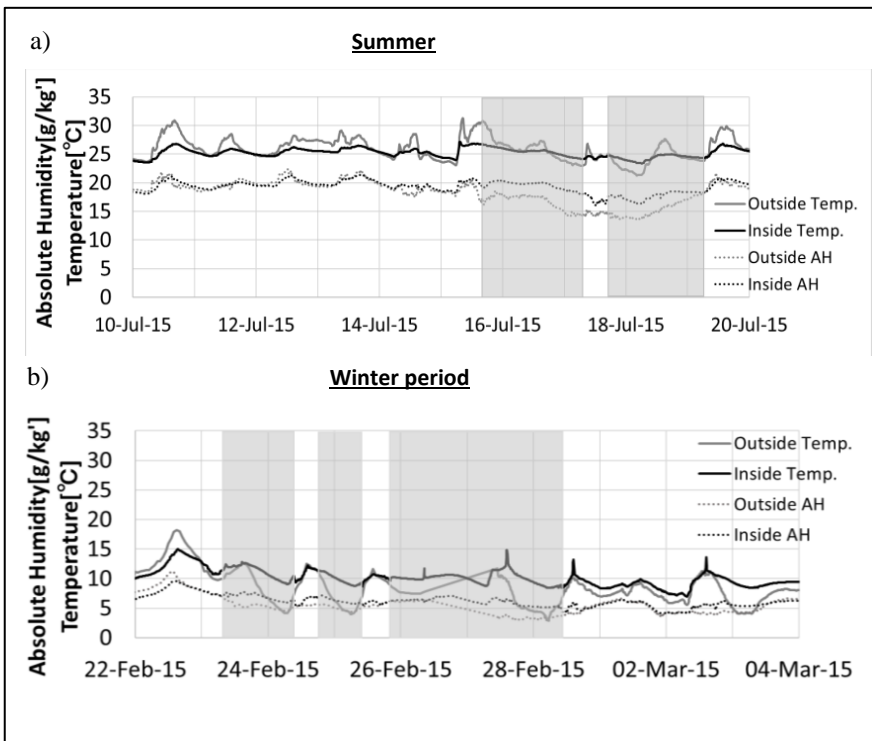


Fig. 6: Absolute humidity and temperature both inside and outside the shelter. The closed-door periods are shaded in grey.

4.3. Effect of groundwater

The result of the analysis of the groundwater is given in Figures 7a and 7b. Sulphate, calcium and sodium ions, that are the origins of gypsum and thenardite, are detected in the water. The concentration of ions dissolved in the observation hole water is prone to be higher than that of the drainage well except for sodium and potassium ions. There are few seasonal changes in the concentration of ions. This means that the inside environment of the shelter has an effect on salt crystallisation in winter. Fig. 8 shows the groundwater table of the observation hole and the precipitation in 2014. The water level seems to be constant at 1-2m above the drainage tunnel except for during continuous rain. The fluctuation within each season cannot be observed. Therefore, the water level may not have an effect on seasonal changes in salt crystallisation (as mentioned in background).

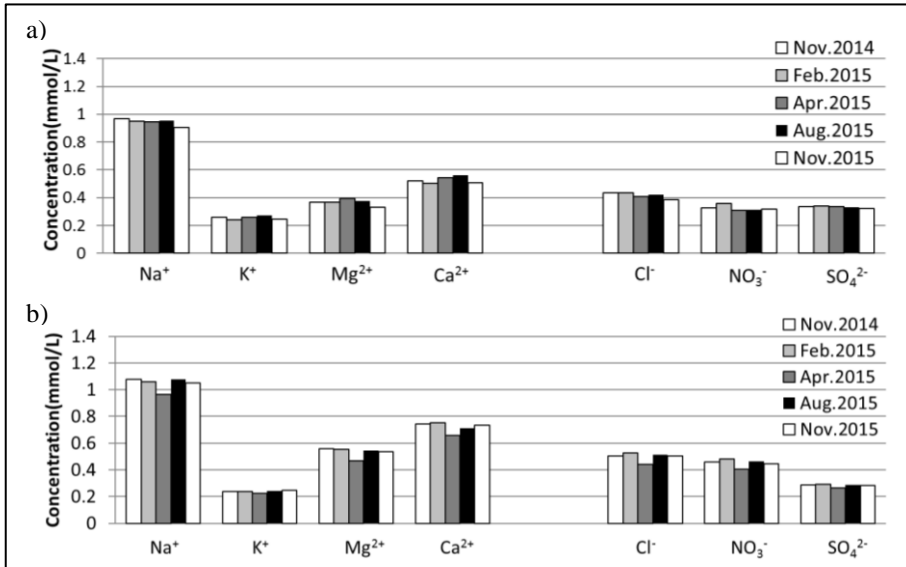


Fig. 7: a) Results of ion chromatography of the water from the drainage well; b) Results of ion chromatography of the water from the observation hole.

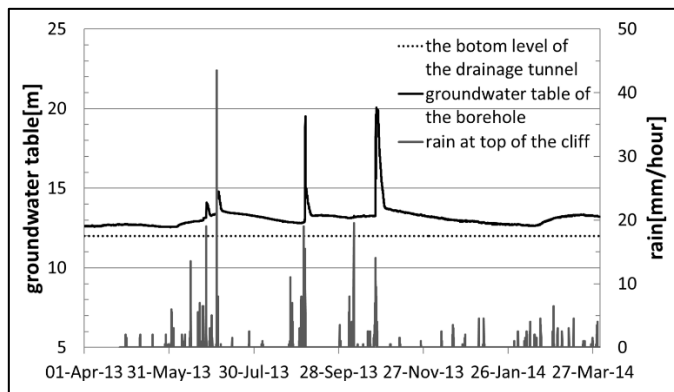


Fig. 8: Groundwater table of the observation hole and precipitation.

4.4. Environmental effects on salt crystallization

The results of the XRD are presented in Tab. 1. Thenardite and gypsum were identified. We could not collect salt at the points where salt crystallisation usually occurs in winter, as these were protected by a paper pulp to desalinate the surface layer. The solubility of calcium sulphate has less temperature dependence. Further, the equilibrium relative humidity of the calcium sulphate saturated solution is around 99% at normal temperatures. Therefore, once it crystallised, it is likely that calcium sulphate could have remained on the surface of the stone in a crystallised state all year long. Therefore, the statement that ‘salt crystallises in winter and disappears in summer’ as stated in a report (Oita city board of education 1996) implies that the salt is the soluble sodium sulphate.

Sodium sulphate has two stable phases at room temperature: thenardite (an anhydride) and mirabilite (a decahydrate). Fig. 9 illustrates a phase diagram for sodium sulphate and the temperature and relative humidity of daily averages inside the shelter. The continuous lines indicate the boundaries of the stable phases (Flatt 2002). The temperature and humidity cross the phase boundary due to annual and diurnal changes. This diagram implies that the inside environment facilitates damage to stone caused by phase changes and crystallisation of sodium sulphate. However, this does not correspond entirely to the accrual situation, which is the disappearance of sodium sulphate crystallisation in the rainy season and in summer. Some reasons to be considered include decreasing solubility with a drop in temperature and the concentration of soluble salt.

As regards calcium sulphate, it could appear to be ineffective as compared to sodium sulphate as it may not repeat the process of crystallisation and disappearance. However, before repairing the shelter, photos show water intrusions from a crack in the roof that wet the stone surface during rains. In addition, the high water content of the stone in the lower parts as well as intrusive water could have made it easy for the slightly soluble calcium sulphate to move to the surface.

Tab. 1: Result of XRD studies.

	01-Aug-14	08-Nov-14	08-Feb-15	18-Apr-15	02-Aug-15	15-Nov-15
No.1	Thenardite	Thenardite, Gypsum	Thenardite	Thenardite, Gypsum	-	-
No.2	Gypsum	Gypsum	Gypsum	Gypsum	Gypsum	Gypsum
No.3	Gypsum	Gypsum	Gypsum	Gypsum	Gypsum	Gypsum
No.4	Gypsum	Gypsum	Gypsum	Gypsum	Gypsum	Gypsum
No.5	Gypsum	Gypsum	Gypsum	Gypsum	Gypsum	Gypsum

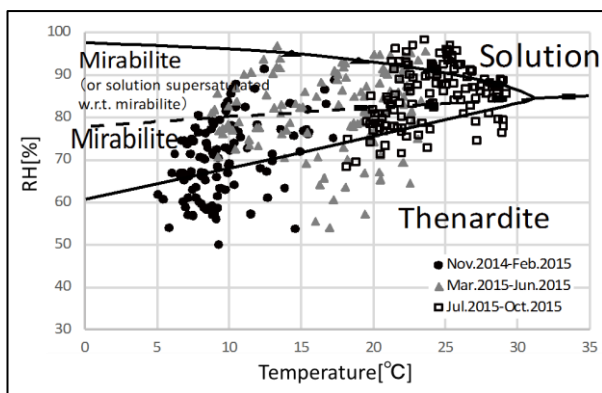


Fig. 9: Phase diagram for sodium sulphate and temperature and relative humidity of daily average inside the shelter, based upon data from Flatt (2002).

5. Conclusion

To investigate the relationship between salt behaviour and the environment, environmental research, dissolved ions analysis of the groundwater and salt analysis were carried out for each season. The results suggest that door-opening, a drop in temperature and water leaking into the high-water-content stone could be the three factors for salt crystallisation to occur at the Motomachi stone-cliff Buddha. Proposal of an ideal environment for the preservation of the stone-cliff Buddha is the subject of further study.

Acknowledgements

We are grateful to the Oita-city board of education for the image of stone-cliff Buddha (Figure5) and the groundwater table of the observation hole. This work was supported by JSPS KAKENHI Grant Number 26709043 [Grant-in-Aid for Young Scientists (A)]

References

- Bionda, D., 2004, Methodology for the preventive conservation of sensitive monuments : microclimate and salt activity in a church, Proceedings of the 10th international congress on deterioration and conservation of stone, Daniel Kwiatkowski and Runo Löfvendahl (eds.), Stockholm, ICOMOS, 2, 627–634.
- Flatt, R. J., 2002, Salt damage in porous materials: how high supersaturations are generated, Journal of Crystal Growth, 242, 435-454.
- Oita city board of education, 1996, *Kunishiteishiseki Oitamotomachisekibutsu Hozonsyurijigyo Hokokusho* (in Japanese), oita, sohrinsha.
- Zehnder, K. and Schoch, O., 2009, Efflorescence of mirabilite, epsomite and gypsum traced by automated monitoring on-site, Journal of Cultural Heritage, 10, 319–330.

THE DURBAR SQUARE AND THE ROYAL PALACE OF PATAN, NEPAL – STONE CONSERVATION BEFORE AND AFTER THE GREAT EARTHQUAKE OF APRIL 2015

G. Krist¹, M. Milchin^{1*} and M. Haselberger¹

Abstract

The Durbar Square and the Royal Palace of Patan (Nepal) constitute one of the seven World Heritage Monument Zones of the Kathmandu Valley. In 2010, the Institute of Conservation, University of Applied Arts Vienna, joined the conservation project of the Royal Palace, run by the Kathmandu Valley Preservation Trust (KVPT). The subsequent cooperation between the Institute and the KVPT has over the years resulted in the conservation of numerous monuments of stone, wood, metal, ivory and other materials. When dealing with the stone monuments, the greatest problems conservators were faced with were structural issues resulting from frequent earthquakes and subsequent inadequate repairs, combined with the extreme climate of the region. Attention was given to the removal of inappropriate materials. A brick dust lime mortar was used for the pointing of the joints, instead of the cement rich mortar which was invariably used in repairs executed in the second half of the 20th century. To improve the resistance to future seismic activities, stainless steel pins and clamps were used when reassembling. This presented a novelty (in the way of doing things). During the severe earthquake of 25th April 2015, also known as the Gorkha earthquake, and the subsequent one of 12th May, many monuments in the Valley were damaged. The impact on the Patan Durbar Square and the Royal Palace was equally devastating. A preliminary survey revealed that the monuments which were recently treated by the Institute, endured without major damage. On the other hand, many of those still carrying marks of old repairs were now in dire need of a treatment. Given this scenario, a conservation project, extending up to 2018, was drafted. Works would be carried out by the Institute together with Nepalese partners, and with the financial support of the Austrian government.

Keywords: conservation, earthquake, Kathmandu Valley, Patan, stone

¹ G. Krist, M. Milchin* and M. Haselberger
Institute of Conservation, University of Applied Arts Vienna, Austria
marija.milcin@uni-ak.ac.at

*corresponding author

1. Introduction

The bilateral relations between Nepal and Austria, especially in the field of heritage preservation, have a long tradition. It started when Eduard Sekler (Harvard University) first visited Kathmandu Valley in 1962. Subsequent trips, in association with UNESCO, resulted in the 'Master Plan for the Preservation of Cultural Heritage of the Kathmandu Valley' and the inclusion on the World Heritage List. The first visit of Gabriela Krist (University of Applied Arts Vienna) and Manfred Trummer (Museum of Applied Arts Vienna) in 2010, kick-started the presently ongoing cooperation between the Institute of Conservation and the Kathmandu Valley Preservation Trust (KVPT). From 2010 to 2014, thirteen small monuments from the Patan Durbar (=Royal) Square and the Royal Palace, one of the seven monument zones of the Valley, were successfully treated and conserved (Krist *et al.* 2010-2014). In 2015, two devastating earthquakes hit the Kathmandu Valley. A new outlining of priorities was required, and a three-year project (2015-2018) to preserve earthquake-damaged cultural heritage was drafted by the Institute of Conservation together with local partners and is funded by Austria. The following report discusses the challenges of the previous conservation campaigns and the solutions which were eventually used, after the severe earthquakes.

2. Nepal's Challenges

The extreme climate conditions, heavy biological colonization, and the distortion of the structures, are among the main problems of the monuments in Patan. The latter is explained by cycles of demolition (partial or total) through frequent earthquakes and the efforts to repair, rebuild and/or restore. The high amount of water available during the monsoon period combined with the stones' physical properties, not only favour the fast growth of microbiology, but also higher plants.

2.1. Material and Structure

Two different stone materials were used for the monuments of the Durbar Square and Palace of Patan. The first one is a very porous and capillary-active siliceous sandstone. The grain is fine and the colour can vary from whitish to ochre. In general, the stone is very homogenous, though some of the blocks show distinct bedding. Tooling marks on the blocks indicate a very fine workmanship which was only possible due to its homogeneity and softness. Analysis on stone samples² in Vienna included thin section microscopy, both in polarized and unpolarized light, SEM investigations, as well as porosity measurements and petrographic characterization. In addition, prisms were used to measure the water absorption after a 24 hour immersion, water absorption coefficient, and the drying rate. The results show water absorption of 10% to 18% and a water absorption coefficient from 5.25 to 30.2 kg/m²h^{0.5} (Fuchs 2013). Despite the big differences in the water uptake, these high values show that the stone is very absorptive in all directions. This property can also be directly related to the usual damage. Decay through microbiological growth and salt contamination presents the biggest problem. Sanding, scaling and alveolar decomposition

¹ Funding partners: Austrian Development Agency (ADA); the Austrian Federal Chancellery (BKA); the Federal Ministry for Europe, Integration and Foreign Affairs (BMEIA V, North South Embassy Project - BMEIA VII); Eurasia-Pacific Uninet (EPU).

² Katharina Fuchs, Institute of Conservation and Prof. Johannes Weber, Section of Conservation Sciences, Institute of Art and Technology, University of Applied Arts Vienna, 2012-2013.

are some of the most common manifestations. Monuments built up of the siliceous sandstone consist mostly of small blocks that can be carried by a single worker. Originally, no mortar pointing or metal pins were used. The bonding between singular blocks was established by simple adding an occasional natural resin dash in the joints. The gaps between the blocks were so small that the carving sometimes continues over more blocks, regardless of their dimensions.



Fig. 1: Decay patterns and typical construction of monuments made of the siliceous sandstone.

The other stone material which was employed, is dense, heavy and grey (light grey to almost black) in colour. It is a weakly metamorphic material containing a high concentration of silicates in foliations, surrounded by a very fine grained siliceous marble. Though the water uptake for this kind of stone was not measured, it can safely be assumed to be very low. All forms of decay that can be traced to the influence of water are very superficial. The majority of damage patterns were in all probability caused by mechanical impact (*e.g.* different cracks and/or missing parts). The structures made from this material consist of blocks which are much larger in scale and often contain stone dowels in vertical structures (*e.g.* columns and pillars). Even in this case, no bedding or pointing mortar was used. Both construction methods make the monuments extremely vulnerable during earthquakes. Distortions are caused as horizontal and/or vertical connections between the single blocks are only partly given.



Fig. 2: Decay patterns and typical construction of monuments made of the metamorphic stone.

2.2. Climate

The climate of the Kathmandu Valley is characterized by heavy rainfall in the monsoon period and no frost in winter; this favours biological growth (Leiner 2011). Stone surfaces are covered not only with algae and bacteria, but also with moss. Plants grow within joints and cracks, where earth and dust has accumulated. Due to the high water uptake and slow drying rate of the porous sandstone, surfaces remain mostly wet during the rainy season (Fuchs 2013). The microbiological growth is much stronger here than on the very dense surfaces of the metamorphic stone.

2.3. Introduced Materials and Recent History

Of the frequent, more-or-less intense earthquakes and apart from the recent quakes of 2015, the one of 1934 was the last disastrous one. It destroyed a large extent of Patan's historical centre. Most of the damage we are faced with today is directly related to materials and methods used in the course of the twenty years it took to rebuild, reconstruct and restore the structures affected by the earthquake of 1934. Blocks were sometimes swapped or completely discarded, and pointing mortar containing very little aggregate – instead of the traditional natural resin mentioned earlier – was introduced in the joints. In all cases, a low quality Portland cement was used as a binder (Leiner 2011). As happened elsewhere at the time, this material was seen as a solution for any situation, and as we now come to expect, the mortars turned out to be too hard, dense and stiff, and over the course of the years, damaged the surrounding stonework. Moreover, the copious amounts of water in combination with the capillary-inactive joints, allowed the blocks to remain wet for a longer period of time, thereby accelerating deterioration through bio-colonization and salts (Leiner 2011).

3. Conservation Campaigns 2010 – 2014

The situation of the stone monuments before the treatments carried out between 2010 and 2014 can be summarized as follows: damage as distortion, cracks, breakages and missing parts are a result of seismic activity. Repair in various phases has caused further decay since inappropriate materials, particularly pointing mortars were used. Due to the mild winter climate and excessive rainfall in the monsoon season, bio-colonization plays an important role in the overall deterioration mechanism. The aim of the conservation programme considered international standards which were adapted for the Nepalese context. The preservation of the structures and surfaces is imperative. The concept for the conservation had to be applicable in the extreme climatic situation of the Kathmandu Valley and consider the restricted availability of conservation materials. Additionally, the appearance of the previously treated surfaces and structures (brick and stone walls, wood constructions and roofing systems) had to be considered and an additional strengthening of structures envisaged. During the first four years, the following stone monuments were treated: the Bhandarkhal Tank pavilion; the stone lions at the Tank; two gate-keeper lions; the Tusha Hiti ritual bath and two stone relief gates. Wherever possible, the treatments were carried out in cooperation with local craftsmen. As the majority of the objects needed a dismantling, a very important first step was the graphic documentation - mapping and labelling of all elements. The dismantled blocks were cleaned with water and brushes; mortar remnants, paint spots and thick biological films were reduced mechanically. A biocide treatment (quaternary ammonium salts, 1-3%) was necessary in preparation for further works. Blocks with obvious salt damage or those with cases of strong salination were treated in water baths using monsoon rain (Fuchs 2013). Missing parts were reconstructed/ carved in stone as indents (Dutchmen) by local stone masons (Fuchs 2013). This proved to be a good solution since a high level of craftsmanship is still widely practiced in Nepal. This type of collaboration has the added advantage of contributing to the preservation of skills as intangible heritage. As a final step, the elements were reassembled. An important aspect of the conservation was to reduce water infiltration and improve the stability of the structures to withstand future earthquakes. Where possible, foundations were dried-out (Leiner 2011) and monuments were reassembled with an air draft separating them from the brick walls behind them (Fuchs 2013). Pins and clamps were used to additionally strengthen the structures. Anti-seismic rings were introduced by connecting the blocks of one specific course with stainless-steel-clamps. The rings themselves were connected to each other at the corners by using pins. For the pointing of the joints, a lime-brick dust mortar was used. It worked well in the climate of the valley and performed satisfactorily with the stone used.

4. The Earthquake and the First Response

In April and May 2015, the Kathmandu Valley experienced two devastating earthquakes, claiming more than nine thousand human lives and injuring over twenty-two thousand people.¹ The 2015 earthquakes can be considered the worst natural disaster in Nepal since 1934. An estimated total of 2,900 structures of cultural and religious value and major monuments of the UNESCO World Heritage - including the Durbar Squares of Kathmandu, Bhaktapur and Patan - were severely damaged or collapsed completely. The emergency

¹ Nepal Earthquake, Post Disaster Needs Assessment, Executive Summary, published by the Government of Nepal, National Planning Commission, 2015.

response, security and clean-up measures in Patan, started immediately after the earthquake. Valuable objects - such as wood carvings, gilded metal sculptures and stone reliefs, and remnants of collapsed temples on the Durbar Square - were brought to the Patan Museum courtyards and documented. With financial support from the Austrian government, temporary storage could be built to safely store these objects. Damaged building structures were secured with wooden beams and roofs were covered with tarpaulins to reduce water infiltration during the coming monsoon. A fact-finding mission in June 2015 by two conservators from the Institute of Conservation recorded the extent of the damage and set priorities for the future work of the Institute. The assessment of the destruction at Patan's Durbar Square and Palace can be summarized as follows: two temples and two rest-houses collapsed completely, several other buildings are still endangered and had to be secured. Additionally, two pillars with important fire-gilded sculptures (Lion and King Yoganarendra) collapsed. The stone pillars themselves are partly broken and/or fissured, the metal sculptures deformed and disfigured. Two roof tops of buildings that are part of the Royal Palace partly collapsed and had to be dismantled. Exterior walls of the Palace have been damaged and parts collapsed.

5. Conservation after the Earthquake 2015

Within a working campaign in August/September 2015 – being already the sixth of the Institute – first important measures on selected objects made of stone as well as metal and ivory could be implemented. Furthermore the seismic performance of the previously treated monuments was evaluated.

5.1. Evaluation of the Performance of Past Treatments

It could be concluded that the treatments done in the period between 2010 and 2014 performed well. All of the monuments are still standing and no major damage could be found. Even after a more detailed investigation only one single crack between the pointing mortar and the stone block on one of the relief gates of the Palace's façade facing the Durbar Square can be associated with the earthquakes.

5.1.1. Treatments

After the earthquake predominantly monuments made of the grey dense marble-like stone required treatment, whereas those made of sandstone represented the problematic cases in the period before 2015. There are three possible reasons for this: firstly, most of the monuments¹ made of the porous sandstone were treated shortly before the earthquake and measures were taken to improve the seismic stability of the structures. This however, seems to have worked quite well. A second reason is due to the nature of the material. While the sandstone is very porous and cracks easily stop in pores, the metamorphic stone is very dense and rigid so that the propagation of cracks and fissures occurs rapidly. Thirdly, blocks of different sizes behave differently during seismic activity. The sandstone monuments are made of rather small blocks and therefore the number of joints in the structure is high. This results in a relatively malleable structure which can deform easily without damage to the single blocks. The structures made of the metamorphic stone contain much larger blocks, and when this is combined with the rigid and dense material, greater

¹ Bhandarkhal Tank pavilion, two lion sculptures in the Palace's garden, two lion sculptures in front of the Mul Chowk, two stone relief gates at the Palace's façade.

cracking and fragmentation occurs. Two objects made out of the grey dense stone and the treatments which were adopted will be discussed.

5.1.2. *Hari Shankar*

The almost one and a half metre sized sculpture of the god Hari Shankar, stood at the heart of the Harishankar Temple on the Durbar Square. This collapsed completely in the course of the earthquake. As a result, the sculpture broke in two. A diagonal crack separated the figure of the god at waist level, and smaller sculptural details broke off. In the campaign of 2015, the two broken parts were glued together with epoxy resin (Akepox 2020, Akemi) and two stainless steel pins. Layers of dust, dirt and remnants of offering were reduced mechanically and with the use of different solvents. A missing attribute of the god was reconstructed using a stone indent (on request of the local authorities) to improve readability. Joints and gaps were pointed with adequate mortar.

5.1.3. *The Pillar of the Lion Statue*

The smallest of the three freestanding pillars on the Durbar Square of Patan partially collapsed during the course of the earthquake(s) and only the lowest part of the shaft remained standing. The large upper part of the shaft was broken in two. Work on the pillar started early to avoid further damage, since the bigger fragments were already being used as an *ad hoc* bench or market stand on occasions. The smaller upper stone parts as well as the metal lion sculpture on its top were recovered from the debris soon after the first earthquake. In the course of the campaign the broken shaft was glued together using the same epoxy resin and three stainless steel pins. The missing parts of the capital were reconstructed in the same stone and mounted with stainless steel pins and epoxy resin. The remaining gaps were pointed with a matching mortar. All surfaces were cleaned with water and solvents.



Fig. 3: Partly collapsed pillar used as market stand (left), gluing of broken parts (right).

During the course of the work, many technological details came to light. For instance, it became amply clear that the column had already collapsed in part during the last big earthquake of 1934. Moreover, the cement paste found in the upper joints was corroborated with the extensive reconstruction phase carried out in the 1950s. It was decided to remove the cement based mortar and to re-use the original construction method without joint mortar. This way, the structure will be rendered less rigid – and consequently more resistant to seismic action. Also, the device used originally to fit the lion sculpture on top of the column was renewed.

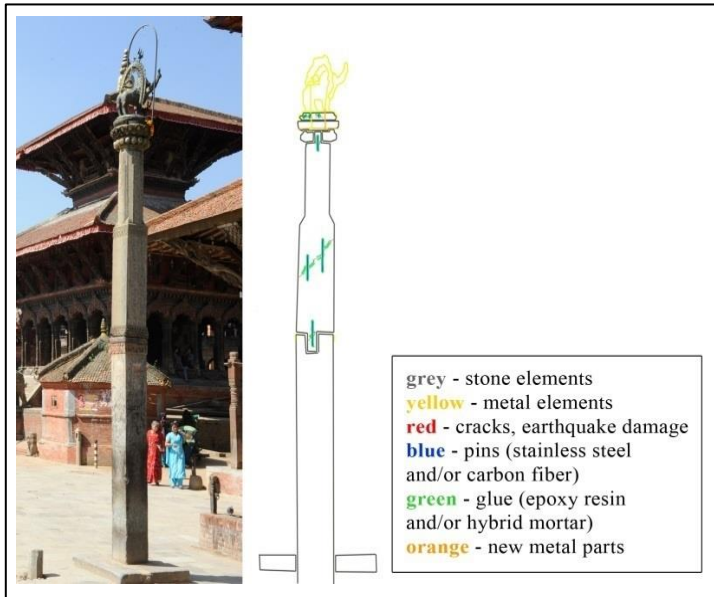


Fig. 4: Concept for the reassembling of the Lion Statue.

It can therefore be concluded that the stone structures treated by the Institute of Conservation between 2010 and 2014 were hardly damaged by the earthquakes of 2015. In general however, monuments made of the metamorphic stone were affected more severely and require more attention than the ones made from the porous sandstone.

6. Outlook

During the campaign of 2015, four metamorphic stone objects damaged during the earthquake were treated. The pillar of the Lion Statue will be reassembled in 2016. Particular attention will be given to the second monument on the Patan Durbar Square which also collapsed - the pillar of King Yoganarendra Malla. Even though the two pillars are different in size, both situations are similar. With a height of about 8 m, the King's pillar is almost double the height of the Lion's. The extreme weight of the singular pieces is of great concern. As good fortune would have it, this pillar did not break, and there is very little mechanical damage to be observed. The greatest issues however, are the numerous cracks and fissures that can be seen on the individual stone blocks, primarily on the shaft pieces. Ultra-sound velocity measurements shall be used to assess the cracks and to decide whether these require treatment before reassembly. In general the treatment should be

similar to the one of the Lion's pillar. The close cooperation with local craftsmen and architects continues to be of great importance after the earthquake, as the understanding of the original constructions and the reconstruction of missing parts prove to be essential. However, the *lacunae* in the field of conservation cannot yet be covered from the Nepalese side - this gap is presently occupied by the team of the Institute of Conservation from the University of Applied Arts Vienna.

Acknowledgements

Many thanks are due to our partners: The Kathmandu Valley Preservation Trust and its staff, particularly Dr Rohit Ranjitkar; the Austrian Development Agency (ADA); the Austrian Federal Chancellery (BKA); the Federal Ministry for Europe, Integration and Foreign Affairs (BMEIA); and Eurasia-Pacific Uninet (EPU). Thanks are due to Prof. Johannes Weber for the microscopic analyses of the different stone materials and mortars. Heartfelt thanks also go to all individuals involved in the project during the past six years.

References

- Fuchs, K., 2013, Bitumen Coating on Stone, a Nepalese Problem? - The Conservation of Two Stone Relief Gates at the Nasal Chowk, Patan Royal Palace, pre-thesis, University of Applied Arts Vienna, Austria.
- Fuchs, K., 2014, The Royal Place in Patan, Nepal - Evaluation of the conservation treatments and recommendation for a maintenance program, diploma thesis, University of Applied Arts Vienna, Austria.
- Government of Nepal/National Planning Commission, 2015, 'Nepal Earthquake, Post Disaster Needs Assessment, Executive Summary' and 'Vol A: Key Findings', reports, Nepal.
- Henry, A., 2006, 'Stone Conservation: Principles and Practice', Donhead Publishing, Dorset, Great Britain, ISBN 978-1-87339-478-6.
- Krist, G., *et al.*, 2014, 'Patan Royal Palace (Nepal) - Conservation campaigns 2010-2014', unpublished reports, University of Applied Arts Vienna, Austria.
- Leiner, S., 2011, Der Pavillon am Bhandarkhal-Tank. Palastkomplex Patan, Nepal, pre-thesis, University of Applied Arts Vienna, Austria.
- Sekler, E.F., 2001, Fragen architektonischer Authentie am Fuss des Himalaya, *ÖZKD*, 4, 389-403.
- Sekler, E.F., 1979, Use of collective space in Patan and other historic towns of the Kathmandu Valley, Nepal, *Monumentum*, XVIII-XIX, 97-107.
- United States Geological Survey (<http://www.usgs.gov>, accessed 2nd October 2015).

This page has been left intentionally blank.

RESTORING THE PAST EXPERIENCE OF STONE MASONRY IN BURKINA FASO FOR FOSTERING THE USE OF LOCAL MATERIALS

A. Lawane¹, A. Pantet^{2*}, R. Vinai³ and J.H. Thomassin¹

Abstract

A number of associations, companies, and research institutions are currently working together in Burkina Faso in order to promote the valorisation and the reuse of laterite dimension stones (LDS). In this study, old masonry constructions such as schools and churches built during colonisation period in the city of Dano, situated near the borders of Ivory Coast and Ghana, were examined. This article gives a description of old and often abandoned constructions, where dimension stones are however generally well conserved. At first, a specific classification for laterite masonry able to describe the observed pathologies is presented. Subsequently, possible cultural causes that could explain the current state of these constructions are derived, through a survey carried out among local people. Eventually, a classification for LDS, based on geo-mechanical studies carried out on material from four local quarries of laterite, is proposed. Three quality grades were defined and agreed according to local technicians and professionals. Therefore, based on the traditional experience and on results from geo-mechanical studies, a revamp of the use of local materials for urban and suburban constructions, both for new buildings and for the restoration of ancient construction in West Africa, should be fostered, in line with general principles of sustainability in building construction.

Keywords: laterite, index quality, masonry, vernacular architecture, guidelines, African local houses

¹ A. Lawane and J.H. Thomassin

LEMC, International Institute for Water and Environmental Engineering, Rue de la Science, 01 BP 594 Ouagadougou, Burkina Faso

² A. Pantet*

LOMC, University Le Havre, COREVA Building, 53 Rue de Prony, BP 540, 76058 Le Havre Cedex, France
anne.pantet@univ-lehavre.fr

³ R. Vinai

School of Planning, Architecture and Civil Engineering, Queen's Univ. Belfast, David Keir Building, 39 Stranmillis Rd., Belfast BT9 5AG, United Kindom

*corresponding author

1. Introduction

Sub-Saharan Africa is undergoing deep demographic changes. People are moving to the cities and African population will be more urban than rural by 2030. Housing has been recognised as one of the most important and essential need after food and water. Housing construction is a major source of employment and can give an economic propulsion with creation of jobs in Africa, as a significant component of developing countries' economies. Building technology is still extremely labour intensive.

The construction of decent housing is a key component of social development and has major impacts on health conditions in urban areas, coupled with access to safe drinking water supplies.

The need for locally manufactured building materials has been emphasized in many countries. Conventional building materials are expensive and have a high environmental impact (Chevalier 2009). In order to address to this situation, attention has been focused on alternative local building materials. In subtropical zone of the Earth, laterites are very common materials. These can be exploited under two forms, as a soft soil or hardened soil respectively. In this latter case, the hardened laterite can be used for masonry purposes. A number of sites exist in the World, like Angkor Temples in Cambodia, the Fortress of Loropéni in Burkina Faso, and the National Monument in Angadipuram in India, which are famous due to the use of laterite. Many quarries have been exploited since long time, initially manually and more recently with mechanical equipment, and laterite dimension stones (LDS) are usually cut for being used as masonry elements (Indian Standard Specification 3620, 1998).

This study focused on the valorisation of this local material. It was carried out with the following objectives:

- To determine the physical and mechanical properties of the material, which can vary in a wide range due to the very complex weathering processes (that have led to the laterite formation or happened in the laterite after deposition) that can vary for each laterite layer. A quality index has been defined, and the best use of LDS was optimised accordingly. Quality control is therefore of primary importance, also considering that today testing procedures are available and easily performed in any civil engineering work.
- To examine the structural behaviour of masonry buildings, taking into account the state of conservation of the materials used for construction. The structural performance of masonry wall structures can only be understood if the history of their construction, their geometry, and the characteristics of the masonry material are known.

This paper provides a relevant case study, demonstrating that laterite stone masonry construction can be developed in Burkina Faso for simple, one-storey housing or, when coupled with concrete frames, for more complex building.

2. Presentation of the site of the study

The investigation focused on a region in the Southwest of Burkina Faso, West Africa. The site, (see Fig. 1), is located in Dano in the IOBA Province, about 230 km southwest of Ouagadougou, on the N12 in Gaoua direction and about 50 km from Loropeni site. In the region, the laterite stone is commonly used for the construction of masonry buildings. Laterite, which has reddish brown colour, is a residual rock, and it is the product of sub-tropical weathering on many rocks. The term laterite is restricted to highly weathered material rich in secondary form of iron, aluminium, poor in organic content. Laterite is usually found as superficial layers such as thick ferricretes, typically observed in the landscape. It is commonly found on top of flat hills or as boulders on slope surfaces. The weathering profiles developing from different parent rocks exhibit the following upward succession of layers: saprolite, mottled clay and ferricrete.

The region has a tropical humid climate characterised by a dry season (November to April) and a rainy season (May to October). Monthly average temperatures ranged from a minimum of 24.7°C in August to maximum values of 31.9°C in May (as measured in 2006). Long term mean annual precipitation is 926 mm. Eighty percent of the annual rainfall was recorded from June to September. Precipitations during this season are characterised by strong and short storms mainly occurring during the evening. The vegetation cover consists of a semi-humid forest and savannah. A hydrographical network developed on the plateau. Vegetable gardening flourished in the flood plain created by an earth dam.

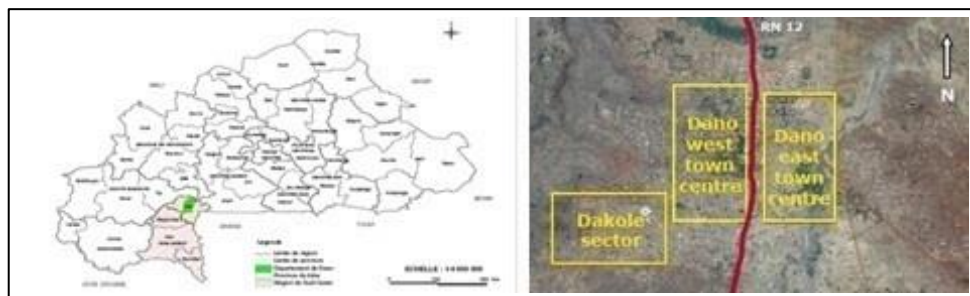


Fig. 1: Site location on Burkina Faso map and Google Earth view of the town of Dano.

The town of Dano was selected for this research due to the existence of several quarries of laterite, either excavated by hand (for local market and simple self-construction housing) or with semi-industrial techniques, for local residential market or for trading.

3. Production of laterite dimension stones (LDS)

Physical properties of LDS vary considerably from place to place (Kasthurba and Santhanam 2005 – Lawane *et al.*, 2014). A careful selection of the laterite stone is necessary in order to ensure its suitability for masonry construction. In order to provide a guidance, many studies indicated minimum requirements in terms of compressive strength. Being soft and porous when freshly extracted, laterite usually hardens if adequate stabilisation is ensured, i.e. under atmospheric conditions but not exposed to rain. The blocks shall be tested for compressive strength, but also for water adsorption, and specific gravity should be measured as well. Stone blocks shall present no cracks, cavities, clay

veins or others imperfections. The shape of the blocks shall be regular and uniform, with straight and rough edges at right angle.

A classification of LDS, with three quality grades, based on geo-mechanical studies carried out on four quarries of laterite and agreed among technicians and professionals was proposed in Tab. 1. The normalised compressive strength is defined by: $fb = Rm \cdot \delta \cdot \chi$ where: Rm , the compressive strength (MPa) - δ , shape factor and χ , curing or drying conditions coefficient, (Eurocode 6, 2013).

During the excavation of laterite stone, a high volume of waste (around 25 to 30 per cent of the total laterite) is generated as scraps. This leads to operational problems, since such material needs to be removed for further excavation. An alternative, added-value option for this waste rock is to use it as aggregate for the manufacture of concrete blocks.

Tab. 1: Quality index for LDS.

f_b (MPa)	> 4	2-4	1-2
compact	Grade 1	Grade 2	Grade 3
granular	Grade 2	Grade 3	Grade 3

4. Survey on housing typology in the Dano town

4.1. Background

The town is developed along a main street, with densely built houses (in the form of buildings with a courtyard), distributed on each side. The spatial structure of the old centre is more or less determined by the related economic life (markets, handicraft, workshops, and bars). The expansion of the centre developed in many peripheral zones such as the administration area (new town hall, school, museum, and hotel), two religious institutions (cathedral and mosque) and many residential areas.

Tab. 2: Summary of results from building survey (for localization see Fig. 1).

Materials	Concrete frame			Masonry	
	LDS	Sand -concrete	Banco	Mix	LDS
Centre	9%	10%	18%	60%	2%
Dakole	34%	18%	17%	9%	23%

Two zones have been investigated to compare construction materials used for the households (or “greater family housing” as defined in Africa). Many households from the extended family (from grandparents to grandchildren) live together in the same courtyard. Two building modes can be identified: masonry, using earth blocks (banco), LDS or mixed techniques, or concrete frame with partition walls in concrete blocks (sand concrete). The distribution and occurrence of each type is reported in Tab. 2. Most houses are built with self-produced materials. Under the influence of modernisation, straw has been replaced by galvanized iron roofing sheets (thatched roofing can still be observed in rural areas),

whereas traditional bricks, produced with a mix of wet earth, dung and straw or vegetable fibres, have been replaced by stabilized earth (soil cement) blocks, and most recently by sand cement blocks.

The majority of housing in the urban centre is composed by buildings partially realised in earth bricks or adobe with possible addition of straw, connected with mortar made of clay and sand. The basement and the lower layer of masonry elements are generally built with LDS. Coating is applied and smoothed to produce a smooth wall surface, which is treated with plaster (mixture: clay- cement or clay – lime) to achieve some weather protection.

The Dakole sector, more residential, is an area where houses are built in LDS masonry or with frame structure in concrete, whereas the partition walls are realised with LDS. The complex of the Drayer Foundationed, a German charity working for children, has been built in LDS. No coating was applied, because the aesthetic effects and the waterproof qualities of the laterite were considered satisfactory.

4.2. Construction techniques with laterite dimension stones (LDS)

The construction system with LDS usually follows horizontal and parallel shelves where medium and large blocks are mainly used. The mortar used to connect the block is either clay or lime based. Only for the outer walls, the earth is removed on many centimeters and replaced by cement mortar, to avoid erosion (water or wind) actions (see detailed photo in Fig. 2). Inner walls are plastered and painted. In the case of building with concrete frame structure, a floor slab is casted and supported by columns, isolating the roof space. Ventilation holes are created in the upper layer of the walls.



Fig. 2: Typical houses in LDS, either load bearing masonry or with frame concrete.

5. Diagnosis survey of laterite constructions

5.1. Description of the state of a colonial building

The oldest building realised in LDS that can be found in Dano is a school, built in the 1930's by the religious Fathers during the last years of colonial period. The building was left without any maintenance during the post-independence era, leading to severe deterioration. The building shows a rectangular plan section sized about 40.5×10.5 m, with a maximum height of 6.25 m. Two corridors, along the northern and southern load-bearing walls, give access to the aligned classrooms.

The construction (see Fig. 3) is composed by thick masonry walls (double walls) built with adobe with lime mortar and coated with plaster (clay and cement), whereas the top layers, which are exposed to rain and wind, are made with LDS. The load-bearing walls are made with a mixed masonry of adobe and stone blocks locally quarried. Stone units are connected together by means of a weak lime and sand mortar. The cohesion between the mortar and the stone is weak. All different types of masonry in the structure can be defined as solid masonry.



Fig. 3: Views of the school and CAD representation.

A layer of lime plaster and one of lime wash paint were applied to create smooth surface. Masonry blocks have small to medium size (L: 20 cm, h: 15 cm, w: 10 cm) with rough surface, rectangular or square shape. Some of them show a flattened surface. Blocks were used according to their strength, being the weaker used for filling or for coating, whereas the stronger were used for structural purposes. A virtual reconstruction view has been obtained with a CAD application as shown above left in Fig. 3.

A continuous vaulted gallery ran along the two long sides (north and south walls) of the building. Pupils accessed the gallery from the courtyard. The arches were built with ashlar, with a stiff structure made up of well carved headers forming a single arch line. The opening between columns is about 2 m. A wood formwork was presumably used during the construction. The eastern and western sides show gables, made up of small headers and long stones on the corners, without openings. The horizontal elements of the flat roof are made of a mixed construction system with steel profiles for the classrooms and with wood beams for the corridors. The whole structure was covered with galvanized iron sheets.

On site visual inspection revealed severe damages. The roof structure of the school was dismantled and partly destroyed. As a result, the vault of the north wall collapsed, and the building was no longer in an operational state. Bricks from demolition were reused for foundations, but also as aggregates in concrete. However, the integrity of the existing arches appears still satisfactory and not affected by the general conditions. No deformation and collapse of gable walls was observed, although these were built as a single layer. There is no evidence that the building collapsed because under dimensioned, or because of insufficient bearing capacity of the construction material or due to any overload on the structure.

5.2. Deterioration processes observed in LDS structures

Masonry defects can be associated with several reasons, from a wrong choice of materials to an insufficient quality of the workmanship (Bromblet and Association MEDISTONE, 2010). The local climatic impact can also have a role. Main categories of defects and related causes were defined by direct observations on the surveyed LDS building (the old school and the houses) in Fig. 4:

- Deterioration of the structure of LDS, by atmospheric agents, such as sandy wind and rain, affecting surface stone (a). The block can also be damaged by the cracking associated with the action of water and temperature variation, which facilitates rock degradation and failure (b),
- Disintegration of lime and sand mortar joints, due to the moisture transfer or water runoff action and also because the excessive mortar width between the layers and loss adherence (c),
- Organic deterioration from musk and other plants growth on the lowermost layer of masonry elements, due lack of drained or ventilated space in the basements (d),
- Cracks due to uneven distribution of the loads.



Fig. 4: Views of the most usual defects observed in LDS structures.

Some of the above mentioned defects can be avoided by controlling the block production. Good ashlar with rough, parallel surfaces are to be preferred, since these features improve the joint strength, contribute to an even distribution of the loads and reduce the potential accumulation of organic material on joints. The quality of the laying of the block is also an important factor for preventing structure failures. The width of the joints should be kept at a minimum, and in some cases the laying should be carried out even without joint. The quality of the LDS is another key point. Top quality LDS seem to be subject to hardening upon exposure to alternate wetting and drying, but poor to medium quality are not, since granular morphologies are disintegrated by drying and wetting cycles. Masons must be careful when choosing the blocks during construction, trying to use them according to their quality in different places of the structure.

6. Conclusions

This study aimed at understanding the potentiality of the utilisation of LDS as building material. The geological study of laterite quarries showed large variability in quality. Such variability influences the stone availability, and, consequently, has an impact on the economic viability and safety of the exploitations. All the material extracted from the quarries (LDS and waste) need to be valorised to their maximum potential.

The fostering of a return of stone masonry constructions poses important challenges because of the variability of the properties of traditional materials. The assessment of the structural conditions of old masonry structures, with the definition of damages or defects categories that can be listed through visual inspections, contribute to indicate the actual potential of the use of LDS in building, provided that a proper choice of the material is carried out and proper construction best practises are followed. The quality grade of LDS must be considered during the construction phase, since higher or lower quality blocks can be used for different purposes, also depending on the typology of building structure (load bearing masonry or concrete frame). When both climatic exposure and thermal properties of the lateritic material are properly considered, masonry structures can provide the required thermal comfort to dwellers in a sustainable and energy efficient way, provided that iron sheet roofing is avoided.

Some requirements for improving design guidelines have been proposed. It is however of utmost importance to increase the knowledge on the building material through laboratory tests on samples cored on site (for each quarry) and loading tests on buildings at realistic scale. Systematic analysis of building defects should also be considered as part of a design approach aimed at overcoming these challenges.

References

- P. Bromblet et Association MEDISTONE, 2010 : Guide "Techniques de conservation de la pierre". Association MEDISTONE.
- Chevalier, J, 2009, Analyse du cycle de vie: Utilisation dans le secteur de la construction, Techniques de l'ingénieur. Environnement, 1 (G5880).
- Eurocode 6, 2013, Calcul des ouvrages en maçonnerie - Partie 1-1 : règles générales pour ouvrages en maçonnerie armée et non armée, NF EN 1996-1-1+A1 Mars 2013.
- Indian Standard Specification 3620, 1998, Indian Standard Specification for Laterite Stone Block for masonry, Bureau of Indian Standards, New Delhi, India, 86, 1-8.
- Kasthurba, A. K., and Santhanam, M., 2005, A re-look into the code specifications for the strength evaluation of laterite stone blocks for masonry purposes, Journal of The Institution of Engineers (India), 86, 1-6.
- Lawane, A., Vinai, R., Pantet, A., Thomassin, J. H., and Messan, A., 2014, Hygrothermal Features of Laterite Dimension Stones for Sub-Saharan Residential Building Construction, Journal of Materials in Civil Engineering, 26 (7).

PROTECTION OF MEDIEVAL TOMBSTONES (STEĆCI) WITH AMMONIUM OXALATE TREATMENT

V. Marinković^{1*} and D. Mudronja²

Abstract

Since 2013 Croatian Conservation Institute has performed research and preliminary conservation works on medieval tombstones (stećci) on the archaeological site Crljivica near Cista Velika in Croatia. During the project, tombstones from several sites in the region of Cista were analysed for provenance study and for protection of stones. Stone characterisation was performed using mineralogical-petrographical analysis on different tombstones and surrounding quarries or rock outcrops. Approximately 80% of analysed stones from tombstones were determined to be biomicritic limestones ranging from wackestone to flintstone (according to Dunham classification). They were all determined to be from the upper Cretaceous. Other analysed tombstones were determined to be dolomites. Some of the surrounding quarries did show the same type of limestones. Concerning the protection of tombstones, one of the main goals was to create a protective layer of artificial calcium oxalate on stone surface through the reaction of ammonium oxalate with calcium carbonate. In order to establish the most effective way of achieving such kind of protection, research included laboratory testing and in-situ testing. Ammonium oxalate was applied on the stone by poultice (24 h), brushing method (1, 2 and 3 hours) and total immersion (24 h). The method of total immersion of stone provided best results, both in laboratory and on site.

Keywords: medieval tombstones (stećci), stone deterioration, calcium-oxalate, ammonium oxalate, limestone

¹ V. Marinković*

Department of Stone Conservation, Croatian Conservation Institute, Croatia
vmarinkovic@h-r-z.hr

² D. Mudronja

Natural Science Laboratory, Croatian Conservation Institute, Croatia

*corresponding author

1. Introduction

Medieval monolithic tombstones called stećci are found on the entire territory of the present Bosnia and Herzegovina, as well as in parts of Serbia, Montenegro and Croatia. Stećci first appeared in the second half of the 12th century, but the period of its most intensive production range from the 14th to the 15th century. One of the most significant sites with stećci in Croatia is the archaeological site of Velika and Mala Crljivica near village of Cista Velika in Dalmatian hinterland. Crljivica is located along the road Trilj-Imotski in a length of 200 meters and contains more than ninety stećci of all types (slabs, chests and ridged monuments). The entire area is an unique complex of archaeology, history and biodiversity.

Since 2013 Croatian Conservation Institute has performed investigation and preliminary conservation works on some tombstones on the site Crljivica. Also, some analyses were done on several other sites with stećci near Crljivica: Lovreć, Zadužbina and Bisko. All the investigations and some preliminary works were done with the intention to create a systematic plan for conservation and protection of stećci in the region.

The research was supposed to provide answers to few main questions:

- 1.) *What is the state of preservation of monuments, and is it necessary to start with conservation works on tombstones?*
- 2.) *What is the origin of stones and do all the tombstones have the same stone provenance?*
- 3.) *If tombstones need conservation treatments, what kind of surface protection is the most compatible with the type of stone, and how to apply it?*

After preliminary review of the situation on the site, several types of damage were observed on the stones. The tombstones on the site are exposed to large temperature changes. In Dalmatian hinterland winters are wet and cold with large diurnal temperature variation (from 0 to -13°C during a night). Summer is dry and the temperatures are very high (the mean is approximately 30°C). Cracks, flanking and lowering of stone surface are mainly caused by frost, acid rain and extreme temperature changes. These types of damage are possible to observe by naked eye. The lowering of surface and pitting are caused by complex mechanisms of biological colonization (lichens, moss and cyanobacteria). This degradation can be seen only after preliminary cleaning treatment and under magnification. The presence of harmful salts in the stones was not recorded and it was not proven by laboratory analysis.

Considering the first analysis it was possible to make plan for materials and methodology supposed to be used during conservation treatment. After finding natural calcium oxalate patina on tombstones, it was decided to create artificial layer of calcium oxalate to protect the stones (Matteini 2008; Doherty *et al.* 2007). Creation of artificial protective layer was tried using several methods (Mudronja *et al.* 2013; Vanmeert *et al.* 2013). In order to establish the most effective way of achieving such protection, research included laboratory testing and in situ testing. Ammonium oxalate was applied on the stone by poultice (24 h), brushing method (1, 2 and 3 hours) and total immersion (24 h). A method by total immersion provided best results, both in laboratory and on site.

2. Materials and methods

From region of Cista, 11 samples of stone from tombstones were taken for mineralogical and petrographic determination of stone. 7 samples from surrounding quarries and stone outcrops were also taken for comparison. Samples were taken by small core-drill, 2 cm in diameter (Tab. 1). After sampling, samples of stone were prepared as thin sections and analysed by mineralogical-petrographic analysis (MPA) using Olympus BX 51 polarised microscope.

Tab. 1: Analysed samples.

Sample No.	Place of origin	Analysis type
19163	Lovreć, <i>stećak</i> no.3	MPA
19164	Lovreć, <i>stećak</i> no.4	MPA
19165	Zadužbina, <i>stećak</i> no.3	MPA
19166	Zadužbina, <i>stećak</i> no.4	MPA
19167	Crlijivica, <i>stećak</i> no. 70	MPA
19168	Crlijivica, <i>stećak</i> no. 691	MPA
19169	Crlijivica, <i>stećak</i> no. 182	MPA
19170	Crlijivica, <i>stećak</i> no. 11	MPA
19171	Crlijivica, <i>stećak</i> no. 12	MPA
19172	Bisko, <i>stećak</i> no. F1	MPA
19173	Crlijivica, <i>stećak</i> no. 2	MPA
19516	Crlijivica, quarry sample C	MPA
19517	Crlijivica, quarry sample D	MPA, XRD
19518	Crlijivica, quarry sample E	MPA
19519	Bisko, quarry sample F	MPA, XRD
19520	Bisko, quarry sample G	MPA
19521	Lovreć, quarry sample A	MPA, XRD
19522	Zadužbina, quarry sample B	MPA
20519	Crlijivica, <i>stećak</i> no. 62	μFT-IR
20520	Crlijivica, <i>stećak</i> no. 62	μFT-IR
20521	Crlijivica, <i>stećak</i> no. 62	μFT-IR

Samples from quarries marked 19517, 19519 and 19521 were determined to be closest match to tombstones samples. Afterwards, these samples were emerged in solution of 5% ammonium oxalate (AmOx). 24 hours after, samples were taken out of AmOx solution and air-dried for 7 days. Subsequently their surface was analysed by phase analysis using X-Ray diffraction (XRD). Phase analysis was done on flat surface of samples using Philips X-Pert diffractometer with graded parabolic X-ray mirror using Cu X-ray tube with 45kv and 40 mA.

After laboratory tests, 3 samples (Tab. 1) from tombstone no. 62 were taken by small core-drill 7 days after soaking in 5% AmOx. These samples were then embedded in polyester resin (Scott Bader A-132 UV), and prepared as cross sections. The cross sections were analysed from the surface to a depth of 1mm with Ge-ATR using Agilent Carry 660 FT-IR spectrometer fitted with Carry 610 FT-IR microscope (μ FT-IR).

3. Results

Mineralogical-petrographic analysis of stone determined that most of the stećci are made of limestone. Most of them were determined as biomicritic limestones ranging from wackestone to floatstone (according to Dunham classification). They were all determined to be from upper Cretaceous. Other analysed stećci were determined as dolomites - dolosparite. Some of the surrounding quarries did show the same type of limestones. They were closest to tombstones sites. We were not successful in finding dolomite quarry. The results of mineralogical petrographic analysis are shown in Tab. 2.

Samples 19517 (biopelmicritic packstone), 19519 (bioclastic roudist floatstone) and 19521 (biopelmicritic packstone – wackestone) were selected as closest match to stećak stones. They were then emerged in 5% AmOx solution for 24 hours. After air drying their surface was analysed by XRD. XRD spectra of samples showed peaks corresponding to whewellite and weddellite. All intensities were approximately the same, meaning that a protective oxalate layer has been probably formed on all the treated samples (Fig. 1, Tab. 3, 4 and 5).

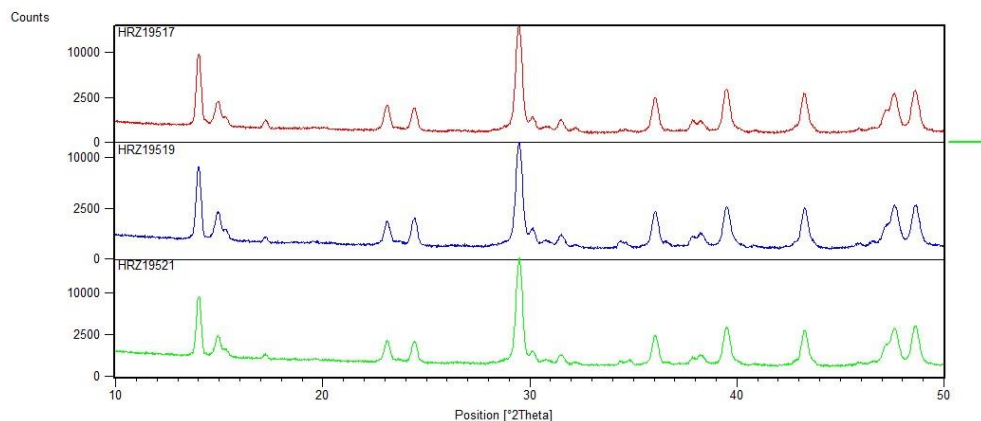


Fig. 1: XRD spectra of treated limestones from quarry.

Tab. 2: Results of mineralogical-petrographic analysis of stone.

Sample No.	Place of origin	Stone type
19163	Lovreć, <i>stećak</i> no.3	Bioclastic packestone
19164	Lovreć, <i>stećak</i> no.4	Biomicritic wackestone
19165	Zadužbina, <i>stećak</i> no.3	Biopelmicritic packestone - wackestone
19166	Zadužbina, <i>stećak</i> no.4	Biopelmicritic packestone - wackestone
19167	Crlijivica, <i>stećak</i> no. 70	Dolomitized limestone (mudstone)
19168	Crlijivica, <i>stećak</i> no. 691	Oncoidic floatstone
19169	Crlijivica, <i>stećak</i> no. 182	Dolosparite
19170	Crlijivica, <i>stećak</i> no. 11	Peloidic bindstone
19171	Crlijivica, <i>stećak</i> no. 12	Biopelmicritic packestone - wackestone
19172	Bisko, <i>stećak</i> no. F1	Biomicritic wackestone
19173	Crlijivica, <i>stećak</i> no. 2	Biomicritic wackestone
19516	Crlijivica, quarry sample C	Breccia
19517	Crlijivica, quarry sample D	Biopelmicritic packestone
19518	Crlijivica, quarry sample E	Dolomitic breccia
19519	Bisko, quarry sample F	Bioclastic roudist floatstone
19520	Bisko, quarry sample G	Bioclastic roudist floatstone
19521	Lovreć, quarry sample A	Biopelmicritic packestone – wackestone
19522	Zadužbina, quarry sample B	Breccia
20519	Crlijivica, <i>stećak</i> no. 62	Biopelmicritic packestone – wackestone
20520	Crlijivica, <i>stećak</i> no. 62	Biopelmicritic packestone – wackestone
20521	Crlijivica, <i>stećak</i> no. 62	Biopelmicritic packestone – wackestone
		Biopelmicritic packestone - wackestone

Tab. 3: XRD data for sample No. 19517.

2θ	d-[Å]	Rel. Int. [%]	Mineral
14.00	6.3226	58	oksammit
14.93	5.9297	10	whewellit
15.29	5.7892	3	whewellit
17.22	5.1455	2	oksammit
19.55	4.5371	1	whewellit
20.05	4.4250	1	weddellit
23.08	3.8499	9	kalcit
24.40	3.6447	8	whewellit
26.37	3.3777	0	whewellit
28.25	3.1565	0	oksammit
29.45	3.0307	100	kalcit
30.12	2.9646	4	whewellit
30.82	2.8991	1	whewellit
31.52	2.8358	3	kalcit; whewellit
32.23	2.7749	1	weddellit
34.64	2.5871	1	oksammit
36.05	2.4895	13	kalcit; whewellit
37.85	2.3752	3	whewellit; oksammit
38.23	2.3521	3	whewellit
39.46	2.2816	19	kalcit
40.86	2.2068	0	whewellit
43.22	2.0914	16	kalcit
45.90	1.9755	1	whewellit
47.25	1.9220	7	kalcit
47.58	1.9095	15	kalcit
48.57	1.8731	18	kalcit
52.79	1.7327	1	whewellit
56.64	1.6238	3	kalcit
57.47	1.6022	8	kalcit
58.15	1.5851	1	kalcit
60.77	1.5229	6	kalcit
61.31	1.5109	3	kalcit

Tab. 4: XRD data for sample No. 19519.

$^{\circ}2\theta$	d-[Å]	Rel. int. [%]	Mineral
13.99	6.3255	62	oksammit
14.93	5.9292	14	whewellit
15.32	5.7796	4	whewellit
17.24	5.1448	1	oksammit
19.60	4.5287	0	whewellit
23.09	3.8519	9	kalcit
24.41	3.6444	11	whewellit
29.46	3.0297	100	kalcit; whewellit
30.12	2.9646	6	whewellit
30.79	2.9043	1	whewellit
31.51	2.8393	3	kalcit; whewellit
32.21	2.7789	1	weddellit
34.43	2.6029	1	oksammit
36.03	2.4910	16	kalcit; whewellit
36.61	2.4526	1	whewellit; oksammit
37.30	2.4089	0	whewellit
37.82	2.3766	3	whewellit; oksammit
38.22	2.3527	4	whewellit
39.48	2.2807	19	kalcit
43.25	2.0918	18	kalcit; whewellit
45.96	1.9748	1	whewellit
46.57	1.9502	1	whewellit
47.13	1.9284	6	kalcit
47.60	1.9087	20	kalcit
48.59	1.8724	20	kalcit
50.99	1.7896	0	whewellit
52.74	1.7344	1	whewellit
56.65	1.6234	4	kalcit
57.48	1.6019	8	kalcit
58.18	1.5844	1	kalcit
60.79	1.5224	5	kalcit
61.36	1.5097	3	kalcit

Tab. 5: XRD data for sample No. 19521.

$^{\circ}2\theta$	d-[Å]	Rel. int. [%]	Mineral
14.00	6.3216	47	oksammit
14.93	5.9292	9	whewellit
15.32	5.7808	3	whewellit
17.21	5.1478	1	oksammit
19.57	4.5325	1	whewellit
23.07	3.8526	7	kalcit
24.41	3.6436	7	whewellit
29.46	3.0291	100	kalcit; whewellit
30.10	2.9663	3	whewellit
30.75	2.9053	1	whewellit
31.49	2.8385	2	kalcit; whewellit
32.18	2.7792	0	weddellit
34.38	2.6065	1	oksammit
34.79	2.5767	1	oksammit
36.03	2.4909	11	kalcit; whewellit
37.82	2.3769	2	oksammit
38.23	2.3526	2	whewellit
39.47	2.2810	16	kalcit
40.87	2.2062	0	whewellit
43.23	2.0909	14	kalcit; whewellit
45.88	1.9764	0	whewellit
46.51	1.9510	1	whewellit
47.17	1.9251	6	kalcit
47.58	1.9096	16	kalcit
48.58	1.8726	17	kalcit
50.06	1.8206	0	whewellit
50.95	1.7909	0	whewellit
52.82	1.7319	0	whewellit
54.36	1.6863	0	whewellit
56.65	1.6234	2	kalcit
57.48	1.6020	6	kalcit
58.20	1.5838	1	kalcit
60.78	1.5227	4	kalcit
61.29	1.5113	2	kalcit

Next step was to treat *stećak* no. 62 by emerging it in 5% AmOx solution for 24h. After that, taken samples were prepared as cross-sections and measured from surface to depth by μ FT-IR spectroscopy. Results showed that calcium oxalate is present only on surface. Measurements at depth of 1 mm showed only presence of calcium carbonate. Results are shown in table 6 and figures 2, 3 and 4.

Tab. 6: Results of μ FT-IR spectroscopy on samples from tombstone no. 62.

Sample No. - depth	Detected calcium oxalate bands	Detected calcium carbonate bands
20519 - surface	1620, 1315, 780, 665 cm^{-1}	1425, 875, 710 cm^{-1}
20519 - 1mm depth	-	1380, 870, 710 cm^{-1}
20520 - surface	1610, 1315, 780, 665 cm^{-1}	1410, 875, 710 cm^{-1}
20520 - 1mm depth	-	1390, 870, 710 cm^{-1}
20521 - surface	1620, 1320, 780, 665 cm^{-1}	1410, 875, 710 cm^{-1}
20520 - 1mm depth	-	1390, 870, 710 cm^{-1}

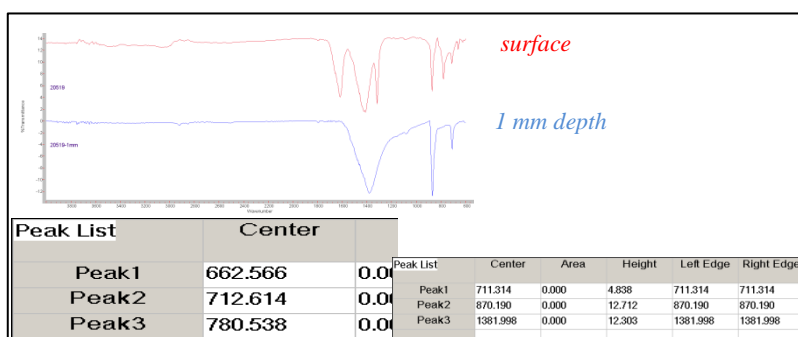


Fig. 2: FT-IR spectra of sample 20519 at surface and 1 mm depth.

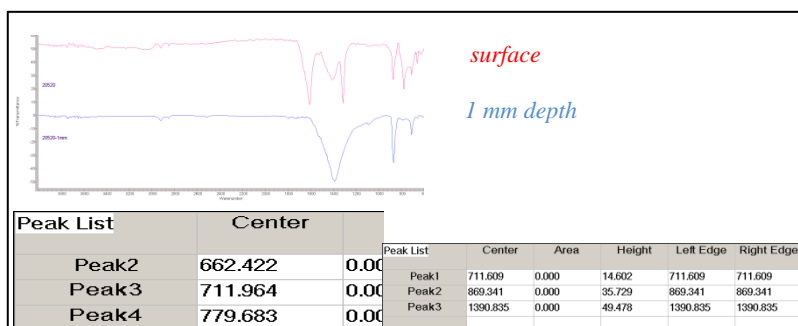


Fig. 3: FT-IR spectra of sample 20520 at surface and 1 mm depth.

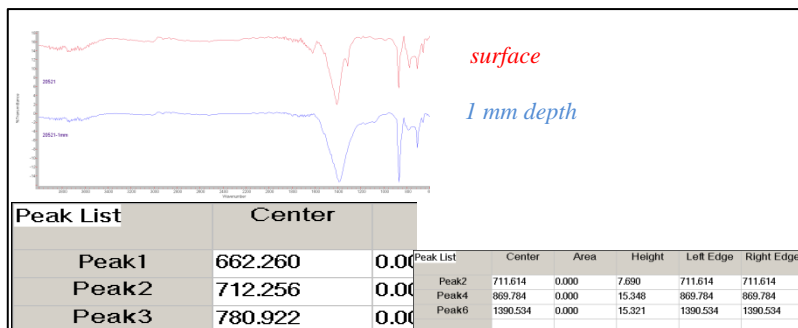


Fig. 4: FT-IR spectra of sample 20521 at surface and 1 mm depth.

4. Discussion

During previous conservation works on stećci (2014), field tests on creation of artificial calcium oxalate layer by poultice (Doherty *et al.* 2007, Pinna *et al.* 2011) or brushing (Mudronja *et al.* 2013) didn't show great results. After finding appropriate or similar "standards" in surrounding quarries, we tried to create protective layer by emerging them in 5% AmOx solution (Mudronja *et al.* 2013; Vanmeert *et al.* 2013). XRD measurements showed similar creation of calcium oxalate layer on surface of all the treated limestones. In addition, some ammonium oxalate (oksammit) bands were detected, which is a left over of the treatment. It will be dissolved with first rain so it does not represent a problem. After successful laboratory tests we immersed the whole stećak in ammonium oxalate bath for 24h using a crane on site (Fig. 5).



Fig. 5: The improvised pool with ammonium oxalate bath, Crljivica.

We tried to measure on site the thickness of created calcium oxalate layer using μ FT-IR fitted with transmission fibers. Results showed creation of protective layer on surface, but mapping of oxalate bands beneath surface was very difficult with this technique because of the resthralen effect (Ricci *et al.* 2006). We determined that below a depth of 1 mm there is no calcium oxalate. For more precise thickness measurements, other techniques like μ XRD (Vanmeert *et al.* 2013) or μ Raman (Doherty *et al.* 2013) could be more appropriate.

5. Conclusion

In order to create a protective layer of artificial calcium oxalate on surface of the tombstones, ammonium oxalate was applied on the stone by poultice (24 h), brushing method (1, 2 and 3 hours) and by total immersion (24 h). Treatment by immersion of stone sample (in laboratory) showed best results. Only with this type of treatment we can say that protective layer of calcium oxalate was created on entire surface, which is needed for protection. After that the same treatment was applied on the whole tombstone on the site. Unfortunately, the investigations was limited because of technical and financial issues. Mentioned limitations of μ FT-IR technique could not resolve depth creation of CaOx, so we could just approximate this value according to literature. Further investigations are planned for future.

Acknowledgements

The project is supported by the Ministry of Culture of the Republic of Croatia.

References

- Doherty, B., Pamplona, M., Selvaggi, R., Milliani, C., Matteini, M., Sgamellotti, A., Brunetti, B., 2007a, Efficiency and resistance of the artificial oxalate protection treatment on marble against chemical weathering, *Applied Surface Science*, 253(10), 4477-4484.
- Doherty, B., Pamplona, M., Matteini, M., Sgamellotti, A., Brunetti, B., 2007b, Durability of the artificial calcium oxalate protective on two Florentine monuments, *Journal of Cultural Heritage*, 8(2), 108-121.
- Matteini, M., 2008, Inorganic treatments for the consolidation and protection of stone artefacts and mural paintings, *Conservation Science in Cultural Heritage*, 13-27.
- Mudronja, D., Vanmeert, F., Hellemans, K., Fazinic, S., Janssens, K., Tibljas, D., Rogosic, M., Jakovljevic, S., 2013, Efficiency of applying ammonium oxalate for protection of monumental limestone by poultice, immersion and brushing methods, *Applied physics. A, Materials science & processing*, 111, 109-119.
- Pinna, D., Salvadori, B., Porcinai, S., 2011, Evaluation of the application conditions of artificial protection treatments on salt-laden limestones and marble, *Construction and Building Materials*, 25, 2723-2732.
- Ricci, C., Miliani, C., Brunetti, B.G., Sgamellotti, A., 2006, Non-invasive identification of surface materials on marble artifacts with fiber optic mid-FTIR reflectance spectroscopy, *Talanta*, 69, 1221-1226.
- Vanmeert, F., Mudronja, D., Fazinic, S., Janssens, K., Tibljas, D., 2013, Semi-quantitative analysis of the formation of a calcium oxalate protective layer for monumental limestone using combined micro-XRF and micro-XRPD, *X-ray spectrometry*, 42, 256-261.

This page has been left intentionally blank.

INFLUENCE OF WATER EVAPORATION ON THE DEGRADATION OF WALL PAINTINGS IN HAGIA SOPHIA, ISTANBUL

E. Mizutani^{1*}, D. Ogura¹, T. Ishizaki², M. Abuku³ and J. Sasaki⁴

Abstract

Hagia Sophia in Istanbul has been suffering from severe degradation such as exfoliation of the wall paintings and interior finishing materials that is mostly associated with salt crystallization at and near the wall surfaces. The purposes of our study are to elucidate the physical mechanism of degradation of the wall paintings and then to propose suitable measures to prevent the degradation. In this study, because degradation by salt crystallization is likely to occur in places where a large amount of moisture evaporates, we performed a numerical analysis of simultaneous heat and moisture transfer using a model of the exedra wall, in which accumulation and evaporation of infiltrated rain are highlighted. The results suggest that evaporation from the middle-layer mortar caused the exfoliation of the interior finishing materials. We also developed a prediction model of the room temperature and humidity of Hagia Sophia, in order to quantify the influences of solar radiation and heat and moisture generation by visitors on evaporation at and near the inner wall surfaces. Based on simulation results, it should be particularly pronounced that reducing the transmission of solar radiation through windows is an efficient way to reduce evaporation and to mitigate the subsequent degradation of the inner wall.

Keywords: porous materials, rain water, salt crystallisation, heat and moisture transfer, evaporation

1. Introduction

Hagia Sophia, in Istanbul, has been suffering from severe degradation such as exfoliation of the wall paintings and interior finishing materials mainly due to salt crystallisation within the walls, especially at the exedras of the second cornice (Sasaki *et al.*, 2012). Moisture accumulation and evaporation significantly affect salt crystallisation. Therefore, in this study, we investigate the influence of the indoor and outdoor climate and wall composition on moisture behavior within the wall. This is done via a field survey and numerical analysis

¹ E. Mizutani* and D. Ogura
Graduate School of Engineering, Kyoto University, Japan
be.etu@archi.kyoto-u.ac.jp

² T. Ishizaki
Tohoku university of Art and Design, Japan

³ M. Abuku
Faculty of architecture, Kindai University, Japan

⁴ J. Sasaki
Center for the Global Study of Cultural Heritage and Culture, Kansai University, Japan

*corresponding author

of heat and moisture transfer. In our previous study, we demonstrated that the main factor of exfoliation of the interior finishing materials due to salt crystallisation was the accumulation and evaporation of infiltrated rainwater at the middle-layer mortar (Mizutani *et al.*, 2015a and b). Ideally, restricting the penetration of rainwater from the outer surface would be an effective countermeasure. However, completely blocking the penetration pathway of rainwater is difficult because of the architectural size and complexity of Hagia Sophia. Besides, accumulated water in a wall might remain even after the countermeasures are applied to the outer walls. Therefore, this study investigates the effectiveness of controlling the indoor climate to limit the evaporation near the interior surfaces using a prediction model to reproduce the room temperature and humidity. In this paper, we discuss the influence of heat and moisture generation from visitors and the transmission of solar radiation and other forms of heat transfer through windows on evaporation at and near the inner wall surfaces.

2. Degradation and moisture content of the inside walls at exedra of the 2nd cornice.

Figures 1 and 2 give respectively a vertical section of Hagia Sophia and photographs of degradation of the inner walls at the exedra of the 2nd cornice. We have conducted deterioration survey and measurement of the moisture content of the outer and the inner walls since 2010. Fig. 3 shows the moisture content measured using a contact-type TDR moisture content sensor at the 2nd cornice. The moisture content tends to be higher at the semicircular-shaped walls called the exedra, and a high moisture content of > 20% was confirmed at all the exedras. As Ogura *et al.* (2012) noted, locations, where remarkable degradation of the inner walls with exfoliation of the inside stucco and middle-layer mortar due to salt crystallisations is confirmed, generally correspond to locations of a high moisture content. The exedras are considered to be corners where rainwater intensively concentrates due to the geometry of the roofs and walls. Therefore, rainwater tends to infiltrate the outer wall surfaces, causing a high moisture content and the consequent degradation of the inner wall surface at the exedras (Mizutani *et al.*, 2015a and b).

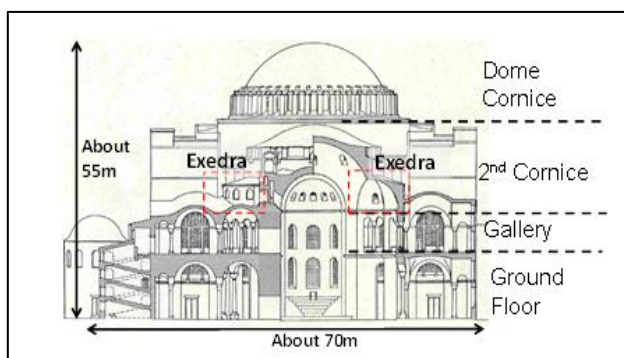


Fig. 1: Section of Hagia Sophia.



Fig. 2: Exfoliation of inner stucco (left) and middle-layer mortar with salt crystallisation (right)

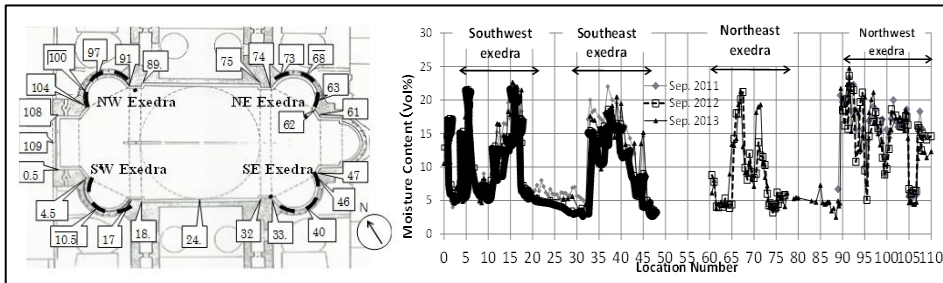


Fig. 3: Location number at 2nd cornice (a) and measured values of moisture content (b).

3. Fundamental equation of heat and moisture transfer

We use simultaneous heat and moisture transfer equations (Matsumoto, 1978) as fundamental equation of numerical analysis of moisture migration and evaporation within wall in Chapter 4 and 5. Heat and moisture balance equations are respectively:

$$c_p dT/dt = \nabla \cdot (\lambda \nabla T) + r \nabla \cdot (\lambda'_{\mu g} \nabla \mu + \lambda'_{Tg} \nabla T) \quad (\text{Eq. 1})$$

$$\rho_w (\partial \psi / \partial \mu) \partial \mu / \partial t = \nabla \cdot (\lambda'_{\mu g} \nabla \mu + \lambda'_{Tg} \nabla T + \lambda'_{\mu l} \nabla \mu + \lambda'_{Tl} \nabla T) \quad (\text{Eq. 2})$$

where c_p , T , λ , r , μ , ρ_w and ψ refer to respectively the specific heat capacity for volume [$\text{J}/\text{m}^3 \text{K}$], the temperature [K], the heat conductivity [$\text{W}/\text{m K}$], the latent heat [J/kg], the water chemical potential [J/kg], the water density [kg/m^3] and the moisture content [m^3/m^3], and λ'_{Tg} and $\lambda'_{\mu g}$ are respectively the water conductivity for the temperature [$\text{kg}/\text{m s K}$] and that for the water chemical potential [$\text{kg}/\text{m s (J/kg)}$]; the subscripts g and l indicate water vapor and liquid water respectively.

4. Investigation of influence of infiltrated rainwater by analysis of wall model

We performed a numerical analysis of the heat and moisture transfer with a model of the exedra wall (Fig. 4), to confirm the relation between the accumulation and evaporation of infiltrated rainwater and degradation of the interior wall surfaces at the exedra. The analysis

conditions (Tab. 1) and hygrothermal material properties are kept the same as the past study (Mizutani *et al.*, 2015a). The severely deteriorated wall of the north-facing exedra is analysed. The vertical radiation for the north-facing walls is calculated by decomposing the total measured horizontal solar radiation into the direct and diffuse components using the equations of Bouguer and Berlarge. Judging by the roof shape, three times the amount of measured precipitation was assumed to flow at the outer surface of the exedra.

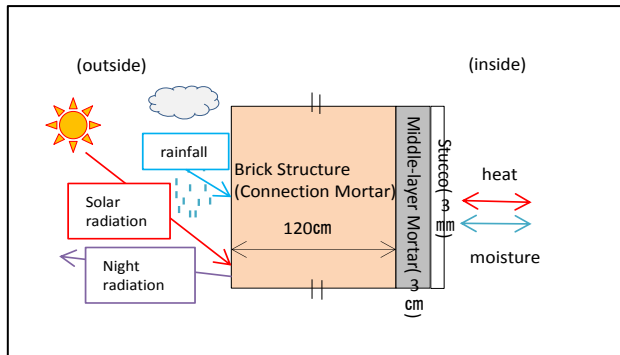


Fig. 4: Schematic diagram of the analysis

Table1: Analysis conditions in Section 4.

Outdoor	Measured Value at Hagia Sophia
Temperature and Humidity	(2010/9/26~2011/9/26)
Indoor Temperature and Humidity	Measured Value at Hagia Sophia (2010/9/26~2011/9/26)
Precipitation	3 times of amount of measured precipitation, (This value was estimated from the roof shape.)
Solar radiation	Calculated Value of vertical radiation at North from measured value of horizontal radiation at Hagia Sophia

Fig. 5 shows the calculated values of moisture content in the cases for which we considered rainfall and no rainfall. In the rainfall case, the moisture content of the connection mortar and middle-layer mortar sharply rose. The annual change of moisture content in the connection mortar is large. Winter is the rainy season, and the moisture content of the connection mortar reaches approximately $0.42 \text{ m}^3/\text{m}^3$ of the saturation of moisture content. On the contrary, the annual change in the moisture content of the middle-layer mortar is slight.

Fig. 6 and shows the average annual distribution of liquid and moisture fluxes near the inner surface as well as the annual change in the amount of evaporation at main evaporation locations near the inner surface, respectively. It can be said that evaporation mainly occurs from the middle-layer mortar. Change of the amount of evaporation between stucco and

middle-layer mortar, namely 0.8cm from the inner surface, is so large that both of evaporation and condensation occur mainly because of the change of indoor temperature and humidity. The amount of evaporation is large in summer, when evaporation occurs not only from the middle-layer mortar but also from the connection mortar. It might be said that evaporation from the middle-layer mortar is related to the exfoliation of the stucco, which is the main symptom of degradation confirmed at the exedra (Mizutani *et al.*, 2015a and b).

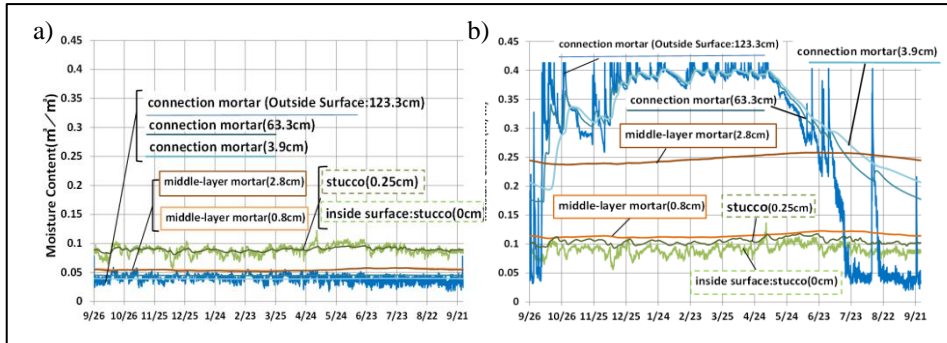


Fig. 5: Annual change of calculated values of moisture content with no rain (a) and with rain (b).

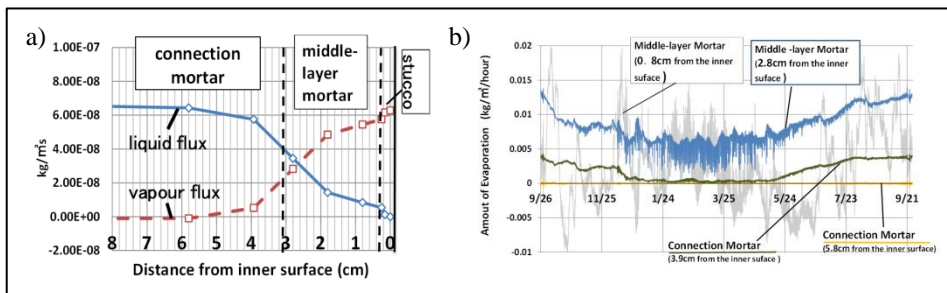


Fig. 6: a) Average annual distribution of liquid and moisture fluxes near the inner surface; b) Annual change in the amount of evaporation near the inner surface

5. Influence of Room Temperature and Humidity on Evaporation

5.1. Modelling for analysis of room temperature and humidity

To estimate an influence of the room temperature and humidity on evaporation at and near the inner wall surface, we develop a numerical model of the room temperature and humidity of Hagia Sofia. Using this model, we investigate how to control the inside climate to restrain the evaporation. This section accounts for the influence of heat and moisture generation from visitors and the transmission of solar radiation and heat through windows on the evaporation. The walls are treated as a one-dimensional uniform structure. The simultaneous heat and moisture transfer equations (Matsumoto, 1978) are used as the fundamental equation of the walls. The analysis model is composed of two rooms, as shown in Fig. 7. The lower room, composed of the ground floor and gallery (see Fig. 1), is

called the visitor zone. The windows and doors are opened during visiting hours. The upper room, composed of the second cornice and dome cornice in Fig. 1, is called the cornice zone. The dimensions of the rooms, openings, walls, floors and roofs are estimated based on the architectural survey of Van Nice (1965). The air of each room are represented as a single mass.

The heat and moisture generated from one person are taken at 80 W and 64 g/h, respectively. The daily number of visitors is based on the monthly average of 2013. It is assumed that the staying time is 30 min. The visitors, who generate heat and moisture, stay in the visitor zone during the opening time.

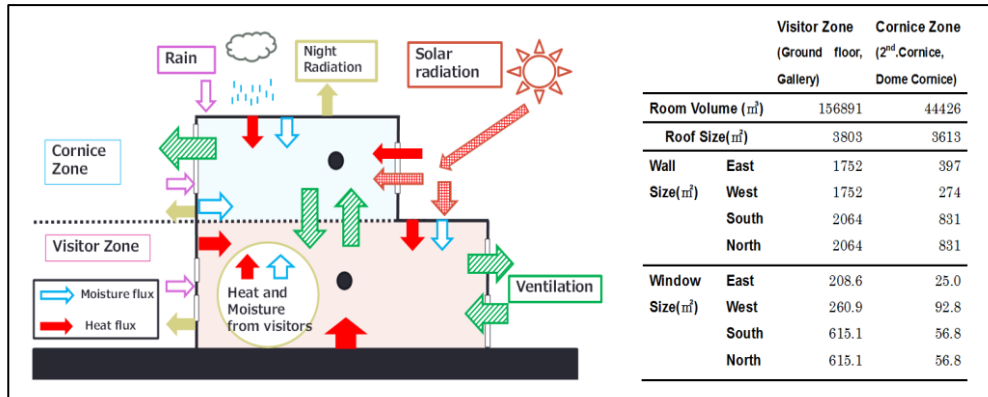


Fig. 7: Schematic diagram of the analysis model.

5.2. Boundary conditions

A third type of boundary condition is applied to the inner and outer wall surfaces. The temperature, humidity and precipitation are based on the data measured every 30 min outside and inside Hagia Sophia from September 26, 2012 to September 25, 2013. Solar radiation on the walls facing each direction is calculated by decomposing the total measured horizontal solar radiation into the direct and diffuse components using the equations of Bouguer and Berlarge. A boundary condition for the bottom of the ground, which is 13.2 m below the floor, is the annual average value of the outside temperature. The air change rates between the inside and outside and between the visitor and cornice zones were determined to identify the measured values of temperature and humidity.

5.3. Comparison of the calculated and measured values of temperature and humidity

Fig. 8 shows the calculated and measured values of room temperature and humidity in the visitor (a) and cornice zones (b). The calculated values of the humidity ratio for the visitor zone and cornice agree with the measured values throughout much of the year. The calculated values of the daily change of temperature are somewhat different in summer, but the annual changes of temperature in the visitor zone and cornice generally agree with the measured ones. We use these analysis conditions and results as reference values for the following investigation.

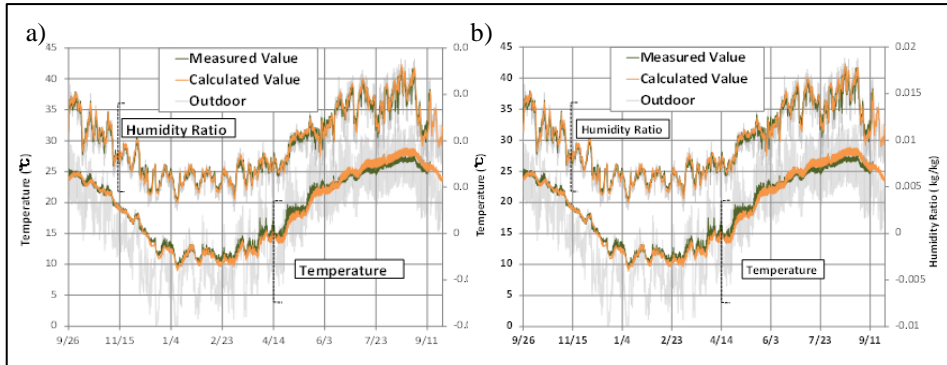


Fig. 8: Annual variation of temperature and humidity ratio in visitor zone (a) and cornice zone (b).

5.4. Influence of heat and moisture generation from visitors on evaporation from the inner wall surface

Hagia Sophia is the most popular sightseeing spot in Istanbul; it has approximately 3 million visitors annually. Our past study observed that the measured values of the annual average temperature on the opening day were $0.2\text{--}0.5^\circ$ higher than that on the closing day. It can be assumed that the heat and moisture generation from visitors influences the indoor climate. Figures 9a and 9b show the number of visitors and provide a comparison between the calculated amount of evaporation at the wall of the cornice zone in the reference case, together with the heat and moisture generation of cases with and without visitors. The relative humidity of the cornice zone in the reference case is slightly higher than that in the case without visitors. Furthermore, the amount of evaporation from the middle-layer mortar in the case without visitors is a slightly higher than that of the reference case, especially in spring. Therefore, it can be said that the heat and moisture generation from visitors restricts water evaporation, although it is quantitatively insignificant.

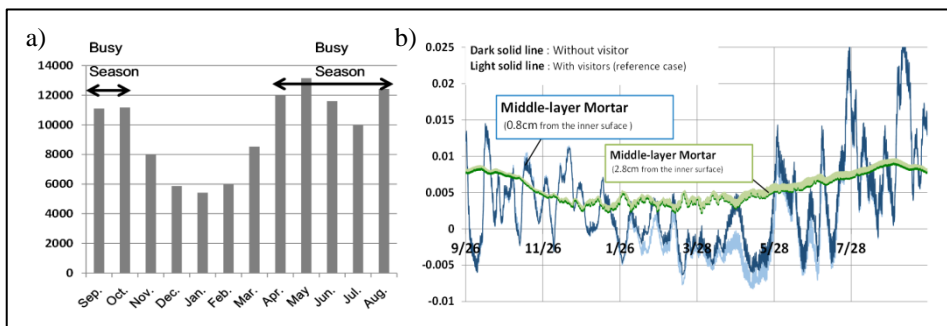


Fig. 9: a) Average daily number of visitors of each month; b) Difference in amount of evaporation due to heat and moisture generation from visitors.

5.5. Influence of heat loss and regain from windows on evaporation

The transmission of solar radiation through many windows that Hagia Sophia has is considered to affect the room and wall surface temperatures, so we investigate the influence of solar transmittance on the room temperature and humidity and the evaporation at and near the wall surfaces. To study the influence of the windows on evaporation, the solar transmittance of the windows is taken at 0.7 as the reference value or one fourth of that. Fig. 10a and 10b show the calculated values of respectively the temperature and amount of evaporation in the cornice zone. With a decrease of solar transmittance, the room temperature decreases, especially in spring and summer because of a relatively large impact of solar radiation. The decrease in the room temperature in these seasons would suppress evaporation in the middle-layer mortar.

Furthermore, the influence of the heat transmission coefficient, i.e. the conductivity of the window, is investigated. The heat transmission coefficient of the window is taken at 6.3 as the reference value or one fourth of that. Fig. 10c and Fig. 10d show the calculated values of the room temperature and the amount of evaporation in the cornice zone, respectively. The room temperature of the case with a lower heat transmission coefficient is significantly higher than that of the reference case in autumn and winter when the outdoor temperature is lower than the indoor temperature. The room temperatures of both cases in spring and summer do not differ. The decrease in the heat transmission can increase the indoor air and wall temperature specially in autumn and winter; as a result, the evaporation would increase throughout the year, when the heat conductivity performance of the window is improved.

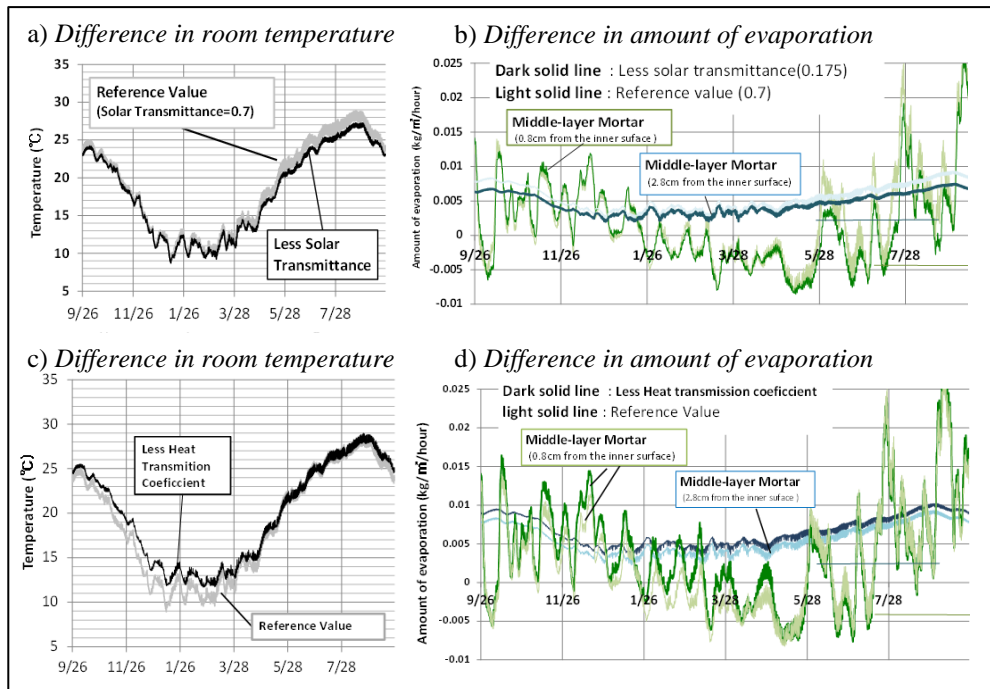


Fig. 11: Difference in room temperature and amount of evaporation.

6. Conclusion

We investigated accumulation of infiltrated rainwater in the masonry and the influence of its subsequent evaporation at and near the interior wall surfaces that would lead to degradation associated mostly with salt crystallisation. This was done by numerical analysis with a model of the exedra wall that takes into account out long-term on-site measurement data of the indoor and outdoor environment. The results showed that infiltrated rainwater mainly evaporates at the middle-layer mortar and would thus cause exfoliation of the inner stucco, which becomes significant in summer. Furthermore, we developed a numerical model that can sufficiently reproduce the room temperature and humidity, in order to investigate the influences of the indoor climate conditions on the evaporation. The simulation results show three main findings:

- Heat and moisture generation by visitors only slightly affects water evaporation.
- Reducing the transmission of solar radiation through the windows can reduce evaporation in spring and summer.
- Increasing the thermal resistance of the windows promotes evaporation.

Based on the simulation results, it should be particularly pronounced that reducing the transmission of solar radiation is an effective way to restrict evaporation at and near the wall surfaces and thus to mitigate the subsequent degradation of the inner walls. On the other hand, the number of visitors is of no importance from a viewpoint of restricting evaporation. The influence of ventilation on the evaporation is to be investigated in the future.

Acknowledgements

This work was partly supported by JSPS KAKENHI grant numbers 21226014 and 26709043. We extend our gratitude to them. We are deeply grateful for understanding and cooperation of this research given by curators and staffs of Aya Sophia Museum.

References

- Sasaki J., Yosida N., Ogura D., Ishizaki T., Hidaka K. 2012. Study of salt crystallization on the inner wall of Hagia Sophia, Istanbul, Turkey, *Science for Conservation* 51: 303-312. (in Japanese)
- Mizutani E., Ogura D., Ishizaki T., Abuku M., Sasaki J. 2015a. Influence of infiltration of rain water on degradation of the wall paintings in Hagia Sophia, *Journal of Environmental Engineering* 80: 1001-1012. (in Japanese)
- Mizutani E., Ogura D., Ishizaki T., Abuku M., Sasaki J. 2015b. Influence of infiltrated rain water on degradation of the wall paintings in Hagia Sophia, *Energy Procedia* 78: 1353-1358.
- Ogura D., Ishizaki T., Koizumi K., Sakaki J., Hidaka D., Kawata K. 2012. Deterioration on the wall and indoor and outdoor environmental conditions in Hagia Sophia, Istanbul, Turkey. *Science for Conservation* 51: 59-76. (in Japanese)
- Matsumoto M. 1978. Energy conservation in heating cooling ventilating building: heat and mass transfer techniques and alternatives (ed. Hoeogendoorn C.J. and Afgan N.H.), Washington : Hemisphere Pub. Corp., pp.1-45.
- Van Nice R.J. 1965. *Saint Sophia in Istanbul: an architectural survey*, Washington, Dumbarton Oaks.

This page has been left intentionally blank.

CONSERVATION OF MAGAI-WAREISHI-JIZO, A BUDDHA STATUE CARVED INTO A GRANITE ROCKFACE ON THE SEASHORE

M. Morii^{1*}, N. Kuchitsu¹, T. Kawaguchi², H. Matsuda³ and S. Tokimoto³

Abstract

The Magai-Wareishi-Jizo statue, carved on granite by stone mason Nenshin in A.D. 1300, is located in Mihara City, Hiroshima Prefecture, Japan. It is located near the seashore now and the whole image sinks under water at high tide. A global sea level change curve indicates that the sea level must have been lower around A.D. 1300 and that the statue was not fully immersed when first built. The present condition of frequent sinking must be due to subsequent sea level change which was not assumed at the beginning. Macroscopically speaking, the weathering rate of this statue is not regarded as so fast because it is carved on a core stone which is hard. However, compared with a replica made 24 years ago, it is revealed that the scaling is advancing little by little. Investigations are required from various viewpoints and appropriate measures are hoped to be executed. The authors carried out the conservation of Magai-Wareishi-Jizo in 2011. In this conservation, they carried out reattachment of loose parts by acrylic resin. As the restored parts were sunk under sea level because of the tide, drain holes were installed in order to help displace sea water in a cavity of the adhesive part.

Keywords: granite, core stone, seashore, scaling, attachment, acrylic resin

1. Introduction

Ever since Buddhism was introduced to Japan in the 6th century, many Buddhist works of art, such as stone pagodas and stone Buddha, have been created out of stone. The techniques for creating these works continued to develop over the years, with influence from overseas and master stonemasons were brought over from China to assist in the reconstruction of the Great Buddha Hall (Daibutsuden) of Nara's Todai-ji temple. At the end of the 12th century, the offspring of those Chinese stonemasons remained in Japan, and it became increasingly common for hard rock, such as granite, to be used in carvings. The Magai-Wareishi-Jizo statue was carved in the 13th century, at a time of much activity in the creation of stone artworks. The statue of Buddha is carved quite deeply into the granite surface, and the inscriptions of "2nd Year of Shoan" (1300) and the name "Nenshin,

¹ M. Morii* and N. Kuchitsu
National Research Institute for Cultural Properties, Tokyo, Japan
morii@tobunken.go.jp

² T. Kawaguchi
Act-Biz Cooperation, Japan

³ H. Matsuda and S. Tokimoto
Mihara city education board

*corresponding author

Buddhist sculptor” still remain to the right of the statue. The fact that it still bears the artist’s name and the year of production makes this statue a valuable piece of cultural heritage.

The statue stands on the shoreline, which means that, as well as the usual effects of the external environment, it is also highly susceptible to the effects of tidal activity and seawater spray. In fact, the sea level at high tide during spring tides comes up to the face of the Buddha and the statue is almost completely submerged in seawater. In contrast, when the tide goes out, the water level recedes to the point where it is possible to climb down to the beach and view the statue from head on (Fig. 1). Considering that it has been standing there, in an environment where stone-made structures are generally susceptible to deterioration, for 710 years, the statue is in remarkably good condition.

In recent years, however, dirt and grime on the surface of the work and some peeling on both the statue and the inscription have been observed. The authors therefore ascertained the current condition of the statue and repaired some of the peeling. In this article, the authors will report on the current condition of the Magai-Wareishi-Jizo statue and policies for its restoration. The article will also report on the methodology for re-attaching the peeling sections as a means of mitigating the effects of seawater, which poses a significant deterioration risk to cultural properties made of stone that are located on the coast, and on the results of field trials of that methodology.

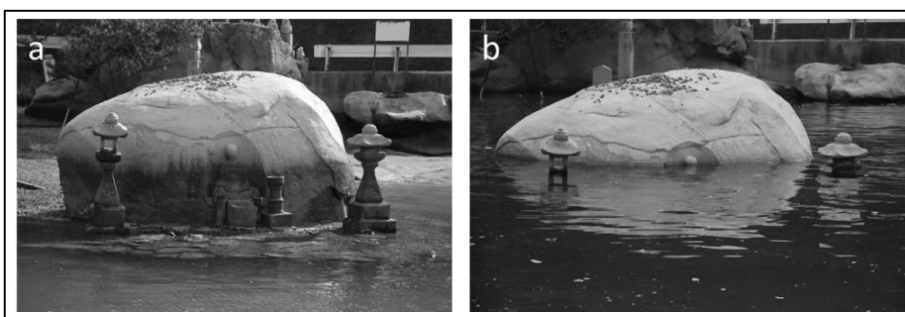


Fig. 1: Magai-Wareishi-jizo statue; a) Situation at low tide; b) Situation at high tide.

2. Overview of the Magai-Wareishi-Jizo

The Magai-Wareishi-Jizo is a 0.88-meter tall relief of a seated Jizo (bodhisattva) facing out to sea, carved into a granite boulder that is about 2.5 meters high, 4.9 meters wide, and 3.7 meters thick. It is located on the shoreline next to the Mukota Port Ferry Terminal on Sagi Island (Mihara, Hiroshima Prefecture) in the Seto Inland Sea. On the right side of the statue, an inscription of kanji characters can also be observed, which reads “2nd Year of Shōan” (1300) and “Nenshin, Buddhist sculptor.” In the city of Mihara, there is a stone pagoda built in 1249, which was said to have been created by a stonemason from Nara, and a number of stone pagodas known to be the work of Nenshin are still in existence in the city. They include the Hokyoin-to pagoda at Beisan-ji temple, which bears the inscription “1st Year of Genō” (1319) and “Nenshin, builder.” It is presumed that the “Nenshin, Buddhist sculptor” who carved the stone Buddha, and the “Nenshin, builder” who built the

stone pagodas in Mihara are one and the same person, and that he may have given himself different titles depending on what he was creating.

Most of Sagi Island is made of granite from the Late Cretaceous period. The granite boulder into which the Buddha has been carved is exceptionally hard and in good condition compared to the cliff faces on the same coast line and nearby stone Kasatoba (carved stone pillars with hat) from the 17th century, which have decomposed badly and become fragile. This granite boulder may be presumed to be an unweathered rock known as a “core stone.” Its outward appearance differs from that of the decomposed surfaces nearby, which often leads to the mistaken impression that it was brought to the site from elsewhere, but it is believed to be an embedded rock that was originally part of a larger rock body (Fig. 2).

Because the statue is situated on the water’s edge, it is currently highly susceptible to the effects of the tides. At low tide, the entire boulder is exposed above the water’s surface, but at high tide, some or all of the statue is submerged. The area submerged at high tide differs greatly day by day, but on most days, it comes up to at least the level of the Buddha’s chest. The surface of the statue up to that point is covered in black algae, making the lower half of the boulder appear black and dirty to the naked eye. During spring tides, however, the water level rises even higher, and at the peak of high tide in those periods, the statue is sometimes observed to be completely submerged to the top of the Buddha’s head.

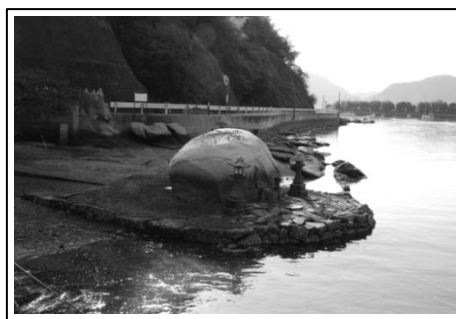


Fig. 2: Comparison between the boulder on which the Magai-Wareishi-Jizo statue is carved and the surrounding granite cliff face.

3. Conservation status of Magai-Wareishi-Jizo

The boulder on which the Magai-Wareishi-Jizo statue is carved is made of granite. Compared to the decomposition of the surrounding cliff faces, which are of a similar geological make-up, and of nearby stone structures that were erected after the statue was carved, it has remained relatively unweathered. On a macroscopic level, if we assume that the current rate of weathering is markedly rapid, the shape of the entire boulder should have changed greatly from that of a core stone. It would have been no surprise, for example, if the rock had taken on a gourd-like shape, with the area closest to the water’s surface at high tide becoming indented. In reality, however, the boulder is believed to have retained the characteristic core stone shape, so it is presumed that that kind of erosion has not been significant. In other words, it is believed that, since 1300, when the statue was carved, there has been no erosion significant enough to change the shape of the boulder, and it is difficult

to believe that weathering is currently taking place at a rate that would cause the boulder itself to disappear in the near future.

However, visual inspection of the statue has confirmed that there has been some partial surface peeling that has obviously occurred in recent years. To identify the peeling sections, the authors attempted a comparison with a replica of the statue that was cast in 1988 and is currently on display at the Hiroshima Prefectural Museum of History. This comparison confirmed deterioration in six places on the statue and the inscription that had occurred in the past twenty years approximately. For example, peeling of about 1 mm diameter was found on the chin of the stone Buddha (Fig. 3). Moreover, the deterioration is concentrated around the peak high water line, and it is believed that the peeling may be caused by tidal activity, that is, the repeated pattern of soaking at high tide and drying out at low tide.

Further, examination of the dark green areas found on the lower half of the Buddha's body confirmed the growth of algae in that area. Algae growth was also observed on the boulder in the area between the ground and about 40 cm above ground, but there was none observed above that line. Algae were also found on the stone lanterns in front of the statue, so the algae growth is believed to be caused by the effects of the sea water.



Fig. 3: Confirmation of deterioration by comparison with replica.

4. Conservation measures

4.1. Past conservation measures

There are records of restoration work having been performed on the Magai-Wareishi-Jizo in 1976. These records show that, at that time, it was believed that there was a great risk that the interaction of a number of influences, such as erosion by the seawater, the repeated drying and soaking caused by tidal activity, the effect of changes in temperature over the course of the day in the sections submerged by the sea and those that are not, and the effects of microorganisms and algae, could accelerate the weathering of the granite rock. It was also believed that it would be impossible to eliminate all of those influences. For this reason, restoration work consisted mainly of reinforcement of the granite with silicone resin, repairs of cracks and peeling with epoxy resins, and injection of bonding agents. However, as far as the authors could confirm during their field survey, it appears that most

of the repairs were done on the back of the rock, and the work on the front was confined to reinforcement alone.

4.2. Restoration policy

Despite the sculpture being regularly submerged under the sea at high tide, the statue itself and the inscription have remained remarkably intact. The main deterioration at this point in time is surface peeling, and the authors determined that a minimal level of measures to prevent peeling was required to protect the statue and the inscription. Also, in terms of bonding the peeling areas back onto the stone, it was decided to keep the use of bonding agents to a minimum, in order to eliminate the impact of the difference in the thermal expansion coefficients of the rock itself and the bonding agent. Moreover, because the bond strength of the bonding agent would be reduced if it were to get wet before manifesting, a restoration schedule was established that took into consideration the properties of the bonding agent and the surrounding environment. Details are as Tab. 1.

4.2.1. Bonding method

Because the loss of the carved sections of the stone statue itself and the inscription would greatly reduce the value of the sculpture, a minimal level of bonding was necessary. It was decided, therefore, to spot-bond the areas affected by peeling and the areas that were lifting away with an acrylic resin (Fig. 4. The black sections are the areas adhered with the acrylic bond). Also, because no salt precipitation or plant growth was observed behind the peeling sections, it was decided to ignore the deterioration caused by water inside the rock (salt weathering, etc.) and to leave holes to allow any water infiltrating the peeling areas at high tide to escape, in particular, for water to escape from the bottom sections.

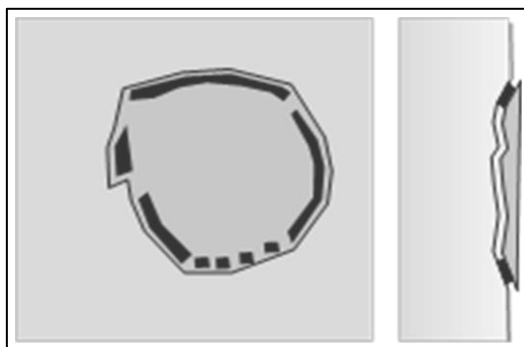


Fig. 4: Method of bonding peeling sections.

4.2.2. Schedule of conservation

Bonding agents generally require time to harden. To prevent any adverse effect of moisture or seawater while it was hardening, a season with a relatively large number of sunny days was chosen, and it was decided to undertake the conservation measures at low tide during neap tide periods, so that the area being worked on would not be submerged during high tide.

4.2.3. *Conservation procedure*

The conservation measures were carried out in November 2011. The areas of surface peeling on the statue and inscription considered most at risk were selected and the bonding agent applied. The procedure was conducted in the following order: (1) advance survey; (2) determination of locations in need of restoration; (3) advance trials; (4) bonding of peeling sections; (5) follow-up observation.

4.2.4. *Advanced survey*

The state of deterioration of the statue and inscription was ascertained before the work was undertaken. As described earlier in this article, compared with when the replica was produced, the authors found many areas of damage. For example, the chin of the *bodhisattva* image is rounded on the replica, but in comparison, there has clearly been peeling on the original sculpture in that area.

4.2.5. *Determination of parts of restoration*

Based on the advance survey, the areas for restoration was confined to the Buddhist image itself and the carved surface of the inscription. Surface peeling was also observed on the areas at the bottom of the Buddha relief that were dark green (algae), but these areas were deemed unsuitable for the use of bonding agents due to their being wet for longer periods, so conservation of those areas was deferred on this occasion. Also, because the purpose of this work was not to reinforce the surface but to adhere the peeling sections, it was decided to defer work on peeling of less than 1 mm in width, where there was a risk of the resin attaching to the surrounding stone, and to only treat sections of 1 mm or more in width which were in danger of falling off completely.

4.2.6. *Advance trials*

Advance trials of the bonding procedure were performed on a section of surface peeling on the left side of the statue. In the trial, the resin's hardening time was measured, and methods for accelerating hardening and the composition of the thickening agent were decided. The state of hardening and changes in colour of the bonded sections after submersion were also checked.

4.2.7. *Bonding of peeling sections*

After the restoration methodology and schedule were decided based on the results of the advance trials, the bonding agent was applied to the peeling sections. The resin was not applied to the entire back surface of the peeling section; instead a hole for seawater that entered the peeling section to drain out was created (Fig. 5). For smaller sections, however, to ensure that the bonded section did not become detached, no drainage hole was made and the surface was closed up completely. Because the area of peeling on the chin of the stone Buddha had expanded, cracks of less than 1 mm were also bonded by filling them in with resin. Subsequently, any grade differences from the surface were filled in with resin mixed with stone powder.

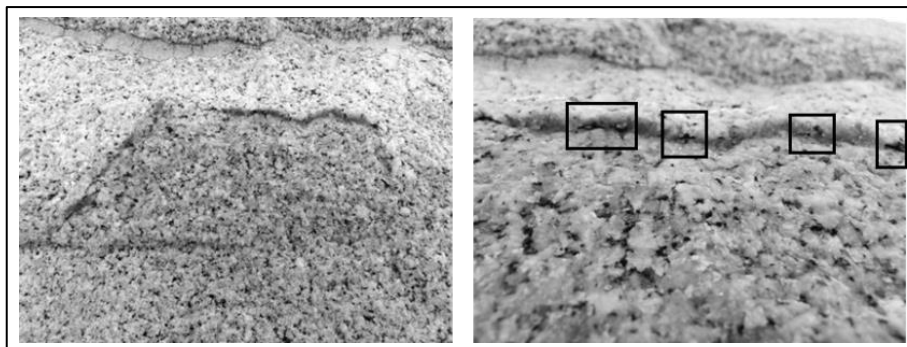


Fig. 5: Bonding peeling sections.

Tab. 1: Restoration policy.

	Detail
Acrylic resin	Acrylate (Liquid A: oxidizing agent, Liquid B: reducing agent)
Thickener	Stone powder
Compounding ratio	1:2 (resin : thickener, capacity ratio) *paste
Bonding	Bonding the edge of the peeling section using bamboo skewer
Acceleration of hardening	Heated with a dryer for 2 hours
Colour tone	4 colours (white, yellow, black and brown) *slightly dark colour

4.3. Follow-up observation

Three months after the restoration work was done, follow-up observations were conducted of the restored areas. No changes in the bond strength or colour tone were observed. However, because these repairs were performed in a special environment, although a bonding agent appropriate to the conditions was used, further regular follow-up observations will be needed to determine whether or not the effectiveness of the repairs can be maintained.

5. How the statue would have looked when it was first carved

The boulder on which the Magai-Wareishi-Jizo was carved is a granite core stone, and in the 700 years since it was created, there has been only slight weathering on a macroscopic scale. So what would the stone Buddha have looked like when it was first carved? If we look at the curve of global sea-level change, the year 1300 coincided with a period of marine regression in the Middle Ages known as the Paria Regression, and on a global average, sea levels may have been around one meter lower than they are today (Fig. 6). Topical elevation and sedimentation in the area would need to be studied, but if it was the same on Sagi Island, then sea levels at the time the statue was carved would have been

lower than they are today, and it is likely that the statue would not have been submerged at high tide. In other words, the original concept may have been that, with the stone Buddha located on the water's edge, the water level would have come up to just below the Buddha himself at high tide, which would make it appear as though the sitting Buddha was floating on the water. With today's higher sea levels, however, the statue is almost completely submerged at high tide, something that the sculptor would not have intended.

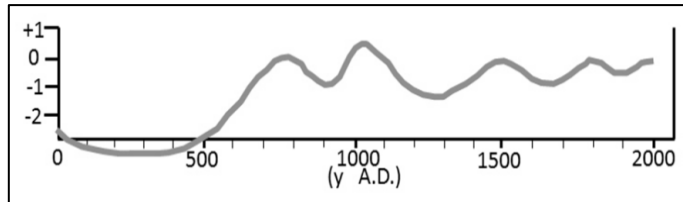


Fig. 6: Global sea level change (from Fairbridge, R. W., 1961).

6. Conclusion

In addition to ascertaining the state of deterioration of the Magai-Wareishi-Jizo visible today as it stands on the shoreline, the authors undertook those conservation measures which were possible to carry out in the given circumstances in which the statue could not be moved. Regarding the bonding of the peeling sections in particular, various innovations were performed, such as including holes for drainage of seawater that had entered behind the peeling section with the tide. As a result of these conservation measures, follow-up observations three months after the work was performed showed that there were no major problems and the work has remained in a good condition to date.

References

- Katayama, K., 1961, "Akikoku Sagi-shima Wareishi-Jizo, Shoan Ninen Mei Magaibutsu", "Shiseki to Bijyutsu", 314, 143-154 (in Japanese).
- Kawakatsu, M., 1998, "Nihon Sekizou Bijyutsu Jiten", Tokyo-do Shuppan, 9784490105032, 418p (in Japanese).
- Ikeda, H., 1998, The World of Granite Landforms, Kokon-shoin, 9784772216791, 206p (in Japanese).
- Mihara City Education Board, 2012, Report of conservation of Magai-Wareishi-Jizo statue, Important Cultural Properties of Hiroshima Prefecture, 30p (in Japanese).
- Hayakawa N. and Kawanobe W., 2001, The Study to Control Water Contents by Various Silicone Derivatives Usuki-magaibutsu, Science for Conservation, National Research Institute for Cultural Properties, Tokyo, Japan, 40, 69-74 (in Japanese).
- Fairbridge, R. W., 1961, Eustatic Changes in sea-level, in L. H. Ahrens, K. Rankama, F. Press and S. K. Runcorn (eds), Physics and Chemistry of the Earth vol 4, London: Pergamon Press, 99-185.

EVALUATION OF THE PRESERVATION STATE OF THE HOLY AEDICULE IN THE HOLY SEPULCHRE COMPLEX IN JERUSALEM

A. Moropoulou¹, K. Labropoulos¹, E. Alexakis^{1*}, E.T. Delegou¹,
P. Moundoulas^{1†}, M. Apostolopoulou¹ and A. Bakolas¹

Abstract

The Church of the Holy Sepulchre (Church of the Resurrection) in the city of Jerusalem is one of the most important historical sites of Christianity and according to tradition is the scene of Jesus Christ's death and resurrection. Holy Aedicule is one of the Holy Pilgrimage Sites of the Complex, and is the place where Jesus has been buried and resurrected. During the British Mandate, the structure of Holy Aedicule was strengthened by the installation of a metal supporting frame to restrain the façades' deformation that was macroscopically observed and is still evident. To evaluate the preservation state of The Holy Aedicule, characterisation of building materials, decay diagnosis and construction phase determination have been performed using Non Destructive Techniques (NDT) in situ, and analytical techniques in lab after sampling. In particular, based upon the historic documentation of the Monument, Ground Penetrating Radar (GPR) measurements provided a satisfactory discrimination of the construction phases. Additionally, samples were investigated by analytical techniques like X-Ray Diffraction (XRD), Simultaneous Differential Thermal and Thermogravimetric Analysis (DTA/TG) and Mercury Intrusion Porosimetry (MIP), to characterize building materials, as well as to diagnose decay and pathology of the historic structure.

Keywords: diagnostic study, non-destructive testing (NDT), building material, analytical techniques, decay

1. Introduction

The Church of the Holy Sepulchre (Church of the Resurrection) is one of the most important historical sites of Christianity. Within this Church, the Holy Aedicule is built, which contains the tomb of Jesus Christ. The current Aedicule structure is the result of various construction phases (Fig. 1), damages and destructions, reconstructions and protection interventions (Lavvas 2009, Mitropoulos 2009, Montefiore 2012, Moropoulou 2016). The Church dates back to 325AD, when Emperor Constantine I ordered the construction of a basilica incorporating the tomb of Christ, within the Holy Aedicule (Fig. 1a). The Tomb was carved outside, possibly in a polygonal form, with an entrance on its eastern side (Fig. 1a), whereas the interior had a rectangular form and on its northern side the arcosolium. At the start of the 7th century, the exterior surfaces of the polygonal

¹ A. Moropoulou, K. Labropoulos, E. Alexakis*, E.T. Delegou, P. Moundoulas,
M. Apostolopoulou and A. Bakolas
School of Chemical Engineering, National Technical University of Athens, Greece
alexman@central.ntua.gr

*corresponding author

monolithic Aedicule were covered by marble plates, columns and metal fences to protect it from the visiting pilgrims. This building was damaged by fire in 614 when the Church of the Holy Sepulchre was damaged by fire in 614 when the Persians invaded and destroyed Jerusalem. The Aedicule's exterior and interior surfaces and decorations were destroyed, including partial destruction of the burial chamber, along its east-west axis (Fig. 1b). In 622, Christians were allowed to rebuild churches and monasteries. Modestus, the abbot of the Monastery of St. Theodosius, rebuilt the Church of the Holy Sepulchre and destroyed parts along the east-west axis of the Aedicule were restored with masonry (Fig. 1c). In 1009, the Caliph of Egypt El-Hakem ordered the complete destruction of the church; the Holy Aedicule is destroyed down to ground level. During the reign of Constantine Monomachus, Patriarch Nikiforos persuaded the Emperor to offer money for the reconstruction of the Holy Sepulchre (1027-1048). Parts destroyed by Al-Hakim were restored with masonry, the Aedicule regaining its former Constantinean plan form, and its exterior surfaces covered with stone plates, enveloped by 12 columns (Fig. 1d). After the arrival of the crusaders (1099) the Church of the Holy Sepulchre was renovated in a Romanesque style and added a bell tower. A vestibule (Chapel of the Angel) was added at the eastern side of the Aedicule in 1119 (Fig. 1e). Following various conquerors, Jerusalem fell in 1517 to the Ottoman Turks, who remained in control until 1917.

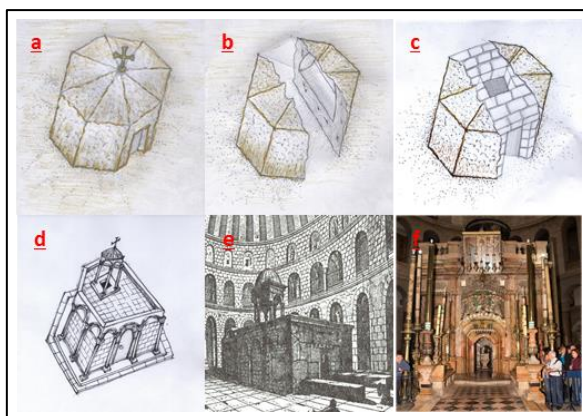


Fig. 1: The construction phases of the Holy Aedicule of the Church of the Holy Sepulchre throughout history (Mitropoulos 2009).

In 1808, an accidental fire became uncontrolled, which caused the dome of the Rotunda to collapse over the Aedicule, inflicting to it severe damage. According to historic sources (Moropoulou 2016), The Holy Tomb remained intact but the Aedicule structure was heavily damaged and buried under the Rotunda dome ruins. After permission, the official architect Nikolaos Komnenos rebuilt the Aedicule in the contemporary Ottoman Baroque style, effectively embedding the remaining core of the burial chamber within the new, larger, Aedicule structure. The restored Church was inaugurated on 13th September 1810 (Fig. 1f).

Since the 1810 reconstruction, in all external faces, except the west end, the marble shell presents a strong buckling. By 1947, the deformation of the external construction of the Aedicule was already as intense as today, forcing the British Authority (to take immediate measures in the form of an iron “frame”, along the flanks, which through strong wooden

wedges prevented any further outward movement of the stones already affected by the buckling mechanism. More recently, the National Technical University of Athens, after invitation from His All Holiness, Beatitude Patriarch of Jerusalem and All Palestine, Theophilos III, signed a programmatic agreement with the Jerusalem Patriarchate and implemented an innovative research titled "*Integrated Diagnostic Research and Strategic Planning for Materials, and Conservation Interventions, Reinforcement and Rehabilitation of the Holy Aedicule in Church of the Holy Sepulchre in Jerusalem*". Within this framework, based upon the historic documentation provided by the Patriarchate Technical Bureau, an array of non-destructive techniques in conjunction with materials characterization were performed to elucidate the construction phases of the Holy Aedicule and the materials they are composed of, in order to assess the preservation state of the Aedicule, and to provide basic layering information for the assessment of its current state against static and seismic loads.

2. Methods and Techniques

2.1. Non Destructive Testing - Ground Penetrating Radar (GPR)

Ground Penetrating Radar (GPR) is an established non-destructive electromagnetic technique that can locate objects or interfaces within a structure. GPR was utilized in order to reveal information about the interior structure of the Aedicule, i.e. the interior layers of its masonries, as well as the assessment of their preservation state and cohesion, in the conjunction with macroscopic deformations. The ground penetrating radar system used in this survey was a MALÅ Geoscience ProEx system with 1.6 GHz and 2.3 GHz antennae. The MALÅ Geoscience Groundvision 2 software was used for data acquisition. The GPR scans were processed with the MALÅ Geoscience RadExplorer v.1.41 software, after application of the following filters: DC removal, Time zero adjustment, Amplitude correction, and Band pass filtering.

2.2. Analytical (in-lab) Techniques

Sieve analysis was performed according to Normal 27/88 (Normal 27/88 1988) in order to analyze the mortar aggregates grain size distribution and to calculate the binder aggregate ratio. The sieves used were according to ISO 565. Differential Thermal and Thermo-Gravimetric Analysis (DTA-TG) provides qualitative and quantitative information regarding the composition of the samples (Mettler Toledo 651e). The temperature range applied was 25-1000°C and the heating rate was selected at 10°C/min (Moropoulou *et al.*, 1995). X-ray diffraction (XRD) provides information regarding the mineralogical composition of the materials (Advance D8 Diffractometer of Bruker Corporation) (Normal 27/88 1988, Moropoulou *et al.*, 1995). The microstructural characteristics of the samples were studied through the use of Mercury Intrusion Porosimetry (MIP) with the use of a Pascal 400 Thermo-Electronics-Corporation (Normal 27/88 1988).

3. Sampling

A number of historical mortar and building stone samples deriving from the façades and the construction faces of the Holy Aedicule were collected for their characterization with the analytical-laboratory techniques. The examined samples that are presented in this study are coming from the South outer façade and the restoration mortar of Architect Komnenos. The samples were obtained by Core Sampling on selected areas in the ground and the façades in order the particular materials to be acquired.

4. Results and Discussion

4.1. Non Destructive Testing

In Fig. 3a, over the plan of the Aedicule, the basic scan areas of the exterior and interior of the Aedicule are presented. The red quadrants represent the basic survey areas. The markings B1-B5 and N1-N5 corresponds to the north and south arch areas at the exterior surfaces of the Aedicule. The description of the analysis of the GPR scans is presented in Fig. 3b, which corresponds to a horizontal scan on area N4 at a height of 130 cm above the interior floor level. For the conversion of the scan in Fig. 3b/A into a two-dimensional section distance - depth (X axis vs. Depth – Z axis), the calculation of the pulse velocities throughout all observed layers is required. For this purpose, stone blocks of the parapet at the roof and stone block from the seat outside the entrance to the Aedicule were used as standards to calibrate the pulse velocities for the GPR analysis, with the aid of, the velocities and dielectric constants were calculated and used in the velocities models of the remaining areas, representing the exterior stone panels and the holy rock, as they have similar synthesis. Based on this calibration, a velocity of $v=11.58$ cm/ns ($\sigma=1.02$ cm/ns) was calculated. It should be noted that the stone ashlars that were used for the construction of the Bell Tower of the Church of the Holy Sepulchre had a velocity of $v=10.48$ cm/ns, as measured during a previous diagnostic study with non-destructive techniques by the research team of NTUA (Labropoulos and Moropoulou 2013).

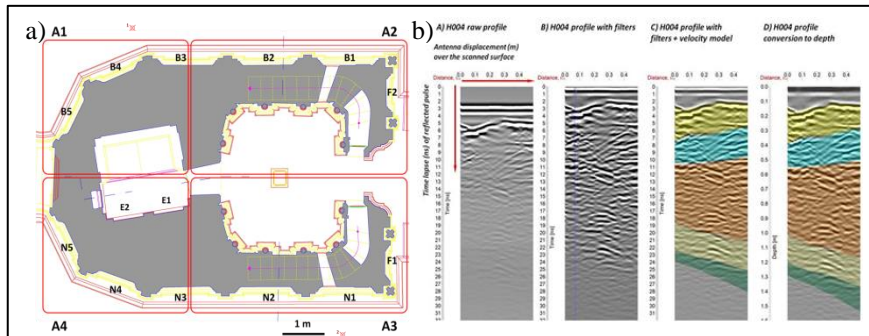


Fig. 2: a) Plan of the Aedicule (at a height of 130cm from the interior floor); b) Overall process of conversion of a GPR scan into a graph distance - depth

It should be noted that the scan after its processing with the aforementioned filters still remains a distance – time graph. Specifically, the horizontal axis corresponds to the displacement of the antenna over the surveyed surface, whereas the vertical axis of the graph corresponds to the time elapsed between the moment when the electromagnetic pulse is emitted from the antenna on the surface, its diffusion within the masonry, its encounter with an interface of materials of different electrical properties, its partial reflection towards the exterior surface, and its detection by the receiver antenna. The amplitude of the reflected pulse is attributed with shades of grey, where black and white correspond to maximum intensity of a pulse with positive or negative polarity correspondingly, whereas grey corresponds to zero intensity of the detected pulse. Figure 3b/B presents with a blue color the palmograph at position $X=0.07$ m from the beginning of the scan, where the various reflections per time lapse (blue line peaks) are visible, and in particular the reflection of the exterior panel / Komnenos construction phase at approximately 3ns. For

the calculation of the pulse velocity of the Komnenos construction phase, scans in the N2 area were calibrated, where most probably the masonry consists mainly by stone/marble panels (exterior and interior) and one internal building phase. Following these, Fig. 3b/C and Fig. 3b/D present the application of the velocity model on scan H004. The various layers are identified by the user and are depicted on the scan. From the exterior surface and inwards, the various layers are shown. Grey: exterior stone panel, Yellow: Komnenos construction phase, Blue: Crusader's construction phase, Brown: Holy Rock of Golgotha, Light Green: Masonry layer between Holy Rock of Golgotha and interior marble panel. Green: Interior marble panel.

Figure 4 presents in a descriptive approach the various layers within the Aedicule structure, as analyzed by GPR and retains the plan of the current structure and the exterior boundary of the 11th/12th century building (red outlines). The BN3 plane and the longitudinal axis conceptually define the four quadrants A1 – A4 of Fig. 3a. Starting from the southwest quadrant A4 of the Aedicule, and analyzing with the aforementioned methodology the various detected internal interfaces, from the south exterior towards the interior of the Holy Sepulchre, the following are revealed: a) exterior panel, b) Komnenos construction phase, c) Crusaders construction phase, d) Holy Rock, e) masonry between Holy Rock and interior panel, and f) interior panel.

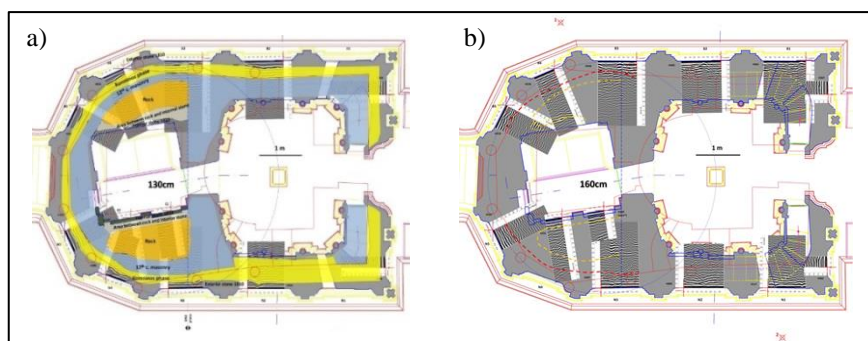


Fig. 3: Layering within the Holy Aedicule (cross-section at height level 130cm and 160 cm, left and right, respectively) as identified by GPR analysis (Moropoulou 2016).

The exterior panel has a varying thickness of 10-15 cm, and corresponds to the first zone (0-15 cm) at the respective GPR scans of the exterior surfaces. Moving towards the interior, an interface is observed at a depth of 30-40 cm. The layer between the exterior panel and this interface corresponds to the Architect Komnenos construction phase, and is indicated in Fig. 3a as a yellow colored zone. Moving further towards the interior, the GPR scans reveal the presence of a second interface, at a depth of approximately 50-60 cm. The layer between the red dashed curve – internal boundary of the Komnenos construction phase – and this second interface, corresponds to the 12th century masonry, i.e. the Crusaders construction phase. It should also be noted that the 12th c. masonry appears to have an increased thickness, approximately 30 cm eastwards (area N3), in comparison with a thickness of 20cm westwards (area N4, as well as throughout quadrant A1). This observation, in conjunction with a) the slight rotation of the Holy Tomb in respect with the longitudinal axis of the Aedicule and b) the different location, towards the north, of the 8th pillar of the Crusaders phase, in relation to its location at the original dodecagon building,

can lead to the theory that the Holy Rock solid volume, or at least whatever remained from its successive carvings, did not have a canonical dodecagon plan in full correspondence with the pillars of the original dodecagon building, but possible had a transverse dimension slightly smaller than the longitudinal one. Therefore, the addition to the Holy Rock of the 12th century masonry, possibly reinstated the canonical geometry on the apparent volume of the Holy Rock. The revealed layers within quadrant A1 of the Aedicule are the same as that of quadrant A4. The 12th century masonry appears, however, to have a thickness of approximately 20cm, throughout quadrant A1, in contrast to the case of quadrant A4.

Regarding the Chapel of the Angel, and based on the analysis of GPR scans, there are indications that on the northern side and on the eastern side parts of the Crusaders' masonry were retained (Fig. 3), on which deep carving was performed to its interior, to facilitate the northward expansion of the Chapel. The old wall was retained – on the north part of the Chapel of the Angel – probably to the full length of the Chapel, up to the façade area (Moropoulou 2016). The retained height is probably approximately up to 1,5m above the interior floor level, this corresponding to the height of the entrance of the northern staircase and its first three steps. Above that height, the masonry is most probably entirely new, constructed during the 1810 restoration works. Correspondingly, at the southern part of the Chapel of the Angel, GPR analysis indicates that retaining of Crusaders' phase masonry occurs only at the southeastern corner (Fig. 3), up to height similar as the one on the northeastern corner.

4.2. Building Material Characterization

4.2.1. South Façade Building Stone

Based upon the XRD pattern of Fig. 4a the sample mainly consists of carbonate minerals (CaCO_3), most particularly micrite calcite, approximately 98%, which in places becomes microsparitic, while quartz crystals, clay minerals, opaque metallic mineral oxides and iron hydroxides are found at < 2%. This stone is characterized as a micritic fossiliferous limestone. With regards to the Microstructural Analysis (Fig. 4b), the building stone's Cumulative Volume 1.21 mm³/g, Bulk Density 2.67 g/cm³, Total Porosity 0.32%, Average Pore Radius 0.005 μm and Special Surface Area 0.39 m²/g.

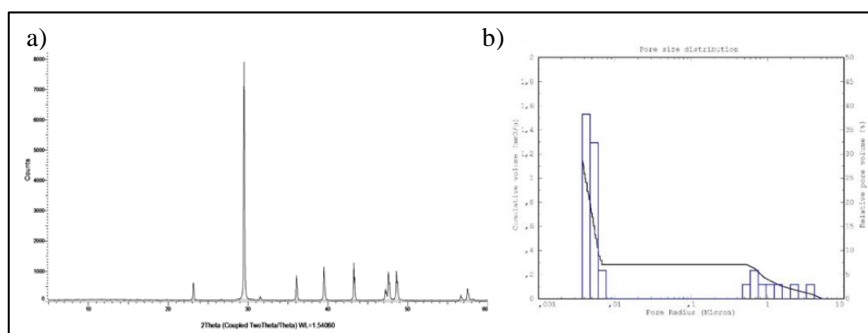


Fig. 4: Outer façade building stonet: a) XRD pattern and b) Pore size distribution.

4.2.2. Architect Komnenos Restoration Mortar

According to the XRD pattern of Fig. 5a and the thermal analysis results (Fig. 6) and, the examined are characterized calcitic with a slightly hydraulic as it presents high or even very high percentages of natural bound water (hygroscopic). The important mass loss observed in the temperature range 200-600°C, is attributed to four factors:

- 1.) Saturation of aluminat compounds of the marly limestone in water, which has led to the intense disintegration of the mortar, simultaneously diminishing its mechanical properties;
- 2.) Presence of organic compounds in the mortar composition which can be validated through FT-IR measurements;
- 3.) Presence of ettringite; ettringite is crystallized with 16 crystalline waters, and it is produced by the corrosion of the crust of larnitic rocks. The characteristic peaks of ettringite can be found in XRD pattern of Fig. 5a;
- 4.) Large mass loss in the temperature range from 200 to 600°C is due to the slightly hydraulic nature of the mortar which provided high mechanical strength to the mortar at the time of its application. With regards to the microstructural analysis (Fig. 5b), the mortar's cumulative volume 570.5 mm³/g, bulk density 0.98 g/cm³, total porosity 56.03%, average pore radius 0.24 µm and special surface area 15.25 m²/g.

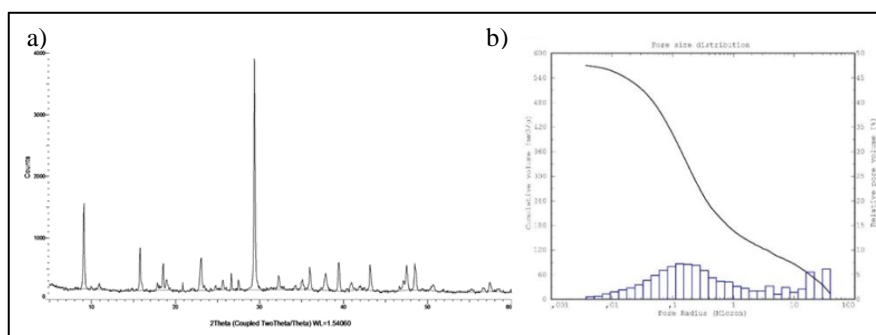


Fig. 5: Restoration mortar: a) XRD pattern; b) Pore size distribution.

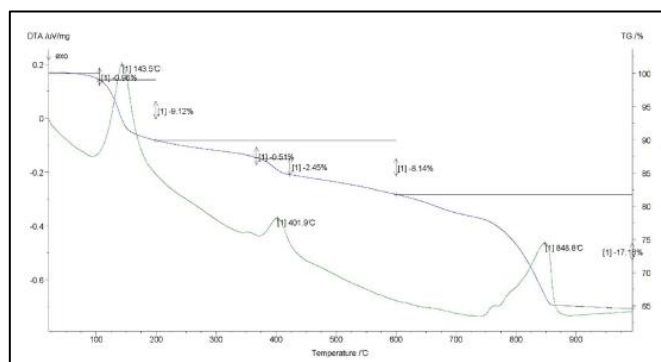


Fig. 6: Differential thermal analysis and thermogravimetry graphs.

Acknowledgements

The authors would like to express the gratitude to His Beatitude the Patriarch of Jerusalem Theophilos III who initiated the program agreement by NTUA with title “*Integrated Diagnostic Research Project and Strategic Planning for Materials, Interventions Conservation and Rehabilitation of the Holy Aedicule of the Church of the Holy Sepulchre in Jerusalem*”, His Paternity the Franciscan Custos of the Holy Land, Rev. f. Pierrebattista Pizzaballa and His Beatitude the Armenian Patriarch in Jerusalem, Nourhan Manougian who that authorized His Beatitude the Patriarch of Jerusalem Theophilos III and NTUA to perform this research.

References

- Labropoulos, K. and Moropoulou, A., 2013, Ground penetrating radar investigation of the bell tower of the church of the Holy Sepulchre, *Int. J. of Construction and Building Materials*, 47, 689-700.
- Lavvas, G., 2009, *The Holy Church of the Resurrection in Jerusalem*, The Academy of Athens; Greece.
- Mitropoulos T., 2009, *The Church of Holy Sepulchre – The Work of Kalfas Komnenos*, European Centre of for Byzantine and Post-Byzantine Monuments, Israel.
- Montefiore, S., 2012, *The Biography Paperback*, Phoenix; Jerusalem, Israel.
- Moropoulou, A., Bakolas, A., Bisbikou, K., 1995, Characterization of ancient, byzantine and later historic mortars by thermal analysis and X-ray diffraction techniques, *Int. J. Thermochemica Acta*, 269/270, pp. 779-795.
- Moropoulou, A., 2016, *Materials & Conservation, Reinforcement and Rehabilitation Interventions in the Holy Edicule of the Holy Sepulchre*, National Technical University of Athens, Greece.
- Normal 27/88, 1988, *Caratterizzazione di una malta*, C.N.R. – I.C.R., Roma, Italy.
- Pringle, D., 2007, *The Churches of the Crusader Kingdom of Jerusalem, A Corpus, Volume III, the City of Jerusalem*, Cambridge University Press, United Kingdom.

CONSERVATION OF MACHU PICCHU ARCHAEOLOGICAL SITE: INVESTIGATION AND EXPERIMENTAL RESTORATION WORKS OF THE “TEMPLE OF THE SUN”

T. Nishiura^{1*}, I. Ono¹, A. Ito², H. Fujita³, M. Morii⁴, F. Astete⁵ and C. Cano⁶

Abstract

Machu Picchu archaeological site, which is called “Ancient capital in the sky”, is one of the most important and famous world-heritage. It was the special place of the Inca Empire in the sixteenth century located on the high ridge in Peru. There are about 200 remaining structures built of stones (granite) at the site of 13,000 km². Systematic conservation measures for the structures has not been applied, except emergency ones by the regional office. Thus, the authors have started the project for the conservation of the remaining structure, especially for the preservation and restoration of “*Temple of the Sun*”, which is one of the most important structures in the site, in cooperation with the Ministry of Culture of Peru. There are three major problems on the *Temple of the Sun*. One is that the stones of the structure have cracks caused probably by lightening thunderbolts. Another problem is that the structure became unstable because some of the joint parts among the stones are open since it was excavated. The third one is the growth of lichens causing chromatic alterations on the surfaces. The main activities of the project are reported.

Keywords: Machu Picchu, world heritage, stone structures, *Temple of the Sun*, granite

1. Introduction

Researches on deterioration and conservation of Machu Picchu archaeological site have typically been approached from geological or civil engineering aspects of study due to its unique setting of its mountain top location. In addition, many anthropological studies have been made.

¹ T. Nishiura* and I. Ono
Professor, Kokushikan University, Japan
nishiura@kokushikan.ac.jp

² A. Ito
Kansai University, Japan

³ H. Fujita
Niigata of International and Information studies, Japan

⁴ M. Morii
National Research Institute for Cultural Properties, Japan

⁵ F. Astete
Office for Conservation and Administration of Machu Picchu Region, Ministry of Culture, Peru

⁶ C. Cano
Cusco University of Art, Peru

*corresponding author

In regard to individual condition of granite dimension stones, a local conservation office had been in charge of taking care of responsive emergency measures, however, a comprehensive survey, research or restoration project has not yet undertaken. Therefore, Japanese cooperation project under the cooperation of Cuzco Regional Office of Ministry of Culture, Peru and Office for Conservation and Administration of Machu Picchu Region was now established to take on *in situ* conservation and restoration technique research particularly for *Temple of the Sun*.

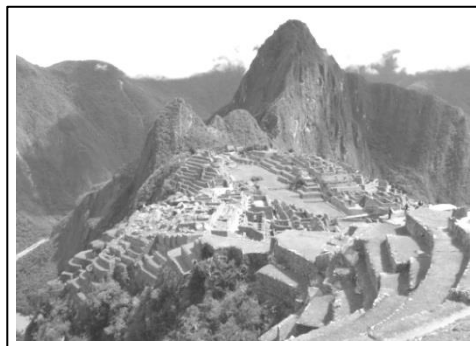


Fig. 1: Machu Picchu site.



Fig. 2: Temple of the Sun.

2. Temple of the Sun

2.1. General

Temple of the Sun is one of the most significant remaining structures in Machu Picchu archaeological sites. The dry stone technique employed to stick up stones on top of natural stone bed is remarkable and considered to be the best construction technology in Machu Picchu ruins. The sacred chamber situated on top of the sacred burial is dedicated to the Sun. On Eastern wall, there are two windows, from one of which the sunlight comes through on the winter solstice and on the summer solstice from another. When the building was in use, it is said that the golden statue was placed on the natural rock pedestal with a large bronze mirror set on the northern window to reflect golden sunlight.

2.2. Present Condition

Granite material degradation is most obvious in the *Temple of the Sun*. Exfoliation, delamination, fissures, cracks of both large and small and missing parts are all detected in the stones used in the structure. The cause for these damages is considered to be heat. Granite as of its mineral composition is sensitive to fire and excess heat (remark: above 573 when quartz changes the structure. Gaps between stones caused by secondary phenomena are bringing the building to a danger of collapse. Recent growing of lichens on the surface is also noted. This is a cause of surface change of appearance.

There are two theories for the cause of hyper heating. One is of man-made fire during the excavation time (1912-15). The excavation team cut down trees and dead branches and burns them during the archaeological excavation survey inside the temple. The high location of the site and circular protected high wall would have offered good conditions for wood burning. It is common hearsay information among the locals.

Another theory is the thunderbolt. After Machu Picchu site was abandoned, the large bronze mirror was said to have attracted the thunderbolt. The area where the mirror was supposed to be situated was damaged most severely. The stones of the area were specially worked on for setting a mirror. If a manmade fire is to be a cause, a lot of substantial black carbon would have been left on the stone surface, but it is not so obvious. This is also a supportive evidence for the thunderbolt theory. However, the large bronze mirror or similar objects have not found.

Close comparisons of historical photographs to present condition do not support evidence of dismantling and reassembling of stones (Fig. 3). Fissures of one area, however, seem to be progressive more aggressively. We continue comparison survey with historic photographs to confirm. If there was no hyper heating damage at the discovery time, thunderbolt must have occurred after the excavation period. Since the mirror was not found at the discovery, the facts may support more for the manmade fire damage theory. We are still investigating and not yet come to a conclusion, but are inclined toward thunderbolt theory.

2.2.1. Extreme damage at the northern opening

There are traces of severe degradation of interior wall of the sacred chamber. Especially surrounding the northern opening is most evident. This opening was said to be the place where a big bronze mirror used to be. The stones used in the area were cracked and many pieces were lost. The movements of the stones are also found that made the structure unstable (Fig. 4). For stabilization of this area, substantial repair and consolidation of stone material is necessary.

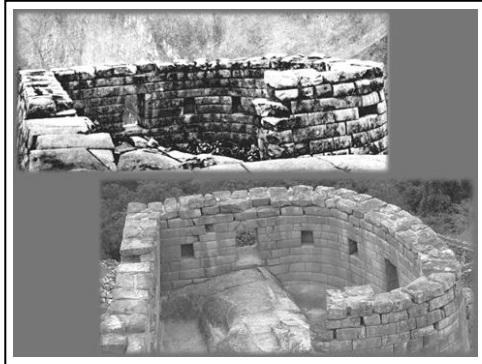


Fig. 3: Upper: 1915, Lower: 2013.



Fig. 4: Severe damage of the northern opening area.

2.2.2. Exfoliations and cracks found on the interior curvilinear wall

Exfoliations and cracks are evident of interior curvilinear wall of the chamber. This is typical damage phenomenon when granite was under hyper heating (Fig. 5).

2.2.3. Missing pieces of the edge stones

Many of the edge stones of the walls lost its pieces due to cracks of the material stones (Fig. 6).

2.2.4. *Stone movement and vertical gaps arising*

Movements of the dimension stones of horizontal directions, due to some kind of shocks such as earthquakes, created vertical gaps among stones. These gaps seem to have already been evident during the time of excavation, but the rate of progress was not yet measured. Peruvian restoration technologists filled these gaps, some of which are as large as 5cm, as emergency measures using special clay mixture of reversible materials.

2.2.5. *Fissures in natural rock pedestal*

Numbers of cracks are found in the natural rock pedestal in the sacred chamber. These cracks pass through the rock completely in longitudinal direction. The upper part must have been detached. The special clay mixture is presently filled in these fissures to prevent excess water to fill the fissures and plants to grow there (Figures 3 and 7).



Fig. 5: Cracks and detachments.

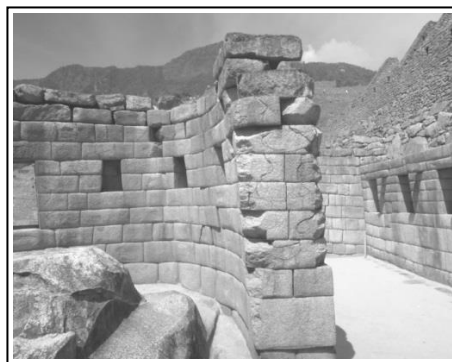


Fig. 6: Missing parts of edge stones.



Fig. 7: Decay of natural rock pedestal.

2.2.6. *Stone surface degradation*

Graining or sugaring is not so evident on these stone surfaces. Growth of lichens evident on the exterior walls changes colors (greying) and appearances of the ruins. The manual cleaning with wire brushes were provided two years ago, but now the situation was brought back to the before cleaning state.

3. Investigations

3.1. Climate Condition

The meteorological observation station is set in the mountainside from the *Sentry Hut* to the *Inca Bridge* in Machu Picchu site. Temperatures, humidity, precipitations, wind velocity and directions, and sunlight amount are recorded at this station. We were able to access the data of the last several years provided by the Peruvian side. In order to analyze fully we need to get an access to the raw data, which is in discussion. The interim analyses with the given data are as follows:

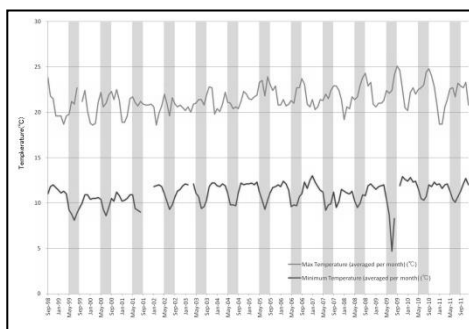


Fig. 8: Monthly maximum and minimum temperature.

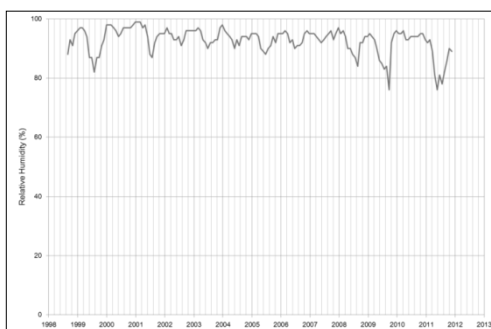


Fig. 9: Monthly average humidity.

Data was of monthly reports since September 1998 until August 2013. Fig. 8 shows monthly highs and lows of the temperature during the recorded period. The rainy season of the region is normally from November till March. The dry season is from May to August. The temperature difference during the rainy season is smaller than the dry season. Fig. 9 shows monthly mean relative humidity. As is in Fig. 8, differences correspond to the rainy and dry seasons, and mean relative humidity of over 80% throughout the year. Fig. 10 shows means of monthly-accumulated precipitation during the recorded period. The total annual precipitation at the observation station records quite high, 2,150 mm, and 70% of which are concentrated during the rainy season. The site is thus said to be in relatively high in humidity, which is the geographical situation surrounded by the mountains with vegetation. The high concentration of heavy precipitation as much as 300 mm in a month during the rainy season is not so uncommon, but that can lead into landslides of the site or to the access roads in the buffer zone.

3.2. Three-Dimensional Surveying of Temple of the Sun

In order to accurately measure the present condition of the *Temple of the Sun*, 3D measuring using total station was made.

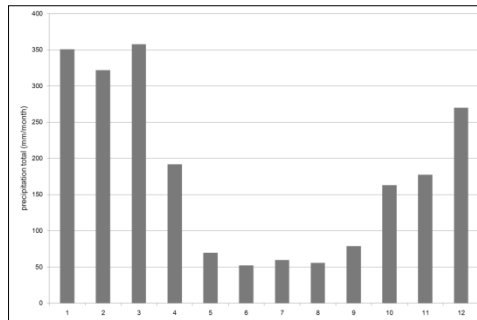


Fig. 10: Monthly precipitation.

Prior to the measuring survey, we went over previous measured datum points closely and utilized all usable points and data. Additional points were then measured from these measured points. Using these newly measured points, we obtained plane table outfits inside of the *Temple of the Sun* and produced a precise contour map of the area. The map is captured by the 3D data points including usable points especially for photographic measuring and scanning.

For the purpose of recording degradation condition of stones, fissures and cracks, we used photogrammetry to produce 3D imaging. By capturing 3D data, scale of stone to stone relationships and sizes of gaps are quantitatively measurable.

We used 3D scanning function of the total station to monitor the rate of displacement degree and to make a model. For scanning, vertical and horizontal measuring pitch degree must be determined. In this case, the exterior pitch is not completely even due to lack of foundation on exterior wall. In order to create an accurate model, additional measuring will become necessary. The model created this time was to adjust visual perception.

3.3. Tests in Situ

3.3.1. Injection of resins into cracks of a rock

As a testing of conservation measure, we injected resin into fissures of a natural rock in the site with a gap opening of 0.6mm. In order to avoid spilling of the resin, we applied ethylene vinyl acetate copolymer adhesives and then to applied stone powder and grains to treat the stone surface before injecting 100 cc of epoxy polymer emulsion using syringe. If we use manual pump injector, agent will reach further and will become more effective.

3.3.2. Application of a biocide against Lichens

In August of 2012, testing of biocide agent was applied on places where lichen infestations are widespread on a natural rock in the site. The biocide was applied on four area (0.1m²) on four sides on north, south, east and west of the natural rock (about 500g/m²). After a year, obvious effect is not yet evident, while another testing place with the same biocide agent set outside of the site in March of 2012 shows more apparent effect (Fig. 11).

3.3.3. *Reattachment of detached stone brocks to the natural rock pedestal in Temple of the Sun*

Stone pieces of the pedestal rock had been detached for the section of about 60 cm in length. There were three detached pieces left as a remnant. We experimentally put these three pieces back to where they had been and filled in missing parts with an artificial stone. The specification used for the experimental restoration is as follows. Technically there was no particular difficulty in application (Fig. 12).

- 1) Wash the surface with water where detachment occurred.
- 2) Apply epoxy adhesive of grease texture and attach the fallen pieces pressing with wooden mullet and then to remove the piece once to see if the adhesive is evenly spread on the joining surface. When uneven application of the adhesive is noticed, add it to even out.
- 3) Set in the piece again with pressure and remove again. Confirm attachment of entire joining surface and press the piece firmly. Leave it until the adhesive completely cured.
- 4) The joint line left at the restored part is camouflaged with powdered artificial stone of a mixture of ethylene vinyl acetate with both fine and grainier granite powder with small amount of lime. This will bring a result of natural appearance and acceleration of curing.



Fig. 11: Application of a biocide against lichens.

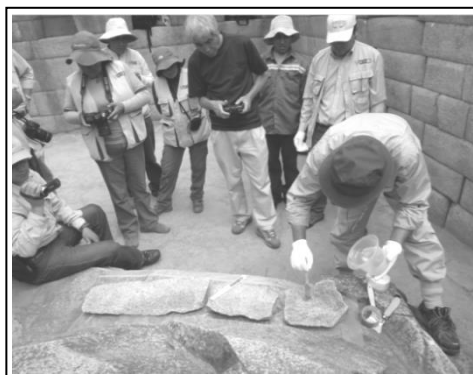


Fig. 12: Reattachment of detached brocks to the original position of the pedestal rock.

4. Measures for the Conservation

4.1. Principle

The primary, but the most substantial issue is whether to disassemble the stone wall or keep it as it is. The both approaches have merits and demerits which have a relation opposite each other. We have been considering the issue from various angles generally together with the Peruvian government, experts for restoration and academic experts. And, presently we plan to respect the discussion between UNESCO and Peruvian government, stabilizing method will be the basic approach.

4.2. Conservation measures

4.2.1. Capping on the top of the structure

In order to avoid further decay of the structure, protection from rainwater to penetrate down into the structure is prim. For that purpose, application of water-proofing layer on the top (capping) is effective. As a possible material for capping, cement mortar is very effective. But, cement is not desirable because it is irreversible, has inappropriate appearance and contains soluble salts which may cause secondary decay.

Clay mixture is then an alternative material for capping. Quality of the base clay must be very high. Mixture should contain lime and water-repellant to increase durability and water-resistance property. In Machu Picchu site, good quality clay mixture prepared by a local technician had been used for filling gaps, cracks and missing parts. Generally speaking, the clay obtained from the granite bed is known to be high in quality. For these reasons, use of this clay is considered to apply.

4.2.2. Consolidation and restoration of stone

Prior to the above mentioned capping, consolidation and restoration treatments to the decayed stones are necessary. The techniques to provide these treatments are available, but they take time and toil when disassembling is not an option

4.2.3. Filling the gaps between stones

Displacements of stone blocks created unwanted gaps among the stones. The opening can be as large as 5cm in width. For such gaps, Clay mixture mentioned above was used to fill in and so far they are working.

A new method, that durable and irreversible synthetic resin is injected into inner part of the gaps and then the clay mixture is apply to the outer part of them, is currently suggested by the Peruvian professional group. This method is easy in technique, but should be discussed from the point of view of conservation philosophy. Now we are considering.

4.2.4. Restoration of the rock pedestal

Large crack found in the rock pedestal is confirmed to be causing complete detachment of upper part. But the condition is stable due to the clay used to fill in these gaps and the weight itself of upper detached piece. However, we noticed that the movement is still progressive and we would have to make a decision on when we remove the detached piece and place it back before the fall. This work requires some kind of heavy machinery or an equivalent. Skilled technicians who are able to maneuver them in the extreme condition are required as well. At that time, the heavy blocks should be jointed and the missing parts filled. The specifications of the method and skilled technicians who could operate the restoration are in search. In this summer, precise investigation *in situ* will be conducted for this work.

4.2.5. Elimination of lichens, and consolidation and hydrophobic treatment of stone surfaces

Since the cohesion of the stones is quite good, impregnation treatment with silicone consolidant is not necessarily needed. It can be applied as preventive treatment against future deteriorations.

As for the elimination of lichens from the surface of the stones, the biocide which has been tested *in situ* is showing good effect. Probably use of this biocide will be suggested. After lichens are disappeared, the surface of the stones will be perhaps impregnated with hydrophobic silicone consolidant, though this treatment is still in discussion.

5. Acknowledgment

The “Project for Conservation of Machu Picchu Archaeological Site” is supported mainly by JSPS KAKENHI Grant Number 24404001, and partly by The *Asahi Shinbun* Foundation (Grants for conservation of cultural properties), The *Sumitomo* Foundation (Grant for the Protection, Preservation & Restoration of Cultural Properties outside Japan) and Center for the Global Study of Cultural Heritage and Culture, Kansai University. We sincerely thank them.

References

- UNESCO, Historic Sanctuary of Machu Picchu, (whc.unesco.org/en/list/274, accessed 10th October 2009).
- Nishiura, T. *et al.*, Conservation of the Machu-Picchu Archaeological Site: Investigation and Experimental Restoration Works of “Temple of the Sun”, The Journal of Center for the Global Study of Cultural Heritage, and Culture, Vol.1, Kansai University, 67-79.
- Nishiura, T. *et al.*, Conservation of Machu-Picchu Archaeological Site: Investigation and Experimental Restoration Works of “Temple of the Sun”, in proceedings of International Symposium on Conservation of Ancient Sites on the Silk Road in 2014, Dunhuang, China, 98-101.

This page has been left intentionally blank.

LAS CASAS TAPADAS DE PLAZUELAS – STRUCTURAL DAMAGE, WEATHERING CHARACTERISTICS AND TECHNICAL PROPERTIES OF VOLCANIC ROCKS IN GUANAJUATO, MEXICO

C. Pötzl^{1*}, R.A. López-Doncel², W. Wedekind¹ and S. Siegesmund¹

Abstract

The building stones of the pyramids of Plazuelas were analysed in terms of their pore space, water transport and retention properties, as well as their mechanical properties and weathering characteristics. Based on mineralogical composition, different types of tuff could be distinguished. In a field survey the structural damages and their intensities were mapped in situ at every wall of the main building. The field investigation uncovered substantial types of damage in the used tuffs. The specimens for the laboratory investigations were prepared parallel and perpendicular to the lamination to distinguish effects of the anisotropy. The data shows that the pore space properties have the largest influence on additional rock properties (e.g. hygric expansion) of the tuffs, and hence the largest influence on the weathering resistance of the stones. Due to the local climatic conditions, some of the building stones, which would be commonly classified as unsuitable, could be classified as a proper building stone.

Keywords: tuff, weathering characteristics, technical properties, damage mapping

1. Introduction

The suitability of tuffs as building stones is strongly dependent on the environmental conditions. Therefore it is not always possible to give a general statement in terms of their application. In Mexico tuffs were used as raw material for the construction of churches, pyramids and other monuments. Due to infrastructure and availability rocks in the immediate vicinity were usually used. In the federal state of Guanajuato (Mexico) the Chichimecas, a sophisticated predecessor culture of the Aztecs that populated the adjacent Bajío region, created the pyramids of Plazuelas at approximately 450 AD (Castañeda López and Gutiérrez Lara, 2014). The central temple complex, which is also known as Casas Tapadas, consists of four pyramids and an adjacent ballgame court (Fig. 1) and is possibly connected to the worship of their gods. Because the pyramids were enlarged at least three times, one can find a minimum of three phases of construction. Around 900 AD the complex was abandoned due to a fire, which has been documented to date in the form of discoloration of the façade leaving considerable structural damages. In 1998, after the

¹ C. Pötzl*, W. Wedekind and S. Siegesmund,
Geoscience Centre of the Georg August University Göttingen, Germany,
christopher.poetzl@gmx.de

² R.A. López Doncel
Geological Institute, Autonomous University of San Luis Potosí, Mexico

*corresponding author

temple complex was buried for several centuries due to sedimentation, the Casas Tapadas were officially rediscovered and excavated in the following years.

The building stones of the pyramids experienced more than a thousand years of weathering processes and show damages and weathering characteristics equivalent to that length of time. To make sustainable and effective protection for the preservation and conservation of these valuable cultural assets, the consolidated scientific findings of the physical and mechanical properties of the building stones as well as their weathering characteristics are indispensable.



Fig. 1: a) View from the south over the ballgame court to the main pyramids; b) West side of the central pyramid with the main entrance; c) South side of the central pyramid.

2. Materials and methods

In this investigation seven different tuffs and volcanic rocks from Guanajuato were analysed. Mineralogical composition and whole rock chemistry were analysed by both optical and geochemical methods (polarized light microscopy, X-ray diffraction (XRD) and X-ray fluorescence (XRF) spectroscopy). Matrix and bulk density as well as the porosity were measured by hydrostatic weighing according to the DIN 52 102. The pore radii distribution was determined by mercury intrusion porosimetry. The capillary water absorption was measured according to DIN ISO 15148. The water vapor diffusion was measured according to DIN ISO 12572. The sorption was measured according to the DIN ISO 12571 in a climate chamber. The tensile strength measurement was determined by means of the Brazilian test. To determine the weathering behavior of the tuffs during temperature changes, a thermal expansion experiment was carried out in a climate chamber under dry and wet conditions. The moisture expansion of the rocks was determined by hydric wetting of cylindrical samples under water-saturated conditions. The specimens for the laboratory experiments were prepared parallel and perpendicular to the lamination to distinguish potential effects of anisotropy. To investigate the resistance of the rocks to salt stress, a salt-weathering test according to the DIN EN 12370 was performed. As an index of salt resistance the numbers of test-cycles were used till a 30 % of weight lost was

established. In a field survey the lithologies, the structural damages and their intensities were mapped in situ at all four sides of the main pyramid of the Casas Tapadas.

3. Results

3.1. Petrology and mineralogy

The volcanic rocks range in age from Paleogene to Quaternary (Cotler Avalos *et al.*, 2006), with chemical compositions that vary from basaltic andesite to rhyolitic tuff. The petrographic analyses of each rock sample were done on orientated thin sections under a polarization microscope (Fig.2).

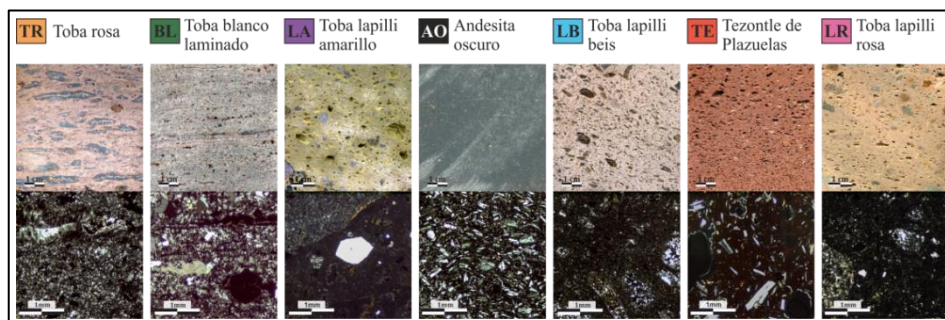


Fig. 2: Illustration of the volcanic rock samples described in detail. Top: Polished section. Bottom: Thin section under polarized light

The Toba rosa (**TR**) is a white to reddish rhyolitic tuff with grey clasts embedded in a characteristic flow texture. It mostly consists of a hypocrySTALLINE matrix of quartz, feldspar with approximately 20 % vitric material and clasts and melting lenses up to 50 mm in length. TR is the most used rock on the pyramid. The Toba blanco laminado (**BL**) is a white to yellowish green rhyolitic tuff with a clearly recognizable lamination. Altered rocks of this type show a reddish colour. The reddish to brown clasts are less than 1 mm in size. Grey, extremely elongated clasts can be found between the layers. The Toba lapilli amarillo (**LA**) is a yellow to greenish porphyritic lapilli tuff with a dacitic composition. The proportion of clasts shows strong variations, while clasts can show sizes over 5 cm and often show andesitic composition. Variations of compact layers of ash and layers mostly consisting of clasts also occur. The rocks appear to be very porous and show many gas inclusions. It is the second most used building stone in the pyramid. The Andesita oscuro de Sierra de Penjamo (**AO**) is a microcrystalline andesite black in colour and only shows up in certain areas of the pyramid in the form of slabs of up to 5 cm of thickness. AO consists of feldspar phenocrysts with an average size of 0,2 mm with a slight orientation. The Toba lapilli beis (**LB**) is a beige porphyritic lapilli tuff with a clearly acidic composition (rhyolitic tuff). It shows slightly orientated brown clasts of pumice with sizes up to 3 cm. The Tezontle de Plazuelas (**TE**) is a red pyroclastic rock with a composition of a basaltic andesite. It appears similar to the basaltic bomb named Tezontle, which can be found nearby Mexico City. Due to many gas inclusions, the rock appears to be very porous and lightweight but strongly welded with a recognizable lamination. The Toba lapilli rosa (**LR**) is a beige to reddish rhyolitic tuff with red to brown clasts of pumice. The clasts are slightly orientated and show sizes up to 5 cm. The cryptocrystalline matrix makes up about 70 % of the rock. The volcanic lithic clasts mostly consist of feldspar.

3.2. Petrophysical properties

Whenever possible the measurements were done in three perpendicular directions of the rocks. The direction parallel to the bedding/lamination is defined as X, the direction parallel to the bedding and perpendicular to the lamination is defined as Y and the direction perpendicular to the bedding is defined as Z.

3.2.1. Pore space properties, water transport and retention properties

AO shows the lowest porosity with 0.63 vol% while having the highest bulk density with 2.73 g/cm³. TR and BL show a medium porosity of 21.1 % and 14.68 vol% and medium bulk densities of 2.05 and 2.23 g/cm³, respectively. The remaining rocks show high porosities up to 32.7 % and low bulk densities ranging between 1.56 to 1.81 g/cm³ (Tab.1). Pore radii distributions show either a unimodal distribution like AO, LB and LR or bimodal unequal like TR, BL, LA and TE (Fig.3). The amount of micropores in the rocks ranges between 9 to 85 % (Tab.1). Microporosity is defined as the pores <0.1 μm and capillary pores are defined as pores between 0.1 to 1,000 μm (Klopfer, 1985). The rock with the highest amount of micropores is LA with 85 %, followed by AO with 81 % and TR with 70 %. The remaining rocks show microporosities less than 30 % (Tab. 1).

Tab. 1: Pore space properties, moisture transport and retention properties.

Stone type	Toba rosa (TR)	Toba blanco laminado (BL)	Toba lapilli amarillo (LA)	Andesita oscuro (AO)	Toba lapilli beis (LB)	Tezontle de Plazuelas (TE)	Toba lapilli rosa (LR)
Effective porosity (vol%)	21.1	14.68	29.98	0.63	32.42	32.7	29.39
Matrix density (g/cm ³)	2.6	2.62	2.23	2.75	2.5	2.63	2.56
Bulk density (g/cm ³)	2.05	2.23	1.56	2.73	1.69	1.77	1.81
Average pore radius (μm)	0.09	0.59	0.04	0.05	0.51	2.24	0.62
Microporosity (%)	70	28	85	81	11	21	9
<i>w</i> value (kg/m ² √h)							
X	14.93	7.79	21.84	0.96	62.85	7.9	56.17
Y	12.41	7.13	35.87	0.99	60.5	7.9	58.36
Z	10.88	4.01	44.49	0.99	59.92	7.13	42.33
Anisotropy (%)	27	49	51	3	5	10	27
<i>μ</i> value							
X	41.39	32.92	14.89	58.66	18.34	18.28	14.3
Y	39.56	22.3	-	-	8.88	32.69	11.36
Z	54.72	33.26	17.51	-	13.27	63.39	14.81
Anisotropy (%)	28	33	15	-	52	71	23
max. moisture content <i>u</i>	0.0097	0.0054	0.0474	0.005	0.0132	0.01	0.02

The *w* value of the investigated rocks varies considerably. LA, LB and LR show the highest values with up to 62.85 kg/m²√h (LB). The lowest *w* value is shown by AO with 0.96 kg/m²√h. The *w* values of TR, BL and TE range between 4.01 to 14.93 kg/m²√h. The rocks show anisotropic behavior up to 51 % (Tab.1). With up to 71 % (TE) the rocks show strong anisotropic behavior of the *μ* value. The highest *μ* values are shown by TR, BL, AO and TE with up to 63.39 (TE). The remaining rocks show *μ* values ranging between 8.88 to 17.51. The highest *u* value is shown by LA with 0.0474, followed by LR with 0.02 and LB with 0.0132. The remaining rocks show *u* values below 0.01. The least *u* value is shown by AO with 0,005. Except for TE, all rocks show higher *w* values with rising porosity and all rocks show higher water vapor diffusion with rising porosity (Tab.1).

3.2.2. Mechanical properties

TR has the highest tensile strength with 13.23 MPa, followed by AO with 11.16 MPa. The remaining rocks show tensile strength ranging from 5.42 to 2.47 MPa (Tab.2). The tuffs show medium to high anisotropic behaviour of up to 48 % (LA). Except for TR, all rocks show lower tensile strength the higher their porosity (Tab. 1 and Tab. 2).

Tab. 2: Mechanical properties.

Stone type	Toba rosa (TR)	Toba blanco laminado (BL)	Toba lapilli amarillo (LA)	Andesita oscuro (AO)	Toba lapilli beis (LB)	Tezontle de Plazuelas (TE)	Toba lapilli rosa (LR)
Splitting tensile strength (Mpa)							
X	13.01	4.51	4.73	11.16	5.3	5.42	4.67
Y	13.23	6	4.07	-	5.2	5	4.74
Z	10.81	4.42	2.47	11.2	3.57	4.53	3.52
Anisotropy (%)	18	26	48	0	33	16	26

3.2.3. Thermal expansion, moisture expansion and salt weathering

The thermal expansion of the rocks under dry conditions shows relatively low values ranging between 0.017 to 0.028 mm/m and low anisotropies (Tab. 3). Under wet conditions the thermal expansion of TR triples, BL doubles and LA quadruples. Even the anisotropic behaviour increases up to 45 % for TR. The thermal expansion of LB, TE and LR does not change much under wet conditions (Tab. 3).

Tab. 1: Thermal expansion under dry conditions and wet conditions, hydric expansion and salt weathering.

Stone type	Toba rosa (TR)	Toba blanco laminado (BL)	Toba lapilli amarillo (LA)	Andesita oscuro (AO)	Toba lapilli beis (LB)	Tezontle de Plazuelas (TE)	Toba lapilli rosa (LR)
therm. expansion (mm/m) dry							
X	0.017	0.022	0.01	-	0.028	-	0.023
Z	0.019	0.021	0.011	0.017	0.026	0.017	0.022
Anisotropy (%)	11	5	9	-	7	-	7
therm. expansion (mm/m) wet							
X	0.0335	0.038	0.038	-	0.0275	-	0.0285
Z	0.0605	0.04	0.0425	0.024	0.03	0.0175	0.0255
Anisotropy (%)	45	5	11	-	8	-	11
hydric expansion (mm/m)							
X	0.351	0.186	0.659	-	0.057	0.085	0.007
Z	0.392	0.183	0.736	0.061	0.054	0.031	0.022
Anisotropy (%)	11	2	10	-	5	64	68
Salt weathering (cycles)	19	19	11	> 40	> 40	> 40	33

The hydric expansion of the rocks in the X and Z direction is shown in Fig. 3. It shows values that are partially multiple times higher than the thermal expansion and ranging between 0.007 mm/m for T10 and 0.736 mm/m for LA. In general the rocks show higher values for the Z direction and the anisotropy is very high for TE with 64 % and LR with 68 % (Tab.3). Every rock reaches the maximal expansion after a short time. The microporosity has a large influence on the hydric expansion (Snethlage *et al.*, 1995). In Fig. 3 we can show a good correlation of the microporosity and the hydric expansion. The

salt weathering test shows a low resistance in TR and BL with 19 cycles and 11 cycles in LA until destruction. LR shows a medium resistance with 33 cycles and AO, LB and TE were not affected by salt bursting even after more than 40 cycles. Except for AO, the rocks show lower resistance against salt weathering when having a high microporosity (Tab. 1 and 3).

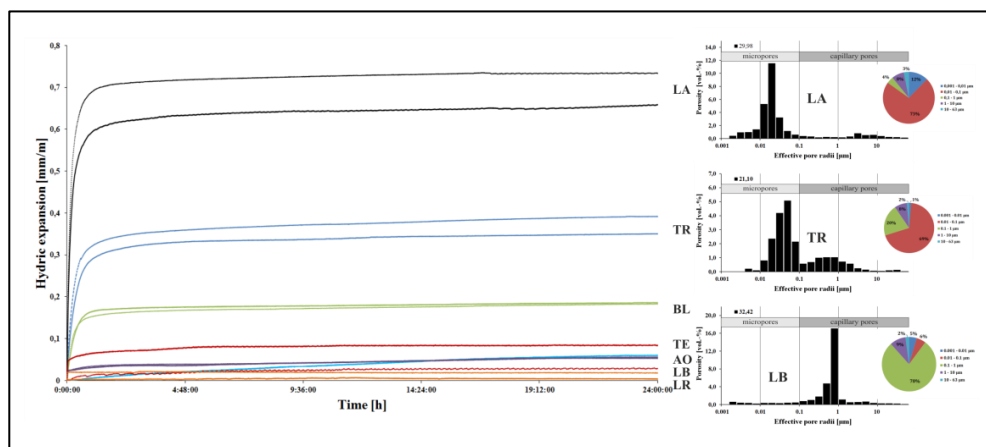


Fig. 3: Hydric expansion correlates with the microporosity on the right.

3.2.4. Salt weathering and moisture expansion related to the pore space properties

A high porosity allows the water uptake and distribution to take place and thus letting the water in the rock interact with the present clay minerals (Ruedrich *et al.*, 2011). Salt weathering is favoured due to high porosity and a bimodal pore radii distribution of the tuffs as capillary pores provides the transport for salt solutions and micropores lower the resistance of the rocks against salt crystallization. We could verify the findings from (Punuru *et al.*, 1990; Fitzner and Basten, 1994; Benavente *et al.*, 2004) that the pore radii distribution affects the stone's durability as a key factor.

3.2.5. Mapping and in situ investigations

Some of the main deterioration and weathering effects are caused by back weathering (Fig. 4a), fracturing (Fig. 4b), salt efflorescence (Fig. 4c) and scaling (Fig. 4d). These phenomena are often found in shady areas or areas close to the ground (Fig. 5), where water or moisture is permanently or temporarily available. The damage types were classified according to the glossary on stone and deterioration patterns of the International Scientific Committee for Stone (ISCS – ICOMOS, Anson-Cartwright, 2010). By mapping all four sides of the pyramid (Fig. 5) and combining the different lithologies with the types of damage and their intensity, we could detect the main damage sources and the building stones most susceptible to it quantitatively. Fig. 6 shows a clear correlation of increased damage intensities and an increased use of the Toba lapilli amarillo (LA) on the north and west side of the pyramid. The percentages of high to very high damage intensities can be related to LA. The rocks of the Toba rosa (TR) mostly show medium damage intensities.

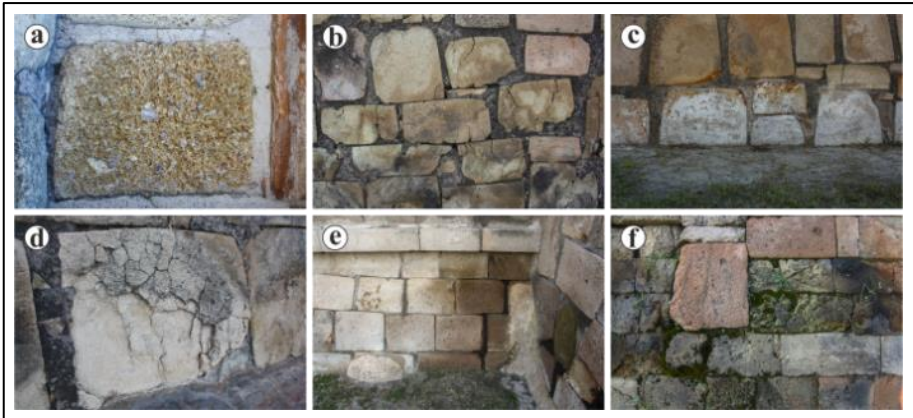


Fig. 4: Some of the main damage phenomena in the building stones of the pyramids of Plazuelas. a) Back weathering of clasts and components; b) Extensive fracturing and craquele; c) Salt efflorescence; d) Scaling; e) Discolouration due to moisture area; f) Biological colonization.

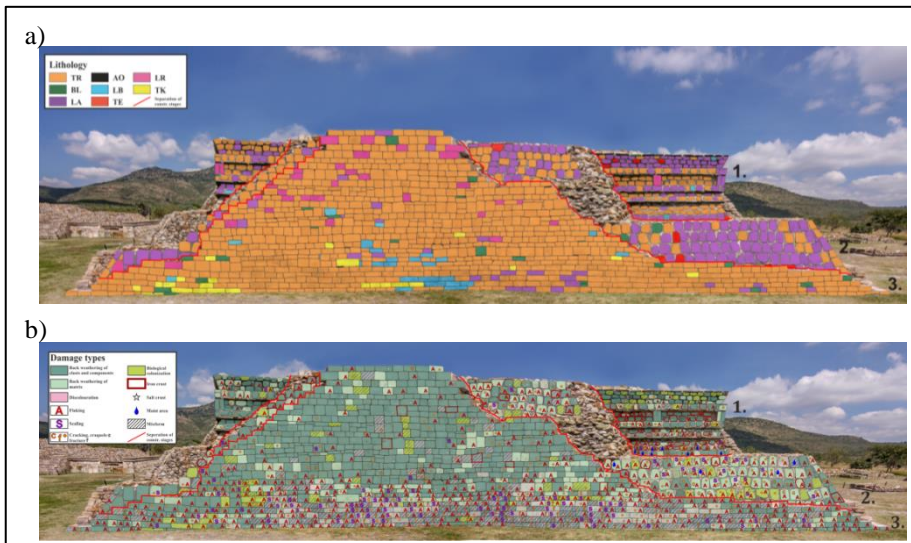


Fig. 5: Mapping of the south side of the pyramid;
 a) Lithographic mapping; b) Mapping of damage types.
 1 = 1st construction stage,
 2 = 2nd construction stage,
 3 = 3rd construction stage.

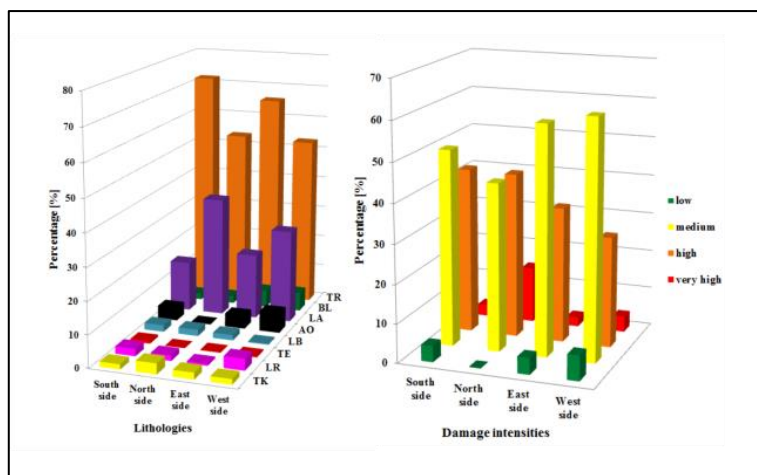


Fig. 6: Quantitative analysis of lithologies and damage intensities.

4. Conclusion

In combination with an increased hydric expansion, the rocks are in a situation where availability of water can mean both an advantage and a disadvantage. Due to precipitation the salt is washed out of the rock surface, which lowers the salt crystallization on the one hand, but increases the hydric expansion on the other hand. By comparing the distribution of the salt crusts at the different sides of the buildings clarifies how these circumstances are connected to the exposition of the building stones in the pyramid. Since the main wind direction is ESE during the rainy period, salt at the south side and east side gets washed out before it can crystallize. According to this, salt weathering only occurs in areas close to the ground where rocks can absorb the salt in solution by capillary water at any time. On the east side this process is lowered due to the influence of the wind. The north and west side of the pyramid shows an extensive distribution of salt efflorescence all over the façade due to the lack of influence from the precipitation. On the other hand, hydric expansion only occurs to a minor degree on these sides.

We were able to show that the building stones of the pyramids of Plazuelas partially suffered serious damage due to salt weathering and hydric expansion. We could approve that the pore space properties have a strong influence on the weathering behaviour of the rocks. Especially the pore radii distribution seems to play an important role. While providing a good water transport due to capillary pores as well as the availability of micropores, which lower the resistance against salt crystallization, a bimodal pore radii distribution with a high amount of micropores has proven to be inappropriate. Despite the fact that laboratory investigations show high hydric expansion and low resistance against salt weathering due to a high amount of micropores, the Toba rosa (TR) has proven to be a suitable building stone under the existing environmental conditions at the Casas Tapadas. Conservation measures will be challenged by the need of minimizing the salt contamination while facing the risk of hydric expansion.

Acknowledgements

Our work was supported by the Consejo Nacional de Ciencia y Tecnología (CONACyT), Projects Ciencia Básica (CB-130282) and Cooperación Bilateral (191044). We are grateful to G. Hartmann and K. Wemmer of the GZG for their help with the mineral analysis.

References

- Anson-Cartwright, T. (Ed.) (2010), *Illustrated glossary on stone deterioration patterns: Illustriertes Glossar der Verwitterungsformen von Naturstein, Monuments and sites Monuments et sites Monumentos y sitios*, Vol. 15, 1st ed., ICOMOS, International Scientific Committee for Stone (ISCS); Imhof, Paris, Petersberg.
- Benavente, D., del Cura, M.G., Fort, R. and Ordóñez, S. (2004), “Durability estimation of porous building stones from pore structure and strength”, *Engineering Geology*, Vol. 74 No. 1, pp. 113–127.
- Castañeda López, C. and Gutiérrez Lara, G. (2014), “La Arquitectura de Plazuelas”, in Viramontes Anzures, C. (Ed.), *Tiempo y Región. Estudios Históricos y Sociales: Volumen VII: Ensayos sobre cultura material entre las sociedades prehispánicas del centro-norte y occidente de México*.
- Cotler Avalos, H., Mazari Hiriart, M., Anda Sánchez, J.d., Garrido Pérez, A. and Pérez Damián, J.L. (Eds.) (2006), *Atlas de la Cuenca Lerma-Chapala: Construyendo una visión conjunta*, Instituto Nacional de Ecología, México, D.F.
- Fitzner, B. and Basten, D. (1994), “Gesteinsporosität--Klassifizierung, meßtechnische Erfassung und Bewertung ihrer Verwitterungsrelevanz”, in *Jahresberichte aus dem Forschungsprogramm Steinzerfall, Steinkonservierung. Band 4, 1992*, Ernst, Wilhelm & Sohn, Verlag für Architektur und technische Wissenschaften GmbH, Berlin, Germany, pp. 19–32.
- Klopfer, H. (1985), “Feuchte”, in Klopfer, H. (Ed.), *Lehrbuch der Bauphysik*.
- Punuru, A.R., Chowdhury, A.N., Kulshreshtha, N.P. and Gauri, K.L. (1990), “Control of porosity on durability of limestone at the Great Sphinx, Egypt”, *Environmental Geology and Water Sciences*, Vol. 15 No. 3, pp. 225–232.
- Ruedrich, J., Bartelsen, T., Dohrmann, R. and Siegesmund, S. (2011), “Moisture expansion as a deterioration factor for sandstone used in buildings”, *Environmental Earth Sciences*, Vol. 63 No. 7-8, pp. 1545–1564.
- Snethlage, R., Wendler, E. and Klemm, D.D. (1995), “Tenside im Gesteinsschutz-bisherige Resultate mit einem neuen Konzept zur Erhaltung von Denkmälern aus Naturstein”, *Denkmalpflege und Naturwissenschaft-Natursteinkonservierung I*. Verlag Ernst & Sohn, Berlin, pp. 127–146.

This page has been left intentionally blank.

DESALINATING THE ASYUT DOG IN THE MUSÉE DU LOUVRE

O. Rolland^{1*}, V. Vergès-Belmin², M. Etienne³, H. Guichard³,
S. Duberson³ and P. Bromblet⁴

Abstract

The Asyut dog is a one meter high sculpture which is part of the collections of the Louvre Museum in Paris, France. It was carved in Egypt during the Ptolemaic period, out of a fine grained limestone, and was found broken into multiple fragments within the frame of an archeologic campaign in the early twentieth century. The sculpture was restored in the twentieth century using plaster of Paris, iron and brass rods. Since at least four decades it shows degradation patterns typical of the action of soluble salts. A general superficial granular disintegration is observed along with little cracks and scales. Deep cracks linked to the corrosion and rust formation on iron rods endanger the structural stability of the sculpture. These deep cracks broke apart the fragments. We took advantage of this dismantling to use some of these fragments for soluble salts analyses and careful desalination trials. Sodium chloride (halite) is the most abundant crystallized phase and most probably takes a prominent role in the degradation, although its equilibrium relative humidity is far higher (75%) than the relative humidity range in the museum showcase where the dog is presented (33-65%). Further analyses of the salts extracted from a fragment of the statue by immersion in water and evaporation at room temperature reveal a contamination by a very hygroscopic mixture (a brine) the equilibrium relative humidity (*ERH*) of which is lower than 33%. We suggest that the unexpected sodium chloride empowerment of the statue deterioration may be due to the presence of this hygroscopic brine, which would facilitate the transfer of sodium and chloride ions toward the surface, thus feeding almost constantly halite crystallization. We propose to call such a hygroscopic mixture a “transporter brine”.

Keywords: limestone, sculpture, salt, desalination, museum, climate, transporter brine

1. Introduction

The Asyut dog is a life sized sculpture, one meter high, which was carved out of a fine grained limestone and painted in Egypt during the Ptolemaic period. It was found broken

¹ O. Rolland*

Independent conservator, 3 rue du Gué, F-37270, Montlouis sur Loire, France,
olivierrolland@wanadoo.fr

² V. Vergès-Belmin

Laboratoire de recherche des monuments historiques (CRC-LRMH USR 3224), France

³ M. Etienne, H. Guichard, S. Duberson

Department of Egyptian Antiquities, Musée du Louvre, Department of Egyptian Antiquities, France

⁴ P. Bromblet

Centre interdisciplinaire de conservation et de restauration du patrimoine, Marseille, France

*corresponding author

into multiple fragments during an archeologic dig close to a burial site for dogs and wolves, sacred animals of the local divine canid *Oupouaout*. Other dog statues are known around this site, but this is the only one close to the burial site. It entered the Louvre collection in 1923, from a gallery, the year after its probable discovery by Wainwright during Lacau's excavations in Asyut. In the 1930's it was already presented in a showcase, which suggest that it was judged fragile. It is supposed to have given its name to the "dog stair" in the museum. After a stay in a box, since 1997 it is one of the jewels of the animal-gods room, the nineteenth room of the ground floor of the ancient Egypt department (Fig. 1a).

It is only since 2001-2002 that powdering was noticed near the tail. However, photos of the dog showed degradation patterns typical of the action of soluble salts since at least four decades. In 2010, superficial granular disintegration and powdering was observed on all the surface of the statue, especially on its back and even more at the lower part of it; besides, little cracks and scales were seen on the head and some very little scales were seen in a whitish zone on the lower part of the back. Stone powder and millimetric fragments were regularly observed on the floor of its showcase (Fig. 1b). In addition to these surface deterioration patterns, deep cracks were observed in the legs (Fig. 2) thus endangering the structural stability of the sculpture. Rust was visible behind the right thigh near the tail.

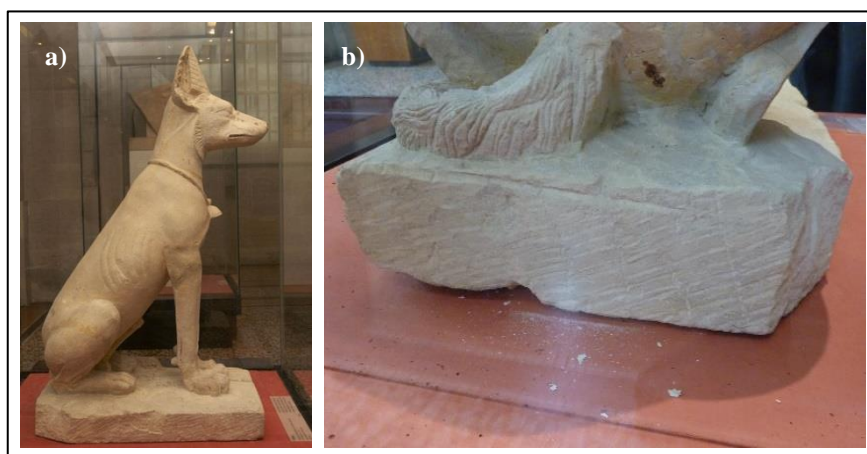


Fig. 1: a) The Asyut dog in its window case in the Musée du Louvre before restoration (Photo: Christian Descamp, Musée du Louvre); b) Stone powder and flakes in the showcase of the Asyut Dog in the Musée du Louvre (Photo: Philippe Bromblet, CICRP).

2. Diagnosis

Radiography and tomography were performed to collect evidence on the metal rods present inside the stone. A metal detector discriminated non-magnetic rods, in the head and front legs, and magnetic rods in the rear part of the animal. UV photos made more visible the fillings and the small plaster of Paris repairs between stone fragments. It appeared clearly that deep cracks developed mainly in these gypsum repairs and that their initial cause was the expansion of the iron rods due to rust development in the rear part of the dog.

To understand powdering and little cracks, we looked at the climatic conditions which had been registered in the showcase during the year before the study: the relative humidity varied between 33% and 65%, the temperature varied between 14°C and 25°C. These conditions were supposed to be the usual ones. We do not know the past climatic conditions but we can suppose that formerly it might have been sometimes much more humid, at least during the probable sea transport.

Four samples were taken from the statue (Fig. 2): two samples (ref PA1 and PA2) are mixes of superficial stone powder and salts collected by brush respectively on the lower part of the back (PA1) and on the left side of the statue (PA2); Sample 3 is a little piece of stone taken in a crack with a chisel; Sample 4 consist of stone powder collected by drilling from 3 to 4 cm depth (Pd1). The little stone fragment was used for petrographic analysis: a fine grained limestone from the Nile Valley was identified.

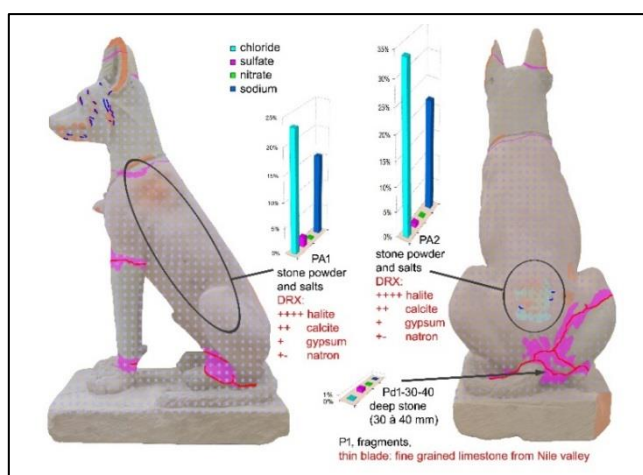


Fig. 3: Localisation and results of the samples and analysis on a decay map of the dog.

Samples PA1-2 were first analysed by X-ray diffraction (Bruker D8 Focus diffractometer (Co K_{α} radiation) equipped with a Lynx'Eye detector operating with an aperture of $1^{\circ}2\theta$): halite (sodium chloride) was detected as the major phase, gypsum (calcium sulphate dihydrate) was detected as a minor phase and natron (sodium carbonate decahydrate) could also be identified as a very minor component. These results suggest that the surface deterioration of the statue is probably mainly due to halite crystallization. The equilibrium relative humidity (*ERH*) of this salt is 75%, and we have seen that the relative humidity in the showcase is always under 65%. In these conditions, halite alone should not be destructive, it should stay its crystallised form.

Soluble sodium and magnesium, chlorides, nitrates and sulphates were quantified in the samples PA1-2 and Pd1, following the solubilisation procedure of the Italian standard NORMAL 13/83. Anions were analysed by ion chromatography (DIONEX DX 500 fitted with an analytical column AS 9 HS) and sodium by Atomic Absorption Spectroscopy (VARIAN AA240FS).

In the surface samples (PA1-2) sodium and chlorides are very abundant while sulphates and nitrates show respectively low and very low concentrations (Tab. 1). At 3-4 cm into the stone (Pd1), sodium and chlorides concentration is divided by 100, sulphates are divided by two, nitrates and magnesium have approximately the same concentration.

Tab. 1: Ionic contents at the stone surface (PA1-2) and at 3-4cm depth (Pd1).

Sample	Sulphate [wt%]	Chloride [wt%]	Nitrate [wt%]	Sodium [wt%]	Magnesium [wt%]
PA1	1.91	23.38	0.23	15.25	0.02
PA2	1.79	33.80	0.11	21.70	0.01
Pd1	0.77	0.19	0.18	0.07	0.02

3. Desalination test

The dog had to be disassembled to remove the iron rods, so we decided to take this opportunity to desalt a part of it. We chose a part without any polychromy, a fragment of the right thigh. The desalination was performed by the bath method. Three successive baths of demineralised water (added with calcium carbonate) were necessary to complete the desalination (Bromblet *et al.* 2011). Water was moved constantly using an aquarium pump.

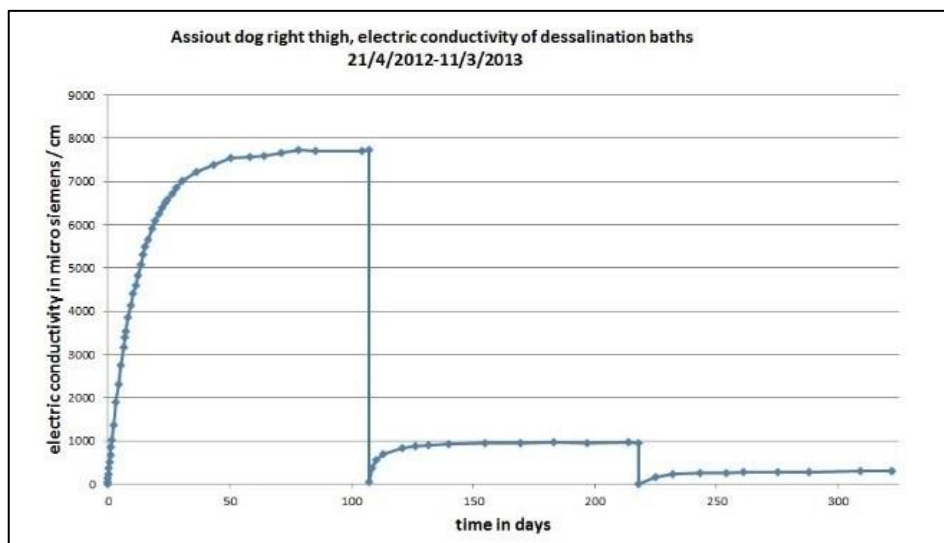


Fig. 3: Conductivity of the three successive desalination baths of the fragment of the right thigh.

The desalination was monitored by electric conductivity measurements (Fig. 3). The fragment was removed from each bath as soon as the conductivity became relatively constant over the time. We used as less water as possible, in order for gypsum and other relatively low soluble components to be less removed than very soluble salts such as chlorides and nitrates. We think that all the salts in the object are part of its history and that

removing only the largest part of the most soluble salts should be sufficient to stop the decay. As expected, the first bath contained much more salt than the second one, which contained more salt than the last one.

4. Characterization of the first bath water

Once the fragment was removed, a sample of the first bath was kept in a fridge for analysis and the rest was left to evaporate at low temperature (between 20 to 32°C on a heater). Drying process started in an open container, and then in a hermetically closed box, using a cup containing calcium chloride oversaturated solution ($ERH=33.3\%$ at 20°C) as a desiccant. In this way we concentrated the soluble salts extracted from the brine of the stone fragment. The obtained extract contained millimetric halite crystals and a brownish precipitate the nature of which remained unidentified (Fig. 4a). Such a mixture containing very soluble and hygroscopic salts in solution was probably present in the statue before desalination.

The brine was separated from the halite crystals and brownish precipitate. Quantitative analyses of the soluble species in the water and in its corresponding brine were performed, using the same analytical techniques as before desalination (Tab. 2). The brine, compared to the bath, is relatively enriched with nitrates and depleted in sodium, chlorides and sulphates (Fig. 4b and 4c), Chloride and sodium drop is logical since crystallized halite has trapped these ions. Sulphates depletion may be due to the crystallization of sulphates (gypsum, apththialite? maybe into the brownish precipitate described above).

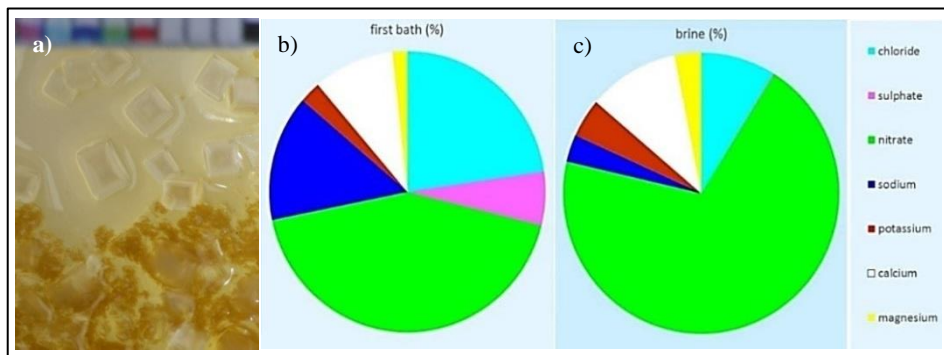


Fig. 4: Macrophotography of the evaporation residue from the first desalination bath showing big halite crystals and smaller brownish crystals (a); Weight proportion of ionic species (% of mass) in the first bath (b) and its corresponding brine (c).

Tab. 2: Ionic composition of the first bath and its corresponding brine in g/l.

	Sodium	Potassium	Magnesium	Calcium	Chloride	Sulphate	Nitrate	pH
Bath	71.5	12.4	8.5	46.85	111.87	30.56	211.98	6.8
Brine	185.6	266.5	184.1	633.2	518.0	1.5	4146.7	7.3

As the brine still contains chlorides, other very hygroscopic chlorides such as calcium chloride might be present. This may at least partly explain why it is not possible to get the brine in a dry state at room climatic conditions ($T \sim 22^\circ\text{C}$, $RH = 50\%$). It is clear that calcium, sodium or potassium nitrates are not sufficiently hygroscopic to be responsible for such a behaviour, as their *ERH* at 20°C are respectively 53.6%, 75.4% (Arnold and Zehnder 1990) and 97.3% (Schwarz H.-J., SaltWiki 2015). The mix has a very low mutual deliquescence relative humidity (Linnow 2007).

5. Discussion and conclusions

The reasons for the structural deterioration of the statue are clear: rust related expansion, likely accelerated by chlorides. The analytical results confirm that salt crystallization is responsible for the surface deterioration of the statue. Halite is the main crystallized salt. Nitrates, although present, are not identified as crystallized phase: this is quite strange as potassium is present in the system and its nitrate is less soluble than halite (313 versus 356 g/L) and has a high equilibrium relative humidity ($ERH = 93.7\%$ at $T = 20^\circ\text{C}$). We observe that the disintegration of the surface heavily contaminated with halite occurs at relative humidity far lower than halite equilibrium relative humidity. The presence of other salts may decrease halite equilibrium relative humidity, but we have raised another interpretation, or maybe just another way to describe the same phenomenon, that we would like to share with the scientific community: the simple fact that water is present into the system due to the hygroscopic salts might make it easier for some ions to move towards the surface at a rate depending on climatic conditions in the showcase and probably on the concentration and distributions of other ions. In other words, the feeding of the stone surface by deleterious ions might be partly due to the transfer of these ions in the brine within the capillary network of the stone. We propose to name this process “transporting brine hypothesis” (Fig. 5). If it is confirmed, it might concern a large number of objects and monuments, indoors as outdoors, probably in more complex ways. Nevertheless this hypothesis has to be confirmed through additional experimental work and investigations such as the measurement of the sorption isotherm of the brine, and of the stone before and after desalination. The way we obtained the brine most probably should be optimized also, as there are some discrepancies between the composition of the bath water and the one of the brine, in terms of cations/anions balance. Those discrepancies might be due for instance to bacterial activity (bacteria may in certain conditions extract sulphur and nitrogen from the salt solution in the form of SO_2 and N_2), to losses in process of brine collection. The very slight *pH* increase of the salt solution from 6.8 to 7.3 during the evaporation process suggests that carbonates may be more present in the brine than in the bath water.

Eventually the bath desalination procedure we followed was efficient and did not damage the stone. Considering these results, it was decided recently to desalinate all the other fragments, of the statue, except the head because of its large polychromy remains. We will wait for the results of current desalination baths on fragments (neck and ears) bearing smaller remains of polychromy before deciding whether the head can be desalinated safely.

Fragments are currently in different baths according to their size, and each bath is monitored by electric conductivity, density and temperature sensors. The data are accessible 24/24 and 7/7 with remote control and transmission by a GSM modem, and a weekly visual control. When we write this paper on December 2015, the ears and front legs, small parts in the same bath, are still immersed in their second bath, whereas the body, the larger part, is

just at the beginning of its first bath. The polychromy remains seem in good condition. We begin to evaporate the first bath of the little parts and we plan to do so with each first bath. Presently the operation goes on as foreseen.

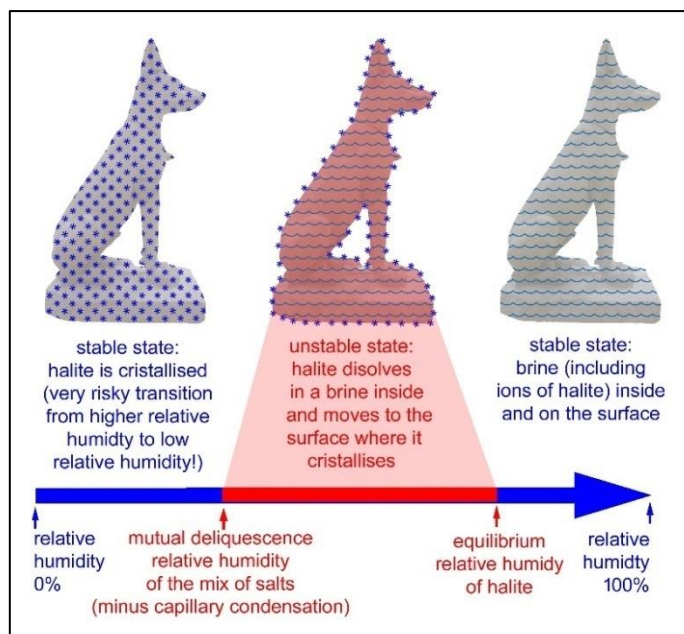


Fig. 5: The transporter brine hypothesis.

References

- Arnold, A. and Zehnder, K., 1990, Salt weathering on monument. First symposium on the conservation of monuments in the Mediterranean basin, ed F. Zezza, Brescia, grafo, p.31-58.
- Bromblet, Ph., Vergès-Belmin, V., Franzen, C., Aze, S., Rolland, O., 2011, Toward an optimization of the specifications for water bath desalination of stone objects, Salt weathering on buildings and stones sculptures, Proceedings from the International Conference, 19-22 october 2011, Limassol, Cyprus , p.397-404.
- Linnow K., 2007, Salt Damage in Porous Materials: An RH-XRD Investigation, Fachbereich Chemie, Universität Hamburg.
- Schwarz H.-J., SaltWiki, <http://193.175.110.91/saltwiki/index.php/Nitrate> (accessed 23/12/2015).

This page has been left intentionally blank.

INVESTIGATION OF SALT CRYSTALLISATION IN A STONE BUDDHA CARVED INTO A CLIFF WITH A SHELTER BY NUMERICAL ANALYSIS OF HEAT AND MOISTURE BEHAVIOUR IN THE CLIFF

N. Takatori^{1*}, D. Ogura¹, S. Wakiya², M. Abuku³,
K. Kiriya⁴ and Y. Kohdzuma²

Abstract

Motomachi Sekibutsu is a stone Buddha statue that was carved into a cliff in Oita City, Japan, around the 11th – 12th century. Salt precipitation, mainly due to a high ground water level, has been observed at Motomachi Sekibutsu. In this study, we elaborate phenomena that the precipitation of crystals is caused by evaporation and a decrease in solubility due to temperature changes. To do so, we examine the heat and moisture behaviour on and near the surface of Motomachi Sekibutsu by numerical analysis and investigate the influence of the environment in the shelter on the damage to the statue. Simulation results show that evaporation generally occurs deep inside the external corner and the surface is mostly dry. In particular, assuming that the amount of water evaporation is proportional to the amount of salt precipitation, salt precipitates deep inside the corner in summer to autumn and near the surface in winter.

Keywords: shelter environment, heat and moisture transfer, water evaporation, sodium sulphate, calcium sulphate

1. Introduction

Motomachi Sekibutsu is a stone Buddha statue carved into a cliff in Oita City, Japan. It has always suffered from the influence of moisture penetration through the cliff because the statue is not and cannot be separated from the cliff. Therefore, at Motomachi Sekibutsu, various preservation measures have been taken: main measures are constructing a shelter to intercept wind and rain and boring a tunnel behind Motomachi Sekibutsu to decrease the ground water level. However, the main factor of degradation, salt damage, has not been prevented yet.

¹ N. Takatori* and D. Ogura
Graduate School of Engineering, Kyoto University, Japan
takatori.nobumitsu.62a@st.kyoto-u.ac.jp

² S. Wakiya and Y. Kohdzuma
National Institutes for Cultural Heritage, Japan

³ M. Abuku
Faculty of Architecture, Kindai University, Japan

⁴ K. Kiriya
Graduate School of Advanced Integrated Studies in Human Survivability, Kyoto University, Japan

*corresponding author

Our ultimate aim is to suppress degradation from salt damage by rebuilding a shelter covering the Buddha statue and controlling the interior environment. The precipitation of crystals is considered to be caused by water evaporation and a decrease in solubility due to temperature changes, the former of which is the main focus of the current study. We examine the heat and moisture behaviour in Motomachi Sekibutsu via numerical analysis and account for the seasonal changes of the position of evaporation.

2. Background

2.1. Surrounding Environment

As shown in Fig. 1a, Motomachi Sekibutsu is covered with a wooden shelter of approximately 7 m wide, 5 m long, and 3.5 m high. However, Motomachi Sekibutsu has suffered from the influence of the surrounding environment, including heat transmission by the roof or walls, ventilation into the front door, solar radiation transmission into windows, and rainfall penetration into the cliff behind the statue.

Motomachi Sekibutsu is composed of tuff, which is a porous material; thus, heat and moisture transfer through the cliff to the statue. In addition, ground water around Motomachi Sekibutsu is located approximately 1 m below the ground level. Therefore, it is estimated that Motomachi Sekibutsu is considerably affected by ground water and remains a high moisture content environment.

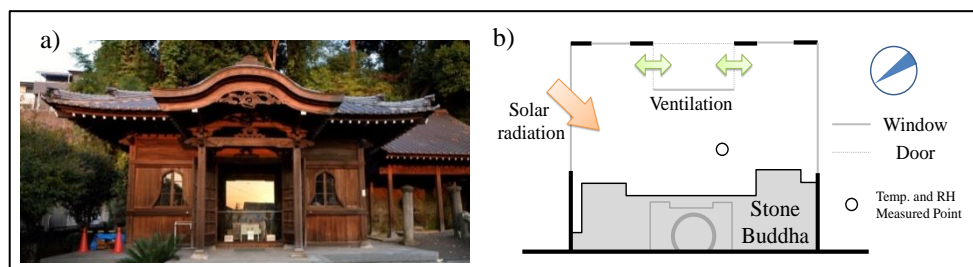


Fig. 1: a) Exterior of the shelter; b) Plan of Motomachi Sekibutsu.

2.2. State of salt precipitation

At the Buddha of healing, which is located at the centre of Motomachi Sekibutsu, salt conspicuously precipitates and deterioration by salt damage is ongoing. Na_2SO_4 and CaSO_4 were mainly found on the statue by the Oita City Board of Education (1996). Na_2SO_4 is considered to be the most destructive salt (Goudie 1997); therefore, deterioration from precipitated Na_2SO_4 is a concern.

On the Buddha of healing shown in Fig. 2a, salt crystals are conspicuously found below the waist. Moreover, there are few salt crystals on the head. Fig. 2b shows the result of ion chromatography analysis of ions absorbed by paper placed on the surface of the statue for desalination (Oita City Board of Education 2014). It can be observed that on the right knee, all ions except Ca^{2+} are detected from November to December. In this study, we consider only heat and moisture transfer and do not consider salt transfer. Therefore, we assume that salt accumulates with water evaporation (Ogura 2013); thus, we investigate the amount of salt precipitation based on the amount of water evaporation.

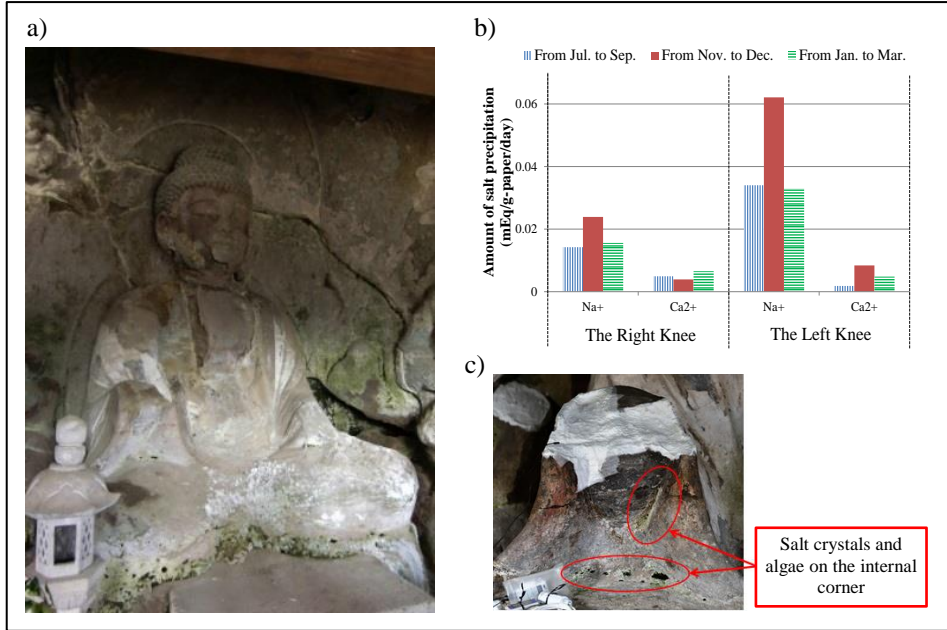


Fig. 2: a) The 'Buddha of Healing', b) Salt precipitation on knees; c) Right knee.

There are some differences in the positions of salt precipitation from the waist to foot because of the difference in shapes. The right hand is in the most conspicuous location where salt precipitation differs at each part. The right hand is convex and contains few salt crystals. Fig. 2c shows that salt precipitates and algae grow on the internal corner, which is the secluded part. Moreover, on the knee, salt crystals are found, although they are on the external corner.

3. Numerical Analysis

3.1. Method for numerical analysis

Here, we present a method of numerical analysis to determine the heat and moisture behaviour in the stone Buddha, including the cliff. Heat and moisture balance equations for porous materials are as follows (Matsumoto 1984):

$$\text{Heat balance} \quad : \quad c\rho \frac{\partial T}{\partial t} = \nabla \cdot \{(\lambda + r\lambda'_{Tg})\nabla T\} + \nabla \cdot (r\lambda'_{\mu g}\nabla \mu),$$

$$\text{Moisture balance} \quad : \quad \rho_w \left(\frac{\partial \psi}{\partial \mu} \right) \frac{\partial \mu}{\partial t} = \nabla \cdot [\lambda'_{\mu}(\nabla \mu - n_x g)] + \nabla \cdot (\lambda'_T \nabla T).$$

In this analysis, we use the explicit finite difference method and the space lattice width is minimized 1 mm near the surface. Moreover, we calculate the amount of evaporation as follows:

$$\text{Amount of evaporation} : W = -\frac{\partial \rho_w \psi}{\partial t} - \nabla J_{2w},$$

where $c\rho$ is the apparent heat capacity of the material [$\text{J}/\text{m}^3\text{K}$], ρ_w is the density of water [kg/m^3], t is time [s], T is temperature [K], ψ is the volumetric moisture content [m^3/m^3], μ

is the chemical potential of water [J/kg], r is the heat of phase change from vapour to liquid [J/kg], λ is the thermal conductivity [W/(m · K)], λ'_T is the moisture conductivity related to temperature [kg/(ms · K)], λ'_{Tg} is the vapour conductivity related to the temperature gradient [kg/(ms · K)], λ'_μ is the moisture conductivity related to the chemical potential gradient of water [kg/(m · s · (J/kg))], $\lambda'_{\mu g}$ is the vapour conductivity related to the chemical potential gradient of water [kg/(m · s · (J/kg))], n_x is the unit vector vertically downward [-] (1 if it is vertically downward and 0 if it is horizontally downward), and J_{2w} is the liquid water flow [kg/m²s].

3.2. Analysis target

In this analysis, we analyze the two-dimensional plane whose centre is the Buddha of healing. The analysis model is the cliff containing the stone Buddha shown in Fig. 3c because Motomachi Sekibutsu is influenced not only by the room environment but also by the temperature and humidity of the cliff behind the stone Buddha.

As shown in Fig. 3c, the cliff, including the stone Buddha statue, consists of two-layered tuff and soil. The heat and moisture properties of tuff and soil are decided in reference to paper which Li Yonghui *et al.* (2010) used; however, we modified the saturated hydraulic conductivity of tuff to be 2.20×10^{-9} [m/s]. The coefficients of heat transfer used are 9.3 W/m² K and 23.3 W/m² K inside and outside the roof, respectively, and the coefficient of moisture transfer was calculated using the Lewis relationship. Fig. 3d shows the space lattice width and the positions used when examining the results.

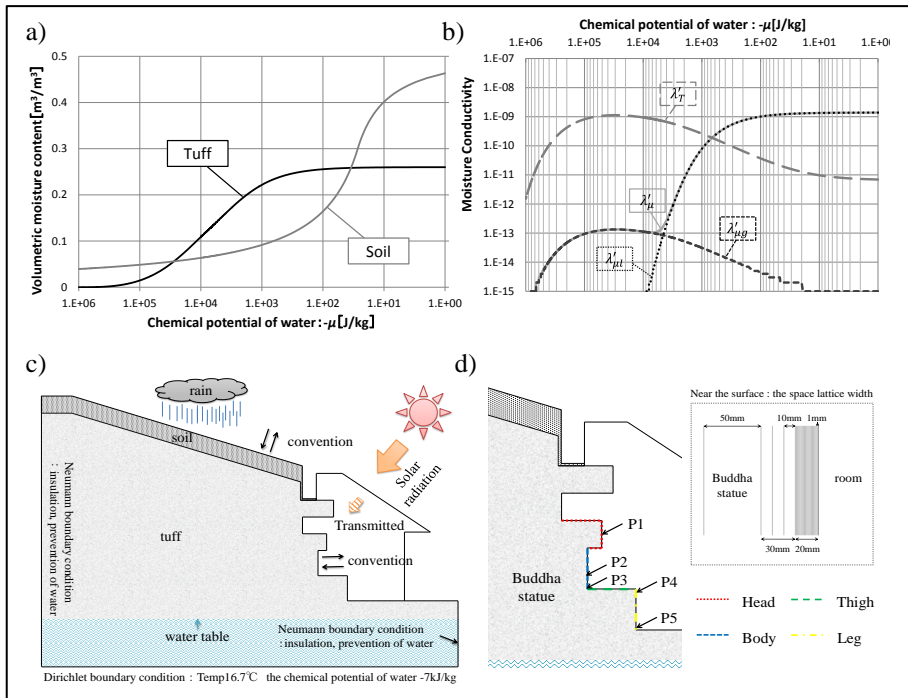


Fig. 3: a) Equilibrium moisture content; b) Moisture conductivity of tuff; c) Analysis model ; d) Analysis positions.

3.3. Analysis conditions

Tab. 1 shows various room conditions used in the analysis. Initially, we performed steady-state analysis to determine the influence of the heat and moisture behaviour arising from the shape of the statue and ground water on the stone Buddha statue. Next, we performed unsteady-state analysis to determine seasonal differences.

Tab. 1: Calculation conditions.

	Temp. and RH inside the roof	Temp. and RH outside the roof	Solar radiation	Rainfall
Steady	Constant ^{*1}	Constant ^{*1}	0	0
Unsteady	Measured ^{*2}	Measured ^{*2}	Estimated ^{*3}	Measured ^{*2}

※1 The constant value is the annual average value in Oita City: Temp 16.4°C, relative humidity (RH) 69%.

※2 The measured value used is the annual value from April 2013 to March 2014. Room temperature and RH in the shelter were measured by Oita City Board of Education (2014), and the outside temperature, RH, and rainfall in Oita City were measured by the Japan Meteorological Agency. Rainfall was applied only to the top of the cliff, and half the measured value was used, considering the influence of rainfall blocking by trees.

※3 The amount of solar radiation was calculated to divide the measured global solar radiation into direct and sky radiation, considering the shape of the roof, the transmittance of the glass, and the solar azimuth.

As boundary conditions, the bottom of the ground is the Dirichlet boundary condition: temperature is 16.7°C at 12 m below the ground level and the chemical potential of water is 7 kJ/kg. As a result of preservation measures, the ground water level is 1 m below the ground level. The vertical plane of the side of the ground is the Neumann boundary condition: there is no heat and moisture flux.

4. Results

4.1. Steady-state analysis

In this section, we present the results of the steady-state analysis. We focus on the influence of the shape of the stone Buddha statue and ground water on the heat and moisture behaviour.

Fig. 4a indicates the temperature, water content, and amount of evaporation on the surface of the statue. The positions corresponding to Fig. 4a are shown in Fig. 3d. The water content on the head and P4 is low; the amount of water evaporation from the same positions is also low. On the other hand, the water content on P3 and P5 is high, and the amount of evaporation is also high. The head and P4 are the external corners that are strongly influenced by room temperature and humidity because a wide portion of these areas is exposed to air. On the other hand, P3 and P5 are the internal corners that are strongly influenced by the deep part of the statue.

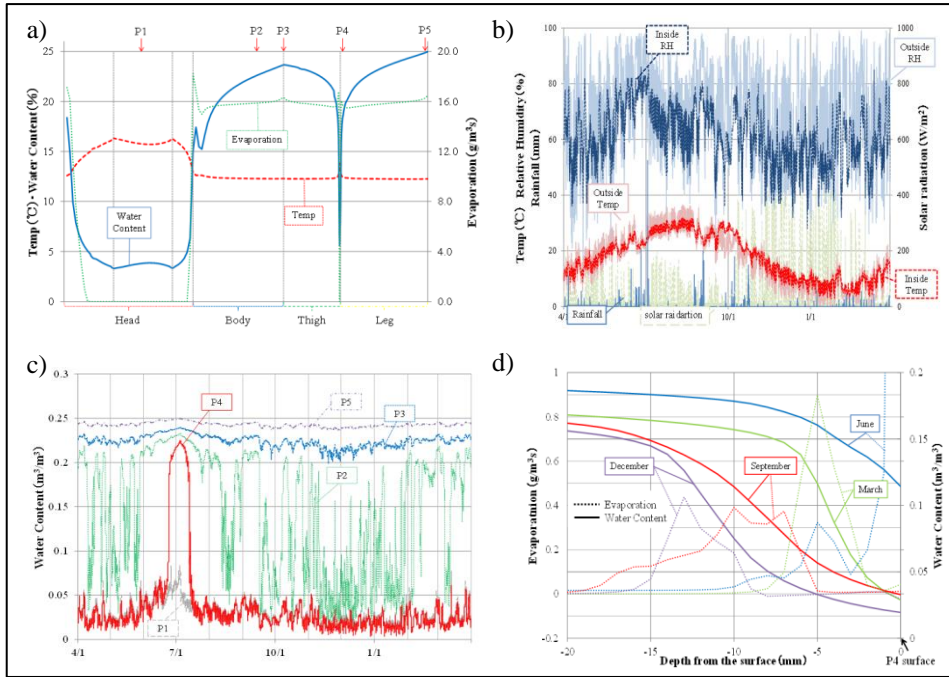


Fig. 4: a) Heat and moisture behaviour on the surface of the Buddha statue; b) Weather conditions from April 2013 to March 2014; c) Annual distribution of moisture content on parts; d) Amounts of evaporation and moisture content with depth from P4.

4.2. Unsteady-state analysis

Next, we present the results of the unsteady-state analysis. We focus on the fluctuation of the water content and evaporation in the statue with seasonal changes of room temperature and humidity. We especially focus on P4, which is strongly influenced by room conditions. Then, we examine changes in the amount of evaporation.

4.2.1. Weather conditions

Fig. 4b shows annual weather conditions used in the unsteady-state analysis as well as the solar radiation that enters P4. As shown in Fig. 4b, the temperature and *RH* inside the shelter fluctuate more slowly than those outside. The amount of solar radiation is the highest during the winter solstice because of the placement of windows.

4.2.2. Depth of evaporation

Fig. 4c shows the annual fluctuation of the water content on parts shown in Fig. 3d. There is a low water content on P1 and P4, and the water content only increases by July. On the other hand, there is a high water content on P3 and P5. The water content intensely fluctuates throughout the year only on P2. The surface of P4 tends to be dry because it is the external corner. Therefore, the water content on P4 increases from June to July when the room humidity increases. It is believed that the water content on P4 is high throughout the year because it is the internal corner and strongly influenced by ground water.

Fig. 4d shows the monthly average value of water content and the amount of water evaporation from the surface to deep part. The horizontal axis indicates the distance from the surface; the 0-mm point is the surface. In July, the water content is high from the depths to surface; therefore, water evaporates mostly on the surface. However, water evaporates only slightly on the surface when the water content is low; it evaporates mostly from the deep part of the statue. Fig. 4d shows that water mostly evaporates where the water content increases rapidly.

5. Discussion

First, we discuss the results of the steady-state analysis. With the fluctuation of room conditions, water evaporates not only on the surface but also from a deep part of the Buddha statue at the external corner; on the other hand, water evaporates near the surface at the internal corner when the ground water level is sufficiently high to keep the deep part of the statue nearly saturated. Consequently, assuming that salt accumulates with water evaporation, it is considered that salt precipitates in the deep parts of the head and P4, which are the external corners. In contrast, on P3, which is the internal corner, salt precipitates mainly near the surface.

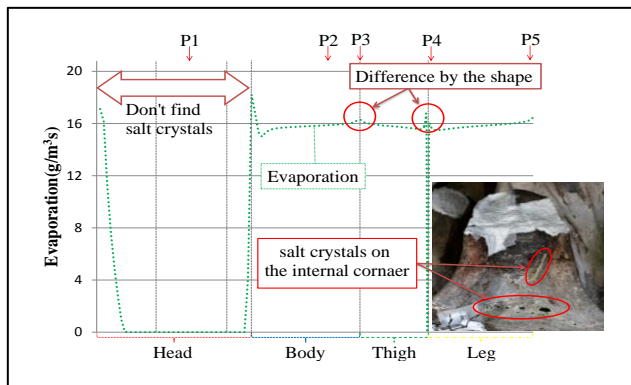


Fig. 5: Positions of salt precipitation.

Next, we discuss the seasonal changes of salt precipitation determined by unsteady-state analysis. On P4, which is the knee of the Buddha of healing, water evaporates mainly from the deep part from summer to autumn and near the surface in winter. Therefore, assuming that the amount of water evaporation has a proportional relation with the amount of salt precipitation, salt precipitates in the deep part from summer to autumn and near the surface in winter. However, Fig. 2b shows that a remarkable amount of Na^{2+} was detected on the knee in winter. This does not correspond with the analyzed results. We believe that this is because the solubility of Na_2SO_4 , which mainly precipitates in Motomachi Sekibutsu, decreases with decreasing temperature. Moreover, the amount of Ca^{2+} detected on the right knee was the highest in winter. This tendency of salt precipitation corresponds with the analyzed results. On the other hand, the amount of Ca^{2+} detected on the left knee was the highest in autumn. This may be because the amount of solar radiation is different on the right and left knees, especially in winter. To confirm these inferences, it is necessary to analyse the amount of solar radiation incident on the right and left knees.

6. Conclusion

With focus on studying the relation between the depth of salt precipitation and that of water evaporation at Motomachi Sekibutsu, we developed a two-dimensional model of Motomachi Sekibutsu. Using this model and assuming that salt precipitation is caused by water evaporation, we analysed the heat and moisture behaviour, and contrasted the simulated moisture distribution with the positions of salt precipitation observed by a field survey. At Motomachi Sekibutsu that is suffering from the strong influence of ground water, evaporation tends to take place deep inside the external corner and near the surface of the internal corner. In particular, on the knee, water evaporates in an area where the water content increases rapidly. Assuming that the amount of water evaporation is proportional to the amount of salt precipitation, it is considered that salt precipitates in the deep part from summer to autumn and near the surface in winter.

References

- Goudie, A.S., Viles, H.A., 1997. Salt weathering hazards, John Wiley and Sons, Chichester, pp.106-107.
- Ogura, D., Abuku, M., Hokoi, S., Iba, C., Wakiya, S. and Uno, T., 2014, Measurement of salt solution uptake by ceramic brick using γ -ray projection, in: Proceedings of the 3rd International Conference on Salt Weathering of Buildings and Stone Sculptures, Brussels, Belgium, October 14-16, 2014, pp.529-532.
- Scherer, G.W., 2004, Stress from crystallization, *Cement and Concrete Research*, 34, pp.323-330.
- Japan Meteorological Agency. 2014. <http://www.jma.go.jp/jma/index.html>, accessed at 27 November, 2014.
- Yonghui, L., Ogura, D., Hokoi, S. and Ishizaki, T., 2010. Effects of excavation and emergency preservation measures after excavation on hygrothermal behavior in stone chamber of Takamatsuzuka tumulus, *Journal of Environmental Engineering*, 658, pp.1041-1050.
- Matsumoto, M., 1984, *Shin Kenchikugaku Taikai*, Chapter 10 (in Japanese), Shokokusya, pp.105-134.
- Oita City Board of Education. 1996. *Kunishiteishiseki Oita Motomachi Sekibutsu Hozonsuyurijigyo Hokokusho* (in Japanese), Oita, Sohrinsha.
- Oita City Board of Education. 2014. *Oita Motomachi Sekibutsu Heisei 25 Nendo Tyosagyomuitaku Hokokusyo* (in Japanese), Oita, Sohrinsha.
- Flatt, R.J., 2002, Salt damage in porous materials: How high supersaturations are generated, *Journal of Crystal Growth*, pp.435-454.

SCIENTIFIC EXAMINATION OF A PAINTED THRACIAN TOMB DISCOVERED NEAR ALEXANDROVO VILLAGE, BULGARIA

V. Todorov^{1*}, K. Frangova² and T. Marinov³

Abstract

The Thracian tomb discovered near the village of Alexandrovo has been dated to the IV century BC. It comprises *dromos*, antechamber and round burial chamber with a false dome. The walls are made of local tuff stone and covered with painted plaster. The construction and its paintings have survived in their original state without any repairs or alterations made at any time of the tomb's existence. Only evidence of processes of natural deterioration is present: lack of adhesion between plaster and stonework, white veils on the paint layer and local damage on the floor plaster due to water percolation. The petrological study revealed that the tomb had been built of crystal-vitroclastic rhyodacitic tuff stone. It also established that there was an ongoing process of zeolitization of the stones closest to the ground, due to permanent moisture exchange. The soluble salts and mineral nanoparticles deposited on the paint surface formed a white veil, the composition and morphology of which were studied by means of SEM/EDX and XRD. Clay particles deposited between the stone and the plaster had caused stratification in the upper parts of the tomb and plaster damage in the lower parts. The mercury porosimetry investigation of the pore size distribution showed the small pores to be entirely filled up. This added to the tomb decoration's uniqueness and presented a rare chance for the modern scientific examination of an authentic encaustic wall painting technique.

Keywords: tuff, zeolitization, damages and causes, painting technique, preservation measures

1. Introduction

In the late 2000, the Bulgarian archaeologist Dr. Georgi Kitov unearthed another Antiquity structure – a painted Thracian tomb buried under a tumulus near the village of Alexandrovo in South-East Bulgaria. According to its discoverer, the tomb dates to the mid IV BC and, although there is no burial inventory (the tomb had been looted prior to its formal discovery), it is of the quality and status of the already internationally renowned tombs in Kazanlak and Sveshtari, included in UNESCO's List of World Heritage Sites (Kitov 2001).

¹ V. Todorov*

National Academy of Art, Department of Conservation, Sofia, Bulgaria
todorov.valentin@abv.bg

² K. Frangova

Royal Danish Academy of Fine Arts, Institute of Conservation, Copenhagen, Denmark

³ T. Marinov

University of Mining and Geology, Sofia, Bulgaria

*corresponding author

All premises within the structure are covered with painted decoration. At the far end of the *dromos*, the traditional battle scenes are depicted, while in the burial chamber, opposite the entrance, the Ancient master has placed the scene “*Welcoming of the Hero*”. At the very centre of the burial chamber itself, there is an unique frieze with hunting scenes – an invaluable evidence of the lifestyle and traditions of the ancient Thracians (Franks 2012).

The universal cultural, historical, artistic and scientific value of the mural paintings prompted the Cultural Fund of the Japanese government to grant financial support (USD 3.5 million) for the creation of the Museum of the Thracian Art in South-East Rhodopes. A full-scale museum copy of the tomb was also erected with this funding in order to meet the needs of cultural tourism. The painting technique used within the tomb places the monument among the very rare examples of use of wax in the Antiquity. Its integrity and authenticity pend no questioning thus making the site one of exceptional interest to science.

A wide-scope research plan to investigate the building and the decorative skills of the ancient masters was developed, aiming at establishing the materials used for both the construction, and the paintings. It also aimed at determining the alterations and decays, as well as the reasons for them. The observations and the research proved that the painting process started on fresh mortar (*buon fresco*) and was finished using wax, identified by GC/MS either as a paint binder or as a coating. The monochrome red and black bands, which also contain wax, were executed in the so-called *stucco lustro* technique. The results of the painting technique research have already been published (Todorov 2011).

2. Condition of the tomb

The tomb near Alexandrovo does not differ in its architectural and constructional characteristics from other tombs from the same period. It comprises approximately 13 m long *dromos*, antechamber with rectangular shape and a round burial chamber (i.e. a beehive tomb) (Fig. 1a). It is built of local stone, native to the area of the East Rhodopes – volcanic tuff. The stone blocks are of different sizes, placed in horizontal layers. Each consecutive layer is smaller in diameter than the previous one, so that a so-called false, or corbelled, dome is formed. The face of each stone in the interior has then been worked up with a flat chisel, so that a smooth 2.5-3 cm wide frame is formed. The rest of the surface has been finely finished with a pointed chisel. The masonry has been laid using a dry building technique, which requires perfect fitting of the building blocks, usually done by additional *in situ* processing of each stone. No traces of additional metal clamps are found.

About 20% of the original mortar in the burial chamber and in the antechamber was discovered highly fragmented and on the floor. The damages on the murals found *in situ* are mainly located in the North half of the burial chamber, up to 1 m above floor level. Interestingly, the size of the damaged area coincides in height with the size of the entrance to the burial chamber. In addition, it is important to note, that at the exact place where the mortar layer is missing from the wall, there is a cavernous damage on the floor rendering (Fig. 2a). This coincidence is explained with water percolating from above. The plaster in the burial chamber is completely separated from the stonework (Fig. 2b).

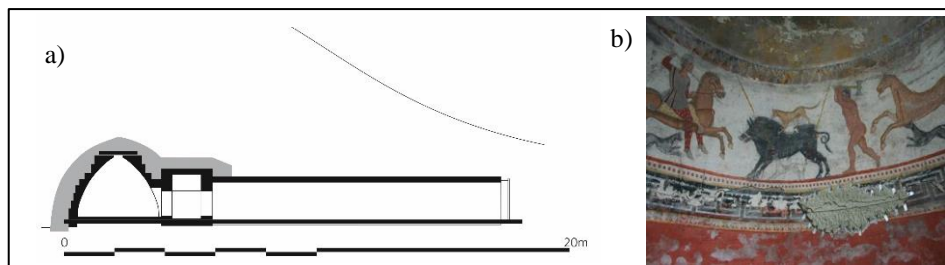


Fig. 1: a) Section of the tomb; b) A hunting scene (detail) with part of the ornamental friezes.

The decorated surfaces in the burial chamber are divided into eight horizontal bands, of which four are monochrome, two have polychrome ornamented friezes and two – figural compositions (Fig. 1a). The main frieze is at eye level and depicts hunting scenes in which four horse riders, four foot-hunters, nine dogs, two boars and two deer can be seen. The paint layer of the swastika frieze is partially missing due to flaking. The scene “*Welcoming the Hero*” situated opposite the entrance of the burial chamber is almost unrecognizable due to powdering of the paint layer. The monochrome-painted areas are affected by salts’ efflorescence and in some areas there is visible spot (pitting) damage, caused by subflorescences. It is obvious that the tomb has been affected by serious natural disasters in the past (i.e. earthquakes), which have caused detachment of large fragments of the building stones, cracking and scaling. In addition to that, human influence is also present, as evidenced by the destruction of the original stone door to the burial chamber by ancient looters.

3. Materials and methods

The samples were collected based on a preliminary research which established the use of wax either as paint binder or as surface treatment (Todorov 2011). Unlike the initial samples collected from the ornamental frieze, the ones for the current research were selected among the detached red band fragments accumulated on the burial chamber’s floor, thus avoiding further damage to the original. Each sample analysed included both paint layer and mortar. Stone samples were collected from the base and approximately 20 cm above the entrance of the burial chamber. Samples for salts investigation were collected from the antechamber from the layer between the detached paint-mortar layer and the stonework. The stone and mortar samples were analysed petrographically using thin sections as well as by SEM/EDS. The porosity of the stone samples was determined by mercury porosimetry. The presence of salts was demonstrated by conductivity measurements of water extracts. These salts were characterised by SEM/EDS and their phase composition determined by XRD.

4. Results

4.1. Petrological characteristics of the stone used to build the tomb

The false dome of the burial chamber is built of crystal-vitroclastic tuffs, astonishingly uniform in their colour, structural and textural characteristics. For the base of the dome, zeolite-containing rocks are used. The tuff is white to light grey with massive texture and crystal-vitroclastic structure comprising vitroclasts (volcanic glass), crystalloclasts and

lithoclasts. The vitroclasts make up to 40% of the rock. They are usually angular or rounded pieces, partially transformed to zeolites and clay minerals. Such transformations are only observed in the periphery and the micro-cracks of the vitroclasts, with the centres of the latter appearing fresh and isotropic under a microscope. The crystalloclasts (or the primary minerals) are represented by quartz, sanidine, plagioclase (oligoclase), biotite, monoclinic pyroxene and amphibole (Fig. 2a). Rhyolitic and middle range vulcanites represent the lithoclasts (Fig. 2b). As supplementary minerals, there are apatite, zircon, titanite, and tourmaline. The rocks are almost entirely transformed to zeolites, with a main mineral being clinoptilolite (63%) (Figures 2c, 3a, 3b and 3c).

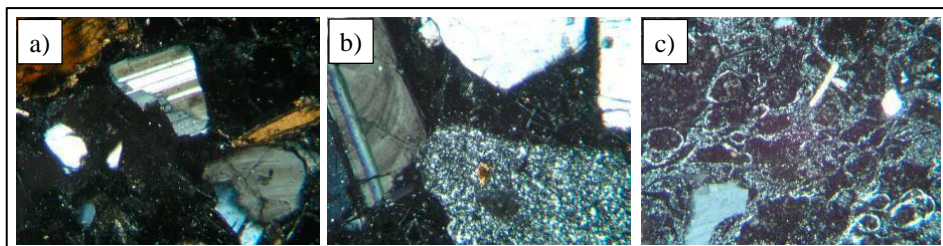


Fig. 2: a) Plagioclase, quartz, biotite, sanidine and vitroclasts; b) Zoned plagioclase, quartz, glassy rocks and rhyolitic lithoclasts; c) Zeolite-containing rock - vitroclasts transformed to zeolite minerals.

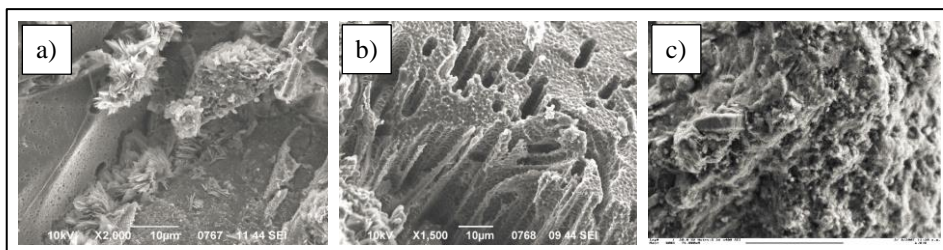


Fig. 3: a) Zeolite: deep narrow crack in a stone from the burial chamber's base. Elemental composition of the needle-like crystals (mass %): C-36.59, O-38.64, Na-0.37, Mg-0.28, Al-3.71, Si-17.56, K-1.35, Ca-1.50; b) Volcanic ash in the same stone. Elemental composition (mass %): C-38.41, O-36.95, Na-0.16, Mg-0.09, Al-17.58, Si-3.66, K-2.72; c) Crystal matter between the mortar and the stonework, antechamber. Oxide composition (mass %): 1) SO_3 -57.53, CaO-42.4 (gypsum) and 2) MgO-1.67, Al_2O_3 -16.85, SiO_2 -65.17, SO_3 -2.08, K_2O -6.28, CaO-4.09 (clinoptilolite).

4.2. Mineral composition of the mortar

The stonework of the two chambers of the tomb and adjoining part of the *dromos* is plastered with two layers of mortar, consisting of lime and mineral filler. Both layers are astonishingly even in their thickness. The first one (laid directly on top of the stone masonry) is about 3-5mm thick, greyish-white in colour and grainy in structure. The filler is mainly crystalloclasts and vitroclasts. At the base of the first mortar layer, there is a fine-grained clay mass, containing clay minerals and sericitic mass. The crystalloclasts and lithoclasts described above are found on top of this layer (Fig. 4a). The second layer is also

of constant thickness (3-4mm), white in colour and with micro-grained structure. A secondary calcite can also be detected, deposited in some of the larger pores as a result of the carbonization of the calcium hydroxide from the binder (Fig. 4b).

The only exceptions of the described stratigraphy are the monochrome (red and black) bands in the burial chamber, executed in stucco lustro technique. They are laid over additional layer of mortar, applied on top of the main one, so that they are different in thickness compared to the other painted areas.

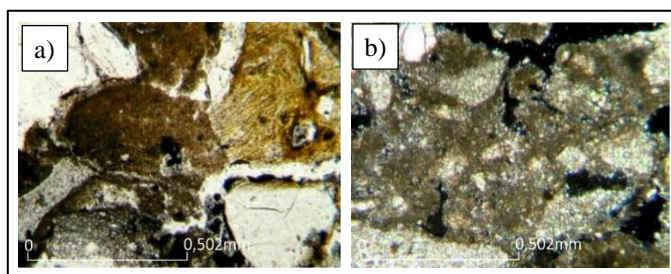


Fig. 4: Burial chamber a) First mortar layer: quartz and traces of clay-carbonate cement; b) Second mortar layer: single quartz grains and carbonate cement.

4.3. Morphology and composition of the white veil and salts

In order to determine the composition of the salts three samples were collected from different areas in the tomb. The measured conductivity of the aqueous extracts of the stone and the mortar samples proved the presence of water-soluble salts. Their composition was determined by XRD (BRUKER E-8 Advance) and EDS. Unfortunately, the salts were present only in micro quantities and the analysis of their composition by x-ray diffraction proved impossible. This necessitated the collection of additional samples, this time consisting of secondary deposits – the white veils on the red band in the burial chamber (sample Al-S1a) and the white powder crystallized between the stone and the mortar in the antechamber (sample Al-S1b). These new samples allowed for better readings, so the actual composition of the salts was determined as containing gypsum, calcium carbonate (both calcite and aragonite), calcium aluminate and clinoptilolite (Fig. 5). The calcite and the aragonite both originated from the lime mortar, the clinoptilolite – from the building stone.

5. Discussion

When the tomb was discovered, the inner temperature measured at 12-14°C and the relative humidity – at 96%. An important issue in the interpretation of the results of the analyses of the materials is the presence of a humidity gradient starting at the peak of the dome and decreasing towards the floor. This phenomenon is explained by the military activities that took place in the region during the Balkan War and WWI around 1915. Those included the digging of a trench and the building of an observation post on top of the tumulus. The trench collected atmospheric moisture (rain and snow) for almost a century, significant part of the water actually penetrating the burial chamber and the antechamber through the soil. There are a few reasons why we should reconsider the generally accepted belief that, when buried underneath a thick layer of soil, the chambers of such constructions exist in an

environment of stable temperature and humidity. In reality, a permanent moisture exchange with the environment takes place, both directly (through the difference between the temperature and the humidity levels in the interior and the external atmosphere), and by diffusion (through the soil layer in front of the *dromos*), while the tomb is still covered. We have no means of guessing the length of these exposure periods. As is obvious from the section of the tumulus (Fig. 1), the *dromos*' entrance is covered with significantly thinner layer of soil compared to the layer over the burial chamber. It is also apparent that there is a temperature and humidity gradient starting from the humid soil of the tumulus through the chambers and the *dromos* out to the atmosphere. The mechanism of humidity transportation is diffusional and is influenced by the daily, seasonal and annual climatic fluctuations. The tomb's construction and position within the tumulus only advances the process, while the long *dromos* functions as a chimney-stack. The missing mortar, detached and fallen off, corresponds with this phenomenon and is to be seen only at the height of the entrances of the chambers and the *dromos*, i.e. it coincides with the path through which the humidity is transported.

In the tomb both subflorescences and efflorescences are present, however the subflorescences are predominant. It can be suggested that the efflorescences are related to the periods when the *dromos* was opened, i.e. when the humidity exchange was more intensive. The presence of two types of damage effects – irregular white veil spots and pitting, could be explained only by the disrupted vapour permeability of the paint layer, related to the use of beeswax.

The building stone itself plays a special part in the weathering processes. Humidity is the worst adversary of tuffs, influencing mainly the susceptible components of the rock, such as clay minerals and zeolites, and causing their degradation. The weathering of vitroclasts (volcanic glass) gives rise to zeolites and clay minerals. In the burial chamber, especially at its base, vitroclasts constitute about 40% of the tuffs' mass and are completely transformed to zeolites and clay minerals. The main mineral in the zeolite-containing rocks is the clinoptilolite, comprising as much as 63% of their contents. In comparison, the sanidine content is about 14%, smectite – 8%, albite – 10% and quartz – 4%. On account of its advanced stage of zeolitization, the rock is identified as tuff containing clinoptilolite and zeolite. Zeolites are natural ion-exchanging minerals, influencing the ionic balance between the stone and the mortar. The diffractogram of sample A1-S2a shows that the clinoptilolite is predominantly present as clinoptilolite-Na and clinoptilolite-K and not as much as clinoptilolite-Ca. This means that the potassium and sodium ions originating from soil salts are trapped i.e. are chemically bound.

Moisture carries and deposits the products of weathering to the border area between the mortar and the stone, to the porous structure of the mortar and to the surface of the paint layer. Their exact location is dependent on the size of the dispersed minerals. Montmorillonite clays are highly susceptible to humidity fluctuations. This explains why the lower parts of the wall paintings bear the worst damage and why most of the mortar in this area is detached.

Analysis of the surface white veils also proves that their origin lies in the weathering products of the tuff and the mortar. A very interesting scientific fact is that the water-carried extracts of the mortar's binder have recrystallized in both polymorphic forms – calcite and aragonite (Fig. 5), while usually either one or the other form would be present.

An interesting phenomenon is the discovery of gypsum among the white efflorescence and at the border area between the stone and the mortar in the antechamber. The location and distribution of the gypsum were obviously related to the path of the moisture's penetration in the tomb. The additional research showed that the gypsum in the white efflorescence was of anthropogenic origin. In the period 1951-1994 in the nearby town of Dimitrovgrad (approximately 10km away as the crow flies), a chemical factory for the production of synthetic fertilizers and sulfuric acid was in operation. The air pollutants from the factory were transported aerially to the site of the tomb. This is yet another proof of the existence of moisture exchange between the tumulus, chambers and *dromos* and their surrounding atmosphere. The analysis of the porous structure by means of mercury porosimetry showed that the total volume of the pores is highly reduced, the finest of the pores of the stone and the mortar (pore sizes under 500 nm) were completely filled up by products of stone decomposition (Fig. 6).

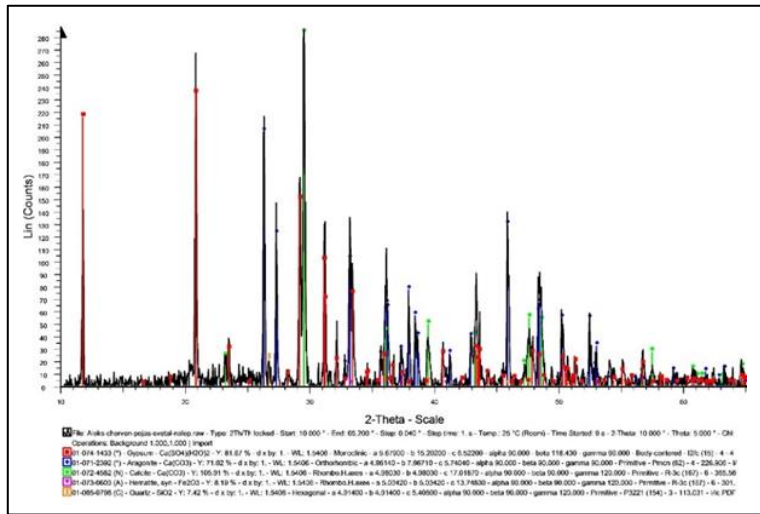


Fig. 5: XRD analysis of Al-S1a. Identified minerals include calcite, aragonite, quartz, gypsum, dolomite; all minerals are secondarily crystallized.

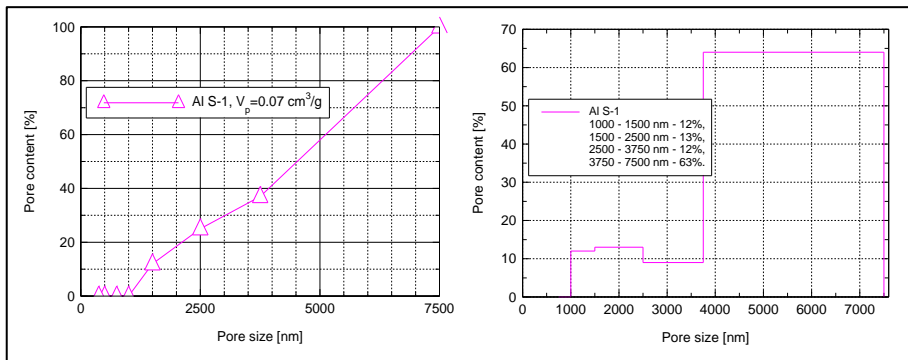


Fig. 6: Integral and differential micro-porosity of sample Al-S1. The finest pores are filled up.

6. Conclusions

The clarification of the decay processes and their mechanisms causing the damaging of the stone and the mural paintings in the tomb allowed for the development of a long-term concept for the preservation of both the built structure and the wall paintings. The main proposed actions are:

- To separate the tomb from the tumulus so that the drying process is redirected from the interior to the exterior. The main goal is to deposit the water-transmitted salts and erosion products into the stone rubble layer around the tomb.
- To stop the moisture exchange and the percolation of water in the burial chamber through insolation.
- To re-install the adhesion between the stonework and the mortar, which would preserve the painted decoration.
- To execute minimal conservation treatment to locally stabilize the powdering paint layer, located in the lower areas of the tomb, close to the floor.
- To preserve the authentic state of the wall paintings as a precious evidence of the ancient painting techniques to be studied in the future. The white veil is not to be removed and no further cleaning is to be undertaken.
- To disallow access to the tomb and to create conditions as close as possible to the historical microclimate by passive measures.
- To develop a plan and methodology for distant observations (monitoring) of the condition and emergency actions when and if needed.

Most of these measures and actions have already been implemented. The recreation of the historic microclimate in the tomb using passive measures is forthcoming.

Acknowledgements

The authors would like to express their sincere gratitude to Mr. Werner Schmidt, wall paintings conservator, ICCROM collaborator, for the cooperation and the encouragement to investigate into the painting technique; to Dr. Dario Camufo, CNR, Italy, and Dr. Thomas Warscheid, LBW Bioconsult, Germany, for the valuable advice on historical microclimates and bio-protection of the tomb; as well as to Dr. Esther von Plehwe-Leisen, Germany, for the discussions on building stone damage.

References

- Kitov, G., 2001, A newly found Thracian tomb with frescoes, *Archaeologia Bulgarica*, 5 (2), 15-29.
- Todorov, V., 2011, The Thracian Tomb at Alexandrovo, SE Bulgaria: Preliminary observations on its painting technique, in *Interdisziplinäre Forschungen zum Kulturerbe auf der Balkanhalbinsel*, Nikolov, V., Bachvarov, K., Popov, H. (eds.), Sofia, 323-334.
- Franks, H.M., 2012, *Hunters, Heroes, Kings: The frieze of the tomb II at Vergina*, The American School of Classical Studies at Athens, ISBN 978-0-87661-966-7.

CASE STUDY OF THE EPISCOPAL GROUP OF FREJUS (FRANCE): DIAGNOSIS AND TREATMENT OF CLAY CONTAINING SANDSTONES IN MARINE ENVIRONMENT

M. Trubert¹, B. Brunet-Imbault^{2*}, P. Bromblet³ and C. Guinamard²

Abstract

The episcopal group of Fréjus concentrating 16 centuries of architecture is located at 2km from the sea. Six different sandstone patterns of local Permian sandstones were identified and a list of damages (granular disintegration, craquele, scaling, moist area and salt efflorescences) was localized on mappings. The analysis of the environmental context and the implementation of the masonries indicate that the damage expression strongly depends on the stone's orientation. Moreover, we can recognize two sandstone patterns which are mainly affected by a high level of decay: an original pattern of coarse sandstone and a restoration pattern of fine sandstone. Petrographic analysis, petrophysic measures (porosity, water capillarity, water vapour permeability and thermo-hydric dilation), salt analysis, micro-scanning observations and clay activity evaluations were conducted. Our results indicate that the on-site scaling thickness can be related to the thermo-hydric dilation values and to the clay swelling capacity. Furthermore, the salt analysis indicates a contamination in chloride and sodium due to the marine environment. The contamination is enlarged by nitrates in capillary rising areas and by sulfates due to the urban environment as well as locally used gypsum mortars. The intrinsic properties, like dilation properties with water, are then the dominant factor in the sandstone damages but the salt contamination and water transfers are aggravating factors. Therefore, solution based on buthylidiammonium chloride was tested to evaluate the feasibility of dilation stabilization. Tests performed on samples in laboratory indicate, for the two main sandstone patterns, the impact of the application protocol on the depth of penetration. The tests show a significant effect of the solution on the hydric dilation decrease. In parallel, a consolidating protocol based on tetraethoxysilane (TEOS) has been tested. These tests are encouraging for the treatment feasibility, they will be extended by an on-site experimental restoration phase.

Keywords: sandstone, clay, swelling, conservation, treatment

¹ M. Trubert
Architecte en Chef des Monuments Historiques, Fontainebleau, France

² B. Brunet-Imbault* and C. Guinamard
Cabinet d'études Studiolo, Paris, France

³ P. Bromblet,
Centre Interdisciplinaire de Conservation et de Restauration du Patrimoine, Marseille, France

*corresponding author

1. Introduction

The episcopal group of Fréjus (Var – France) is composed of the baptistery, the cathedral church, the canonical buildings including the cloister and the bishop's residence. This remarkable group presents a subtle range of colors due to the use of various local Permian sandstones. The Mediterranean sea is located 2 km south from the building. The conservation issue of the episcopal group is to define protocols permitting conservation and restoration of damaged sandstones. The main issue is to distinguish the influence of the marine environment from the intrinsic properties of the sandstones in the degradation process. Damages can, indeed, be caused by the components and microstructure of the stone itself, more specifically the clay inclusions. Although the effect of clays on the sandstone, and especially swelling clays, is well-known, the discrimination of the predominant factor leading to the observed damages and the feasibility of long-term stone preservation is yet an unsolved issue, especially in the marine environment. Firstly, we focused on the identification and classification of the factors involved in the development of different damages. Secondly, we tested stabilization and consolidation protocols.

2. Materials and methods

2.1. Building stones and degradation patterns

The episcopal group was built with local Permian sandstones. The macroscopic examination of the building's stones allows distinguishing six different sandstone patterns.



Fig. 1: details of the 6 different sandstone patterns.

The detailed sandstones on the previous photos are:

- a) Type 1: fine wine lees colour sandstone
- b) Type 2: coarse wine lees colour sandstone including rock fragments of several cm
- c) Type 3: fine red sandstone of restoration
- d) Type 4: yellow sandstone
- e) Type 5: grey-green sandstone
- f) Type 6: grey-green restoration sandstone

The episcopal group presents pathologies affecting stones in terms of sandstones reactivity in their environment but does not present structural disorder of masonries. Pathologies affect the different sandstone patterns, main damages consist of granular disintegration, craquele, scaling, moist area and salt resurgences.



Fig. 2: Details of craquele, scaling and granular disintegration patterns.

Craquele is a degradation level which evolves towards the scaling (Fig.2a and 2f); it is due to constraints which occur in stone subsurface, under the superficial epidermis part, on the total stone surface. The observed craquele pattern seems to be characteristic of a degradation mechanism due to intrinsic properties of the stone. The picture f detail shows that it is not significant of interactions with joint mortars. The picture e documents the yellow type 4 sandstone scaling. It shows that the more the stone is exposed to the imbibition-evaporation phenomena, the more it scales. The stone cutting in bumps on the bell tower enhances the degradation. Scaling affects the 6 sandstone patterns of the episcopal group of Fréjus; nevertheless, the grey-green of types 5 and 6 sandstones are particularly damaged. So craquele and scaling affect as much, and even in a spectacular way, the type 6 grey-green sandstone used in a recent restoration (less than 30 years ago). Besides, granular disintegration is a phenomena which widely affects the type 2 coarse wine lees sandstone (Fig. 2c), especially in capillary rising zones.

The analysis of the environmental context and the implementation of the masonries indicates that the damage expression strongly depends on the stone's orientation. Indeed, if epidermis are locally remained undamaged on the north and east façades, all of the sandstones of the south and west façades have scaled. Moreover, very important granular disintegrations occur in the lower part of the south baptistery façade, in possible area of capillary rising. We can also recognize two sandstone patterns which are mainly affected by a high level of decay: an original pattern of coarse sandstone (type 2) and a restoration pattern of fine sandstone (type 6).

2.2. Sampling

Type 1 sandstone being the most present on the episcopal group and particularly affected by damages and type 2 sandstones being the most strongly affected by damages, they can be considered as representative of the conservation issue of the episcopal group. So they have been used for the first characterization of the building sandstones. In addition, each specific sandstone pattern has been sampled to characterize stone properties and specific fraction in order to try to highlight discrimination factors. Sandstone fragments sampling

includes the different degradation stages in order to search the degrading agents. Stone powders have then been sampled in various areas of the episcopal group as well as in different heights and different depths to evaluate the salt contamination of the masonries.

2.3. Analysis

The characterization of the building sandstones includes petrographic analysis, vapour permeability, porosity and water capillarity according to the NF EN 1936 and NF EN 1625 (1999) standards. Microscopic observations have been performed on craquele and scaling patterns with a scanning electron microscope coupled with an EDX Phenom Pro X probe. In order to determine the dimensional variations of the different sandstone patterns with temperature and water exposures, the thermo-hydric dilations were measured. Clay activity of fine sandstone fraction (< 2mm) has been evaluated. The test consists in adding methylene blue to an aqueous suspension of the 0-2mm size fraction of the crushed sandstone, the solution adsorption is verified after each addition by determination of free colouring agent on filter paper according to the recommendations of the NF 933-9 standard. Salt analyses were performed with an ionic chromatography Dionex DX 120 according to the Italian "Normal 13/83" standard. Analyses have been performed by BPE laboratory (France).

2.4. Treatment tests

Clay stabilization and stone consolidation were tested on the types 1 and 2 sandstones. The size of the treated samples was of 10×10 cm² and type 1 and 2 sandstone samples with cohesive surface were selected.

Tab. 1: Protocol of the treatment tests.

Sample	Stone	1 st application	2 nd application
I EP-2	Type 1	Estel 1000 40% - Solvent 60%	Estel 1000 70% - Solvent 30%
II EP-2	Type 2	Brush in saturation	Brush in saturation
I KC-2	Type 1	Estel 1000 25% - Solvent 75%	Estel 1000 50% - Solvent 50%
II KC-2	Type 2	Cellulose compress (Arbocell)	Cellulose compress (Arbocell)
I AP-2	Type 1	Antihygro	Antihygro
II AP-2	Type 2	Brush in saturation	Brush in saturation

The used products for the trials are:

- Antihygro (Remmers) : solution based on buthlyldiammonium chloride permitting the stabilisation of swelling clays
- Estel 1000 (CTS) : consolidant based on tetraethoxysilane (TEOS) in solution with White-Spirit solvent; concentration is calculated in volume
- Compresses are made with cellulose fibers of type Arbocell BW40

3. Results

3.1. Sandstone characterization

3.1.1. Petrography and petrophysic

Type 1 sandstone is an arkosic and type 2 is a protoquartzite sandstone including 5 to 25 % of rock fragments, orthoses, micas and clays.

Tab. 2: Summary of petrographic and petrophysic analysis.

Parameters	Unit	Type 1	Type 2
Open porosity	%	10.5	15.3
Bulk density	kg/m ³	2216	2130
Water capillarity	g·m ⁻² ·s ^{-0.5}	37.7	24.7
Vapour permeability	g/m ² ·h·mmHg	0.167	0.457
Petrographic class		Arkosic sandstone	Lithic sandstone

Results are significant of distinct properties of the type 1 and type 2 sandstones. For an open porosity value 50% more important, the type 2 sandstone presents a vapour permeability 3 times more important than the type 1 sandstone, with a capillarity 30% lower. The comparative analysis of type 2 sandstone porosity and capillarity provides indications of the pore geometry that is a macroporal microstructure fitting with the coarse macroscopic appearance of this sandstone type.

3.1.2. Thermo-hydric dilation

The thermos-hydric dilation measures allow to evaluate the rock deformation potential under water and temperature exposures. Samples are gradually plunged into water and measures are made during 96 hours using a retractometer and a digital micrometric comparator. Concerning the thermic dilation, samples were exposed to a thermal interval of 60°C (from 20°C to 80°C).

Tab. 2 provides the reached values for the asymptote in stabilization phase for the 5 sandstone patterns; we cannot have a sample of sufficient size for the type 6 sandstone only present on the sculptures of the portal.

Tab. 3: Hydric and thermic dilation values.

Sandstone	Hydric dilation at saturation (mm/m)	Thermic dilation (K ⁻¹)
Type 1	0.20	3.16·10 ⁻⁵
Type 2	0.24	3.30·10 ⁻⁵
Type 3	0.11	2.60·10 ⁻⁵
Type 4	0.17	3.21·10 ⁻⁵
Type 5	0.14	3.88·10 ⁻⁵

The thermal dilation values are homogeneous while the hydric dilation values are very different according to the various sandstone patterns. The type 3 red sandstone used in restoration has a hydric dilation lower 45% than the type 1 wine lees sandstone and 54% than the type 2 wine lees sandstone which presents the most important hydric dilation value.

3.1.3. Clay fraction

The clay activity has been evaluated with the methylene blue test. The table 3 provides the adsorbed colouring agent weight for 100 g of dry 0-2 mm sandstone fraction. This try indicates at the same time the presence of clays in significant proportion in the different sandstone patterns and the swelling capacity of these clays adsorbing the colouring agent.

Tab. 4: Blue methylene values.

Sandstone	Blue methylene value (MB)
Type 1	0.40
Type 2	0.99
Type 3	0.34
Type 4	0.42
Type 5	0.34
Type 6	0.63

Moreover, the scanning electron microscope (SEM) permits to observe the in situ clay figures. Observations in the damaged areas of scaling indicate fracture formation where clay layers are opened (Fig. 3c).

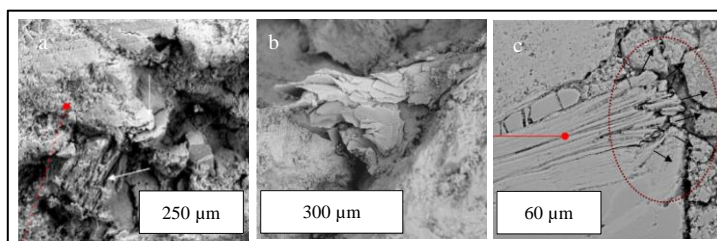


Fig. 3: SEM images of clays inside type 2, 5 and 6 sandstones.

3.2. Salt contamination

Quantification of cations (sodium and potassium) and anions (chloride, sulfates and nitrates) indicates a salt contamination especially on west and south exposures. Sodium (until 0.16% on scaling patterns) is associated to chloride (until 0.24%), indicating by there even the origin of the contamination due to the marine environment. Local contaminations, over stone conservation thresholds, are determined for the sulfates in the baptistery, on the south baptistery wall and under the bell tower cornice, in the bell opening intrados. Lastly, nitrates over threshold in the lower part of the façades and in the baptistery are significant of capillary rising.

3.3. Efficiency of the treatment and feasibility

Measurements of consolidant absorption and action depth by reaction to dithizone after reticulation show that microstructural differences between types 1 and 2 sandstones require specific application protocols; brush can be used for the type 1 sandstone but compresses must be used to reach a significant penetration depth for the type 2 sandstone which is significantly less capillary.

Tab. 5: Consolidation and clay stabilization effects on sandstone.

Sample	Absorption (g/cm ²)	Action depth (mm)	Porosity (%)	Water capillarity (g.m ⁻² .s ^{-0.5})	Vapour permeability, <i>D</i> (g/m ² .H.mmHg)
Type 1			10.5	37.7	0.167
I EP-2	0.0625	3	9.8	8.9	0.139
I KC-2	0.25	4	10.4	3.1	0.135
Type 2			15.3	24.7	0.457
II EP-2	0.0625	2	11.2	6.2	0.358
II KC-	0.25	5	9.4	4.5	0.363
			Penetration depth	Hydric dilation (mm/m)	
Type 1				0.20	
I AP-2	0.0625	5		0.13	
Type 2				0.24	
II AP-2	0.0625	3		0.15	

Consolidation test provides until 38% of porosity decrease for the type 2 while it provides until 7% of porosity decrease for type 1 sandstone. Vapour permeability is preserved in all consolidating protocols with around 20% of decrease which allows to preserving the fluid transfers. However, consolidation with tetraethoxysilane has a strong effect on water capillarity reducing it of 80-90%. Clay stabilization tests indicate a significant hydric dilation decrease of 35%.

4. Result analysis

Analytical investigations show that damages are due to combined factors. The saline contamination due to the marine environment, some local gypsum mortar use and capillary rising enhance the damages. Nevertheless important scaling is observed even in areas where the salt contamination is not significant.

	<i>Type 3</i> <i>Red</i>	<i>Type 5</i> <i>Grey-green</i>	<i>Type 4</i> <i>Yellow</i>	<i>Type 1</i> <i>Wine lees</i>	<i>Type 2</i> <i>Coarse</i> <i>wine lees</i>
Scaling thickness (mm)	a few mm	a few mm	2 to 5 mm	until 10 mm	until 15 mm
Hydric dilation (mm/m)	0.11	0.14	0.17	0.20	0.24

Fig. 4: Sandstone classification according to scaling thickness and hydric dilation.

Classification of the various sandstone patterns according to their common scaling thickness determined by on-site reading is correlated to the hydric dilation. More the scaling is thick or more the disintegration is strong, more higher the hydric dilation is; this is an intrinsic factor of the stones which is in relation with the clay activity. Indeed, most low clay activities are measured for types 3 and 5 sandstone and largely strongest clay activity is determined for the type 2 sandstone. The bar chart shows that the blue methylene value is a discriminant factor. If the various sandstone patterns have important clay activities, type 2 and 6 sandstones have significantly the most important values and these are the ones which react in the most spectacular way.

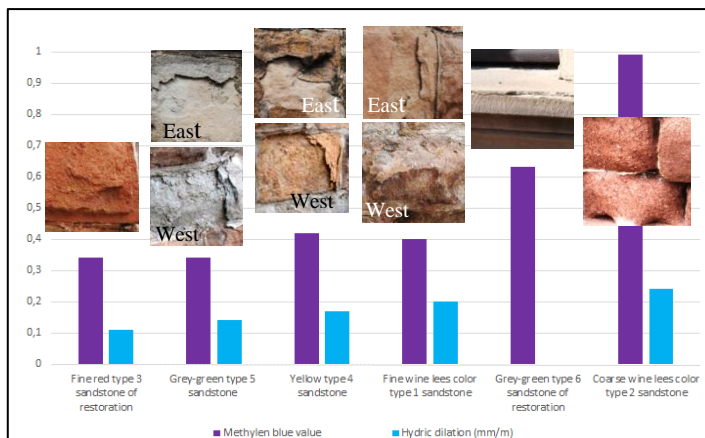


Fig. 5: Bar chart according to hydric dilation and methylene blue values.

5. Conclusions

Intrinsic property, especially hydric dilation related to clay activity, is the dominant factor in the damage mechanisms particularly craquele and scaling patterns but salt contamination and water transfers, such as capillary rising, are aggravating factors. Our study shows the feasibility of dilation stabilization by application of a solution based on buthlydiammonium chloride. Furthermore, the consolidating protocol tested to enhance the sandstone cohesion leads to capillarity reduction while preserving fluid transfers thanks to permeability. Capillarity reduction is a side effect of the tetraethoxysilane treatment which is favorable to the conservation of such sandstones containing swelling clays. However, tests indicate the impact of the application protocol on the depth of penetration. Buthyldiammonium chloride has a significant effect on the hydric dilation decrease but the penetration depth remains weak with regard to the scaling thickness. Laboratory tests are encouraging for the treatment feasibility; nevertheless, they will be extended by a next on-site experimental restoration phase on several limited areas of masonries which must be desalinated before the treatment.

References

- Berthonneau J., 2014, Le rôle des minéraux argileux dans la dégradation de la pierre, Ph.D. thesis, University of Aix-Marseille, France.
- Mertz J.D., 2006, Salt damage, dilation and actual practices in sandstone conservation, Colloque des architectes de cathedrals à Strasbourg, 153-156.
- Furlan V., Félix C., Queisser A., 2000, La pierre du portail peint de la cathédrale de Lausanne : nature, état de conservation et consolidation, 9th Int. Congress on Deterioration and Conservation of Stone, Venice, vol 2, 633-640.
- Félix C., 1995, Peut-on consolider les grès tendres du plateau Suisse avec le silicate d'éthyle, "Conservation et restauration des biens culturels, Montreux, 266-274.

THE POLYCHROMED BETHLEHEM PORTAL OF HUY, BELGIUM: EVALUATION AND MAINTENANCE OF A 25 YEAR OLD TREATMENT

J. Vereecke^{1*}, L. Rossen², K. Raymakers² and M. Stillhammerova¹

Abstract

Built around 1430 at the entrance of the cemetery of the Collegial of Huy, the Bethlehem portal has been modified and restored many times. The Royal Institute for Cultural Heritage (KIK/IRPA) carried out the last restoration in 1988-1989. Twenty five years later, in 2014, a maintenance treatment of the portal was decided upon at the end of the global restoration of this side of the collegiate church. In addition to the conservation treatment, this was also a unique opportunity to evaluate the efficiency of the previous 1988-89 treatment. We examined the reports and work site diaries to have a clear idea of the state of conservation before this treatment and to understand the materials, methods and techniques of the treatment itself. The conservation state of the portal, and therefore the efficiency of the past treatment was firstly evaluated through visual observation. To the unaided eye it appeared perfect except for decolouration of the blue wash layer applied on the background. The purpose of this maintenance treatment was to return the portal to its condition after the restoration of 1988-89 by light removal of dust and a soft superficial cleaning. Even if the 25 years old treatment might nowadays be considered as quite “heavy” (products used and the methods applied) and would not be employed these days, we must admit that it did, and still does work perfectly well.

Keywords: ethyl silicate and epoxy consolidations, acrylic and PVA as fixatives for polychromies, water repellent, old treatment evaluations

1. Introduction

Built around 1430, the Bethlehem portal has been modified and restored many times. The last restoration realised by the IRPA/KIK in 1988-1989 was published in de VI international congress on deterioration and conservation of stone of Torun in 1988 (De Henau *et al.*, 1988). Twenty-five years later, in 2014, a maintenance treatment of the portal was decided upon at the end of the global restoration of this side of the collegiate church. In addition to the conservation treatment, this was also a unique opportunity to evaluate the efficiency of the previous 1988-89 treatment. We examined the reports and work site

¹ J. Vereecke* and M. Stillhammerova
Jacques Vereecke sprl, Belgium
jacquesvereeckesprl@hotmail.com

² L. Rossen and K. Raymakers
Vof Raymakers-Rossen, Belgium

*corresponding author

diaries to have a clear idea of the state of conservation before this treatment and to understand the materials, methods and techniques of the treatment.

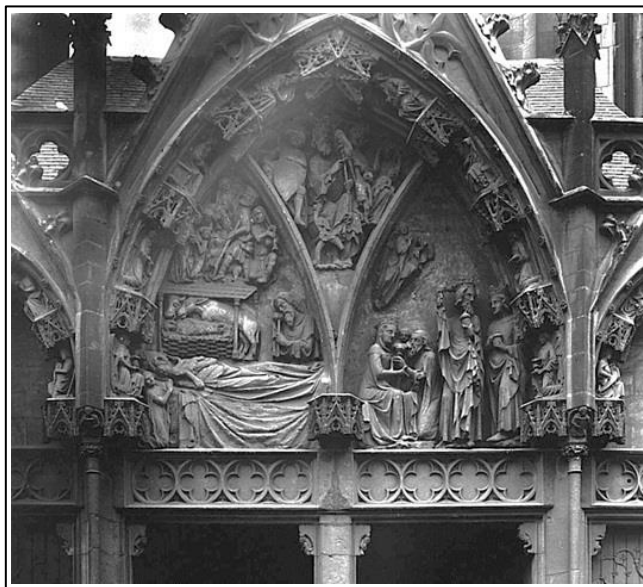


Fig. 1: Portal in the 1930, © KIK/IRPA, Bruxelles.

2. Conservation state before 1988-89 and this treatment

The portal is originally built with three kinds of stone. The base and lintel was carved from local blue limestone. For the arches and sculptures, a softer material was chosen: an organoclastic Bajocian yellow limestone quarried in Dom-le-Mesnil. The background of the portal consists of Maastrichtian limestone (soft bioclastic calcarenite of the Upper-Cretaceous) briquette carefully jointed. The bed of the Virgin is also carved in this stone. When restored in 1890, they substituted deteriorated original stone with an oolitic Bajocian limestone (French Jaumont limestone). The blue stone and the stone of Jaumont were in good condition. The Maastrichtian limestone did not suffer from sulfatation but shows disintegration and was strongly eroded. The Dom-le-Mesnil stones show a lot of sulfatation decay such as blistering and micro cracks. Salts analyses showed the presence of sodium, ammonium and calcium phosphates and sulphates. Layers of whitewashes covered the original polychromy, all sensitive to water.

The first step of the treatment consisted of taking away pigeon's nests and excreta. Then the salt crystals on the surface, the encrustation of dust and the whitewashes were removed mechanically. During this procedure, the original polychromy was fixed, and the stone was consolidated where necessary. At first, the stone consolidation was carried out by injecting ethyl silicate (Goldschmidt Tegovacom V). After unsatisfactory result, it was decided to consolidate with injections of epoxy resins (Araldite AY 103-HY956 diluted with methanol 10%). These operations were repeated until the desired result was achieved. A mortar composed of lime stone powder mixed with pva emulsion (10%) was used. The background

was overpainted with a blue paint composed of a mixture of casein and lime with blue pigments. As finishing layer, a water-diluted silicone was applied over all the surfaces of the portal. For protection against pigeons, a nylon net with 3 centimetres square was placed.



Fig. 2: Portal after treatment in 1989, © KIK/IRPA, Bruxelles.

3. Understanding the methodology of treatments applied in 1988-89

Given the very good state of conservation after 25 years where no evidence of any kind of decay was visible, we decided it was too interventionist to make any destructive analyses. However, for a better understanding of the conservation status we thought it was important to map in diagram form the treatment done in 1988-89. In the interest of continuity and comprehension we employ the same format used at that time in the treatment reports and worksite diaries including written notes and drawings / diagrams. This compilation concerns only information about the consolidation of the stone and fixing polychromy and the application of the water repellent.

3.1. Stone consolidation

It was carried out in several partial stages corresponding to the areas where the restorers were working. Some areas have been consolidated once, others up to five times, with a minimum period of three weeks between applications, which mean that the silicate was completely polymerized before the new application. We find also mentions of a much-localized consolidation with a mixture of ethyl silicate (Wacker OH) supplemented with Paraloid B72. We do not know when that treatment was performed: before, during or after the individual impregnation with ethyl silicate, but we think it is probably just a test and that this type of treatment was not used. Some elements were not consolidated with ethyl silicate (based on documents consulted). The result after five campaigns of impregnations was considered insufficient and (after testing), consolidation with epoxy resin (AY103 / HY956) diluted in methanol (100 cc resin diluted with 20 cc of solvent) was decided upon. The consolidation with the epoxy resin was not applied everywhere, which implies that the condition of some of the stones were found to be sufficiently good (unless there is a gap in the reports).

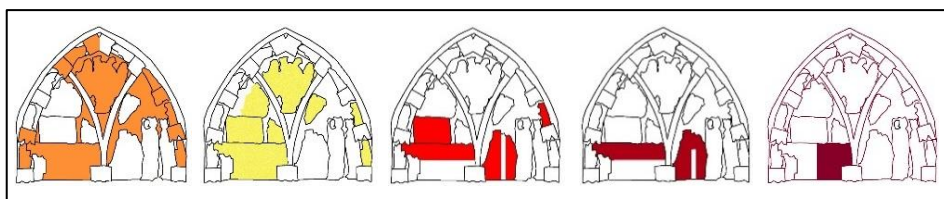


Fig. 3: Localisation of the five treatments with ethyl silicate.

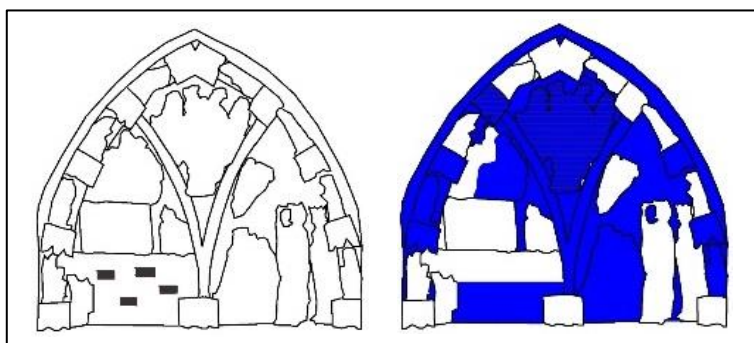


Fig. 4: Localisation of the treatment with a mixture of ethyl silicate supplemented with Paraloid B72 (left) and consolidation with epoxy resins (right).

3.2. Fixation of the Polychromy

Polychromy was fixed with PVA glue. When necessary, the fixing was repeated, so some areas have been treated many times. It is mentioned that following repeated fixing there was the formation of a whitish film on "Joseph". One restorer used an acrylic adhesive (Primal AC33) to carry out fixation. The diagrams show the areas mentioned in the documents. It must also be considered that these are maybe local fixings and therefore not

necessarily the complete 'shaded' area was treated. From our observations, not all the areas treated have been recorded in the treatment documentation. The current state of the polychromy is very good. We have not found any lifting paint, or a disturbing whitish veil (bloom).

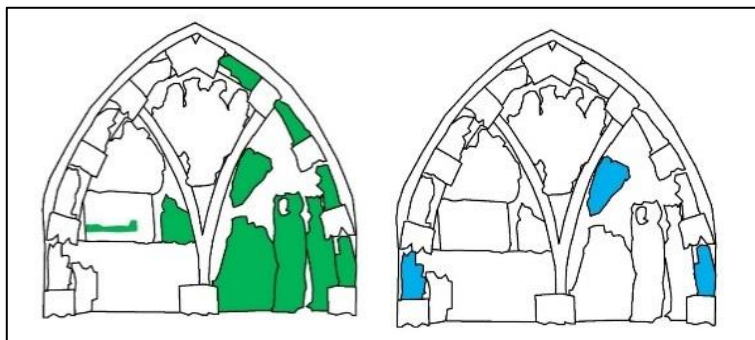


Fig. 5: Localisation of the treatment with PVA (left) and Acrylic (right).

3.3. Water-repellent treatment

After a satisfactory test, it was decided to apply the water-repellent on all surfaces of the portal. The product used was R d sil S. We found the water repellent present and active on all surfaces. It certainly played an important inhibitory role against weathering elements, the formation of black crusts (sulfatation) and the attachment of dirt deposit.

3.4. The blue background

The blue lime wash applied on the background is the only intervention that has not aged well. It has discoloured to a green-greyish tone. Lime wash, made with lime caseinate and a blue pigment was applied in order to restore a sufficiently homogeneous background to push the sculptures into relief.

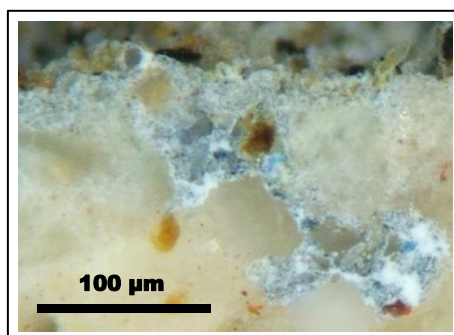


Fig. 6: Microphotograph of cross-section of blue background (optical microscopy using reflected light).

The pigment used was not mentioned in the report but SEM/EDX and Micro Raman spectroscopy analyses of the rests of blue still preserved in the depth of the stone proved the presence of cerulean blue and titanium IV oxide (rutile type). As Cerulean blue, cobalt tin

oxide CoSnO_3 is considered to be a very stable pigment, the discoloration of surface paint layer could only be explained by degradation and yellowing of the lime-casein medium used.

4. Maintenance treatment in 2014

The goal of the maintenance treatment was to return the portal to the state in which it was immediately after the 1988-89 treatment. The dirt was superficial and not compact and had little cohesion. We tested soft, dry pencil erasers. After several tests, we selected the 'Firm gum Milan, the pan miga 4020'. This is a pencil eraser made from a synthetic rubber compound having a neutral ph. The entire portal was cleaned using this method except the background, which was too fragile. The three lower baldaquins, having more compact dirt, could not be successfully treated with the erasers. Areas where superficial dirt showed greater cohesion, mainly in the lower part of the ogive and more particularly in areas with horizontal surfaces, another cleaning method had to be determined in order to achieve a uniform cleaning of the whole portal. First we tested solvents and solvent mixtures based on Dr. Masschelein-Kleiner's list (1981). Despite the water sensitivity of polychromy layers as described in the reports we dared test solvents and gels containing water because of the presence of a water repellent. Only mixtures of isopropanol / ammonium hydroxide and water (90/10/10 and 50/25/25) gave results, dissolution of dirt, but the friction of the cotton swab caused a significant abrasion of the polychromy layer. Secondly, we tested solvent gels with the idea to limit the friction. Gels posed the problem of their elimination: gel residue remained on polychromy surfaces. Following the disappointing and unsatisfactory result, we decided to test the micro sandblasting with low pressure and mild abrasives (calcite and glass micro balls) or very fine alumina oxide (240 mesh, 320 mesh and 400 mesh). This proved a good solution: regular and easily controllable. The cleaning was performed with a Sand master machine speed of 3, an outlet nozzle with a diameter of 1.2 mm, a pressure of 1 bar and an alumina oxide 320 mesh.

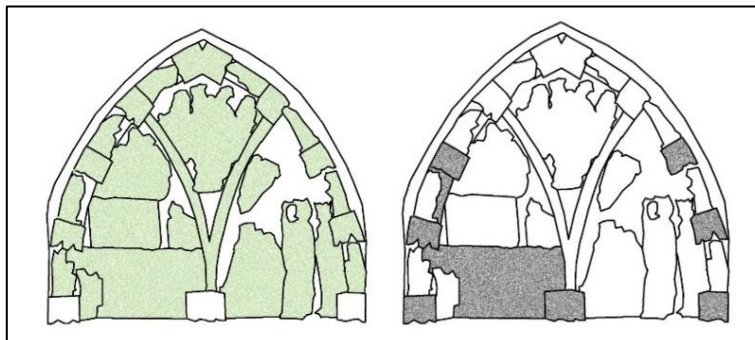


Fig. 7: Localisation of the treatment with 'soft rubber pencil eraser' (left) and micro sandblasting (right).

Before retouching the background, it was important to evaluate the effectiveness of the repellent. To do this, we initially made a water flow test on the surface. In view of the rapid percolation without water absorption, we decided to place Karsten pipes. They were applied for ten minutes without any absorption! This proves that the repellent was still active. Due to the presence of the water repellent, retouching, usually made with water-based products, was problematic. They were restricted to a reintegration of the current green / blueish

background. Retouching with lime wash was not considered because of the water repellent. We tested silicates products (Beeck), acrylic (Golden), but they formed an unsightly film which remained visible after drying. We tested gouache paint which gave a satisfactory cosmetic result. However, because of worries concerning the adhesion of the gouache to the background, we tested this by rubbing the dry gouache with a wet micro-sponge: the gouache was resistant to this. Therefore we retouched the most important gaps with gouache.

5. Conclusions

Following the conventions of today, we probably would not use the same methods, materials and techniques as in this 1988-89 treatment, however, one cannot fault their results. The fixing of the polychromy is still good; stones and mortars repair are in a good state of preservation; the water repellent is still active. Only the painted background presents colour alterations from blue to greenish grey. There are few localized zones, well protected, which present a blue appearance probably close to the original state of the whitewash applied in 1989. The maintenance treatment with its main goal of going back to the state after the restoration of 1988-89, was achieved with a light removal of dust, soft superficial cleaning treatment and a retouching treatment of the discoloured blue background.



Fig. 8: Portal after maintenance treatment in 2014.

Acknowledgements

We would like to thank the restorers of the stone workshop of the KIK/IRPA to allow us to consult all the data concerning the treatment executed in 1988-89.

References

- De Henau, P., Van Molle, M. and Annaert, M., 1988, Etude et conservation du portail polychrome dit de Bethléem à Huy”, Proceedings of the 6th international congress on deterioration and conservation of stone, Torun, Ciabach, J. (ed), Nicholas Copernicus University Press Department, 680-686.
- De Henau, P., Annaert, M., Kockaert, L. and Van Molle, M., 1995, in Le portail polychrome dit “Le Bethléem” à Huy, Extrait du Bulletin de l’Institut royal du Patrimoine artistique, XXV, 1993, Bruxelles.
- Masschelein-Kleiner, L., 1981, Les solvants, Cours de conservation 2, Institut Royal du Patrimoine Artistique, Bruxelles.

EXPLORING THE PERFORMANCE OF POMPIGNAN LIMESTONE AS EXTERIOR CLADDING AND PAVERS IN THE MID-ATLANTIC REGION OF THE UNITED STATES

R. Wentzel^{1*} and M. Coggin¹

Abstract

Herein presented is a case study outlining an investigation of the suitability of Pompignan limestone as an exterior finish at an unnamed, architecturally significant installation. Included in this study are the forensic investigation techniques employed as well as results from petrographic examination and analysis involved. Also provided are descriptions of the methods by which the stone was installed as exterior pavers and as exterior wall cladding. Ultimately, this case study concludes that Pompignan limestone has several inherent characteristics which negatively affect its performance and durability in exterior exposures in regions subject to freeze/thaw cycles matching that of the mid-Atlantic region of the United States. Specifically, stylolite features found in the limestone enable moisture entrapment, leading to freeze/thaw damage. The freeze/thaw expansion propagates parallel with the face of the stone along microscopic vein features filled with secondary mineralization. The net result of both occurrences is a reduction in strength and durability of the Pompignan limestone installed and exposed per this case study.

Keywords: limestone, Mid-Atlantic, Pompignan, performance, stylolite

1. Introduction

This paper discusses the findings and conclusions of an investigation into the causes and origins of catastrophic cracking in Pompignan limestone installed as exterior pavers, cladding, and capstones in the Mid-Atlantic geographic region of the United States. Both installed and attic stock examples of pavers and cladding from the project were acquired for purposes of petrographic analysis. This analysis was undertaken with the goal of determining both the causes of the cracking and the appropriateness of Pompignan limestone for use as an exterior finish within the region in which it was installed. Capstones were not removed for analysis.

2. Existing Conditions

Thermally finished Pompignan limestone pavers sized 55.9 cm square by 5.1 cm thick (22" square by 2" thick), mounted on plastic composite shims atop pedestals, with open joints, were encountered at the project location. Failed pavers exhibited cracking and/or delamination.

¹ R. Wentzel* and M. Coggin,
Thornton Tomasetti, Inc., United States of America
rwentzel@thorntontomasetti.com

*corresponding author



Fig. 1: Typical failed paver.

Thermally finished Pompignan limestone cladding sized 55.9 cm by 29.8 cm by 4.13 cm thick (22" × 11 3/4" × 1 5/8") installed on stainless steel anchors grouted into field cut kerfs were encountered at the project location. Façades featuring Pompignan limestone were built as cavity walls, acknowledging the fact that moisture will work its way through the limestone veneer. Approximately 3.5 cm (1 3/8") of air space was left between the veneer and waterproofed insulation board on CMU serving as a structural exterior wall. A flexible backer rod was installed in each joint between each individual stone, and silicone sealant applied in front of the backer rod to a plane virtually flush with the surface of the stone cladding. Failed cladding stones exhibited vertical cracking or semi-circular cracking at the kerfs.

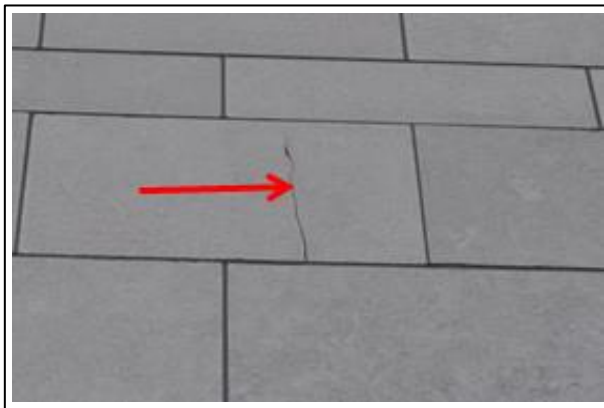


Fig. 2: Typical failed cladding.

Encountered at the project location, but not analysed, were thermally finished Pompignan limestone coping stones. Featuring various lengths, the coping stones measured 27.9 cm (11") wide, 9.4 cm (3 11/16") thick on the high side and 8.1 cm (3 3/16") on the low side.

3. Material Testing

Based on observations of deterioration in the paving, cladding, and cap stones, petrographic analysis of pavers and cladding stones was undertaken in an effort to determine causation of observed deterioration. Selected representative samples of cladding and pavers were acquired from the project owners on site attic stock. Two fragments from broken kerf spalls, a piece of cladding, and a paver removed from in situ were also acquired. Tab. 1 describes 12 pieces submitted for petrographic analysis.

Tab. 1: Matrix showing material application, area from which it was obtained and size.

Sample ID	Location	Dimensions (cm)	Dimensions (in)
Cladding 1	Attic Stock	55.9×29.8×4.1	22×11.75×1.6
Cladding 2	Attic Stock	55.9×29.8×4.1	22×11.75×1.6
Cladding 3	Attic Stock	55.9×29.8×4.1	22×11.75×1.6
Cladding 4	Attic Stock	55.9×29.8×4.1	22×11.75×1.6
Cladding 5	Attic Stock	55.2×29.8×4.1	21.75×11.75×1.6
Cladding 6	Attic Stock	55.2×29.8×4.1	21.75×11.75×1.6
Paver 1	In situ	55.9×55.9×5.1	22×22×2
Paver 2	Attic Stock	55.9×55.9×5.1	22×22×2
Paver 3	Attic Stock	55.9×55.9×5.1	22×22×2
Sample #1 (Shard)	In situ	Spall – 15.9 length	Spall – 6.25 length
Sample #2 (Shard)	In situ	Spall – 15.2 length	Spall – 6 length
Cladding 7 (Stone)	In situ	30.5×22.9×4.1	12×9×1.6

3.1. Petrographic Facilities

Highbridge Materials Consulting, Inc., Pleasantville NY provided petrographic examination and analysis of the stone pavers and cladding.

3.2. Analysis/Test Sample Selection Criteria

The cladding from the Owner's attic stock had been stored outside in a vertical orientation. These unit items were highly desirable for analysis purposes as they shared both of those characteristics with installed cladding, although kerfs for anchors had not been cut.

Owner's paving attic stock was also stored outside stacked in a horizontal orientation, again mimicking the installed position of these units and again providing a highly desirable item for analysis.

Units selected from attic stock represented the most pristine examples remaining in stock and featured undamaged edges and no visible cracking. Units removed from in situ were selected due to obvious cracking. Analysis of attic stock material presented an opportunity

to view stone characteristics with stresses limited to those related to water absorption, thermal cycling and in situ stress relief following quarrying.

4. Analysis and Testing Results

4.1. Petrographic Analysis

Petrographic examination was conducted in accordance with ASTM C 1721. The analysis and interpretation was performed by an ASTM C 956 Section 4 qualified petrographer.

4.1.1. Visual Appearance

All samples received were similar in appearance, presenting as a dense, compact limestone with medium greenish grey colour. Fresh surfaces (intended for exposure when installed) were uniform with a lithographic to slightly grainy texture. Fresh surfaces also showed as roughly planar with a slight textured relief. Faint linear ripples with very low relief were just visible at the surface when viewed under low angled lighting:

- The remaining five surfaces in full dimensioned samples were cleanly saw cut.
- No bedding surfaces, sedimentary laminations, or other depositional structures were visible in the samples. Veins or other secondary mineralizations were not visible in the samples.

4.1.2. General Summary of Petrographic Findings

Sample analysis revealed a dense calcitic limestone with no petrographically observable microscopic pore structure. The stone exhibited a fine grain, homogeneous texture. No distinct bedding fabric was found to be present.

Original geological structures were noted to be present as two localized planar elements. Both elements can be considered as discrete planes of relative weakness and also as avenues for moisture infiltration through an otherwise dense and cohesive limestone matrix. Stylolitic cleavage is one structural element present in an orientation both parallel and perpendicular to the stone face, though the former appears dominant. Microscopically thin calcite veins represent the other type of structure present; however these veins manifest strictly in a perpendicular orientation to the stone face and are not visible to the eye in the samples.

4.1.2.1. Stylolites

A stylolite is a type of geological cleavage across which dissolution has occurred during compaction of the original sediment. Insoluble matter such as clay and other silicates collect at the dissolution plane. Stylolites in the stones examined manifested as saw toothed bands in both horizontal and, less commonly, vertical planes as oriented to the intended exposed face of the stone. The more notable stylolites usually presented as a single continuous to semi-continuous seam located somewhere between mid-depth and the inside surface of the stone. Stylolites within the plane of paving stones were noted to exhibit a series of incipient microcracks oriented parallel to the stone face in its installed position.



Fig. 3: Microcracks parallel to stone face.

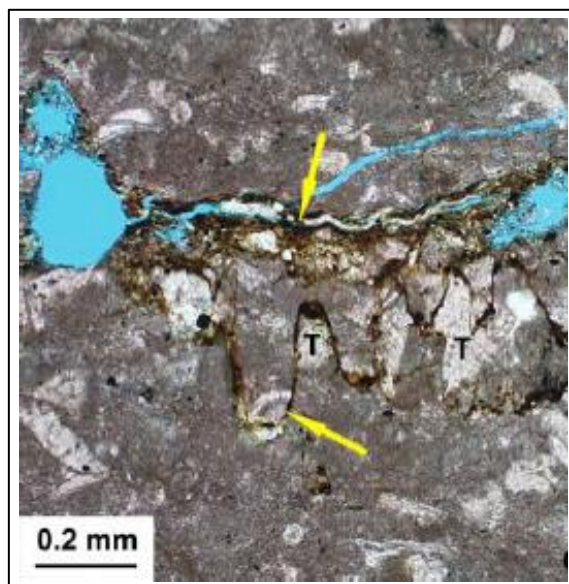


Fig. 4: Stylolite feature. Arrows indicate saw tooth nature of stylolite.

4.1.2.2. Veins

Veins are geological crack openings that have healed with secondary mineralization. These are not visible to the eye in the samples and were only identified petrographically. Veins manifested in the stone roughly perpendicular to the finished stone surface in thin sets of two or three closely spaced planes. Vein spacing is unknown; however one set is found in almost every linear inch of material subjected to petrographic study. Vein thickness ranges from approximately 0.025 to 0.075 millimetres (0.00098 to 0.00029 inches).

All veins are filled with secondary calcium carbonate that is coarser grained than the calcite found in the adjacent host stone. Due to the thinness of the vein structure, only two or three crystals are generally found across the vein width. It was observed in examples exhibiting cracking from service that said cracks almost always follows a path between individual crystals.

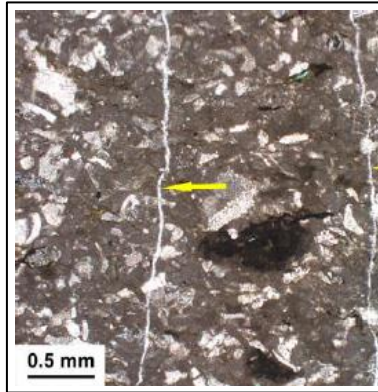


Fig. 5: Calcite healing at petrographically observed vein (shown at arrow).

5. Failure Modes

5.1. Paver Cracking

Two failure modes were identified in paving stones; both are closely related to the pre-existing geological structure. One is a fracture that splits the stone coincidental with a microscopic vein set. The other is an incipient in-plane crack with secondary gypsum crystallization coincidental with main stylolitic surfaces.

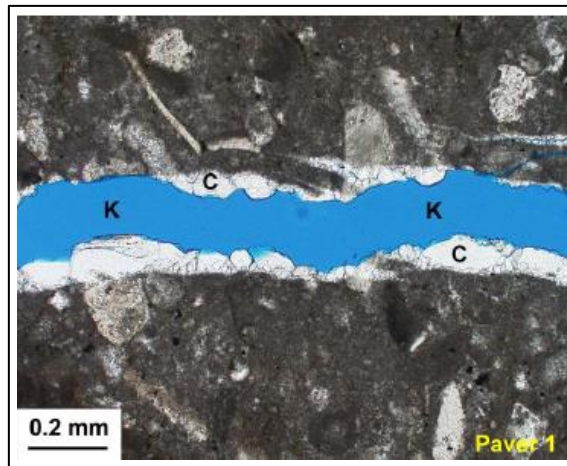


Fig. 6: PPL photomicrograph revealing nature of failure at paver crack. The crack was epoxied together (blue area) for sample preparation.



Fig. 7: Typical delaminated Paver.

5.2. Cladding Cracking

Microcracks present within the stone structure represent an incipient plane of weakness oriented parallel to the stone face. Crack opening thicknesses are approximately 0.025 millimetres (0.00098 inches).

5.3. Miscellaneous

Pyrite and glauconite are present in all of the petrographically examined stone. Both minerals are capable of oxidative weathering producing a red iron oxide that could manifest as “rust” spots.

6. Conclusions

Based on the petrographic analysis completed at our direction, it is apparent that Pompignan limestone used as exterior paving and cladding in the Mid-Atlantic region of the United States exhibits several characteristics that negatively impact its performance and durability. These undesirable characteristics include stylolite and vein geologic features.

As Pompignan limestone is exposed to moisture and cyclical freeze/thaw, the stylolite features allow moisture to penetrate the stone. This moisture freezes and expands, opening a crack at the stylolite which results in more moisture being able to penetrate the stone. The typical multicyclic freeze/thaws that occur in the winter and spring in the Mid-Atlantic region of the United States exacerbate this condition.

Pompignan veining features have lower-strength value than the surrounding stone. At the case study location, paver failure was always coincidental with veining, as was coping stone failure, said failures which occurred solely under the self-weight of the stone.

Based on the forensic efforts outlined in this case study in combination with the relative petrographic analysis, we opine that the presence of open seams is fully attributable to the characteristics of the stone and not to failures in the installation method. The use of Pompignan limestone for exterior paver installations on pedestals and as exterior cladding in regions with a climate similar to the Mid-Atlantic region of the United States is not recommended.

This page has been left intentionally blank.

ABSTRACTS

This page has been left intentionally blank.

CONSERVATION:

**MECHANISMS OF CARBONATE-OXALATE
TRANSFORMATION:
EFFECTIVENESS OF PROTECTIVE TREATMENTS FOR
MARBLE BASED ON OXALATE SURFACE LAYERS**

A. Burgos-Cara^{1*}, C. Rodríguez-Navarro¹ and E. Ruiz-Agudo¹

Abstract

The widespread distribution and the severity of the weathering processes suffered by numerous stone-built historical and artistic complexes of our cultural heritage make it crucial to undertake conservation strategies for the stone materials in these monuments, in order to preserve them for future generations. In particular, the design of treatments that protect the surface of carbonate rocks (e.g. marble) from etching by acidic or saline solutions is an urgent need. Current urban atmospheres, with a high concentration of pollutants such as SO₂ and NO_x, are a significant hazard for building elements made of carbonate stone due to their susceptibility to chemical attack. Since ancient times, oxalate patinas formed on building elements have had an important protective role over these materials. Nowadays, because of the current high levels of pollution in urban and industrial centres, the proliferation of microorganisms that excrete oxalic acid during their metabolism and the formation of protective oxalate patinas related to the activity of such microorganisms has declined, which adds to the own negative side effects of harmful contaminants. The poor knowledge on the mechanisms controlling the carbonate–oxalate transformation at the nanoscale, as well as the lack of an in-depth understanding of the factors that determine the extent of coverage or adhesion of the oxalate layers to the carbonate substrate has limited the development of effective procedures for marble conservation that mimic the natural process of oxalate patina formation. It is the aim of this work to investigate the mechanism of the replacement of calcite and dolomite by calcium oxalate, as well as to evaluate the effects of pH, oxalate concentration, and fluid-to solid ratio on this transformation. With this idea, the formation of calcium oxalate protective layers on the surface of two types of marble (a calcitic marble -Macaoel White- and a dolomitic marble -Yellow Triana-) as a possible protective treatment to chemical dissolution processes are studied in this work. This has been done by a combination of Scanning Electron Microscopy (SEM), bidimensional X-Ray Diffraction (2D-XRD) and Atomic Force Microscopy (AFM) techniques. Finally, the efficacy of such a treatment as a protective protocol for marble surfaces was assessed by performing water absorption and drilling resistance tests, by determining the resistance to acidic solutions and the colour variation after the oxalate treatment. The textural evidence found in this research show that the replacement of calcite and dolomite by calcium oxalate (whewellite) is an interface-coupled dissolution-precipitation reaction. Calcite and dolomite pseudomorphs were

¹ A. Burgos-Cara*, C. Rodríguez-Navarro and E. Ruiz-Agudo
Departamento de Mineralogía y Petrología, Universidad de Granada, Spain
aburgoscara@ugr.es

*corresponding author

obtained under acidic conditions, when spatial coupling between the dissolution of carbonates and nucleation and growth of whewellite occurs. Also, the existence of structural similarities between calcite and whewellite appears to result in the promotion of whewellite crystallization, since the formation of other Ca-oxalate phases was not detected in our experiments. Experiments performed using marbles cubes as substrates demonstrate that these layers effectively protect carbonate surfaces from chemical weathering, without significantly affecting the water properties of the stone, maintaining the coherence with the substrate and being only slightly perceptible to the human eye.

Keywords: oxalate, marble, protective patinas

CONSERVATION:

PRESERVATION OF BUILT CULTURAL HERITAGE USING NANOTECHNOLOGY BASED COATINGS: RESPONDING TO CONSERVATION VALUES?

J.J. Hughes^{1*}, L.P. Singh², P.C. Thapliyal², T. Howind¹ and W. Zhu¹

The application of surface treatments on buildings is common, to protect or to functionalise surfaces (e.g. consolidation, water repellence, self-cleaning). Many applications clearly have performance and sustainability benefits for mainstream construction. This is also the case for the built Cultural Heritage, though inappropriate application of materials has been blamed in the past for damage to buildings. Conservation philosophy emphasises the safeguarding of original material fabric, and the preservation of age value, through the maintenance of authenticity and integrity, and often appearance and function. This implies that the replacement of old materials with new in cultural heritage objects, is a special case. The same criteria for specification or for measuring a successful outcome compared with repairs to non-historic structures, where newness or visibly improved function is valued, do not apply. The application of coatings and treatments that penetrate into a surface layer to alter the properties of a material is a sensitive subject for heritage objects. Such material applications are subject to (well established) criteria for the selection of treatments, including that it has no effect on appearance, be re-treatable or that it should even be reversible. Any surface treatment should of course also achieve the desired physical affect, which is usually to overcome loss of cohesion between constituents, to improve durability and to be compatible with the historic fabric. However this is achieved, the application of any treatment should not adversely affect the authenticity of the object or building. Drawing on other work, we can show that perceptions of authenticity are however, contextual, and that practitioners attach great importance to operational parameters such as health and safety alongside material performance characteristics. Therefore decision support for choosing treatments, may need to accommodate this variability in the criteria for selection, not just on the basis of material performance characteristics. In addition, a full understanding of the aesthetic, mechanical and physical properties of surface coatings, in addition to the practical application methods and risks is important and needs to be defined for untried coating formulations, especially in Cultural Heritage applications.

Keywords: coating, conservation values, cultural heritage, nanotechnology

¹ J.J. Hughes*, T. Howind and W. Zhu
School of Engineering and Computing, University of the West of Scotland, Paisley, Scotland,
United Kingdom
john.hughes@uws.ac.uk

² L.P. Singh and P.C. Thapliyal
Organic Building Materials Group, CSIR-Central Building Research Institute, Roorkee, India

*corresponding author

CONSERVATION:

**INNOVATIVE DEVELOPMENTS IN THE FIELD OF STONE
CONSERVATION BY THE ACRYLIC RESIN TOTAL
IMPREGNATION PROCESS OF NATURAL STONES BY THE
JBACH COMPANY**

G. Scholz¹, R.J.G. Sobott², H.W. Ibach¹

Abstract

The complete saturation of historically and culturally valuable stone monuments and sculptures with MMA (methylmethacrylate) and the subsequent polymerization in the pore space of the object is carried out by the JBACH company for 40 years. More than 20,000 stone objects with a wide range of petrophysical parameters were conserved in this time period. Well-known examples are sculptures from the Cologne Cathedral, Sanssouci Palace in Potsdam or the Royal Palace of Huis ten Bosch in The Hague. Compared to the standard impregnation process with 100% MMA the new development is based on a decrease of the monomer content in the impregnation solvent (formulations A and B) which as a principal innovative feature reduces the polymerization temperature below 80°C and consequently the thermal strain in the objects. The petrophysical properties of weathered rocks, sandstone as well as marble, benefit very much from the conservation process with respect to the mechanical strength and capillary water uptake. For instance, the flexural strength of the fine-grained Udelfanger sandstone is raised from 4 to more than 34 N/mm², while the capillary water uptake is reduced from 9 kg/m²·h^{0.5} to practically nil. The optical microscopy of thin sections of this sandstone after conservation reveals a lining of the pore walls with PMMA which effectively seals the pore throats against the infiltration of water, while the central parts of larger pores remain open. In the case of marble we no longer observe a complete filling of the slit-like pores with PMMA containing small vacuoles but delicate cellular PMMA structures instead. The results are no less than a great improvement of the already very successful and efficient acrylic resin total impregnation process and of great importance for the preservation of cultural heritage in the form of stone objects. The successful conservation must be completed by a professional installation of the objects at their original site which avoids rigid emplacement and guarantees compensation of possible thermal strain by expansion joints.

Keywords: acrylic resin, marble, conservation, Udelfanger sandstone, total impregnation

¹ G. Scholz* and H.W. Ibach
JBACH GmbH, Scheßlitz, Germany
g.scholz@ibach.eu

² R.J.G Sobott
Labor für Baudenkmalpflege Naumburg, Naumburg (Saale), Germany

*corresponding author

DIGITISATION:
MONUMENTUM:
DIGITAL 3D MODELLING AND DATA MANAGEMENT
FOR THE CONSERVATION OF DECORATED STONE BUILDINGS

L. De Luca¹, J.-M. Vallet^{2*}, P. Bromblet², M. Pierrot-Desseilligny³,
X. Brunetaud⁴, F. Dubois⁵, M. Bagneris¹, M. Al Mukhtar⁴,
F. Cherblanc⁵, O. Guillon² and J. Tugas⁶

Abstract

The investigations that are made on a building for conservation purposes need an important work that is transcribed in a variety of numerical and printed data: surveying data and scientific imagery, damage mapping, photographic collections, historical archives, physical and chemical data etc. Given the difficulty to collect, compare, analyse and validate data prior to restoration, the approach we present aims to mobilize various disciplines (architecture, conservation, mechanics, and computer sciences) to define a novel information processing chain including metric surveys, analysis of surfaces, geometric models of structures, heterogeneous documentary sources management, temporal data, etc. By the way of MONUMENTUM project which is an on-going research project (2013-2017) funded by ANR (French National Agency for Research), we are designing and developing an open and expandible web platform for the capitalisation and the management of knowledge needed for the understanding and analysis of degradation phenomena affecting historic buildings. This objective requires the definition of a common and continuous process that establish a technological and conceptual interconnection between the stages of 3D digitization, semantic annotation and structuring of the geometric model (including multi-layers analysis of surfaces), characterisation of the state of the building and management of restoration actions. Based on three case studies that present conservation issues on stones (Castle of Chambord and Caromb's church in France) and wall paintings (Notre-Dames des Fontaines' chapel in France), it concerns the image-based-modelling of architectural heritage, the development of a 3D information system for the

¹ L. De Luca and M. Bagneris
UMR CNRS/MCC « MAP », Marseille, France

² J.-M. Vallet*, P. Bromblet and O. Guillon
CICRP, Marseille, France.
jean-marc.vallet@cicrp.fr

³ M. Pierrot-Desseilligny
ENSG/IGN, Marne la Vallée, France

⁴ X. Brunetaud and M. Al Mukhtar
UPRES PRISME, France

⁵ F. Dubois and F. Cherblanc
UMR CNRS/ Université Montpellier 2 « LMGC », Montpellier, France

⁶ J. Tugas
CRMH, DRAC-PACA, Aix-en-Provence, France

*corresponding author

management of conservation data and also a numerical modelling tool (FEM-DEM) for the physical and structural analysis.

Keywords: conservation, stone, 3D information system, modelling, web platform

CASE STUDIES:

INVESTIGATION OF BUILDING STONES USED IN THE AL-AZHAR MOSQUE (HISTORIC CAIRO, EGYPT)

N. Aly^{1*}, A. Hamed¹, Á. Török², M. Gomez-Heras³ and M. Alvarez de Buergo³

Abstract

Al-Azhar was the first mosque built in Fatimid Cairo and the first theological college, and has played a continuous role in the history of Cairo from its foundation to the present day. A long series of restorations and enlargements were made at Al-Azhar during the Mamluk and Ottoman periods. More additions and restorations were carried out in the nineteenth and twentieth centuries. Mokattam Limestone is the main building material used in the construction of the Al-Azhar mosque and all Historic Cairo. The site in the center of Cairo makes it susceptible to various factors of weathering and pollution. Limestone core samples were extracted from different facades of the Al-Azhar Mosque, including new and old stones. The samples investigated and analyzed by means of different techniques, such as Polarizing microscopy, Scanning Electron Microscope (SEM), Ion Chromatography (IC) and Unconfined Compression Strength (UCS) besides, non-destructive techniques [i.e. Ultrasound Pulse Velocity (UPV) and Rebound Hardness (Leeb)]. The analyses revealed that all the samples contain different amounts of salts mainly chlorides, sulphates and nitrates which also noticed filling the stone pores in SEM images. The presence of salts affects the strength, P-wave velocity and rebound hardness measurements and indicates that the Al-Azhar building stone is under deterioration.

Keywords: cultural heritage buildings, stone decay, non-destructive testing (NDT)

¹ N. Aly and A. Hamed
Faculty of Petroleum and Mining Engineering, Suez University, Egypt
neven.ali@suezuniv.edu.eg

² A. Török
Department of Construction Materials and Engineering Geology,
Budapest Technical University, Hungary

³ M. Gomez-Heras and M. Alvarez de Buergo
Geosciences Institute IGEO (CSIC, UCM) Madrid, Spain

*corresponding author

CASE STUDIES:

**THE EFFECT OF REBURIAL ON STONE DETERIORATION:
EXPERIMENTAL CASE STUDY, OXFORD, ENGLAND**

N. Zaman^{1*} and H. Viles¹

Abstract

The practice of reburial/backfilling, either partially or fully, of stone ruins is a method of site management and preservation that is of interest to cultural heritage site managers worldwide due to the expense and limited resources agencies often face in site maintenance and restoration. Some sites have implemented reburial to some degree, including Chaco Canyon National Historical Park (United States), Aztec Ruins National Monument (United States), Rose Theatre (England), Laetoli hominid trackway (Tanzania), and at various sites in Italy, Israel, and North Africa for the preservation of ancient mosaics. This method of site preservation is dependent upon the assumption that soil conditions that were conducive to preservation of the ruins pre-excavation are reestablished upon reburial/backfilling. Yet to date there has been extremely limited research done to assess whether this is the case and being cause for the primary hesitation on the part of site managers in implementing partial or full reburial/backfilling of sites. This research aims to bridge this gap by investigating whether soils used to protect cultural stone through the method of reburial/backfilling of sites are benign or likely to cause alteration to the stones due to the environment they facilitate. The effects of a reburial/backfilled soil environment versus surface exposure on the weathering of stone materials are examined through a case study at Wytham Woods in Oxford, England. Limestone and sandstone blocks were buried at differing depths for two years in fill material consisting of the native soil on site, a clay rich silt loam. The limestone and sandstone samples were pre-weathered in the laboratory prior to burial in order to simulate weathered cultural stone. A corresponding set of limestone and sandstone blocks were left exposed at the surface for two years. Weathering of the limestone and sandstone blocks were assessed by examination of changes in weight, the Young's modulus of elasticity, and surface hardness after burial and surface exposure. *In situ* soil moisture and temperature measurements were monitored continuously with emplaced soil sensors connected to dataloggers and soil samples were taken for chemical and physical analysis before burial and upon excavation. An on-site weather station was used to obtain above ground environmental data including temperature, relative humidity, rainfall, and solar radiation. Results from all stone and soil analyses were used to assess whether burial in this case enhanced preservation or promoted alteration of cultural stone to a stronger degree than being left exposed to surface conditions.

Keywords: reburial, backfill, stone weathering, soil

¹ N. Zaman* and H. Viles

School of Geography and the Environment, University of Oxford, United Kingdom
nooren.zaman@ouce.ox.ac.uk

*corresponding author

LIST OF AUTHORS

A

Abdel-Wahab, M. 1041
 Abuku, M. 1201, 1255
 Aguiar, J. 653
 Al Mukhtar, M. 1301
 Alexakis, E. 1219
 Aloiz ,E. 1069
 Alonso, J. 663
 Alvarez de Buergo, M. 1303
 Aly, N. 1303
 Andraud, C. 785
 Apostolopoulou, M. 1219
 Araiza-Garaygordobil, G. 1051
 Arnold, T. 879
 Arosio, F. 1089
 Astete, F. 1227
 Auras, M. 1077

B

Bagneris, M. 1301
 Bakolas, A. 1219
 Ball, R.J. 671
 Balloi, A. 1089
 Barov, Z. 679
 Bartoli, F. 915
 Benchiarin, S. 1111
 Bianchi, S. 847, 855
 Bîrzu, C. 1097
 Böhm, K. 879
 Bonazza, A. 1137
 Bourgon, J. 785
 Boyes, N. 1103
 Bracci, S. 653
 Bresciani, V. 1089
 Bromblet, P. 1247, 1271, 1301
 Brunetaud, X. 1301
 Brunet-Imbault, B. 1271
 Burgos-Cara, A. 1297

C

Cabello-Briones, C. 695
 Caner, E. 839

Caner-Saltık, E.N. 839
 Caneva, G. 915
 Cano, C. 1227
 Carmona-Quiroga, P.M. 703
 Caruso, F. 923
 Casanova Muncicchia, A. 915
 Castelvetro, V. 847, 855
 Charalambous, C. 711
 Charola, A.E. 1069, 1129
 Cherblanc, F. 1301
 Chiantore, O. 847, 855
 Coggin, M. 1287
 Colella, M. 1089
 Coltelli, M.-B. 847, 855
 Çömez, S. 839

D

D'Amen, E. 761
 Dağ, F.K. 839
 Dajnowski, A. 719
 Dajnowski, B. 719
 De Luca, L. 1301
 De Roy, J. 999
 Del Lama, E.A. 811
 Delegou, E.T. 1219
 Ďoubal, J. 729
 Downes, S. 963
 Drdácáký, M. 687
 Duberson, S. 1247
 Dubois, F. 1301

E

Erdil, M. 839
 Espinosa-Gaitán, J. 745
 Etienne, M. 1247
 Ettl, H. 1077

F

Fassina, V. 1111
 Fermo, P. 1137
 Flatt, R.J. 923
 Fontaine, L. 999

Forster, A. 769
 France, C. 1129
 Frangova, K. 1263
 Franković, M. 663
 Franzen, C. 753, 1119
 Franzoni, E. 761, 803, 947
 Fregni, A. 761
 Frühwirt, T. 955
 Fujita, H. 1227

G

Gabrielli, R. 761
 Gembinski, C. 1009
 Gerdwilker, C. 769
 Gerns, E. 777
 Ghaffari, E. 889
 Gherardi, F. 847, 855
 Giaccai, J. 1129
 Godet, M. 785
 Gomez-Heras, M. 1303
 Górnjak, A. 793
 Graham, C.A. 1017
 Graziani, G. 761, 803, 947
 Grissom, C. 1069, 1129
 Grossi, C.M. 817
 Grossi, D. 811
 Guichard, H. 1247
 Guillon, O. 1301
 Guinamard, C. 1271
 Gulotta, D. 1137
 Güney, B.A. 839

H

Hamed, A. 1303
 Hartleitner, W. 1077
 Haselberger, M. 1171
 He, L. 905
 Henry, A. 671
 Hoornaert, L. 999
 Howind, T. 1299
 Hughes, J.J. 1299
 Hunt, B.J. 817
 Huysmans, S. 999
 Hyslop, E. 769

I

Iba, C. 1145
 Ibach, H.W. 1300
 Ioannou, I. 711
 Ishizaki, T. 825, 1201
 Ito, A. 1227

J

Jablonski, M. 1153
 Jakutajć, J. M. 831
 Jandejsek, I. 687

K

Kang, S. 703
 Karacsonyi, S. 889
 Karbowska-Berent, J. 831
 Kardara, E. 1025
 Kawaguchi, T. 1211
 Kiesewetter, A. 1119
 Kiriyama, K. 1255
 Kohdzuma, Y. 1255
 Koizumi, K. 1145
 Kozub, B. 1031
 Kozub, P. 1031
 Kraus, K. 753
 Krist, G. 889, 1171
 Kuchitsu, N. 1211

L

Labropoulos, K. 1219
 Lawane, A. 1181
 Lawrie, K. 1059
 Lazzeri, A. 847, 855
 Leroy, E. 785
 Lezzerini, M. 847, 855
 Little, N.C. 1129
 Livingston, R.A. 1069, 1129
 Long, E.S. 863
 López-Doncel, R.A. 981, 1051, 1237
 Łukaszewicz, J.W. 793, 831
 Luxford, N. 963

M

Marelli, I. 1089

Marinković, V. 1189
 Marinov, T. 1263
 Martín-Chicano, A. 745
 Mas-Barberà, X. 871
 Matsuda, H. 1211
 McGibbon, S. 1041
 Meier, T. 1077
 Meinhardt, J. 879
 Milchin, M. 889, 1171
 Mısır, Ç.T. 839
 Mizutani, E. 1201
 Molin, G. 1111
 Monnier, J. 785
 Morii, M. 1211, 1227
 Moropoulou, A. 1219
 Moundoulas, P. 1219
 Mudronja, D. 1189

N

Niccolai, L. 847
 Nishiura, T. 1227
 Nuño, M. 671

O

Odgers, D. 671
 Ogura, D. 1201, 1255
 Ono, I. 1227
 Ottosen, L.M. 897

P

Pan, A. 905
 Pantet, A. 1181
 Pascucci, S. 915
 Pérez, L. 871
 Pesce, G.L. 671
 Pfefferkorn, S. 1119
 Piao, C. 1145
 Pierrot-Desseilligny, M. 1301
 Polí, T. 855
 Pomonis, T. 1025
 Pötl, C. 1237
 Praticò, Y. 923
 Pummer, E. 931

Q

Quarto, A. 1089

R

Raymakers, K. 1279
 Rieffel, Y. 981
 Rodríguez, M.A. 871
 Rodríguez-Navarro, C. 1297
 Rohatsch, A. 847
 Rolland, O. 1247
 Rossen, L. 1279
 Roveri, N. 761
 Rüdrieh, J. 981
 Ruiz Bazán, I. 1089
 Ruiz, S. 871
 Ruiz-Agudo, E. 1297

S

Sacchi, B. 653
 Saheb, M. 785
 Salvadori, B. 653
 Salvini, S. 939
 Sano, K. 1145
 Sasaki, J. 1201
 Sassoni, E. 761, 803, 947
 Scherer, G.W. 803, 811, 947
 Scholz, G. 1300
 Siedel, H. 955, 1119
 Siegesmund, S. 1237
 Signori, F. 855
 Simon, S. 1017
 Singh, L.P. 1299
 Smacchia, D. 855
 Smith, N. 1059
 Sobott, R.J.G. 1300
 Sotgia, C. 1089
 Soto-Zamora, M.Á. 1051
 Šperl, M. 687
 Stanley, B. 963
 Stillhammerova, M. 1279

T

Takatori, N. 1255
 Taniguchi, Y. 1145

Tavukçuoğlu, A. 839
Thapliyal, P.C. 1299
Thomassin, J.H. 1181
Thorn, A. 971
Todorov, V. 1263
Tokimoto, S. 1211
Toniolo, L. 847, 855, 1137
Torney, C. 769
Török, Á. 1303
Tracey, E.A. 1059
Trubert, M. 1271
Tugas, J. 1301

V

Vallet, J.-M. 1301
Verecke, J. 1279
Vergès-Belmin, V. 785, 1247
Verhulst, N. 999
Vicenzi, E. 1129
Viles, H. 1304
Viles, H.A. 695, 703
Vinai, R. 1181
Vizcaino-Hernández, I.E. 1051

W

Wakiya, S. 1255
Wangler, T. 923
Watanabe, K. 1145
Weber, J. 847, 889
Wedekind, W. 981, 1237
Weise, S. 1119
Wentzel, R. 1287
Wichert, J. 955
Will, R. 777
Wiśniewska, B. 793

Y

Yang, S. 905
Yoshioka, M. 1145
Young, D. 991
Young, D.A. 863

Z

Zaman, N. 1304
Zhu, W. 1299

LIST OF KEYWORDS
3

3D information system 1302
 3D photo monitoring 1031
 3D surface geometry 1017
 3D survey 1089
 3D-modelling 1051

A

ablation 719
 acid attack 803
 acrylic and PVA as fixatives for
 polychromies 1279
 acrylic resin 1211, 1300
 additives 663
 adhesives 663
 African local houses 1181
 ageing 703
 alveolar weathering 981
 ammonium citrate 653
 ammonium oxalate 803, 1189
 analytical techniques 1219
 application 889
 application techniques 679
 archaeological sites 695
 architectural heritage 848
 attachment 1211

B

bacillus cereus 831
 backfill 1304
 bedrock 879
 benzalkonium chloride 863
 biocide 863, 915
 biodeterioration 915
 biological growth 863
 biomineralisation 745, 831
 bio-restoration 1089
 black crust 999, 1077
 block copolymer 855
 building material 1219
 burial 817

C

calcareous stone 793
 calcination 1129
 calcite 803
 calcium phosphate 803, 947
 calcium sulphate 1255
 calcium-oxalate 1189
 captive-head washing 991
 carbonate stones 831
 Carthage marble 777
 cemetery 1153
 cemetery conservation 939
 Central Park Obelisk 1009
 clay 1271
 cleaning 729, 785, 1077, 1089
 climate 1247
 Close-Range Digital Photogrammetry
 1051
 coating 1299
 compatibility 769
 compatible treatment 729
 conservation 663, 719, 729, 939,
 981, 1059, 1119, 1137, 1171, 1271,
 1300, 1302
 conservation of stone 1077
 conservation planning 769
 conservation practice 1017
 conservation treatment 839, 1009
 conservation values 1299
 consolidants 811
 consolidation 687, 745, 769, 793,
 831, 839, 848, 855, 889, 923, 931,
 955, 1279
 convergent photogrammetry 1089
 core stone 1211
 cracks in stone 687
 crust 999, 1077
 cultural heritage 663, 817, 1031,
 1299, 1303
 cultural heritage buildings 1303
 cyanobacteria 915
 Cyprus 711

D

damage mapping 1237
 damages and causes 1263
 database schema 1025
 decay 695, 897, 1137, 1219
 decorated stone elements 1097
 delamination 999, 1069
 demineralisation 931
 dense limestone 831
 deposition 1137
 desalination 981, 991, 1247
 design of experiment (DoE) 923
 deterioration 1189
 deterioration mapping 999
 deterioration patterns 1111
 diagnostic study 1219
 diammonium hydrogen phosphate (DAP)
 793
 digital documentation 1009
 digitalisation 1051
 digitisation 1041
 dissolution 803
 dolomite 839
 drilling resistance 671
 durability 1111

E

earthquake 1171
 efficiency tests for conservation
 treatment 839
 efflorescence 1103
 Elbe sandstone 1119
 electro-desalination 897
 environmental monitoring 1145
 environmental pollution soiling 1103
 epoxy consolidation 1279
 ethanol 947
 ethyl silicate 923, 971, 1111
 ethyl silicate consolidation 1279
 evaluation 729
 evaporation 1201, 1255
 exhibition 1097
 existing conditions 1009

F

façade cladding 777
 fatty acid 711
 field recording 1009
 film properties 905
 fire 1129
 fragile tuff 1145
 fragments 871
 freeze thaw 671
 frost 817
 frost damage 825
 frost heave phenomenon 825

G

GC-1 719
 geospatial data capture 1059
 Gotland sandstone 793
 grain loss 947
 granite 719, 1211, 1227
 gravestones 1017
 green conservation 939
 grouting repairs 1153
 guidelines 1181
 gypsum crust 785

H

Hagar Qim 695
 heat and moisture transfer 1201,
 1255
 heritage management 1059
 historic building materials 761
 hybrid latex 855
 hydric properties 955
 hydrogen peroxide 963
 hydroxyapatite 793

I

index quality 1181
 infilling cracks 831
 injectable grout 971
 interactive re-lighting 1017
 iron yellowing 785
 Itararé sandstone 811

J

Joliet limestone 777

K

Kathmandu Valley 1171

KSE 879

L

laser 785

laser ablation 1103

laser cleaning 719, 1077

laser scanning 1041

laterite 1181

leaching 761

lime 663

limestone 711, 719, 777, 793, 831,
889, 963, 1189, 1247, 1287

limestone decay 695

lithium silicate injectable grout 971

M

Machu Picchu 1227

magnetism 871

magnets 871

maintenance 1041

maintenance and repair 1059

mapping 999, 1031, 1237

marble 777, 1089, 1129, 1153, 1298,
1300

marble decay 1137

masonry 1181

mechanical properties 955

medieval tombstones (stećci) 1189

metadata 1025

Metigo *MAP* 999

Mid-Atlantic 1287

mobile applications 1009

modelling 1302

moisture transfer 1255

monitoring 695, 817, 879, 1137,
1145

monitoring and care concept 879

monument 1103

monument mapping 1031

mould 963

museum 1247

Nnano-dispersive calcium hydroxide
solutions 839

nanolime 671, 745

nanomaterials 848

nanoparticle 785

nanotechnology 1299

natural weathering 703

non-destructive testing (NDT) 1219,
1303**O**

obelisk 719

old treatment evaluations 1279

onsolidation of calcareous stones
793

oxalate 1298

P

painting technique 1263

Patan 1171

penetration depth 955

performance 1287

permeability 905

photocatalytic activity 703

photogrammetry 1129

Pińczów limestone 793

pinning repairs 1153

Platteville limestone 777

point cloud 1031

Pompignan 1287

porous limestone 831, 889

porous materials 1201

POSS-based copolymer 905

poultice 863

poultices 879

pre-consolidants 811

pre-investigation 1119

preservation 817

preservation measures 1263

preventive conservation 753, 1137

projects 1025

- protection 753, 761, 848, 855
 protective measure 825
 protective patinas 1298
 protective performance 905
 Puerto stone 745
- R**
- rain 761
 rain water 1201
 reburial 1304
 recarbonation 1129
 repair 1041, 1153
 resin 1211
 reversible stone adhesive 679
 risk assessment 753, 769
 rock weathering 1145
 Romanesque portals 999
 RTI 1017
 rust removal 653
- S**
- salt 981, 1247
 salt attack 991
 salt crystallisation 671, 1201
 salt decay 897
 salt deterioration 1119
 salt reduction 879
 salt weathering 991
 sandstone 769, 793, 811, 897, 955,
 971, 1069, 1119, 1153, 1271, 1300
 scaling 1211
 scheduled monument 1103
 sculpture 871, 1089, 1247
 seashore 1211
 self-cleaning 761
 self-cleaning coating 703
 self-stabilisation 855
 SEM/EDS 793, 839
 shelter 825, 1255
 shelter environment 1255
 shelters 695
 siloxane polymers 1111
 skills development 1041
 smart ventilation 963
 sodium dithionite 653
 sodium hexametaphosphate 653
 sodium sulphate 1255
 soft nanomaterials 905
 soil 1304
 soiling 1103
 sorptivity 711
 stone 653, 663, 719, 729, 817, 1171,
 1211, 1302
 stone blackening 1137
 stone conservation 848, 931, 939,
 1025, 1097, 1119
 stone consolidation 745
 stone decay 1303
 stone deterioration 1051, 1189
 stone restauration 1097
 stone structures 1227
 stone weathering 1304
 stonemasonry 1041
 strengthening 931
 stylolite 1287
 sulphate 897
 surface erosion 1137
 surface treatment 1145
 surfactants 811
 survey 1103
 sustainability 939
 swelling 1271
 swelling clay 811, 1271
 swelling clay-bearing sandstones
 923
 swelling inhibitor 923
- T**
- technical investigations 679
 technical properties 1237
 TEM 785
 Temple of the Sun 1227
 TEOS 745, 889
 thermal ageing 947
 thermal diffusivity 947
 thermosetting polymethyl methacrylate
 679
 TiO₂ 703
 tombstones 1189
 total impregnation 1300
 toughness 687
 Tournai cathedral 999
 Tournai stone 999

transporter brine 1247
travertine 915
treatment 1271
tuff 1145, 1237, 1263

U

Udelfanger sandstone 1300
ultra-violet 963
unions 871

V

vacuum 889, 931
vacuum circulation process 955
Vermont marble 1129
vernacular architecture 1181

W

water content 825
water evaporation 1255

water repellency 711
water repellent 915, 1145, 1279
weathered stone degradation 671
weathering 753, 981, 1145
weathering characteristics 1237
web platform 1302
wettability 711
winter cover 753
world heritage 1227

X

XRD 839

Z

zeolitization 1263

Conference sponsor and partners



HISTORIC
ENVIRONMENT
SCOTLAND

ÀRAINNEACHD
EACHDRAIDHEIL
ALBA



**British
Geological Survey**

NATURAL ENVIRONMENT RESEARCH COUNCIL



fokus
GmbH Leipzig

GC  **LASER SYSTEMS**



Surface Measurement Systems
World Leader in Sorption Science

UWS UNIVERSITY OF THE
WEST of SCOTLAND